frontiers
RESEARCH TOPICS

DESIGN PRINCIPLES OF SENSORY RECEPTORS

Topic Editor
Dieter Wicher

frontiers in
CELLULAR NEUROSCIENCE

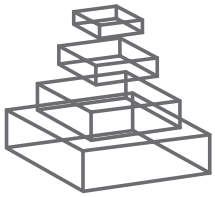

frontiers

FRONTIERS COPYRIGHT STATEMENT

© Copyright 2007-2013
Frontiers Media SA.
All rights reserved.

All content included on this site, such as text, graphics, logos, button icons, images, video/audio clips, downloads, data compilations and software, is the property of or is licensed to Frontiers Media SA ("Frontiers") or its licensees and/or subcontractors. The copyright in the text of individual articles is the property of their respective authors, subject to a license granted to Frontiers.

The compilation of articles constituting this e-book, as well as all content on this site is the exclusive property of Frontiers. Images and graphics not forming part of user-contributed materials may not be downloaded or copied without permission.

Articles and other user-contributed materials may be downloaded and reproduced subject to any copyright or other notices. No financial payment or reward may be given for any such reproduction except to the author(s) of the article concerned.

As author or other contributor you grant permission to others to reproduce your articles, including any graphics and third-party materials supplied by you, in accordance with the Conditions for Website Use and subject to any copyright notices which you include in connection with your articles and materials.

All copyright, and all rights therein, are protected by national and international copyright laws.

The above represents a summary only. For the full conditions see the Conditions for Authors and the Conditions for Website Use.

Cover image provided by Ibbl sarl, Lausanne CH

ISSN 1664-8714
ISBN 978-2-88919-113-0
DOI 10.3389/978-2-88919-113-0

ABOUT FRONTIERS

Frontiers is more than just an open-access publisher of scholarly articles: it is a pioneering approach to the world of academia, radically improving the way scholarly research is managed. The grand vision of Frontiers is a world where all people have an equal opportunity to seek, share and generate knowledge. Frontiers provides immediate and permanent online open access to all its publications, but this alone is not enough to realize our grand goals.

FRONTIERS JOURNAL SERIES

The Frontiers Journal Series is a multi-tier and interdisciplinary set of open-access, online journals, promising a paradigm shift from the current review, selection and dissemination processes in academic publishing.
All Frontiers journals are driven by researchers for researchers; therefore, they constitute a service to the scholarly community. At the same time, the Frontiers Journal Series operates on a revolutionary invention, the tiered publishing system, initially addressing specific communities of scholars, and gradually climbing up to broader public understanding, thus serving the interests of the lay society, too.

DEDICATION TO QUALITY

Each Frontiers article is a landmark of the highest quality, thanks to genuinely collaborative interactions between authors and review editors, who include some of the world's best academicians. Research must be certified by peers before entering a stream of knowledge that may eventually reach the public - and shape society; therefore, Frontiers only applies the most rigorous and unbiased reviews.
Frontiers revolutionizes research publishing by freely delivering the most outstanding research, evaluated with no bias from both the academic and social point of view.
By applying the most advanced information technologies, Frontiers is catapulting scholarly publishing into a new generation.

WHAT ARE FRONTIERS RESEARCH TOPICS?

Frontiers Research Topics are very popular trademarks of the Frontiers Journals Series: they are collections of at least ten articles, all centered on a particular subject. With their unique mix of varied contributions from Original Research to Review Articles, Frontiers Research Topics unify the most influential researchers, the latest key findings and historical advances in a hot research area!
Find out more on how to host your own Frontiers Research Topic or contribute to one as an author by contacting the Frontiers Editorial Office: researchtopics@frontiersin.org

DESIGN PRINCIPLES OF SENSORY RECEPTORS

Topic Editor:
Dieter Wicher, Max Planck Institute for Chemical Ecology, Germany

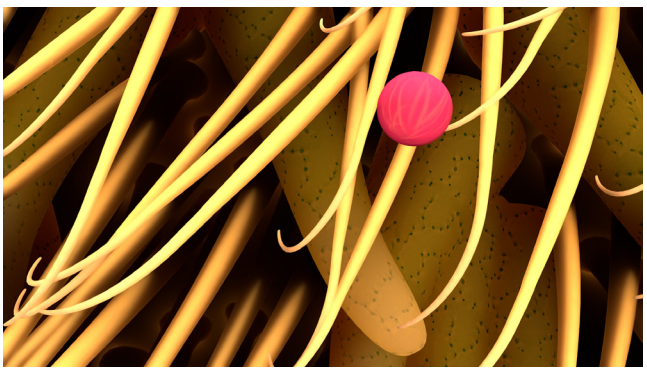

Odor molecule navigating towards a fly nose. Copyright: © 2012 Kimberly Falk

This Research Topic is aimed towards collecting the present knowledge of structure and function of sensory receptors in the animal kingdom, as well as the mechanisms of signal transduction and downstream signal amplification. The term sensory receptor applies for sensory modalities reflecting the outer world (vision, audition, olfaction etc.), the inner world (pH, osmolarity, glucose level etc.) or both such as temperature and pain.

Table of Contents

05 ***Design Principles of Sensory Receptors***
Dieter Wicher

08 ***Sensory Receptors—Design Principles Revisited***
Dieter Wicher

10 ***Drosophila Photoreceptors and Signaling Mechanisms***
Ben Katz and Baruch Minke

28 ***Daily Rhythm of Melanopsin-Expressing Cells in the Mouse Retina***
Irene Gonzalez-Menend, Felipe Contreras, Rafael Cernuda-Cernuda and Jose M Garcia-Fernandez

35 ***A New Photosensory Function for Simple Photoreceptors, the Intrinsically Photoresponsive Neurons of the Sea Slug Onchidium***
Tsukasa Gotow and Takako Nishi

41 ***Functional and Evolutionary Aspects of Chemoreceptors***
Dieter Wicher

45 ***Mammalian Olfactory Receptors***
Joerg Fleischer, Heinz Breer and Joerg Strotmann

55 ***Odorant and Pheromone Receptors in Insects***
Tal Soo Ha and Dean P. Smith

61 ***Molecular and Cellular Designs of Insect Taste Receptor System***
Kunio Isono and Hiromi Morita

77 ***Pheromone Transduction in Moths***
Monika Stengl

92 ***Temporal Response Dynamics of Drosophila Olfactory Sensory Neurons Depends on Receptor Type and Response Polarity***
Merid N. Getahun, Dieter Wicher, Bill S. Hansson and Shannon B. Olsson

103 ***Plant Odorants Interfere with Detection of Sex Pheromone Signals by Male Heliothis Virescens***
Pablo Pregitzer, Marco Schubert, Heinz Breer, Bill S. Hansson, Silke Sachse and Jürgen Krieger

115 ***A First Glance on the Molecular Mechanisms of Pheromone-Plant Odor Interactions in Moth Antennae***
Sylvia Anton and Michel Renou

117 Ric-8A, a Gαα Protein Guanine Nucleotide Exchange Factor Potentiates Taste Receptor Signaling

Claire J Fenech, Iila Patrikainen, Daniel S Kerr, Sylvie Grall, Zhenhui Liu, Fabienne Laugerette, Bettina Malnic and Jean-Pierre Montmayeur

126 Identification of New Binding Partners of the Chemosensory Signaling Protein Gγ13 Expressed in Taste and Olfactory Sensory Cells

Zhenhui Liu, Claire Fenech, Hervé Cadiou, Sylvie Grall, Esmerina Tili, Fabienne Laugerette, Anna Wiencis, Xavier Grosmaitre and Jean-Pierre Montmayeur

frontiers in
CELLULAR NEUROSCIENCE

EDITORIAL
published: 07 July 2010
doi: 10.3389/fncel.2010.00025

Design principles of sensory receptors

Dieter Wicher*

Laboratory of Neurophysiology, Department of Evolutionary Neuroethology, Max Planck Institute for Chemical Ecology, Jena, Germany
**Correspondence: dwicher@ice.mpg.de*

Organisms continuously detect and process physical and chemical signals from their external and internal world, and they monitor their interaction with the environment. Aristotle was the first who defined the five external senses in humans: sight, hearing, smell, taste, and touch. In addition, we consider balance as the sixth external sense. Similarly important for the control of movement is the sense of body position, the proprioception. The physiological state of the organism is reported by a variety of internal receptors including those for gases, temperature, or pH. According to the activating stimulus sensory receptors can be classified into electromagnetic receptors (photoreceptor, thermoreceptor), mechanoreceptors (hearing, touch, balance, osmoreceptor), and chemoreceptors (odorant receptor, gustatory receptor). Sensory signals are perceived by specialized neurons equipped with one type of receptor molecules as photoreceptor cells or with various types of receptors as nociceptive neurons to detect different noxious stimuli including heat, pressure, pH, or chemical signals. Most receptor molecules are tuned to a single sensory modality but some are polymodal as the vanilloid receptor VR1 which is activated by heat, pungent chemicals, acids, or lipids. Activation of receptor molecules by an adequate stimulus initiates a signal transduction process in the sensory neuron in which the physical or chemical signal is amplified and converted into an electrical signal that depolarizes or hyperpolarizes the cell. The properties of the stimulus such as strength and duration are then translated into a specific temporal pattern of action potentials which is further processed in the brain.

In recent years the research on design and function of sensory receptors and their signal transduction machinery has largely extended our knowledge in this field. The present special issue is aimed of presenting an actual view on photoreceptors and chemoreceptors.

Photoreceptors and many chemoreceptors belong to the G protein-coupled receptor (GPCR) family. GPCRs are seven transmembrane (7-TM)-spanning proteins that interact with heterotrimeric G proteins. According to structural similarities GPCRs are grouped into families. Photoreceptors and most vertebrate olfactory receptors belong to the rhodopsin receptor/class A family. Ligand binding to a GPCR causes a conformational change thereby activating a trimeric G protein which disensembles into the G_{α}- and the $G_{\beta\gamma}$-subunit. Independently, both subunits can affect various targets such as enzymes or ion channels. G protein signaling is usually associated with signal amplification. An exception are mammalian olfactory receptors in which the dwell time of odorant molecules is too short to efficiently activate G proteins (Bhandawat et al., 2005). The signal amplification takes place downstream by interaction of ion channels.

In the classical view a monomeric protein with 7-TM topology constitutes a metabotropic receptor (**Figure 1A**) which interacts with a trimeric G protein. However, in the case of the channelrhodopsins the 7-TM protein does not couple to a G protein. Instead, it functions as an ionotropic receptor (**Figure 1B**) since its activation gates an ion channel (Nagel et al., 2005). GPCRs may form homomeric (**Figure 1C**) as well as heteromeric dimers (**Figure 1D**). For class A GPCRs instable homodimerization has been observed for M1 muscarinic acetylcholine receptors (Hern et al., 2010) or an oligomerization to higher orders as for β2-adrenergic receptors (Fung et al., 2009). Class C GPCRs built stable heterodimers such as the mammalian taste receptors for sweet and umami (Palmer, 2007). In heterodimeric $GABA_B$ receptors, $GABA_B$R1 binds the ligand while $GABA_B$R2 couples to the G protein and is required for targeting $GABA_B$R1 to the membrane (Brauner-Osborne et al., 2007). Intriguingly, a similar principle is observed in insect odorant receptors. These 7-TM proteins are heterodimers of a conventional odorant receptor (OR) protein and an ubiquitous co-receptor (Neuhaus et al., 2005) (**Figure 1E**). The OR protein binds the odorant and couples to the G protein which in turn stimulates cAMP production (Wicher et al., 2008). The co-receptor is required for membrane targeting of the OR protein (Larsson et al., 2004) and is a non-selective cation channel activated by cAMP (Wicher et al., 2008). In addition to this metabotropic pathway of insect OR activation there is also a G protein independent, ionotropic one (Sato et al., 2008; Wicher et al., 2008). These findings raised a controversial discussion how to classify insect ORs, as ionotropic or metabotropic. One view is "In insects, most odorant receptors consist of a heteromeric complex that serves both as the receptor for the ligand and as the ion channel that is gated by binding of the ligand – a mechanism that is referred to as ionotropic" (Kaupp, 2010). The other view is "The design principle of insect ORs of being composed of an odorant-sensitive protein and of a protein finally transducing the chemical message into an electrical signal ensures very rapid recognition of high odor concentrations via the ionotropic pathway as well as a somewhat slower but prolonged and highly sensitive odor detection via the G protein-mediated signal amplification" (Wicher et al., 2008). Per definition an ionotropic receptor is an ion channel directly gated by ligand binding. This is not the case for insect ORs at low odor concentration where channel opening requires G protein activation and second messenger production – hallmarks of metabotropic signaling. This kind of signal transduction is quite similar to the olfactory signaling in vertebrates. The only difference is that in vertebrates the activated ion channel is separated from the receptor while in insects it is part of the receptor. At high odor concentration the metabotropic pathway is accompanied and sped up by the ionotropic one. Thus, a more appropriate classification of insect ORs might be "combined metabotropic and ionotropic receptors". A detailed discussion on insect ORs is given by Ha and Smith.

In *Drosophila* photoreceptors the signal transduction machinery is highly organized. Their elements are held together by the

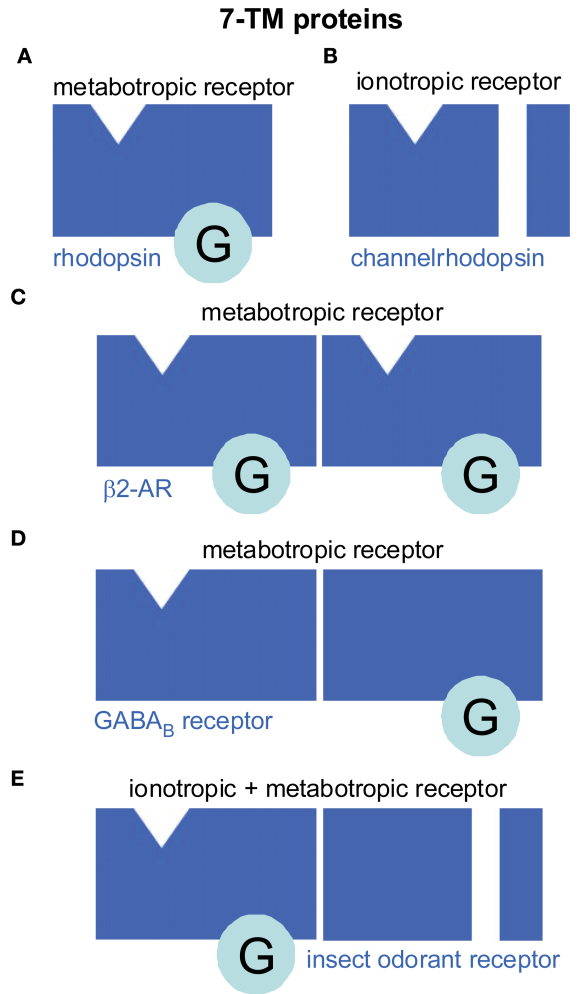

FIGURE 1 | Seven transmembrane (7-TM) proteins function as monomers but can also dimerize (or oligomerize). Although most 7-TM proteins are metabotropic receptors (**A**, **C–E**) there are a few examples of ionotropic 7-TM receptors (**B**, **E**). **(A)** Most common for a 7-TM protein is to function as G protein-coupled receptor (GPCR). For example, monomeric rhodopsin in vertebrate rods forms a metabotropic receptor such as bearing the light-sensitive retinal as ligand which activates trimeric G proteins upon light-dependent activation of its associated ligand retinal. **(B)** However, channelrhodopsins are 7-TM ionotropic receptors in green algae. Ligand binding directly gates an ion channel while there is no G protein interaction. **(C**, **D)** GPCRs can form homodimers **(C)** as the β2-adrenoceptor (β2-AR) or heterodimers **(D)** as the $GABA_B$ receptor. In the $GABA_B$ receptor the subunits have distinct function. One is responsible for ligand binding, the other for G protein interaction. **(E)** Insect odorant receptors are heterodimers composed of inversely oriented 7-TM proteins (Benton et al., 2006). The odorant-specific protein contains the ligand-binding site and a so far undescribed G protein interaction site. The other protein forms a channel that can be activated by odorant binding either directly via an ionotropic pathway or via a metabotropic pathway including G protein activation.

scaffolding protein InaD which enables fast processing of the sensory input. The delay between photon absorption by rhodopsin and activation of the receptor current is only 20 ms. The ion channel conducting this current was the first member of the TRP channel superfamily to be detected. Mutant flies with disrupted channel function show the phenotype of Transient Receptor Potential upon constant light stimulus (Cosens and Manning, 1969). Various members of the TRP superfamily form sensory receptors including mechanoreceptors, thermoreceptors, chemoreceptors, and pain receptors (Damann et al., 2008), some of which are polymodal (Belmonte and Viana, 2008). Katz and Minke review anatomy and function of fly photoreceptors and provide a current view on details of sensory transduction.

Retinal ganglion cells expressing melanopsin are photosensitive cells that do not contribute to image-processing vision but are involved in the entrainment of circadian rhythms. Gonzalez-Menendez et al. demonstrate in their research report that melanopsin-expressing cells themselves are subjected to circadian regulation. They found a circadian oscillation of the number of these cells in the mouse retina which required synchronization by the light/dark cycle.

A review related to non-visual photoreception is presented by Gotow and Nishi on photosensitive interneurons modulating the behavior of a sea slug. These neurons are localized in central ganglia and respond to light either with depolarizations or with hyperpolarizations. The type of the photoresponse depends on coupling to G proteins which lead either to cGMP hydrolysis or synthesis subsequently closing or opening a cGMP-dependent K^+ channel, respectively.

Chemoreceptors are another class of sensory receptors using GPCRs – though not exclusively – to detect chemical signaling molecules. An update on mammalian olfactory receptors is given by Fleischer et al. According to structure and distribution these receptor proteins are grouped into families including ORs, vomeronasal receptors (VRs), trace amine-associated receptors (TAARs), formyl peptide receptors (FPRs), and guanylyl cylase D (GCD). Except for the GCDs all other receptors form GPCRs. ORs, TAARs and the VR1 subgroup belong to the rhodopsin/class A family. The VR2 subgroup belongs to the class C family, whether their members dimerize remains to be shown.

Insect ORs, as reviewed by Ha and Smith, differ from classical GPCRs in various aspects. Although the receptor proteins have a 7-TM structure like GPCRs they do not share sequence similarity with them. In addition, insect odorant receptor proteins show an inverted orientation in the membrane, i.e., the N-terminus is intracellular and the C-terminus extracellular. Finally, these ORs are heterodimers composed of a conventional, odor-specific receptor protein and an ubiquitous protein such as Or83b in *Drosophila* (**Figure 1E**). There is a distinct class of putative chemosensory receptors that are akin to ionotropic glutamate receptors. *Drosophila* pheromone receptors are composed of a conventional OR and Or83b. But in contrast to ORs another, receptor-associated sensory neuron membrane protein (SNMP) with 2-TM topology is required to form a functional complex. Intriguingly, it is SNMP that binds the ligand which is not the pheromone itself but the pheromone-binding protein LUSH when activated by the pheromone.

The review by Stengl on moth pheromone receptors demonstrates how the high sensitivity of male moth pheromone receptor neurons is obtained which is necessary to perceive the intermittently

released sex-pheromone blend. It becomes apparent that depending on the stimulus properties different signal transduction pathways are recruited. Furthermore, the sensitivity of receptor neurons is regulated in a circadian manner to achieve highest sensitivity during the moth's activity phase and to allow for a phase of rest.

The contribution by Isono and Morita reviews the present knowledge on insect gustatory receptors (GRs) which are distantly related to the insect ORs. While in the olfactory system one neuron expresses one receptor, various GRs may be expressed in taste neurons. Moreover, these neurons also express other sensory receptors such as the TPR channel *painless*. This principle allows one neuron to perceive different sensory modalities.

The function of GPCRs and downstream signaling is subject to extensive modulation, for example by RGS proteins (regulator of G protein signaling). Fenech et al. present an original article on Ric-8A, a guanine nucleotide exchange factor. This G protein interacting protein is localized in taste receptor cells and is able to amplify the response to a taste signal by promoting the exchange of GDP by GTP.

This special issue comprises various examples how the receptor design is adapted to the physiological demands of an organism to perceive sensory signals in different intensity and temporal resolution. There is accumulating evidence that often a sensory receptor is part of a signal processing network including scaffolding proteins or RGS proteins.

REFERENCES

Belmonte, C., and Viana, F. (2008). Molecular and cellular limits to somatosensory specificity. *Mol. Pain* 4, 14.

Benton, R., Sachse, S., Michnick, S. W., and Vosshall, L. B. (2006). Atypical membrane topology and heteromeric function of *Drosophila* odorant receptors *in vivo*. *PLoS Biol.* 4, e20. doi:10.1371/journal.pbio.0040020.

Bhandawat, V., Reisert, J., and Yau, K. W. (2005). Elementary response of olfactory receptor neurons to odorants. *Science* 308, 1931–1934.

Brauner-Osborne, H., Wellendorph, P., and Jensen, A. A. (2007). Structure, pharmacology and therapeutic prospects of family C G-protein coupled receptors. *Curr. Drug Targets* 8, 169–184.

Cosens, D. J., and Manning, A. (1969). Abnormal electroretinogram from a *Drosophila* mutant. *Nature* 224, 285–287.

Damann, N., Voets, T., and Nilius, B. (2008). TRPs in our senses. *Curr. Biol.* 18, R880–R889.

Fung, J. J., Deupi, X., Pardo, L., Yao, X. J., Velez-Ruiz, G. A., Devree, B. T., Sunahara, R. K., and Kobilka, B. K. (2009). Ligand-regulated oligomerization of beta(2)-adrenoceptors in a model lipid bilayer. *EMBO J.* 28, 3315–3328.

Hern, J. A., Baig, A. H., Mashanov, G. I., Birdsall, B., Corrie, J. E., Lazareno, S., Molloy, J. E., and Birdsall, N. J. (2010). Formation and dissociation of M1 muscarinic receptor dimers seen by total internal reflection fluorescence imaging of single molecules. *Proc. Natl. Acad. Sci. U.S.A.* 107, 2693–2698.

Kaupp, U. B. (2010). Olfactory signalling in vertebrates and insects: differences and commonalities. *Nat. Rev. Neurosci.* 11, 188–200.

Larsson, M. C., Domingos, A. I., Jones, W. D., Chiappe, M. E., Amrein, H., and Vosshall, L. B. (2004). Or83b encodes a broadly expressed odorant receptor essential for *Drosophila* olfaction. *Neuron* 43, 703–714.

Nagel, G., Szellas, T., Kateriya, S., Adeishvili, N., Hegemann, P., and Bamberg, E. (2005). Channelrhodopsins: directly light-gated cation channels. *Biochem. Soc. Trans.* 33, 863–866.

Neuhaus, E. M., Gisselmann, G., Zhang, W., Dooley, R., Störtkuhl, K., and Hatt, H. (2005). Odorant receptor heterodimerization in the olfactory system of *Drosophila* melanogaster. *Nat. Neurosci.* 8, 15–17.

Palmer, R. K. (2007). The pharmacology and signaling of bitter, sweet, and umami taste sensing. *Mol. Interv.* 7, 87–98.

Sato, K., Pellegrino, M., Nakagawa, T., Nakagawa, T., Vosshall, L.B., and Touhara, K. (2008). Insect olfactory receptors are heteromeric ligand-gated ion channels. *Nature* 452, 1002–1006.

Wicher, D., Schäfer, R., Bauernfeind, R., Stensmyr, M. C., Heller, R., Heinemann, S.H., and Hansson, B. S. (2008). *Drosophila* odorant receptors are both ligand-gated and cyclic-nucleotide-activated cation channels. *Nature* 452, 1007–1011.

Received: 02 June 2010; accepted: 15 June 2010; published online: 07 July 2010.
*Citation: Wicher D (2010) Design principles of sensory receptors. Front. Cell. Neurosci. **4**:25. doi: 10.3389/fncel.2010.00025*
Copyright © 2010 Wicher. This is an open-access article subject to an exclusive license agreement between the authors and the Frontiers Research Foundation, which permits unrestricted use, distribution, and reproduction in any medium, provided the original authors and source are credited.

frontiers in
CELLULAR NEUROSCIENCE

EDITORIAL
published: 24 January 2013
doi: 10.3389/fncel.2013.00001

Sensory receptors—design principles revisited

Dieter Wicher*

Laboratory of Reception and Transduction, Department of Evolutionary Neuroethology, Max Planck Institute for Chemical Ecology, Jena, Germany
**Correspondence: dwicher@ice.mpg.de*

Edited by:
Egidio D'Angelo, University of Pavia, Italy

This research topic was aimed toward collecting the present knowledge of structure and function of sensory receptors in animal kingdom as well as the mechanisms of signal transduction and amplification. To translate external signals such as light, sound, smell, etc., into an appropriate intracellular signal, sensory receptors use either a fast, direct or a slow, indirect way. These qualitatively different signal transduction pathways are now usually called ionotopic or metabotropic. Historically, the term metabotropic receptor has been introduced to distinguish a subtype of glutamate receptors that triggers chemical reactions (cell metabolism) in the postsynaptic cell from other glutamate receptors that pass an ion current (ionotropic) (Eccles and McGeer, 1979). Metabotropic glutamate receptors were found to be linked to inositol phospholipid metabolism (Sugiyama et al., 1987), and were subsequently identified as G-protein-coupled receptors (GPCRs) (Masu et al., 1991). The terminology ionotropic/metabotropic has been extended to other neurotransmitter receptors, such as for nicotinic/muscarinergic acetyl choline or $GABA_A$/$GABA_B$ receptors. All metabotropic neurotransmitter receptors are GPCRs. There are, however, a large number of non-GPCRs that also fulfill the original definition for a metabotropic receptor, namely "that the transmitter acts *indirectly*, by triggering a chemical reaction or a series of reactions" (Eccles and McGeer, 1979). Accordingly, it has been used to extent the term metabotropic receptor to receptor kinases, receptor cyclases, etc., as well.

Sensory receptors are often part of complex signal transduction cascades. An ion current through an ionotropic receptor may initiate metabotropic signaling, as well as a metabotropic receptor may downstream affect the function of ion channels. An example for protein–protein interaction in chemosensation is given in the original article by Liu et al. (2012). The authors identified so far unknown binding partners of Gγ13, a G-protein subunit expressed in mammalian taste and olfactory receptor cells. These binding partners are PDZ-domain containing proteins assumed to target Gγ13 to specific subcellular locations or represent parts of the chemosensory signal transduction cascade.

The evolution of chemoreceptors shows that—from bacteria to mammals—both, ionotropic as well as metabotropic mechanisms were conserved. Functional aspects of chemoreceptors, including the interaction of electrical and chemical signaling, and the amplification of sensory information are discussed in the perspective article (Wicher, 2012). Intriguingly, insect chemoreceptors operate as ionotropic receptors, namely odorant receptors (ORs), ionotropic glutamate-like receptors (IRs), and gustatory receptors (GRs). Getahun et al. (2012) investigate the temporal response dynamics of insect chemoreceptors and demonstrate that olfactory sensory neurons (OSNs) expressing ORs, GRs, or IRs differ in their response kinetics to brief stimuli. OR-expressing neurons respond faster and with higher sensitivity, while IR-expressing neurons do not adapt to long stimulations. Although ORs primarily operate as ionotropic receptors, metabotropic signaling was seen to modulate the ionotropic odor response (Olsson et al., 2011; Sargsyan et al., 2011). Stimulation of cAMP production enhanced the response to a given odor concentration, corresponding to an increased sensitivity. This type of modulation may constitute the mechanistic basis for the higher sensitivity of ORs compared with IRs.

Chemical information released from different sources may interfere during processing in the nervous system and affect the response of an organism. Odor mixtures can act in synergistic or in an inhibitory way. On the level of the chemoreceptors the existence of a huge number of different chemical signal molecules leads to the intriguing question of receptor specificity and whether a given chemical signal is perceived independent of the background. The interaction of odorant and pheromone detection in moths is reported by Pregitzer et al. (2012) and commented by Anton and Renou (2012). Certain plant odors are known to inhibit the activation of pheromone receptors. The reported investigations provide evidence that the odorant-pheromone interaction already takes place at the receptor level.

Since the first editorial to this topic was written in 2010 recent progress shed new light on structure and function of certain receptors. Channelrhodopsins, for example, are photoreceptors in green algae which conduct a current upon illumination. They are seven transmembrane (7-TM)-spanning proteins as typical for GPCRs but do not couple to a heterotrimeric G-protein. With the given 7-TM topology it was as yet not clear how the channelrhodopsin proteins have to arrange to form an ion channel. Recently, the non-selective cation channel, channelrhodopsin-2 from *Chlamydomonas reinhardtii* has been successfully crystallized (Müller et al., 2011; Kato et al., 2012). The channelrhodopsin-2 proteins were found to stably dimerize in such an arrangement that the third and the fourth TM helix of each protein align to a tetramer thereby lining the cation-permeable pore. Another example for ion channel-forming 7-TM proteins are the above mentioned insect ORs. In contrast to homodimeric channelrhodopsin channels they are heterodimers, composed of variable, odorant-binding protein OrX, and an ubiquitous co-receptor OrCo. There is growing evidence that both OR proteins contribute to channel pore formation and determine their properties such as the ion permeability and pharmacological properties (Nichols et al., 2011; Pask et al., 2011; Nakagawa et al., 2012). It remains to be established whether OrCo form homomeric channels in the receptor neurons as seen in the heterologous expression system and whether they represent

the metabotropic pathway used to tune the sensitivity of the ionotropic receptor (Olsson et al., 2011; Sargsyan et al., 2011). The role of stimulatory G-proteins in olfactory signaling has been demonstrated (Deng et al., 2011), and also downstream signaling such as cAMP production were seen to affect the odor response of receptor neurons (Olsson et al., 2011). These recent findings on insect OR function modify the view to classify them. While in the first editorial they have been considered as combined metabotropic and ionotropic receptors, they might now be more appropriately characterized as metabotropically regulated ionotropic receptors. This change of view illustrates the highly dynamic development in the field.

REFERENCES

Anton, S., and Renou, M. (2012). A first glance on the molecular mechanisms of pheromone-plant odor interactions in moth antennae. *Front. Cell. Neurosci.* 6:46. doi: 10.3389/fncel.2012.00046

Deng, Y., Zhang, W., Farhat, K., Oberland, S., Gisselmann, G., and Neuhaus, E. M. (2011). The stimulatory Galpha(s) protein is involved in olfactory signal transduction in *Drosophila*. *PLoS ONE* 6:e18605. doi: 10.1371/journal.pone.0018605

Eccles, J. C., and McGeer, P. L. (1979). Ionotropic and metabotropic neurotransmission. *Trends Neurosci.* 2, 39–40.

Getahun, M. N., Wicher, D., Hansson, B. S., and Olsson, S. B. (2012). Temporal response dynamics of Drosophila olfactory sensory neurons depends on receptor type and response polarity. *Front. Cell. Neurosci.* 6:54. doi: 10.3389/fncel.2012.00054

Kato, H. E., Zhang, F., Yizhar, O., Ramakrishnan, C., Nishizawa, T., Hirata, K., et al. (2012). Crystal structure of the channelrhodopsin light-gated cation channel. *Nature* 482, 369–374.

Liu, Z., Fenech, C., Cadiou, H., Grall, S., Tili, E., Laugerette, F., et al. (2012). Identification of new binding partners of the chemosensory signaling protein Ggamma13 expressed in taste and olfactory sensory cells. *Front. Cell. Neurosci.* 6:26. doi: 10.3389/fncel.2012.00026

Masu, M., Tanabe, Y., Tsuchida, K., Shigemoto, R., and Nakanishi, S. (1991). Sequence and expression of a metabotropic glutamate receptor. *Nature* 349, 760–765.

Müller, M., Bamann, C., Bamberg, E., and Kühlbrandt, W. (2011). Projection structure of channelrhodopsin-2 at 6 A resolution by electron crystallography. *J. Mol. Biol.* 414, 86–95.

Nakagawa, T., Pellegrino, M., Sato, K., Vosshall, L. B., and Touhara, K. (2012). Amino acid residues contributing to function of the heteromeric insect olfactory receptor complex. *PLoS ONE* 7:e32372. doi: 10.1371/journal.pone.0032372

Nichols, A. S., Chen, S., and Luetje, C. W. (2011). Subunit contributions to insect olfactory receptor function: channel block and odorant recognition. *Chem. Senses* 36, 781–790.

Olsson, S. B., Getahun, M. N., Wicher, D., and Hansson, B. S. (2011). Piezo-controlled microinjection: an *in vivo* complement for *in vitro* sensory studies in insects. *J. Neurosci. Methods* 201, 385–389.

Pask, G. M., Jones, P. L., Rützler, M., Rinker, D. C., and Zwiebel, L. J. (2011). Heteromeric anopheline odorant receptors exhibit distinct channel properties. *PLoS ONE* 6:e28774. doi: 10.1371/journal.pone.0028774

Pregitzer, P., Schubert, M., Breer, H., Hansson, B. S., Sachse, S., and Krieger, J. (2012). Plant odorants interfere with detection of sex pheromone signals by male *Heliothis virescens*. *Front. Cell. Neurosci.* 6:42. doi: 10.3389/fncel.2012.00042

Sargsyan, V., Getahun, M. N., Llanos, S. L., Olsson, S. B., Hansson, B. S., and Wicher, D. (2011). Phosphorylation via PKC regulates the function of the *Drosophila* odorant coreceptor. *Front. Cell. Neurosci.* 5:5. doi: 10.3389/fncel.2011.00005

Sugiyama, H., Ito, I., and Hirono, C. (1987). A new type of glutamate receptor linked to inositol phospholipid metabolism. *Nature* 325, 531–533.

Wicher, D. (2012). Functional and evolutionary aspects of chemoreceptors. *Front. Cell. Neurosci.* 6:48. doi: 10.3389/fncel.2012.00048

Received: 27 November 2012; accepted: 05 January 2013; published online: 24 January 2013.

Citation: Wicher D (2013) Sensory receptors—design principles revisited. Front. Cell. Neurosci. 7:1. doi: 10.3389/fncel.2013.00001

Copyright © 2013 Wicher. This is an open-access article distributed under the terms of the Creative Commons Attribution License, which permits use, distribution and reproduction in other forums, provided the original authors and source are credited and subject to any copyright notices concerning any third-party graphics etc.

frontiers in
CELLULAR NEUROSCIENCE

REVIEW ARTICLE
published: 11 June 2009
doi: 10.3389/neuro.03.002.2009

Drosophila photoreceptors and signaling mechanisms

Ben Katz and Baruch Minke*

Department of Physiology, Kühne Minerva Center for Studies of Visual Transduction, Faculty of Medicine, The Hebrew University, Jerusalem, Israel

Edited by:
Dieter Wicher, Max Planck Institute for Chemical Ecology, Germany

Reviewed by:
Satpal Singh, University of New York, USA
Monika Stengl, Philipps-Universitat Marburg, Germany

***Correspondence:**
Baruch Minke, Department of Physiology, Faculty of Medicine, The Hebrew University, Jerusalem 91120, Israel.
e-mail: baruchm@ekmd.huji.ac.il

Fly eyes have been a useful biological system in which fundamental principles of sensory signaling have been elucidated. The physiological optics of the fly compound eye, which was discovered in the *Musca*, *Calliphora* and *Drosophila* flies, has been widely exploited in pioneering genetic and developmental studies. The detailed photochemical cycle of bistable photopigments has been elucidated in *Drosophila* using the genetic approach. Studies of *Drosophila* phototransduction using the genetic approach have led to the discovery of novel proteins crucial to many biological processes. A notable example is the discovery of the inactivation no afterpotential D scaffold protein, which binds the light-activated channel, its activator the phospholipase C and it regulator protein kinase C. An additional protein discovered in the *Drosophila* eye is the light-activated channel transient receptor potential (TRP), the founding member of the diverse and widely spread TRP channel superfamily. The fly eye has thus played a major role in the molecular identification of processes and proteins with prime importance.

Keywords: optics of compound eyes, bistable pigments, phosphorylated arrestin, G-protein, phospholipase C, TRP channels, phosphoinositide cycle, INAD scaffold protein

INTRODUCTION

Vision of invertebrate species has been one of the first senses to be thoroughly studied, and many fundamental principles relevant to all senses have been first discovered in invertebrate eyes. A notable example is the discovery of lateral inhibition in the compound eye of the *Limulus* by the Nobel Prize Laurie, Haldan Keffer Hartline (Ratliff, 1990). Surprisingly, invertebrate phototransduction, the process by which light quanta are translated into electrical signal is still not entirely understood in terms of its underlying molecular mechanism. The pioneering experiments, which exploited the size of giant photoreceptor cells in some invertebrate species like the *Limulus* (reviewed in Dorlochter and Stieve, 1997), were followed by studies on *Drosophila melanogaster*, exploiting its great molecular genetics power (reviewed in Minke and Hardie, 2000; Montell, 1989; Pak, 1995; Ranganathan et al., 1995). In the present review, we focus on processes and molecules that have been discovered in invertebrate eyes in general and in the *Drosophila* eye in particular, which shed light on crucial functions of other cells and tissues. These landmark discoveries include: (i) Structural and optical properties of *Diptera* compound eyes. (ii) Bistable photopigments in which both the rhodopsin (R) and metarhodopsin (M) states of the photopigment are dark stable and photoconvertible. (iii) The photochemical cycle in which phosphorylated arrestin (ARR) and ARR translocation play a major role. (iv) Light-induced translocation of $G_q\alpha$ and the excess of $G_q\beta$ over $G_q\alpha$, which prevents spontaneous activation of the G_q-protein in the dark. (v) The dual role of light-activated phospholipase Cβ (PLCβ) in vivo as a G-protein-mediated activator and negative regulator of phototransduction via its action as a GTPase activating protein (GAP). (vi) Unitary signaling events (e.g. single photon responses, quantum bumps). (vii) The light-activated channels, TRP and TRPL, the founding members of the TRP superfamily channel proteins. (viii) Light-induced translocation of the TRPL channel. (ix) The inactivation no afterpotential D (INAD) multimolecular signaling complex, which binds the TRP channel, its activator, the PLC and its regulator, eye-specific protein kinase C (ePKC).

Abbreviation: ARR, arrestin; CaMKII, Ca^{2+} calmodulin-dependent kinase II; DAG, diacylglycerol; ePKC, eye-specific protein kinase C; INAC, inactivation no afterpotential C (eye-specific PKC); GAP, GTPase activating protein; GDP, guanosine diphosphate; GTP, guanosine triphosphate; GPCR, G-protein-coupled receptor; INAD, inactivation no afterpotential D (scaffold protein); $InsP_3$, inositol 1,4,5-trisphosphate; R, rhodopsin; M, metarhodopsin; Rpp, phosphorylated rhodopsin; Mpp, phosphorylated metarhodopsin; NINAC, no inactivation no afterpotential C (Myosin III which contains a protein kinase domain); NORPA, no receptor potential A (PLCβ); PDA, prolonged depolarizing afterpotential; PDZ, initials of PSD95, DLG and ZO1; PIP_2, phosphatidylinositol 4,5-bisphosphate; PLC, phospholipase C; PUFA, polyunsaturated fatty acid; RDGA, retinal degeneration A (DAG kinase); SMC, submicrovillar cisternae; TRP, transient receptor potential (channel); TRPL, transient receptor potential-like (channel).

STRUCTURAL AND OPTICAL PROPERTIES OF THE *DIPTERA* COMPOUND EYE

GENERAL ANATOMY

Two distinct types of eyes have evolved through evolution; the lens eye (or camera eye) typically encountered in vertebrates, and the compound eye typically encountered in arthropods. Many insects encompass both types of eyes. While, the compound eye is the primary image forming organ, the ocelli lens eye is small and primitive (Kirschfeld and Franceschini, 1968, 1969). The compound eyes are composed of many repeat and well-organized units termed ommatidia (**Figure 1B**) embedded in a sphere (**Figure 1A**). The number of ommatidia in insects vary from just a handful in the primitive *Archaeognatha* (jumping bristletails) and *Thysanura* (silverfish or bristletails) to several hundred up to thousands in *Diptera* (which includes the house fly *Musca* and the fruit fly *Drosophila*). In *Drosophila*, the ommatidium consists of about 20 cells, in which 8 (6–21 in different insect species) are the photoreceptor cells (RZ, **Figure 1A**). Each ommatidium contains a dioptric apparatus composed of transparent chitinous cuticle, which forms the cornea (C, **Figure 1A**) and an extracellular fluid-filled cavity, called the pseudocone (PC, **Figure 1A**). The floor of the cavity is formed by four

Semper cells (SZ, **Figure 1A**) and the walls by primary pigment cells (PZ, **Figure 1A,** red), which together circle the pseudocone, shielding the photoreceptor from stray light coming from adjacent ommatidia. The photoreceptor cells are highly polarized epithelial cells, with a specialized compartment known as the rhabdomere (Rh, **Figure 1A**), consisting of a stack of ~30,000–50,000 microvilli each ~2 μm long and ~60 nm in diameter. The transduction machinery is located in these tightly dense structures, while the nucleus and cellular organelles (N, **Figure 1C**), such as submicrovillar cisternae (SMC, **Figure 1C**) reside in the cell body. Pioneering studies conducted by Franceschini and Kirschfeld in *Diptera* (mainly in *Musca*) have elucidated the remarkable optics of the compound eye. In their studies, they showed that the highly ordered rhabdomeres form light guides (Kirschfeld and Snyder, 1976) that have been widely exploited experimentally (**Figure 3**). For example, the screening for retinal degeneration mutants of *Drosophila* has used the optical phenomenon designated deep pseudopupil (dpp), by Franceschini and Kirschfeld (1971), that is associated with their light guide property (see **Figure 3**). The dpp, which disappears in retinal degeneration mutant flies such as in R defective mutants, has been used as an efficient tool for a fast screen of large populations of putative mutant flies. Other examples are spectral measurement of the compound eye such as the eye shine, resulting from tapetal reflection, transmittance spectra of photopigments and fluorescent measurements of M.

OPEN AND CLOSED RHABDOM

Two kinds of rhabdomere architecture exist: closed rhabdom, in which all rhabdomeres are fused at the center of the ommatidium (**Figures 2A,C**) and open rhabdom, in which the rhabdomeres are separated (**Figures 2A,B**), forming a polygon pattern depending on the number of photoreceptors (hexagonal in *Drosophila*). Each ommatidium is connected by axons to the ganglionic layers providing a single or several image elements of space, depending on the rhabdomere architecture (**Figure 1A**). In open rhabdomere, the repeated elements are arranged in a specific geometrical patterning and spacing, ensuring visual connectivity between adjacent ommatidia. Accordingly, the angles between the individual rhabdomeres in one ommatidium are identical to those between adjacent ommatidia. As a result, each of the seven rhabdomeres in one ommatidium portrays the same field of view as a rhabdomere in a neighboring ommatidium (**Figures 2D,E;** Kirschfeld, 1967). In addition, all six rhabdomeres that share a common field of view send their axons to the same place in the first ganglionic layer – the lamina (La, **Figures 1A and 2E**). The central rhabdomeres send their axons to the second ganglionic layer – the medulla (Me, **Figure 1A**). In *Drosophila*, the seven rhabdomeres of each ommatidium are separated from each other and function as independent light guides (**Figure 1D**) forming open rhabdomere architecture (**Figures 2A,B**). In contrast, bees, beetles and various mosquitoes have a closed rhabdom architecture, in which rhabdomeres within each ommatidium are fused to each other, thus sharing the same visual axis (**Figures 2A,C**). Recently, the power of *Drosophila* genetics was exploited to elucidate the molecular factors participating in the transition between open and closed rhabdom architecture by screening, isolating and characterizing *Drosophila* genes involved in this process. The study identified two genes, *spacemaker* (*spam*) and *prominin* (*prom*) which when mutated cause the collapse of the intra-rhabdomere space (IRS; **Figure 2B**) resulting in the conversion of an open rhabdom system into a closed rhabdom architecture. Further analysis showed that SPAM is a secreted protein

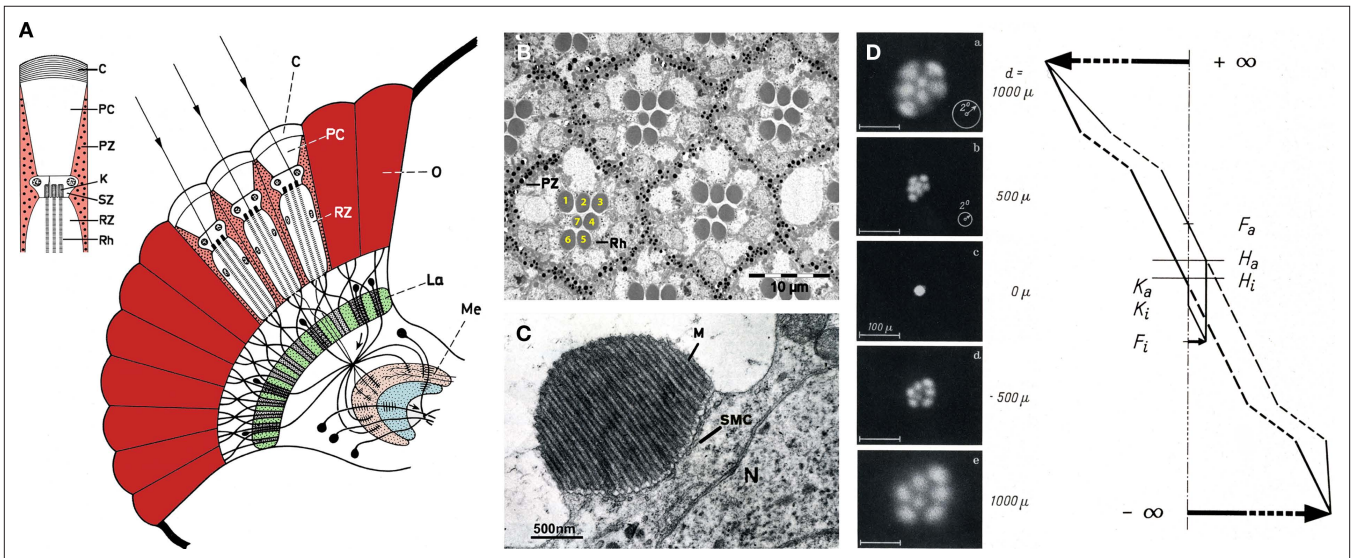

FIGURE 1 | The morphology and optics of the compound eye. (A) The compound eye of *Musca* and the visual ganglionic layers: a schematic representation of a horizontal section. Inset – Schematic representation of the distal area of a single ommatidium. C – corneal lens, PC – pseudocone, RZ – retinula cells (photoreceptor), PZ – pigment cells, K – rhabdomere cap, SZ – Semper cells, Rh – rhabdomere, La – lamina, Me – medulla (modified from Kirschfeld, 1967). **(B,C)** Electron microscopic (EM) cross-section of *Drosophila* ommatidia and a rhabdomere at the upper region of the photoreceptors respectively. M – microvilli, SMC – submicrovillar cisternae, N – nucleus (modified from Minke and Selinger, 1996). **(D)** Optical properties of a single ommatidium demonstrated by "antidromic" illumination in *Musca* when a 30 μm diaphragm is placed over a single ommatidium seen when focused at the cornea (0 μm). Inverted images of the rhabdomere tips are seen when focusing above the cornea (1000 μm and 500 μm) and upright images below the cornea (–500 μm and –1000 μm). The optical path is shown on the right, F – focal plane, H – main plane, K – junction, a – outer, i – inner (modified from Kirschfeld and Franceschini, 1968).

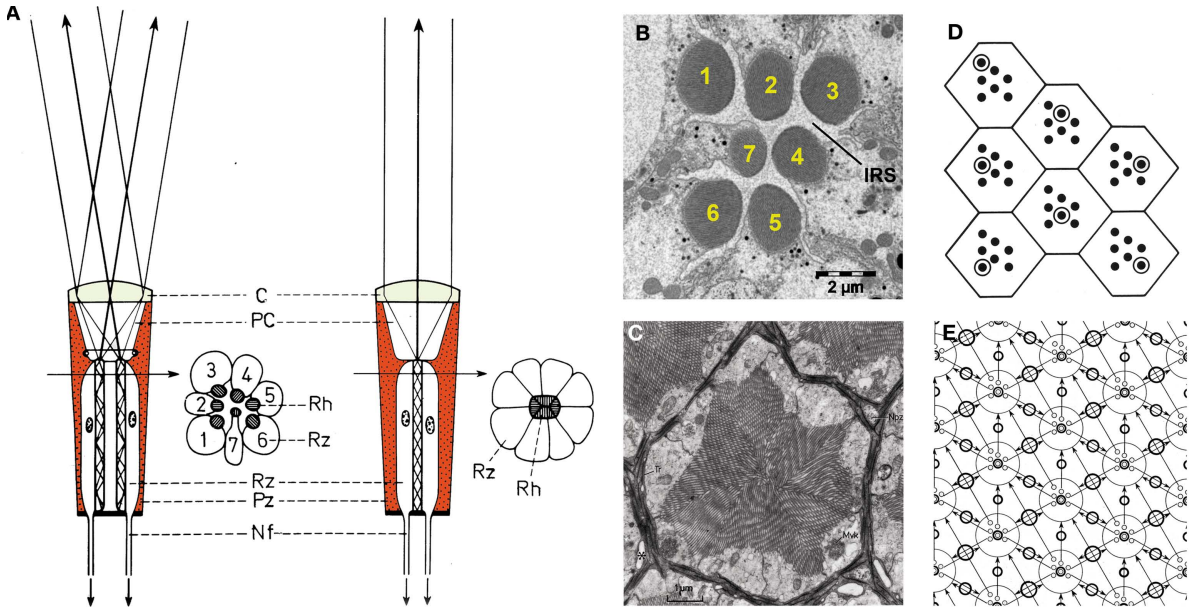

FIGURE 2 | Compound eyes with closed and open rhabdoms. (A) Schematic representation of an ommatidium with open rhabdom (left) and closed rhabdom architecture (right) (modified from Kirschfeld, 1971). **(B)** EM cross-section of *Drosophila* ommatidium with open rhabdom architecture. **(C)** EM cross-section of *Ephestia* ommatidium in the region of distal tracheole ends with closed rhabdom architecture (from Fischer and Horstmann, 1971). **(D)** Diagram of seven facets of the compound eye. The encircle rhabdomeres receive light from one and the same point in space (modified from Kirschfeld, 1967). **(E)** Diagram of axonal connections between ommatidia. Axons of photoreceptor cells one to six receiving light from the same point in space are drawn converging on one and the same cartridge of the lamina (modified from Kirschfeld, 1967).

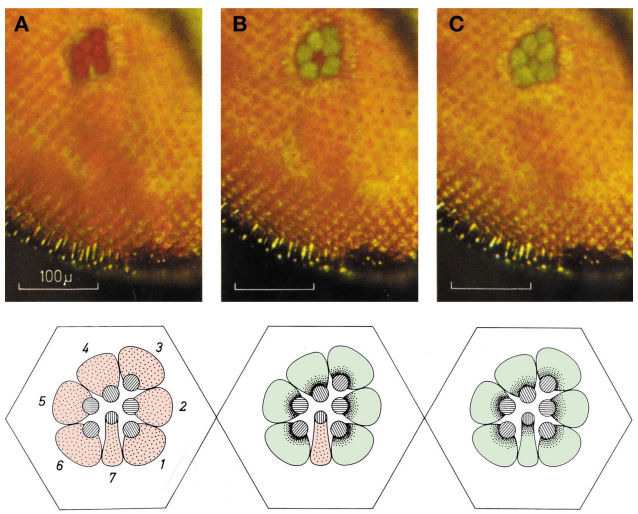

FIGURE 3 | Deep pseudopupil (dpp) observed in the eye of a living *Drosophila* under white orthodromic illumination. The dpp is the superposition of virtual images of adjacent ommatidia observed when a low power microscope is focused at the center of the curvature of the compound eye of *Diptera*. **(A)** Dark adapted. **(B)** After 60 s of medium intense illumination. Note that the central image corresponding to R7/R8 still appears red while the six peripheral images corresponding to R1–R6 reflect green light. **(C)** After 60 s of intense illumination (twofold higher). Note that all images reflect green light. The disparity between **(B)** and **(C)** arises from the difference in the absorption spectra between rhodopsin expressed in R1–R6 compared to R7 (upper panels). Schematic representation of the positioning of the pigment granules at each of the above states (lower panels) (modified from Franceschini and Kirschfeld, 1971).

expressed in the IRS, which acts together with PROM, which is an evolutionary conserved transmembrane (TM) protein often associated with microvilli. Secretion of SPAM into the IRS forces the separation of the stalk membrane, pushing the rhabdomere apart, and the recruitment of SPAM to the microvilli surface by the binding to PROM prevents inter-rhabdomere adhesion. Furthermore, targeted expression of *spam* to photoreceptors of a closed system markedly reorganizes the architecture of the compound eyes to resemble an open system (Zelhof et al., 2006).

The unusual stiffness of SPAM has been exploited in mechanoreceptors of *Drosophila*. Accordingly, a recent study has demonstrated the involvement of SPAM in maintaining cell shape and tone, crucial for integrity of the mechanosensory neurons. The authors argued that for poikilothermic organisms, like insects, changes in temperature may impact the function of mechanoreceptor neurons. SPAM role was found as protective of mechanosensory organ from massive cellular deformation caused by heat-induced osmotic imbalance, by forming an extracellular shield that guards mechanosensory neurons from environmental insult (Cook et al., 2008).

FUNCTIONAL RETINAL ORGANIZATION

Drosophila ommatidia consist of eight photoreceptors that can be divided into two functional groups according to their position, functional involvement, spectral specificity and axonal projection. The R1–R6 cells (marked 1–6 in **Figure 1B**) represent the major class of photoreceptors in the retina and are involved in image formation and motion detection. These cells have peripherally located rhabdomeres extending from the basal to the apical side of the retina. They express a single opsin called Rh1, which when

combined with 11-*cis* 3-hydroxy retinal, forms a blue-absorbing R and orange-absorbing M. The R1–R6 cells (**Figure 1B**) project their axons to the first optic lobe, the lamina (La, **Figure 1A** green). The second group consists of two cells in the center of each ommatidium termed, R7 (marked 7 in **Figure 1B**) and R8 (located below R7) each spanning only half of the retina in length. The central cells R7 and R8 are involved in color vision and detection of polarized light and project their axons to the second optic lobe, the medulla (Me, **Figure 1A,** pink; Wernet et al., 2006).

Color vision requires comparison between the electrical signals of photoreceptors that are sensitive to different ranges of wavelengths of light. In *Drosophila*, this is achieved by the inner photoreceptors (R7 and R8) that contain different Rs. The R7 rhabdomere is located distally in the retina and expresses one of two opsins, Rh3 or Rh4, characterized by a UV-absorbing R and blue-absorbing M. The R8 rhabdomere is located proximally in the retina, beneath the R7 rhabdomere (not shown) and expresses one of three opsins, Rh3, Rh5 or Rh6, characterized by a UV-, blue- or green-absorbing R, respectively. On the basis of opsin expression in the R7 and R8 cells, three ommatidia subtypes can be distinguished. The R7 and R8 cells in ommatidia, residing in the dorsal rim area of the eye, which functions as a polarized light detector, both express Rh3 opsin. The "pale" ommatidia subtype express Rh3 in R7 cells and Rh5 in R8 cells and constitute ~30% of the total ommatidia, while the "yellow" ommatidia subtype express Rh4 in R7 cells and Rh6 in R8 cells and constitute ~70% of the total ommatidia. Two types of comparisons, required for color vision, can thus occur in the fly: between the R7 (UV sensitive) and R8 (blue or green sensitive) photoreceptor cells within one ommatidium or between different ommatidia that contain spectrally distinct inner photoreceptors (Wernet et al., 2006).

The intriguing repeated structure of fly compound eye has been a major scientific preparation for research of various aspects of cell differentiation and development. For example, in *Drosophila*, the hexagonal chiral orientation of the six rhabdomeres in the ommatidia is identical at the upper hemisphere of the compound eye and is reverted by 180° at the equator (**Figure 1D**).This phenomenon is generally referred to as the planar cell polarity (PCP) of a tissue, a unique polarization within the plane of epithelium. Genetic screens in *Drosophila* pioneered the discovery of core PCP factors, which subsequently were found to be evolutionarily conserved. In vertebrate, the PCP factors participate in several developmental processes such as convergence extension, neural tube closure, eyelid closure, hair bundle orientation in inner ear sensory cells, and hair follicle orientation in the skin (for review see Wang and Nathans, 2007).

PUPIL MECHANISM

The pupil-like mechanism of the compound eye was first discovered and studied by Franceschini and Kirschfeld. Upon bright light illumination, tiny pigment granules about 0.2 μm in diameter migrate from dispersed areas of the cell body to the cytoplasmic face of the rhabdomere (**Figure 3;** Kirschfeld and Franceschini, 1969). The accumulation of pigment granules attenuates propagation of light along the rhabdomere by reducing the refractive index of the interface between the rhabdomere and the adjacent cell body region, thereby changing the waveguide property of the rhabdomere. As a consequence, the amount of light traveling through the rhabdomere is attenuated, activating less photopigment, much like a pupil. This mechanism can attenuate the light flux in the rhabdomere by up to one order of magnitude and operates in a time scale of seconds, making it an elegant adaptation mechanism. The pigment granule migration is Ca^{2+}-dependent, as evidenced by injecting Ca^{2+} chelators into flies eye, resulting in the inhibition of pupil closure (Kirschfeld and Vogt, 1980). The pupil mechanism was later found to occur transiently in the *trp* mutant fly (Lo and Pak, 1981; Zuidervaart et al., 1979) and was used by Minke as supporting evidence for his hypothesis that TRP is a major route for Ca^{2+} entry into the photoreceptor cell (see below, Minke and Selinger, 1991). Recently, the molecular mechanism of pigment granules migration has been elaborated. It was shown that pigment migration is myosin V (MyoV), lightoid, calmodulin (CaM) and cytoplasmic myosin light chain dependent. A model of pigment migration has been put forward by Ready, in which MyoV pulls the pigment granules to the base of the rhabdomere upon Ca^{2+} elevation. Accordingly, lightoid, a Rab-related protein, links MyoV to pigment granules while both CaM and myosin light chain bind the long, multi-IQ domain of MyoV lever arms. Together, this Ca^{2+}-dependent protein complex migrates to the plus ends (+) of the actin microfilaments, designated the rhabdomere terminal web, at the base of the rhabdomere upon Ca^{2+} influx induced by illumination (Satoh et al., 2008).

THE PHOSPHOINOSITIDE CASCADE OF VISION

The signaling proteins of the phototransduction cascade are tightly assembled in the microvillar structure and linked to the actin cytoskeleton (F-actin) via two proteins: Dmoesin, which binds the TRP and TRPL channels, at the base of the microvilli to F-actin (Chorna-Ornan et al., 2005), and no inactivation no afterpotential C (NINAC), that associates INAD to F-actin (Li et al., 1998). The only protein that diffuses during the phototransduction cascade is $G_q\alpha$ (**Figure 4**).

Upon absorption of a photon, R is converted into the active state of the photopigment, M (**Figure 4**). This leads to the activation of heterotrimeric G-protein (DG_q) by promoting the guanosine diphosphate (GDP) to guanosine triphosphate (GTP) exchange. In turn, this leads to activation of PLCβ, which hydrolyzes the minor phospholipid, phosphatidylinositol 4,5-bisphosphate (PIP_2) into the soluble inositol 1,4,5-trisphosphate ($InsP_3$) and the membrane-bound diacylglycerol (DAG). Subsequently, two classes of light-sensitive channels, TRP that is highly permeable to Ca^{2+} and TRPL that is a non-selective cation channel, open by a still unknown mechanism. PLC also promotes hydrolysis of the bound GTP, resulting in $G_q\alpha$ bound to GDP and this ensures the termination of $G_q\alpha$ activity. The TRP and TRPL channel openings lead to elevation of calcium ions extruded by the Na^+/Ca^{2+} exchanger CALX. Elevation of DAG and Ca^{2+} promote ePKC activity, which regulates channel activity. PLC, ePKC and the TRP ion channel form a supramolecular complex with the scaffolding protein INAD (for reviews on the phototransduction cascade see Hardie and Raghu, 2001; Minke and Cook, 2002; Montell, 1989).

UNITARY EVENTS

Dim light stimulation induces discrete voltage (or current) fluctuations in most invertebrate species, which are called quantum bumps (Yeandle and Spiegler, 1973; see **Figure 5A**). Each bump is assumed to be evoked by the absorption of a single photon. The

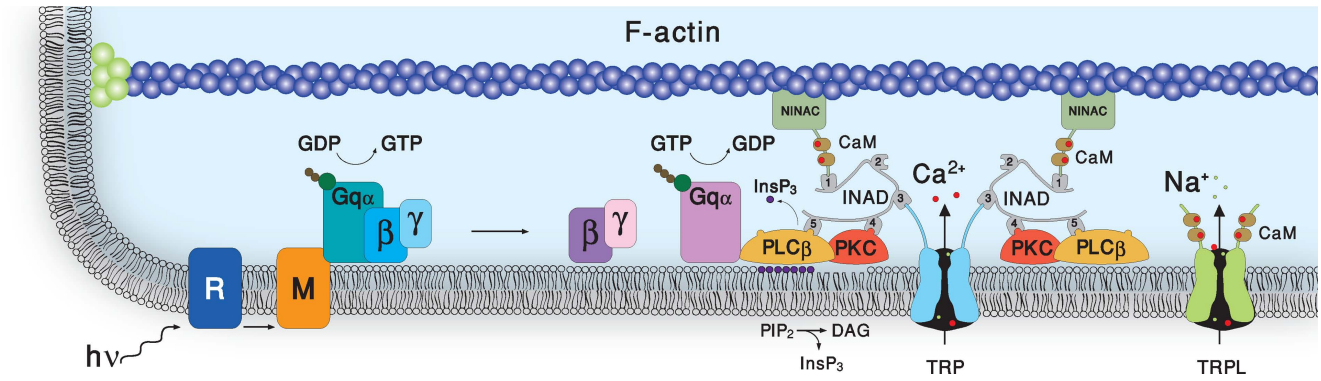

FIGURE 4 | Schematic representation of the molecular components of the signal transduction cascade of *Drosophila*. Upon absorption of a photon, rhodopsin (R) is converted into metarhodopsin (M). This photoconversion leads to the activation of heterotrimeric G-protein ($G_q\alpha$) by promoting the GDP to GTP exchange. In turn, this leads to activation of phospholipase Cβ (PLCβ), which hydrolyzes PIP_2 into the soluble $InsP_3$ and the membrane-bound DAG. Subsequently, two classes of light-sensitive channels, the TRP and TRPL open by a still unknown mechanism. PLC also promotes hydrolysis of the bound GTP, resulting in $G_q\alpha$ bound to GDP and this ensures the termination of $G_q\alpha$ activity. The TRP and TRPL channel openings lead to elevation of cellular Ca^{2+}. Elevation of DAG and Ca^{2+} promote eye-specific protein kinas C activity, which regulates channel activity. PLC, PKC and the TRP ion channel form a supramolecular complex with the scaffolding protein INAD.

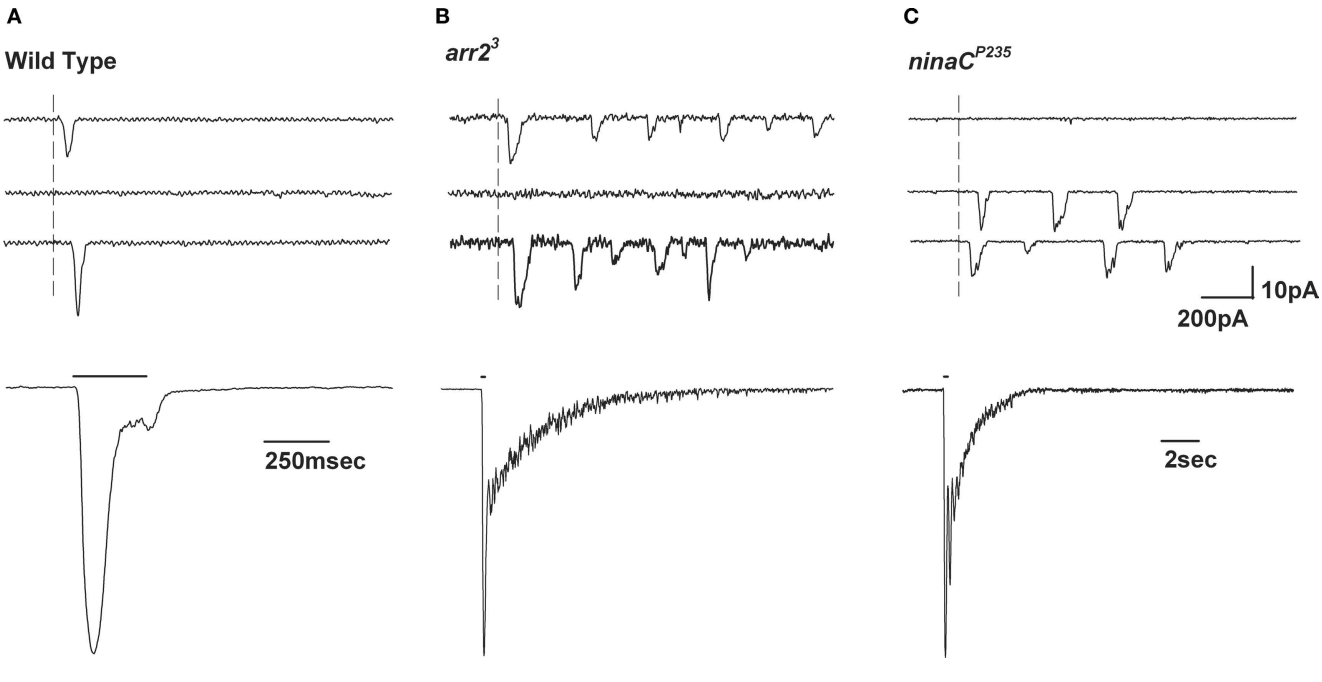

FIGURE 5 | Slow response termination in *arr2* and *ninaC* null mutants. **(A–C)** Upper panels: Whole-cell voltage clamp recordings of quantum bumps in response to brief (1 ms) dim flashes of light with intensity sufficient to activate only a single rhodopsin molecule upon photon absorption in wild-type (WT), $arr2^3$ and $ninaC^{P235}$ null *Drosophila* mutant flies. In WT, only a single bump is induced by a single flash and some flashes do not elicit any bump (middle trace). In contrary, a single flash in $arr2^3$ and $ninaC^{P235}$ mutant flies elicits a train of bumps. **(A–C)** Lower panels: Whole-cell voltage clamp recordings of normalized macroscopic responses of WT and the corresponding mutants in response to 500-ms light pulses. A slow termination of macroscopic response is observed in $arr2^3$ and $ninaC^{P235}$ mutant flies relative to WT.

discrete nature of the unitary events of the photoreceptor cells is not due to the quantized nature of light. This has been demonstrated by the application of a non-quantized stimulus such as GTPγS, which elicit quantum bump-like events (Fein and Corson, 1981). The bumps vary in latency, time course and amplitude for identical stimulation and are the consequence of synchronized activation of many light-sensitive channels. The number of channels, which are activated to produce a bump vary greatly in different species: few tens in *Drosophila* and up to several thousands in *Limulus* ventral photoreceptors (Nasi et al., 2000). Bump generation is a stochastic process described by Poisson statistics where each effective absorbed photon elicits only one bump (Yeandle and Spiegler, 1973). However

in at least two *Drosophila* mutants (*ninaC* and *arr*, see **Figure 5**), absorption of a single photon elicits a train of bumps which do not overlap but are separated by intervals (**Figures 5B,C**). This train of bumps is thought to be caused by a failed R inactivation process and a refractory period of the microvilli (Scott et al., 1997).

A detailed study in *Limulus* photoreceptors has indicated that the latency of the bump is not correlated with the bump waveform, thus strongly suggesting that the triggering mechanism of the bump arises from different molecular processes than those determining the bump waveform (Dorlochter and Stieve, 1997). These findings are partly explained by models in which the amplification process is preceded by a series of non-amplifying latency producing steps. To produce realistic bumps by such a model means that no step in the transduction cascade could have a life time greater than the duration of a bump generating mechanism which includes the latency, bump duration and bump refractory period. The single photon-single bump relationship requires that each step in the cascade must have not only an efficient "turn-on" mechanism, but also an equally effective "turn-off" mechanism (see below). The functional advantage of such a transduction mechanism is obvious; it produces a sensitive photon counter, very well suited for both the sensitivity and the temporal resolution required by the visual system.

A recent study has presented a quantitative model explaining how bumps emerge from stochastic non-linear dynamics of the signaling cascade. Three essential "modules" govern the production of bumps in this model: (i) an "activation module" downstream of PLC but upstream of the channels, (ii) a "bump-generation module" including channels and Ca^{2+}-mediated positive feedback and (iii) a Ca^{2+}-dependent "negative-feedback module". The model shows that the cascade acts as an "integrate and fire" device conjectured formerly by Henderson et al. (2000) much like the generation of spikes. The model explains both the reliability of bump formation and low background noise in the dark and is able to capture mutant bump behavior and explains the dependence on external calcium, which controls feedback regulation (Pumir et al., 2008).

THE PHOTOCHEMICAL CYCLE: THE "TURN-ON" AND "TURN-OFF" OF THE PHOTOPIGMENT

BISTABLE PIGMENTS

The G-protein-coupled receptor (GPCR), R, is composed of a 7-TM protein, opsin and the chromophore, 11-*cis* 3 hydroxy retinal (in *Diptera*; Vogt and Kirschfeld, 1984). Isomerization of the chromophore by photon absorption induces conformational change in the opsin, which is photoconverted into the dark stable physiologically active photoproduct, M. The action spectrum of this reaction depends on the R type (see above) and spans a wavelength range between UV and green lights. To ensure high sensitivity, high temporal resolution and low dark noise of the photoresponse, the active M has to be quickly inactivated and recycled (**Figure 6**). The latter requirement is achieved, in invertebrates, by two means: the

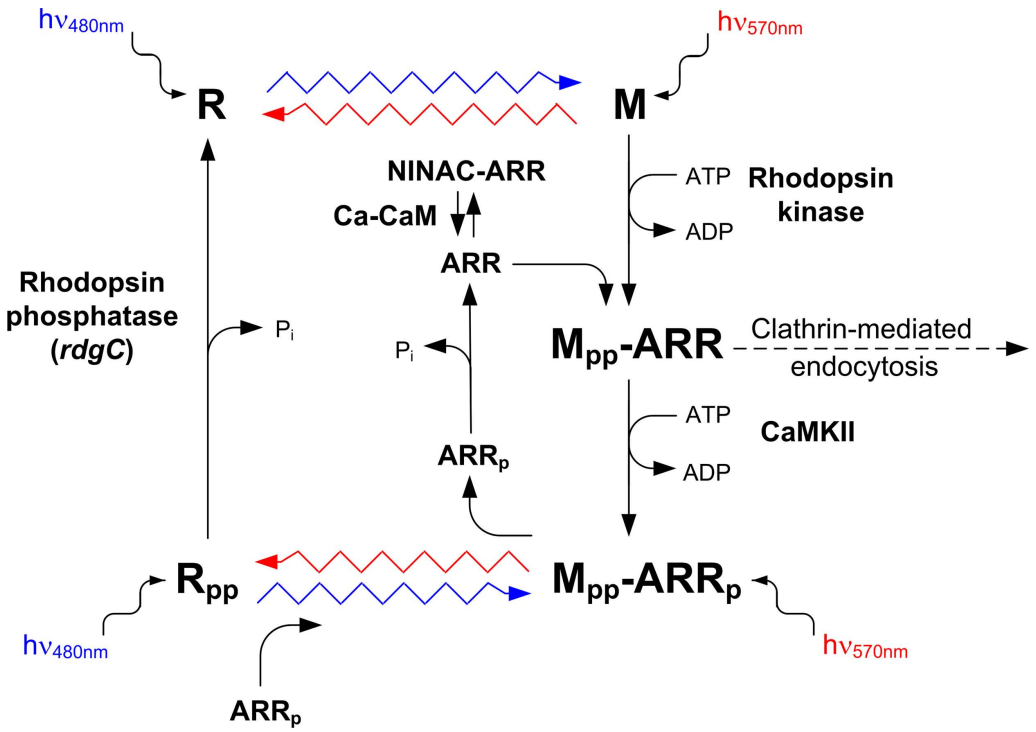

FIGURE 6 | The photochemical cycle: the "turn-on" and "turn-off" of the photopigment. Upon photoconversion of rhodopsin (R) to metarhodopsin (M), by illuminating with blue light (wavy blue arrow), M is phosphorylated at multiple sites by rhodopsin kinase and the fly ARR2 binds to phosphorylated M. ARR2 is then phosphorylated by Ca^{2+} calmodulin-dependent kinase (CaMKII). Photoconversion of phosphorylated M (Mpp) back to phosphorylated R (Rpp) is achieved by illuminating with orange light (wavy red arrow). Upon photoregeneration of Mpp to Rpp, phosphorylated ARR2 is released and the phosphorylated rhodopsin (Rpp) is exposed to phosphatase activity by rhodopsin phosphatase (encoded by the *rdgC* gene). Unphosphorylated ARR2 also binds to myosin III (NINAC) in a Ca^{2+} calmodulin (Ca-CaM)-dependent manner (modified from Liu et al., 2008; Selinger et al., 1993).

absorption of an additional photon by the dark stable M, which photoconverts M back to R (Hillman et al., 1972, 1983), or by a multistep photochemical cycle (**Figure 6**). The action spectrum of M to R conversion in the R1–R6 cells of *Drosophila* is in the orange range. The red screening pigment of the *Drosophila* eye prevents massive conversion of R to M, by formation of a red filter, which is preferential for M to R conversion. Genetic removal of the red screening pigment and application of blue light (which is preferentially absorbed by the R state) enables a large net photoconversion of R to its dark stable photoproduct M with a minimal conversion of M back to R (**Figure 6**). A large net photoconversion of R to M, prevents phototransduction termination at the photopigment level when light is turned off (Minke et al., 1975a). This is because the net photoconversion of R to M exceeds the amount of ARR (see below) and thereby its ability to inactivate M, resulting in a large amount of dark stable M, which does not undergo inactivation and thus remains physiologically active in the dark (Byk et al., 1993; Dolph et al., 1993). This brings the capacity of the phototransduction process to its upper limit and results in a phenomenon called prolonged depolarizing afterpotential (PDA; Hillman et al., 1972, 1983). Illumination with red light photoconverts M back to R and terminates the PDA after the light is turned off. The PDA protocol has been used efficiently to screen for phototransduction defective *Drosophila* mutants (Pak, 1995) and has been widely exploited in studies of *Drosophila* phototransduction.

THE ROLE OF ARRESTIN IN PHOTOINACTIVATION

The ARR family of proteins plays a key role in regulating the activity of GPCRs (Violin and Lefkowitz, 2007). In *Drosophila*, two homologues of vertebrate ARR exist, which participate through binding, in M inactivation. Both ARRs undergo light-dependent phosphorylation by Ca^{2+} calmodulin-dependent kinase II (CaMKII) originally discovered by Matsumoto (Kahn and Matsumoto, 1997). This phosphorylation is unique to the invertebrate visual ARRs and crucial for ARR dissociation from M (Alloway and Dolph, 1999; Kiselev et al., 2000; Yamada et al., 1990).

The study, which clarified the regulatory role of ARR2, used in vitro assays of ARR2 and M, in *Drosophila* and *Musca* eyes. Upon photoconversion of R to M, by illumination with blue light (wavy blue arrow, **Figure 6**), the fly ARR2 is found predominantly in the membrane fraction, while photoconversion of phosphorylated M (Mpp) back to phosphorylated R (Rpp), by illumination with orange light (wavy red arrow), result in the detection of ARR2 in the supernatant fraction (cytosol). ARR1 on the other hand, always remains membrane bound. The in vitro studies indicated that the functional role of ARR2 binding to M is to terminate its activity (Byk et al., 1993). The isolation of *Drosophila* mutant fly *arrestin2* (*arr2*), enabled demonstrating the physiological effect, in vivo, of ARR2 on the light response (Dolph et al., 1993). Accordingly, these flies showed a slow response termination at the macroscopic level (**Figure 5B**). Further investigations have shown that single photon absorption in these flies results in a train of quantum bumps while in wild-type flies it elicits a single bump (**Figure 5B**). The train of bumps is a manifestation of the M's incapability to inactivate, and explains the slow response termination seen at the macroscopic level (Scott et al., 1997). Moreover, under the assumption that each bump is produced in a single microvillus, the train of bumps separated by intervals suggests a possible inactivation process of the microvilli (Hardie and Raghu, 2001).

The binding of ARR2 also protects the Mpp from phosphatase activity (**Figure 6**). Only upon photoregeneration of Mpp to Rpp, is ARR2 released and the Rpp is exposed to phosphatase activity by rhodopsin phosphatase, encoded by the *rdgC* gene (Steele et al., 1992). These combined actions are crucial for preventing reinitiating of phototransduction in the dark, as the dissociation of ARR2 is coupled to conversion of Mpp to Rpp, thereby directing the protein phosphatase only towards the inactive Rpp (Byk et al., 1993). Subsequent studies have revealed that both CaMKII-dependent phosphorylation of ARR2 at Ser366 and photoconversion of Mpp are required to release phosphorylated ARR2. They furthermore showed that the phosphorylation of ARR2 is required for its dissociation from Mpp upon photoconversion and that ARR2 phosphorylation prevents endocytotic internalization of the ARR2-Mpp complex by a clathrin-mediated mechanism (Alloway and Dolph, 1999; Alloway et al., 2000; Kiselev et al., 2000).

Upon illumination, ARR2 translocates from the cell body to the rhabdomere, thereby elevating its concentration in the signaling compartment (Byk et al., 1993). This process enables the ARR2-dependent inactivation of M, operating in massive photoconversion of R to M in bright daylight, thus preventing response saturation and ensures sufficient time resolution of the light response. A further study has shown that ARR2 translocation requires a phosphoinositide-mediated interaction with myosin III (NINAC; Lee and Montell, 2004). Interestingly, the electrophysiological phenotype of the *ninaC* mutant is similar to that of *arr2* mutant (**Figures 5B,C**) and may be the consequence of reduced ARR2 concentration in the rhabdomere caused by the *ninaC* mutation. A recent study suggests that under low Ca^{2+} conditions, ARR2 binding to M is slowed down by its sequestration to NINAC. Accordingly, in physiological conditions, light-induced Ca^{2+} influx acting via CaM (Ca-CaM), rapidly releases ARR2 from NINAC and allows its binding to M and consequently, M inactivation (Liu et al., 2008; **Figure 6**).

LIGHT-ACTIVATED G_q-PROTEIN: THE ROLES OF $G_q\alpha$ AND $G_q\beta$

It has been well established in photoreceptors of several invertebrate species that photoexcited R activates a heterotrimeric G-protein (Fein, 1986). The first experiments, conducted on fly photoreceptors, showed that when pharmacological agents, known to activate G-proteins, are applied to *Musca* photoreceptors in the dark, they mimic the light-dependent activation of the photoreceptor cells (Minke and Stephenson, 1985). Later studies using genetic screens isolated two genes encoding visual specific G-protein subunits. These genes, *dgq* (Lee et al., 1990) and *gβe* (Dolph et al., 1994), encode a $G_q\alpha$ and $G_q\beta$ subunit, respectively. The isolated eye-specific $DG_q\alpha$, shows ~75% identity to mouse $G_q\alpha$, which is known to activate PLC (Lee et al., 1990). The most direct demonstration that $DG_q\alpha$ participates in the phototransduction cascade came from studies of mutants defective in $G_q\alpha$ which showed highly reduced sensitivity to light. In the isolated $G\alpha q^1$ mutant, $DG_q\alpha$ protein levels are reduced to ~1%, while $G_q\beta$, PLC and R protein levels are virtually normal. The $G\alpha q^1$ mutant exhibits a ~1000-fold reduced sensitivity to light and slow response termination (Scott et al., 1995), strongly suggesting that there is no parallel pathway mediated by the G-protein, as proposed for the

Limulus eye (Dorlochter and Stieve, 1997). Manipulations of the $DG_q\alpha$ protein levels by the inducible heat-shock promoter made it possible to show a strong correlation between the sensitivity to light and $DG_q\alpha$ protein levels, further establishing its major role in *Drosophila* phototransduction (Scott et al., 1995).

The *Drosophila* fly has an eye-specific $G_q\beta$ ($G_q\beta_e$) which shares 50% amino acid identity with other Gβ homologue proteins. Two defective $G_q\beta_e$ ($G\beta_e^1$ and $G\beta_e^2$) mutants with highly reduced $G_q\beta$ levels were isolated and showed a greatly (~100-fold) decreased sensitivity to light and slow response termination (Dolph et al., 1994). Studies conducted on these mutants revealed that $G_q\alpha$ is dependent on $G_q\beta\gamma$ for both membrane attachment and targeting to the rhabdomere, suggesting that the decreased light sensitivity of these mutants may result from the mislocalization of the $G_q\alpha$ subunit (Elia et al., 2005). Attachment of $G_q\alpha$ to $G_q\beta\gamma$ prevents spontaneous GDP-GTP exchange and anchors $G_q\alpha$ to the plasma membrane. Therefore, in $G\beta_e$ mutants $G_q\alpha$ concentration is highly reduced in the rhabdomere (**Figures 7A,B**). Analysis of the stoichiometry between the $G_q\alpha$ and $G_q\beta$ subunits revealed a twofold excess of $G_q\beta$ over $G_q\alpha$. Genetic elimination of the $G_q\beta$ excess leads to spontaneous activation of the visual cascade in the dark, demonstrating that $G_q\beta$ excess is essential for the suppression of dark electrical activity produced by spontaneous GDP-GTP exchange of $G_q\alpha$. Reestablishing the excess of $G_q\beta$ over $G_q\alpha$, by a double hetrozygote mutant fly, suppresses the dark electrical activity (Elia et al., 2005; **Figures 7C** bottom trace and **D**). These studies show a dual role for $G_q\beta$: retention of $G_q\alpha$ in the signaling membrane and prevention of spontaneous activation of $G_q\alpha$ in the dark.

Heterotrimeric G-proteins relay signals between membrane-bound receptors and downstream effectors. Little is known, however, about the regulation of Gα subunit localization within the natural endogenous environment of a specialized signaling cell. Studies using *Drosophila* flies showed that prolonged lights cause massive and reversible translocation of $G_q\alpha$ to the cytosol (Kosloff et al., 2003), in similar manner to light-induced translocation of the vertebrate $G_t\alpha$ transducin (Arshavsky, 2003; Trojan et al., 2008). A long exposure to light followed by minutes of darkness resulted in reduction in the efficiency with which each absorbed photon elicited single photon responses, while the size and shape of each single photon response did not change. To dissect the physiological significance of $G_q\alpha$ translocation by light, a series of *Drosophila* mutants were used. Genetic dissection showed a pivotal role for light-induced translocation of $G_q\alpha$ from the signaling membrane and the cytosol. Biochemical studies revealed that the sensitivity to light depends on the membrane $G_q\alpha$ concentration, which can be modulated either by light or by mutations that impair its membrane targeting. Thus, long-term adaptation is mediated by the movement of $G_q\alpha$ from the signaling membrane to the cytosol, thereby reducing the probability of each photon to elicit a bump (Frechter et al., 2007).

DUAL ROLE FOR LIGHT-ACTIVATED PLC

PLC ROLE IN LIGHT EXCITATION

Evidence for a light-dependent $G_q\alpha$-mediated PLC activity in fly photoreceptors came from combined biochemical and electrophysiological experiments. These experiments, conducted in membrane preparations and intact *Musca* and *Drosophila* eyes, showed illumination and $G_q\alpha$-dependent accumulation of $InsP_3$ and $InsP_2$, derived from PIP_2 hydrolysis by PLC (Devary et al., 1987; **Figure 4**).

The key evidence for the participation of PLC in visual excitation of the fly was achieved by the isolation and analysis of *Drosophila* PLC gene, designated no receptor potential A (*norpA*). The *norpA* gene encodes a β-class PLC, predominately expressed in the rhabdomeres. Mutant flies in the *norpA* gene show a drastically reduced receptor potential. Transgenic *Drosophila*, carrying the *norpA* gene on a null *norpA* background, rescued the transformant flies from all the physiological, biochemical and morphological defects, which are associated with the *norpA* mutants (Bloomquist et al., 1988). The *norpA* mutant thus provides essential evidence for the critical role of inositol-lipid signaling in phototransduction, by showing that no excitation takes place in the absence of functional PLC (Bloomquist et al., 1988; Minke and Selinger, 1992). However, the events required for light excitation downstream of PLC activation remain unresolved.

PLC ROLE IN RESPONSE TERMINATION

In general, the cytoplasmic GTP concentration in cells is much higher than GDP, making the inactivation process of Gα by hydrolysis of Gα-GTP to Gα-GDP unfavorable. In order to accelerate the GTPase reaction and terminate Gα activity, a specific GAP exists (Mukhopadhyay and Ross, 1999). In vitro studies of mammalian PLC-β1 reconstituted into phospholipid vesicles with recombinant M1 muscarinic receptor and $G_{q/11}$ (Berstein et al., 1992) have shown that, upon receptor stimulation, the addition of PLC-β1 increases the rate at which G_q hydrolyses GTP by three orders of magnitude, suggesting its action as GAP. A reduction in the levels of PLC in mutant flies affects the amplitude and activation kinetics of the light response (Pearn et al., 1996), but also mysteriously slows response termination (compare **Figure 8A** to **Figure 8B**, lower panels). Biochemical and physiological studies conducted in *Drosophila* have revealed the requirement for PLC in the induction of GAP activity in vivo. Using several *Drosophila norpA* mutant flies, a high correlation between PLC protein level, GAP activity and response termination was observed (Cook et al., 2000). The virtually complete dependence of GAP activity on PLC provides an efficient mechanism for ensuring the one photon, one bump relationship (Yeandle and Spiegler, 1973), which is critical for the fidelity of phototransduction in dim light. The apparent inability to hydrolyze GTP without PLC ensures that every activated G-protein eventually encounters a PLC molecule and thereby produces a response by the downstream mechanisms. The instantaneous inactivation of the G-protein by its target, the PLC, guarantees that every G-protein produces no more than one bump (Cook et al., 2000). This apparently complete dependence of GTPase activity on its activator PLC, in flies, differs from the partial dependence of GTPase activity on additional GAP factors in vertebrate phototransduction (Chen et al., 2000). Vertebrate phototransduction depends on specific GAPs (Arshavsky and Pugh-EN, 1998; Makino et al., 1999). Accordingly, genetic elimination of regulators of G-protein signaling (RGS) proteins reduces and slows down GAP activity and leads to slow response termination to light (Chen et al., 2000).

The dual action of PLC as an activator and a negative regulator nicely accounts for all features of the PLC-deficient mutants. A

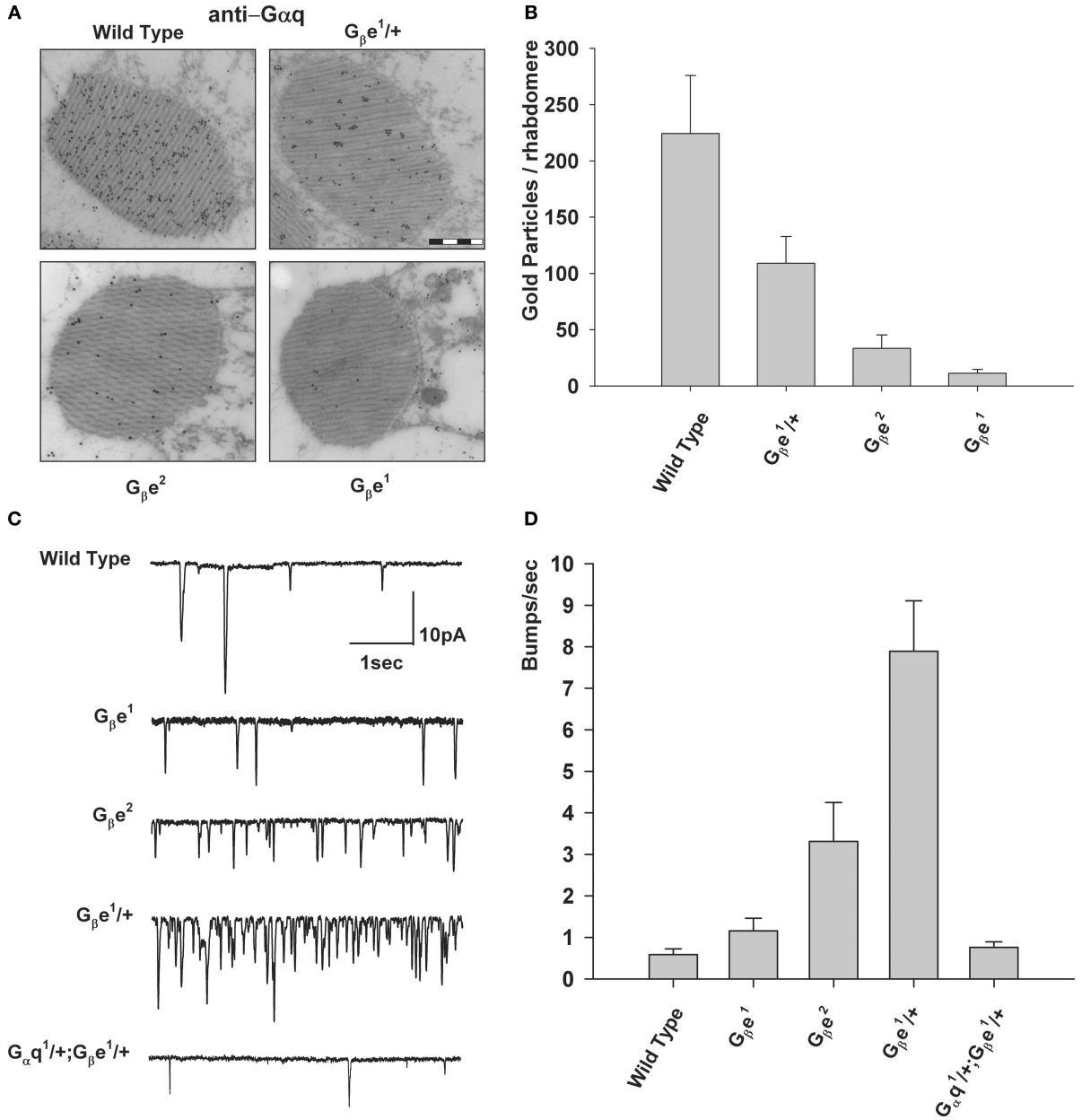

FIGURE 7 | Excess of $G_q\beta$ over $G_q\alpha$ is required to prevent production of spontaneous bumps in the dark. (A) Immunogold EM analysis of a cross-section of a single rhabdomere, using a $G_q\alpha$ antibody that was applied to dark adapted wild-type flies and Gβ mutants (bar 500 nm). **(B)** Number of mean gold particles in cross-sections of 20 different single rhabdomeres. Error bars are SEM. **(C)** Whole-cell voltage clamp recordings of spontaneous bumps observed in complete darkness of various mutants as indicated. **(D)** Histogram plotting the mean bump frequency of the various mutants. Error bars are SEM. Note the high spontaneous bump frequency of Gβ hetrozygote compared to the reduced bump frequency of the $G_q\alpha$/Gβ double hetrozygote mutant (modified from Elia et al., 2005).

striking demonstration of the poor temporal resolution of mutants with reduced PLC levels relative to wild-type flies is shown in **Figure 8C**, which compares the ability of wild type and the PLC-deficient mutant *norpA*^{P76} to discriminate between intense lights of different durations (flash, red arrow, pulse, blue line). In contrast to the wild-type fly, where there is a pronounced difference between the responses to a flash compared with a long stimulus, no such difference is observed in the *norpA* mutants, where the two responses overlap (**Figure 8C**). This result indicates that the PLC-deficient mutants cannot discriminate between long and short light stimuli. When PLC levels in the signaling membranes are low relative to the amount of the active G-protein, light induces production of $G_q\alpha$-GTP at a higher rate than it is inactivated by PLC. The $G_q\alpha$-GTP that has accumulated during illumination continues to produce bumps in the dark until all active $G_q\alpha$-GTP molecules are hydrolyzed via GAP activity of the scarce PLC (**Figure 8B,** lower panel, inset). Hence, the flies' temporal resolution is reduced and become virtually blind at low levels of PLC (Cook et al., 2000).

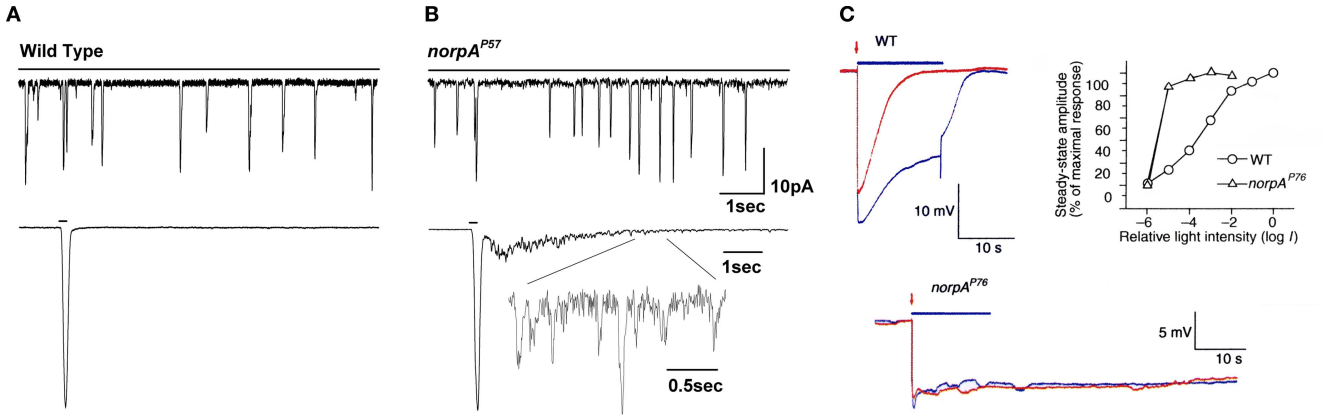

FIGURE 8 | Slow response termination composed of bumps characterizes *norpA* mutants. (A,B) Upper panels: Whole-cell voltage clamp recordings of quantum bumps in response to continues dim light in wild-type and the weak allele of *norpA*, *norpA*^{P57} mutant flies. **(A,B)** Lower panels: Whole-cell voltage clamp recordings of normalized macroscopic responses of wild-type and the corresponding mutants in response to 200-ms light pulses. In contrast to the fast response termination of wild-type, slow termination of the light response of *norpA*^{P57} mutant flies is revealed. This slow response termination can be resolved into continuous production of bumps in the dark at a later time (inset, at higher magnification). **(C)** Electroretinogram (ERG) responses showing superimposed traces recorded from wild-type and *norpA*^{P76} (a weak *norpA* allele) to a brief flash (red arrow) and continuous light. The graph plots the relative steady state amplitude of the ERG to prolonged lights as a function of relative light intensity. The ERG responses of *norpA*^{P76} to a brief flash and to continuous light are indistinguishable.

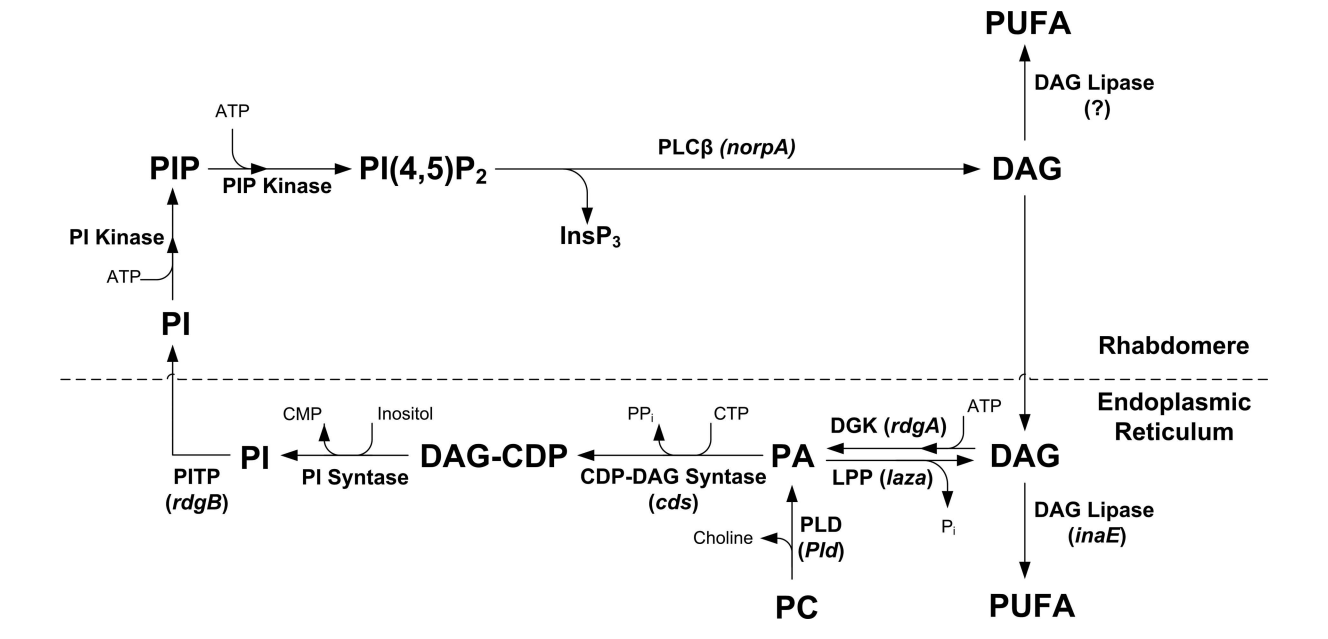

FIGURE 9 | The phosphoinositide cycle. In the phototransduction cascade, light triggers the activation of phospholipase Cβ (PLCβ). This catalyzes hydrolysis of the membrane phospholipid PIP_2 into $InsP_3$ and DAG. DAG is transported by endocytosis to the endoplasmic reticulum and inactivated by phosphorylation converting it into phosphatidic acid (PA) via DAG kinase (DGK) and to CDP-DAG via CDP-DAG syntase. Subsequently, CDP-DAG is converted into phosphatidylinositol (PI), which is transferred back to the microvillar membrane, by the PI transfer protein. PIP and PIP_2 are produced at the microvillar membrane by PI kinase and PIP kinase, respectively. There are probably two PIP kinases (PIPK I, PIPK II, which are unified in the scheme). PA can also be converted back to DAG by lipid phosphate phosphohydrolase. PA is also produced from phosphatidylcholine (PC) by phospholipase D (PLD). DAG is also hydrolyzes by DAG lipase into poly unsaturated fatty acids (PUFA).

THE PHOSPHOINOSITIDE (PI) CYCLE

In the phototransduction cascade of *Drosophila*, light triggers the activation of PLCβ. This catalyzes hydrolysis of the membrane phospholipid PIP_2 into water soluble $InsP_3$ and membrane-bound DAG (Berridge, 1993). The continuous functionality of the photoreceptors during illumination is maintained by rapid regeneration of PIP_2 in a cyclic enzymatic pathway (the PI pathway, **Figure 9**). Moreover, the PI pathway has emerged to be most important for activation of the TRP and TRPL channels (Hardie, 2003; Raghu and Hardie, 2009).

The phospholipid branch of the PI cycle, following PLC activation, begins by DAG transport through endocytosis to the endoplasmic reticulum (SMC) and subsequently, inactivation by phosphorylation and conversion into phosphatidic acid (PA), via DAG kinase (DGK), encoded by the retinal degeneration A (*rdgA*) gene (Masai et al., 1993, 1997). Then, CDP-DAG syntase encoded by the *cds* gene (Wu et al., 1995) produces DAG-CDP from PA. Both RDGA and CDS are located in the SMC (**Figure 1C**). Subsequently, DAG-CDP is converted into phosphatidylinositol (PI), which is transferred back to the microvillar membrane, by the PI transfer protein (PITP), encoded by the *rdgB* gene (Vihtelic et al., 1991) located in the SMC. PIP and PIP_2 are produced at the microvillar membrane by PI kinase and PIP kinase, respectively. PA can be reconverted back to DAG by lipid phosphate phosphohydrolase, LPP, also designated phosphatidic acid phosphatase, PAP, encoded by the *laza* gene (Garcia-Murillas et al., 2006; Kwon and Montell, 2006) or produced from phosphatidylcholine (PC) by phospholipase D, PLD, encoded by the *Pld* gene (LaLonde et al., 2005). DAG is also hydrolyzed by DAG lipase encoded by the *inaE* gene (Leung et al., 2008) predominantly localized outside the rhabdomeres, into polyunsaturated fatty acid (PUFA, **Figure 9**).

Mutations in most proteins of the PI pathway result in retinal degeneration. For example, *rdgA* mutant flies show light-independent retinal degeneration, thought to occur due to a sustained Ca^{2+} influx through the light-activated TRP and TRPL channels, making the PI pathway crucial for understanding phototransduction and TRP channels activation. Although it is possible to partially rescue the degeneration phenotypes by reducing the level of TRP (Raghu et al., 2000b), it is still unclear whether this mutation promotes channel opening directly or through an indirect change in the photoreceptor, leading to channel opening.

THE LIGHT-ACTIVATED CHANNELS, TRP AND TRPL, THE FOUNDING MEMBERS OF THE TRP SUPERFAMILY

THE *trp* MUTANT AND THE DISCOVERY OF THE TRP CHANNEL

A spontaneously occurring *Drosophila* mutant, showing a decline in the receptor potential to baseline during prolonged illumination (Cosens and Manning, 1969), was designated transient receptor potential (*trp*) by Minke et al. (1975b) (**Figure 10B,** right). Minke and Selinger suggested in a review article, that the *trp* gene encodes a Ca^{2+} channel/transporter, mainly because application of the Ca^{2+} channel blocker La^{3+} to wild-type photoreceptors mimicked the *trp* phenotype (Minke and Selinger, 1991). The cloning of the *trp* locus by Montell and Rubin (1989) revealed a novel membrane protein. The available sequence of the *trp* gene led, several years later, to the discovery of mammalian TRPs and the TRP superfamily (Wes et al., 1995; Zhu et al., 1995). However, the significance of the *trp* sequence, as a gene encoding a putative channel protein, was only first appreciated after a *trp* homolog, the *trp-like* (*trpl*) gene was cloned. This was done by a screen for calmodulin-binding proteins which identified a TM protein. A comparison of its TM domain to that of voltage gated Ca^{2+} channels and the TRP protein led to the conclusion that this protein is a putative channel protein with high identity to TRP (Phillips et al., 1992). The first direct physiological evidence for the notion that TRP is the major light-activated channel came from a comparative patch clamp study of isolated ommatidia of wild type and the *trp* mutant (Hardie and Minke, 1992). The use of Ca^{2+} indicator dyes and Ca^{2+}-selective microelectrodes, directly demonstrated that the TRP channel is the major route for Ca^{2+} entry into the photoreceptor cell (Peretz et al., 1994a,b). The final evidence showing that TRP and TRPL are the light-activated channels came from the isolation of a null mutant of the *trpl* gene and the construction of the double mutant, *trpl;trp*, which is blind (Niemeyer et al., 1996). A third TRP homolog channel designated TRPγ has been cloned and sequenced (Xu et al., 2000). Heterologous expression in HEK293 cells has revealed a functional channel (Jors et al., 2006; Xu et al., 2000). However, in *Drosophila* photoreceptors this channel cannot generate any light-activated conductance in isolation as revealed in the *trpl;trp* double null mutant and therefore its role in phototransduction, if any, is not clear.

BIOPHYSICAL PROPERTIES OF THE TRP AND TRPL CHANNELS

The *Drosophila* light-sensitive channels, TRP and TRPL, can be studied separately by utilizing the $trpl^{302}$ and trp^{P343} null mutants, respectively (Scott et al., 1997; **Figure 10**). The channels are permeable to a variety of monovalent and divalent ions including Na^+, K^+, Ca^{2+} and Mg^{2+} and even to large organic cations such as TRIS and TEA (Ranganathan et al., 1991). The reversal potential of the light-induced current (LIC) shows a marked dependence on extracellular Ca^{2+} indicating a high permeability for this ion. Permeability ratio measurement for a variety of divalent and monovalent ions, determined under bi-ionic conditions, confirmed a high Ca^{2+} permeability of ~57:1 = Ca^{2+}:Cs^+ in the *trpl* mutant and ~4.3:1 = Ca^{2+}:Cs^+ for the *trp* mutant (Reuss et al., 1997). The large Ca^{2+} permeability of TRP is reflected in its positive reversal potential (E_{rev}; **Figures 10C,D**).

The TRP and TRPL channels show voltage-dependent conductance during illumination. An early study revealed that the light response can be blocked by physiological concentrations of Mg^{2+} ions (Hardie and Mojet, 1995). The block mainly influenced the TRP channel and affected its voltage dependence. Later, detailed analyses described the voltage dependence of heterologously expressed TRPL channels in S2 cells and of the native TRPL channels, using the *Drosophila trp* null mutant. These studies indicated that the voltage dependence of the TRPL channel is not an intrinsic property, as is thought for some other members of the TRP family, but arises from divalent cations open channel block that can be removed by depolarization. The open channel block by divalent cations is thought to play a role in improving the signal to noise ratio of the response to intense light and may function in light adaptation and response termination (Parnas et al., 2007).

A comparison with voltage-gated K^+ channels and cyclic nucleotide gated (CNG) channels, postulates that both TRP and TRPL are assembled as tetrameric channels, thus raising the question whether they assemble as homomultimers or as heteromultimers. Since null *trp* and *trpl* mutants both respond to light, each can clearly function without the other. However, heterologous co-expression studies and co-immunoprecipitation, led to the suggestion that the TRP and TRPL channels can assemble into heteromultimers (Xu et al., 1997). Detailed

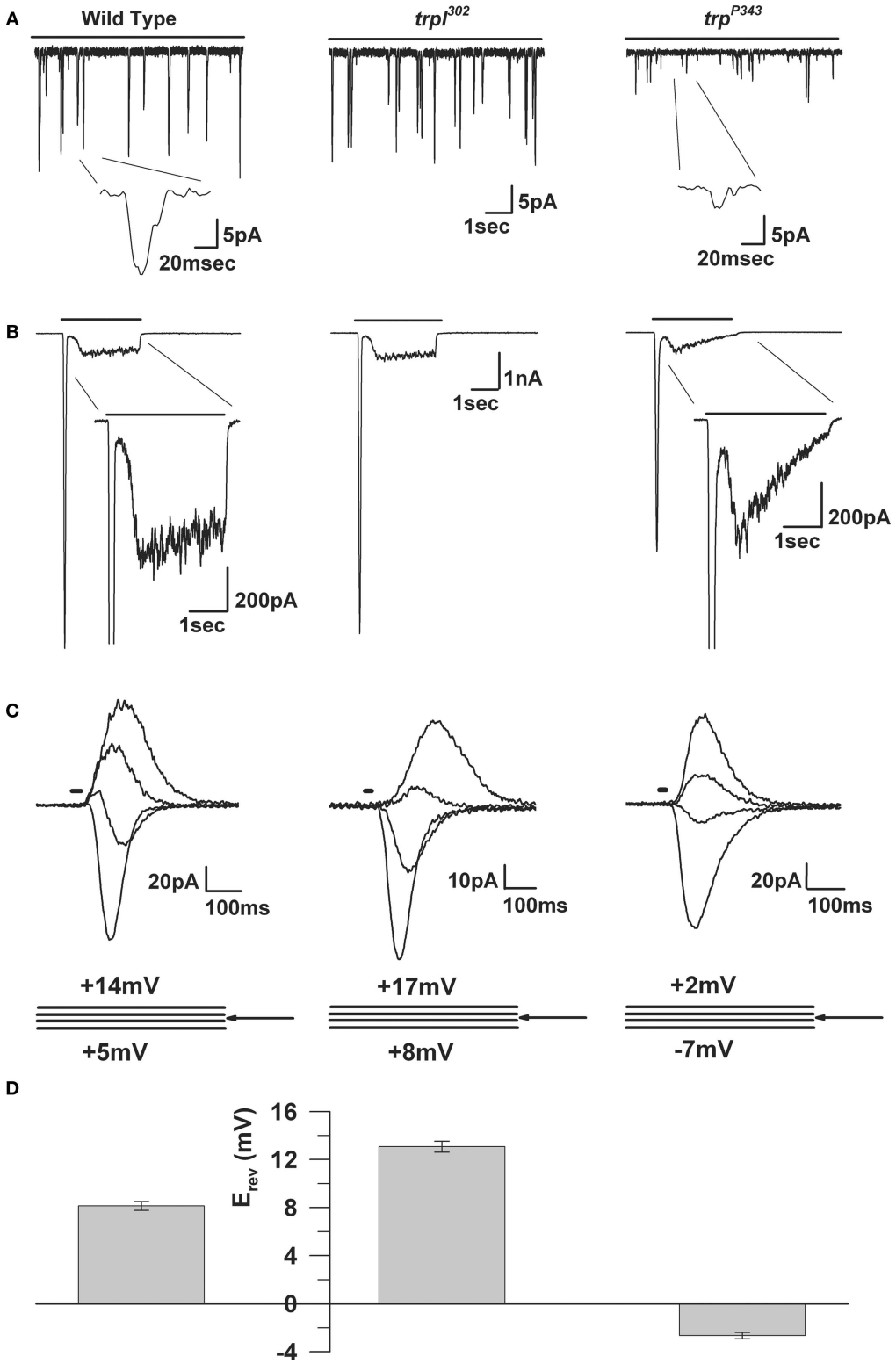

FIGURE 10 | The electrophysiological properties of WT, *trp* and *trpl* mutants. **(A)** Whole-cell voltage clamp recordings of quantum bumps in response to continuous dim light in wild-type, *trpl*^{302} and *trp*^{P343} null mutant flies. Highly reduced amplitude of *trp*^{P343} bumps is observed. **(B)** Whole-cell voltage clamp recordings in response to a 3-s light pulse of WT and the corresponding mutants. The transient response of the *trp*^{P343} mutant is observed. **(C)** A family of light-induced currents to 20-ms light pulse at voltage steps of 3 mV measured around E_{rev}. **(D)** Histogram plotting the mean E_{rev} of WT and the various mutants, error bars are SEM. E_{rev} of wild-type is between the positive E_{rev} of *trpl*^{302}, which expresses only TRP and the E_{rev} of *trp*^{P343} mutant, which expresses only TRPL.

measurements of biophysical properties, questioned this conclusion since they found that the wild-type conductance could be quantitatively accounted for by the sum of the conductances determined in the *trp* and *trpl* mutants (Reuss et al., 1997). In addition, a study demonstrated that the TRPL, but not the TRP channel reversibly translocates from the rhabdomere to the cell body upon illumination (Bahner et al., 2002) further imply that TRPL assemble as homomers.

LIGHT-REGULATED SUBCELLULAR TRANSLOCATION OF *DROSOPHILA* TRPL CHANNELS

In neurons the expression pattern of ion channels determines the physiological properties of the cell. Besides regulation at the level of gene expression that determines which channels are present in a given neuron, trafficking of ion channels into and out of the plasma membrane is an important mechanism for manipulating the number of channels at a specific cellular site (for reviews see Lai and Jan, 2006; Sheng and Lee, 2001). In *Drosophila* photoreceptors activation of the phototransduction cascade and the influx of Ca^{2+} through the TRP channels initiate the translocation of the TRPL but not the TRP channels from the signaling compartment, the rhabdomere, to the cell body (Bahner et al., 2002; Meyer et al., 2006). The TRPL translocation process occurs in two stages, a fast translocation (5 min) to the neighboring stalk membrane and a slow translocation (over 6 h) to the basolateral membrane (Cronin et al., 2006). Thus, the TRPL translocation timescale conforms to day night cycle and act in light adaptation (Bahner et al., 2002). While, Ca^{2+} influx has been shown to be necessary for TRPL translocation the molecular mechanism and structural determinants of the TRPL involved in translocation, are still unknown. Signal dependent translocation of mammalian TRP channels was found to be a widespread phenomenon (Bezzerides et al., 2004; Kanzaki et al., 1999; Zhang et al., 2005). Nevertheless, many of these researches are conducted on TRP channels expressed in tissue culture cells. This makes the *Drosophila* photoreceptors a unique system in which TRPL channels translocation can be studied in vivo.

ACTIVATION MECHANISMS OF TRP AND TRPL CHANNELS

It has been well established that hydrolysis of PIP_2 by PLC, encoded by the *norpA* gene, activates the light-sensitive channels TRP and TRPL in *Drosophila* photoreceptors. However, the mechanism by which PLC activity results in channels opening is still under debate. Several hypotheses have been presented through the years. (i) The $InsP_3$ hypothesis, suggested that the elevation of $InsP_3$, following PIP_2 hydrolysis, activates the $InsP_3R$ ($InsP_3$ receptor) resulting in Ca^{2+} store depletion and activation of the channels in a store-operated mechanism (Hardie and Minke, 1993). This mechanism of activation has also been suggested for a number of mammalian TRPC channels (Putney, 2007; Yuan et al., 2007). In addition, direct activation of the channels as in the *Limulus* ventral photoreceptors (Payne et al., 1986) using caged Ca^{2+} or $InsP_3$ to elevate Ca^{2+} did not activate the channels (Hardie, 1995; Hardie and Raghu, 1998). Rather, direct application of Ca^{2+} in excised inside-out patches inhibits expressed TRPL channels in S2 cells by an open channel block mechanism (Parnas et al., 2007), suggesting an inhibition rather than activation effect of Ca^{2+}. Furthermore, genetic elimination of the only $InsP_3R$ in *Drosophila* had no effect on the light response (Acharya et al., 1997; Raghu et al., 2000a). Therefore, the $InsP_3$ hypothesis was abundant. It therefore became evident that the alternative branch of PLC, DAG production should be investigated. The most familiar action of DAG is to activate the classical protein kinase C (PKC) synergistically with Ca^{2+}. However, mutations in the ePKC, encoded by the *inaC* gene lead to defects in response termination with no apparent effects on activation (Hardie et al., 1993; compare **Figure 11A** to **Figure 11B**). (ii) The PUFA or DAG hypothesis argues that the elevation of DAG and consequently of PUFA acting as second messengers results in channel opening. This hypothesis emerged from a detailed pharmacological study which tested the effect of various fatty acids (including PUFAs) on TRP and TRPL channels activation in vivo and TRPL expressed in *Drosophila* S2 cells (Chyb et al., 1999). In addition, a detailed analysis of the *rdgA* mutant encoding DAG kinase has established the importance of the DAG branch in channel activation. This mutant shows light-independent retinal degeneration and constitutive activity of the light-activated channels, while a partial rescue of the degeneration is achieved by eliminating the TRP channel in the double mutant $rdgA;trp^{P343}$ (Raghu et al., 2000b). Furthermore, it has been shown that the double mutant $norpA^{P24}$, *rdgA* partially rescues the light response in the almost null $norpA^{P24}$ mutant. This finding further supports the hypothesis that DAG or its surrogate PUFA are involved in channel activation (Hardie et al., 2003). Several lines of evidence challenge this hypothesis: first, application of DAG to intact ommatidia does not activate the channels (unpublished data), while application of DAG analogs 1-oleoyl-2-acetyl-sn-glycerol (OAG) at low concentration (2 μM) in inside-out patches excised from the microvilli of dissociated ommatidia result in activation of the TRP and TRPL channels in kinetics slower by three orders of magnitude (~60 s after application) compared to the light stimuli (Delgado and Bacigalupo, 2009). Second, the localization of RDGA in the SMC, a relatively distant cellular compartment from the transduction machinery (Masai et al., 1997) makes it unlikely that DAG could act as a second messenger without considerably slowing response termination kinetics, which does not fit to the fast termination of the response to light. Further establishment of this hypothesis requires identification of a functional-binding domain for DAG or PUFA on the TRP and TRPL channel and further elucidating the complex enzymatic machinery of PUFA production by DAG lipases. Recently, the *inaE* gene was identified as encoding a homologue of mammalian *sn-1* type DAG lipase and was shown to be expressed predominantly in the cell body of *Drosophila* photoreceptors (**Figure 9**). Mutant flies, expressing low levels of the *inaE* gene product, have an abnormal light response, while the activation of the light-sensitive channels was not prevented (Leung et al., 2008). The discovery of the *inaE* gene is a first step in an endeavor to elucidate lipids regulation of the channels (see review, Raghu and Hardie, 2009). Thus, the participation of DAG or PUFAs in TRP and TRPL activation in vivo needs further exploration. (iii) The PIP_2 depletion and DAG accumulation hypothesis argues that PIP_2 acts as a negative modulator, while DAG or its surrogates acts as positive modulators of the TRPL channel. Schilling and colleagues demonstrated

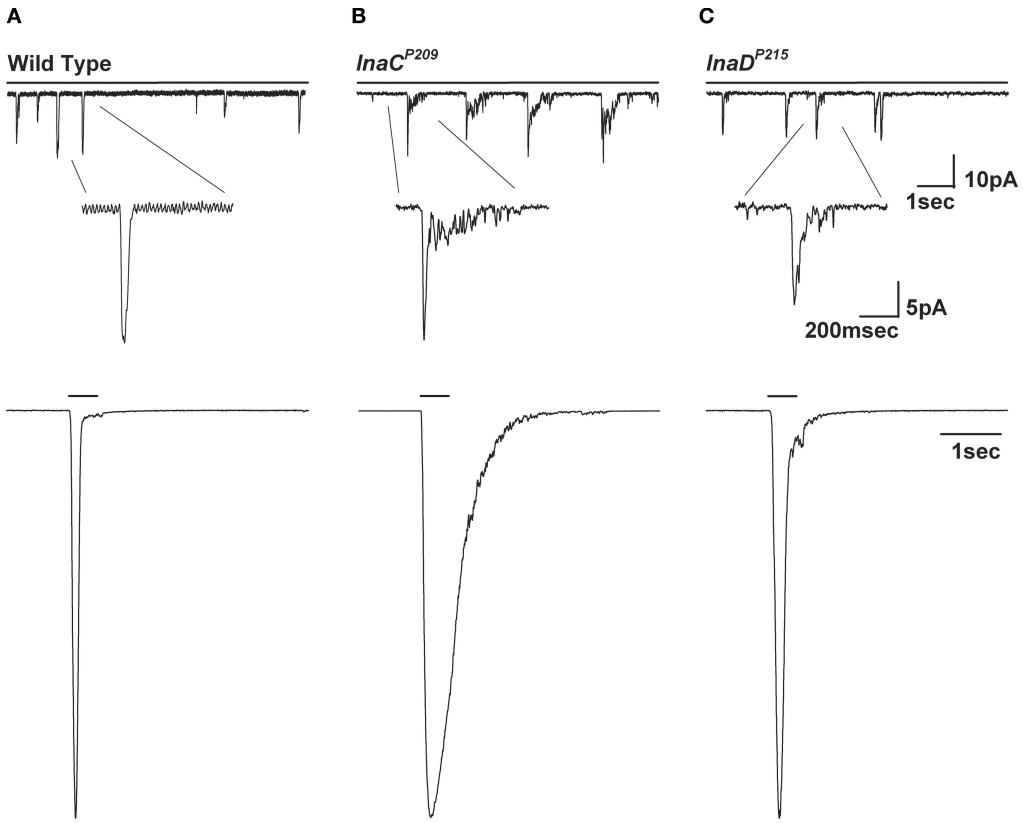

FIGURE 11 |The *inaC*^{P209} and *inaD*^{P215} mutants reveal slow response termination of the macroscopic response to light and of the single bumps. **(A–C)** Upper panels: Whole-cell voltage clamp quantum bump responses to continues dim light in wild-type, *inaC*^{P209} and *inaD*^{P215} mutant flies. A slow termination of the bumps is observed in *inaC*^{P209} and *inaD*^{P215} mutant flies. **(A–C)** Lower panels: Whole-cell voltage clamp recordings of normalized responses to a 500-ms light pulse of the above mutants. A slow termination of macroscopic response is observed in *inaC*^{P209} null mutant and in the *inaD*^{P215} mutant in which the binding of INAD to TRP is disrupted (Chevesich et al., 1997; Shieh and Zhu, 1996).

in Sf9 cells expressing TRPL that application of DAG or PUFA activates the channels, while application of PIP_2 in inside-out patches inhibit their activity (Estacion et al., 2001). However, Hardie et al. (2001) showed that the *trp*^{P343} mutant phenotype (in which the light response decays to baseline) is a result of PIP_2 depletion which is not compatible with a PIP_2 inhibitory action. In addition, a PIP_2-binding domain has not been functionally identified in the TRP or TRPL channels. Together, the above arguments put the PIP_2 depletion and DAG accumulation hypothesis in question. (iv) A recently new hypothesis was formulated, suggesting that plasma membrane lipid–channel interaction controls channel gating. Accordingly, disruption of this interaction by membrane lipid modification through PLC activation causes the opening of the channels (Parnas et al., 2009). It is important to realize that PLC activation, which converts PIP_2, a charged molecule, containing a large hydrophilic head-group, into DAG, devoid of the hydrophilic head-group, is known to cause major changes in lipid packing and lipid–channel interactions (Janmey and Kinnunen, 2006). It is therefore possible that neither PIP_2 hydrolysis nor DAG production affect the TRP and TRPL channel as second messengers, but rather act as modifiers of membrane lipid–channel interactions. This may in turn act as a possible mechanism of channel activation (Parnas et al., 2009). This hypothesis evades the two main problems of the DAG or PUFA hypothesis: the need of RDGA at closed proximity to the channels and a channel-binding domain for DAG and/or PUFA. This hypothesis suffers from insufficient direct demonstration both in cell expression systems and in vivo.

ORGANIZATION IN A SUPRAMOLECULAR SIGNALING COMPLEX VIA THE SCAFFOLD PROTEIN INAD

An important step towards understanding *Drosophila* phototransduction has been achieved by the finding that some of the key elements of the phototransduction cascade are incorporated into supramolecular signaling complexes via a scaffold protein, INAD (**Figure 4**). The INAD protein was discovered using a PDA screen which isolated a defective *Drosophila* mutant (*inaD*). The first discovered *inaD* mutant, the *inaD*^{P215}, was isolated by Pak (1995) and was subsequently cloned and sequenced by Shieh and Niemeyer (1995). Later studies in *Calliphora* have shown that INAD binds not only TRP but also PLC (NORPA) and ePKC (INAC) (Huber et al., 1996). The interaction of INAD with TRP, NORPA and INAC was later confirmed in *Drosophila* (Tsunoda et al., 1997). It was further found that *inaD* is a scaffold protein, which consists

of five ~90 amino acid (aa) protein interaction motifs called PDZ (PSD95, DLG, ZO1) domains. These domains are recognized as protein modules which bind to a diversity of signaling, cell adhesion and cytoskeletal proteins (Dimitratos et al., 1999; Schillace and Scott, 1999) by specific binding to target sequences typically, though not always, in the final three residues of the C-terminal. The PDZ domains of INAD bind to the signaling molecules as follows: PDZ1 and PDZ5 bind PLC (Shieh et al., 1997; van Huizen et al., 1998), PDZ2 or PDZ4 bind ePKC (Adamski et al., 1998) and PDZ3 binds TRP (Chevesich et al., 1997; Shieh and Zhu, 1996). This binding pattern is still under debate due to several contradictory reports. Contrary to TRP, TRPL appears not to be a member of the complex, since unlike INAC, NORPA and TRP it remains strictly localized to the microvilli in the *inaD*^{1} null mutant (Tsunoda et al., 1997). Several studies have suggested that, in addition to PLC, PKC and TRP, other signaling molecules such as CaM, R, TRPL and NINAC bind to the INAD signaling complex. Such binding, however, must be dynamic. Biochemical studies conducted in *Calliphora* have revealed that both INAD and TRP are targets for phosphorylation by the nearby ePKC (Huber et al., 1998). Accordingly, the association of TRP into transduction complexes may be related to increasing speed and efficiency of transduction events as reflected by the immediate vicinity of TRP to its upstream activator, PLC, and its possible regulator, ePKC (Huber et al., 1998). Indeed, genetic elimination of INAC affected the shape of the quantum bump of the *inaC* null mutant, by inducing slow termination of the bump, composed of dumped oscillating current noise of an unclear underlying mechanism (Hardie et al., 1993; Henderson et al., 2000; **Figure 11B**). Interestingly, a similar phenotype was observed in the *inaD*^{P215} mutant, whereby the INAD complex and TRP channel are dissociated (Henderson et al., 2000; **Figure 11C**), also with a still unclear underlying mechanism.

TRP plays a major role in localizing the entire INAD multimolecular complex. Association between TRP and INAD is essential for correct localization of the complex in the rhabdomeres, as found in other signaling systems (Arnold and Clapham, 1999). This conclusion was derived from the use of *Drosophila* mutants in which the signaling proteins, which constitute the INAD complex, were removed genetically, and also by deletions of the specific binding domains, which bind TRP to INAD. These experiments showed that INAD is correctly localized to the rhabdomeres in *inaC* mutants (where ePKC is missing) and in *norpA* mutants (where PLC is missing), but severely mislocalized in null *trp* mutants (Li and Montell, 2000; Tsunoda et al., 2001), thus indicating that TRP but not PLC or PKC is essential for localization of the signaling complex to the rhabdomere. To demonstrate that a specific interaction of INAD with TRP is required for rhabdomeric localization of the complex, the binding site at the C-terminal of TRP was removed or three conserved residues in PDZ3, which are expected to disrupt the interaction between PDZ domains and their targets were modified. As predicted, both TRP and INAD were mislocalized in these mutants. The study of the above mutants was also used to show that TRP and INAD do not depend on each other for targeting to the rhabdomeres. Thus, INAD–TRP interaction is not required for targeting but for anchoring of the signaling complex (Li and Montell, 2000; Tsunoda et al., 2001). Additional experiments on TRP and INAD further showed that INAD has other functions in addition to anchoring the signaling complex. One important function is to preassemble the proteins of the signaling complex. Another important function, at least in the case of PLC, is to prevent degradation of the unbound signaling protein.

A recent study by Ranganathan and colleagues has suggested that the binding of signaling proteins to INAD may be a dynamic process that allows an additional level of phototransduction regulation. Their study showed two crystal structural states of isolated INAD PDZ5 domain, differing mainly by the formation of a disulfide bond. This conformational change has light-dependent dynamics that was demonstrated by the use of transgenic *Drosophila* flies expressing INAD with a point mutation disrupting the formation of the disulfide bond. They proposed a model in which, ePKC phosphorylation at a still unknown site promotes the light-dependent conformational change of PDZ5, distorting its ligand-binding groove to PLC and thus regulating phototransduction (Mishra et al., 2007).

CONCLUDING REMARKS

The study of fly photoreceptors has opened new avenues in biological research, mainly through the exploitation of the power of *Drosophila* molecular genetics. Processes and proteins that were discovered in *Drosophila* have been found to be highly conserved through evolution and thus paved the way for the discovery of important proteins and mechanisms in development and cell signaling in mammals. A striking example is the discovery of the TRP channel protein in the *Drosophila* photoreceptors, which led to the discovery of the widespread TRP superfamily, which plays crucial roles in sensory signaling of insects and mammals. The activation and regulation of *Drosophila* TRPs by the inositol-lipid signaling pathway and the major role of PLC in the activation of these channels has wide implications for understanding the activation and regulations of mammalian TRPs. Even today *Drosophila* photoreceptors are one of the few systems in which TRP channels are studied in vivo. Another novel molecule that was discovered in *Drosophila* photoreceptors is the INAD scaffold protein which forms a supramolecular signaling complex. This protein has introduced new concepts in cell signaling dynamics which are still under investigations. An additional advantage of using the fly for research on cellular signaling is that frequently the fly system is less evolutionary evolved relative to mammals, making it simpler to study, while maintaining its core function. It is therefore anticipated that research using the *Drosophila* sensory and motor systems will continue to identify new proteins and mechanisms of high biological importance.

ACKNOWLEDGMENTS

We thank Shaya Lev, Moshe Parnas and Daniela Dadon for critical reading of the manuscript. The research part of this review was supported by grants from the National Institute of Health (EY 03529), the Israel Science Foundation (ISF), the US-Israel Binational Science Foundation (BSF), the Moscona Foundation and the Minerva Foundation.

REFERENCES

Acharya, J. K., Jalink, K., Hardy, R. W., Hartenstein, V., and Zuker, C. S. (1997). $InsP_3$ receptor is essential for growth and differentiation but not for vision in *Drosophila*. *Neuron* 18, 881–887.

Adamski, F. M., Zhu, M. Y., Bahiraei, F., and Shieh, B. H. (1998). Interaction of eye protein kinase C and INAD in *Drosophila*. Localization of binding domains and electrophysiological characterization of a loss of association in transgenic flies. *J. Biol. Chem.* 273, 17713–17719.

Alloway, P. G., and Dolph, P. J. (1999). A role for the light-dependent phosphorylation of visual arrestin. *Proc. Natl. Acad. Sci. U. S. A.* 96, 6072–6077.

Alloway, P. G., Howard, L., and Dolph, P. J. (2000). The formation of stable rhodopsin-arrestin complexes induces apoptosis and photoreceptor cell degeneration. *Neuron* 28, 129–138.

Arnold, D. B., and Clapham, D. E. (1999). Molecular determinants for subcellular localization of PSD-95 with an interacting K^+ channel. *Neuron* 23, 149–157.

Arshavsky, V. Y. (2003). Protein translocation in photoreceptor light adaptation: a common theme in vertebrate and invertebrate vision. *Sci. STKE* 2003, E43.

Arshavsky, V. Y., and Pugh-EN, J. (1998). Lifetime regulation of G protein-effector complex: emerging importance of RGS proteins. *Neuron* 20, 11–14.

Bahner, M., Frechter, S., Da, S. N., Minke, B., Paulsen, R., and Huber, A. (2002). Light-regulated subcellular translocation of *Drosophila* TRPL channels induces long-term adaptation and modifies the light-induced current. *Neuron* 34, 83–93.

Berridge, M. J. (1993). Inositol trisphosphate and calcium signalling. *Nature* 361, 315–325.

Berstein, G., Blank, J. L., Jhon, D. Y., Exton, J. H., Rhee, S. G., and Ross, E. M. (1992). Phospholipase C-β1 is a GTPase-activating protein for $G_{q/11}$, its physiologic regulator. *Cell* 70, 411–418.

Bezzerides, V. J., Ramsey, I. S., Kotecha, S., Greka, A., and Clapham, D. E. (2004). Rapid vesicular translocation and insertion of TRP channels. *Nat. Cell Biol.* 6, 709–720.

Bloomquist, B. T., Shortridge, R. D., Schneuwly, S., Perdew, M., Montell, C., Steller, H., Rubin, G., and Pak, W. L. (1988). Isolation of a putative phospholipase C gene of *Drosophila*, *norpA*, and its role in phototransduction. *Cell* 54, 723–733.

Byk, T., Bar Yaacov, M., Doza, Y. N., Minke, B., and Selinger, Z. (1993). Regulatory arrestin cycle secures the fidelity and maintenance of the fly photoreceptor cell. *Proc. Natl. Acad. Sci. U. S. A.* 90, 1907–1911.

Chen, C.-K., Burns, M. E., He, W., Wensel, T. G., Baylor, D. A., and Simon, M. I. (2000). Slowed recovery of rod photoresponse in mice lacking the GTPase accelerating protein RGS9-1. *Nature* 403, 557–560.

Chevesich, J., Kreuz, A. J., and Montell, C. (1997). Requirement for the PDZ domain protein, INAD, for localization of the TRP store-operated channel to a signaling complex. *Neuron* 18, 95–105.

Chorna-Ornan, I., Tzarfaty, V., Ankri-Eliahoo, G., Joel-Almagor, T., Meyer, N. E., Huber, A., Payre, F., and Minke, B. (2005). Light-regulated interaction of Dmoesin with TRP and TRPL channels is required for maintenance of photoreceptors. *J. Cell Biol.* 171, 143–152.

Chyb, S., Raghu, P., and Hardie, R. C. (1999). Polyunsaturated fatty acids activate the *Drosophila* light-sensitive channels TRP and TRPL. *Nature* 397, 255–259.

Cook, B., Bar, Y. M., Cohen-Ben, A. H., Goldstein, R. E., Paroush, Z., Selinger, Z., and Minke, B. (2000). Phospholipase C and termination of G-protein-mediated signalling in vivo. *Nat. Cell Biol.* 2, 296–301.

Cook, B., Hardy, R. W., McConnaughey, W. B., and Zuker, C. S. (2008). Preserving cell shape under environmental stress. *Nature* 452, 361–364.

Cosens, D. J., and Manning, A. (1969). Abnormal electroretinogram from a *Drosophila* mutant. *Nature* 224, 285–287.

Cronin, M. A., Lieu, M. H., and Tsunoda, S. (2006). Two stages of light-dependent TRPL-channel translocation in *Drosophila* photoreceptors. *J. Cell Sci.* 119, 2935–2944.

Delgado, R., and Bacigalupo, J. (2009). Unitary recordings of TRP and TRPL channels from isolated *Drosophila* retinal photoreceptor rhabdomeres: activation by light and lipids. *J. Neurophysiol.* 101, 2372–2379.

Devary, O., Heichal, O., Blumenfeld, A., Cassel, D., Suss, E., Barash, S., Rubinstein, C. T., Minke, B., and Selinger, Z. (1987). Coupling of photoexcited rhodopsin to inositol phospholipid hydrolysis in fly photoreceptors. *Proc. Natl. Acad. Sci. U. S. A.* 84, 6939–6943.

Dimitratos, S. D., Woods, D. F., Stathakis, D. G., and Bryant, P. J. (1999). Signaling pathways are focused at specialized regions of the plasma membrane by scaffolding proteins of the MAGUK family. *Bioessays* 21, 912–921.

Dolph, P. J., Man Son Hing, H., Yarfitz, S., Colley, N. J., Deer, J. R., Spencer, M., Hurley, J. B., and Zuker, C. S. (1994). An eye-specific Gβ subunit essential for termination of the phototransduction cascade. *Nature* 370, 59–61.

Dolph, P. J., Ranganathan, R., Colley, N. J., Hardy, R. W., Socolich, M., and Zuker, C. S. (1993). Arrestin function in inactivation of G protein-coupled receptor rhodopsin in vivo. *Science* 260, 1910–1916.

Dorlochter, M., and Stieve, H. (1997). The *Limulus* ventral photoreceptor: light response and the role of calcium in a classic preparation. *Prog. Neurobiol.* 53, 451–515.

Elia, N., Frechter, S., Gedi, Y., Minke, B., and Selinger, Z. (2005). Excess of $G\beta_e$ over $G_q\alpha_e$ in vivo prevents dark, spontaneous activity of *Drosophila* photoreceptors. *J. Cell Biol.* 171, 517–526.

Estacion, M., Sinkins, W. G., and Schilling, W. P. (2001). Regulation of *Drosophila* transient receptor potential-like (TrpL) channels by phospholipase C-dependent mechanisms. *J. Physiol.* 530, 1–19.

Fein, A. (1986). Blockade of visual excitation and adaptation in *Limulus* photoreceptor by GDP-β-S. *Science* 232, 1543–1545.

Fein, A., and Corson, D. W. (1981). Excitation of *Limulus* photoreceptors by vanadate and by a hydrolysis-resistant analog of guanosine triphosphate. *Science* 212, 555–557.

Fischer, A., and Horstmann, G. (1971). Fine structure of the eye of the meal moth, *Ephestia kuehniella* Zeller (Lepidoptera, Pyralididae). *Z. Zellforsch. Mikrosk. Anat.* 116, 275–304.

Franceschini, N., and Kirschfeld, K. (1971). In vivo optical study of photoreceptor elements in the compound eye of *Drosophila*. *Kybernetik* 8, 1–13.

Frechter, S., Elia, N., Tzarfaty, V., Selinger, Z., and Minke, B. (2007). Translocation of $G_q\alpha$ mediates long-term adaptation in *Drosophila* photoreceptors. *J. Neurosci.* 27, 5571–5583.

Garcia-Murillas, I., Pettitt, T., Macdonald, E., Okkenhaug, H., Georgiev, P., Trivedi, D., Hassan, B., Wakelam, M., and Raghu, P. (2006). *lazaro* encodes a lipid phosphate phosphohydrolase that regulates phosphatidylinositol turnover during *Drosophila* phototransduction. *Neuron* 49, 533–546.

Hardie, R. C. (1995). Photolysis of caged Ca^{2+} facilitates and inactivates but does not directly excite light-sensitive channels in *Drosophila* photoreceptors. *J. Neurosci.* 15, 889–902.

Hardie, R. C. (2003). Regulation of TRP channels via lipid second messengers. *Annu. Rev. Physiol.* 65, 735–759.

Hardie, R. C., Martin, F., Chyb, S., and Raghu, P. (2003). Rescue of light responses in the *Drosophila* "null" phospholipase C mutant, $norpA^{P24}$, by the diacylglycerol kinase mutant, *rdgA*, and by metabolic inhibition. *J. Biol. Chem.* 278, 18851–18858.

Hardie, R. C., and Minke, B. (1992). The *trp* gene is essential for a light-activated Ca^{2+} channel in *Drosophila* photoreceptors. *Neuron* 8, 643–651.

Hardie, R. C., and Minke, B. (1993). Novel Ca^{2+} channels underlying transduction in *Drosophila* photoreceptors: implications for phosphoinositide-mediated Ca^{2+} mobilization. *Trends Neurosci.* 16, 371–376.

Hardie, R. C., and Mojet, M. H. (1995). Magnesium-dependent block of the light-activated and *trp*-dependent conductance in *Drosophila* photoreceptors. *J. Neurosci.* 74, 2590–2599.

Hardie, R. C., Peretz, A., Suss-Toby, E., Rom-Glas, A., Bishop, S. A., Selinger, Z., and Minke, B. (1993). Protein kinase C is required for light adaptation in *Drosophila* photoreceptors. *Nature* 363, 634–637.

Hardie, R. C., and Raghu, P. (1998). Activation of heterologously expressed *Drosophila* TRPL channels: Ca^{2+} is not required and $InsP_3$ is not sufficient. *Cell Calcium* 24, 153–163.

Hardie, R. C., and Raghu, P. (2001). Visual transduction in *Drosophila*. *Nature* 413, 186–193.

Hardie, R. C., Raghu, P., Moore, S., Juusola, M., Baines, R. A., and Sweeney, S. T. (2001). Calcium influx via TRP channels is required to maintain PIP_2 levels in *Drosophila* photoreceptors. *Neuron* 30, 149–159.

Henderson, S. R., Reuss, H., and Hardie, R. C. (2000). Single photon responses in *Drosophila* photoreceptors and their regulation by Ca^{2+}. *J. Physiol.* 524, 179–194.

Hillman, P., Hochstein, S., and Minke, B. (1972). A visual pigment with two physiologically active stable states. *Science* 175, 1486–1488.

Hillman, P., Hochstein, S., and Minke, B. (1983). Transduction in invertebrate photoreceptors: role of pigment bistability. *Physiol. Rev.* 63, 668–772.

Huber, A., Sander, P., Bahner, M., and Paulsen, R. (1998). The TRP Ca^{2+} channel assembled in a signaling complex by the PDZ domain protein INAD is phosphorylated through the interaction with protein kinase C (ePKC). *FEBS Lett.* 425, 317–322.

Huber, A., Sander, P., Gobert, A., Bahner, M., Hermann, R., and Paulsen, R. (1996). The transient receptor potential protein (Trp), a putative store-operated Ca^{2+} channel essential for phosphoinositide-mediated photoreception, forms a signaling

complex with NorpA, InaC and InaD. *EMBO J.* 15, 7036–7045.

Janmey, P. A., and Kinnunen, P. K. (2006). Biophysical properties of lipids and dynamic membranes. *Trends Cell Biol.* 16, 538–546.

Jors, S., Kazanski, V., Foik, A., Krautwurst, D., and Harteneck, C. (2006). Receptor-induced activation of *Drosophila* TRPγ by polyunsaturated fatty acids. *J. Biol. Chem.* 281, 29693–29702.

Kahn, E. S., and Matsumoto, H. (1997). Calcium/calmodulin-dependent kinase II phosphorylates *Drosophila* visual arrestin. *J. Neurochem.* 68, 169–175.

Kanzaki, M., Zhang, Y. Q., Mashima, H., Li, L., Shibata, H., and Kojima, I. (1999). Translocation of a calcium-permeable cation channel induced by insulin-like growth factor-I. *Nat. Cell Biol.* 1, 165–170.

Kirschfeld, K. (1967). The projection of the optical environment on the screen of the rhabdomere in the compound eye of the *Musca*. *Exp. Brain Res.* 3, 248–270.

Kirschfeld, K. (1971). Uptake and processing of optic data in the complex eye of insects. *Naturwissenschaften* 58, 201–209.

Kirschfeld, K., and Franceschini, N. (1968). Optical characteristics of ommatidia in the complex eye of *Musca*. *Kybernetik* 5, 47–52.

Kirschfeld, K., and Franceschini, N. (1969). A mechanism for the control of the light flow in the rhabdomeres of the complex eye of *Musca*. *Kybernetik* 6, 13–22.

Kirschfeld, K., and Snyder, A. W. (1976). Measurement of a photoreceptor's characteristic waveguide parameter. *Vision Res.* 16, 775–778.

Kirschfeld, K., and Vogt, K. (1980). Calcium ions and pigment migration in fly photoreceptors. *Naturwissenschaften* 67, 516–517.

Kiselev, A., Socolich, M., Vinos, J., Hardy, R. W., Zuker, C. S., and Ranganathan, R. (2000). A molecular pathway for light-dependent photorecptor apoptosis in *Drosophila*. *Neuron* 28, 139–152.

Kosloff, M., Elia, N., Joel-Almagor, T., Timberg, R., Zars, T. D., Hyde, D. R., Minke, B., and Selinger, Z. (2003). Regulation of light-dependent $G_q\alpha$ translocation and morphological changes in fly photoreceptors. *EMBO J.* 22, 459–468.

Kwon, Y., and Montell, C. (2006). Dependence on the Lazaro phosphatidic acid phosphatase for the maximum light response. *Curr. Biol.* 16, 723–729.

Lai, H. C., and Jan, L. Y. (2006). The distribution and targeting of neuronal voltage-gated ion channels. *Nat. Rev. Neurosci.* 7, 548–562.

LaLonde, M. M., Janssens, H., Rosenbaum, E., Choi, S. Y., Gergen, J. P., Colley, N. J., Stark, W. S., and Frohman, M. A. (2005). Regulation of phototransduction responsiveness and retinal degeneration by a phospholipase D-generated signaling lipid. *J. Cell Biol.* 169, 471–479.

Lee, S. J., and Montell, C. (2004). Light-dependent translocation of visual arrestin regulated by the NINAC myosin III. *Neuron* 43, 95–103.

Lee, Y. J., Dobbs, M. B., Verardi, M. L., and Hyde, D. R. (1990). dgq: a *Drosophila* gene encoding a visual system-specific G a molecule. *Neuron* 5, 889–898.

Leung, H. T., Tseng-Crank, J., Kim, E., Mahapatra, C., Shino, S., Zhou, Y., An, L., Doerge, R. W., and Pak, W. L. (2008). DAG lipase activity is necessary for TRP channel regulation in *Drosophila* photoreceptors. *Neuron* 58, 884–896.

Li, H. S., and Montell, C. (2000). TRP and the PDZ protein, INAD, form the core complex required for retention of the signalplex in *Drosophila* photoreceptor cells. *J. Cell Biol.* 150, 1411–1422.

Li, H. S., Porter, J. A., and Montell, C. (1998). Requirement for the NINAC kinase/myosin for stable termination of the visual cascade. *J. Neurosci.* 18, 9601–9606.

Liu, C. H., Satoh, A. K., Postma, M., Huang, J., Ready, D. F., and Hardie, R. C. (2008). Ca^{2+}-dependent metarhodopsin inactivation mediated by calmodulin and NINAC myosin III. *Neuron* 59, 778–789.

Lo, M. V., and Pak, W. L. (1981). Light-induced pigment granule migration in the retinular cells of *Drosophila melanogaster*. Comparison of wild type with ERG-defective mutants. *J. Gen. Physiol.* 77, 155–175.

Makino, E. R., Handy, J. W., Li, T., and Arshavsky, V. Y. (1999). The GTPase activating factor for transducin in rod photoreceptors is the complex between RGS9 and type 5 G protein β subunit. *Proc. Natl. Acad. Sci. U. S. A.* 96, 1947–1952.

Masai, I., Okazaki, A., Hosoya, T., and Hotta, Y. (1993). *Drosophila* retinal degeneration A gene encodes an eye-specific diacylglycerol kinase with cysteine-rich zinc-finger motifs and ankyrin repeats. *Proc. Natl. Acad. Sci. U. S. A.* 90, 11157–11161.

Masai, I., Suzuki, E., Yoon, C. S., Kohyama, A., and Hotta, Y. (1997). Immunolocalization of *Drosophila* eye-specific diacylgylcerol kinase, *rdgA*, which is essential for the maintenance of the photoreceptor. *J. Neurobiol.* 32, 695–706.

Meyer, N. E., Joel-Almagor, T., Frechter, S., Minke, B., and Huber, A. (2006). Subcellular translocation of the eGFP-tagged TRPL channel in *Drosophila* photoreceptors requires activation of the phototransduction cascade. *J. Cell Sci.* 119, 2592–2603.

Minke, B., and Cook, B. (2002). TRP channel proteins and signal transduction. *Physiol Rev.* 82, 429–472.

Minke, B., and Hardie, R. C. (2000). Genetic dissection of *Drosophila* phototransduction. In Molecular Mechanisms in Visual Transduction, D. G. Stavenga, D. J. N. van der Hope, and E. Pugh, eds (North Holland, Elsevier), pp. 449–525.

Minke, B., and Selinger, Z. (1991). Inositol lipid pathway in fly photoreceptors: excitation, calcium mobilization and retinal degeneration. In Progress in Retinal Research, N. A. Osborne and G. J. Chader, eds (Oxford, Pergamon Press), pp. 99–124.

Minke, B., and Selinger, Z. (1992). The inositol-lipid pathway is necessary for light excitation in fly photoreceptors. In Sensory Transduction, D. Corey and S. D. Roper, eds (New York, The Rockofeller University Press), pp. 202–217.

Minke, B., and Selinger, Z. (1996). The roles of *trp* and calcium in regulating photoreceptor function in *Drosophila*. *Curr. Opin. Neurobiol.* 6, 459–466.

Minke, B., and Stephenson, R. S. (1985). The characteristics of chemically induced noise in *Musca* photoreceptors. *J. Comp. Physiol.* 156, 339–356.

Minke, B., Wu, C.-F., and Pak, W. L. (1975a). Isolation of light-induce response of the central retinular cells from the electroretinogram of *Drosophila*. *J. Comp. Physiol.* 98, 345–355.

Minke, B., Wu, C., and Pak, W. L. (1975b). Induction of photoreceptor voltage noise in the dark in *Drosophila* mutant. *Nature* 258, 84–87.

Mishra, P., Socolich, M., Wall, M. A., Graves, J., Wang, Z., and Ranganathan, R. (2007). Dynamic Scaffolding in a G Protein-Coupled Signaling System. *Cell* 131, 80–92.

Montell, C. (1989). Molecular genetics of *Drosophila* vision. *Bioessays* 11, 43–48.

Montell, C., and Rubin, G. M. (1989). Molecular characterization of the *Drosophila trp* locus: a putative integral membrane protein required for phototransduction. *Neuron* 2, 1313–1323.

Mukhopadhyay, S., and Ross, E. M. (1999). Rapid GTP binding and hydrolysis by G_q promoted by receptor and GTPase-activating proteins. *Proc. Natl. Acad. Sci. U. S. A.* 96, 9539–9544.

Nasi, E., del Pilar Gomez, M., and Payne, R. (2000). Phototransduction mechanims in microvillar and ciliary photoreceptors of invertebrate. In Molecular Mechanisms in Visual Transduction, D. G. Stavenga, D. J. N. van der Hope, and E. Pugh, eds (North Holland, Elsevier), pp. 389–448.

Niemeyer, B. A., Suzuki, E., Scott, K., Jalink, K., and Zuker, C. S. (1996). The *Drosophila* light-activated conductance is composed of the two channels TRP and TRPL. *Cell* 85, 651–659.

Pak, W. L. (1995). *Drosophila* in vision research. The Friedenwald Lecture. *Invest. Ophthalmol. Vis. Sci.* 36, 2340–2357.

Parnas, M., Katz, B., Lev, S., Tzarfaty, V., Dadon, D., Gordon-Shaag, A., Metzner, H., Yaka, R., and Minke, B. (2009). Membrane lipid modulations remove divalent open channel block from TRP-like and NMDA channels. *J. Neurosci.* 29, 2371–2383.

Parnas, M., Katz, B., and Minke, B. (2007). Open channel block by Ca^{2+} underlies the voltage dependence of *Drosophila* TRPL channel. *J. Gen. Physiol.* 129, 17–28.

Payne, R., Corson, D. W., and Fein, A. (1986). Pressure injection of calcium both excites and adapts *Limulus* ventral photoreceptors. *J. Gen. Physiol.* 88, 107–126.

Pearn, M. T., Randall, L. L., Shortridge, R. D., Burg, M. G., and Pak, W. L. (1996). Molecular, biochemical, and electrophysiological characterization of *Drosohpila norpA* mutannts. *J. Biol. Chem.* 271, 4937–4945.

Peretz, A., Sandler, C., Kirschfeld, K., Hardie, R. C., and Minke, B. (1994a). Genetic dissection of light-induced Ca^{2+} influx into *Drosophila* photoreceptors. *J. Gen. Physiol.* 104, 1057–1077.

Peretz, A., Suss-Toby, E., Rom-Glas, A., Arnon, A., Payne, R., and Minke, B. (1994b). The light response of *Drosophila* photoreceptors is accompanied by an increase in cellular calcium: effects of specific mutations. *Neuron* 12, 1257–1267.

Phillips, A. M., Bull, A., and Kelly, L. E. (1992). Identification of a *Drosophila* gene encoding a calmodulin-binding protein with homology to the *trp* phototransduction gene. *Neuron* 8, 631–642.

Pumir, A., Graves, J., Ranganathan, R., and Shraiman, B. I. (2008). Systems analysis of the single photon response in invertebrate photoreceptors. *Proc. Natl. Acad. Sci. U. S. A.* 105, 10354–10359.

Putney, J. W. Jr (2007). Inositol lipids and TRPC channel activation. *Biochem. Soc. Symp.* 74, 37–45.

Raghu, P., Colley, N. J., Webel, R., James, T., Hasan, G., Danin, M., Selinger, Z., and Hardie, R. C. (2000a). Normal phototransduction in *Drosophila* photoreceptors lacking an $InsP_3$ receptor gene. *Mol. Cell Neurosci.* 15, 429–445.

Raghu, P., and Hardie, R. C. (2009). Regulation of *Drosophila* TRPC channels by lipid messengers. *Cell Calcium*. [Epub ahead of print].

Raghu, P., Usher, K., Jonas, S., Chyb, S., Polyanovsky, A., and Hardie, R. C. (2000b). Constitutive activity of the light-sensitive channels TRP and TRPL in the *Drosophila* diacylglycerol kinase mutant, *rdgA*. *Neuron* 26, 169–179.

Ranganathan, R., Harris, G. L., Stevens, C. F., and Zuker, C. S. (1991). A *Drosophila* mutant defective in extracellular calcium-dependent photoreceptor deactivation and rapid desensitization. *Nature* 354, 230–232.

Ranganathan, R., Malicki, D. M., and Zuker, C. S. (1995). Signal transduction in *Drosophila* photoreceptors. *Annu. Rev. Neurosci.* 18, 283–317.

Ratliff, F. (1990). Haldan Keffer Hartline: December 22, 1903–March 18, 1983. *Biogr. Mem. Natl. Acad. Sci.* 59, 197–213.

Reuss, H., Mojet, M. H., Chyb, S., and Hardie, R. C. (1997). In vivo analysis of the *Drosophila* light-sensitive channels, TRP and TRPL. *Neuron* 19, 1249–1259.

Satoh, A. K., Li, B. X., Xia, H., and Ready, D. F. (2008). Calcium-activated myosin V closes the *Drosophila* pupil. *Curr. Biol.* 18, 951–955.

Schillace, R. V., and Scott, J. D. (1999). Organization of kinases, phosphatases, and receptor signaling complexes. *J. Clin. Invest.* 103, 761–765.

Scott, K., Becker, A., Sun, Y., Hardy, R., and Zuker, C. (1995). $G_q\alpha$ protein function in vivo: genetic dissection of its role in photoreceptor cell physiology. *Neuron* 15, 919–927.

Scott, K., Sun, Y., Beckingham, K., and Zuker, C. S. (1997). Calmodulin regulation of *Drosophila* light-activated channels and receptor function mediates termination of the light response in vivo. *Cell* 91, 375–383.

Selinger, Z., Doza, Y. N., and Minke, B. (1993). Mechanisms and genetics of photoreceptors desensitization in *Drosophila* flies. *Biochim. Biophys. Acta* 1179, 283–299.

Sheng, M., and Lee, S. H. (2001). AMPA receptor trafficking and the control of synaptic transmission. *Cell* 105, 825–828.

Shieh, B. H., and Niemeyer, B. (1995). A novel protein encoded by the *InaD* gene regulates recovery of visual transduction in *Drosophila*. *Neuron* 14, 201–210.

Shieh, B. H., and Zhu, M. Y. (1996). Regulation of the TRP Ca^{2+} channel by INAD in *Drosophila* photoreceptors. *Neuron* 16, 991–998.

Shieh, B. H., Zhu, M. Y., Lee, J. K., Kelly, I. M., and Bahiraei, F. (1997). Association of INAD with NORPA is essential for controlled activation and deactivation of *Drosophila* phototransduction in vivo. *Proc. Natl. Acad. Sci. U. S. A.* 94, 12682–12687.

Steele, F. R., Washburn, T., Rieger, R., and O'Tousa, J. E. (1992). *Drosophila* retinal degeneration C (*rdgC*) encodes a novel serine/threonine protein phosphatase. *Cell* 69, 669–676.

Trojan, P., Krauss, N., Choe, H. W., Giessl, A., Pulvermuller, A., and Wolfrum, U. (2008). Centrins in retinal photoreceptor cells: regulators in the connecting cilium. *Prog. Retin. Eye Res.* 27, 237–259.

Tsunoda, S., Sierralta, J., Sun, Y., Bodner, R., Suzuki, E., Becker, A., Socolich, M., and Zuker, C. S. (1997). A multivalent PDZ-domain protein assembles signalling complexes in a G-protein-coupled cascade. *Nature* 388, 243–249.

Tsunoda, S., Sun, Y., Suzuki, E., and Zuker, C. (2001). Independent anchoring and assembly mechanisms of INAD signaling complexes in *Drosophila* photoreceptors. *J. Neurosci.* 21, 150–158.

van Huizen, R., Miller, K., Chen, D. M., Li, Y., Lai, Z.-C., Raab, R. W., Stark, W. S., Shortridge, R. D., and Li, M. (1998). Two distantly positioned PDZ domains mediate multivalent INAD-phospholipase C interactions essential for G protein-coupled signaling. *EMBO J.* 17, 2285–2297.

Vihtelic, T. S., Hyde, D. R., and O'Tousa, J. E. (1991). Isolation and characterization of the *Drosophila* retinal degeneration B (*rdgB*) gene. *Genetics* 127, 761–768.

Violin, J. D., and Lefkowitz, R. J. (2007). Beta-arrestin-biased ligands at seven-transmembrane receptors. *Trends Pharmacol. Sci.* 28, 416–422.

Vogt, K., and Kirschfeld, K. (1984). Chemical identity of the chromophores of fly visual pigment. *Naturwissenschaften* 77, 211–213.

Wang, Y., and Nathans, J. (2007). Tissue/planar cell polarity in vertebrates: new insights and new questions. *Development* 134, 647–658.

Wernet, M. F., Mazzoni, E. O., Celik, A., Duncan, D. M., Duncan, I., and Desplan, C. (2006). Stochastic spineless expression creates the retinal mosaic for colour vision. *Nature* 440, 174–180.

Wes, P. D., Chevesich, J., Jeromin, A., Rosenberg, C., Stetten, G., and Montell, C. (1995). TRPC1, a human homolog of a *Drosophila* store-operated channel. *Proc. Natl. Acad. Sci. U. S. A.* 92, 9652–9656.

Wu, L., Niemeyer, B., Colley, N., Socolich, M., and Zuker, C. S. (1995). Regulation of PLC-mediated signalling in vivo by CDP-diacylglycerol synthase. *Nature* 373, 216–222.

Xu, X. Z., Chien, F., Butler, A., Salkoff, L., and Montell, C. (2000). TRPγ, a *Drosophila* TRP-related subunit, forms a regulated cation channel with TRPL. *Neuron* 26, 647–657.

Xu, X. Z. S., Li, H. S., Guggino, W. B., and Montell, C. (1997). Coassembly of TRP and TRPL produces a distinct store-operated conductance. *Cell* 89, 1155–1164.

Yamada, T., Takeuchi, Y., Komori, N., Kobayashi, H., Sakai, Y., Hotta, Y., and Matsumoto, H. (1990). A 49-kilodalton phosphoprotein in the *Drosophila* photoreceptor is an arrestin homolog. *Science* 248, 483–486.

Yeandle, S., and Spiegler, J. B. (1973). Light-evoked and spontaneous discrete waves in the ventral nerve photoreceptor of *Limulus*. *J. Gen. Physiol.* 61, 552–571.

Yuan, J. P., Zeng, W., Huang, G. N., Worley, P. F., and Muallem, S. (2007). STIM1 heteromultimerizes TRPC channels to determine their function as store-operated channels. *Nat. Cell Biol.* 9, 636–645.

Zelhof, A. C., Hardy, R. W., Becker, A., and Zuker, C. S. (2006). Transforming the architecture of compound eyes. *Nature* 443, 696–699.

Zhang, X., Huang, J., and McNaughton, P. A. (2005). NGF rapidly increases membrane expression of TRPV1 heat-gated ion channels. *EMBO J.* 24, 4211–4223.

Zhu, X., Chu, P. B., Peyton, M., and Birnbaumer, L. (1995). Molecular cloning of a widely expressed human homologue for the *Drosophila trp* gene.. *FEBS Lett.* 373, 193–198.

Zuidervaart, H., Stavenga, D. G., Stark, W. S., and Bernard, G. D. (1979). Pupillary responses revealing receptors characteristics in wild-type and mutant *Drosophila*. *Abstr. Soc. Neurosci.* 5, 814.

Conflict of Interest Statement: The authors declare that the research was conducted in the absence of any commercial or financial relationships that could be construed as a potential conflict of interest.

Received: 18 March 2009; paper pending published: 07 April 2009; accepted: 11 May 2009; published online: 11 June 2009.
*Citation: Katz B and Minke B (2009) Drosophila photoreceptors and signaling mechanisms. Front. Cell. Neurosci. (2009) **3**:2. doi: 10.3389/neuro.03.002.2009*
Copyright © 2009 Katz and Minke. This is an open-access article subject to an exclusive license agreement between the authors and the Frontiers Research Foundation, which permits unrestricted use, distribution, and reproduction in any medium, provided the original authors and source are credited.

frontiers in
CELLULAR NEUROSCIENCE

ORIGINAL RESEARCH ARTICLE
published: 15 June 2009
doi: 10.3389/neuro.03.003.2009

Daily rhythm of melanopsin-expressing cells in the mouse retina

Irene González-Menéndez, Felipe Contreras, Rafael Cernuda-Cernuda and José M. García-Fernández*

Department of Morphology and Cell Biology, Oviedo University, Oviedo, Spain

Edited by:
Dieter Wicher, Max Planck Institute for Chemical Ecology, Germany

Reviewed by:
Jane L. Witten, University of Wisconsin Milwaukee, USA
Monika Stengl, Philipps Universität Marburg, Germany

****Correspondence:***
José M. García-Fernández, Department of Morphology and Cell Biology, University of Oviedo, C/Julián Clavería s/n, Oviedo 33006, Asturias, Spain.
e-mail: jmgf@uniovi.es

In addition to some other functions, melanopsin-expressing retinal ganglion cells (RGCs) constitute the principal mediators of the circadian photoentrainment, a process by which the suprachiasmatic nucleus (the central clock of mammals), adjusts daily to the external day/night cycle. In the present study these RGCs were immunohistochemically labelled using a specific polyclonal antiserum raised against mouse melanopsin. A daily oscillation in the number of immunostained cells was detected in mice kept under a light / dark (LD) cycle. One hour before the lights were on (i.e., the end of the night period) the highest number of immunopositive cells was detected while the lowest was seen 4 h later (i.e., within the first hours of the light period). This finding suggests that some of the melanopsin-expressing RGCs "turn on" and "off" during the day/night cycle. We have also detected that these daily variations already occur in the early postnatal development, when the rod/cone photoreceptor system is not yet functional. Two main melanopsin-expressing cell subpopulations could be found within the retina: M1 cells showed robust dendritic arborization within the OFF sublamina of the inner plexiform layer (IPL), whilst M2 cells had fine dendritic processes within the ON sublamina of the IPL. These two cell subpopulations also showed different daily oscillations throughout the LD cycle. In order to find out whether or not the melanopsin rhythm was endogenous, other mice were maintained in constant darkness for 6 days. Under these conditions, no defined rhythm was detected, which suggests that the daily oscillation detected either is light-dependent or is gradually lost under constant conditions. This is the first study to analyze immunohistochemically the daily oscillation of the number of melanopsin-expressing cells in the mouse retina.

Keywords: retina, melanopsin, circadian rhythm, postnatal development, mouse

INTRODUCTION

Circadian rhythms are oscillations with a period of about 24 h. Animals express these rhythms in their behavior and their physiology. The main role of the so-called circadian system is to set the time at which physiological and behavioral events occur with respect to the 24-h period, i.e. the day/night cycle. By anticipating physiological processes, organisms get ready for predictable changes in the environment. The period of the inner clock is not exactly 24 h and, hence, it must be entrained everyday. Twilight transition provides the most reliable indicator of environmental time and mediates this synchronization, a process that has been called photoentrainment. The principal pacemaker in mammals is the hypothalamic suprachiasmatic nucleus (SCN) (Foster and Hankins, 2002).

The perception of the external day/night cycle, which is perhaps the most important function of the so-called non-image-forming visual system, is mediated by rod/cone photoreceptors and by intrinsically photosensitive retinal ganglion cells (ipRGCs) whose phototransduction is based on the photopigment melanopsin (Berson et al., 2002; Hattar et al., 2003). These ipRGCs transmit light information to the SCN through a monosynaptic pathway called the retinohypothalamic tract (RHT), allowing the photoentrainment to the external light-dark cycle (Gooley et al., 2001; Hankins et al., 2008; Hannibal et al., 2002; Hattar et al., 2002; Panda et al., 2002). Some other major projections of these cells include the olivary pretectal nucleus, which controls pupil constriction and the intergeniculate leaflet, in which photic and non-photic circadian cues converge (Fu et al., 2005). Minor innervation from the ipRGCs is also received in brain areas involved in the promotion of sleep (the ventrolateral preoptic nucleus), gaze control (superior colliculus), image-forming vision (dorsal lateral geniculate nucleus), etc. (Fu et al., 2005). Apart from perceiving light, melanopsin-expressing RGCs are also the principal conduits for rod-cone input to the mentioned responses (Güler et al., 2008), and in fact, their targeted destruction altered the effects of light on circadian rhythms (Göz et al., 2008).

The retina itself behaves as a clock, showing circadian oscillations. Which cells contribute to the clock mechanism that drives the inner retinal rhythm, as well as to what extent the ipRGCs are involved in such mechanism, is still unknown. Hannibal et al. (2005) and Sakamoto et al. (2004, 2005) demonstrated that melanopsin mRNA shows a daily oscillating pattern, with a peak in the transitional phase from day to night, whilst the minimum was observed at the end of the night. This rhythm appears to be influenced by rod/cone inputs, since melanopsin expression in rats with retinal degeneration, lacking rod and cone photoreceptors, is lower than in controls and also arrhythmic (Sakamoto et al., 2004). Moreover, the elimination of dopamine in the rat retina provoked an alteration in the expression of melanopsin mRNA (Sakamoto et al., 2005),

which means that dopamine is also involved in this daily oscillation. Under constant darkness pigmented rats (Sakamoto et al., 2005) showed an attenuated oscillation of melanopsin mRNA expression; however, Hannibal et al. (2005) and Mathes et al. (2007) showed that this daily rhythm was abolished by exposure to constant conditions.

The melanopsin daily rhythm could be observed in the early postnatal development, when rods and cones are not functional yet (Hannibal et al., 2007), which means that, at least at this early stage, is independent of the rod/cone input. Also, the ipRGCs were seen to be responsive to light stimulation since postnatal day (P) 0 (Sekaran et al., 2005; Tu et al., 2005). Moreover, it has been reported that the SCN begins to respond to stimulation of the retina at P0–1 (Lupi et al., 2006), or at P4 (Muñoz-Llamosas et al., 2000) depending on intensity of the light administered, suggesting that functional connections between the retina and the SCN are already established on the day of birth.

Two main different morphological types of melanopsin-expressing RGCs have been previously described: M1 and M2 cells, which show different dendritic arborisation in different sublayers of the inner plexiform layer (IPL). Baver et al. (2008) demonstrated that these cell subpopulations have different brain projections, and in a recent study by Schmidt and Kofuji (2009) electrophysiological differences between them were also reported.

In the present work we have analyzed for the first time the daily variation of the number of the mouse melanopsin-expressing ipRGCs and of their main subpopulations, by means of immunohistochemistry, as well as the effects of darkness on such variation.

MATERIALS AND METHODS

ANIMALS AND EXPERIMENTAL DESIGN

Male pigmented mice *C3H/He* were used in the present study. Although commercially available *C3H/He* mice are retinally degenerate (*rd/rd*), we only studied *C3H/He* mice with normal retinas, i.e. wild-type at the *rd* locus (+/+), which were kindly donated by Dr. R. G. Foster (Oxford University, UK).

All the animals were maintained in the central animal care facilities under constant temperature conditions (20 ± 2°C), fed with standard food and tap water *ad libitum* and maintained under a 12-h light/12-h dark cycle (LD). As we will indicate below, a group of animals were also exposed to continuous darkness (DD). Under LD conditions the illumination source was a white light fluorescent lamp, so that the animals were exposed to an intensity of 200 lux at cage level.

Within the 24-h period two timing systems were considered in the present study: zeitgeber time (ZT), when the rhythms of the animals are synchronised with the external cycle (LD conditions); and circadian time (CT), when the animals show their endogenous rhythms (DD conditions).

In order to study the possible oscillation of melanopsin-expressing cells under the LD cycle or the effects of DD, several groups of mice were analyzed.

LD mice

Mice aged 1–3 months kept under 12-h light/ 12-h dark were used. Animals were killed at ZT3, ZT8, ZT13, ZT18, ZT23 (ZT0 = lights on, ZT12 = lights off, $n = 4$ animals at each time point). In order to analyze the postnatal development of this daily rhythm pups of P1 and P5 were used. Pups were kept with their mothers under LD conditions until P1 and P5. Two time points were analyzed: ZT3 and ZT23.

DD mice

To study the effects of constant darkness (DD), a group of adult mice were maintained in DD conditions for 6 days and killed at CT3, CT8, CT13, CT18 and CT23 ($n = 4$ animals at each time point). To calculate the CT of these animals we considered that the period length was 23.5 h, as estimated in previous publications (Hatori et al., 2008; Rollag et al., 2003).

TISSUE PREPARATION

In order to minimize pain, animals were anaesthetized prior to sacrifice. Experiments were performed in accordance with the European Communities Council Directive of 24 November 1986 (86/609/EEC). Eyes from decapitated animals were removed and fixed in a 4% paraformaldehyde solution in 0.1 M phosphate buffer (PB), pH 7.4, for 24 h, and then washed in PB for 24 h at 4°C. Then, the cornea and lens were removed and the eyecup was dehydrated through a graded series of ethanol and embedded in paraffin. Only one eyecup per animal was used for the present study. 10 µm–thick sections covering the whole eyecup were obtained from the paraffin blocks with a microtome and then mounted onto slides in six parallel series, of which only one was used. Paraffin sections were collected on gelatine-coated slides, deparaffined in xylene, hydrated in ethanol and placed in phosphate-buffered saline solution (PBS 0.01 M phosphate, 0.15 M NaCl) for 10 min.

For immunohistochemical labelling, endogenous peroxidase activity was blocked by immersion in a solution of 0.3% hydrogen peroxide in PBS at room temperature (RT) for 30 min. Then they were washed twice for 5 min in PBS containing 0.4% Triton-100 (PBS-T) at RT to enhance permeability. Unspecific binding was blocked with normal goat serum (Vector Labs) diluted in PBS for 30 min. at RT. This was followed by incubation with the UF006 anti-mouse melanopsin polyclonal antibody at a dilution 1:5000 at 4°C for 3 days. This antiserum, which was raised in rabbit against the N-terminus peptide of the mouse melanopsin, was generously donated by Dr. Ignacio Provencio (University of Virginia, USA). Immunoreaction was visualized via the avidin–biotin–peroxidase method (Elite ABC kit, Vector Labs), using 0.025% DAB (3-3 diaminobenzidine tetrahydrochloride; Sigma) in 0.003% hydrogen peroxide Tris–HCl (0.05 M, pH 7.5) buffer as chromogen. Finally, the sections were dehydrated in an ethanol series, cleared in eucalyptol, and coverslipped.

CELL COUNT AND CLASSIFICATION

Retinal sections were observed in a bright-field microscope (Nikon Eclipse E400). The somata of melanopsin-immunopositive cells were counted in the whole area of all the retinal sections of the series analyzed (1 out of 6 series per retina were used). Immunopositive cells were classified in M1 or M2 cells attending to the location of their soma and dendritic processes.

STATISTICAL ANALYSIS

The SPSS 15 software was used for all the statistical analyses of the present study. Kolmogorov–Smirnov test was used to confirm

the normality of the data. The homogeneity of the variances was assessed with Levene's test. Student's *t*-tests were performed when the groups to be compared were only two. One-way ANOVA tests were used to analyse the total number of melanopsin-immunopositive cells, as well as the numbers of M1 and M2 cell subpopulations, throughout the LD cycle and throughout the DD cycle. *Post hoc* tests were performed to detect differences between specific time-points. In order to study possible interactions between the variables "cell subpopulation" and "time-point" throughout the LD cycle or the DD cycle, factorial ANOVA tests were performed. The number of melanopsin-expressing cells per retinal sample was presented as mean ± SEM. $p < 0.05$ was considered statistically significant.

RESULTS

Melanopsin immunostaining could be observed in somata, dendrites and proximal segments of axons. Melanopsin-expressing cells were located throughout the retina and their somata were found either in the ganglion cell layer (GCL) or displaced in the inner nuclear layer (INL). Two dendritic plexuses could be distinguished in the inner plexiform layer (IPL) (**Figure 1**): one in the innermost sublamina (ON) and another in the outermost sublamina (OFF).

Two clearly distinguishable cell populations were considered for the present study attending to the different location of their somata and dendritic processes (**Figure 1**):

- **M1 cells**, with robust dendrites arborizing in the outer margin of the IPL (OFF-sublayer). Within this group, most of the cells, which were frequently heavily stained, had their somata located in the GCL. Some other cells had their somata displaced in the amacrine cell sublayer (i.e., the inner margin of the INL). Among the latter, heavily and weakly stained cells could be observed (not shown in the figure).
- **M2 cells** had their somata located in the GCL and their dendritic processes, which were finer and more numerous that those of M1 cells, were placed in the inner margin of the IPL (ON-sublayer). These cells usually showed weak staining.

Some other cell populations (not shown) were only occasionally seen and, hence, were not considered for our analysis: a few immunostained cells had their somata located in the amacrine cell layer and their processes in the inner margin of the IPL (ON sublayer) and some other cells seemed to arborize in both the inner and outer plexuses of the IPL.

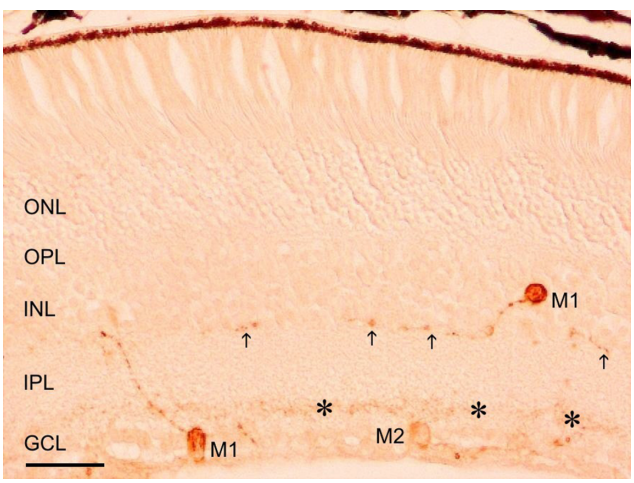

FIGURE 1 | A representative micrograph of melanopsin immunostained retina of adult mice. Two plexuses can be observed in the IPL, one in the innermost layer (OFF sublayer, asterisks) and the other in the outermost layer (ON sublayer, arrows). Three immunostained cells can be seen: two M1 cells (with dendritic arborization in the OFF sublayer) and one M2 cell (with dendritic arborization in the ON sublayer). GCL, ganglion cell layer; IPL, inner plexiform layer; INL, inner nuclear layer; OPL, outer plexiform layer; ONL, outer nuclear layer. Scale bar: 50 µm.

NUMBER OF MELANOPSIN-IMMUNOSTAINED CELLS THROUGH THE LD CYCLE

Under LD conditions an oscillation in the total number of cells that expressed melanopsin was detected in adult mice retinas (**Figure 2**). The highest number of immunopositive cells was found 1 h before lights were on (ZT23), while the lowest was seen 4 h later (ZT3) ($p < 0.001$). Then, a small increase of the number of immunopositive cells, which is maintained during the late day and the early night, was observed (not significative). The increase of melanopsin-expressing cells was found at the late night ($p < 0.05$).

In order to find out whether such differences between ZT23 and ZT3 were also present at the early postnatal stages, the retinas of newborn mice of P1 and P5 were also analyzed. In this case, a significant increase between ZT23 and ZT3 was found at P5 ($p < 0.01$). Such increase was not so marked as in adults. At P1 no statistical difference was detected between these time-points (**Figure 3**).

When M1 and M2 cells were counted separately under LD conditions, factorial ANOVA revealed an interaction between "cell subpopulation" and "time-point" ($p < 0.001$), which indicates that variations of both cell subpopulations were significantly different. One-way ANOVA tests for each subpopulation revealed that both of them had different oscillations throughout the period analyzed (M1 cells, $p < 0.001$; M2 cells, $p < 0.01$). In fact, as can be seen in **Figure 4**, the M1 cell oscillation is more pronounced than that of

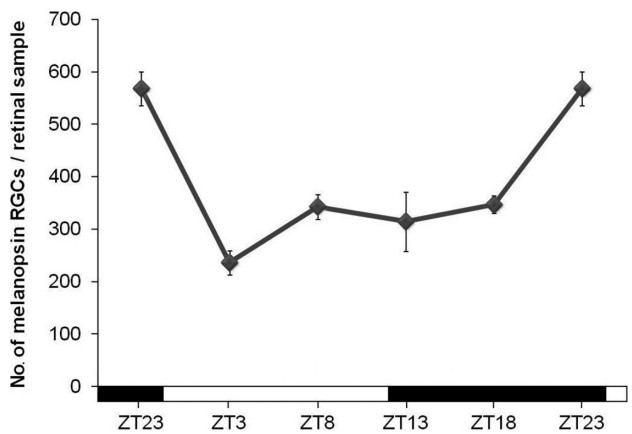

FIGURE 2 | Number of immunopositive cells throughout the 12 h L/12 h D cycle. The ANOVA test revealed a daily significant oscillation ($p < 0.001$). *Post hoc* tests detected a significant decrease at the beginning of the light period ($p < 0.001$) and an increase at the end of the night ($p < 0.05$). ($n = 4$ at each time-point).

M2 cells, in which just a significant difference was found between ZT18 and ZT23 ($p < 0.05$). Also, the ratio between these two cell types changed at some time-points: at ZT3 M2 cells were more abundant than M1 ($p < 0.001$), and at ZT18, vice versa ($p < 0.01$), as revealed by Student's *t*-tests performed to compare both cell subpopulations in parallel at the same time points. The maxima were observed at ZT23 and, after the onset of the light period (ZT3), the decrease of M1 cells was stronger than that of M2 cells (**Figure 4**).

We also analyzed whether M1 and M2 cells presented a similar oscillation between ZT23 and ZT3 at P5. Student's *t*-tests revealed that while M2 cells showed no fluctuation between these time-points at this early postnatal age, M1 cells did show a fluctuation ($p < 0.001$), which was parallel to that found in adults (**Figure 5**).

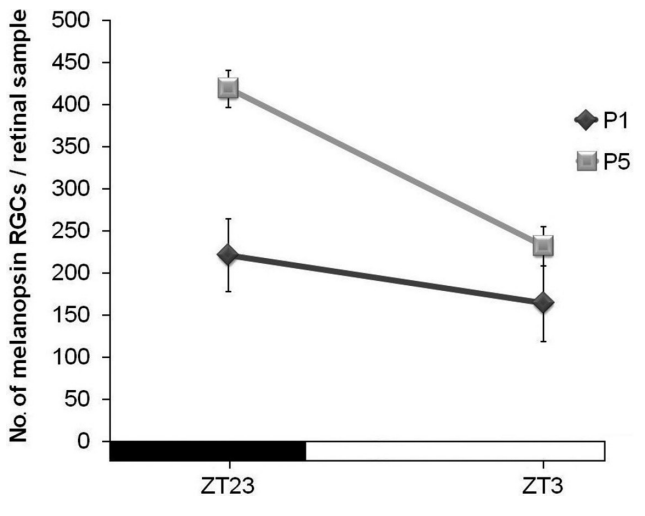

FIGURE 3 | Number of immunostained cells at ZT23 and ZT3 in the early postnatal development (mice were maintained under an LD cycle). Significant differences could be detected at P5 ($p < 0.01$), but not at P1. ($n = 4$ per group at both time-points).

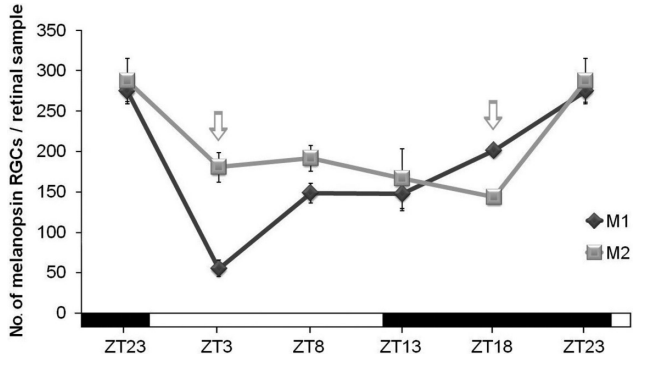

FIGURE 4 | M1 and M2 cell subpopulations counts under LD conditions. One-way ANOVA tests revealed significant oscillation during the LD cycle for M1 cells ($p < 0.001$) and for M2 cells ($p < 0.01$). M1 cells showed a sharp decrease ($p < 0.001$) at the onset of the light period and then an increase between ZT3 and ZT8 ($p < 0.01$). For M2 cells, a significant difference was only detected between ZT18 and ZT23 ($p < 0.05$). Arrows indicate the two time-points in which the numbers of both cell subpopulations were significantly different ($p < 0.001$ at ZT3 and $p < 0.01$ at ZT18). ($n = 4$ per group at all the time-points analyzed).

NUMBER OF MELANOPSIN-IMMUNOSTAINED CELLS IN DD CONDITIONS

With the aim to study whether or not the melanopsin oscillation was endogenous, animals were maintained in DD for 6 days. Under DD, differences between the highest and the lowest numbers disappeared ($p > 0.05$) and no rhythm could be detected (**Figure 6**).

When analyzed separately under these DD conditions, the ratio between both cell subtypes changed with regard to those in LD conditions: M1 cells maintained a higher number than M2 cells at all the time-points studied (**Figure 7**). Factorial ANOVA test

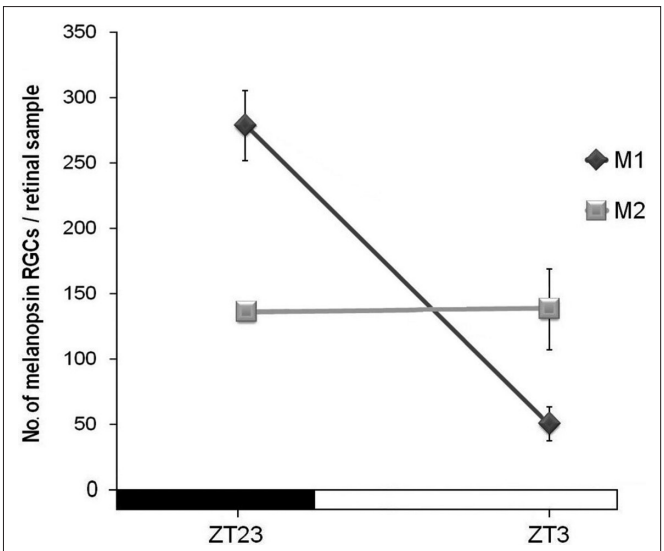

FIGURE 5 | Number of M1 and M2 melanopsin cells of P5 mice at ZT23 and ZT3. Only M1 cells showed significant difference between these time-points ($p < 0.001$). ($n = 4$ per group at both time-points).

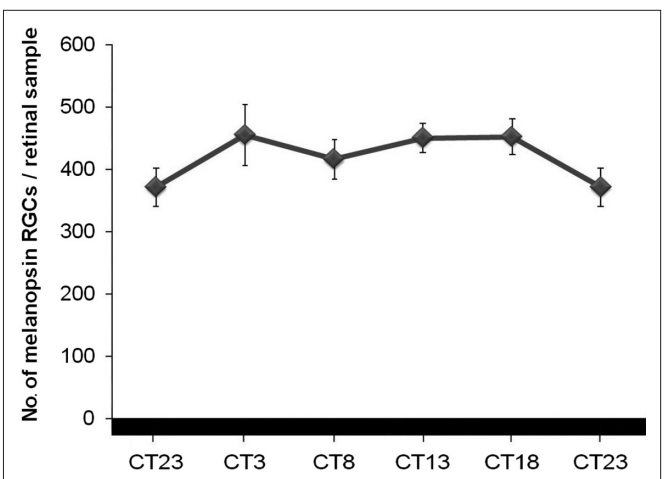

FIGURE 6 | No rhythm was detected in the number of melanopsin cells in DD conditions (ANOVA test: $p >$ 0.05). ($n = 4$ at each time-point).

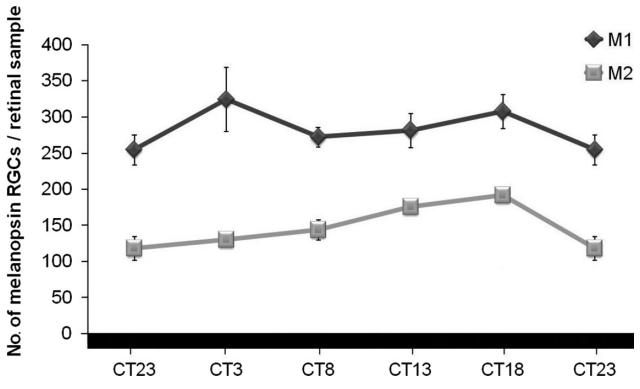

FIGURE 7 | Numbers of M1 and M2 cells under DD conditions. While M1 cells maintained rather constant values, significant oscillation was observed for M2 cells (one-way ANOVA test: $p < 0.01$). A decrease in the number of M2 cells at the end of the subjective night ($p < 0.05$) was detected by a *post hoc* test. ($n = 4$ per group at each time-point).

did not reveal interaction between "cell subpopulation" and "time-point", which means that both cell populations behave similarly throughout the period analyzed. One-way ANOVA tests and *post hoc* tests for each cell subpopulation revealed that M1 cells maintained rather constant values throughout the period, but curiously M2 cells did show a daily oscillation ($p < 0.01$), with a small but significant diminution at the end of the subjective night between CT18 and CT23 ($p < 0.05$).

DISCUSSION

In addition to environmental cyclic fluctuations, rhythms are present in organisms, organs and cells. Some of these oscillations even persist in absence of external cues and constitute a way by which the organisms are prepared to predictable variations of the environment. These autonomous oscillators are considered biological clocks. Other organs and cells oscillate because they are governed by primary autonomous oscillators or simply as a response to environmental fluctuations. The retinal circadian clock was the first extra-SCN oscillator to be discovered in mammals (Tosini and Menaker, 1996). The endogenous oscillators of the retina are supposed to constitute an organized network to control many of the physiological, cellular and molecular rhythms that are present within this organ (Tosini et al., 2008). The nature of the cells that constitute such network has not been yet completely established. As an example, cone/rod photoreceptors, which release melatonin that peaks at night, and a subpopulation of amacrine/interplexiform cells that produce dopamine peaking at day, are known to form an intercellular feedback loop that regulate circadian retinal physiology (Green and Besharse, 2004). The C3H/He mice used in the present study, unlike some other mouse strains, have robust retinal melatonin rhythms that persist even after several days under continuous darkness (Tosini and Menaker, 1998), indicating that the retinal clock is fully operative and, therefore, this murine strain constitutes an appropriate model to study oscillations within the retina.

Since they were discovered a decade ago, melanopsin-expressing cells have continuously been subject of thorough study. Together with the cone/rod photoreceptors, these photosensitive neurons contribute to circadian photoentrainment, but also have other remarkable roles (Fu et al., 2005; Göz et al., 2008; Hattar et al., 2003), including the modulation of some classical image-forming visual pathways. Barnard et al. (2006) demonstrated that the differences between the electroretinographic responses of the cone cell pathway at midday and at midnight are related to the presence of melanopsin-expressing RGCs. This suggests that these cells are somehow involved in the fluctuations occurring within the retina. Daily oscillations of both the melanopsin mRNA and the melanopsin protein have been previously reported in the rat (Hannibal et al., 2005; Sakamoto et al., 2004). In these studies, the total content of mRNA and the total amount of protein, by means of RT-PCR and Western-blot analyses, respectively, were measured. However, to date no previous studies had been done with regard to the possible variation in number of melanopsin-expressing cells through the 24-h cycle. The results presented in this paper clearly demonstrate that this number does oscillate throughout the day/night cycle, with a maximum at the end of the dark period (ZT23) and a minimum within the first hours of the light period (ZT3). A remarkable conclusion can be immediately extracted from this finding: at least some ipRGCs turn on and off during the LD cycle. When we analyzed these two time points (ZT3 and ZT23) at P1 and P5, i.e. the early postnatal stage when the rod/cone photoreceptors are not yet functional, we only could detect significant difference between them at P5, which suggests that the melanopsin system gradually develops within the early postnatal period. In the previous studies mentioned (Hannibal et al., 2005; Sakamoto et al., 2004) the maximum levels of melanopsin mRNA and protein in the rat occur at the transition from day to night, which is difficult to fit with our results in the mouse, in which the peak occurs in the transition from night to day. It must be taken into account that two mammalian species may have a different physiology and also that the total amount of protein detected by Western-blot analyses need not reflect the number of immunostained cells.

It is important to remark that the present work analyses for the first time the daily oscillation of M1 and M2 cells, which are the main morphologically and physiologically different subpopulations recognised among the melanopsin-expressing RGCs (Baver et al., 2008; Schmidt and Kofuji, 2009). In adult mice the numbers of both cell types reached the maximum and the minimum at similar times of the day; however, these numbers did not run parallel, which means that the ratio of the two cell types varied throughout the day/night cycle. This finding might be related to their likely distinct functional roles, since they have different dendritic stratification and physiology (Schmidt and Kofuji, 2009), as well as different brain projections (Baver et al., 2008); however, further data are required to discuss the meaning of their different oscillation through the LD cycle.

When M1 and M2 cells were analyzed separately at P5, difference between ZT3 and ZT23 was only significant for M1 cells, which indicates that this cell subpopulation develops earlier than the M2 cells, a fact that might also be related to their distinct central connectivity and functional roles. Of the two cell subpopulations described above, only one has been reported to date in the rat and this makes any comparison between the two species more difficult. Such cell population in the rat retina likely correspond to the mouse

M1 cells, due to their common dendritic arborization in the OFF sublamina, and also to the fact that antibodies raised against the C-terminus of the rat melanopsin specifically labeled the M1 cells in the mouse (Baver et al., 2008). Hannibal et al. (2007) detected a daily rhythm in neonatal rats (P5) that could correspond to the oscillation described in this paper for the mouse M1 cells at the same postnatal day. Our finding, like theirs, supports the idea that at least the oscillation of M1 cells during the 24-h cycle is independent of the rod/cone input, since it was detected even before these photoreceptors were developed. On the other hand, Sakamoto et al. (2004) observed that cone/rod photoreceptor loss in RCS-rdy rats abolishes melanopsin production by the ipRGCs. Curiously, in a mouse model Semo et al. (2003) did not observe any significant diminution of melanopsin production after retinal degeneration, which again reveals the variability between species. M2 cell oscillation, which was only detected in adults in our experiments, might depend on the development of other retinal neurons, like rod/cone photoreceptors or the dopaminergic amacrine cells, which are not functional at the early postnatal stage.

After 6 days under constant darkness, we did not detect any rhythm in the total number of melanopsin-immunostained cells, which suggests that the oscillation is not endogenous, but subjected to the day/night cycle. When M1 and M2 cells were analyzed separately, their ratio was roughly maintained at all the time-points analyzed, with the exception that M2 cells showed a small but significant decrease at the end of the subjective night in such experimental conditions. This finding is difficult to explain, but suggests that the physiology of the two subpopulations is different and still poorly understood. Whether the melanopsin oscillation through the 24-h period is endogenous or not is a controversial matter. Sakamoto et al. (2005) detected an attenuated circadian oscillation in melanopsin mRNA in rats after 2 days in constant darkness. In contrast, Mathes et al. (2007) reported in a different rat strain that the daily rhythm of melanopsin mRNA was abolished after both constant light or constant darkness exposure, suggesting that the regulation of the melanopsin gene does not rely on a circadian oscillator but is directly illumination-dependent. Therefore, no comparisons can be established between our results in mice and any of these studies. Moreover, only M2 cells showed a small fluctuation in constant conditions. Therefore, no comparisons can be established between our results in mice and any of these studies. Moreover, only M2 cells showed a small fluctuation in constant conditions. If the melanopsin-expressing RGCs had an endogenous rhythm, they should work in a synchronized way. If this was the case, exposure to continuous darkness might induce disruption of the coupling among them and, thus, a loss of their circadian oscillation. Additional analyses on each cell subpopulation, administering shorter periods of exposure to constant conditions, are needed to clarify this issue.

Our study contributes to understanding the physiology of melanopsin-expressing cells and their two subpopulations, which respond differently to changes in environmental conditions. Some of these retinal neurons seem to turn on and off during the LD cycle. Moreover, the effects that these cells exert on different brain areas might be additive, i.e., dependent on the number of cells being active at a certain time. Apart from the physiological importance that this finding may have on its own, this could also explain some quantitative differences reported in previous studies by other authors regarding the melanopsin content of the retina, and why some retinal ganglion cells that project to the SCN do not show melanopsin immunostaining (Sollars et al., 2003). These cells that do not apparently express the melanopsin photopigment might correspond to retinal samples taken at hours in which such cells were switched off, but still might transmit inputs from the cone/rod pathway to the brain. Differences found in previous studies regarding the total number of melanopsin-expressing cells in the retina, or the numbers of M1 and M2 cell subpopulations, might also be derived from different times of the day for sample collection. Further research is needed to answer questions related to the networks established among neurons within the retina and to what extent the melanopsin-expressing neurons contribute to the circadian physiology of this organ.

ACKNOWLEDGEMENTS

The UF006 antiserum was generously donated by Dr. Ignacio Provencio, University of Virginia, USA. The C3H/He mice (wild-type at the *rd* locus) were kindly donated by Dr. Russell G. Foster (Oxford University, UK). This study was supported by Grant BFU2006-15576 (from the Spanish Ministry of Science and Innovation) to J.M. García-Fernández, I. González-Menéndez was supported by fellowship BP07-088 (from the Spanish FICYT).

REFERENCES

Barnard, A. R., Hattar, S., Hankins, M. W., and Lucas, R. J. (2006). Melanopsin regulates visual processing in the mouse retina. *Curr. Biol.* 16, 389–395.

Baver, S. B., Pickard, G. E., Sollars, P. J., and Pickard, G. E. (2008). Two types of melanopsin retinal ganglion cell differentially innervate the hypothalamic suprachiasmatic nucleus and the olivary pretectal nucleus. *Eur. J. Neurosci.* 27, 1763–1770.

Berson, D. M., Dunn, F. A., and Takao, M. (2002). Phototransduction by retinal ganglion cells that set the circadian clock. *Science* 295, 1070–1073.

Foster, R. G., and Hankins, M. W. (2002). Non-rod, non-cone photoreception in the vertebrates. *Prog. Retin. Eye Res.* 21, 507–527.

Fu, Y., Liao, H. W., Do, M. T., and Yau, K. W. (2005). Non-image-forming ocular photoreception in vertebrates. *Curr. Opin. Neurobiol.* 15, 415–422.

Gooley, J. J., Lu, J., Chou, T. C., Scammell, T. E., and Saper, C. B. (2001). Melanopsin in cells of origin of the retinohypothalamic tract. *Nat. Neurosci.* 12, 1165.

Göz, D., Studholme, K., Lappi, D. A., Rollag, M. D., Provencio, I., and Morin, L. P. (2008). Targeted destruction of photosensitive retinal ganglion cells with a saporin conjugate alters the effects of light on mouse circadian rhythms. *PLoS ONE* 3, e3153.

Green, C. B., and Besharse, J. C. (2004). Retinal circadian clocks and control of retinal physiology. *J. Biol. Rhythms* 19, 91–102.

Güler, A. D., Ecker, J. L., Lall, G. S., Haq, S., Altimus, C. M., Liao, H. W., Barnard, A. R., Cahill, H., Badea, T. C., Zhao, H., Hankins, M. W., Berson, D. M., Lucas, R. J., Yau, K. W., and Hattar, S. (2008). Melanopsin cells are the principal conduits for rod-cone input to non-image-forming vision. *Nature* 453, 102–105.

Hankins, M. W., Peirson, S. N., and Foster, R. G. (2008). Melanopsin: an exciting photopigment. *Trends Neurosci.* 31, 27–36.

Hannibal, J., Georg, B., and Fahrenkrug, J. (2007). Melanopsin changes in neonatal albino rat independent of rods and cones. *Neuroreport* 18, 81–85.

Hannibal, J., Georg, B., Hindersson, P., and Fahrenkrug, J. (2005). Light and darkness regulate melanopsin in the retinal ganglion cells of the albino Wistar rat. *J. Mol. Neurosci.* 27, 147–155.

Hannibal, J., Hindersson, P., Knudsen, S. M., Georg, B., and Fahrenkrug, J. (2002). The photopigment melanopsin is exclusively

present in pituitary adenylate cyclase-activating polypeptide-containing retinal ganglion cells of the retinohypothalamic tract. *J. Neurosci.* 22, 191–197.

Hatori, M., Le, H., Vollmers, C., Keding, S. R., Tanaka, N., Schmedt, C., Jegla, T., and Panda, S. (2008). Inducible ablation of melanopsin-expressing retinal ganglion cells reveals their central role in non-image forming visual responses. *PLoS ONE* 3, e2451.

Hattar, S., Liao, H. W., Takao, M., Berson, D. M., and Yau, K. W. (2002). Melanopsin-containing retinal ganglion cells. *Science* 295, 1065–1075.

Hattar, S., Lucas, R. J., Mrosovsky, N., Thompson, S., Douglas, R. H., Hankins, M. W., Lem, J., Biel, M., Hofmann, F., Foster, R. G., and Yau, K. W. (2003). Melanopsin and rod-cone photoreceptive systems account for all major accessory visual functions in mice. *Nature* 424, 76–81.

Lupi, D., Sekaran, S., Jones, S. L., Hankins, M. W., and Foster, R. G. (2006). Light-evoked FOS induction within the suprachiasmatic nuclei (SCN) of melanopsin knockout (Opn4–/–) mice: a developmental study. *Chronobiol. Int.* 23, 167–179.

Mathes, A., Engel, L., Holthues, H., Wolloscheck, T., and Spessert, R. (2007). Daily profile in melanopsin transcripts depends on seasonal lighting conditions in the rat retina. *J. Neuroendocrinol.* 19, 952–957.

Muñoz-Llamosas, M., Huerta, J. J., Cernuda-Cernuda, R., and García-Fernández, J. M. (2000). Ontogeny of a photic response in the retina and suprachiasmatic nucleus in the mouse. *Brain Res. Dev. Brain Res.* 15, 1–6.

Panda, S., Sato, T. K., Castrucci, A. M., Rollag, M. D., DeGrip, W. J., Hogenesch, J. B., Provencio, I., and Kay, S. A. (2002). Melanopsin (Opn4) requirement for normal light-induced circadian phase shifting. *Science* 298, 2213–2216.

Rollag, M. D., Berson, D. M., and Provencio, I. (2003). Melanopsin, ganglion-cell photoreceptors, and mammalian photoentrainment. *J. Biol. Rhythms* 18, 227–234.

Sakamoto, K., Liu, C., Kasamatsu, M., Pozdeyev, N. V., Iuvone, P. M., and Tosini, G. (2005). Dopamine regulates melanopsin mRNA expression in intrinsically photosensitive retinal ganglion cells. *Eur. J. Neurosci.* 22, 3129–3136.

Sakamoto, K., Liu, C., and Tosini, C. (2004). Classical photoreceptors regulate melanopsin mRNA levels in the rat retina. *J. Neurosci.* 24, 9693–9697.

Schmidt, T. M., and Kofuji, P. (2009). Functional and morphological differences among intrinsically photosensitive retinal ganglion cells. *J. Neurosci.* 29, 476–482.

Sekaran, S., Lupi, D., Jones, S. L., Sheely, C. J., Hattar, S., Yau, K. W., Lucas, R. J., Foster, R. G., and Hankins, M. W. (2005). Melanopsin-dependent photoreception provides earliest light detection in the mammalian retina. *Curr. Biol.* 15, 1099–1107.

Semo, M., Peirson, S., Lupi, D., Lucas, R. J., Jeffery, G., and Foster, R. G. (2003). Melanopsin retinal ganglion cells and the maintenance of circadian and pupillary responses to light in aged rodless/coneless (rd/rd cl) mice. *Eur. J. Neurosci.* 17, 1793–1801.

Sollars, P. J., Smeraski, C. A., Kaufman, J. D., Ogilvie, M. D., Provencio, I., and Pickard, G. E. (2003). Melanopsin and non-melanopsin expressing retinal ganglion cells innervate the hypothalamic suprachiasmatic nucleus. *Vis. Neurosci.* 20, 601–610.

Tosini, G., and Menaker, M. (1996). Circadian rhythms in cultured mammalian retina. *Science* 272, 419–421.

Tosini, G., and Menaker, M. (1998). The clock in the mouse retina: melatonin synthesis and photoreceptor degeneration. *Brain Res.* 789, 221–224.

Tosini, G., Pozdeyev, N., Sakamoto, K., and Iuvone, P. M. (2008). The circadian clock system in the mammalian retina. *Bioessays* 30, 624–633.

Tu, D. C., Zhang, D., Demas, J., Slutsky, E. B., Provencio, I., Holy, T. E., and Van Gelder, R. N. (2005). Physiologic diversity and development of intrinsically photosensitive retinal ganglion cells. *Neuron* 48, 987–999.

Conflict of Interest Statement: The authors declare that the research was conducted in the absence of any commercial or financial relationships that could be construed as a potential conflict of interest.

Received: 14 April 2009; paper pending published: 08 May 2009; accepted: 05 June 2009; published online: 15 June 2009.
*Citation: González-Menéndez I, Contreras F, Cernuda-Cernuda R and García-Fernández JM (2009) Daily rhythm of melanopsin-expressing cells in the mouse retina. Front. Cell. Neurosci. (2009) **3**:3. doi:10.3389/neuro.03.003.2009*
Copyright © 2009 González-Menéndez, Contreras, Cernuda-Cernuda and García-Fernández. This is an open-access article subject to an exclusive license agreement between the authors and the Frontiers Research Foundation, which permits unrestricted use, distribution, and reproduction in any medium, provided the original authors and source are credited.

frontiers in
CELLULAR NEUROSCIENCE

REVIEW ARTICLE
published: 09 December 2009
doi: 10.3389/neuro.03.018.2009

A new photosensory function for simple photoreceptors, the intrinsically photoresponsive neurons of the sea slug *Onchidium*

Tsukasa Gotow*[1] *and Takako Nishi*[2]

[1] *Laboratory for Neuroanatomy, Department of Neurology, Graduate School of Medical and Dental Sciences, Kagoshima University, Kagoshima, Japan*
[2] *Laboratory of Physiology, Institute of Natural Sciences, Senshu University, Kawasaki, Japan*

Edited by:
Dieter Wicher, Max Planck Institute for Chemical Ecology, Germany

Reviewed by:
Christian Derst, Institut für Integrative Neuroanatomie der Charité, Germany
Ulf Bickmeyer, Alfred Wegener Institute, Germany

***Correspondence:**
Tsukasa Gotow, Laboratory for Neuroanatomy, Department of Neurology, Graduate School of Medical and Dental Sciences, Kagoshima University, 8-35-1 Sakuragaoka, Kagoshima 890-8520, Japan.
e-mail: tsukasa@m.kufm.kagoshima-u.ac.jp

Simple photoreceptors, namely intrinsically light-sensitive neurons without microvilli and/or cilia, have long been known to exist in the central ganglia of crayfish, *Aplysia, Onchidium,* and *Helix.* These simple photoreceptors are not only first-order photosensory cells, but also second-order neurons (interneurons), relaying several kinds of sensory synaptic inputs. Another important issue is that the photoresponses of these simple photoreceptors show very slow kinetics and little adaptation. These characteristics suggest that the simple photoreceptors of the *Onchidium* have a function in non-image-forming vision, different from classical eye photoreceptors used for cording dynamic images of vision. The cited literature provides evidence that the depolarizing and hyperpolarizing photoresponses of simple photoreceptors play a role in the long-lasting potentiation of synaptic transmission of excitatory and inhibitory sensory inputs, and as well as in the potentiation and the suppression of the subsequent behavioral outputs. In short, we suggest that simple photoreceptors operate in the general potentiation of synaptic transmission and subsequent motor output; i.e., they perform a new photosensory function.

Keywords: molluscan simple photoreceptors, photoresponsive neurons similar to ipRGC, phototransduction, photosensory synaptic potentiation, potentiated sensory inputs

INTRODUCTION

It has been known since the 1930s that photoresponsive neurons that are intrinsically sensitive to light exist in the central ganglia of some invertebrates besides the photoreceptor cells (photoreceptors) in classical bilateral eyes. For instance, there are photoresponsive neurons in the sixth abdominal ganglion of the crayfish (Kennedy, 1963) and the visceral (abdominal) or pleuro-parietal ganglia of the sea slugs *Aplysia* (Arvanitaki and Chalazonitis, 1961; Brown and Brown, 1973) and *Onchidium verruculatum* (Hisano et al., 1972; Gotow, 1989).

We refer to these neurons as simple photoreceptors, in view of their lack of any specialized structures, such as microvilli and/or cilia, that are characteristic of classical eye photoreceptors (see review, Gotow and Nishi, 2008). In addition, it is known that these simple photoreceptors are not only first-order photosensory cells, but are also second-order neurons (interneurons), relaying several kinds of sensory inputs (Kennedy, 1963; Frazier et al., 1967; Gotow, 1975).

Recently, similar simple photoreceptors, the intrinsically photosensitive retinal ganglion cells (ipRGC), were discovered in mammalian retinas (Berson et al., 2002; Hattar et al., 2002), and their relevance will be discussed later.

A considerable amount of information has been obtained about the phototransduction mechanisms underlying the first-order photosensory responses of invertebrates, especially that of the simple photoreceptors of *Onchidium* (for review, Gotow and Nishi, 2008). However, little has yet been established about how their simple photoreceptor functions as second-order neurons (interneurons) *in vivo.*

This review examines the non-image-forming visual functions of simple photoreceptors acting as second-order neurons. In addition, we survey the profiles of the cell membrane channels that mediate related receptor potentials and the phototransduction mechanisms of the simple photoreceptors studied to date.

CHARACTERISTICS OF SIMPLE PHOTORECEPTORS (PHOTORESPONSIVE NEURONS)

Several simple photoreceptors (photoresponsive neurons) have been identified on the dorsal aspect of the central ganglia of *Onchidium verruculatum*, a species closely related to *Aplysia* (Hisano et al., 1972; Gotow, 1989; Nishi and Gotow, 1998). Of these simple photoreceptors, which were designated Ep-2, Ep-3, Es-1, A-P-1, Ip-1, and Ip-2, A-P-1 and Es-1 respond to light with a depolarizing receptor potential, which is associated with a decrease in membrane K^+ conductance (Gotow, 1989; Nishi and Gotow, 1992); whereas, Ip-1 and Ip-2 are hyperpolarized by light, owing to an increase in membrane K^+ conductance (Nishi and Gotow, 1998). These intrinsic photoresponses persist even when synaptic transmission is blocked either chemically or by ligation of the axo-somatic junction. Ep-2 and Ep-3 are depolarized by light, but their depolarizing mechanism is still unknown. However, we have evidence that Ep-2 and Ep-3 are also depolarized by a similar mechanism to that of A-P-1 and Es-1. Both of these depolarizing and hyperpolarizing photoresponses take 20 to 30 s to reach their peak after a latency of 300 to 500 ms following a brief light stimulus and then decline gradually. This contrasts with the fast and adaptive photoresponses of a few milliseconds to a few seconds in classical eye photoreceptors, e.g. the proximal and distal cells of *Pecten* (McReynolds and Gorman,

1970) and the stalk eyes of *Onchidium* (Katagiri et al., 1985). When eliciting electrophysiological responses, the action spectrum peaked at about 490 nm in A-P-1 (Gotow, 1989) and at about 580 nm in Es-1 (Nishi and Gotow, 1992), while those in Ip-1 and Ip-2 both peaked at about 510 nm, suggesting that each of their photoresponses is mediated by a single photopigment. Unfortunately, this photopigment has not yet been found in the *Onchidium* simple photoreceptors, although the presence of a rhodopsin-like protein was suggested in the *Aplysia* photoresponsive neuron R2 (Robles et al., 1986). On the other hand, the *Onchidium* photoresponsive neurons as well as the above mentioned *Aplysia* neurons are indistinguishable from the other light insensitive neurons in the ganglion by visual inspection. Electron microscopic observation showed that these photoresponsive neurons lack morphologically specialized structures, such as microvilli or cilia, that are characteristic of classical eye photoreceptors (Frazier et al., 1967; Kubozono, 1988). Thus, we consider that these photoresponsive neurons should be termed "simple photoreceptors". In addition, the simple photoreceptors in the *Onchidium* and *Aplysia* ganglia are not only first-order photosensory cells, but are also second-order neurons (interneurons), relaying several kinds of sensory inputs (Frazier et al., 1967; Gotow, 1975; Nishi et al., 2006), similar to those in the crayfish ganglion.

Recently, similar simple photoreceptors without microvilli or cilia, the ipRGC, were discovered in mammalian rat and mouse retinas (Berson et al., 2002; Hattar et al., 2002). Their studies suggested that their visual pigment may be melanopsin, an invertebrate-like photopigment, which was first identified in frog skin by Provencio et al. (1998). The latest studies have provided compelling evidence that melanopsin is the photopigment of the ipRGC (Melyan et al., 2005; Panda et al., 2005; Qiu et al., 2005). According to Berson (2003) and Do et al. (2009), the ipRGC show a delayed, slow, and lasting depolarizing photoresponse (in the order of a few seconds to tens of seconds) following a suitably brief light stimulation, which is different from the fast and adaptive hyperpolarizing response (in the order of a few milliseconds to tens of milliseconds) seen in cones and rods. In addition to being primary photosensory cells, the ipRGC are also second-order interneurons, relaying photic inputs from rods/cones to the brain. These characteristics of a lack of morphologically specialized structures, morphological arrangement as second-order neurons, and slow photoresponse kinetics in the ipRGC parallel those of the invertebrate *Onchidium* simple photoreceptors mentioned above. This reminds us that the mammalian ipRGC seem to be homologous to the invertebrate *Onchidium* simple photoreceptors.

PHOTOTRANSDUCTION MECHANISM

The primary function of simple photoreceptors and eye photoreceptors is to convert light energy into an electrical response, namely the receptor potential that is generated by light-dependent conductance or channels. Little work has been done on the ionic conductance mechanism in the excitatory, depolarizing photoresponses of the simple photoreceptors in crayfish (Kennedy, 1963) and *Aplysia* (Arvanitaki and Chalazonitis, 1961) ganglia.

A single-channel analysis showed that the depolarizing photoresponses of A-P-1 and Es-1 cells are produced by the closing of one class of K^+ -selective channel (Gotow, 1989; Gotow et al., 1994; Gotow and Nishi, 2002). Later, it was reported that the *Helix* simple photoreceptors also respond to light with membrane depolarization, due to a decrease in K^+ conductance (Pasic and Kartelija, 1995). On the other hand, we demonstrated that the hyperpolarizing receptor potential of Ip-2 and Ip-1 cells results from the opening of the same K^+ -selective channel that induces hyperpolarizing receptor potentials in A-P-1 and Es-1 cells (Nishi and Gotow, 1998; Gotow and Nishi, 2002).

It is thought that the hyperpolarizing photoresponses of most vertebrate eye photoreceptors (rods and cones) are produced by the closing of non-selective cation channels or by a decrease in membrane cation conductance (Tomita, 1972; Owen, 1986; Matthews and Watanabe, 1987). Only one known exception has been found, the lizard parietal eye photoreceptors, which responds to light with depolarization resulting from the opening of non-selective cation channels similar to those of the above mentioned vertebrate eye photoreceptors (Solessio and Engbretson, 1993). Except for this parietal photoreceptor, the above mentioned mechanism contrasts with that in the eye photoreceptors studied to date in invertebrates, which are present in most members of the animal kingdom; i.e., a depolarizing or a hyperpolarizing photoresponse is produced by the opening of membrane cation channels or by an increase in membrane cation conductance (Fuortes, 1963; Washizu, 1964; Brown et al., 1970; Pinto and Brown, 1977; Bacigalupo and Lisman, 1983; Nagy and Stieve, 1990; Nasi and Gomez, 1992; Gomez and Nasi, 1994). Thus, the simple photoreceptors of *Onchidium*, A-P-1 and Es-1, are the first invertebrate eye or simple photoreceptor in which it has been demonstrated that their photoresponses result from the "closing of channels" or "decreases in conductance".

The cGMP-gated channels in the vertebrate photoreceptors that close in light are non-selective cation channels permeable to Na^+, K^+, and Ca^{2+} (for review, Finn et al., 1996). However, the cGMP-gated channels in the simple photoreceptors of *Onchidium* that close and open in the light are predominantly K^+ selective under physiological ionic conditions such as of K^+, Na^+, Ca^{2+}, Mg^{2+} and Cl^-; i.e., the contributions of these ions except for K^+ to these channels is negligible (Gotow, 1989; Gotow et al., 1994; Nishi and Gotow, 1998; Gotow and Nishi, 2002). Interestingly, we have found that the K^+ -selective channels of the simple photoreceptors of *Onchidium* can be specifically blocked by the external addition of 0.1–0.2 mM 4-aminopyridine (4-AP) or 0.2–0.4 mM L-cis-diltiazem (L-DIL) (Gotow et al., 1997; Nishi and Gotow, 1998). L-DIL, a stereoisomer of the D-type Ca^{2+} channel blocker, specifically blocks the non-selective cation channels in vertebrate rod and cone cells (Stern et al., 1986; Rispoli and Menini, 1988; Haynes, 1992; McLatchie and Matthews, 1994) and light -dependent K^+ conductance in *Pecten* hyperpolarizing eye (ciliary) cells (Gomez and Nasi, 1997). 4-AP is another well-known blocker of K^+ channels, e.g., the I_A or K_A channels, which are transiently activated in the subthreshold range of membrane potentials (Hagiwara et al., 1961; Hermann and Gorman, 1981; Hille, 1992).

As described above, the simple photoreceptors A-P-1 and Es-1, which are depolarized by light, seem to be homologous to the vertebrate eye photoreceptors in the sense that both of their cGMP-gated channels are closed by light, although the polarity of their receptor potentials is reversed. This homology prompted us to examine whether the phototransduction cGMP cascade model used for vertebrate rod and cone photoreceptors (Fesenko et al.,

1985, for review, Finn et al., 1996; Kaupp and Seifert, 2002) can be applied to that of A-P-1 or Es-1. According to the cGMP cascade model, cGMP acts as a second messenger that opens cGMP-gated non-selective cation channels, allowing the channels to close when light activates PDE (phosphodiesterase) in order to reduce internal cGMP levels through a Gt-type G-protein (transducin), thereby leading to a hyperpolarizing response (**Table 1**). As in the above mentioned vertebrate cGMP cascade, we also concluded that cGMP acts as a second messenger that opens the cGMP-gated K^+-selective channels of the simple photoreceptors A-P-1 and Es-1, allowing the channels to close when light activates PDE (phosphodiesterase) in order to reduce cGMP levels through a Gt-type G-protein (Gt), thereby leading to depolarization (Gotow et al., 1994; Gotow and Nishi, 2002), as shown in **Table 1**.

On the other hand, we found that the hyperpolarizing photoresponses of other types of simple photoreceptor, Ip-2 and Ip-1 cells, are produced by the opening of the same type of channel that is closed in A-P-1 and Es-1 cells (Gotow and Nishi, 2002). Thus, Gotow and Nishi (2007) have proposed a new type of cGMP cascade model in which Ip-2 and Ip-1 cells are hyperpolarized when light activates GC (guanylate cyclase) through a Go-type G-protein (Go), leading to an increase in the level of the second messenger cGMP, thereby producing the opening of the same channels opened in A-P-1 and Es-1 cells (see also **Table 1**). A similar phototransduction model has also been suggested to operate in a different system, the scallop ciliary eye photoreceptor (Kojima et al., 1997; Gomez and Nasi, 1995, 2000). Unfortunately, no molecular identification of the visual pigment or G-protein involved in phototransduction has yet been undertaken in the simple photoreceptors of *Onchidium*.

In the related *Aplysia* simple photoreceptor R2, it has long been known that when illuminated, R2 hyperpolarizes due to an increase in membrane K^+ conductance and that this light-dependent K^+ conductance is activated by a rise in the intracellular levels of Ca^{2+}; i.e., the light-dependent K^+ conductance is equivalent to this Ca^{2+}-activated K^+ conductance (Meech, 1972; Brown and Brown, 1973; Brown et al., 1977). However, no single-channel analysis of the hyperpolarizing photoresponse in R2 has been undertaken.

Furthermore, a considerable amount of information has been obtained about the photochemistry of melanopsin in ipRGC (for review, He et al., 2003; Peirson and Foster, 2006). For example, it has been suggested that melanopsin activates phospholipase C through the Gq G-protein, as in *Drosophila* rhabdomeric photoreceptors (Raghu et al., 2000; for review, Hardie, 2003). However, the cell membrane channels and their channel-gating mechanism that mediate the photoreceptor potential of ipRGC have not yet been identified, so the phototransduction mechanism that couples melanopsin to its photoreceptor potential remains unknown (for review, Berson, 2007).

PHOTOSENSITIVITY OF SIMPLE PHOTORECEPTORS *IN VIVO*

The simple photoreceptors in the central ganglia, which are well covered by the animal's body wall, seem to be unsuitable as a classical photosensory system, but these simple photoreceptors may have adapted to serve as a new photosensory modality; i.e., non-image-forming vision.

The amount of light energy transmitted through the *Onchidium* body wall, which is composed of the mantle and foot, was measured and compared with the energy required for a minimally detectable photoresponse in their simple photoreceptors. The spectral energy of incident sunlight was also measured in the centre of Kagoshima, which corresponds to that at Sakurajima beach, the home of the *Onchidium* tested.

These analyses supported the assertion that the transmittance of daylight through the animal's body wall is high enough to stimulate the simple photoreceptors of the *Onchidium in vivo* (Gotow et al.,

Table 1 | Phototransduction cGMP cascade models of simple photoreceptors.

Simple photoreceptors	Final transducing molecules (cGMP-gated K^+-selective channels)	Receptor potentials
A-P-1/Es-1	(hυ) Rh → Gt → PDE(Hydrolysis); (5′GMP) ← cGMP : Closing of channel	Depolarization
Ip-1/Ip-2	(hυ) Rh → Go → GC(Synthesis); (GTP) → cGMP : Opening of channel	Hyperpolarization
Vertebrate eye photoreceptors	**(cGMP-gated non-selective cation channels)**	
*Rod/Cone	(hυ) Rh → Gt (Transducin) → PDE(Hydrolysis); (5′GMP) ← cGMP : Closing of channel	Hyperpolarization

**The Rod/Cone (Eye photoreceptors) phototransduction cascade is shown for comparison: Derived from the review by Finn et al. (1996), Kaupp and Seifert (2002). A-P-1/Es-1: Depolarizing A-P-1 and Es-1 cells. Ip-1/Ip-2: Hyperpolarizing Ip-1 and Ip-2 cells. Rh: Visual pigments, PDE: Phosphodiesterase, GC: Guanylate cyclase.*

2005). Brown et al. (1977) have also reported that the amount of light energy required to stimulate the simple photoreceptors of the *Aplysia in vivo* can be provided by the transmittance through the animal's body wall.

Non-image-forming visual function:

1. Depolarizing Ep-2, Ep-3, and Es-1 cells
2. Hyperpolarizing Ip-1 and Ip-2 cells

Little has been definitively established about the functional significance of simple photoreceptors. In spite of a concerted effort to elucidate the functions of the 6th abdominal ganglion simple photoreceptors of crayfish, many questions remain (for review, Wilkens, 1988). It has only been postulated that the simple photoreceptors of crayfish operate in the general regulation of synaptic transmission (Kennedy, 1963; Wilkens and Larimer, 1972; Pei et al., 1996). The function of the simple photoreceptors of *Aplysia* (Arvanitaki and Chalazonitis, 1961; Brown and Brown, 1973) is also unknown. However, it has been reported that *Aplysia* demonstrate light-entrained behavior in the absence of bilateral eyes and that simple photoreceptors such as R2 may be involved in such behavior (Block and Lickey, 1973; Block et al., 1974).

Onchidium are intertidal and amphibian mollusks. Thus, they use gill-trees at high tide, but at low tide they begin to use their lung (pulmonary sac) for respiration and crawl over the rocks on the exposed seashore in order to obtain food or to reproduce. Occasionally, *Onchidium* slip and turn over, while rock-crawling. In such cases, these animals pick themselves up through a chain of behavioral responses, such as the mantle-levating reflex (Gotow et al., 1973). This mantle-levating reflex is also reproducibly triggered by tactile stimulation of the animal's dorsal surface, the mantle.

On the other hand, Gotow (1975) and Gotow et al. (1973) have shown that the first-order depolarizing simple photoreceptors Ep-2, Ep-3, and Es-1 are not only second-order neurons relaying tactile sensory inputs from the mantle through the specified peripheral nerves, but are also motoneurons innervating the mantle and foot (mesopodium) so the combined spike activity evoked by tactile synaptic transmission in these three cell types results in a levation movement of the mantle equivalent to the mantle-levating reflex (**Figure 1A**). They have also shown that all excitatory synaptic transmissions and potentials induced by tactile sensory inputs in these cells are potentiated during light illumination, even when the preceding light stimulus is subthreshold. Thus, it has been suggested that the depolarizing photoresponses of Ep-2, Ep-3, and Es-1 cells play a role in the potentiation of the excitatory synaptic transmission and potentials related tactile sensory inputs and the subsequent mantle-levating reflex (Gotow et al., 1973) and so may be involved in a new photosensory modality, non-image-forming vision.

At low tide, the amphibian mollusks *Onchidium* open their pneumostome, the orifice of their pulmonary sac, in order to begin aero-respiration, although they close the pneumostome at high tide. The opening of the pneumostome; i.e., an aero- breathing behavior, can also be reproducibly triggered by removal of the surrounding seawater from the animal's body surface such as the mantle, pneumostome, etc. or by moving the animal from underwater to air.

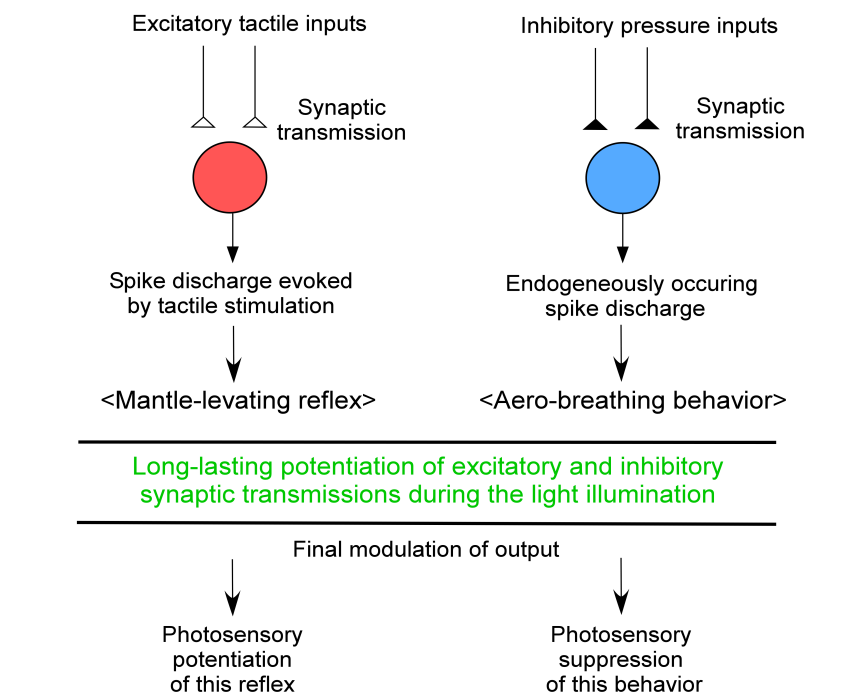

FIGURE 1 | Chart showing a new photosensory function of *Onchidium* simple photoreceptors, (A) depolarizing and (B) hyperpolarizing cells. See text for details.

On the other hand, Nishi et al. (2006) and Gotow and Nishi (2008) have found that the first-order hyperpolarizing simple photoreceptors Ip-1 and Ip-2 are not only second-order neurons that receive inhibitory presynaptic inputs, such as water pressure and/or tactile signals arising from the animal's body surface, but are also interneurons (motor-like neurons) involved in aero-breathing behavior. Thus, they suggested that at low tide these cells are released from inhibitory sensory synaptic inputs such as water pressure and/or touch and begin to produce endogenous spike discharges, thereby leading to opening of the pneumostome (**Figure 1B**).

An attempt to examine the effects of light on the hyperpolarizing Ip-1 and Ip-2 cells showed that inhibitory synaptic transmissions and potentials related to pressure and/or tactile sensory inputs in these cells are potentiated during light illumination, even if the preceding light stimulus is subthreshold. This result suggested that the hyperpolarizing photoresponse of Ip-1 and Ip-2 cells operates in the potentiation of inhibitory synaptic transmission as well as in the suppression of subsequent aero-breathing behavior (Nishi et al., 2006; Gotow and Nishi, 2008) and so may also be involved in the above mentioned new photosensory modality.

The above mentioned potentiation of excitatory and inhibitory synaptic transmission by simple photoreceptors occurred even when their photoresponses were subthreshold, demonstrating true "potentiation" rather than only "summation"; i.e., the sum of synaptic potentials and photoreceptor potentials. Furthermore, we refer to this potentiation as "long-lasting potentiation". As the photoresponses of simple photoreceptors can last for hours and even days, they are effective during most daylight hours.

On the other hand, it has been reported that ipRGC operate in non-visual functions such as the pupillary light reflex and circadian photoentrainment (Panda et al., 2002, 2003; Ruby et al., 2002; Hattar et al., 2003; Lucas et al., 2003). However, nothing is known about their light-sensing functions as interneurons. Most recently, Do et al. (2009) reported that the ipRGC in transgenic mice modulated rod/cone response and synaptic signal transmission from amacrine and bipolar cells, etc. to the brain.

CONCLUSION

Simple photoreceptors similar to those of *Onchidium* have been known to exist in the central ganglion of crayfish, *Aplysia*, and *Helix* since the 1930s. Recently, similar simple photoreceptors, ipRGC, have been discovered in the ganglion cells of mammalian retinas. It was suggested that the simple photoreceptors of *Onchidium* as well as ipRGC function as a new sensory modality, non-image-forming vision, which is different from the image-forming vision of classical eye photoreceptors. As non-image-forming functions of ipRGC, it is known that they contribute to pupillary light reflex and circadian clocks. However, their light-sensing function as interneurons has not been ascertained. An *Onchidium* study showed that simple photoreceptors (Ep-2, Ep-3, A-P-1, Es-1, Ip-1, and Ip-2) play roles in the long-lasting potentiation of synaptic transmission of excitatory and inhibitory sensory inputs as well as in the potentiation and suppression of the subsequent behavioral responses. **Figure 1** shows a chart that explains these non-image-forming functions of simple photoreceptors. Interestingly, it seems that both simple photoreceptors and classical eye photoreceptors use the same phototransduction and channel-gating mechanisms (see **Table1**), in spite of the great difference in the functions of these two types of photoreceptors.

REFERENCES

Arvanitaki, A., and Chalazonitis, N. (1961). Excitatory and inhibitory processes initiated by light and infrared radiations in single identifiable nerve cells (giant ganglion cells of *Aplysia*). In Nervous inhibition, E. Florey ed. (Oxford, Pergamon), pp. 194–231.

Bacigalupo, J., and Lisman, J. E. (1983). Single-channel currents activated by light in Limulus ventral photoreceptors. *Nature* 304, 268–270.

Berson, D. M. (2003). Strange vision: ganglion cells as circadian photoreceptors. *Trends Neurosci.* 26, 314–320.

Berson, D. M. (2007). Phototransduction in ganglion-cell photoreceptors. *Pflugers Arch.* 454, 849–855.

Berson, D. M., Dunn, F. A., and Takao, M. (2002). Phototransduction by retinal ganglion cells that set the circadian clock. *Science* 295, 1070–1073.

Block, G. D., Hudson, D. J., and Lickey, M. E. (1974). Extraocular photoreceptors can entrain the circadian oscillator in the eye of *Aplysia*. *J. comp. Physiol.* 89, 237–249.

Block, G. D., and Lickey, M. E. (1973). Extraocular photoreceptors and oscillators can control the circadian rhythm of behavioral activity in *Aplysia*. *J. comp. Physiol.* 84, 367–374.

Brown, A. M., Brodwick, M. S., and Eaton, D. C. (1977). Intracellular calcium and extra-retinal photoreception in *Aplysia* giant neurons. *J. Neurobiol.* 8, 1–18.

Brown, A. M., and Brown, H. M. (1973). Light response of a giant *Aplysia* neuron. *J. Gen. Physiol.* 62, 239–254.

Brown, H. M., Hagiwara, S., Koike, H., and Meech, R. M. (1970). Membrane properties of a barnacle photoreceptor examined by the voltage clamp technique. *J. Physiol.* 208, 385–413.

Do, M. T., Kang, S. H., Xue, T., Zhong, H., Liao, H. W., Bergles, D. E., and Yau, K. W. (2009). Photon capture and signalling by melanopsin retinal ganglion cells. *Nature* 457, 281–287.

Fesenko, E. E., Kolesnikov, S. S., and Lyubarsky, A. L. (1985). Induction by cyclic GMP of cationic conductance in plasma membrane of retinal rod outer segment. *Nature* 313, 310–313.

Finn, J. T., Grunwald, M. E., and Yau, K. W. (1996). Cyclic nucleotide-gated ion channels: an extended family with diverse functions. *Annu. Rev. Physiol.* 58, 395–426.

Frazier, W. T., Kandel, E. R., Kuppermann, I., Waziri, R., and Coggeshall, R. E. (1967). Morphological and functional properties of identified neurons in the abdominal ganglion of *Aplysia californica*. *J. Neurophysiol.* 30, 1288–1351.

Fuortes, M. G. F. (1963). Visual responses in the eye of the dragonfly. *Science* 142, 69–70.

Gomez, M., and Nasi, E. (1994). The light-sensitive conductance of hyperpolarizing invertebrate photoreceptors: a patch-clamp study. *J. Gen. Physiol.* 103, 939–956.

Gomez, M., and Nasi, E. (1995). Activation of light-dependent K^+ channels in ciliary invertebrate photoreceptors involves cGMP but not the IP^3/Ca^2+ cascade. *Neuron* 15, 607–618.

Gomez, M., and Nasi, E. (1997). Antagonists of the cGMP-gated conductance of vertebrate rods block the photocurrent in scallop ciliary photoreceptors. *J. Physiol.* 500, 367–378.

Gomez, M., and Nasi, E. (2000). Light transduction in invertebrate hyperpolarizing photoreceptors: possible involvement of a Go-regulated guanylate cyclase. *J. Neurosci.* 20, 5254–5263.

Gotow, T. (1975). Morphology and function of the photoexcitable neurones in the central ganglion of *Onchidium verruculatum*. *J. Comp. Physiol.* 99, 139–152.

Gotow, T. (1989). Photoresponses of an extraocular photoreceptor associated with a decrease in membrane conductance in an opisthobranch mollusc. *Brain Res.* 479, 120–129.

Gotow, T., and Nishi, T. (2002). Light-dependent K^+ channels in the mollusc *Onchidium* simple photoreceptors are opened by cGMP. *J. Gen. Physiol.* 120, 581–597.

Gotow, T., and Nishi, T. (2007). Involvement of a Go-type G-protein coupled to guanylate cyclase in the phototransduction cGMP cascade of molluscan simple photoreceptors. *Brain Res.* 1144, 42–51.

Gotow, T., and Nishi, T. (2008). Simple photoreceptors in some invertebrates: physiological properties of a new photosensory modality. *Brain Res.* 1225, 3–16.

Gotow, T., Nishi, T., and Kijima, H. (1994). Single K^+ channels closed by light and opened by cyclic GMP in molluscan extra-ocular photoreceptor cells. *Brain Res.* 662, 268–272.

Gotow, T., Nishi, T., and Murakami, M. (1997). 4-Aminopyridine and

L-cis-diltiazem block the cGMP-activated K^+ channels closed by light in the molluscan extra-ocular photoreceptors. *Brain Res.* 745, 303–308.

Gotow, T., Shimotsu, K., and Nishi, T. (2005). Non-image forming function of the extraocular photoreceptors in the ganglion of the sea slug *Onchidium*. Brain, vision, and artificial intelligence. In Proceedings of First International Symposium, M. D. Gregorio, V. D. Maio, M. Frucci, and C. Musio, eds (Berlin, Springer), pp. 136–145.

Gotow, T., Tateda, H., and Kuwabara, M. (1973). The function of photoexcitive neurones in the central ganglia for behavioral activity of the marine mollusc *Onchidium verruculatum*. *J. comp. Physiol.* 83, 361–376.

Hagiwara, S., Kusano, K., and Saito, N. (1961). Membrane changes of *Onchidium* nerve cell in potassium-rich media. *J. Physiol.* 155, 470–489.

Hardie, R. C. (2003). Regulation of TRP channels via lipid second messengers. *Annu. Rev. Physiol.* 65, 735–759.

Hattar, S., Liao, H.-W., Takao, M., Berson, D. M., and Yau, K. W. (2002). Melanopsin-containing retinal ganglion cells: architecture, projections, and intrinsic photosensitivity. *Science* 295, 1065–1070.

Hattar, S., Lucas, R. J., Mrosovsky, N., Thompson, S., Douglas, R. H., Hankins, M. W., Lem, J., Biel, M., Hofmann, F., Foster, R. G., and Yau, K. W. (2003). Melanopsin and rod-cone photoreceptive systems account for all major accessory visual functions in mice. *Nature* 424, 76–81.

Haynes, L. W. (1992). Block of the cyclic GMP-gated channel of vertebrate rod and cone photoreceptors by L-cis-diltiazem. *J. Gen. Physiol.* 100, 783–801.

He, S., Dong, W., Deng, Q., Weng, S., and Sun, W. (2003). Seeing more clearly: Recent advances in understanding retinal circuitry. *Science* 302, 408–411.

Hermann, A., and Gorman, A. L. F. (1981). Effects of 4-aminopyridine on potassium currents in a molluscan neurons. *J. Gen. Physiol.* 78, 63–86.

Hille, B. (1992). Ionic Channels of Excitable Membranes, 2nd Edn. Sunderland, MA, Sinauer.

Hisano, N., Tateda, H., and Kuwabara, M. (1972). A Photosensitive neurones in the marine pulmonate mollusc *Onchidium verruculatum*. *J. Exp. Biol.* 57, 651–660.

Katagiri, Y., Katagiri, N., and Fujimoto, K. (1985). Morphological and electrophysiological studies of a multiple photoreceptive system in a marine gastropod, *Onchidium*. *Neurosci. Res. Suppl.* 2, S1–S15.

Kaupp, U. B., and Seifert, R. (2002). Cyclic nucleotide-gated ion channels. *Physiol. Rev.* 82, 769–824.

Kennedy, D. (1963). Physiology of photoreceptor neurons in the abdominal nerve cord of the crayfish. *J. Gen. Physiol.* 46, 551–572.

Kojima, D., Terakita, A., Ishikawa, T., Tsukahara, Y., Maeda, A., and Shichida, Y. (1997). A novel Go-mediated phototransduction cascade in scallop visual cells. *J. Biol. Chem.* 272, 22979–22982.

Kubozono, T. (1988). A study on an extraocular photoreceptor in the central ganglia of the marine gastropod mollusc, *Onchidium verruculatum*. (in Japanese). *Med. J. Kagoshima Univ.* 40, 161–178.

Lucas, R. J., Hattar, S., Takao, M., Berson, D. M., Foster, R. G., and Yau, K. W. (2003). Diminished pupillary light reflex at high irradiances in melanopsin-knockout mice. *Science* 299, 245–247.

Matthews, G., and Watanabe, S. (1987). Properties of ion channels closed by light and opened by guanosine 3′,5′-cyclic monophosphate in toad retinal rods. *J. Physiol.* 389, 691–715.

McLatchie, L. M., and Matthews, H. R. (1994). The effect of pH on the block by L-cis-diltiazem and amiloride of the cyclic GMP-activated conductance of salamander rods. *Proc. R. Soc. Lond., B, Biol. Sci.* 255, 231–236.

McReynolds, J. S., and Gorman, A. L. (1970). Photoreceptor potentials of opposite polarity in the eye of the scallop, *Pecten irradians*. *J. Gen. Physiol.* 56, 376–391.

Meech, R. W. (1972). Intracellular calcium injection causes increased potassium conductance in *Aplysia* nerve cells. *Comp. Biochem. Physiol., A* 42, 493–499.

Melyan, Z., Tarttelin, E. E., Bellingham, R. J., Lucas, M., and Hankins, W. (2005). Addition of human melanopsin renders mammalian cells photoresponsive. *Nature* 433, 741–745.

Nagy, K. and Stieve, H. (1990). Light-activated single channel currents in Limulus ventral nerve photoreceptors. *Euro. Biophys. J.* 18, 220–224.

Nasi, E., and Gomez, M. (1992). Light-activated ion channels in solitary photoreceptors from the eye of the scallop Pecten irradians. *J. Gen. Physiol.* 99, 747–769.

Nishi, T., and Gotow, T. (1992). A neural mechanism for processing colour information in molluscan extra-ocular photoreceptors. *J. Exp. Biol.* 168, 77–91.

Nishi, T., and Gotow, T. (1998). Light-increased cGMP and K^+ conductance in the hyperpolarizing receptor potential of *Onchidium* extra-ocular photoreceptors. *Brain Res.* 809, 325–336.

Nishi, T., Gotow, T., and Nakagawa, S. (2006). Non-image-forming visual function of the simple photoreceptors in the sea slug *Onchidium* ganglion. *Neurosci. Res.* 55, S176.

Owen, W. G. (1986). The light-induced conductance change in the vertebrate rod. In The Molecular Mechanism of Photoreception, H. Stieve, ed. (Berlin, Springer-Verlag) pp. 171–187.

Panda, S., Nayak, K. S., Campo, B., Walker, J. R., Hogenesch, J. B., and Jegla, T. (2005). Illumination of the melanopsin signaling pathway. *Science* 307, 600–604.

Panda, S., Provencio, I., Tu, D. C., Pires, S. S., Rollag, M. D., Castrucci, A. M., Pletcher, M. T., Sato, T. K., Wiltshire, T., Steve, A., Kay, S. A., Van Gelder, R. N., and Hogenesch, J. B. (2003). Melanopsin is required for non-image-forming photic responses in blind mice. *Science* 301, 525–527.

Panda, S., Sato, T. K., Castrucci, A. M., Rollag, M. D., DeGrip, W. J., Hogenesch, J. B., Provencio, I., and Kay, S. A. (2002). Melanopsin (Opn4) requirement for normal light-induced circadian phase shifting. *Science* 298, 2213–2216.

Pasic, M., and Kartelija, G. (1995). The reaction of Helix photosensitive neurons to light and cyclic GMP. *Neuroscience* 69, 557–565.

Pei, X., Wilkens, L. A., and Moss, F. (1996). Light enhances hydrodynamic signaling in the multimodal caudal photoreceptor interneurons of the crayfish. *J. Neurophysiol.* 76, 3002–3011.

Peirson, S., and Foster, R. G. (2006). Melanopsin: another way of signaling light. *Neuron* 49, 331–339.

Pinto, L. H. and Brown, J. E. (1977). Intracellular recordings from photoreceptors of the squid (*Loligo pealii*). *J. Comp. Physiol. A.* 122, 241–250.

Provencio, I., Jiang, G., De Grip, W. J., Hayes, W. P., and Rollag, M. D. (1998). Melanopsin: an opsin in melanophores, brain, and eye. *Proc. Natl. Acad. Sci. U.S.A.* 95, 340–345.

Qiu, X., Kumbalasiri, T., Carlson, S. M., Wong, K. Y., Krshna, V., Provencio, I., and Berson, D. M. (2005). Induction of photosensitivity by heterologous expression of melanopsin. *Nature* 433, 745–749.

Raghu, P., Usher, K., Jonas, S., Chyb, S., Polyanovsky, A., and Hardie, R. C. (2000). Constitutive activity of the light-sensitive channels TRP and TRPL in the Drosophila diacylglycerol kinase mutant, rdgA. *Neuron* 26, 169–179.

Rispoli, G., and Menini, A. (1988). The blocking effect of L-cis-diltiazem on the light-sensitive current of isolated rods of the tiger salamander. *Eur. Biophys. J.* 16, 65–71.

Robles, L. J., Breneman, J. W., Anderson, E. O., Nottoli, V. A., and Kegler, L. L. (1986). Immunocytochemical localization of a rhodopsin-like protein in the lipochondria in photosensitive neurons of *Aplysia californica*. *Cell Tissue Res.* 244, 115–120.

Ruby, N. F., Brennan, T. J., Xie, X., Cao, V., Franken, P., Heller, H. C., and O'Hara, B. F. (2002). Role of melanopsin in circadian responses to light. *Science* 298, 2211–2213.

Solessio, E., and Engbretson, G. A. (1993). Antagonistic chromatic mechanisms in photoreceptors of the parietal eye of lizards. *Nature* 364, 442–445.

Stern, J. H., Kaupp, U. B., and MacLeish, P. R. (1986). Control of the light-regulated current in rod photoreceptors by cyclic GMP, calcium, and L-cis-diltiazem. *Proc. Natl. Acad. Sci. U.S.A.* 83, 1163–1167.

Tomita, T. (1972). Light-induced potential and resistance changes in vertebrate photoreceptors. In Handbook of Sensory Physiology. VII/2, M. G. F. Fuortes, ed. (Berlin, Springer-Verlag), pp. 483–511.

Washizu, Y. (1964). Electrical activity of single retinula cells in the compound eye of the blowfly *Calliphora erythrocephala* Meig. *Comp. Biochem. Physiol.* 12, 369–387.

Wilkens, L. A. (1988). The crayfish caudal photoreceptor: advances and questions after the first half century. *Comp. Biochem. Physiol.* 91C, 61–68.

Wilkens, L. A., and Larimer, J. L. (1972). The CNS Photoreceptor of crayfish: morphology and synaptic activity. *J. comp. Physiol.* 80, 389–407.

Conflict of Interest Statement: The authors declare that the research was conducted in the absence of any commercial or financial relationships that could be construed as a potential conflict of interest.

Received: 27 August 2009; paper pending published: 24 September 2009; accepted: 24 November 2009; published online: 09 December 2009.

Citation: Gotow T and Nishi T (2009) A new photosensory function for simple photoreceptors, the intrinsically photoresponsive neurons of the sea slug Onchidium. Front. Cell. Neurosci. ***3****:18. doi: 10.3389/neuro.03.018.2009*

Copyright © 2009 Gotow and Nishi. This is an open-access article subject to an exclusive license agreement between the authors and the Frontiers Research Foundation, which permits unrestricted use, distribution, and reproduction in any medium, provided the original authors and source are credited.

frontiers in
CELLULAR NEUROSCIENCE

PERSPECTIVE ARTICLE
published: 26 October 2012
doi: 10.3389/fncel.2012.00048

Functional and evolutionary aspects of chemoreceptors

Dieter Wicher*

Department of Evolutionary Neuroethology, Max Planck Institute for Chemical Ecology, Jena, Germany

Edited by:
Michael Hausser, University College London, UK

Reviewed by:
Mala Shah, University of London, UK
Jean-Pierre Montmayeur, The Coca-Cola Company, USA

****Correspondence:***
Dieter Wicher, Department of Evolutionary Neuroethology, Max Planck Institute for Chemical Ecology, Hans-Knöll-St. 8, D-07745 Jena, Germany.
e-mail: dwicher@ice.mpg.de

The perception and processing of chemical signals from the environment is essential for any living systems and is most probably the first sense developed in life. This perspective discusses the physical limits of chemoreception and gives an overview on the receptor types developed during evolution to detect chemical signals from the outside world of an organism. It discusses the interaction of chemoreceptors with downstream signaling elements, especially the interaction between electrical and chemical signaling. It is further considered how the primary chemosignal is appropriately amplified. Three examples of chemosensory systems illustrate different strategies of such amplification.

Keywords: ionotropic receptor, metabotropic receptor, receptor kinase, GPCR, TRP channel

INTRODUCTION

Chemoreceptors transduce an external signal, a volatile molecule (olfaction) or a molecule in solution (gustation) into an intracellular signal. There are two major types of chemoreceptors, ionotropic and metabotropic receptors. Ionotropic receptors (IRs) are ion channels activated by ligand binding. The chemical messenger elicits an immediate electrical signal in the sensory cell. By contrast, activation of metabotropic receptor activates an intracellular signaling cascade which may include enzyme activation, second messenger production or activation of ion channels. Receptor function and sensitivity are usually regulated by interaction with accessory proteins. A high sensitivity of the chemoreceptive machinery results from signal amplification which may take place at various levels of signal processing.

While most chemoreceptors in mammals are metabotropic receptors, chemoreception in insects is ionotropic. The authors of a recent review thus asked whether the choice of a mechanism for a sensory task is "chance or design" (Silbering and Benton, 2010), and concluded that the choice of ionotropic mechanisms for insect chemoreception probably reflects a special mechanistic advantage. For a detailed review on the evolution of insect olfaction see (Hansson and Stensmyr, 2011).

PHYSICAL LIMITS OF CHEMOSENSATION

To detect low pheromone concentrations released in the order of magnitude of ng per hour male insects have expanded the surface area of their antennae (Hansson and Stensmyr, 2011). How are receptor size and resolution related? Analysing bacterial chemotaxis Berg and Purcell (1977) calculated the maximum precision in sensing the concentration of a chemoattractant. The limit is set by the noise due to Brownian motion when sensing a few molecules. *Escherichia coli* can detect amino acids at nanomolar concentration (Mao et al., 2003) which corresponds to only a few molecules per cell volume. The fractional accuracy $\delta c/c$ in determining the concentration c is given by:

$$\delta c/c = 1/\sqrt{Drc_m t}$$

where D is the diffusion coefficient of the chemoattractant, r the receptor radius (e.g., cell radius), c_m the mean concentration and t the detection time (Berg and Purcell, 1977). This formula is valid for a single receptor as well as for a receptor array such as a cell surface equipped with receptors (Bialek and Setayeshgar, 2005). To determine a molecule with a diffusion coefficient of 10^{-5} cm^2/s at a mean concentration of 1 μM with an accuracy of 1%, a cell with a radius of 1 μm requires a measuring time of 10 ms. For a single receptor with a radius of 1 nm a detection time of 17 s would be required. Considering a fixed detection time increasing the receptive surface indeed enhances the resolution as in the above case of pheromone detection.

CHEMOSIGNAL PROCESSING AND AMPLIFICATION

External molecules bind to chemoreceptors located in the plasma membrane, the subsequent receptor activation transduces the external signal across the plasma membrane. For ligand-gated or IRs, binding of the signal molecule opens an ion channel and produces an electrical signal. This process is usually fast (micro to milliseconds). The ion flux changes the membrane potential and thus the electrical activity of the chemosensory neurons. Signals transferred by excitatory IRs are amplified by depolarization which activates various voltage-gated cation channels leading to further depolarizion of OSNs. Another type of amplification may take place when receptor activation leads to Ca^{2+} influx, either directly such as for the Ca^{2+}-permeable TRP channels or indirectly when the depolarization activates voltage-gated Ca^{2+}-channels. A rise in the free intracellular Ca^{2+} concentration may activate various intracellular signaling cascades thereby amplifying the chemical signal.

For metabotropic receptors binding of the signal molecule initiates changes in intracellular chemical signaling such as enzyme activation and production of second messengers. This process is slower than ionotropic signaling and requires typically 50–150 milliseconds. However, for a tightly packed signaling cascade this delay can be much shorter as in *Drosophila* photoreception where

the receptor current activates 20 ms after photon absorption by rhodopsin (Katz and Minke, 2009).

Since metabotropic signaling often involves G protein activation, stimulation of enzymatic activity, and production of second messengers, i.e., processes potentially contributing to a signal amplification, this type of signaling may achieve a high sensitivity of chemodetection. For example, in G protein-coupled receptors (GPCRs) ligand binding activates a number of G proteins setting a first level of signal amplification. This amplification relies on a sufficient long dwelling time of the ligand to the receptor. The residence time of the ligand which is inversely related to the dissociation rate constant is thought to determine the effect of receptor activation under *in vivo* conditions far from thermodynamic equilibrium rather than the affinity defined as the reciprocal of the equilibrium dissociation constant (Tummino and Copeland, 2008). Another mechanism that may restrict the number of activated G proteins is receptor desensitization (Kato and Touhara, 2009). Furthermore, the signal amplification at G protein level is controlled by proteins regulating their activity cycle such as RGS proteins (regulators of G protein signaling), AGS proteins (activators of G protein signaling) and GEFs (guanine nucleotide exchange factors), for example in *C. elegans* RGS proteins (Fukuto et al., 2004; Ferkey et al., 2007). G proteins downstream activate enzymes such as adenylyl cyclases. The cAMP production sets the second level of amplification since each molecule may affect further downstream targets such as protein kinases which might add another level of amplification.

Primary electrical signals can elicit secondary chemical signaling, and vice versa, primary chemical signals can be transformed into electrical signals as metabotropic receptors downstream often target ion channels. For example, activation of the vanilloid receptor VR1, a member of the TRP channel family, by capsaicin induces a Ca^{2+} influx in the receptor cell. Ca^{2+} as a universal intracellular signaling molecule can then activate Ca^{2+}-dependent proteins such as cyclases and kinases. In mammalian olfactory sensory neurons, odor binding activates the olfactory receptor (OR), a GPCR bound to a stimulatory G_{olf} protein which in turn enhances the cAMP production via adenylyl cyclase stimulation. cAMP binds to and opens cyclic nucleotide gated (CNG) channels which depolarize the neuron and also conduct Ca^{2+}. Finally, Ca^{2+} activates Ca^{2+}-dependent Cl^- channels thereby further depolarizing the cell (Kaupp, 2010). Similarly, receptor guanylyl cyclases catalyze the production of cGMP which also activate CNG channels to depolarize cells and enhance the free Ca^{2+} concentration.

SPECIAL EXAMPLES FOR CHEMOSIGNAL AMPLIFICATION

BACTERIAL CHEMORECEPTORS

In *Escherichia coli*, chemoreceptors transmembrane methyl-accepting chemotaxis proteins (MCPs). They couple via a signal conversion module to histidine autokinases CheA which are inhibited upon chemoattractant and activated upon repellent binding (Hazelbauer et al., 2008). The receptors for attractants bind serine (Tsr), aspartate and maltose (Tar) ribose, glucose and galactose (Trg), and dipeptides (Tap). The phosphorylation state of CheA controls the flagellar motor. The chemoreceptors form dimers which assemble to hexagonally packed trimers. These arrays are concentrated in patches of about 250 nm diameter, corresponding to 1% of the cell surface, and contain nearly half the number of expressed chemoreceptors.

Within the signaling complex chemoreceptor/CheA there is a signal amplification of ∼36, i.e., one receptor controls 36 kinase molecules. Moreover, the receptors show strong cooperativity, for attractant stimulation a Hill coefficient of 10 was observed (Hazelbauer et al., 2008). Taken together, the lattice structure of receptor arrangement allows a high degree of interaction within the signaling complexes. This allows the bacteria to detect nanomolar amino acid concentrations (Mao et al., 2003).

SEA URCHIN SPERM CELLS

The chemoattractant resact is released from the egg and binds to a transmembrane receptor guanylyl cyclase on a sperm cell. One ligand molecule gives rise to the production of ∼45 cGMP molecules (Bönigk et al., 2009). One cGMP molecule is able to activate CNGK, an atypical CNG channel with exclusive K^+ permeability that forms a pseudotetramer like voltage-gated Na^+ or Ca^{2+} channels. Conventional CNG channels operate in the micromolar concentration range and are activated in cooperative manner, CNGK operates in the nanomolar range and is activated by binding of a single molecule to the third repeat. CNGK activation produces a transient hyperpolarization followed by activation of voltage-gated Ca^{2+} channels allowing Ca^{2+} to enter the flagellum. At least 25 cGMP molecules were found to be required for eliciting a Ca^{2+} signal. Thus, binding of one chemoattractant molecule is sufficient to produce a number of cGMP molecules that activate the highly cGMP-sensitive CNGK channels which in turn elicit a behavioral response.

MAMMALIAN OLFACTORY RECEPTORS

Odor binding on mouse OR is extremely short. A dwelling time of ∼1 ms is not sufficient to activate on average one G protein, similar as previously observed in frog ORs (Bhandawat et al., 2005; Ben-Chaim et al., 2011). Thus, there is no signal amplification at this level. Multiple binding of odor molecules to the same receptor integrates odor signaling, and together with sufficient receptor expression that multiplies binding events and thus the probability of G protein activation leads to a stimulation of adenylyl cyclase III. This raises the cAMP level to activate CNG channels thereby depolarizing the cell and importing Ca^{2+}. The signal amplification takes place when Ca^{2+} activates Ca^{2+}-dependent Cl^- channels which further depolarize the cell (Kaupp, 2010).

The delay between binding of odor molecules to the receptor and the development of the receptor potential depends on the odor concentration and can range between 100 ms at submicromolar concentration and 25–40 ms at concentrations up to 100 μM (Ghatpande and Reisert, 2011). A delay in this order of magnitude seems to be not limiting since a behavioral response appears already 200 ms after odor stimulation (Abraham et al., 2004).

CHEMORECEPTOR TYPES IN EVOLUTION

From bacteria to men both types of receptors, metabotropic and ionotropic, are used to perceive chemical signals (**Table 1**) (Biswas et al., 2009; Gees et al., 2010; Nordström et al., 2011). Most of them are conserved during evolution, yet there are cases of receptor gene degeneration such as the CO_2-sensing guanylyl

Table 1 | Chemoreceptors in model organisms operating via a metabotropic or an ionotropic mechanism.

	Metabotropic		Ionotropic		
	RC/RK	GPCR	GR/OR	TRP	IR
E. coli	X	–	–	–	X
S. cerevisae	–	X	–	X	–
C. elegans	X	X	X	X	X
D. melanogaster	–	–	X*	X	X
M. musculus	X	X	–	X	–

*RC/RK, receptor cyclase/receptor kinase; GPCR, G protein-coupled receptor; GR/OR, gustatory receptor, olfactory receptor; TRP, ion channel family named according to the first member to be discovered ("transient receptor potential" channel in Drosophila photoreceptors); IR, "ionotropic receptor", a variant ionotropic glutamate receptor protein serving as olfactory receptor. * GR/ORs in insects are 7-TM proteins as GPCRs, but are inversely oriented in the membrane. They do not belong to the GPCR superfamily according to a bioinformatics analysis (Benton et al., 2006; Nordström et al., 2011), and form ionotropic receptors. X, receptor type reported for that species.*

cyclase D in primates (Young et al., 2007) or TRPC2, a channel part of the pheromone signaling cascade, in men (Zufall, 2005).

Bacteria obtain nutrient information for chemotaxis from receptor-associated kinases (Hazelbauer et al., 2008) and sense amino acids using precursors of ionotropic glutamate receptors (iGluRs, Chiu et al., 1999). Yeast express GPCRs to detect sugar and pheromones (Versele et al., 2001) as well as TRP channels for sensing aromatic compounds (Nilius and Owsianik, 2011). Highly sugar-sensitive receptors are the 12-TM proteins Snf3/Rgt2 which regulate the expression of sugar transporters (Gancedo, 2008).

In more complex organisms, specialized chemosensory neurons detect volatile or external chemical messengers in solution. Receptor activation induces a change in the electrical activity of sensory neurons. IRs form ion channels gated by ligand binding to the receptor. Metabotropic receptors couple to intracellular signaling systems regulating the activity of targets such as ion channels thereby changing the neuronal activity.

In nematodes metabotropic chemoreceptors comprise receptor guanylyl cyclases and a large number of GPCRs (Bargmann, 2006). Receptors operating via an ionotropic mechanism are TRP channels (Nilius and Owsianik, 2011), and "Ionotropic Receptors" (IRs), ORs sensing general odors which are related to iGluRs (Croset et al., 2010).

In insects, ORs are heterodimers composed of two proteins with 7-transmembrane topology like GPCRs (Neuhaus et al., 2005). However, there is no sequence similarity to other GPCRs and the proteins are inversely oriented in the membrane (Benton et al., 2006). One of these proteins is odor-specific, the other one a co-receptor with chaperone function (Larsson et al., 2004). While there are indications that odors initiate metabotropic signaling (Wicher et al., 2008; Deng et al., 2011), the primary odor response is ionotropic (Sato et al., 2008; Wicher et al., 2008). Other IRs in insects are gustatory receptors [GRs, (Sato et al., 2011), IRs (Benton et al., 2009), and TRP channels (Nilius and Owsianik, 2011)].

In mammals metabotropic chemoreceptors comprise receptor tyrosine kinases (Petersen et al., 2011), guanylyl cyclases (Fülle et al., 1995; Sun et al., 2009), and a large number of GPCRs (Kaupp, 2010). Most olfactory and pheromone receptors are GPCRs (Fleischer et al., 2009). Taste receptors for sweet, bitter, and umami are GPCRs whereas those for sour and salty are thought to be ionotropic (Chandrashekar et al., 2006). Receptors for hot and spicy compounds as capsaicin, for cool compounds as menthol or pungent compounds as mustard oil are also ionotropic TRP channels (Damann et al., 2008). IRs are not expressed in mammals (Croset et al., 2010). Instead, mammalian central synapses express various subtypes of the related iGluRs.

CONCLUSION

Chemosensory systems are functional complexes of receptors and downstream signaling elements. There seems to be no preference for the use of either metabotropic or IRs for the detection of chemicals during evolution. Moreover, receptors for a given sense might be both metabotropic and ionotropic as seen above for mammalian taste receptors. There is a pronounced conservation of chemoreceptors during evolution. It is rather rare that receptors disappear at a certain stage like the IRs in vertebrates. As seen in mammalian ORs, there is no selection toward perfection. It is possible to neglect the potential of G proteins for a signal amplification. Although the chemosensory system was not optimized for fast processing, the organism as a whole is capable of behaviorally responding to odor stimulation in astonishingly short time. A high sensitivity of chemosensory systems can be achieved by spatial arrangements such as the chemosensory patches in bacteria which provide the basis for high cooperativity of signaling elements. On the other hand, the capability of sea urchin sperm cells to react to single resact molecules demonstrates that high sensitivity can also be obtained in a remarkably simple way unless the internal signaling cascade allows a sufficiently high amplification of the external signal.

ACKNOWLEDGMENTS

This study was supported by the Max Planck Society.

REFERENCES

Abraham, N. M., Spors, H., Carleton, A., Margrie, T. W., Kuner, T., and Schaefer, A. T. (2004). Maintaining accuracy at the expense of speed: stimulus similarity defines odor discrimination time in mice. *Neuron* 44, 865–876.

Bargmann, C. I. (2006). Chemosensation in *C. elegans*. *WormBook*. doi: 10.1895/wormbook.1.123.1

Ben-Chaim, Y., Cheng, M. M., and Yau, K. W. (2011). Unitary response of mouse olfactory receptor neurons. *Proc. Natl. Acad. Sci. U.S.A.* 108, 822–827.

Benton, R., Sachse, S., Michnick, S. W., and Vosshall, L. B. (2006). Atypical membrane topology and heteromeric function of *Drosophila* odorant receptors *in vivo*. *PLoS Biol.* 4:e20. doi: 10.1371/journal.pbio.0040020

Benton, R., Vannice, K. S., Gomez-Diaz, C., and Vosshall, L. B. (2009). Variant ionotropic glutamate receptors as chemosensory receptors in *Drosophila*. *Cell* 136, 149–162.

Berg, H. C., and Purcell, E. M. (1977). Physics of chemoreception. *Biophys. J.* 20, 193–219.

Bhandawat, V., Reisert, J., and Yau, K. W. (2005). Elementary response of olfactory receptor neurons to odorants. *Science* 308, 1931–1934.

Bialek, W., and Setayeshgar, S. (2005). Physical limits to biochemical signaling. *Proc. Natl. Acad. Sci. U.S.A.* 102, 10040–10045.

Biswas, K. H., Shenoy, A. R., Dutta, A., and Visweswariah, S. S. (2009). The evolution of guanylyl cyclases as multidomain proteins: conserved features of kinase-cyclase domain fusions. *J. Mol. Evol.* 68, 587–602.

Bönigk, W., Loogen, A., Seifert, R., Kashikar, N., Klemm, C., Krause, E., et al. (2009). An atypical CNG channel activated by a single cGMP molecule controls sperm chemotaxis. *Sci. Signal* 2, ra68.

Chandrashekar, J., Hoon, M. A., Ryba, N. J., and Zuker, C. S. (2006). The receptors and cells for mammalian taste. *Nature* 444, 288–294.

Chiu, J., DeSalle, R., Lam, H. M., Meisel, L., and Coruzzi, G. (1999). Molecular evolution of glutamate receptors: a primitive signaling mechanism that existed before plants and animals diverged. *Mol. Biol. Evol.* 16, 826–838.

Croset, V., Rytz, R., Cummins, S. F., Budd, A., Brawand, D., Kaessmann, H., et al. (2010). Ancient protostome origin of chemosensory ionotropic glutamate receptors and the evolution of insect taste and olfaction. *PLoS Genet.* 6:e1001064. doi: 10.1371/journal.pgen.1001064

Damann, N., Voets, T., and Nilius, B. (2008). TRPs in our senses. *Curr. Biol.* 18, R880–R889.

Deng, Y., Zhang, W., Farhat, K., Oberland, S., Gisselmann, G., and Neuhaus, E. M. (2011). The stimulatory Galpha(s) protein is involved in olfactory signal transduction in *Drosophila*. *PLoS ONE* 6:e18605. doi: 10.1371/journal.pone.0018605

Ferkey, D. M., Hyde, R., Haspel, G., Dionne, H. M., Hess, H. A., Suzuki, H., et al. (2007). *C. elegans* G protein regulator RGS-3 controls sensitivity to sensory stimuli. *Neuron* 53, 39–52.

Fleischer, J., Breer, H., and Strotmann, J. (2009). Mammalian olfactory receptors. *Front. Cell. Neurosci.* 3:9. doi: 10.3389/neuro.03.009.2009

Fukuto, H. S., Ferkey, D. M., Apicella, A. J., Lans, H., Sharmeen, T., Chen, W., et al. (2004). G protein-coupled receptor kinase function is essential for chemosensation in *C. elegans*. *Neuron* 42, 581–593.

Fülle, H. J., Vassar, R., Foster, D. C., Yang, R. B., Axel, R., and Garbers, D. L. (1995). A receptor guanylyl cyclase expressed specifically in olfactory sensory neurons. *Proc. Natl. Acad. Sci. U.S.A.* 92, 3571–3575.

Gancedo, J. M. (2008). The early steps of glucose signalling in yeast. *FEMS Microbiol. Rev.* 32, 673–704.

Gees, M., Colsoul, B., and Nilius, B. (2010). The role of transient receptor potential cation channels in Ca^{2+} signaling. *Cold Spring Harb. Perspect. Biol.* 2, a003962.

Ghatpande, A. S., and Reisert, J. (2011). Olfactory receptor neuron responses coding for rapid odour sampling. *J. Physiol.* 589, 2261–2273.

Hansson, B. S., and Stensmyr, M. C. (2011). Evolution of insect olfaction. *Neuron* 72, 698–711.

Hazelbauer, G. L., Falke, J. J., and Parkinson, J. S. (2008). Bacterial chemoreceptors: high-performance signaling in networked arrays. *Trends Biochem. Sci.* 33, 9–19.

Kato, A., and Touhara, K. (2009). Mammalian olfactory receptors: pharmacology, G protein coupling and desensitization. *Cell. Mol. Life Sci.* 66, 3743–3753.

Katz, B., and Minke, B. (2009). *Drosophila* photoreceptors and signaling mechanisms. *Front. Cell. Neurosci.* 3:2. doi: 10.3389/neuro.03.002.2009

Kaupp, U. B. (2010). Olfactory signalling in vertebrates and insects: differences and commonalities. *Nat. Rev. Neurosci.* 11, 188–200.

Larsson, M. C., Domingos, A. I., Jones, W. D., Chiappe, M. E., Amrein, H., and Vosshall, L. B. (2004). Or83b encodes a broadly expressed odorant receptor essential for *Drosophila* olfaction. *Neuron* 43, 703–714.

Mao, H., Cremer, P. S., and Manson, M. D. (2003). A sensitive, versatile microfluidic assay for bacterial chemotaxis. *Proc. Natl. Acad. Sci. U.S.A.* 100, 5449–5454.

Neuhaus, E. M., Gisselmann, G., Zhang, W., Dooley, R., Störtkuhl, K., and Hatt, H. (2005). Odorant receptor heterodimerization in the olfactory system of *Drosophila melanogaster*. *Nat. Neurosci.* 8, 15–17.

Nilius, B., and Owsianik, G. (2011). The transient receptor potential family of ion channels. *Genome Biol.* 12, 218.

Nordström, K. J., Almen, M. S., Edstam, M. M., Fredriksson, R., and Schioth, H. B. (2011). Independent HHsearch, Needleman-Wunsch-based and motif analyses reveals the overall hierarchy for most of the G protein-coupled receptor families. *Mol. Biol. Evol.* 28, 2471–2480.

Petersen, C. I., Jheon, A. H., Mostowfi, P., Charles, C., Ching, S., Thirumangalathu, S., et al. (2011). FGF signaling regulates the number of posterior taste papillae by controlling progenitor field size. *PLoS Genet.* 7:e1002098. doi: 10.1371/journal.pgen.1002098

Sato, K., Pellegrino, M., Nakagawa, T., Nakagawa, T., Vosshall, L. B., and Touhara, K. (2008). Insect olfactory receptors are heteromeric ligand-gated ion channels. *Nature* 452, 1002–1006.

Sato, K., Tanaka, K., and Touhara, K. (2011). Sugar-regulated cation channel formed by an insect gustatory receptor. *Proc. Natl. Acad. Sci. U.S.A.* 108, 11680–116805.

Silbering, A. F., and Benton, R. (2010). Ionotropic and metabotropic mechanisms in chemoreception: 'chance or design'? *EMBO Rep.* 11, 173–179.

Sun, L., Wang, H., Hu, J., Han, J., Matsunami, H., and Luo, M. (2009). Guanylyl cyclase-D in the olfactory CO_2 neurons is activated by bicarbonate. *Proc. Natl. Acad. Sci. U.S.A.* 106, 2041–2046.

Tummino, P. J., and Copeland, R. A. (2008). Residence time of receptor-ligand complexes and its effect on biological function. *Biochemistry* 47, 5481–5492.

Versele, M., Lemaire, K., and Thevelein, J. M. (2001). Sex and sugar in yeast: two distinct GPCR systems. *EMBO Rep.* 2, 574–579.

Wicher, D., Schäfer, R., Bauernfeind, R., Stensmyr, M. C., Heller, R., Heinemann, S. H., et al. (2008). *Drosophila* odorant receptors are both ligand-gated and cyclic-nucleotide-activated cation channels. *Nature* 452, 1007–1011.

Young, J. M., Waters, H., Dong, C., Fulle, H. J., and Liman, E. R. (2007). Degeneration of the olfactory guanylyl cyclase D gene during primate evolution. *PLoS ONE* 2:e884. doi: 10.1371/journal.pone.0000884

Zufall, F. (2005). The TRPC2 ion channel and pheromone sensing in the accessory olfactory system. *Naunyn Schmiedebergs Arch. Pharmacol.* 371, 245–250.

Conflict of Interest Statement: The author declares that the research was conducted in the absence of any commercial or financial relationships that could be construed as a potential conflict of interest.

Received: 31 July 2012; accepted: 08 October 2012; published online: 26 October 2012.

*Citation: Wicher D (2012) Functional and evolutionary aspects of chemoreceptors. Front. Cell. Neurosci. **6**:48. doi: 10.3389/fncel.2012.00048*

Copyright © 2012 Wicher. This is an open-access article distributed under the terms of the Creative Commons Attribution License, which permits use, distribution and reproduction in other forums, provided the original authors and source are credited and subject to any copyright notices concerning any third-party graphics etc.

frontiers in
CELLULAR NEUROSCIENCE

REVIEW ARTICLE
published: 27 August 2009
doi: 10.3389/neuro.03.009.2009

Mammalian olfactory receptors

Joerg Fleischer, Heinz Breer and Joerg Strotmann*

Institute of Physiology, University of Hohenheim, Stuttgart, Germany

Edited by:
Dieter Wicher, Max Planck Institute for Chemical Ecology, Germany

Reviewed by:
Bernd Grunewald, Johann-Wolfgang-Goethe University, Germany
Klemens F. Störtkuhl, Ruhr Universität Bochum, Germany

***Correspondence:**
Joerg Strotmann, Institute of Physiology, University of Hohenheim, Garbenstr. 30, 70599 Stuttgart, Germany.
e-mail: strotman@uni-hohenheim.de

Perception of chemical stimuli from the environment is essential to most animals; accordingly, they are equipped with a complex olfactory system capable of receiving a nearly unlimited number of odorous substances and pheromones. This enormous task is accomplished by olfactory sensory neurons (OSNs) arranged in several chemosensory compartments in the nose. The sensitive and selective responsiveness of OSNs to odorous molecules and pheromones is based on distinct receptors in their chemosensory membrane; consequently, olfactory receptors play a key role for a reliable recognition and an accurate processing of chemosensory information. They are therefore considered as key elements for an understanding of the principles and mechanisms underlying the sense of smell. The repertoire of olfactory receptors in mammals encompasses hundreds of different receptor types which are highly diverse and expressed in distinct subcompartments of the nose. Accordingly, they are categorized into several receptor families, including odorant receptors (ORs), vomeronasal receptors (V1Rs and V2Rs), trace amine-associated receptors (TAARs), formyl peptide receptors (FPRs), and the membrane guanylyl cyclase GC-D. This large and complex receptor repertoire is the basis for the enormous chemosensory capacity of the olfactory system.

Keywords: olfaction, G protein-coupled receptor, odorant, pheromone, vomeronasal, trace amine-associated receptor, formyl peptide receptor, guanylyl cyclase

INTRODUCTION

For survival and reproduction, animals have to recognize a multitude of odorous substances related to food, predators and mating partners. Accordingly, their sense of smell has the capacity to detect and discriminate an almost unlimited number of chemical compounds. This is accomplished by an elaborated olfactory system composed of several chemosensory subsystems, including the main olfactory epithelium (MOE), the vomeronasal organ (VNO), the septal organ (SO), and the Grueneberg ganglion (GG) (**Figure 1**; reviewed by Breer et al., 2006; Spehr et al., 2006; Ma, 2007; Munger et al., 2009). In these nasal compartments, the recognition of odorous compounds is based on highly specialized chemosensory cells, the olfactory sensory neurons (OSNs). The observation that a given odorant stimulates only a subset of OSNs (Sicard and Holley, 1984) has led to the concept that the responsiveness of individual OSNs to distinct odorants is determined by specialized receptors in their chemosensory membranes. Comprehensive research throughout the past two decades has led to the discovery of an unexpected large repertoire of olfactory receptors which is considered as the molecular basis for the enormous capacity of the olfactory system to detect and discriminate myriads of odorous compounds. Based on their structure and topographic distribution, this repertoire of olfactory receptors is categorized into several receptor families which include the odorant receptors (ORs), the vomeronasal receptors (V1Rs and V2Rs), trace amine-associated receptors (TAARs), formyl peptide receptors (FPRs), and the guanylyl cyclase GC-D (**Figure 1**). In line with the finding that odor detection depends on G protein-mediated pathways (Pace et al., 1985; Pace and Lancet, 1986; Sklar et al., 1986; Belluscio et al., 1998), most of these receptors belong to the large superfamily of G protein-coupled receptor proteins (GPCRs) which are characterized by seven transmembrane domains (**Figure 2**). Nevertheless, olfactory receptors constitute a highly divergent group of receptors, consistent with the structural diversity of odorous compounds. In this review, structural features and functional implications of the olfactory receptor families are discussed and their common as well as their specific features are summarized.

ODORANT RECEPTORS (ORs)

STRUCTURAL FEATURES OF RECEPTOR PROTEINS

The structure of OR proteins is characterized by seven hydrophobic, putative membrane-spanning domains, the hallmark of all GPCRs. Based on their primary sequence, GPCRs are categorized into three classes: A, B or C (Jacoby et al., 2006). According to this classification, due to their domain organization, the ORs belong to GPCR class A, like e.g. rhodopsin (Jacoby et al., 2006). OR proteins have an average length of about 320 ± 25 amino acids residues; the differences in length result mainly from variable N- and C-terminal stretches. The N-terminal region which is exposed extracellularly contains a well conserved NXS/T consensus for N-linked glycosylation.

ORs are distinguishable from other GPCRs by several conserved amino acid motifs; these include an LHTPMY motif within the first intracellular loop, the most characteristic MAYDRYVAIC motif at the end of transmembrane (TM) domain 3 (TM3), a very short SY motif at the end of TM5, an FSTCSSH stretch at the beginning of TM6 and PMLNPF in TM7. Although these sequences are slightly different between species they were used to identify OR genes from many genomes. Extensive comparative analyses have identified more than 80 short motifs (Liu et al., 2003; Zhang et al., 2007), some of which are specific for distinct subfamilies or species and have been implicated in ligand binding. Seven cysteine residues are well conserved, a couple of them are thought to play a

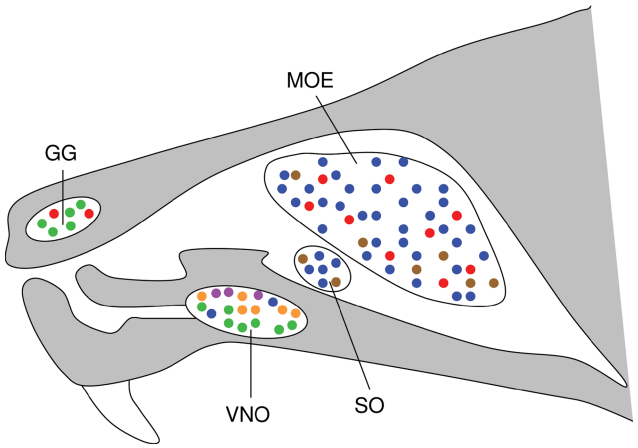

FIGURE 1 | Different olfactory compartments in the nose express distinct types of olfactory receptors. Schematic representation of the murine nose and its olfactory subsystems, including the main olfactory epithelium (MOE), the vomeronasal organ (VNO), the septal organ (SO), and the Grueneberg ganglion (GG). The olfactory receptor types expressed in each of these organs are indicated by color: ORs in blue, V1Rs in orange, V2Rs in green, TAARs in red, FPRs in purple, GC-D in brown (modified from Fleischer et al., 2007).

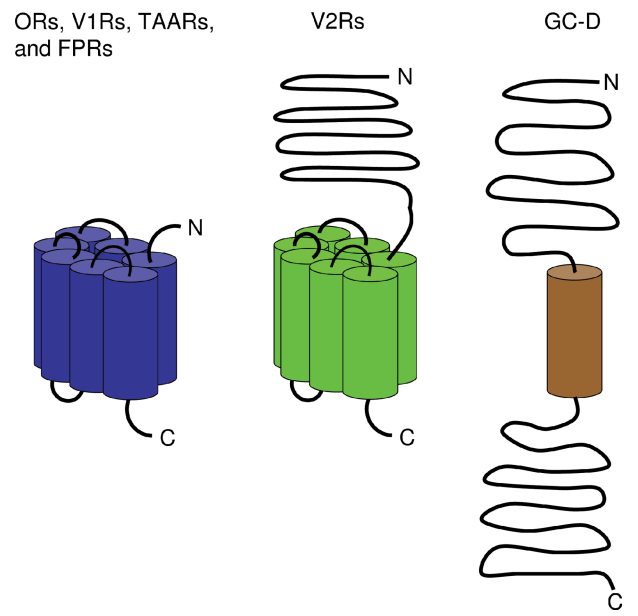

FIGURE 2 | Membrane topology of olfactory receptors. While ORs, V1Rs, V2Rs, TAARs, and FPRs belong to the GPCRs which encompass seven transmembrane domains (indicated by cylinders), guanylyl cyclase GC-D comprises only one transmembrane domain. In all these receptor types, the N-terminus is localized to the extracellular face of the cell membrane whereas the C-terminal end resides intracellularly. Unlike other olfactory receptors and similar to GC-D, V2Rs are endowed with a large N-terminal extracellular domain. In contrast to other olfactory receptors, GC-D also possesses a large C-terminal intracellular region.

role in maintaining the structural integrity of the protein. Two of these (at positions 97 and 179) are common to all GPCRs and are believed to form a disulfide link between extracellular loops 1 and 2; the other five are unique to ORs.

Although ORs in general are rather uniform in size and membrane topology, there are exceptions to this rule. A prominent one is represented by the so-called 'OR37' subfamily, which is characterized by an unusual third extracellular loop, which is six residues longer than in all other ORs (Kubick et al., 1997). Although only a few additional residues are present, they extend this loop – which is generally short – by about one-third.

Odor binding

Since the discovery of the OR genes by Buck and Axel (1991), many studies have been performed to identify the binding sites of the receptor proteins for odorous ligands. The first indications which protein domains are relevant for ligand interaction came already from the very initial sequence alignments which revealed that transmembrane domains were the most variable ones (Buck and Axel, 1991); this notion was subsequently confirmed employing larger receptor repertoires and bioinformatic approaches (Singer et al., 1996; Krautwurst et al., 1998; Zhao et al., 1998). The sequence variability of these domains thus was considered as the basis for the wide spectrum of odorous ligands that can be recognized by the receptor repertoire. Subsequent studies revealed that the most variable residues are oriented towards the inner surface of the receptor protein, whereas hydrophobic residues tended to point towards the protein/lipid interface. Using bioinformatic approaches, distinct residues have been defined which might be involved in ligand binding (Pilpel and Lancet, 1999; Lapidot et al., 2001; Katada et al., 2005; Khafizov et al., 2007); several of them could be confirmed experimentally by site-directed mutagenesis (Katada et al., 2005; Abaffy et al., 2007). All these data indicate that amino acid positions mainly in TM3, TM5 and TM6 are essential and strongly support the concept that predominantly the transmembrane domains of the OR protein form the binding pocket for odorants. The notion that a particular OR type may have a rather broad receptive range is supported by the finding that almost all analyzed ORs recognize not only a single, but multiple chemical compounds (e.g. Raming et al., 1993; Malnic et al., 1999; Araneda et al., 2000; Bozza et al., 2002; Gaillard et al., 2002; Mombaerts, 2004; Grosmaitre et al., 2006; Malnic, 2007; Touhara, 2007; Saito et al., 2009).

Activation/signaling

With respect to ligand binding, ORs seem to resemble rhodopsin and related GPCRs. These GPCRs exist in one of two main conformations: an inactive and an active conformation which interacts with an intracellular heterotrimeric G protein. The transition between these conformations occurs through a movement of membrane-spanning domains. The conformational changes of a receptor that are elicited upon an interaction with a suitable odor molecule are not fully understood; however, a recent study has indicated the important role of distinct residues in an intracellular loop and the C-terminal domain (Kato et al., 2008). In this context also the DRY motif positioned at the cytoplasmic end of TM3 appears to be essential for G protein activation. Mutations within this motif caused either a constitutive activity or abolished G protein coupling (Imai et al., 2006). Based on this activation pattern, it has been proposed that upon ligand binding to the receptor, the third helix is displaced, thereby exposing the DRY motif and initiating the signal transduction pathway (Vaidehi et al., 2002; Katada et al., 2005).

Interestingly, *in vitro*, ORs can couple to various G proteins, such as $G\alpha_{olf}$, $G\alpha_{s}$ and $G\alpha_{15}$ (Kajiya et al., 2001) and there are indications that the interaction of a receptor with a non-typical G protein, such as $G\alpha_{15}$ instead of $G\alpha_{olf}$, can alter the ligand specificity of an OR (Shirokova et al., 2005). However, although various Gα genes are expressed in OSNs, it is well established that $G\alpha_{olf}$ plays the major role in the chemo-electrical transduction process (Belluscio et al., 1998): odorant-activated ORs signal through $G\alpha_{olf}$ which then stimulates the adenylyl cyclase type III (ACIII), leading to a rise in cAMP concentration and opening of calcium-permeable cyclic nucleotide-gated (CNG) channels.

GENE STRUCTURE AND ORGANIZATION

OR genes have a rather unusual structure with an intronless coding region. The up- and down-stream non-coding exons are usually short, as well as the corresponding introns. Thus the transcription start site on one end and the polyadenylation signal on the other side are located in close proximity (1–10 kb) to the coding sequence. By these features, OR genes form very compact units; such an organization is supposed to favor the evolutionary dynamics of this gene family (see below). The upstream exons of several OR genes were shown to be alternatively spliced, resulting in different isoforms of OR mRNAs which, however, lead to the same protein (Asai et al., 1996; Sosinsky et al., 2000; Hoppe et al., 2003; Volz et al., 2003; Young et al., 2003).

OR genes are widely dispersed in the mammalian genomes and found on virtually all chromosomes. They generally reside at numerous locations with largely differing numbers of genes at each locus. In general, the OR clusters do not include non-OR interspersed genes. The intergenic distances vary from less than 5 kb to more than 50 kb depending on the amount of inserted repetitive sequences. Numerous clusters have meanwhile been analyzed in detail (Ben Arie et al., 1994; Glusman et al., 1996; Brand-Arpon et al., 1999; Sosinsky et al., 2000; Xie et al., 2000; Lane et al., 2001; Zhang and Firestein, 2002) indicating that each of them may contain members of several subfamilies or even families, suggesting that OR clusters have evolved through duplication of ancient precursor genes, as well as more recent duplications within gene clusters. Alternatively, genes of a given subfamily may be found in several clusters, suggesting that clusters may have been partly or completely duplicated. A high proportion of cluster sequences belongs to various families of interspersed repetitive elements. These repeats are believed to play a role in the numerous transposition/duplication events encountered in the OR repertoire during evolution.

RECEPTOR REPERTOIRES

OR genes have meanwhile been identified from numerous vertebrate species including many mammals like human, mouse, rat, dog, cow, opossum, and platypus.

Classes

Based on phylogenetic analyses, the mammalian ORs can be classified into two different groups: class I and class II. This classification is based on the original finding that the frog (*Xenopus laevis*) has two different groups of ORs: one (class I) that is similar to fish ORs and a second (class II) similar to mammalian ORs (Freitag et al., 1995). Interestingly, a comparison of the structural features of both receptor classes from various species revealed that they differ mainly in the sequence of the second extracellular loop, and it was suggested that this loop may contribute to their ligand specificity (Freitag et al., 1998). In mammals the majority of the ORs belong to class II, but mammals do also have class I ORs (Zhang and Firestein, 2002; Tsuboi et al., 2006). Actually, more than 100 class I ORs are present e.g. in humans and mice; surprisingly, a large fraction of them are potentially functional (Niimura and Nei, 2005), suggesting that some ancient ORs were maintained and may even serve a special role in mammals.

Families and subfamilies

The complete OR gene repertoires have been characterized in several mammalian species (e.g. human, chimpanzee, mouse, rat, dog, cow, opossum, and platypus) (Glusman et al., 2001; Young and Trask, 2002; Zhang and Firestein, 2002; Godfrey et al., 2004; Malnic et al., 2004; Olender et al., 2004; Zhang et al., 2004, 2007; Quignon et al., 2005; Grus et al., 2007) demonstrating that the OR gene family is by far the largest in vertebrate genomes. ORs have been grouped in families (sequence similarity > 40%) and subfamilies (similarity > 60%). Due to the level of receptor diversification, there are large numbers of subfamilies.

Evolution

The number of OR sequences (functional and nonfunctional genes) present in the genome ranges between about 1,500 in macrosmatic species like e.g. dog or mouse and about 800 in the microsmatic primates. A rather small repertoire of functional OR genes exists in human (387) and platypus (262) (Young and Trask, 2002; Grus et al., 2007), the largest are currently known from rat (1,284) and mouse (1,194) (Zhang et al., 2007).

During mammalian evolution, many OR genes have been gained and lost (Niimura and Nei, 2007). The large turnover of OR genes in vertebrate evolution probably reflects the functional requirement for different olfactory abilities in different evolutionary lineages. The largest gene family expansion occurred in the marsupial lineage, with at least 750 novel genes. Similarly, more than 400 genes were gained in the rodent lineage. On the other hand, in the primate lineage, the number of genes that were lost is much greater than that in other lineages (Gilad et al., 2003).

EXPRESSION

OR genes are mainly expressed in OSNs of the MOE. The consensus view is that only one OR gene is expressed per OSN (monogenic). It has been shown in mice that this expression is also monoallelic, i.e. either the maternal or the paternal allele is expressed in one particular OSN (Chess et al., 1994; Mombaerts et al., 1996; Strotmann et al., 2000; Shykind, 2005). A given OR gene is expressed by a few thousand OSNs, which are usually widely scattered within a particular spatial zone of the MOE (Ressler et al., 1993; Vassar et al., 1993; Iwema et al., 2004; Miyamichi et al., 2005). Only for a few OR genes, a different pattern has been shown (Strotmann et al., 1992; Pyrski et al., 2001). A small subset of OR genes is not only expressed in the MOE, but also in other chemosensory organs, like the VNO (Levai et al., 2006) and the septal organ (Kaluza et al., 2004; Tian and Ma, 2004) or even broadly in tissues which are not involved in chemsosensation (Feldmesser et al., 2006), like e.g. sperm cells

(Parmentier et al., 1992; Branscomb et al., 2000; Spehr et al., 2003; Fukuda and Touhara, 2006), autonomic ganglia (Weber et al., 2002) or cells of the cortex (Otaki et al., 2003); their functional role in these tissues is largely elusive.

VOMERONASAL RECEPTORS (VRs)

Vomeronasal receptors (VRs) are classified into two major groups, V1Rs and V2Rs.

V1Rs

STRUCTURAL FEATURES OF RECEPTOR PROTEINS

The V1Rs, like the ORs, belong to class A of the GPCRs; however, they lack significant sequence homology to any other receptor from this rhodopsin-like receptor group, except for a weak relationship with the so-called T2Rs, the bitter taste receptors. In retrospect, it is therefore obvious that the V1R genes could not be uncovered by employing the homology-based approaches which had been successful for identifying the OR gene family. Instead, comparative hybridization of cDNA libraries from individual vomeronasal sensory neurons (VSNs) led to the discovery of this receptor family (Dulac and Axel, 1995). A characteristic feature of the V1Rs is their high degree of sequence diversity; only TM3 is rather well conserved and this domain is in fact under a strong negative selection pressure, i. e. selection against amino acid changes (Lane et al., 2002; Rodriguez et al., 2002). Also, a potential glycosylation site in extracellular loop 2 is rather well conserved. However, characteristic sequence motifs common to all V1R family members, as found for the ORs, are basically missing. Those that have been described are largely specific for distinct V1R families (Zhang et al., 2007). The highest sequence variability is found in TM2 and in the extracellular loops 2 and 3. The highest positive selective pressure, i.e. selection in favour of change, was surprisingly found in the first intracellular loop (Lane et al., 2002). The reason for this is currently unclear, since this domain is most likely not involved in ligand interaction.

Ligand binding and downstream signaling

Due to the similarities of the V1R membrane topology with that of the ORs, it is currently believed that the ligand binding sites – like in ORs – are located within the transmembrane regions; however, no residues that represent docking sites for ligands have been defined. Altogether, the knowledge about ligands for distinct V1Rs is still very sparse, which is mainly due to the fact that no mammalian V1R could be expressed in heterologous cells, yet. However, by means of single cell imaging and patch-clamp recordings from identified VSNs that co-express the V1R2b along with green fluorescent protein (GFP), Boschat et al. (2002) could identify 2-heptanone as a compound that activates these cells. Based on the concept that each VSN expresses only one V1R type, 2-heptanone was thus allotted as a ligand to this receptor. Interestingly, compounds which are structurally related to 2-heptanone did not activate V1R2b-expressing cells, arguing in favour of a high selectivity of this receptor. Optical imaging experiments on VNO sections independently demonstrated that distinct VSNs are activated only by very few, in the extreme by a single compound (Leinders-Zufall et al., 2000), suggesting that the respective V1Rs expressed by these cells are rather narrowly tuned. Increasing the concentrations of compounds did not activate more VSNs (Leinders-Zufall et al., 2000) – in contrast to what is generally observed for OSNs in the MOE (Duchamp-Viret et al., 1999; Malnic et al., 1999) – further supporting this concept. Altogether, this contrasts with the relatively unspecific ligand spectrum of ORs which are generally activated by many different molecules. It thus seems conceivable that structural features of V1Rs are distinct from ORs, making their binding pocket rather rigid compared to the binding pocket of ORs which can accommodate several ligands.

In V1R-expressing VSNs several subunits of heterotrimeric G proteins have been indentified including $G\alpha_{i2}$, $G\alpha_{o}$, $G\alpha_{q/11}$, $G\beta_{2}$ and $G\gamma_{2}$ (Berghard and Buck, 1996; Jia and Halpern, 1996; Runnenburger et al., 2002; Wekesa et al., 2003). In fact, $G\alpha_{i2}$, $G\alpha_{o}$ and $G\alpha_{q/11}$ have been found to be located in the microvilli of VSNs (Berghard and Buck, 1996; Liman et al., 1999; Menco et al., 2001). Nevertheless, it is currently not known which of these subunits is actually directly interacting with the V1Rs; thus, their precise roles in the transduction process are still elusive.

GENE STRUCTURE AND ORGANIZATION

Similar to what is known for the OR genes, the coding region of the V1R genes spans about 900 basepairs and is included in a single exon. Although additional 5′ non-coding exons have been identified for several V1R genes (Lane et al., 2002), the transcriptional start site is generally positioned only a few (~5) kilobases upstream of the coding region; thus, V1R genes represent equally compact units as OR genes.

The genomic organization of the V1R repertoire has been studied most comprehensively in rodents (Rodriguez et al., 2002; Zhang et al., 2004, 2007). In the mouse, almost all V1R genes are arranged in clusters; there are only a few exceptions. The clusters rarely contain non-V1R genes, however, they appear to be densely populated with repetitive elements, mostly members of the *Line1* (L1) repeat family (Lane et al., 2002; Kambere and Lane, 2009). In one cluster residing on chromosome 6, an additional homology region of almost 1 kb length was found upstream of the transcription start site of each V1R gene; this observation led to the hypothesis that these conserved elements may be involved in controlling the expression of the respective V1R genes. The fact that they are associated exclusively with the V1R genes from this particular cluster suggested some kind of locus-specific transcriptional regulation.

RECEPTOR REPERTOIRES

The size of the V1R repertoire in most mammalian species investigated to date is significantly smaller than that of ORs; nevertheless, the 100–300 members found e.g. in rodents and marsupials (Zhang et al., 2004; Young et al., 2005; Shi and Zhang, 2007) still represent a relatively large group. Interestingly, the most 'ancient' mammal – the platypus – has the largest currently known repertoire with more than 800 V1R genes (Grus et al., 2007). Even in species with a pronounced communication by pheromones, like rodents, a large fraction of the V1R genes are pseudogenes. Extreme examples are humans and dogs which have only 5 or 8 potentially functional V1R genes (Rodriguez et al., 2000; Rodriguez and Mombaerts, 2002; Grus et al., 2005). There is substantial evidence that the VNO is not functional in adult humans, e.g. no axonal connections of VSNs to the brain were found (Meredith, 2001) and the gene encoding the TRPC2 channel, which is crucial for the VNO function,

is a pseudogene in humans (Liman and Innan, 2003; Zhang and Webb, 2003). In this context, it is not at all surprising that most V1R genes are pseudogenes in humans and the question arises what may be the function of the five potentially intact V1R genes. The finding that one of them is expressed in the MOE (Rodriguez et al., 2000) could be meaningful. A limited role of the VNO has also been proposed for the dog, and may even be pertinent for all carnivores (Grus et al., 2005). There is yet no final answer to the question why the V1R repertoires are so different in size; it has been speculated that rodents with their high numbers of V1Rs might be the exception rather than the rule.

Evolution

The V1Rs of a particular species can be grouped into distinct families which – in sharp contrast to the OR families – are phylogenetically very divergent from each other with amino acid identities of only about 15%. Within each family, however, a greater identity of up to 70% is found. As mentioned before, the size of the V1R repertoires in different species is highly divergent. A detailed study performed by Lane et al. (2002) suggested that the *L1* repeats may have promoted rearrangement events which led to the V1R expansion in the mouse. Interestingly, the activity of these *L1* elements appeared to coincide with the mouse/rat divergence and it was therefore proposed that such molecular events played a role in the speciation process by generating the species-specific V1R repertoires. In fact most V1Rs do not have orthologs in other species; in other words, the V1R repertoires are not only largely different in size, but moreover also in sequence.

EXPRESSION

The V1Rs are expressed in VSNs whose cell bodies are located in the apical layer of the VNO (Dulac and Axel, 1995). Each VSN expresses a single subtype from the repertoire, furthermore – as with the OR genes – only one allele is chosen by an individual cell (Rodriguez et al., 1999). The V1R proteins are found in the dendritic endings of VSNs (Takigami et al., 1999) such that they are in contact with the VNO lumen which is a liquid-filled, blind-ending tube (Halpern and Martinez-Marcos, 2003). A few V1R transcripts have been detected in the MOE of humans and goats (Rodriguez et al., 2000; Wakabayashi et al., 2002); however, it is currently uncertain whether there are in fact V1R proteins.

V2Rs

The fact that V1R genes are expressed exclusively in the apical $G\alpha_{i2}$-positive layer of the VNO suggested that the $G\alpha_o$-positive VNS in the basal layers may express other GPCR subtypes. Indeed, an additional multigene GPCR family was discovered which is expressed in $G\alpha_o$-positive VSNs (Herrada and Dulac, 1997; Matsunami and Buck, 1997; Ryba and Tirindelli, 1997); accordingly, they were named V2Rs. In these cells, the V2R proteins are localized to the dendritic terminals (Martini et al., 2001). One particular V2R subtype – V2r83 – is also expressed outside the VNO in neurons of the GG (Fleischer et al., 2006).

STRUCTURAL FEATURES OF RECEPTOR PROTEINS

Unlike ORs and V1Rs, the V2Rs belong to the class C of GPCRs. A characteristic feature of class C receptors, which also include the taste receptors for sweet/umami, the metabotropic glutamate receptors, and the Ca^{2+}-sensing receptor is their large (~70 kDa) N-terminal extracellular domain (Pin et al., 2003); this domain is joined to the heptahelical transmembrane part of the receptor protein via a cysteine-rich linker region. Typically, class C receptors dimerize via hydrophobic stretches which are present within the long N-terminal domain. It has therefore been proposed that also the V2Rs dimerize (Martini et al., 2001); a direct proof for this concept is still missing. Most of the V2R genes are expressed in a mutually exclusive manner in small subpopulations of VSNs. In these cells, they appear to be co-expressed with a receptor belonging to the so-called V2R2 family of V2Rs – a distinct family of V2Rs (also designated as family C of V2Rs) – whose members are present in an exceptionally high number of VNO neurons (Martini et al., 2001; Yang et al., 2005; Silvotti et al., 2007), indicating that VSNs in the basal layer express two distinct V2Rs.

Some V2Rs seem to require additional interaction partners. It was found that individual V2R-expressing VSNs also express particular members of non-classical major histocompatibility complex (MHC) class Ib genes (Ishii et al., 2003; Loconto et al., 2003). It has been demonstrated that these MHC molecules, together with the β2-microglobulin, are necessary for escorting distinct V2Rs to the plasma membrane and it was proposed that they might form a multimolecular complex at the membrane (Loconto et al., 2003). More recently, it was reported, however, that defined V2Rs are correctly targeted to the plasma membrane also in the absence of MHC1b proteins (Ishii and Mombaerts, 2008) and furthermore, that MHC1b genes are present only in rodents (Shi and Zhang, 2007). These findings suggest that the concept of V2Rs forming complexes with immune system-related proteins may not be generally applicable.

Ligand binding

V2Rs possess a long extracellular N-terminus (Herrada and Dulac, 1997; Matsunami and Buck, 1997; Ryba and Tirindelli, 1997), suggesting a special mode of ligand recognition. Indeed, it has been shown for GPCRs of class C that this domain forms a Venus flytrap-like structure to which the ligand can bind (Bridges and Lindsley, 2008). Whether V2Rs employ the same mechanism is unclear. Specific ligands for distinct V2Rs have not even been identified, yet. In view of other class C GPCRs, V2R ligands are probably well soluble in water, rather than very hydrophobic molecules. In this context, it is intriguing that many other class C receptors bind amino acids, even the Ca^{2+}-sensing receptor (Conigrave et al., 2000). Consistent with this knowledge an *in vitro* study has provided evidence that in the rat VNO, protein pheromones activated the $G\alpha_o$ subunit (Krieger et al., 1999). Due to these considerations, the major urinary proteins (MUPs) have been viewed as promising candidates for V2R ligands (Dulac and Torello, 2003; Cheetham et al., 2007; Sherborne et al., 2007); however, the MUPs belong to the group of lipocalins which are rather carriers of small hydrophobic molecules; so this concept is still under debate. A recent study revealed, however, that purified MUPs alone are in fact sufficient to activate dissociated $G\alpha_o$-positive VSNs (Chamero et al., 2007). It is noteworthy that in the V2R2s – but not in the other V2Rs – the residues to which amino acids bind and which are thus present in almost all other class C GPCRs, are conserved (Silvotti et al., 2005).

Other potential V2R ligands identified so far are peptides. Two distinct groups of peptides were shown to activate V2R-expressing VSNs: on one hand members from the exocrine gland-secreting peptide (ESP) family (Kimoto et al., 2005) and on the other hand, the MHC class I peptides (Leinders-Zufall et al., 2004), small peptides that are presented by MHC proteins at the cell surface. This finding may be relevant for the fact that mice can discriminate the body odors of conspecifics which are genetically different only in the MHC haplotype (Yamaguchi et al., 1981).

GENE STRUCTURE AND ORGANIZATION

V2R genes are also organized in clusters which are distributed on several chromosomes. The organization of individual V2R genes, however, is much more complex. The coding sequence of V2Rs is comprised of several exons, a unique feature among the olfactory GPCRs; this greatly increases the length (~20 kb) of individual genes and complicates the extraction of V2R coding sequences from genomic databases (Yang et al., 2005). Therefore, our current knowledge about the repertoires and evolution of V2R genes in mammals are still rather limited. The V2R repertoire in rodents comprises more than 200 members; it is slightly smaller in marsupials and in platypus (Shi and Zhang, 2007; Young and Trask, 2007). Again, similar to what has been found for the V1R repertoire, a very large part of the respective V2R genes are pseudogenes. In each species, the genes can be grouped into distinct families. Interestingly, in the mouse, one family is extremely large and comprises almost all (80%) of the V2R genes, whereas another one is very small with only four members. Surprisingly, in some mammalian species, like dog and cow, the V2R repertoire is completely degenerated (Young and Trask, 2007). In those species which have lost all of their functional V2R genes, usually one member from the V2R2 family is still present and contains only very few mutations, indicating a very recent pseudogenization event (Young and Trask, 2007).

TRACE AMINE-ASSOCIATED RECEPTORS (TAARs)

Searching for novel receptors, Borowsky et al. (2001) accidentally identified a group of GPCRs which are characterized by distinct sequence motifs (Lindemann and Hoener, 2005; Lindemann et al., 2005; Hussain et al., 2009; see below). Due to their activation by trace amines (Borowsky et al., 2001; Bunzow et al., 2001), such as β-phenylethylamine, p-tyramine, tryptamine, and octopamine, they were initially designated as trace amine receptors (TAs or TARs). Since it is more than doubtful that all members of this receptor family are sensitive to trace amines (Borowsky et al., 2001; Lindemann et al., 2005), they are now designated as trace amine-associated receptors (TAARs) (Lindemann and Hoener, 2005; Lindemann et al., 2005; Lewin, 2006). The coding sequence of TAAR genes – like those for ORs and V1Rs – encompasses about 1 kb and represents a single exon (Lindemann et al., 2005). TAARs reveal structural hallmarks characteristic of the rhodopsin/β-adrenergic receptor superfamily, including short N- and C-terminal domains. Nevertheless, in line with their clustered genomic localization and a characteristic fingerprint motif in TM7, TAARs represent a well-defined, coherent receptor family (Lindemann et al., 2005). Compared to ORs, the number of distinct TAAR subtypes is rather low (15 TAARs in mice and 6 TAARs in humans; Lindemann et al., 2005).

TAARs are strongly expressed in the murine MOE and each TAAR subtype (except TAAR1) is expressed by a small subset of OSNs in a mutually exclusive manner, i.e., each cell expresses one TAAR type only. OSNs expressing a given TAAR subtype are distributed in the MOE in a manner reminiscent of the zonal expression pattern of ORs (Liberles and Buck, 2006). In addition to the MOE, some TAARs are also present in a distinct population of neurons in the GG (Fleischer et al., 2007). TAARs are activated by certain amine ligands (Borowsky et al., 2001; Bunzow et al., 2001; Liberles and Buck, 2006). Some of these amines are present in mouse urine in gender- or stress-dependent concentrations, leading to speculations that TAARs might be involved in the detection of some 'urine-borne' pheromones (Liberles and Buck, 2006). The signaling elements downstream of TAARs are unknown. In the murine MOE, TAARs are co-expressed with the $G\alpha_s$-related G protein $G\alpha_{olf}$ (Liberles and Buck, 2006); in the GG, however, TAARs are co-expressed with $G\alpha_{i2}$ (Fleischer et al., 2007).

FORMYL PEPTIDE RECEPTORS (FPRs)

Two decades ago, a novel group of GPCRs called formyl peptide receptors (FPRs) was discovered (Boulay et al., 1990). FPR-encoding genes are clustered on a single chromosome (human chromosome 19 and mouse chromosome 17; reviewed by Migeotte et al., 2006). Their coding sequences are intronless and their open reading frames encode proteins of about 350 amino acid residues (Gao et al., 1998; Wang and Ye, 2002) with highly conserved transmembrane domains and more variable extracellular domains; the latter are supposed to be involved in ligand binding (Migeotte et al., 2006). FPRs were reported to be expressed in diverse tissues (reviewed by Migeotte et al., 2006; Panaro et al., 2006). Most recently, it has been shown that out of the seven murine FPR subtypes, some are predominantly expressed in the VNO. In fact, each of these FRP subtypes is expressed in about 1% of the VNO sensory neurons; apparently, these cells do not co-express vomeronasal receptors (Riviere et al., 2009).

In cells of the immune system, FPRs were found to be activated by their name-giving ligands, formylated peptides, which are released by bacteria; moreover, FPRs also bind to some other peptides and proteins associated with disease or inflammation (reviewed by Migeotte et al., 2006; Panaro et al., 2006; Le et al., 2007). For the FPR subtypes expressed in the VNO, it was observed that they are also activated by formylated peptides and other disease-related compounds which also induced responses in subsets of VNO sensory neurons, indicating that these cells might allow detection of infected conspecifics or contaminated food (Riviere et al., 2009).

MEMBRANE GUANYLYL CYCLASE GC-D

Among the various membrane guanylyl cyclases, subtype GC-D was found to be expressed in a subset of OSNs in the MOE which are therefore designated as GC-D neurons (Fülle et al., 1995; Juilfs et al., 1997). These cells lack signaling elements characteristic of the canonical cAMP pathway in OSNs of the MOE. Instead, they are endowed with the cGMP-dependent phosphodiesterase PDE2A and a cGMP-sensitive cyclic nucleotide-gated ion channel (Juilfs et al., 1997; Meyer et al., 2000; Hu et al., 2007). In addition to GC-D neurons in the MOE, GC-D is also expressed in some neurons of the septal organ (Walz et al., 2007). Similar to other OSNs, GC-D

neurons project their axons to the olfactory bulb where they converge on distinct glomeruli; these glomeruli encircle the caudal olfactory bulb and are therefore called 'necklace glomeruli' (Juilfs et al. 1997; Hu et al., 2007; Leinders-Zufall et al., 2007; Walz et al., 2007). In GC-D neurons, GC-D is mainly localized to apical cilia which are considered as the principal site of odor detection; this finding suggests an olfactory role of GC-D (Juilfs et al., 1997). In search of the chemosensory role of GC-D, it was found that the urinary peptides uroguanylin and guanylin activate GC-D neurons in a GC-D-dependent manner (Leinders-Zufall et al., 2007). The notion that GC-D is a receptor for such peptides was lately supported by studies on cells heterologously expressing GC-D (Duda and Sharma, 2008). Other findings indicate that GC-D may also be involved in the detection of carbon dioxide (CO_2), since GC-D neurons – in contrast to other OSNs – respond to low concentrations of CO_2 (Hu et al., 2007; Sun et al., 2009). It is supposed that CO_2 is converted into bicarbonate in GC-D neurons via carbonic anhydrase and that bicarbonate then activates GC-D (Hu et al., 2007; Guo et al., 2009; Sun et al., 2009). In contrast to rodents, CO_2 is odorless to humans. In this context, it is interesting to note that in humans and several other primate species, the GC-D gene is a pseudogene (Young et al., 2007).

ACKNOWLEDGEMENTS

This work was supported by the Deutsche Forschungsgemeinschaft.

REFERENCES

Abaffy, T., Malhotra, A., and Luetje, C. W. (2007). The molecular basis for ligand specificity in a mouse olfactory receptor: a network of functionally important residues. *J. Biol. Chem.* 282, 1216–1224.

Araneda, R. C., Kini, A. D., and Firestein, S. (2000). The molecular receptive range of an odorant receptor. *Nat. Neurosci.* 3, 1248–1255.

Asai, H., Kasai, H., Matsuda, Y., Yamazaki, N., Nagawa, F., Sakano, H., and Tsuboi, A. (1996). Genomic structure and transcription of a murine odorant receptor gene: differential initiation of transcription in the olfactory and testicular cells. *Biochem. Biophys. Res. Commun.* 221, 240–247.

Belluscio, L., Gold, G. H., Nemes, A., and Axel, R. (1998). Mice deficient in G(olf) are anosmic. *Neuron* 20, 69–81.

Ben Arie, N., Lancet, D., Taylor, C., Khen, M., Walker, N., Ledbetter, D. H., Carrozzo, R., Patel, K., Sheer, D., Lehrach, H., and North, M. A. (1994). Olfactory receptor gene cluster on human chromosome 17: possible duplication of an ancestral receptor repertoire. *Hum. Mol. Genet.* 3, 229–235.

Berghard, A., and Buck, L. B. (1996). Sensory transduction in vomeronasal neurons: evidence for G alpha o, G alpha i2, and adenylyl cyclase II as major components of a pheromone signaling cascade. *J. Neurosci.* 16, 909–918.

Borowsky, B., Adham, N., Jones, K. A., Raddatz, R., Artymyshyn, R., Ogozalek, K. L., Durkin, M. M., Lakhlani, P. P., Bonini, J. A., Pathirana, S., Boyle, N., Pu, X., Kouranova, E., Lichtblau, H., Ochoa, F. Y., Branchek, T. A., and Gerald, C. (2001). Trace amines: identification of a family of mammalian G protein-coupled receptors. *Proc. Natl. Acad. Sci. U.S.A.* 98, 8966–8971.

Boschat, C., Pelofi, C., Randin, O., Roppolo, D., Luscher, C., Broillet, M. C., and Rodriguez, I. (2002). Pheromone detection mediated by a V1r vomeronasal receptor. *Nat. Neurosci.* 5, 1261–1262.

Boulay, F., Tardif, M., Brouchon, L., and Vignais, P. (1990). The human N-formylpeptide receptor. Characterization of two cDNA isolates and evidence for a new subfamily of G-protein-coupled receptors. *Biochemistry* 29, 11123–11133.

Bozza, T., Feinstein, P., Zheng, C., and Mombaerts, P. (2002). Odorant receptor expression defines functional units in the mouse olfactory system. *J. Neurosci.* 22, 3033–3043.

Brand-Arpon, V., Rouquier, S., Massa, H., de Jong, P. J., Ferraz, C., Ioannou, P. A., Demaille, J. G., Trask, B. J., and Giorgi, D. (1999). A genomic region encompassing a cluster of olfactory receptor genes and a myosin light chain kinase (MYLK) gene is duplicated on human chromosome regions 3q13-q21 and 3p13. *Genomics* 56, 98–110.

Branscomb, A., Seger, J., and White, R. L. (2000). Evolution of odorant receptors expressed in mammalian testes. *Genetics* 156, 785–797.

Breer, H., Fleischer, J., and Strotmann, J. (2006). The sense of smell: multiple olfactory subsystems. *Cell. Mol. Life Sci.* 63, 1465–1475.

Bridges T. M., and Lindsley, C. W. (2008). G-protein-coupled receptors: from classical modes of modulation to allosteric mechanisms. *ACS Chem. Biol.* 3, 530–541.

Buck, L., and Axel, R. (1991). A novel multigene family may encode odorant receptors: a molecular basis for odor recognition. *Cell* 65, 175–187.

Bunzow, J. R., Sonders, M. S., Arttamangkul, S., Harrison, L. M., Zhang, G., Quigley, D. I., Darland, T., Suchland, K. L., Pasumamula, S., Kennedy, J. L., Olson, S. B., Magenis, R. E., Amara, S. G., and Grandy, D. K. (2001). Amphetamine, 3,4-methylenedioxymethamphetamine, lysergic acid diethylamide, and metabolites of the catecholamine neurotransmitters are agonists of a rat trace amine receptor. *Mol. Pharmacol.* 60, 1181–1188.

Chamero, P., Marton, T. F., Logan, D. W., Flanagan, K., Cruz, J. R., Saghatelian, A., Cravatt, B. F., and Stowers, L. (2007). Identification of protein pheromones that promote aggressive behaviour. *Nature* 450, 899–902.

Cheetham, S. A., Thom, M. D., Jury, F., Ollier, W. E., Beynon, R. J., and Hurst, J. L. (2007). The genetic basis of individual-recognition signals in the mouse. *Curr. Biol.* 17, 1771–1777.

Chess, A., Simon, I., Cedar, H., and Axel, R. (1994). Allelic inactivation regulates olfactory receptor gene expression. *Cell* 78, 823–834.

Conigrave, A. D., Quinn, S. J., and Brown, E. M. (2000). L-amino acid sensing by the extracellular Ca2+-sensing receptor. *Proc. Natl. Acad. Sci. U.S.A.* 97, 4814–4819.

Duchamp-Viret, P., Chaput, M. A., and Duchamp, A. (1999). Odor response properties of rat olfactory receptor neurons. *Science* 284, 2171–2174.

Duda, T., and Sharma, R. K. (2008). ONE-GC membrane guanylate cyclase, a trimodal odorant signal transducer. *Biochem. Biophys. Res. Commun.* 367, 440–445.

Dulac, C., and Axel, R. (1995). A novel family of genes encoding putative pheromone receptors in mammals. *Cell* 83, 195–206.

Dulac, C., and Torello, A. T. (2003). Molecular detection of pheromone signals in mammals: from genes to behaviour. *Nat. Rev. Neurosci.* 4, 551–562.

Feldmesser, E., Olender, T., Khen, M., Yanai, I., Ophir, R., and Lancet, D. (2006). Widespread ectopic expression of olfactory receptor genes. *BMC Genomics* 7, 121.

Fleischer, J., Schwarzenbacher, K., Besser, S., Hass, N., and Breer H. (2006). Olfactory receptors and signalling elements in the Grueneberg ganglion. *J. Neurochem.* 98, 543–554.

Fleischer, J., Schwarzenbacher, K., and Breer, H. (2007). Expression of trace amine-associated receptors in the Grueneberg ganglion. *Chem. Senses* 32, 623–631.

Freitag, J., Krieger, J., Strotmann, J., and Breer, H. (1995). Two classes of olfactory receptors in *Xenopus laevis*. *Neuron* 15, 1383–1392.

Freitag, J., Ludwig, G., Andreini, I., Rossler, P., and Breer, H. (1998). Olfactory receptors in aquatic and terrestrial vertebrates. *J. Comp. Physiol. A* 183, 635–650.

Fukuda, N., and Touhara, K. (2006). Developmental expression patterns of testicular olfactory receptor genes during mouse spermatogenesis. *Genes Cells* 11, 71–81.

Fülle, H. J., Vassar, R., Foster, D. C., Yang, R. B., Axel, R., and Garbers, D. L. (1995). A receptor guanylyl cyclase expressed specifically in olfactory sensory neuron. *Proc. Natl. Acad. Sci. U.S.A.* 92, 3571–3575.

Gaillard, I., Rouquier, S., Pin, J. P., Mollard, P., Richard, S., Barnabe, C., Demaille, J., and Giorgi, D. (2002). A single olfactory receptor specifically binds a set of odorant molecules. *Eur. J. Neurosci.* 15, 409–418.

Gao, J. L., Chen, H., Filie, J. D., Kozak, C. A., and Murphy, P. M. (1998). Differential expansion of the N-formylpeptide receptor gene cluster in human and mouse. *Genomics* 51, 270–276.

Gilad, Y., Man, O., Paabo, S., and Lancet, D. (2003). Human specific loss of olfactory receptor genes. *Proc. Natl. Acad. Sci. U.S.A.* 100, 3324–3327.

Glusman, G., Clifton, S., Roe, B., and Lancet, D. (1996). Sequence analysis in the olfactory receptor gene cluster on human chromosome 17: recombinatorial events affecting receptor diversity. *Genomics* 37, 147–160.

Glusman, G., Yanai, I., Rubin, I., and Lancet, D. (2001). The complete human olfactory subgenome. *Genome Res.* 11, 685–702.

Godfrey, P. A., Malnic, B., and Buck, L. B. (2004). The mouse olfactory receptor

gene family. *Proc. Natl. Acad. Sci. U.S.A.* 101, 2156–2161.

Grosmaitre, X., Vassalli, A., Mombaerts, P., Shepherd, G. M., and Ma, M. (2006). Odorant responses of olfactory sensory neurons expressing the odorant receptor MOR23: a patch clamp analysis in gene-targeted mice. *Proc. Natl. Acad. Sci. U.S.A.* 103, 1970–1975.

Grus, W. E., Shi, P., and Zhang, J. (2007). Largest vertebrate vomeronasal type 1 receptor gene repertoire in the semiaquatic platypus. *Mol. Biol. Evol.* 24, 2153–2157.

Grus, W. E., Shi, P., Zhang, Y. P., and Zhang, J. (2005). Dramatic variation of the vomeronasal pheromone receptor gene repertoire among five orders of placental and marsupial mammals. *Proc. Natl. Acad. Sci. U.S.A.* 102, 5767–5772.

Guo, D., Zhang, J. J., and Huang, X. Y. (2009). Stimulation of guanylyl cyclase-D by bicarbonate. *Biochemistry* 48, 4417–4422.

Halpern, M., and Martinez-Marcos, A. (2003). Structure and function of the vomeronasal system: an update. *Prog. Neurobiol.* 70, 245–318.

Herrada, G., and Dulac, C. (1997). A novel family of putative pheromone receptors in mammals with a topographically organized and sexually dimorphic distribution. *Cell* 90, 763–773.

Hoppe, R., Frank, H., Breer, H., and Strotmann, J. (2003). The clustered olfactory receptor gene family 262: genomic organization, promotor elements, and interacting transcription factors. *Genome Res.* 13, 2674–2685.

Hu, J., Zhong, C., Ding, C., Chi, Q., Walz, A., Mombaerts, P., Matsunami, H., and Luo, M. (2007). Detection of near-atmospheric concentrations of CO2 by an olfactory subsystem in the mouse. *Science* 317, 953–957.

Hussain, A., Saraiva, L. R., and Korsching, S. I. (2009). Positive Darwinian selection and the birth of an olfactory receptor clade in teleosts. *Proc. Natl. Acad. Sci. U.S.A.* 106, 4313–4318.

Imai, T., Suzuki, M., and Sakano, H. (2006). Odorant receptor-derived cAMP signals direct axonal targeting. *Science* 314, 657–661.

Ishii, T., Hirota, J., and Mombaerts, P. (2003). Combinatorial coexpression of neural and immune multigene families in mouse vomeronasal sensory neurons. *Curr. Biol.* 13, 394–400.

Ishii, T., and Mombaerts, P. (2008). Expression of nonclassical class I major histocompatibility genes defines a tripartite organization of the mouse vomeronasal system. *J. Neurosci.* 28, 2332–2341.

Iwema, C. L., Fang, H., Kurtz, D. B., Youngentob, S. L., and Schwob, J. E. (2004). Odorant receptor expression patterns are restored in lesion-recovered rat olfactory epithelium. *J. Neurosci.* 24, 356–369.

Jacoby, E., Bouhelal, R., Gerspacher, M., and Seuwen, K. (2006). The 7 TM G-protein-coupled receptor target family. *Chem. Med. Chem.* 1, 761–782.

Jia, C., and Halpern, M. (1996). Subclasses of vomeronasal receptor neurons: differential expression of G proteins (Gi alpha 2 and G(o alpha)) and segregated projections to the accessory olfactory bulb. *Brain Res.* 719, 117–128.

Juilfs, D. M., Fülle, H. J., Zhao, A. Z., Houslay, M. D., Garbers, D. L., and Beavo, J. A. (1997). A subset of olfactory neurons that selectively express cGMP-stimulated phosphodiesterase (PDE2) and guanylyl cyclase-D define a unique olfactory signal transduction pathway. *Proc. Natl. Acad. Sci. U.S.A.* 94, 3388–3395.

Kajiya, K., Inaki, K., Tanaka, M., Haga, T., Kataoka, H., and Touhara, K. (2001). Molecular bases of odor discrimination: reconstitution of olfactory receptors that recognize overlapping sets of odorants. *J. Neurosci.* 21, 6018–6025.

Kaluza, J. F., Gussing, F., Bohm, S., Breer, H., and Strotmann, J. (2004). Olfactory receptors in the mouse septal organ. *J. Neurosci. Res.* 76, 442–452.

Kambere, M. B., and Lane, R. P. (2009). Exceptional LINE density at V1R loci: the Lyon repeat hypothesis revisited on autosomes. *J. Mol. Evol.* 68, 145–159.

Katada, S., Hirokawa, T., Oka, Y., Suwa, M., and Touhara, K. (2005). Structural basis for a broad but selective ligand spectrum of a mouse olfactory receptor: mapping the odorant-binding site. *J. Neurosci.* 25, 1806–1815.

Kato, A., Katada, S., and Touhara, K. (2008). Amino acids involved in conformational dynamics and G protein coupling of an odorant receptor: targeting gain-of-function mutation. *J. Neurochem.* 107, 1261–1270.

Khafizov, K., Anselmi, C., Menini, A., and Carloni, P. (2007). Ligand specificity of odorant receptors. *J. Mol. Model.* 13, 401–409.

Kimoto, H., Haga, S., Sato, K., and Touhara, K. (2005). Sex-specific peptides from exocrine glands stimulate mouse vomeronasal sensory neurons. *Nature* 437, 898–901.

Krautwurst, D., Yau, K. W., and Reed, R. R. (1998). Identification of ligands for olfactory receptors by functional expression of a receptor library. *Cell* 95, 917–926.

Krieger, J., Schmitt, A., Lobel, D., Gudermann, T., Schultz, G., Breer, H., and Boekhoff, I. (1999). Selective activation of G protein subtypes in the vomeronasal organ upon stimulation with urine-derived compounds. *J. Biol. Chem.* 274, 4655–4662.

Kubick, S., Strotmann, J., Andreini, I., and Breer, H. (1997). Subfamily of olfactory receptors characterized by unique structural features and expression patterns. *J. Neurochem.* 69, 465–475.

Lane, R. P., Cutforth, T., Axel, R., Hood, L., and Trask, B. J. (2002). Sequence analysis of mouse vomeronasal receptor gene clusters reveals common promoter motifs and a history of recent expansion. *Proc. Natl. Acad. Sci. U.S.A.* 99, 291–296.

Lane, R. P., Cutforth, T., Young, J., Athanasiou, M., Friedman, C., Rowen, L., Evans, G., Axel, R., Hood, L., and Trask, B. J. (2001). Genomic analysis of orthologous mouse and human olfactory receptor loci. *Proc. Natl. Acad. Sci. U.S.A.* 19;98, 7390–7395.

Lapidot, M., Pilpel, Y., Gilad, Y., Falcovitz, A., Sharon, D., Haaf, T., and Lancet, D. (2001). Mouse-human orthology relationships in an olfactory receptor gene cluster. *Genomics* 71, 296–306.

Le, Y., Wang, J. M., Liu, X., Kong, Y., Hou, X., Ruan, L., and Mou, H. (2007). Biologically active peptides interacting with the G protein-coupled formyl-peptide receptor. *Protein Pept. Lett.* 14, 846–853.

Leinders-Zufall, T., Brennan, P., Widmayer, P., Chandramani, P. S., Maul-Pavicic, A., Jager, M., Li, X. H., Breer, H., Zufall, F., and Boehm, T. (2004). MHC class I peptides as chemosensory signals in the vomeronasal organ. *Science* 306, 1033–1037.

Leinders-Zufall, T., Cockerham, R. E., Michalakis, S., Biel, M., Garbers, D. L., Reed, R. R., Zufall, F., and Munger, S. D. (2007). Contribution of the receptor guanylyl cyclase GC-D to chemosensory function in the olfactory epithelium. *Proc. Natl. Acad. Sci. U.S.A.* 104, 14507–14512.

Leinders-Zufall, T., Lane, A. P., Puche, A. C., Ma, W., Novotny, M. V., Shipley, M. T., and Zufall, F. (2000). Ultrasensitive pheromone detection by mammalian vomeronasal neurons. *Nature* 405, 792–796.

Levai, O., Feistel, T., Breer, H., and Strotmann, J. (2006). Cells in the vomeronasal organ express odorant receptors but project to the accessory olfactory bulb. *J. Comp. Neurol.* 498, 476–490.

Lewin, A. H. (2006). Receptors of mammalian trace amines. *AAPS. J.* 8, E138–E145.

Liberles, S. D., and Buck, L. B. (2006). A second class of chemosensory receptors in the olfactory epithelium. *Nature* 442, 645–650.

Liman, E. R., Corey, D. P., and Dulac, C. (1999). TRP2: a candidate transduction channel for mammalian pheromone sensory signaling. *Proc. Natl. Acad. Sci. U.S.A.* 96, 5791–5796.

Liman, E. R., and Innan, H. (2003). Relaxed selective pressure on an essential component of pheromone transduction in primate evolution. *Proc. Natl. Acad. Sci. U.S.A.* 100, 3328–3332.

Lindemann, L., Ebeling, M., Kratochwil, N. A., Bunzow, J. R., Grandy, D. K., and Hoener, M. C. (2005). Trace amine-associated receptors form structurally and functionally distinct subfamilies of novel G protein-coupled receptors. *Genomics* 85, 372–385.

Lindemann, L., and Hoener, M. C. (2005). A renaissance in trace amines inspired by a novel GPCR family. *Trends Pharmacol. Sci.* 26, 274–281.

Liu, A. H., Zhang, X., Stolovitzky, G. A., Califano, A., and Firestein, S. J. (2003). Motif-based construction of a functional map for mammalian olfactory receptors. *Genomics* 81, 443–456.

Loconto, J., Papes, F., Chang, E., Stowers, L., Jones, E. P., Takada, T., Kumanovics, A., Fischer, L. K., and Dulac, C. (2003). Functional expression of murine V2R pheromone receptors involves selective association with the M10 and M1 families of MHC class Ib molecules. *Cell* 112, 607–618.

Ma, M. (2007). Encoding olfactory signals via multiple chemosensory systems. *Crit. Rev. Biochem. Mol. Biol.* 42, 463–480.

Malnic, B. (2007). Searching for the ligands of odorant receptors. *Mol. Neurobiol.* 35, 175–181.

Malnic, B., Godfrey, P. A., and Buck, L. B. (2004). The human olfactory receptor gene family. *Proc. Natl. Acad. Sci. U.S.A.* 101, 2584–2589.

Malnic, B., Hirono, J., Sato, T., and Buck, L. B. (1999). Combinatorial receptor codes for odors. *Cell* 96, 713–723.

Martini, S., Silvotti, L., Shirazi, A., Ryba, N. J., and Tirindelli, R. (2001). Co-expression of putative pheromone receptors in the sensory neurons of the vomeronasal organ. *J. Neurosci.* 21, 843–848.

Matsunami, H., and Buck, L. B. (1997). A multigene family encoding a diverse array of putative pheromone receptors in mammals. *Cell* 90, 775–784.

Menco, B. P., Carr, V. M., Ezeh, P. I., Liman, E. R., and Yankova, M. P. (2001). Ultrastructural localization of G-proteins and the channel protein TRP2 to microvilli of rat vomeronasal receptor cells. *J. Comp. Neurol.* 438, 468–489.

Meredith, M. (2001). Human vomeronasal organ function: a critical review of best and worst cases. *Chem. Senses* 26, 433–445.

Meyer, M. R., Angele, A., Kremmer, E., Kaupp, U. B., and Muller, F. (2000). A

cGMP-signaling pathway in a subset of olfactory sensory neurons. *Proc. Natl. Acad. Sci. U.S.A.* 97, 10595–10600.

Migeotte, I., Communi, D., and Parmentier, M. (2006). Formyl peptide receptors: a promiscuous subfamily of G protein-coupled receptors controlling immune responses. *Cytokine Growth Factor Rev.* 17, 501–519.

Miyamichi, K., Serizawa, S., Kimura, H. M., and Sakano, H. (2005). Continuous and overlapping expression domains of odorant receptor genes in the olfactory epithelium determine the dorsal/ventral positioning of glomeruli in the olfactory bulb. *J. Neurosci.* 25, 3586–3592.

Mombaerts, P. (2004). Genes and ligands for odorant, vomeronasal and taste receptors. *Nat. Rev. Neurosci.* 5, 263–278.

Mombaerts, P., Wang, F., Dulac, C., Chao, S. K., Nemes, A., Mendelsohn, M., Edmondson, J., and Axel, R. (1996). Visualizing an olfactory sensory map. *Cell* 87, 675–686.

Munger, S. D., Leinders-Zufall, T., and Zufall, F. (2009). Subsystem organization of the mammalian sense of smell. *Annu. Rev. Physiol.* 71, 115–140.

Niimura, Y., and Nei, M. (2005). Evolutionary dynamics of olfactory receptor genes in fishes and tetrapods. *Proc. Natl. Acad. Sci. U.S.A.* 102, 6039–6044.

Niimura, Y., and Nei, M. (2007). Extensive gains and losses of olfactory receptor genes in Mammalian evolution. *PLoS ONE* 2, e708. doi: 10.1371/journal.pone.0000085.

Olender, T., Fuchs, T., Linhart, C., Shamir, R., Adams, M., Kalush, F., Khen, M., and Lancet, D. (2004). The canine olfactory subgenome. *Genomics* 83, 361–372.

Otaki, J. M., Yamamoto, H., and Firestein, S. (2003). Odorant receptor expression in the mouse cerebral cortex. *J. Neurobiol.* 58, 315–327.

Pace, U., Hanski, E., Salomon, Y., and Lancet, D. (1985). Odorant-sensitive adenylate cyclase may mediate olfactory reception. *Nature* 316, 255–258.

Pace, U., and Lancet, D. (1986). Olfactory GTP-binding protein: signaltransducing polypeptide of vertebrate chemosensory neurons. *Proc. Natl. Acad. Sci. U.S.A.* 83, 4947–4951.

Panaro, M. A., Acquafredda, A., Sisto, M., Lisi, S., Maffione, A. B., and Mitolo V. (2006). Biological role of the N-formyl peptide receptors. *Immunopharmacol. Immunotoxicol.* 28, 103–127.

Parmentier, M., Libert, F., Schurmans, S., Schiffmann, S., Lefort, A., Eggerickx, D., Ledent, C., Mollereau, C., Gerard, C., Perret, J., Grootegoed, A., and Vassart, G. (1992). Expression of members of the putative olfactory receptor gene family in mammalian germ cells. *Nature* 355, 453–455.

Pilpel, Y., and Lancet, D. (1999). The variable and conserved interfaces of modeled olfactory receptor proteins. *Protein Sci.* 8, 969–977.

Pin, J. P., Galvez, T., and Prezeau, L. (2003). Evolution, structure, and activation mechanism of family 3/C G-protein-coupled receptors. *Pharmacol. Ther.* 98, 325–354.

Pyrski, M., Xu, Z., Walters, E., Gilbert, D. J., Jenkins, N. A., Copeland, N. G., and Margolis, F. L. (2001). The OMP-lacZ transgene mimics the unusual expression pattern of OR-Z6, a new odorant receptor gene on mouse chromosome 6: implication for locus-dependent gene expression. *J. Neurosci.* 21, 4637–4648.

Quignon, P., Giraud, M., Rimbault, M., Lavigne, P., Tacher, S., Morin, E., Retout, E., Valin, A. S., Lindblad-Toh, K., Nicolas, J., and Galibert, F. (2005). The dog and rat olfactory receptor repertoires. *Genome Biol.* 6, R83.

Raming, K., Krieger, J., Strotmann, J., Boekhoff, I., Kubick, S., Baumstark, C., and Breer, H. (1993). Cloning and expression of odorant receptors. *Nature* 361, 353–356.

Ressler, K. J., Sullivan, S. L., and Buck, L. B. (1993). A zonal organization of odorant receptor gene expression in the olfactory epithelium. *Cell* 73, 597–609.

Riviere, S., Challet, L., Fluegge, D., Spehr, M., and Rodriguez, I. (2009). Formyl peptide receptor-like proteins are a novel family of vomeronasal chemosensors. *Nature* 459, 574–577.

Rodriguez, I., Del Punta, K., Rothman, A., Ishii, T., and Mombaerts, P. (2002). Multiple new and isolated families within the mouse superfamily of V1r vomeronasal receptors. *Nat. Neurosci.* 5, 134–140.

Rodriguez, I., Feinstein, P., and Mombaerts, P. (1999). Variable patterns of axonal projections of sensory neurons in the mouse vomeronasal system. *Cell* 97, 199–208.

Rodriguez, I., Greer, C. A., Mok, M. Y., and Mombaerts, P. (2000). A putative pheromone receptor gene expressed in human olfactory mucosa. *Nat. Genet.* 26, 18–19.

Rodriguez, I., and Mombaerts, P. (2002). Novel human vomeronasal receptor-like genes reveal species-specific families. *Curr. Biol.* 12, R409–R411.

Runnenburger, K., Breer, H., and Boekhoff, I. (2002). Selective G protein beta gamma-subunit compositions mediate phospholipase C activation in the vomeronasal organ. *Eur. J. Cell Biol.* 81, 539–547.

Ryba, N. J., and Tirindelli, R. (1997). A new multigene family of putative pheromone receptors. *Neuron* 19, 371–379.

Saito, H., Chi, Q., Zhuang, H., Matsunami, H., and Mainland, J. D. (2009). Odor coding by a Mammalian receptor repertoire. *Sci. Signal.* 2, ra9.

Sherborne, A. L., Thom, M. D., Paterson, S., Jury, F., Ollier, W. E., Stockley, P., Beynon, R. J., and Hurst, J. L. (2007). The genetic basis of inbreeding avoidance in house mice. *Curr. Biol.* 17, 2061–2066.

Shi, P., and Zhang, J. (2007). Comparative genomic analysis identifies an evolutionary shift of vomeronasal receptor gene repertoires in the vertebrate transition from water to land. *Genome Res.* 17, 166–174.

Shirokova, E., Schmiedeberg, K., Bedner, P., Niessen, H., Willecke, K., Raguse, J. D., Meyerhof, W., and Krautwurst, D. (2005). Identification of specific ligands for orphan olfactory receptors. G protein-dependent agonism and antagonism of odorants. *J. Biol. Chem.* 280, 11807–11815.

Shykind, B. M. (2005). Regulation of odorant receptors: one allele at a time. *Hum. Mol. Genet.* 14(Spec No. 1), R33–R39.

Sicard, G., and Holley, A. (1984). Receptor cell responses to odorants: similarities and differences among odorants. *Brain Res.* 292, 283–296.

Silvotti, L., Giannini, G., and Tirindelli, R. (2005). The vomeronasal receptor V2R2 does not require escort molecules for expression in heterologous systems. *Chem. Senses* 30, 1–8.

Silvotti, L., Moiani, A., Gatti, R., and Tirindelli, R. (2007). Combinatorial co-expression of pheromone receptors, V2Rs. *J. Neurochem.* 103, 1753–1763.

Singer, M. S., Weisinger-Lewin, Y., Lancet, D., and Shepherd, G. M. (1996). Positive selection moments identify potential functional residues in human olfactory receptors. *Receptors. Channels* 4, 141–147.

Sklar, P. B., Anholt, R. R., and Snyder, S. H. (1986). The odorant-sensitive adenylate cyclase of olfactory receptor cells. Differential stimulation by distinct classes of odorants. *J. Biol. Chem.* 261, 15538–15543.

Sosinsky, A., Glusman, G., and Lancet, D. (2000). The genomic structure of human olfactory receptor genes. *Genomics* 70, 49–61.

Spehr, M., Gisselmann, G., Poplawski, A., Riffell, J. A., Wetzel, C. H., Zimmer, R. K., and Hatt, H. (2003). Identification of a testicular odorant receptor mediating human sperm chemotaxis. *Science* 299, 2054–2058.

Spehr, M., Spehr, J., Ukhanov, K., Kelliher, K. R., Leinders-Zufall, T., and Zufall, F. (2006). Parallel processing of social signals by the mammalian main and accessory olfactory systems. *Cell. Mol. Life Sci.* 2006 63, 1476–1484.

Strotmann, J., Conzelmann, S., Beck, A., Feinstein, P., Breer, H., and Mombaerts, P. (2000). Local permutations in the glomerular array of the mouse olfactory bulb. *J. Neurosci.* 20, 6927–6938.

Strotmann, J., Wanner, I., Krieger, J., Raming, K., and Breer, H. (1992). Expression of odorant receptors in spatially restricted subsets of chemosensory neurones. *Neuroreport* 3, 1053–1056.

Sun, L., Wang, H., Hu, J., Han, J., Matsunami, H., and Luo, M. (2009). Guanylyl cyclase-D in the olfactory CO2 neurons is activated by bicarbonate. *Proc. Natl. Acad. Sci. U.S.A.* 106, 2041–2046.

Takigami, S., Osada, T., Yoshida-Matsuoka, J., Matsuoka, M., Mori, Y., and Ichikawa, M. (1999). The expressed localization of rat putative pheromone receptors. *Neurosci. Lett.* 272, 115–118.

Tian, H., and Ma, M. (2004). Molecular organization of the olfactory septal organ. *J. Neurosci.* 24, 8383–8390.

Touhara, K. (2007). Deorphanizing vertebrate olfactory receptors: recent advances in odorant-response assays. *Neurochem. Int.* 51, 132–139.

Tsuboi, A., Miyazaki, T., Imai, T., and Sakano, H. (2006). Olfactory sensory neurons expressing class I odorant receptors converge their axons on an antero-dorsal domain of the olfactory bulb in the mouse. *Eur. J. Neurosci.* 23, 1436–1444.

Vaidehi, N., Floriano, W. B., Trabanino, R., Hall, S. E., Freddolino, P., Choi, E. J., Zamanakos, G., and Goddard, W. A., III (2002). Prediction of structure and function of G protein-coupled receptors. *Proc. Natl. Acad. Sci. U.S.A.* 99, 12622–12627.

Vassar, R., Ngai, J., and Axel, R. (1993). Spatial segregation of odorant receptor expression in the mammalian olfactory epithelium. *Cell* 74, 309–318.

Volz, A., Ehlers, A., Younger, R., Forbes, S., Trowsdale, J., Schnorr, D., Beck, S., and Ziegler, A. (2003). Complex transcription and splicing of odorant receptor genes. *J. Biol. Chem.* 278, 19691–19701.

Wakabayashi, Y., Mori, Y., Ichikawa, M., Yazaki, K., and Hagino-Yamagishi, K. (2002). A putative pheromone receptor gene is expressed in two distinct olfactory organs in goats. *Chem. Senses* 27, 207–213.

Walz, A., Feinstein, P., Khan, M., and Mombaerts, P. (2007). Axonal wiring of guanylate cyclase-D-expressing olfactory neurons is dependent on

neuropilin 2 and semaphorin 3F. *Development* 134, 4063–4072.

Wang, Z. G., and Ye, R. D. (2002). Characterization of two new members of the formyl peptide receptor gene family from 129S6 mice. *Gene* 299, 57–63.

Weber, M., Pehl, U., Breer, H., and Strotmann, J. (2002). Olfactory receptor expressed in ganglia of the autonomic nervous system. *J. Neurosci. Res.* 68, 176–184.

Wekesa, K. S., Miller, S., and Napier, A. (2003). Involvement of G(q/11) in signal transduction in the mammalian vomeronasal organ. *J. Exp. Biol.* 206, 827–832.

Xie, S. Y., Feinstein, P., and Mombaerts, P. (2000). Characterization of a cluster comprising approximately 100 odorant receptor genes in mouse. *Mamm. Genome* 11, 1070–1078.

Yamaguchi, M., Yamazaki, K., Beauchamp, G. K., Bard, J., Thomas, L., and Boyse, E. A. (1981). Distinctive urinary odors governed by the major histocompatibility locus of the mouse. *Proc. Natl. Acad. Sci. U.S.A.* 78, 5817–5820.

Yang, H., Shi, P., Zhang, Y. P., and Zhang, J. (2005). Composition and evolution of the V2r vomeronasal receptor gene repertoire in mice and rats. *Genomics* 86, 306–315.

Young, J. M., Kambere, M., Trask, B. J., and Lane, R. P. (2005). Divergent V1R repertoires in five species: amplification in rodents, decimation in primates, and a surprisingly small repertoire in dogs. *Genome Res.* 15, 231–240.

Young, J. M., Shykind, B. M., Lane, R. P., Tonnes-Priddy, L., Ross, J. A., Walker, M., Williams, E. M., and Trask, B. J. (2003). Odorant receptor expressed sequence tags demonstrate olfactory expression of over 400 genes, extensive alternate splicing and unequal expression levels. *Genome Biol.* 4, R71.

Young, J. M., and Trask, B. J. (2002). The sense of smell: genomics of vertebrate odorant receptors. *Hum. Mol. Genet.* 11, 1153–1160.

Young, J. M., and Trask, B. J. (2007). V2R gene families degenerated in primates, dog and cow, but expanded in opossum. *Trends Genet.* 23, 212–215.

Young, J. M., Waters, H., Dong, C., Fülle, H. J., and Liman, E. R. (2007). Degeneration of the olfactory guanylyl cyclase D gene during primate evolution. *PLoS ONE* 2, e884. doi: 10.1371/journal.pone.0000884.

Zhang, J., and Webb, D. M. (2003). Evolutionary deterioration of the vomeronasal pheromone transduction pathway in catarrhine primates. *Proc. Natl. Acad. Sci. U.S.A.* 100, 8337–8341.

Zhang, X., and Firestein, S. (2002). The olfactory receptor gene superfamily of the mouse. *Nat. Neurosci.* 5, 124–133.

Zhang, X., Rodriguez, I., Mombaerts, P., and Firestein, S. (2004). Odorant and vomeronasal receptor genes in two mouse genome assemblies. *Genomics* 83, 802–811.

Zhang, X., Zhang, X., and Firestein, S. (2007). Comparative genomics of odorant and pheromone receptor genes in rodents. *Genomics* 89, 441–450.

Zhao, H., Ivic, L., Otaki, J. M., Hashimoto, M., Mikoshiba, K., and Firestein, S. (1998). Functional expression of a mammalian odorant receptor. *Science* 279, 237–242.

Conflict of Interest Statement: The authors declare that the research was conducted in the absence of any commercial or financial relationships that could be construed as a potential conflict of interest.

Received: 22 June 2009; paper pending published: 14 July 2009; accepted: 07 August 2009; published online: 27 August 2009.
*Citation: Fleischer J, Breer H and Strotmann J (2009) Mammalian olfactory receptors. Front. Cell. Neurosci. **3**:9. doi: 10.3389/neuro.03.009.2009*
Copyright © 2009 Fleischer, Breer and Strotmann. This is an open-access article subject to an exclusive license agreement between the authors and the Frontiers Research Foundation, which permits unrestricted use, distribution, and reproduction in any medium, provided the original authors and source are credited.

frontiers in
CELLULAR NEUROSCIENCE

REVIEW ARTICLE
published: 09 September 2009
doi: 10.3389/neuro.03.010.2009

Odorant and pheromone receptors in insects

Tal Soo Ha*[†] *and Dean P. Smith*

Department of Pharmacology and Neuroscience, University of Texas Southwestern Medical Center, Dallas, TX, USA

Edited by:
Dieter Wicher, Max Planck Institute for Chemical Ecology, Germany

Reviewed by:
Peter Kloppenburg, University of Cologne, Germany
Klemens F. Störtkuhl, Ruhr-Universität Bochum, Germany

***Correspondence:**
Dean P. Smith, Department of Pharmacology and Neuroscience, University of Texas Southwestern Medical Center, 5323 Harry Hines Blvd., Dallas, TX 75390-9111, USA. e-mail: Dean.Smith@Utsouthwestern.edu

[†]***Current address:***
Tal Soo Ha, Department of Molecular Biology, College of Natural Science, Daegu University, 15 Naeri, Jillyang, Gyeongsan, Gyeongbuk 712-714, South Korea.

Since the emergence of the first living cells, survival has hinged on the ability to detect and localize chemicals in the environment. Modern animal species ranging from insects to mammals express large odorant receptor repertoires to detect the structurally diverse array of volatile molecules important for survival. Despite the essential nature of chemical detection, there is surprising diversity in the signaling mechanisms that different species use for odorant detection. In vertebrates, odorant receptors are classical G-protein coupled, seven transmembrane receptors that activate downstream effector enzymes that, in turn, produce second messengers that open ion channels. However, recent work reveals that insects have adopted different strategies to detect volatile chemicals. In *Drosophila*, the odorant receptors, predicted to have seven transmembrane domains, have reversed membrane topology compared to classical G-protein coupled receptors. Furthermore, insect odorant receptors appear to form odorant-gated ion channels. Pheromone detection in insects is even more unusual, utilizing soluble, extracellular receptors that undergo conformational activation. These alternate olfactory signaling strategies are discussed in terms of receptor design principles.

Keywords: olfaction, pheromone, odorant, odorant receptor, odorant binding proteins

Olfaction, the detection and discrimination of air-borne chemicals, is probably the most important sense for the survival of most animal species. Detection and localization of food, avoidance of toxins and predators, and communication with cohorts and mating partners through volatile pheromones are examples of the range of olfactory-dependent behaviors. In contrast to the visual system, where a handful of receptor genes are sufficient to cover the relevant range of the electromagnetic spectrum, modern animals require large repertoires of receptors to detect the structurally diverse array of odorant molecules important for survival.

All animals detect chemical information with olfactory neurons exposed to the environment. Individual vertebrate olfactory neurons in the olfactory epithelium are tuned to a small fraction of 'odor space' (the total range of chemicals that can be detected). The restricted chemical tuning of individual olfactory neurons occurs because these neurons express a single allele of a single odorant receptor gene that is only activated by specific chemical features of odorant molecules (reviewed in Axel, 1995). In mammals, several hundred receptor genes are present in the genome, and all the olfactory neurons expressing the same receptor gene converge to a single pair of glomeruli in the olfactory bulb (Vassar et al., 1994; Sullivan et al., 1995). Thus, activation of a single odorant receptor type corresponds to activation of specific glomeruli. Individual odorants activate subsets of receptors tuned to various facets of chemical structure. Therefore, the unique activity pattern produced among the thousands of glomeruli elicited by a particular odorant is relayed to higher processing centers by the second order mitral cells where a unique odor image is formed.

Odorant signal transduction in vertebrate primary olfactory neurons utilizes a cAMP second messenger mechanism (**Figure 1**). Seven-transmembrane odorant receptors activate a G_s heterotrimeric G-protein homolog called G_{olf} that in turn activates adenylyl cyclase III to produce cAMP (Jones and Reed, 1989; Bakalyar and Reed, 1990). cAMP, in turn, binds and opens cyclic nucleotide-gated cation channels (Dhallan et al., 1990). These channels allow sodium and calcium to enter the dendrite, and the calcium influx triggers a second phase of depolarization mediated by calcium activated chloride channels (Lowe and Gold, 1993). Indeed, these later channels pass the majority of the depolarizing current (Lowe and Gold, 1993). This multistep signaling cascade is rather slow, requiring hundreds of milliseconds from odor interaction with receptors to full depolarization of the olfactory neurons, but offers the potential advantage that there are multiple steps that can be regulated to control the gain of the neuron.

The odorant receptor family in insects proved difficult to identify, because there was virtually no sequence similarity with the vertebrate odorant receptor gene family. Insect odorant receptor genes were finally discovered in *Drosophila*. A bioinformatic screen of the *Drosophila* genome sequence identified genes predicted to encode seven transmembrane proteins that were expressed in subsets of antennal neurons (Clyne et al., 1999; Gao and Chess, 1999). Large scale sequencing of cDNAs produced from antenna RNA also hit upon this receptor family (Vosshall et al., 1999). The insect odorant receptors, while predicted to encode seven transmembrane segments, were as similar to ion channels as they were to members of the vertebrate odorant receptor family. Anatomic studies confirmed that *Drosophila* olfactory neurons expressing the same odorant receptor converge to the same glomerulus in the antennal lobe; the equivalent of the vertebrate olfactory bulb (Vosshall et al., 2000). Therefore, odorant-specific patterns of glomerular activity probably underlie odorant discrimination in both insect and vertebrates. Despite the conservation in odorant processing implied by the similarity in

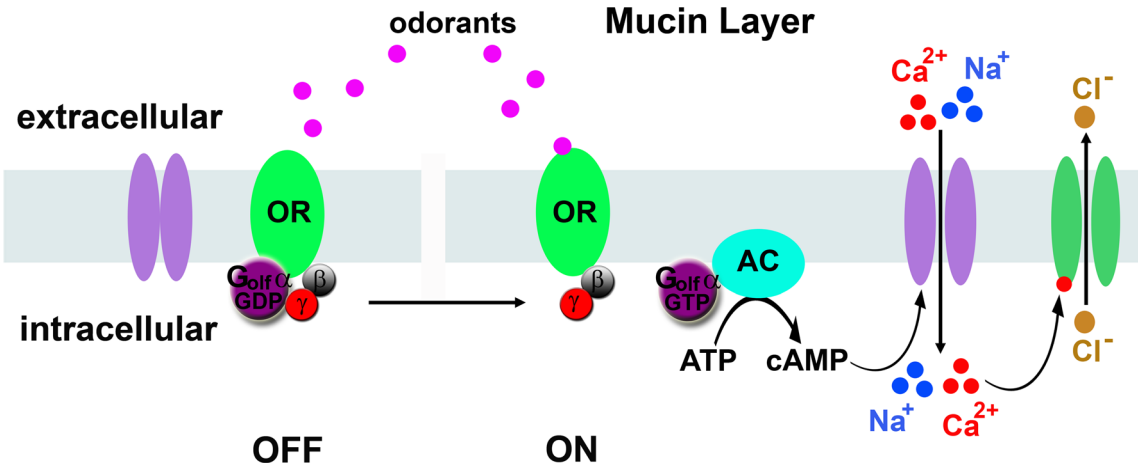

FIGURE 1 | Model of vertebrate olfactory signal transduction. In the absence of odorant (left), the odorant receptor (OR) is bound to the GDP-bound form of G_{olf}. Activation by odorants (right) causes exchange of GDP for GTP by the alpha subunit of G_{olf}, which activates adenylyl cyclase (AC) to produce cAMP. cAMP binds cyclic nucleotide-gated ion channels that conduct sodium and calcium ions into the neuron. The calcium ions bind calcium-activated chloride channels that allow chloride ions to exit the neurons, further depolarizing the neuron.

neuroanatomy and the presence of seven transmembrane receptors, the *Drosophila* olfactory signal transduction mechanisms turned out to be surprisingly unconventional.

Beginning with the odorant receptors, the first surprise was that these seven-transmembrane receptors are reversed in the membrane compared to all known G-protein-coupled receptors. Benton et al. (2006) using LacZ fusions and split GFP constructs showed that the topology of the loops between transmembrane domains was reversed relative to the classical G-protein coupled receptor, rhodopsin. The same conclusion was reached by introducing glycosylation sites in different loops and determining which loops were exposed to the glycosylation machinery in the golgi apparatus (Lundin et al., 2007). While classical G-protein coupled receptors have their C-termini inside the cell, the C-termini of the *Drosophila* odorant receptors appeared to be outside the cell! If these receptors are reversed, how do they trigger action potentials in the olfactory neurons? Do they activate effector enzymes that produce second messengers?

The second surprise was that the insect receptors are capable of forming odor-activated ion channels capable of depolarizing the olfactory neurons without needing a G-protein-activated second messenger system. Recent work indicates that insect odorant receptors form these odorant-gated ion channels as dimers between a 'tuning' receptor that binds odorants, and Or83b, an unusual member of the Or family. (**Figure 2**) (Sato et al., 2008; Smart et al., 2008; Wicher et al., 2008).

Or83b IS A COMMON SUBUNIT OF ODOR-GATED ION CHANNELS

Or83b is unusual in several aspects. First, it is the only odorant receptor that is highly conserved among insect species (Jones et al., 2005). Second, Or83b is expressed in most olfactory neurons. This is in stark contrast to the 'tuning' odorant receptors that are each expressed in small subsets of olfactory neurons that innervate a common glomerulus (Vosshall et al., 2000; Couto et al., 2005). One function of Or83b is to deliver tuning receptors to the olfactory neuron dendrites. In the absence of Or83b, the tuning receptors are trapped in the cell bodies of the olfactory neurons (Larsson et al., 2004). In the absence of a tuning receptor, Or83b is still transported to the dendrites of olfactory neurons, but these neurons are unresponsive to odorants, revealing Or83b itself is not an odorant receptor (Dobritsa et al., 2003; Elmore et al., 2003; Neuhaus et al., 2005). Is Or83b a simple chaperone, or does it have a more essential role in olfaction?

It turns out that Or83b is actually an ion channel that dimerizies with tuning receptors to form odorant-gated ion channels! Two groups independently showed that Or83b confers a novel cation conductance when expressed in heterologous tissue culture cells, and when co-expressed with a tuning odorant receptor, made this conductance odorant dependent (Sato et al., 2008; Wicher et al., 2008). Mutations in the pore-forming regions of Or83b modulated this conductance, directly implicating this protein in ion flux (Wicher et al., 2008). These findings suggest insect odorant receptors form odorant-gated ion channels with Or83b and that odorants trigger the opening of the ion channels without requiring a second messenger system. Why do mammals use a G-protein mechanism and insects use a direct ion channel gating mechanism? One possibility is response time. Signaling through a second messenger requires activation of the G protein, activation of the effector enzyme and production and diffusion of a second messenger before the ion channels are opened. A direct gating mechanism bypasses these steps and theoretically should respond faster. This might be relevant to insects that are flying through odorant plumes in the air trying to localize odorant sources.

Is there no role for second messengers in insect olfaction? Controversy lingers. There are a number of reports in the literature suggesting second messenger pathways underlie olfactory transduction in *Drosophila*. Indeed, olfactory neurons may share components with the phototransduction cascade, a Gq-coupled signaling pathway, as several phototransduction mutants have olfactory defects (Hotta and Benzer, 1969; Riesgo-Escovar et al., 1995; Kain et al., 2008). Furthermore, rapid production of cyclic nucleotides and phosphoinositide (PI) metabolites have been observed in

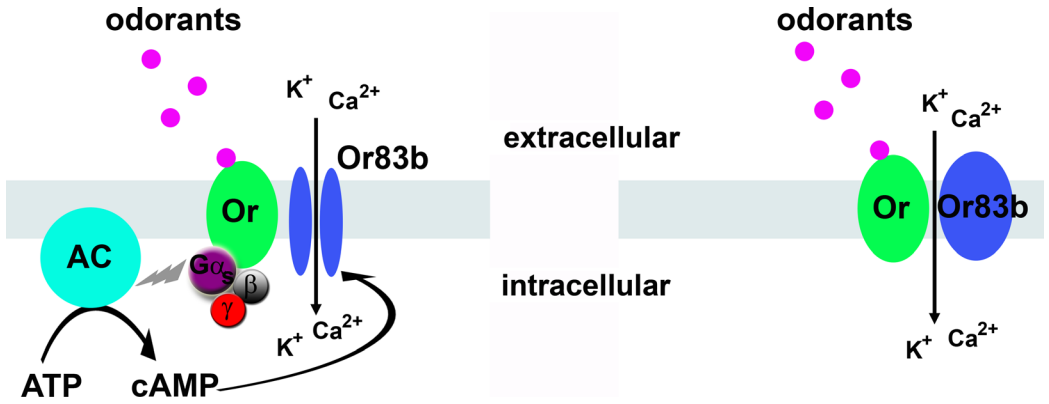

FIGURE 2 |Two possible models for odorant-gated channels. Left, possible role for G-protein mediated cyclic nucleotides in Or83b activation. Right, direct odorant gating of the Or/Or83b receptor complex. The major monovalent cation in the sensillum lymph is potassium.

response to odorants in insect olfactory neurons (Zufall and Hatt, 1991). Together, these studies highlight the importance of PI and possibly cyclic nucleotide signaling for olfactory neuron function, but they do not implicate these second messengers as direct mediators of olfactory signal transduction. For example, these second messengers may underlie long-term homeostatic responses to neuronal activity. Perhaps there is a role for second messengers in insect olfaction by modulating the odorant-gated ion channels.

Work with the insect receptors expressed in heterologous cells showed there is a cytoplasmic rise in cyclic nucleotides that was dependent on expression of a tuning odorant receptor but not Or83b, while there was a cyclic nucleotide-gated conductance that was dependent on expression of Or83b. This suggests the possibility that tuning receptors can activate a cyclase to produce cyclic nucleotides, and that Or83b can be gated by the cyclic nucleotides (Wicher et al., 2008). GDP-β-S, an inhibitor of G-protein activation, dramatically decreased the odor-activated current. This led to a transduction model in which low odorant concentrations trigger cyclic nucleotide production through the tuning receptor that subsequently gates the Or83b ion channel, while at higher odorant concentrations, the direct gating mechanism operates (**Figure 2**). However, work from others showed insect Or/Or83b receptors expressed in heterologous cells loaded with calcium indicators were unaffected by application of inhibitors of G proteins (GDP-β–S), adenylyl cylcase (SQ22536), guanylyl cyclase (ODQ), phosphodiesterases (IBMX) or phospholipase Cβ (U73122) (Smart et al., 2008). However, it should be noted that none of these studies examined the role of second messengers in insect primary olfactory neurons, and future studies will be required to confirm or exclude a direct role for second messengers in insect odorant detection and to elucidate how their formation is triggered if they are important. What is clear is that Or83b is required for dendritic localization of tuning receptors, and when dimerized with a tuning receptor, forms odorant-gated ion channels.

IONOTROPIC RECEPTORS COMPRISE A NEW CLASS OF CHEMOSENSORY RECEPTORS IN *DROSOPHILA*

Recent findings hinted at other types of chemosensory receptors in olfactory organs in *Drosophila*. CO_2 detection by a class of olfactory neuron occurs via two gustatory receptors that function without Or83b (Jones et al., 2007; Kwon et al., 2007). Expression mapping of the odorant receptor genes assigned receptors to specific olfactory neurons, allowing a detailed map of the chemosensory system to be established (Couto et al., 2005; Yao et al., 2005). However, with the exception of Or35a, none of the neurons located in the coeloconic sensilla expressed a member of the Or gene family. Indeed, Or83b, which is required as an obligate co-receptor for members of the Or family, is not expressed in 20% of the olfactory neurons. Most of the olfactory neurons that lack Or83b expression are located in the coeloconic sensilla, a class of small sensilla located on the antenna that normally respond to general odorants like alcohols, acids, but also to humidity (Yao et al., 2005). What is the Or83b-independent signaling mechanism in these olfactory neurons?

Using a bioinformatics approach, a set of antenna-specific genes were found, including a family of genes encoding proteins that resembled ionotropic glutamate receptors (iGluR). A total of 61 genes and 2 pseudogenes were discovered. While rather distantly related to classical ionotropic glutamate receptors, there is strong conservation in the pore forming loops and M2 transmembrane domains when compared to the vertebrate iGluR members (Benton et al., 2009). Fifteen of 60 iGluR mRNAs are expressed in the adult *Drosophila* antenna and are localized to the dendrites of olfactory neurons located in coeloconic sensilla. Or83b is not expressed in most of the iGluR-expressing neurons, with the exception of IR76b, which is co-expressed with Or35a and Or83b in one coeloconic ORN class. It is not clear if Or35a and the glutamate receptor IR76b operate independently to detect distinct ligands, or if they act in concert to sensitize the neurons to specific odors. However, for the other coeloconic neurons lacking Or83b, the expression of specific glutamate receptors correlated perfectly with the chemical sensitivity of the neurons. Importantly, mis-expression of individual glutamate receptors conferred the odorant sensitivity of the mis-expressed glutamate receptor to other neurons (Benton et al., 2009). Finally, for at least one iGluR, neurons expressing that receptor project axons to the same glomerulus in the antennal lobe, confirming these neurons are functionally related. Together, these data provide strong evidence that some of these glutamate receptors have evolved to perform as odorant receptors. It will be interesting

to determine where the other 45 members of the iGluR family are expressed, and if they also function as chemical detectors, and if any correspond to the humidity detector.

PHEROMONE DETECTION IN *DROSOPHILA*: AN EXTRACELLULAR RECEPTOR MEDIATES cVA PHEROMONE RESPONSES

Pheromones are chemicals produced by one individual to influence the behavior of another individual of the same species and are common in animals ranging from *C. elegans* to mammals. Pheromones are odorants with extraordinary biological significance. In insects, pheromones trigger a number of hardwired behaviors, including mating. Pheromone detection is highly sensitive and exquisitely specific so that low levels of pheromone are detected, and random environmental odorants are not mistaken for pheromone cues. Not surprisingly, specialized machinery has evolved for pheromone detection in insects that is not shared with olfactory neurons that detect food odorants. Recent work indicates that pheromone detection can occur through a unique pathway utilizing secreted, extracellular receptors. Once completely unraveled, knowledge of pheromone signal transduction may lead to new 'greener' approaches to control insect pest populations in a species-specific manner.

There is extensive literature describing elegant work with moth sex pheromone detection, a system where single pheromone molecule sensitivity has been reported (Kaissling and Priesner, 1970). Extracellular pheromone-binding proteins were first identified in male moth antenna as 14–16 kD extracellular proteins that bind directly to pheromones (Vogt and Riddiford, 1981). However, it was not clear if pheromone-binding proteins were important for detection of pheromone or for removal of pheromone from the extracellular lymph bathing the dendrites of the pheromone-sensitive neurons.

Insight into pheromone signal transduction mechanisms came from a genetic dissection of volatile pheromone detection in *Drosophila*. The *Drosophila* pheromone, 11-cis vaccenyl acetate (cVA) is a male-specific pheromone that mediates aggregation and recognition of sex among fruit flies (reviewed in Dickson, 2008; Vosshall, 2008). A pheromone-binding protein, LUSH is secreted by non-neuronal support cells into the fluid bathing the pheromone sensitive neuron dendrites (Kim et al., 1998). The importance of pheromone binding proteins was highlighted when it was shown that cVA detection is abolished in mutants lacking LUSH over all physiological levels of cVA (Xu et al., 2005; Laughlin et al., 2008). However, weak responses can still be elicited in *lush* mutant pheromone-sensitive neurons by intense, supra-physiological cVA doses (Laughlin et al., 2008). These findings are consistent with models suggesting LUSH acts as a carrier or transporter that shuttles the hydrophobic pheromone through the aqueous sensillum lymph to the olfactory neuron dendrites (Wojtasek and Leal, 1999; Horst et al., 2001). However, LUSH has a more interesting role than a simple carrier. In mutants lacking LUSH there is a striking loss of spontaneous activity (i.e. the basal neuronal firing rate in the absence of pheromone) specifically in the cVA sensing neurons (Xu et al., 2005). Wild type pheromone sensitive neurons have spontaneous firing rates of approximately 1 spike per second in the absence of pheromone (Clyne et al., 1997; Xu et al., 2005). However, *lush* mutants have spontaneous firing rates of only 1 spike every 400 s – a dramatic reduction in the normal spontaneous activity (Xu et al., 2005). Why would a pheromone carrier alter the firing rate of a neuron in the absence of pheromone? The surprising answer is that an activated conformation of LUSH is the real ligand for pheromone receptors present on pheromone-sensitive neurons.

X-ray crystal structures of LUSH with and without cVA bound were solved by John Laughlin and David Jones at the University of Colorado Heath Sciences Center (Laughlin et al., 2008). These structures revealed that LUSH undergoes a conformational shift upon binding cVA. Mutations in LUSH that enhanced or inhibited that conformational shift without altering cVA binding had large effects on the activity of LUSH, suggesting the conformational shift in LUSH is the true signal activating receptors on pheromone sensitive neurons (Laughlin et al., 2008). This was confirmed when a particular LUSH mutant, $LUSH^{D118A}$, was found to adopt the activated conformation in the absence of cVA and constitutively activate pheromone-sensitive neurons in the absence of cVA (Laughlin et al., 2008). Thus, the actual cVA pheromone receptor appears to be an extracellular binding protein.

THE NEURONAL RECEPTOR FOR ACTIVATED LUSH IS A COMPLEX OF Or67d, Or83b AND SNMP

How is the conformational shift in LUSH transduced into activation of the pheromone-sensitive olfactory neurons? There must be a specific receptor complex expressed exclusively by the pheromone-sensitive neurons, because dominant $LUSH^{D118A}$ only activates pheromone-sensitive neurons, and not any other class of olfactory neuron (Laughlin et al., 2008). Like detection of general odorants, cVA signaling requires Or83b (Jin et al., 2008) and a specific odorant receptor, Or67d (Ha and Smith, 2006; Kurtovic et al., 2007). Loss of either of these factors results in low spontaneous activity in the pheromone sensitive neurons and loss of cVA sensitivity, as observed in *lush* mutants. Further, dominant $LUSH^{D118A}$ fails to activate pheromone sensitive neurons missing either of these components (Jin et al., 2008; Laughlin et al., 2008). However, there is at least one additional factor required for activation of pheromone sensitive neurons, SNMP.

SNMP was identified in moths as a dendritic protein expressed in a subset of pheromone-sensitive neurons (Rogers et al., 2001a,b). SNMP is a homolog of CD36, a protein family important for many biological processes, including cholesterol uptake by macrophages (reviewed in Vogt et al., 2009). CD36 has also been implicated in the signal to convert macrophages into foam cells (Guest et al., 2007; Thorne et al., 2007), possibly through tyrosine kinase signaling (Rahaman et al., 2006). Mice lacking CD36 are defective for uptake of free fatty acids by adipose tissue and muscle (Coburn et al., 2000). *Drosophila* SNMP has the domain structure common to this family-a large extracellular domain flanked by two transmembrane domains with two short intracellular domains. SNMP is essential for pheromone signal transduction. When mutants lacking this gene product were analyzed they were insensitive to cVA at all concentrations, yet had normal responses to food odorants (Benton et al., 2007; Jin et al., 2008). Interestingly, unlike mutants lacking Or67d, Or83b or LUSH that have reduced spontaneous activity when absent, SNMP mutants have increased spontaneous activity. This suggests that SNMP may be an inhibitory subunit in the receptor complex (Benton et al., 2007; Jin et al., 2008). A working model is cVA-activated LUSH binds to SNMP, releasing

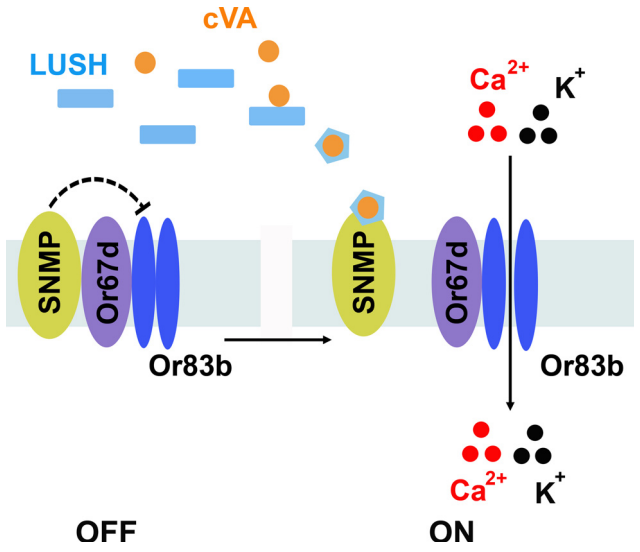

FIGURE 3 | Model for pheromone detection. The extracellular receptor LUSH binds cVA pheromone and undergoes an activating conformational shift. Activated LUSH binds SNMP and relieves SNMP-mediated inhibition of the Or67d/Or83b receptor complex, allowing cations to enter the neurons.

Or67d/Or83b from SNMP inhibition, resulting in activation of the neurons (**Figure 3**). However, there are likely to be addition factors required for pheromone signaling that remain unidentified that are not required for general odorants. Expression of Or67d, Or83b, SNMP together with LUSH in food-sensing olfactory sensilla fails to confer cVA sensitivity to these neurons (Laughlin et al., 2008). Thus, there are likely additional components yet to be discovered in this pheromone signaling mechanism.

What is the logic for using an extracellular binding protein in pheromone detection? We suggest this strategy has the potential to increase the sensitivity and specificity of the pheromone detection process. For example, if pheromone binding induces a stable, activated conformation in LUSH, this species could diffuse in the sensillum lymph until it interacts with a receptor complex on the dendrites and induces action potentials. This could, in theory, robustly increase pheromone detection to single molecule sensitivity. Utilizing an extracellular binding protein could also increase the specificity of pheromone detection. LUSH is able to bind to a wide variety of chemicals (Zhou et al., 2004), but only cVA interacts with LUSH in just the right way to induce the activated conformation of the binding protein. Thus a bona fide pheromone must not only bind LUSH, but also induce the relevant conformational shift in the binding protein in order to activate the pheromone-sensitive neurons. This mechanism may prevent pheromone-like odorants from activating pheromone-sensitive neurons.

DESIGN PRINCIPLES

Olfactory neurons in vertebrates use second messenger signaling to amplify odorant-triggered signals, whereas insects appear to use odorant-gated ion channels for general odorants with a possible role for second messengers as well. Insect pheromone detection utilizes conformational activation of soluble pheromone receptors to confer sensitivity and specificity to pheromone perception. Recent studies indicate vertebrate pheromones may also be detected through binding proteins (Chamero et al., 2007; Sherborne et al., 2007). While extracellular binding proteins functioning as odorant receptors were only recently uncovered, we note that bacteria produce periplasmic receptors that work in a similar manner. Thus, bacteria appear to have discovered this elegant solution for detecting rare chemicals in the environment long ago.

In summary, the neuronal strategy for odorant discrimination appears to be conserved between vertebrates and insects, but the underlying signal transduction mechanisms are surprisingly different. From a design standpoint, the biochemistry of how specific odorant cues are transduced by an olfactory neuron is not as important as having specific receptors to detect essential compounds expressed in labeled lines and a neuronal network to integrate this information so the animal can respond appropriately. Olfactory neurons in both insects and vertebrates converge onto glomeruli where multiple primary olfactory neurons synapse onto a relatively small number of second-order neurons. Convergence converts the relatively noisy, stochastic signals from individual primary olfactory neurons into a high fidelity information transfer by summing simultaneous inputs (Bhandawat et al., 2007). Individual odorants activate reproducible subsets of olfactory neurons expressing single tuning receptors, allowing the nervous system to deconstruct odorants into receptor-activating epitopes in both mammals and insects. How this information is processed into the sensation of 'odor' remains a mystery.

ACKNOWLEDGMENTS

The authors apologize to our colleagues whose contributions could not be cited here due to limited space requirements. We thank Helmut Kramer and Robin Hiesinger for critical review of the manuscript.

REFERENCES

Axel, R. (1995). The molecular logic of smell. *Sci. Am.* 273, 154–159.

Bakalyar, H. A., and Reed, R. R. (1990). Identification of a specialized adenylyl cyclase that may mediate odorant detection. *Science* 250, 1403–1406.

Benton, R., Sachse, S., Michnick, S. W., and Vosshall, L. B. (2006). Atypical membrane topology and heteromeric function of *Drosophila* odorant receptors *in vivo*. *PLoS Biol.* 4, e20. doi: 10.1371/journal.pbio.0040020

Benton, R., Vannice, K. S., Gomez-Diaz, C., and Vosshall, L. B. (2009). Variant ionotropic glutamate receptors as chemosensory receptors in *Drosophila*. *Cell* 136, 149–162.

Benton, R., Vannice, K. S., and Vosshall, L. B. (2007). An essential role for a CD36-related receptor in pheromone detection in *Drosophila*. *Nature* 450, 289–293.

Bhandawat, V., Olsen, S. R., Gouwens, N. W., Schlief, M. L., and Wilson, R. I. (2007). Sensory processing in the *Drosophila* antennal lobe increases reliability and separability of ensemble odor representations. *Nat. Neurosci.* 10, 1474–1482.

Chamero, P., Marton, T. F., Logan, D. W., Flanagan, K., Cruz, J. R., Saghatelian, A., Cravatt, B. F., and Stowers, L. (2007). Identification of protein pheromones that promote aggressive behaviour. *Nature* 450, 899–902.

Clyne, P., Grant, A., O'Connell, R., and Carlson, J. R. (1997). Odorant response of individual sensilla on the *Drosophila* antenna. *Invert. Neurosci.* 3, 127–135.

Clyne, P. J., Warr, C. G., Freeman, M. R., Lessing, D., Kim, J., and Carlson, J. R. (1999). A novel family of divergent seven-transmembrane proteins: candidate odorant receptors in *Drosophila*. *Neuron* 22, 327–338.

Coburn, C. T., Knapp, F. F., Jr., Febbraio, M., Beets, A. L., Silverstein, R. L., and Abumrad, N. A. (2000). Defective uptake and utilization of long chain fatty acids in muscle and adipose tissues of CD36 knockout mice. *J. Biol. Chem.* 275, 32523–32529.

Couto, A., Alenius, M., and Dickson, B. J. (2005). Molecular, anatomical, and functional organization of the *Drosophila* olfactory system. *Curr. Biol.* 15, 1535–1547.

Dhallan, R. S., Yau, K. W., Schrader, K. A., and Reed, R. R. (1990). Primary structure and functional expression of a cyclic nucleotide-activated channel from olfactory neurons. *Nature* 347, 184–187.

Dickson, B. J. (2008). Wired for sex: the neurobiology of *Drosophila* mating decisions. *Science* 322, 904–909.

Dobritsa, A. A., van der Goes van Naters, W., Warr, C. G., Steinbrecht, R. A., and Carlson, J. R. (2003). Integrating the molecular and cellular basis of odor coding in the *Drosophila* antenna. *Neuron* 37, 827–841.

Elmore, T., Ignell, R., Carlson, J. R., and Smith, D. P. (2003). Targeted mutation of a *Drosophila* odor receptor defines receptor requirement in a novel class of sensillum. *J. Neurosci.* 23, 9906–9912.

Gao, Q., and Chess, A. (1999). Identification of candidate olfactory receptors from genomic DNA sequence. *Genomics* 60, 31–39.

Guest, C. B., Hartman, M. E., O'Connor, J. C., Chakour, K. S., Sovari, A. A., and Freund, G. G. (2007). Phagocytosis of cholesteryl ester is amplified in diabetic mouse macrophages and is largely mediated by CD36 and SR-A. *PLoS ONE* 2, e511. doi: 10.1371/journal.pone.0000511

Ha, T. S., and Smith, D. P. (2006). A pheromone receptor mediates 11-cis-vaccenyl acetate-induced responses in *Drosophila*. *J. Neurosci.* 26, 8727–8733.

Horst, R., Damburger, F., Peng, G., Lunigbuhl, P., Guntert, P., Nikonova, L., Leal, W. S., and Wuthrich, K. (2001). NMR structure reveals intramolecular regulation mechanism for pheromone binding and release. *Proc. Natl. Acad. Sci. U.S.A.* 98, 14374–14379.

Hotta, Y., and Benzer, S. (1969). Abnormal electroretinograms of visual mutants in *Drosophila*. *Nature* 222, 354–356.

Jin, X., Ha, T. S., and Smith, D. P. (2008). SNMP is a signaling component required for pheromone sensitivity in *Drosophila*. *Proc. Natl. Acad. Sci. U.S.A.* 105, 10996–11001.

Jones, D. T., and Reed, R. R. (1989). Golf: an olfactory neuron specific-G protein involved in odorant signal transduction. *Science* 244, 790–795.

Jones, W. D., Cayirlioglu, P., Kadow, I. G., and Vosshall, L. B. (2007). Two chemosensory receptors together mediate carbon dioxide detection in *Drosophila*. *Nature* 445, 86–90.

Jones, W. D., Nguyen, T. A., Kloss, B., Lee, K. J., and Vosshall, L. B. (2005). Functional conservation of an insect odorant receptor gene across 250 million years of evolution. *Curr. Biol.* 15, R119–R121.

Kain, P., Chakraborty, T. S., Sundaram, S., Siddiqi, O., Rodrigues, V., and Hasan, G. (2008). Reduced odor responses from antennal neurons of G(q)alpha, phospholipase Cbeta, and *rdgA* mutants in *Drosophila* support a role for a phospholipid intermediate in insect olfactory transduction. *J. Neurosci.* 28, 4745–4755.

Kaissling, K.-E., and Priesner, E. (1970). Die riechschwelle des seidenspinners. *Naturwissenschaften* 57, 23–28.

Kim, M.-S., Repp, A., and Smith, D. P. (1998). LUSH odorant binding protein mediates chemosensory responses to alcohols in *Drosophila melanogaster*. *Genetics* 150, 711–721.

Kurtovic, A., Widmer, A., and Dickson, B. J. (2007). A single class of olfactory neurons mediates behavioural responses to a *Drosophila* sex pheromone. *Nature* 446, 542–546.

Kwon, J. Y., Dahanukar, A., Weiss, L. A., and Carlson, J. R. (2007). The molecular basis of CO_2 reception in *Drosophila*. *Proc. Natl. Acad. Sci. U.S.A.* 104, 3574–3578.

Larsson, M. C., Domingos, A. I., Jones, W. D., Chiappe, M. E., Amrein, H., and Vosshall, L. B. (2004). Or83b encodes a broadly expressed odorant receptor essential for *Drosophila* olfaction. *Neuron* 43, 703–714.

Laughlin, J. D., Ha, T. S., Jones, D. N., and Smith, D. P. (2008). Activation of pheromone-sensitive neurons is mediated by conformational activation of pheromone-binding protein. *Cell* 133, 1255–1265.

Lowe, G., and Gold, G. H. (1993). Nonlinear amplification by calcium-dependent chloride channels in olfactory receptor cells. *Nature* 366, 283–286.

Lundin, C., Kall, L., Kreher, S. A., Kapp, K., Sonnhammer, E. L., Carlson, J. R., Heijne, G., and Nilsson, I. (2007). Membrane topology of the *Drosophila* OR83b odorant receptor. *FEBS Lett.* 581, 5601–5604.

Neuhaus, E. M., Gisselmann, G., Zhang, W., Dooley, R., Störtkuhl, K., and Hatt, H. (2005). Odorant receptor heterodimerization in the olfactory system of *Drosophila melanogaster*. *Nat. Neurosci.* 8, 15–17.

Rahaman, S. O., Lennon, D. J., Febbraio, M., Podrez, E. A., Hazen, S. L., and Silverstein, R. L. (2006). A CD36-dependent signaling cascade is necessary for macrophage foam cell formation. *Cell Metab.* 4, 211–221.

Riesgo-Escovar, J., Raha, D., and Carlson, J. R. (1995). Requirement for a phospholipase C in odor response: overlap between olfaction and vision in *Drosophila*. *Proc. Natl. Acad. Sci. U.S.A.* 92, 2864–2868.

Rogers, M. E., Krieger, J., and Vogt, R. G. (2001a). Antennal SNMPs (sensory neuron membrane proteins) of Lepidoptera define a unique family of invertebrate CD36-like proteins. *J. Neurobiol.* 49, 47–61.

Rogers, M. E., Steinbrecht, R. A., and Vogt, R. G. (2001b). Expression of SNMP-1 in olfactory neurons and sensilla of male and female antennae of the silkmoth *Antheraea polyphemus*. *Cell Tissue Res.* 303, 433–446.

Sato, K., Pellegrino, M., Nakagawa, T., Nakagawa, T., Vosshall, L. B., and Touhara, K. (2008). Insect olfactory receptors are heteromeric ligand-gated ion channels. *Nature* 452, 1002–1006.

Sherborne, A. L., Thom, M. D., Paterson, S., Jury, F., Ollier, W. E., Stockley, P., Beynon, R. J., and Hurst, J. L. (2007). The genetic basis of inbreeding avoidance in house mice. *Curr. Biol.* 17, 2061–2066.

Smart, R., Kiely, A., Beale, M., Vargas, E., Carraher, C., Kralicek, A. V., Christie, D. L., Chen, C., Newcomb, R. D., and Warr, C. G. (2008). *Drosophila* odorant receptors are novel seven transmembrane domain proteins that can signal independently of heterotrimeric G proteins. *Insect Biochem. Mol. Biol.* 38, 770–780.

Sullivan, S. L, Bohm, S., Ressler, K. J., Horowitz, L. F., and Buck, L. B. (1995). Target-independent pattern specification in the olfactory epithelium. *Neuron* 15, 779–789.

Thorne, R. F., Mhaidat, N. M., Ralston, K. J., and Burns, G. F. (2007). CD36 is a receptor for oxidized high density lipoprotein: implications for the development of atherosclerosis. *FEBS Lett.* 581, 1227–1232.

Vassar, R., Chao, S. K., Sitcheran, R., Nunez, J. M., Vosshall, L. B., and Axel, R. (1994). Topographic organization of sensory projections to the olfactory bulb. *Cell* 79, 981–991.

Vogt, R. G., Miller, N. E., Litvack, R., Fandino, R. A., Sparks, J., Staples, J., Friedman, R., and Dickens, J. C. (2009). The insect SNMP gene family. *Insect Biochem. Mol. Biol.* 39, 448–456.

Vogt, R. G., and Riddiford, L. M. (1981). Pheromone binding and inactivation by moth antennae. *Nature* 293, 161–163.

Vosshall, L. B. (2008). Scent of a fly. *Neuron* 59, 685–689.

Vosshall, L. B., Amrein, H., Morozov, P. S., Rzhetsky, A., and Axel, R. (1999). A spatial map of olfactory receptor expression in the *Drosophila* antenna. *Cell* 96, 725–736.

Vosshall, L. B., Wong, A. M., and Axel, R. (2000). An olfactory sensory map in the fly brain. *Cell* 102, 147–159.

Wicher, D., Schafer, R., Bauernfeind, R., Stensmyr, M. C., Heller, R., Heinemann, S. H., and Hansson, B. S. (2008). *Drosophila* odorant receptors are both ligand-gated and cyclic-nucleotide-activated cation channels. *Nature* 452, 1007–1011.

Wojtasek, H., and Leal, W. S. (1999). Conformational change in the pheromone-binding protein from Bombyx mori induced by pH and by interaction with membranes. *J. Biol. Chem.* 274, 30950–30956.

Xu, P.-X., Atkinson, R., Jones, D. N. M., and Smith, D. P. (2005). *Drosophila* OBP LUSH is required for activity of Pheromone-sensitive neurons. *Neuron* 45, 193–200.

Yao, C. A., Ignell, R., and Carlson, J. R. (2005). Chemosensory coding by neurons in the coeloconic sensilla of the *Drosophila* antenna. *J. Neurosci.* 25, 8359–8367.

Zhou, J. J., Zhang, G. A., Huang, W., Birkett, M. A., Field, L. M., Pickett, J. A., and Pelosi, P. (2004). Revisiting the odorant binding protein LUSH of *Drosophila melanogaster*: evidence for odour recognition and discrimination. *FEBS Lett.* 558, 23–26.

Zufall, F., and Hatt, H. (1991). Dual activation of a sex pheromone-dependent ion channel from insect olfactory dendrites by protein kinase C activators and cyclic GMP. *Proc. Natl. Acad. Sci. U.S.A.* 88, 8520–8524.

Conflict of Interest Statement: The authors declare that the research was conducted in the absence of any commercial or financial relationships that could be construed as a potential conflict of interest.

Received: 16 May 2009; paper pending published: 01 June 2009; accepted: 22 August 2009; published online: 09 September 2009.

Citation: Ha TS and Smith DP (2009) Odorant and pheromone receptors in insects. Front. Cell. Neurosci. ***3****:10. doi: 10.3389/neuro.03.010.2009*

Copyright © 2009 Ha and Smith. This is an open-access article subject to an exclusive license agreement between the authors and the Frontiers Research Foundation, which permits unrestricted use, distribution, and reproduction in any medium, provided the original authors and source are credited.

frontiers in
CELLULAR NEUROSCIENCE

REVIEW ARTICLE
published: 18 June 2010
doi: 10.3389/fncel.2010.00020

Molecular and cellular designs of insect taste receptor system

Kunio Isono* and Hiromi Morita

Graduate School of Information Sciences, Tohoku University, Sendai, Japan

Edited by:
Dieter Wicher, Max Planck Institute for Chemical Ecology, Germany

Reviewed by:
Satpal Singh, University of New York, USA
Ulf Bickmeyer, Alfred Wegener Institute, Germany

****Correspondence:***
Kunio Isono, Graduate School of Information Sciences, Tohoku University, Aramaki, Aoba-ku, Sendai, Miyagi 980-8579, Japan.
e-mail: iisono@m.tains.tohoku.ac.jp

The insect gustatory receptors (GRs) are members of a large G-protein coupled receptor family distantly related to the insect olfactory receptors. They are phylogenetically different from taste receptors of most other animals. GRs are often coexpressed with other GRs in single receptor neurons. Taste receptors other than GRs are also expressed in some neurons. Recent molecular studies in the fruitfly *Drosophila* revealed that the insect taste receptor system not only covers a wide ligand spectrum of sugars, bitter substances or salts that are common to mammals but also includes reception of pheromone and somatosensory stimulants. However, the central mechanism to perceive and discriminate taste information is not yet elucidated. Analysis of the primary projection of taste neurons to the brain shows that the projection profiles depend basically on the peripheral locations of the neurons as well as the GRs that they express. These results suggest that both peripheral and central design principles of insect taste perception are different from those of olfactory perception.

Keywords: insect, Drosophila, gustatory receptor (GR), taste ligand, taste neuron, taste sensillum, subesophageal ganglion complex (SOG), feeding behavior

INTRODUCTION

Insect taste organs were first described in the early 20th century as hair-like structures on the distal legs that induce feeding reflex reaction to sugar stimulations in butterflies (Minnich, 1921). The simplicity of insect taste organs innervated by only a few taste neurons was ideal for physiological studies. Single-unit action potentials, sensitivity to taste ligands and other physiological properties were studied intensively during 1950s–1970s using various flies including housefly *Musca domestica*, blowfly *Phormia regina*, fleshfly *Calliphora erythrocephala* and fruitfly *Drosophila melanogaster* (Dethier, 1976). Morphological or developmental studies were also carried out in flies in 1980s–1990s (Pollack and Balakrishnan, 1997; Singh, 1997).

Molecular studies of insect taste receptors started around the 2000s. Searching the *Drosophila* genome successfully led to the first discoveries of a large gustatory receptor (GR) gene family and characterization of taste receptor neurons that express divergent GRs (Clyne et al., 2000). The accumulated knowledge in flies from more than half a century of study thus describes various aspects of the insect taste receptor system. However, molecular profiles of fly taste neurons turned out to be much more complex than earlier physiologists predicted. Therefore we are not yet ready to fully understand design principles of taste systems in insects. To gain an insight into how insect taste receptor systems are designed to encode gustatory information, we will focus mainly on the functional aspects of the insect taste receptors and taste receptor neurons. For recent research advances on *Drosophila* taste receptors and taste perception see other reviews (Amrein and Thorne, 2005; de Bruyne and Warr, 2005; Scott, 2005; Montell, 2009). This review is composed of two parts. Various taste receptor molecules are compared, summarized and discussed in the Section "Insect Taste Receptors". Physiological, morphological, developmental and molecular properties of taste neurons are compared and discussed in the Section "Insect Taste Neurons".

INSECT TASTE RECEPTORS

EVOLUTION OF INSECT GUSTATORY RECEPTORS

Identification of a large family of olfactory G-protein coupled receptor (GPCR) genes by Buck and Axel (1991) provoked searches for taste GPCR genes by molecular biology. A novel family of candidate taste GPCR genes was thus found from the *Drosophila* genome by a computer algorithm to hit seven-transmembrane domain when the *Drosophila* genome project was nearly completed (Clyne et al., 2000). They showed that a total of more than 40 GR genes that belong to a novel family and share a signature motif with *Drosophila* odorant receptor (OR) genes are expressed specifically in taste tissues. Later analysis of the whole *Drosophila* genome predicted a total of 68 GR genes (Robertson et al., 2003; **Table 1**). Subsequent molecular and functional studies showed that most of them encode GRs. The genes are given the name "Gr" (gustatory receptor) followed by a chromosomal locus number. When GR genes are tandemly clustered, an alphabet starting from "a" was appended at the end like *Gr5a* or *Gr10b*.

Among *Drosophila* GR genes, 6 are located on the X chromosome while 38 and 24 are found on the second and the third *Drosophila* chromosome, respectively. Each GR gene encodes a seven-transmembrane receptor protein of about 350–550 amino residues in length. The overall sequences are very divergent with homologies between two randomly chosen GRs as low as 15–25% on the average, which is significantly lower than those for ORs. However, GRs and ORs share a common amino residue motif in the seventh transmembrane plus C terminal domain, indicating that they have evolved from an ancestral chemoreceptor family.

Genome analysis suggests that a robust expansion of GR/OR genes has occurred only in the class Insecta. The nematode *Caenorhabditis elegans* is an exception since the animal carries a few functional GR genes as will be discussed later. The majority of chemoreceptors in *C. elegans*, all chemoreceptors in sea urchin (*Strongylocentrotus purpuratus*) or all gustatory and olfactory receptors in vertebrates do not have GR genes.

Insects like mosquito, moth, beetle, wasp, bee, aphid and louse are shown to carry both GR and OR genes in the genome (FlyBase, http://flybase.org/). The honey bee *Apis mellifera* has 163 intact OR genes but only 10 intact GR genes (Robertson and Wanner, 2006). A dipteran insect, the malaria vector mosquito *Anopheles gambiae* carries 79 and 76 OR and GR genes, respectively (Hill et al., 2002). Numbers of GR genes are therefore similar between the two dipteran insects but their GRs are so distinct that it is often difficult to find common orthologs between the two insects.

Odorant receptor and GR genes of five *D. melanogaster* subgroup species, *D. simulans, D. sechellia, D. melanogaster, D. yakuba* and *D. erecta* have been compared recently (McBride and Arguello, 2007). They estimated that the ancestor of the five species carried a total of 64 ancestral ORs and 74 GRs ~12 million years ago. Interestingly, two ecological specialists, *D. sec* exclusively depending on *Morinda citrifolia* as a host plant and *D. ere* depending on *Pandanus candelabrum* have lost 14 GRs while three other generalist species have lost only 3 to 6 GRs. GR receptors for CO_2 (*Gr21a* and *Gr63a*) and for sugars (*Gr5a, Gr61a* and six *Gr64* genes from *Gr64a* to *Gr64f*) are more conserved than other GRs including GRs for bitter substances.

Thorne and Amrein (2008) and Kent and Robertson (2009) reported that there are no orthologs of a sugar receptor *Gr5a* even in some *drosophilid* species. A BLAST search for *Gr5a* orthologs and paralogs using the genome assembly data from all available insect species revealed only nine *drosophilid* species possessing both *Gr5a* orthologs and paralogs. Other insects including *D. pseudoobscura*, *D. persimilis*, *D. grimshawi*, three mosquitoes, a silkworm moth, a red flour beetle, a honeybee, a wasp and a pea aphid have only *Gr5a* paralogs but no orthologs. A human body louse carries neither paralogs nor orthologs. Gain and loss events of *Gr5a* orthologs within 15 dipteran species are estimated and illustrated in **Figure 1**. Taking into consideration that GR gene family has expanded only in the class *Insecta*, it seems likely that *Gr5a* orthologs appeared recently, probably differentiated from *Gr64f*.

Ueno et al. (2001) showed that a polymorphism of the 218th amino residue Thr^{218} (*Tre*^{01}) and Ala^{218} (*Tre*$^{+}$) in *Gr5a* leads to a low and a high trehalose taste sensitivity in *D. melanogaster*, respectively. Thr^{218} allele is more frequent than Ala^{218} allele in wild populations (Inomata et al., 2004). The 218th residue of the *Gr5a* ortholog in *D. simulans* and other *Drosophila* is fixed to Thr^{218}, indicating that Thr^{218} is ancestral to Ala^{218}, which appeared less than five million years ago only in *D. melanogaster*. Since Thr^{218} is almost a null mutation with respect to trehalose sensitivity (Isono et al., 2005), Ala^{218} must be a gain of function mutation, which seems to be unusual. Other explanations like a second residue polymorphism that compensates the low sugar sensitivity in Thr^{218} are also possible. Future structure–function studies are necessary to understand the molecular evolution of GRs.

LIGANDS OF INSECT TASTE RECEPTORS

Attempts to isolate taste receptor proteins biochemically from taste organs of various animals, i.e., bovine, rat and flies, have failed so far although photoreceptor proteins have been successfully isolated from the retina. Taste receptor proteins may be expressed in low amounts in the tissue or the affinity to taste ligands may be too low for affinity-based isolations.

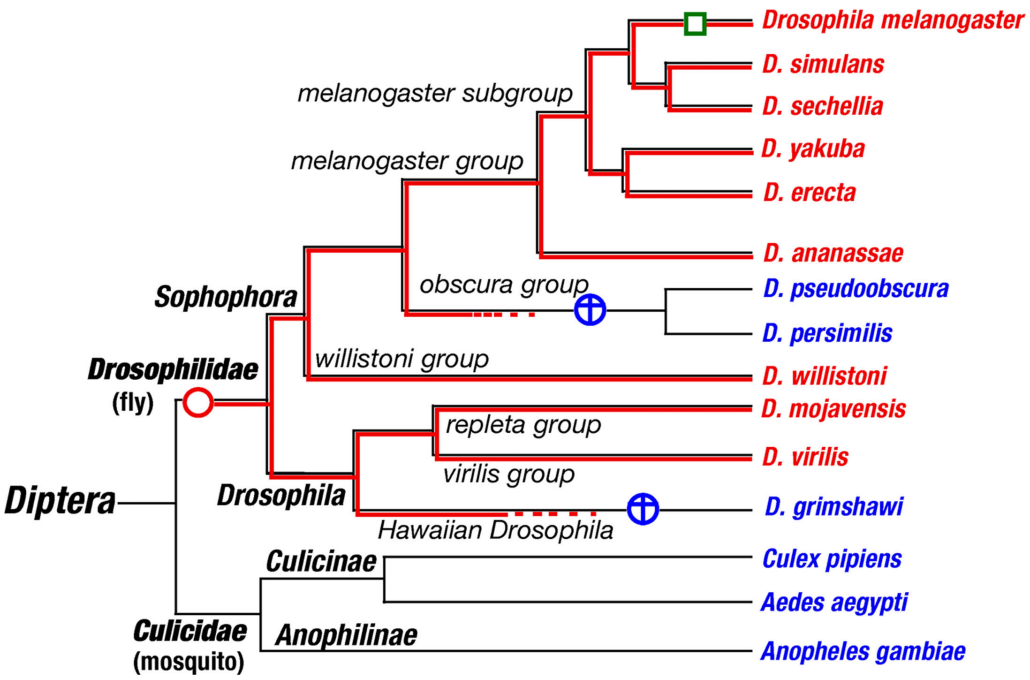

FIGURE 1 | Gain and loss events of *Gr5a*, a sugar receptor, based on phylogenetic analysis of *Gr5a* orthologs from 15 dipteran insects in which the whole genome assemblies are available. The phylogenetic tree is modified from BLAST homepage of FlyBase (http://flybase.org/blast/). Species names in red and blue italics illustrate species with or without *Gr5a* orthologs, respectively. Red and blue circles represent gain and loss events of *Gr5a* orthologs, respectively. A green box represents a functional mutation from ancestral Thr^{218} to Ala^{218} that occurred only in *Drosophila melanogaster* branch.

Ligand profiles of taste receptors have been analyzed using *Drosophila* mutants or transformants of a specific GR gene except for the sugar receptor *Gr5a* using a heterologous expression system (Chyb et al., 2003). As shown in **Table 1**, the ligands are not yet characterized for many insect GRs. The GR ligands are classified into three groups: sugars, bitter substances and pheromones.

Sugar receptors

For many insects, including flies, butterflies and bees, the stimulation of taste organs with a sugar solution not only induces neuronal response but also a robust feeding reflex called proboscis extension response (**Figure 2**) and various appetitive behaviors. Electrophysiological and morphological studies show that the sugar response of a taste sensillum derives from a single sugar-sensitive neuron while other neurons respond to other taste stimulations (Dethier, 1976). Gustatory mutations in *Drosophila* affecting the neuronal responses were isolated by many laboratories (Isono and Kikuchi, 1974; Falk and Atidia, 1975; Tompkins et al., 1979; Rodrigues and Siddiqi, 1981; Tanimura et al., 1982; Arora et al., 1987). Among them a mutation, *Tre (Trehalose-sensitivity,* 1-13.6), on the X chromosome was shown to control sensitivity to a disaccharide trehalose (Tanimura et al., 1982). Among the 68 GRs in *Drosophila*, *Gr5a* that locates near the *Tre* locus became the genomic candidate for *Tre* and indeed was shown that *Tre* is identical to *Gr5a* by disrupting the gene or by genomic rescue experiments (Dahanukar et al., 2001; Ueno et al., 2001; Isono et al., 2005). *Tre* was also shown to be a single nucleotide polymorphism in *Gr5a* leading to a substitution of 218th amino residues Ala^{218} (=Tre^{+}) and Thr^{218} (=Tre^{01}).

The ligand profile of *Gr5a* has been analyzed electrophysiologically and behaviorally using *Gr5a* mutants (Tanimura et al., 1982; Dahanukar et al., 2001, 2007; Ueno et al., 2001; Chyb et al., 2003; Thorne et al., 2004; Wang et al., 2004; Isono et al., 2005; Jiao et al., 2008). Spontaneous (Tre^{01}) or induced genomic deletion mutants of *Gr5a* are shown to reduce the sensitivity to trehalose, glucose, melezitose, methyl-a-glucoside and some other saccharides.

Another type of sugar receptor was identified by disrupting the six tandemly clustered *Gr5a* paralogs, *Gr64a, Gr64b, Gr64c, Gr64d, Gr64e and Gr64f* (**Table 1**). In contrast to *Gr5a*, disruptions of the Gr64 cluster lead to a loss of sensitivity to various sugars including sucrose and maltose (Dahanukar et al., 2007; Jiao et al., 2007; Slone et al., 2007). Since disruption of *Gr64a* alone causes loss of the sugar sensitivity, *Gr64a* is essential for the sensitivity to sucrose. A more detailed ligand analysis revealed that *Gr64a* contributes a wide sugar sensitivity not only to sucrose and maltose but also to various di- and trisaccharides or alcohols including turanose, maitotriose, maltitol, palatinose, stachyose, raffinose and leucrose (Dahanukar et al., 2007).

On the other hand, Slone et al. (2007) showed that deletion of all six Gr64 genes leads to a drastic loss of all sugar sensitivity including trehalose and sucrose. Rescue by *Gr64a* cDNA restored the ligand profile of *Gr64a* but did not restore the ligand profile of *Gr5a* receptor (Jiao et al., 2007). The enigmatic interaction of the two sugar receptors was uncovered by the observation that coexpression of *Gr64f* receptor is essential for the two complementary profiles of *Gr5a* and *Gr61a* receptor functions (Jiao et al., 2008). Thus, *Drosophila* sugar receptors form heterodimers with *Gr64f* receptor as a common co-receptor interacting with *Gr5a* or with *Gr64a* receptor. The heterodimeric chemoreceptor model is also suggested for *Drosophila* caffeine receptors (Lee et al., 2009), *Drosophila* olfactory CO_2 receptors (Suh et al., 2004; Kwon et al., 2007), all olfactory receptors that function with the co-receptor OR83b or its orthologs (Neuhaus et al., 2005), as well as mammalian taste receptors, T1R2/T1R3 sugar reception and T1R2/T1R3 umami reception (Nelson et al., 2001, 2002).

The other five *Gr5a*-related GR genes, *Gr61a, Gr64b, Gr64c, Gr64d* and *Gr64e* have not yet been characterized. Deletions, insertions or suppression by RNAi constructs do not seem to induce significant changes in sugar sensitivity. They may be functional receptors expressed in a limited subset of taste neurons or may simply be nonfunctional receptors as is the case for Tre^{01}, the ancestral form of *Gr5a*.

Bitter receptors

Properties of bitter taste GRs and bitter taste neurons were studied by Thorne et al. (2004) and Wang et al. (2004). They showed that selective inactivation of taste neurons expressing some GRs by neurotoxins leads to reduction in sensitivity to bitter substances without affecting sugar sensitivity. Thorne et al. (2004) showed that inactivation of *Gr66a* expressing neurons (hereafter called simply *Gr66a* neurons) or *Gr22e* neurons reduces sensitivity to caffeine solutions but not to quinine hydrochloride, denatonium benzoate or berberine solutions at low concentrations in a two-choice behavioral preference assay (**Figure 3**). However, Wang et al. (2004) showed by a proboscis extension assay (**Figure 2**) that sensitivity to the four tested bitter substances is simultaneously reduced at wide concentrations in flies where *Gr66a* neurons are inactivated.

Ligand profile of *Gr66a* receptor, rather than *Gr66a* neurons, was later directly analyzed using a *Gr66a* gene knockout mutant (Moon et al., 2006). The mutant showed reduced sensitivity to wide concentrations of caffeine solutions in the two-choice preference assay (**Figure 3**) and also in the electrophysiological response of the labellar sensilla (**Figure 4**). Caffeine is a methylxanthine derivative multiply methylated at three positions (1,3,7-trimethylxanthine). Response to two other derivatives, theophylline (1,3-dimethylxanthine) and 1,7-dimethylxanthine was also reduced in the mutant while the response to theobromine (3,7-dimethylxanthine) was normal, suggesting that a strict ligand structure is required for *Gr66a* receptor.

Gr66a alone is not sufficient to function as a caffeine receptor (Lee et al., 2009). Ablation of the *Gr93a* gene also reduced the behavioral and electrophysiological caffeine response without affecting the response to many other bitter substances. Since *Gr93a* mutant flies show exactly the same phenotype as *Gr66a* mutants, the two GRs may function as heterodimeric co-receptors as was shown for sugar receptors (Jiao et al., 2008). Interestingly, misexpression of both *Gr66a* and *Gr93a* cDNAs in *Gr5a* neurons does not induce response to caffeine, suggesting that the two GRs are not yet sufficient for the caffeine response. Moon et al. (2009) recently showed that *Gr33a* which is widely expressed in bitter neurons is essential for the neuronal and behavioral response to bitter substances including caffeine, suggesting that caffeine and other bitter receptors are trimeric or multimeric rather than dimeric. Since many GR genes are coexpressed in bitter neurons,

Table 1 | Gustatory receptor genes in the genome assembly of *Drosophila melanogaster* with their phylogenetic relations, functions and neuronal expression profiles.

	Gene name	Group	Ligand	Tissue expression*	Coexpressed with	Not coexpressed with	References
1	Gr5a	A	Sugars	L, Tp, T	Gr28a, Gr28bC, Gr61a, Gr64a, Gr64b, Gr64c, Gr64d, Gr64e, Gr64f	Gr22e, Gr32a, Gr33a, Gr39aD, Gr59f, Gr63a, Gr66a, Gr98a	Thorne et al. (2004), Wang et al. (2004), Fishilevich et al. (2005), Dahanukar et al. (2007), Jiao et al. (2007, 2008), Thorne and Amrein (2008)
2	Gr61a	A		L, T	Gr5a, Gr64a, Gr64f	Gr66a	Dahanukar et al. (2007), Jiao et al. (2007)
3	Gr64a	A	Sugars	L, P	Gr5a, Gr61a, Gr64f	Gr66a	Thorne et al. (2004), Dahanukar et al. (2007), Jiao et al. (2007, 2008)
4	Gr64b	A		L	Gr5a	Gr66a	Jiao et al. (2007)
5	Gr64c	A		L	Gr5a	Gr66a	Jiao et al. (2007)
6	Gr64d	A		L	Gr5a	Gr66a	Jiao et al. (2007)
7	Gr64e	A		L, P	Gr5a	Gr66a	Thorne et al. (2004), Jiao et al. (2007)
8	Gr64f	A	Sugars	L, T	Gr5a, Gr61a, Gr64a	Gr66a	Dahanukar et al. (2007), Jiao et al. (2007, 2008)
9	Gr21a	A	CO_2	A, L	Gr63a	Gr10a	Clyne et al. (2000), Scott et al. (2001), Suh et al. (2004), Couto et al. (2005), Fishilevich and Vosshall (2005), Jones et al. (2007), Kwon et al. (2007)
				To**	Gr63a	Gr66a	Scott et al. (2001), Fishilevich et al. (2005), Faucher et al. (2006), Colomb et al. (2007), Jones et al. (2007), Kwon et al. (2007)
10	Gr63a	A	CO_2	A	Gr21a	Gr5a, Gr10a, Gr66a	Scott et al. (2001), Jiao et al. (2007), Jones et al. (2007), Kwon et al. (2007)
				To**	Gr21a		Fishilevich et al. (2005), Jones et al. (2007), Kwon et al. (2007)
11	Gr10a	B		A	Or10a, Or83b	Gr21a, Gr63a	Scott et al. (2001), Fishilevich and Vosshall (2005), Jones et al. (2007)
12	Gr59e	B					

Table 1

	Gene name	Group	Ligand	Tissue expression*	Coexpressed with	Not coexpressed with	References
13	Gr59f	B		L	Gr66a	Gr5a	Jiao et al. (2007)
				To**		Gr66a	Colomb et al. (2007)
14	Gr94a	B					
15	Gr97a	B					
16	Gr10b	C					
17	Gr77a	C					
18	Gr89a	C					
19	Gr92a	D					
20	Gr93a	D	Caffeine	L, P, T	Gr33a, Gr66a		Lee et al. (2009)
21	Gr93b	D					
22	Gr93c	D					
23	Gr93d	D					
24	Gr22a	E		L, W, T			Clyne et al. (2000), Scott et al. (2001)
25	Gr22b	E		L, P, T	Gr22e, Gr28bE, Gr32a, Gr59b, Gr66a		Thorne et al. (2004), Wang et al. (2004)
				Po**	Gr66a, Gr68a		Colomb et al. (2007)
26	Gr22c	E		P, T			Dunipace et al. (2001), Wang et al. (2004)
27	Gr22d	E					
28	Gr22e	E		A, L, P, W, T	Gr22b, Gr22f, Gr28a, Gr28bC, Gr28bD, Gr28bE, Gr32a, Gr59b, Gr66a	Gr5a, Gr47a, Gr68a	Dunipace et al. (2001), Bray and Amrein (2003), Thorne et al. (2004), Wang et al. (2004), Jiao et al. (2007), Thorne and Amrein (2008)
				To, Po**	Gr66a		Fishilevich et al. (2005), Colomb et al. (2007)
29	Gr22f	E		L	Gr22e, Gr59b, Gr66a		Dunipace et al. (2001), Thorne et al. (2004)
30	Gr36a	E					
31	Gr36b	E					
32	Gr36c	E					
33	Gr47a	E		L, P	Gr66a	Gr22e, Gr28a, Gr32a, Gr59b	Clyne et al. (2000), Scott et al. (2001), Wang et al. (2004)
34	Gr58a	E		L			Clyne et al. (2000)
35	Gr58b	E		L			Clyne et al. (2000)
36	Gr58c	E		L			Clyne et al. (2000)
37	Gr59a	E		L			Clyne et al. (2000), Wang et al. (2004)

(Continued)

Table 1

	Gene name	Group	Ligand	Tissue expression*	Coexpressed with	Not coexpressed with	References
38	Gr59b	E		L	Gr22b, Gr22e, Gr22f, Gr32a, Gr66a	Gr47a	Clyne et al. (2000), Dunipace et al. (2001), Thorne et al. (2004), Wang et al. (2004)
				To			Colomb et al. (2007)
39	Gr59c	E		W			Clyne et al. (2000)
40	Gr59d	E		L			Clyne et al. (2000)
41	Gr85a	E					
42	Gr32a	F	Pheromone	L, P,T	Gr22b, Gr22e, Gr28a, Gr28bE, Gr33a, Gr59b, Gr66a	Gr5a, Gr47a	Clyne et al. (2000), Scott et al. (2001), Thorne et al. (2004), Wang et al. (2004), Jiao et al. (2007), Miyamoto and Amrein (2008), Lee et al. (2009)
				To**		Gr66a	Scott et al. (2001), Fishilevich et al. (2005), Colomb et al. (2007)
43	Gr39aA	F		L			Clyne et al. (2000)
44	Gr39aB	F		L			Clyne et al. (2000)
45	Gr39aC	F		L			Clyne et al. (2000)
46	Gr39aD	F		L, W	Gr66a	Gr5a	Clyne et al. (2000), Jiao et al. (2007)
47	Gr47b	F					
48	Gr57a	F					
49	Gr68a	F	Pheromone sound	A, L, W, T		Gr22e, Gr66a	Bray and Amrein (2003), Ejima and Griffith (2008)
				To, Po**	Gr22b, Gr66a		Colomb et al. (2007)
50	Gr2a	G		P			Scott et al. (2001), Wang et al. (2004)
				To, Do, Vo, Po, Vp**		Gr66a	Scott et al. (2001), Python and Stocker (2002), Fishilevich et al. (2005), Colomb et al. (2007)
51	Gr8a	G					
52	Gr9a	G					
53	Gr23aA	G		L			Clyne et al. (2000)
54	Gr23aB	G		L			Clyne et al. (2000)
55	Gr39b	G		L			Clyne et al. (2000)
56	Gr98a	G		L		Gr5a, Gr66a	Scott et al. (2001), Jiao et al. (2007)
57	Gr98b	G					
58	Gr98c	G					
59	Gr98d	G					
60	Gr28a	H		L, P,T	Gr5a, Gr22e, Gr32a	Gr47a	Wang et al. (2004), Thorne and Amrein (2008)

Table 1

	Gene name	Group	Ligand	Tissue expression*	Coexpressed with	Not coexpressed with	References
				To, Vp**			Thorne and Amrein (2008)
61	Gr28bA	H		L, P, T	Gr28bE		Scott et al. (2001), Thorne and Amrein (2008)
				To**			Thorne and Amrein (2008)
62	Gr28bB	H					Scott et al. (2001), Thorne and Amrein (2008)
63	Gr28bC	H		L, P, W	Gr5a, Gr22e		Scott et al. (2001), Thorne and Amrein (2008)
				To, Po**			Scott et al. (2001), Thorne and Amrein (2008)
64	Gr28bD	H		L, P, T	Gr22e		Scott et al. (2001), Thorne and Amrein (2008)
65	Gr28bE	H		L, P, T	Gr22b, Gr22e, Gr28bA, Gr32a, Gr66a,		Thorne and Amrein (2008), Scott et al. (2001), Thorne et al. (2004)
				To, Po**	Gr66a		Colomb et al. (2007), Thorne and Amrein (2008)
66	Gr33a	H	Caffeine, quinine, denatonium, berberine, lobeline papaverine, strychinine	L, P, T	Gr32a, Gr66a, Gr93a	Gr5a	Scott et al. (2001), Jiao et al. (2007), Lee et al. (2009), Moon et al. (2009)
67	Gr43a	H		L, W, T			Clyne et al. (2000)
68	Gr66a	H	Caffeine	L, P, T	Gr22b, Gr22e, Gr22f, Gr28bE, Gr32a, Gr33a, Gr39aD, Gr47a, Gr59b, Gr59f, Gr93a	Gr5a, Gr61a, Gr63a, Gr64a, Gr64b, Gr64c, Gr64d, Gr64e, Gr64f, Gr68a, Gr98a	Dunipace et al. (2001), Scott et al. (2001), Bray and Amrein (2003), Thorne et al. (2004), Wang et al. (2004), Moon et al. (2006, 2009), Jiao et al. (2007), Thorne and Amrein (2008), Lee et al. (2009)
				To, Do, Po**	Gr22b, Gr22e, Gr28bE, Gr68a	Gr2a, Gr21a, Gr32a, Gr59f	Scott et al. (2001), Fishilevich et al. (2005), Colomb et al. (2007)

**Expression data in non-chemosensory cells are not indicated. Abbreviations are as follows: for adult tissues: A, antenna;, L, labellum; Tp, taste peg; P, pharynx; W, wing; T, tarsal leg segments. For larval tissues: to, terminal organ; Do, dorsal organ; Vo, ventral organ; Po, pharyngeal organ; Vp, ventral pit.*

***When GR gene is expressed in both adult and larval tissues, each expression profile is given in the first and the second row, respectively.*

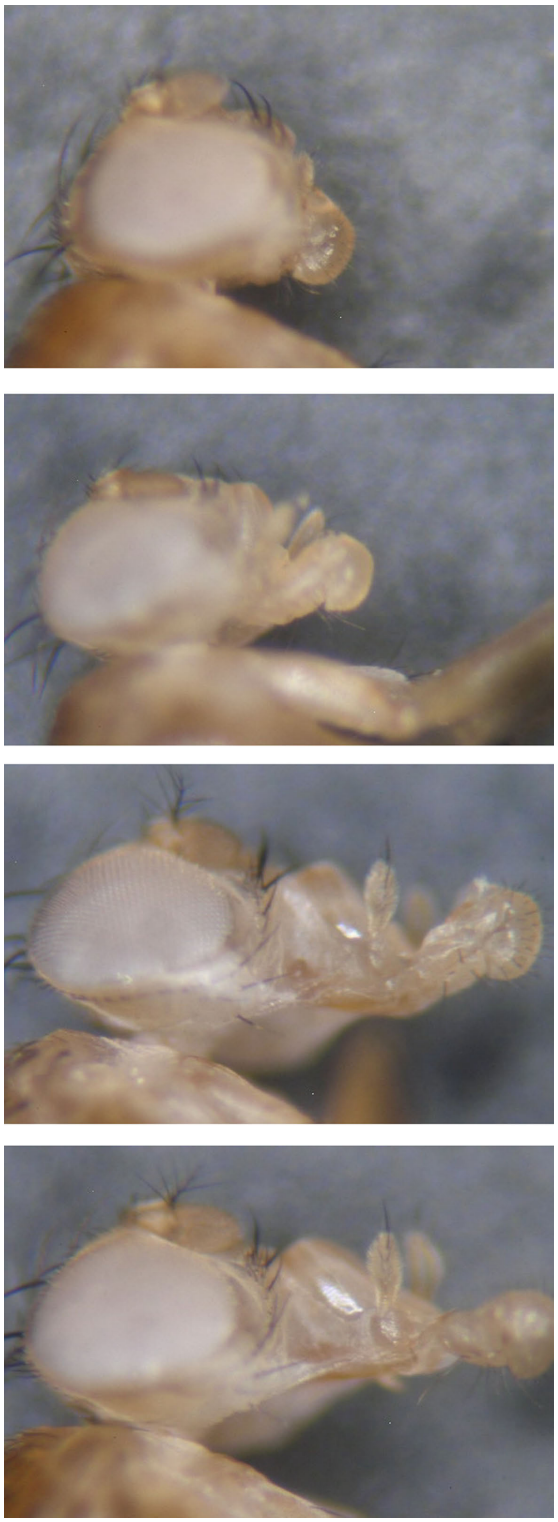

FIGURE 2 | Increasing magnitude of proboscis extension response (from up to down) in *Drosophila*.

future systematic analysis of GR gene complex may be necessary to understand how each GR contributes to bitter-taste reception in *Drosophila*.

Pheromone receptors

Pheromones are volatile and non-volatile chemical substances that are produced for sexual and non-sexual social communications between species members. Two large GPCR families consisting of about 140 V1Rs and 60 V2Rs, respectively, are expressed in the receptor neurons of the vomeronasal organ in the mouse for pheromone communication (Zufall and Leinders-Zufall, 2007). In insects, however, volatile pheromone-sensing receptors are part of the conventional olfactory receptor system. Sakurai et al. (2004) and Nakagawa et al. (2005) showed that two olfactory pheromone receptors, *BmOR1* and *BmOR3*, are expressed only in the male olfactory neurons of the silk moth *Bombyx mori* for the detection of female sex pheromones bombykol, (E, Z)-10,12-hexadecadien-1-ol, and bombykal, (E, Z)-10,12-hexadecadien-1-al, respectively. Another example in the honeybee is *AmOr10*, that detects a main component of the queen substance, 9-oxo-2-decenoic acid (Wanner et al., 2007).

In *Drosophila* a lipid, cis-vaccenyl acetate, has been known to be a male-specific component of the cuticle but is transferred to females upon mating. The lipid acts as an aggregation pheromone for flies of both sexes as well as an inhibitory sex pheromone that suppresses courtship by males (Ejima et al., 2007). Two olfactory receptor genes, *Or67d* and *Or65a*, expressed in olfactory neurons of trichoid type olfactory sensilla are shown to encode receptors for cis-vaccenyl acetate. Two other receptors, *Or47b* and *Or88a*, do not respond to cis-vaccenyl acetate but respond to male and female extracts, suggesting that sex pheromones and receptors are complex in *Drosophila* (van der Goes van Naters and Carlson, 2007).

In addition to volatile sex pheromones, *Drosophila* also uses gustatory information in male courtship behavior. *Gr68a* is expressed in male-specific taste neurons of the forelegs and is necessary for normal courtship since inactivation of *Gr68a* neurons and RNA interference of *Gr68a* mRNA lead to a reduction in the courtship performance (Bray and Amrein, 2003). Cuticle non-volatile hydrocarbons like cis, cis-7,11-hepta cosadiene are structurally divergent between sexes and also among *Drosophila* species and known to promote or suppress courtship in *Drosophila* males depending on the chemical structures (Jallon, 1984; Ferveur and Jallon, 1996). However, it is not yet clear that *Gr68a* encodes a hydrocarbon pheromone receptor. *Gr68a* is broadly expressed in mechanosensory neurons (Ejima and Griffith, 2008). Wild type males show only a poor courtship toward immobilized, silent females in dim light. The performance is greatly improved when they were given a noise arising from fly movements or even artificial white noise. However, the improvement is not observed for transgenic males where *Gr68a* neurons are inactivated, suggesting that *Gr68a* receptor and/or *Gr68a* neurons contribute to mechanoreceptive rather than chemoreceptive function.

A second candidate pheromone receptor gene, *Gr32a*, is closely related to *Gr68a* and was recently shown to be involved in courtship suppression toward males and mated females (Miyamoto and Amrein, 2008). *Gr32a* may be a long-chain hydrocarbon receptor for inhibitory hydrocarbons like cis-7 tricosene that are shown to inhibit male-male courtship (Ferveur and Jallon, 1996).

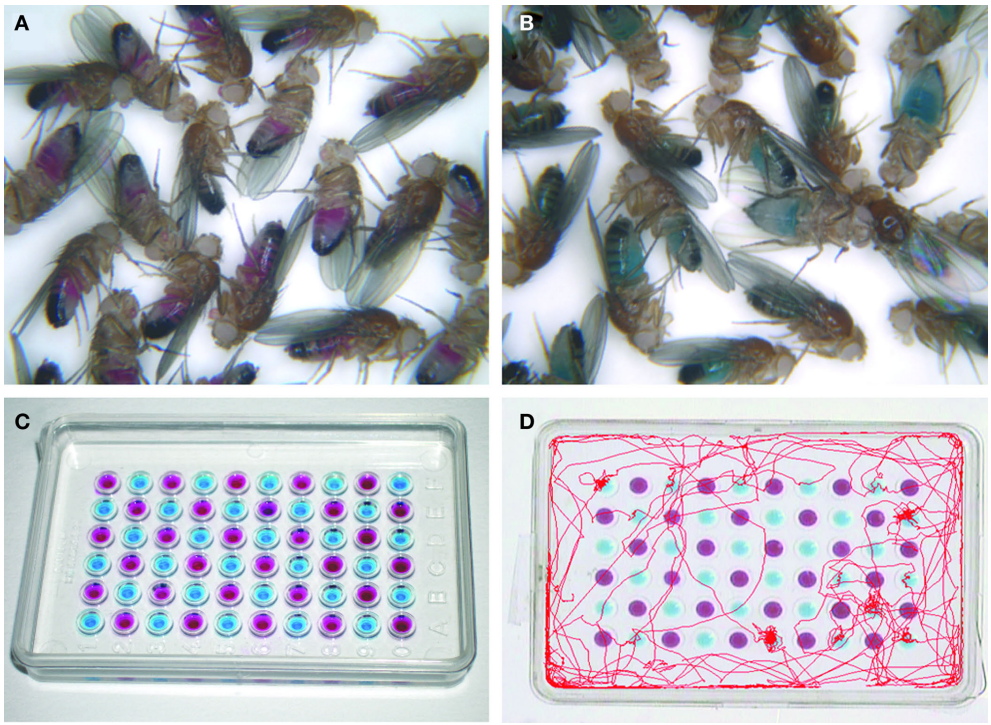

FIGURE 3 | An example of feeding choice test to behaviorally evaluate taste sensitivity and feeding preference in *Drosophila*. **(A,B)** Hungry flies after 20 h of food deprivation ingest a maximum amount of 100 mM sucrose + 1% agar solutions mixed with red or blue food dyes, respectively, and can be visually inspected after feeding. **(C)** A microtiter dish containing two different solutions containing the two food dyes to test for the feeding preference. **(D)** A video analysis simultaneously monitoring the locomotor traces of three individual flies in the choice of 100 mM sucrose + 1% agar solution (marked with a blue dye) and a plain 1% agar solution (marked with a red dye). The traces show that more frequent visits or stays were made on wells containing 100 mM sucrose than on wells containing plain water. The video analysis was provided courtesy of Dr. M. Koganezawa).

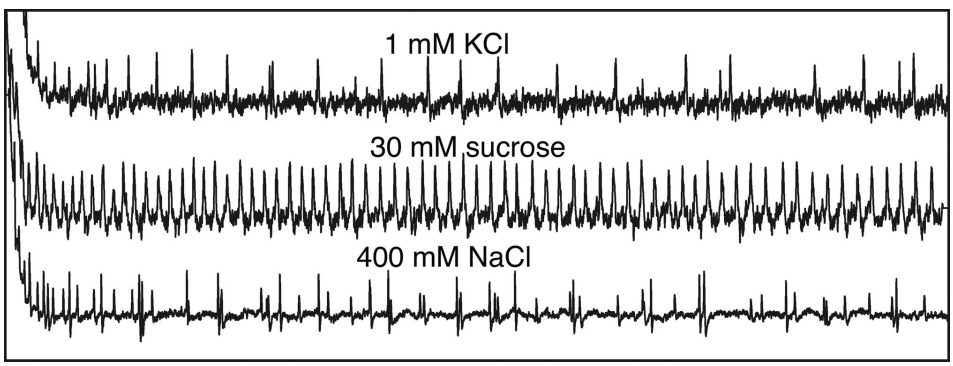

FIGURE 4 | Electrophysiological recordings from a single L-type taste sensillum of the labellum in *Drosophila*. Different types of neurons are activated by different taste stimulations. See explanations in the text. Recordings provided courtesy of Dr. N. Tanabe.

Suh et al. (2004) identified CO_2 as a novel nonsexual olfactory pheromone released by stressed *Drosophila* flies. They found that the released CO_2 induces avoidance in nearby flies. The stress OR is encoded by *Gr21a*, an olfactory GR gene in *Drosophila*. Jones et al. (2007) showed that the CO_2 response is also unique in that *Gr21a* neurons do not coexpress *Or83b*, an essential cofactor for all other ORs, but instead coexpress *Gr63a*. Kwon et al. (2007) showed that the coexpression of *Gr21a* and *Gr63a* is necessary and sufficient for CO_2 response by ectopic expression of the two GRs in other olfactory neurons. The malaria mosquito *A. gambiae*, also coexpresses the two orthologs, *GPRGR22* and *GPRGR24*, respectively, in the antennal neurons. Since CO_2 is a potent attractant for mosquitoes, the differing behavioral response to CO_2 may indicate that the peripheral design of chemoreceptors is more conserved than the central design which is flexible and species-specific in the evolution of the whole insect chemosensory system.

Receptors tuned to non-gustatory stimuli

Phylogenetic analysis suggested that insect OR family arose from an expansion of ancestral GR superfamily (Robertson et al., 2003). Therefore it is not surprising that some GRs like *Gr10a, Gr21a* or *Gr63a* are expressed and function in olfactory neurons. Some other GRs seem to be expressed even in non-chemosensory neurons as shown for *Gr68a* in auditory/mechanosensory neurons (Ejima and Griffith, 2008). Thorne and Amrein (2008) showed that six highly conserved GR genes (*Gr28a* and five *Gr28b* genes, *Gr28bA* to *Gr28bE,* or subgroup H in **Table 1**) are expressed in non-chemosensory neurons including abdominal multidendritic neurons, putative hygroreceptive neurons of the aristae, neurons in Johnston's organ of the antenna, proprioceptive neurons of the legs or even the larval and adult brain neurons. *Gr28bB* and *Gr28bC* are expressed in central neurosecretory cells that release insulin-like peptides (Ikeya et al., 2002), indicating that the two GRs detect internal sugar levels. Coexpression of a sugar receptor *Gr5a* with *Gr28a* or *Gr28bC* also supports that trehalose taste receptor also function as internal sugar detector of the neurosecretory cells. *Gr28bB* is also expressed in non-neural cells like enocytes in adults and larvae that detects nutrient levels to regulate metabolism. The expression profiles suggest that Gr28 receptors are multimodal somatosensory receptors tuned to proprioception, nociception, thermoreception or internal chemoreception. Therefore they may be comparable to mammalian TRP family members (Minke and Parnas, 2006; Ramsey et al., 2006) or divergent, MAS-related GPCRs expressed in the nociceptive neurons of the dorsal root ganglion (Dong et al., 2001).

A photosensitive insect GR homolog, *lite-1,* was recently identified as one of the three insect GR-related genes in the nematode *C. elegans* (Edwards et al., 2008). Mutations in *lite-1* disrupt light-induced locomotor activity. Interestingly, *lite-1* shows homology to *Drosophila Gr28b* gene with the highest homology in their C termini (26% identical over a 68 amino residue length) as are generally the case among GRs in flies. Though no functional studies have yet been carried out for *Gr28b* receptors in flies, it is possible that some Gr28 receptors in flies encode extraocular, non-visual photoreceptor molecules.

Gustatory TRP channels

In addition to GR receptors, other types of receptors are also shown to be expressed in taste neurons and contribute to chemoreception. One is *painless*, a fly homolog of mammalian TRPA1/ANKTM1 ion channel protein. *painless* in flies is involved in the rejection of allyl and benzyl isothiocyanate, the pungent taste and insecticidal component of wasabi (Al-Anzi et al., 2006). Like GR receptors *painless* is expressed in taste neurons of the labellum, pharynx, legs and wings. A subset of labellar *painless* neurons also coexpress caffeine receptor *Gr66a* and, conversely, subset of *Gr66a* neurons coexpress *painless*. A similar relation was also obtained between *painless* neurons and *Gr32a* or *Gr47a* bitter neurons of the legs in an agreement with the fact that both bitter substances and isothiocyanate are aversive stimuli and induce food rejection. Interestingly, *painless* neurons are also involved in the post feeding larval avoidance of food media for pupation (Xu et al., 2008). They showed that peripheral sensory neurons located in the ventral side of the larval body express *painless* and respond to sugar stimulations and that *painless* mutations or inactivation of *painless* neurons reduces the food avoidance and also the neuronal response to sugar stimulations. Chemoreceptors involved in the behavioral sugar/food aversion are not known but it is possible that they are identical to adult sugar receptor GRs. If so, *painless* neurons should provide a neural model as a developmentally controlled taste evaluation system from acceptance to rejection.

Capsaicin is a hot chili pepper component that activates TRPV1, another type of TRP ion channel in mammals. Capsaicin also induces gustatory response in flies but does not involve *painless* receptor or *painless* neurons since it evokes a positive feeding preference in both wild type and *painless* mutants. Therefore capsaicin receptor in flies, though it has not been identified, may be expressed in food acceptance neurons, rather than in bitter neurons. Other TRP ion channel proteins involve *painless* subfamily (TRPA) members PYREXIA and dTRPA1 for heat-protection (Tracey et al., 2003; Lee et al., 2005; Xu et al., 2008) and TRPC subfamily members TRP and TRPL for cold protection (Rosenzweig et al., 2008). Future studies may provide evidence that some TRP ion channels are expressed in taste neurons.

Some bitter neurons express a GPCR receptor for an insecticide L-canavaline (2-amnio-4-guanidinooxybutyric acid), a toxin structurally similar to L-arginine, which interferes with normal protein synthesis. The receptor, named DmXR, does not belong to GR but is a family C member GPCR with a homology to mammalian metabotropic glutamate receptors (mGluRs) and with a long N-terminal extracellular domain. DmXR is expressed in *Gr66a* neurons of the labellum and the tarsus (Mitri et al., 2009), suggesting that non-GR GPCR receptors are also coexpressed in bitter neurons in addition to multiple bitter GRs.

Uncharacterized taste receptors

In addition to taste neurons that express known receptor molecules, there are other types of neurons in which no GRs are yet to be identified. For example, electrophysiological analysis showed that there are usually two L1 and L2 neurons in a single taste hair, both responsive to monovalent cations of salts (Dethier, 1976). No GR receptors have yet been shown to be involved in the salt responses. Instead of GRs, another molecular mechanism has been proposed for the salt response. In some mammals degenerin/epithelial Na^+ channels (DEG/ENaC) are known to be suppressed by the inhibitor amiloride. Since amiloride also suppresses taste response to salts in mammals, DEG/ENaC Na^+ channel has been a candidate molecular mechanism that directly triggers receptor potential without GPCR or transduction cascades (Halpern, 1998; Herness and Gilbertson, 1999). DEG/ENaC amiloride-sensitive channels are widely conserved ion channels throughout animals. Liu et al. (2003) showed that mutations or disruptions of two *Drosophila* DEG/ENaC homologs, *Pickpocket11* and *Pickpocket19*, affect taste sensitivity to salts in larval and adult *Drosophila* without affecting sugar or olfactory sensitivities.

Another example is the W neuron that responds to water and low osmolarity solutions found in many types of taste sensilla. Meunier et al. (2009) showed in *Drosophila* tarsal taste sensilla that W neuron response is pharmacologically inhibited by lanthanum ion (known to inhibit calcium channels) and also by calmodulin antagonists, suggesting that an osmolarity-dependent calcium channel is the osmolarity sensor.

The reception of carbonated water reported by Fischler et al. (2007) may be the most unexpected. A *Gal4* enhancer trap line with an expression profile in the taste peg neurons are defective in neuronal response to, and in behavioral preference for soluble CO_2 but are normal in detecting and avoiding gaseous CO_2 by olfactory CO_2 receptors. Conversely, a mutant in *Gr63a*, one of the essential olfactory CO_2 receptors, is defective in detecting and avoiding CO_2 by olfaction but normal in detecting and preferring soluble CO_2. Gustatory and olfactory detection of CO_2 are therefore independent with respect to the chemoreceptors as well as the central signaling process.

How many species of different taste receptors are present in *Drosophila*? Insect taste response seems to be divergent, including many GRs, non-GR GPCRs, TRP ion channels and other types of receptor molecules. The total number of GR receptors would be increased considerably if functional taste receptors are composed of dimers or multimers of all the possible combinations of coexpressed GRs. However, the number of taste receptors would be much less if specific combinations of GRs are required as were shown for sugar receptors, bitter receptors or CO_2 receptors in *Drosophila*. Future experiments using heterologous expression systems are necessary to understand how different combinations of GRs and other taste receptors modify, disrupt or confer ligand profiles of taste receptors.

INSECT TASTE NEURONS

Adult and larval taste neuron expresses a specific subset of GR receptors and other types of taste receptors. Coexpression of taste receptors is sometimes required for receptor function as discussed in the previous section but is also important for taste signaling since it affects taste coding and taste discrimination. Here we will summarize and discuss the molecular aspects of taste neurons viewed from their receptor expression profiles as well as their morphological, developmental or physiological profiles.

STRUCTURE, DEVELOPMENT AND PHYSIOLOGY OF TASTE NEURONS

In contrast to taste buds, the mammalian taste organs, insect taste organs are usually distributed widely on the external surface of the body including the labella in the proboscis, legs, wings (**Figure 5**) and even the female ovipositors. They belong to sensilla trichodea and often called "taste hair" or "taste bristle" (Wilczek, 1967; Stocker and Schorderet, 1981; Nayak and Singh, 1983). Taste sensilla are also found on the internal labellum and the pharynx. They belong to sensilla basiconica and are sometimes called "taste papillae". A trichodea-type taste sensillum is usually composed of seven to nine cells including two to four taste neurons, a single mechanosensory neuron and a total of four non-neural cells, a trichogen cell, a tormogen cell, thecogen cell and a glial cell. The trichogen and tormogen cell produce hair shaft and socket cuticle materials, respectively. The thecogen and the glial cell wrap the cell bodies of the neuron cluster and their axons, respectively. A taste neuron sends a single, thin dendrite into the sensilla to the terminal pore opening where physical contact with external fluid takes place (Falk and Atidia, 1975). Each neuron also sends an axon proximally to the central nervous system.

Taste sensilla belong to poly-innervated external sensory organs accommodating multiple bipolar neurons (Kankel et al., 1980). Most bristles that cover the cuticle surface, on the other hand, are

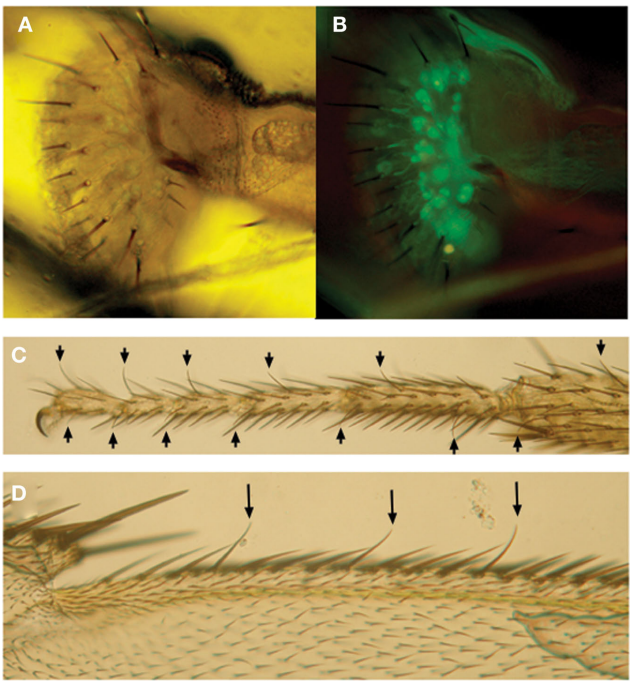

FIGURE 5 | Examples showing taste sensilla and labeled taste neurons in *Drosophila*. (A,B) Taste sensilla along the peripheral labella of a transformant fly expressing a cytoplasmic GFP marker protein driven by *Gr5a* promotor-*Gal4* (Gr5a-Gal4/Gr5a-Gal4, UAS-2xEGFP/UAS-2xEGFP). Pictures were taken under microscope by transmission light **(A)** or by fluorescence microscope **(B)**. Arrows in **(C)** and **(D)** show other types of taste sensilla along the tarsal segments of the distal legs **(C)** and wing margins in **(D)**.

mono-innervated bristles containing only a single mechanosensory neuron at the base that detects bristle movement. They both belong to the larger sensory organ category "external sensory bristles" and are developmentally derived from a common ancestral sensory mother cell in the imaginal discs. There are internal sense organs like chordotonal organs of the internal cuticle surface or multiple dendritic neurons in epidermal tissues that are mechanosensory and function as proprioceptive organs. These internal neurons are also derived from the sensory mother cells but by developmentally distinct programs. Sensory organs like olfactory trichoid, basiconic or coeloconic sensilla, or the compound eyes are also external sensory organs but are derived from the eye-antennal imaginal disc by different developmental programs.

While most adult taste organs are newly formed after eclosion, three pharyngeal taste organs – dorsal and ventral cibarial sense organs and labral sense organs – are embryonic and survive throughout the life stages (Gendre et al., 2004).

The identity of a sensory organ is developmentally determined by neurogenic genes and neuron-type selector genes. For example, activities of proneural genes in the *achaete-scute* gene complex are essential for the formation of sensory organs (García-Bellido and Santamaria, 1978). Once the sensory mother cells are formed, the choice between the external organ or chordotonal organ is regulated by the activity of a neuron-type selector gene *cut* (Bodmer et al., 1987). The choice between mono-innervated and poly-innervated external sensory organ is regulated by the activity of another

neuron-type selector gene *pox-neuro* (*poxn*) (Dambly-Chaudière et al., 1992). In *poxn* mutants all external sensory organs become mono-innervated mechanosensory organs (Awasaki and Kimura, 1997). Expression studies of GRs showed that different taste neurons express a distinct GR or a set of GRs. Therefore it is likely that additional, unknown neuron-type selector genes further determine the final taste neuron identities. The final decision seems to be independent from its receptor expression profile since inactivation or ectopic expression of GRs do not affect their projection or other neuronal identities as is true for *Drosophila* olfactory neurons (Hummel et al., 2003; Komiyama et al., 2004).

The observation that the choice between mechanosensory and taste neurons is regulated by only a single developmental gene *poxn* also suggests a common ancestral neuron between taste and mechanosensory neurons. In fact, as discussed in the previous section, some GRs are expressed in mechanosensory or proprioceptive non-gustatory neurons (Ejima and Griffith, 2008; Thorne and Amrein, 2008).

There are basically four chemosensory neurons plus one mechanosensory neuron in the external taste organs of adult flies. Electrophysiological studies showed that the four chemosensory neurons are (1) a S neuron that responds to sugar stimuli, (2) a W neuron that responds to water or solutions at low osmolarities, (3) an L1 neuron that responds to salt solutions at lower threshold concentrations and (4) an L2 neuron that responds to salt solutions at higher threshold concentrations (Pollack and Balakrishnan, 1997; see also records in **Figure 4**). Among them, S neurons are most extensively studied (Dethier and Hanson, 1968; Morita, 1972; Shimada et al., 1974; Fujishiro et al., 1984). S neurons express sugar receptor GRs and positively control feeding by triggering proboscis extension response. L2 neurons also respond to bitter substances (Meunier et al., 2003; Hiroi et al., 2004) and negatively control feeding and suppress the proboscis response. L1 neurons respond to lower concentrations of salt solutions. No GRs are known to be expressed in L1 neurons. It is not known if they are positively or negatively involved in feeding. W neurons respond to pure water, which also induce proboscis extension response when flies are deprived of water. W neurons may also positively control feeding.

Therefore, except for some sensilla that lack W and L1 neurons, all taste sensilla in the labellum had been considered physiologically identical with only four types of taste neurons until the expression and the functional studies of GRs began in this century.

RECEPTOR EXPRESSION AND FUNCTION IN TASTE NEURONS

Except for a few GRs that are expressed in the olfactory neurons or in the mechanosensory neurons, most GRs are expressed in various taste neurons innervating the adult or larval peripheral taste organs (**Figure 5**). Expression of GRs is unexpectedly divergent depending on each GR. Tissue expression profile for each GR is summarized in the third column of **Table 1**. Among 46 GRs so far studied for their expression out of 68 GRs in the fly genome, 40 GRs (~80%) are expressed in the labella of the proboscis, the major gustatory organs in adults, supporting the view that most GRs are taste receptors. In addition, a total of 17 GRs are expressed in the tarsal segments of the legs, 16 GRs in the internal taste peg or the pharyngeal taste neurons of the mouth and 7 GRs on the wing margin taste neurons. Since some GRs are expressed widely in the labellum, pharynx and the leg while other GRs are expressed only in one tissue, the overall tissue expression profiles are divergent and complex depending on each GR. In addition some GRs are expressed only in single or a limited numbers of taste neurons or sensilla within a given tissue. Despite the divergence in GR expression, however, the expression profiles are conserved between different individuals and the expression profile is dependent exclusively on GR genes themselves, suggesting that they are developmentally regulated.

GRs are also expressed in larval chemosensory organs. Larval GR expression is less complex since the majority of chemoreceptor neurons are localized in the dorsal and terminal organs of the head compartment. Among GR genes expressed in larvae, two genes, *Gr21a* and *Gr63a*, are olfactory CO2 receptor genes. All other GRs expressed in larvae are also expressed in adults, especially in the pharyngeal neurons, supporting that pharyngeal taste organs are of larval origin (Gendre et al., 2004). It is also important to note that the expression studies provide the first molecular evidence that different taste neurons express different taste receptors to process different taste information.

Functional studies were also carried out by mutational analysis of GR genes and by inactivation analysis of GR neurons (Dahanukar et al., 2001, 2007; Ueno et al., 2001; Thorne et al., 2004; Wang et al., 2004; Moon et al., 2006; Jiao et al., 2007; Slone et al., 2007; Jiao et al., 2008; Lee et al., 2009). Physiological and behavioral analyses were carried out. **Figure 3** shows a frequently used device to evaluate behavioral taste sensitivity and preference in *Drosophila*.

Combined studies of the expression and functional analysis of GRs showed that considerable numbers of GRs are coexpressed in one of the two groups, one related to sugar response, another to bitter response, respectively. GRs that are expressed in one neuron type are not usually expressed in other neuron types. The coexpression/ non-coexpression relations among GRs are summarized in the sixth and seventh columns of **Table 1**. The expression is often compared with caffeine receptor *Gr66a* in bitter neurons or with trehalose receptor *Gr5a* in sugar neurons because they are functionally characterized and are expressed widely in various types of taste sensilla.

In the labellar taste neurons a total of 12 GR genes belonging to various GR subgroups are coexpressed in bitter neurons expressing *Gr66a*. They are *Gr22b, Gr22e, Gr22f, Gr28bE, Gr32a, Gr33a, Gr39aD, Gr47a, Gr59b, Gr59f, Gr68a* and *Gr93a*. Even more GRs may be expressed in bitter neurons. Among them *Gr33a* is unique since it is essential for many bitter response as described in the Section "Insect Taste Receptors". Most other GR genes may be involved for specific sensitivity to bitter substances by encoding a bitter receptor or a monomeric component of a multimeric receptor.

Sugar neurons belong to the other coexpression group, expressing a subset of eight sugar receptor subgroup A GR genes, *Gr5a, Gr61a, Gr64a, Gr64b, Gr64c, Gr64d, Gr64e* and *Gr64f*. Among them *Gr64f* is shown to be essential for sugar receptor function (Jiao et al., 2008). *Gr5a* and *Gr64a* are shown to be required for distinct sugar sensitivity, respectively as described in the Section "Insect Taste Receptors".

Coexpression of multiple receptor molecules in single receptor cells is also observed in mammals. Multiple expression of taste receptors seems to be a common strategy in taste system, as was previously discussed (Adler et al., 2000; Dunipace et al., 2001). In flies, however,

coexpression profiles of GRs are more complex depending on GRs and taste neurons. For examples, *Gr59f*, *Gr22f*, *Gr59b* are coexpressed with *Gr66a* in the labellar neurons but are not expressed in other tissues while *Gr22c* and *Gr2a* are expressed in the pharynx *Gr66a* neurons but not expressed in the labellar neurons (Wang et al., 2004).

Some *Gr66a*-expressing L2 neurons were shown to respond also to the hydrocarbon *Z*-7-tricosene, an inhibitory sex pheromone that is involved in suppressing male homosexual courtship (Lacaille et al., 2007). Bitter substances in fact inhibit male courtship and, *vice versa*, *Z*-7-tricosene behaviorally induces bitter taste response. The contribution by *Gr66a* neurons to courtship, however, seems to be controversial. *Gr32a* is a candidate inhibitory pheromone receptor gene since males with a mutated or inactivated *Gr32a* neurons show abnormally high courtship activity toward males or mated females (Miyamoto and Amrein, 2008). *Gr32a is* coexpressed in the labellar *Gr66a*- or *Gr22e*-expressing bitter neurons while the expression of *Gr32a* and *Gr66a* in tarsal neurons do not overlap (**Table 1**). Since disruption of *Gr66a* neurons do not lead to the high courtship activity toward males or mated females, they argue that tarsal *Gr32a* neurons, but not the labellar *Gr32a*/*Gr66a* neurons are responsible for the mating suppression.

Studies of bitter taste response in the herbivorous caterpillar *Manduca sexta* support that discrimination of signals from different bitter neurons are possible. In the caterpillar feeding is robustly suppressed by bitter substances as in flies. However, the caterpillar does not show any suppression by a bitter substance when they are previously kept on a medium containing the same or similar bitter substance. The habituation occurs through a central mechanism, rather than a peripheral adaptation mechanism of the bitter neurons (Glendinning et al., 2001). The animal has only four types of taste organs, or eight pairs of taste sensilla in which a single bitter neuron is innervated. Habituation to a bitter ligand does not generalize to a ligand that stimulates different type of bitter neurons. Therefore it is suggested that the discrimination of bitter ligands is based on distinct higher-order neurons and signaling pathways among qualitatively different bitter substances (Glendinning et al., 2002). Since primary projection of bitter neurons are studied in detail in *Drosophila* as will be discussed in the next section, similar experiments using *Drosophila* would be useful to analyze whether the discrimination is based on segregation of the primary projections.

Another type of coexpression was reported by Thorne and Amrein (2008). They showed that *Gr5a* and *Gr22e* are coexpressed with *Gr28a* or *Gr28b.c* in the neurosecretary cells that produce insulin-like peptides. Since *Gr5a* is tuned to trehalose, it is possible that *Gr5a* is not only a taste receptor for trehalose but also an internal detector for the blood sugar trehalose. Similarly, some GRs like *Gr22e* may be expressed in non-taste neurons and function as internal nutrient detectors. In fact, a polycystic-kidney-disease-like ion channel (PKD2L1), a candidate mammalian sour taste sensor, is also a cerebrospinal fluid sensor in specific neurons surrounding the central canal of the spinal chord to detect decreases in extracellular pH in the mouse (Huang et al., 2006).

PRIMARY PROJECTIONS OF TASTE NEURONS

Taste projections in insects have been studied by Golgi staining and dye labeling of taste neurons in adult and larval central nervous systems of flies, bees, butterflies and other insects (Stocker and Schorderet, 1981; Nayak and Singh, 1983; Shanbhag and Singh, 1989, 1992; Stocker, 1994; Pollack and Balakrishnan, 1997; Mitchell et al., 1999). Gustatory primary centers thus identified were located in the tritocerebral–subesophageal ganglion complex (SOG) or in the thoracic–abdominal ganglion complex of the ventral nerve chord. In flies, chemosensory as well as mechanosensory neurons project to SOG through one of the three major nerve tracts. (1) The pharyngeal taste neurons send their axons through the pharyngeal or accessory pharyngeal nerve tracts and enter anterior SOG from the dorsolateral direction and terminate in anterior and dorsolateral SOG. (2) Labellar and taste peg neurons send their axons through the labial nerve tract and enter medial SOG from the ventrolateral direction. Labeling single labellar neurons show several projection types within SOG. (3) A subset of tarsal taste neurons of the legs directly send their axons through cervical connectives to posterior SOG while other tarsal taste neurons terminate in thoracic–abdominal ganglions. The ascending axons that enter SOG further proceed to anterior and dorsal direction and arborize in the medial or anterior SOG (Rajashekhar and Singh, 1994). Earlier morphological studies supported the view that the projection of taste neurons is organotopic, depending basically on the location of the peripheral taste organs. They also showed that there are several different types of projection within taste neurons sharing similar peripheral locations. However, these observations did not conclusively show that functionally segregated taste neurons are also segregated for their projection.

One of the important contributions by molecular studies was the observation that projections of sugar neurons and bitter neurons are also segregated (Dunipace et al., 2001; Scott et al., 2001; Thorne et al., 2004; Wang et al., 2004; Dahanukar et al., 2007). Based on these studies and our unpublished data, the basic projection profiles of the two types of taste neurons are schematically illustrated in **Figure 6**. Pharyngeal taste neurons expressing sugar and bitter receptor GRs send their axons through the pharyngeal nerve and/or the accessory pharyngeal nerve tract and terminate in an anterior and dorsolateral region in SOG, as have been previously described by earlier morphological studies. Tarsal axons of both sugar and bitter taste neurons enter posterior SOG and proceed along similar thin, two-pronged pathways and arborize along the tracts. Labellar bitter neurons and sugar neurons that enter medial SOG also follow the labial nerve projection profile. Therefore, all bitter neurons and sugar neurons follow the organotopic projection rule. However, fine details in the projection between the two types of neurons are different. Bitter neurons from the left and the right side of the labellum arborize bilaterally and converge to form a single cluster in the central region of the medial SOG. Axons of the bitter neurons from the pharyngeal tract and the tarsal taste neurons project to different regions in SOG. The projections are also bilateral. On the contrary, sugar neurons are mostly, if not all, ipsilateral (Thorne et al., 2004; Wang et al., 2004). In addition, the main projection areas of the sugar neurons are spatially segregated from the bitter projections. These observations first provided structural evidence for distinct locations of the synaptic region to higher-order neurons to process different taste qualities.

Therefore taste information seems to be processed according to two basic principles, organotopic and functional. Since taste neurons basically process chemical information, the latter map

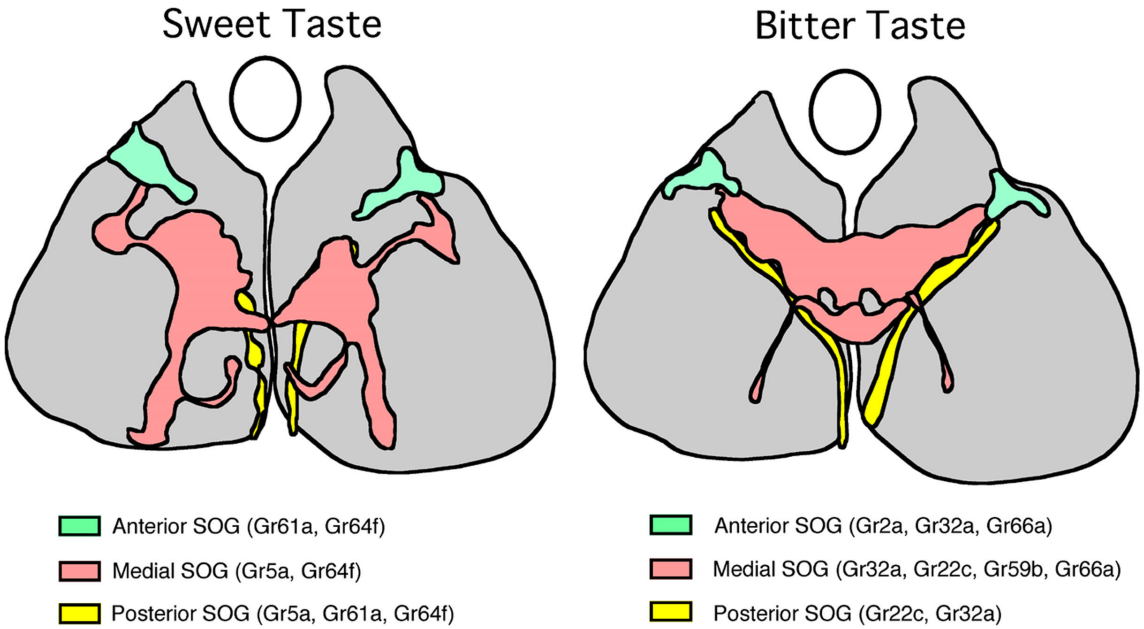

FIGURE 6 | A schematic drawing of the primary projection areas in the subesophageal ganglion (SOG) of sugar taste neurons (left) and bitter taste neurons (right). Frontal views of the anterior (blue), medial (pink) and posterior (yellow) projection areas in the SOG are superimposed in the same plane. Upward direction is dorsal. An oval represents the location of the esophagus. A subset of sugar receptor genes are indicated for each projection (Dahanukar et al., 2007; Wang et al., 2004). Note distinct projection areas for sugar and bitter neurons.

in SOG should reflect distinct pathways of higher-order neurons among different taste qualities. The role of organotopic map in SOG, however, is not so evident. The map may reflect processing of positional information to locate the source of gustatory stimulants as discussed by Wang et al. (2004). Alternatively, the map may reflect distinct output signaling circuits according to different peripheral inputs. For example, leg taste neurons may trigger searching or avoidance behavior while labellar or pharyngeal taste neurons control initiation or rejection of feeding behavior. The organotopic map may also be useful to discriminate between subtle differences in chemical information since neurons from different taste organs are known to express different combinations of GRs. For example, as is shown in **Figure 6**, labellar sugar neurons express *Gr5a* and *Gr64a* while tarsal sugar neurons express *Gr5a*, *Gr64a* and also *Gr61a* so that labellar and tarsal sugar neurons may be tuned to different sugar ligands. Similarly, bitter neurons in different taste organs may be tuned to different bitter ligands by expressing different combinations of bitter GRs. The insects may be able to discriminate details among stimulants by integrating gustatory information from different taste organs. Future studies of secondary taste neurons in SOG are necessary to understand how taste information is further processed in the central brain.

CONCLUSIONS

Insect taste neurons are chemosensory neurons expressing not only taste receptor GRs but also other types of sensory receptors. Since multiple, different subset of GRs are expressed in different types of taste neurons, the overall profiles of receptor expression in the insect taste system are complex in contrast to one receptor – one neuron expression profiles in the olfactory system. By allowing expression of multiple different receptors in single taste neurons insects may be able to expand the ligand spectrum. However, the design would sacrifice performance in discrimination. Future studies on the central mechanism of taste in the insect brain are necessary to understand how insect taste neurons process chemical information and control behavioral outputs.

ACKNOWLEDGMENTS

We thank Dr. Soh Kohatsu for unpublished GR expression data, Dr. Ryota Adachi for discussions, Dr. Masayuki Koganezawa for providing video analysis in Figure 3 and Dr. Noriko Tanabe for electrophysiological recordings in Figure 4. This work is supported by a grant to K. Isono from the Ministry of Education, Culture, Sports, Science and Technology of Japan.

REFERENCES

Adler, E., Hoon, M. A., Mueller, K. L., Chandrashekar, J., Ryba, N. J., and Zuker, C. S. (2000). A novel family of mammalian taste receptors. *Cell* 100, 693–702.

Al-Anzi, B., Tracey, W. D. Jr., and Benzer, S. (2006). Response of *Drosophila* to wasabi is mediated by painless, the fly homolog of mammalian TRPA1/ANKTM1. *Curr. Biol.* 16, 1034–1040.

Amrein, H., and Thorne, N. (2005). Gustatory perception and behavior in *Drosophila melanogaster*. *Curr. Biol.* 15, R673–R684.

Arora, K., Rodrigues, V., Joshi, S., Shanbhag, S., and Siddiqi, O. (1987). A gene affecting the specificity of the chemosensory neurons of *Drosophila*. *Nature* 330, 62–63.

Awasaki, T., and Kimura, K. (1997). pox-neuro is required for development of chemosensory bristles in *Drosophila*. *J. Neurobiol.* 32, 707–721.

Bodmer, R., Barbel, S., Sheperd, S., Jack, J. W., Jan, L. Y., and Jan, Y. N. (1987). Transformation of sensory organs by mutations of the cut locus of *D. melanogaster*. *Cell* 51, 293–307.

Bray, S., and Amrein, H. (2003). A putative *Drosophila* pheromone receptor expressed in male-specific taste neurons is required for efficient courtship. *Neuron* 39, 1019–1029.

Buck, L., and Axel, R. (1991). A novel multigene family may encode odorant receptors: a molecular basis for odor recognition. *Cell* 65, 175–187.

Chyb, S., Dahanukar, A., Wickens, A., and Carlson, J. R. (2003). *Drosophila* Gr5a encodes a taste receptor tuned to trehalose. *Proc. Natl. Acad. Sci. U.S.A.* 100, 14526–14530.

Clyne, P. J., Warr, C. G., and Carlson, J. R. (2000). Candidate taste receptors in *Drosophila*. *Science* 287, 1830–1834.

Colomb, J., Grillenzoni, N., Ramaekers, A., and Stocker, R. F. (2007). Architecture of the primary taste center of *Drosophila melanogaster* larvae. *J. Comp. Neurol.* 502, 834–847.

Couto, A., Alenius, M., and Dickson, B. J. (2005). Molecular, anatomical, and functional organization of the *Drosophila* olfactory system. *Curr. Biol.* 15, 1535–1547.

Dahanukar, A., Foster, K., van der Goes van Naters, W. M., and Carlson, J. R. (2001). A Gr receptor is required for response to the sugar trehalose in taste neurons of *Drosophila*. *Nat. Neurosci.* 4, 1182–1186.

Dahanukar, A., Lei, Y. T., Kwon, J. Y., and Carlson, J. R. (2007). Two Gr genes underlie sugar reception in *Drosophila*. *Neuron* 56, 503–516.

Dambly-Chaudière, C., Jamet, E., Burri, M., Bopp, D., Basler, K., Hafen, E., Dumont, N., Spielmann, P., Ghysen, A., and Noll, M. (1992). The paired box gene pox neuro: a determinant of poly-innervated sense organs in *Drosophila*. *Cell* 69, 159–172.

De Bruyne, M., and Warr, C. G. (2005). Molecular and cellular organization of insect chemosensory neurons. *Bioessays* 28, 23–34.

Dethier, V. G. (1976). *The Hungry Fly: A Physiological Study of the Behavior Associated with Feeding*. Cambridge, MA: Harvard University Press.

Dethier, V. G., and Hanson, F. E. (1968). Electrophysiological responses of the chemoreceptors of the blowfly to sodium salts of fatty acids. *Proc. Natl. Acad. Sci. U.S.A.* 60, 1296–1303.

Dong, X., Han, S., Zylka, M. J., Simon, M. I., and Anderson, D. J. (2001). A diverse family of GPCRs expressed in specific subsets of nociceptive sensory neurons. *Cell* 106, 619–632.

Dunipace, L., Meister, S., McNealy, C., and Amrein, H. (2001). Spatially restricted expression of candidate taste receptors in the *Drosophila* gustatory system. *Curr. Biol.* 11, 822–835.

Edwards, S. L., Charlie, N. K., Milfort, M. C., Brown, B. S., Gravlin, C. N., Knecht, J. E., and Miller, K. G. (2008). A novel molecular solution for ultraviolet light detection in *Caenorhabditis elegans*. *PLoS Biol.* 6, e198. doi: 10.1371/journal.pbio.0060198.

Ejima, A., and Griffith, L. C. (2008). Courtship initiation is stimulated by acoustic signals in *Drosophila melanogaster*. *PLoS ONE* 3, e3246. doi: 10.1371/journal.pone.0003246.

Ejima, A., Smith, B. P. C., Lucas, C., van der Goes van Naters, W., Miller, C. J., Carlson, J. R., Levine, J. D., and Griffith, L. C. (2007). Generalization of courtship learning in *Drosophila* is mediated by cis-vaccenyl acetate. *Curr. Biol.* 17, 599–605.

Falk, R., and Atidia, J. (1975). Mutation affecting taste perception in *Drosophila melanogaster*. *Nature* 254, 325–326.

Faucher, C., Forstreuter, M., Hilker, M., and de Bruyne, M. (2006). Behavioral responses of *Drosophila* to biogenic levels of carbon dioxide depend on life-stage, sex and olfactory context. *J. Exp. Biol.* 209, 2739–2748.

Ferveur, J. F., and Jallon, J. M. (1996). Genetic control of male cuticular hydrocarbons in *Drosophila melanogaster*. *Genet. Res.* 67, 211–218.

Fischler, W., Kong, P., Marella, S., and Scott, K. (2007). The detection of carbonation by the *Drosophila* gustatory system. *Natutr* 448, 1054–1057.

Fishilevich, E., Domingos, A. I., Asahina, K., Naef, F., Vosshall, L. B., and Louis, M. (2005). Chemotaxis behavior mediated by single larval olfactory neurons in *Drosophila*. *Curr. Biol.* 15, 2086–2096.

Fishilevich, E., and Vosshall, L. B. (2005). Genetic and functional subdivision of the *Drosophila* antennal lobe. *Curr. Biol.* 15, 1548–1553.

Fujishiro, N., Kijima, H., and Morita, H. (1984). Impulse frequency and action potential amplitude in labellar chemosensory neurons of *Drosophila melanogaster*. *J. Insect Physiol.* 30, 317–325.

García-Bellido, A., and Santamaria, P. (1978). Developmental analysis of the achaete-scute system of *Drosophila melanogaster*. *Genetics* 88, 469–486.

Gendre, N., Lüer, K., Friche, S., Grillenzoni, N., Ramaekers, A., Technau, G. M., and Stocker, R. F. (2004). Integration of complex larval chemosensory organs into the adult nervous system of *Drosophila*. *Development* 131, 83–92.

Glendinning, J. I., Davis, A., and Ramaswamy, S. (2002). Contribution of different taste cells and signaling pathways to the discrimination of "bitter" taste stimuli by an insect. *J. Neurosci.* 22, 7281–7287.

Glendinning, J. I., Domdom, S., and Long, E. (2001). Selective adaptation to noxious foods by a herbivorous insect. *J. Exp. Biol.* 204, 3355–3367.

Halpern, B. P. (1998). Amiloride and vertebrate gustatory responses to NaCl. *Neurosci. Biobehav. Rev.* 23, 5–47.

Herness, M. S., and Gilbertson, T. A. (1999). Cellular mechanisms of taste transduction. *Annu. Rev. Physiol.* 61, 873–900.

Hill, C. A., Fox, A. N., Pitts, R. J., Kent, L. B., Tan, P. L., Chrystal, M. A., Cravchik, A., Collins, F. H., Robertson, H. M., and Zwiebel, L. J. (2002). G protein-coupled receptors in *Anopheles gambiae*. *Science* 298, 176–178.

Hiroi, M., Meunier, N., Marion-Poll, F., and Tanimura, T. (2004). Two antagonistic gustatory receptor neurons responding to sweet-salty and bitter taste in *Drosophila*. *J. Neurobiol.* 61, 333–342.

Huang, A. L., Chen, X., Hoon, M. A., Chandrashekar, J., Guo, W., Tränkner, D., Ryba, N. J., and Zuker, C. S. (2006). The cells and logic for mammalian sour taste detection. *Nature* 442, 934–938.

Hummel, T., Vasconcelos, M. L., Clemens, J. C., Fishilevich, Y., Vosshall, L. B., and Zipursky, S. L. (2003). Axonal targeting of olfactory receptor neurons in *Drosophila* is controlled by Dscam. *Neuron* 37, 221–231.

Ikeya, T., Galic, M., Belawat, P., Nairz, K., and Hafen, E. (2002). Nutrient-dependent expression of insulin-like peptides from neuroendocrine cells in the CNS contributes to growth regulation in *Drosophila*. *Curr. Biol.* 12, 1293–1300.

Inomata, N., Goto, H., Itoh, M., and Isono, K. (2004). A single-amino-acid change of the gustatory receptor gene, Gr5a, has a major effect on trehalose sensitivity in a natural population of *Drosophila melanogaster*. *Genetics* 167, 1749–1758.

Isono, K., and Kikuchi, T. (1974). Autosomal recessive mutation in sugar response of *Drosophila*. *Nature* 248, 243–244.

Isono, K., Morita, H., Kohatsu, S., Ueno, K., Matsubayashi, H., and Yamamoto, M. T. (2005). Trehalose sensitivity of the gustatory neurons expressing wild-type, mutant and ectopic Gr5a in *Drosophila*. *Chem. Senses* 30, i275–i276.

Jallon, J. M. (1984). A few chemical words exchanged by *Drosophila* during courtship and mating. *Behav. Genet.* 14, 441–478.

Jiao, Y., Moon, S. J., and Montell, C. (2007). A *Drosophila* gustatory receptor required for the responses to sucrose, glucose, and maltose identified by mRNA tagging. *Proc. Natl. Acad. Sci. U.S.A.* 104, 14110–14115.

Jiao, Y., Moon, S. J., Wang, X., Ren, Q., and Montell, C. (2008). Gr64f is required in combination with other gustatory receptors for sugar detection in *Drosophila*. *Curr. Biol.* 18, 1797–1801.

Jones, W. D., Cayirlioglu, P., Kadow, I. G., and Vosshall, L. B. (2007). Two chemosensory receptors together mediate carbon dioxide detection in *Drosophila*. *Nature* 445, 86–90.

Kankel, D. R., Ferrus, A., Garen, S. H., Harte, P. J., and Lewis, P. E. (1980). "The structure and development of the nervous system," in *The Genetics and Biology of Drosophila*, Vol. 2d, eds M. Ashburner and T. R. F. Wright (London and New York: Academic Press), 295–368.

Kent, L. B., and Robertson, H. M. (2009). Evolution of the sugar receptors in insects. *BMC Evol. Biol.* 9, 41. doi: 10.1186/1471-2148-9-41.

Komiyama, T., Carlson, J. R., and Luo, L. (2004). Olfactory receptor neuron axon targeting: intrinsic transcriptional control and hierarchical interactions. *Nat. Neurosci.* 7, 819–825.

Kwon, J. Y., Dahanukar, A., Weiss, L. A., and Carlson, J. R. (2007). The molecular basis of CO2 reception in *Drosophila*. *Proc. Natl. Acad. Sci. U.S.A.* 104, 3574–3578.

Lacaille, F., Hiroi, M., Twele, R., Inoshita, T., Umemoto, D., Manière, G., Marion-Poll, F., Ozaki, M., Francke, W., Cobb, M., Everaerts, C., Tanimura, T., and Ferveur, J. F. (2007). An inhibitory sex pheromone tastes bitter for *Drosophila* males. *PLoS ONE* 2, e661. doi: 10.1371/journal.pone.0000661.

Lee, Y., Lee, Y., Lee, J., Bang, S., Hyun, S., Kang, J., Hong, S. T., Bae, E., Kaang, B. K., and Kim, J. (2005). Pyrexia is a new thermal transient receptor potential channel endowing tolerance to high temperatures in *Drosophila melanogaster*. *Nat. Genet.* 37, 305–310.

Lee, Y., Moon, S. J., and Montell, C. (2009). Multiple gustatory receptors required for the caffeine response in *Drosophila*. *Proc. Natl. Acad. Sci. U.S.A.* 106, 4495–4500.

Liu, L., Leonard, A. S., Motto, D. G., Feller, M. A., Price, M. P., Johnson, W. A., and Welsh, M. J. (2003). Contribution of *Drosophila* DEG/ENaC genes to salt taste. *Neuron* 39, 133–146.

McBride, C. S., and Arguello, J. R. (2007). Five *Drosophila* genomes reveal nonneutral evolution and the signature of host specialization in the chemoreceptor superfamily. *Genetics* 177, 1395–1416.

Meunier, N., Marion-Poll, F., and Lucas, P. (2009). Water taste transduction pathway is calcium dependent in *Drosophila*. *Chem. Senses* 34, 441–449.

Meunier, N., Marion-Poll, F., Rospars, J. P., and Tanimura, T. (2003). Peripheral

coding of bitter taste in *Drosophila*. *J. Neurobiol.* 56, 139–152.
Minke, B., and Parnas, M. (2006). Insights on TRP channels from in vivo studies in *Drosophila*. *Annu. Rev. Physiol.* 68, 649–684.
Minnich, D. E. (1921). An experimental study of the tarsal chemoreceptors of two nymphalid butterflies. *J. Exp. Zool.* 33, 173–203.
Mitchell, B. K., Itagaki, H., and Rivet, M. P. (1999). Peripheral and central structures involved in insect gustation. *Microsc. Res. Tech.* 47, 401–415.
Mitri, C., Soustelle, L., Framery, B., Bockaert, J., Parmentier, M. L., and Grau, Y. (2009). Plant insecticide L-canavanine repels *Drosophila* via the insect orphan GPCR DmX. *PLoS Biol.* 7, e1000147. doi: 10.1371/journal.pbio.1000147.
Miyamoto, T., and Amrein, H. (2008). Suppression of male courtship by a *Drosophila* pheromone receptor. *Nat. Neurosci.* 11, 874–876.
Montell, C. (2009). A taste of the *Drosophila* gustatory receptors. *Curr. Opin. Neurobiol.* 19, 345–353.
Moon, S. J., Köttgen, M., Jiao, Y., Xu, H., and Montel, C. (2006). A taste receptor required for the caffeine response in vivo. *Curr. Biol.* 16, 1812–1817.
Moon, S. J., Lee, Y., Jiao, Y., and Montell, C. (2009). A *Drosophila* gustatory receptor essential for aversive taste and inhibiting male-to-male courtship. *Curr. Biol.* 19, 1623–1627.
Morita, H. (1972). Primary processes of insect chemoreception. *Adv. Biophys.* 3, 161–198.
Nakagawa, T., Sakurai, T., Nishioka, T., and Touhara, K. (2005). Insect sex-pheromone signals mediated by specific combinations of olfactory receptors. *Science* 307, 1638–1642.
Nayak, S. Y., and Singh, R. N. (1983). Sensilla on the tarsal segments and mouthparts of adult *Drosophila melanogaster meigen* (Diptera: Drosophilidae). *Int. J. Insect Morphol. Embryol.* 12, 273–291.
Nelson, G., Chandrashekar, J., Hoon, M. A., Feng, L., Zhao, G., Ryba, N. J. P., and Zuker, C. S. (2002). An amino-acid taste receptor. *Nature* 416, 199–202.
Nelson, G., Hoon, M. A., Chandrashekar, J., Zhang, Y., Ryba, N. J. P., and Zuker, C. S. (2001). Mammalian sweet taste receptors. *Cell* 106, 381–390.
Neuhaus, E. M., Gisselmann, G., Zhang, W., Dooley, R., Störtkuhl, K., and Hatt, H. (2005). Odorant receptor heterodimerization in the olfactory system of *Drosophila melanogaster*. *Nat. Neurosci.* 8, 15–17.
Pollack, G., and Balakrishnan, R. (1997). Taste sensilla of flies: function, central neuronal projections, and development. *Microsc. Res. Tech.* 39, 532–546.
Python, F., and Stocker, R. F. (2002). Adult-like complexity of the larval antennal lobe of *D. melanogaster despite markedly low numbers of odorant receptor neurons. J. Comp. Neurol.* 445, 374–387.
Rajashekhar, K. P., and Singh, R. N. (1994). Neuroarchitecture of the tritocerebrum of *Drosophila melanogaster*. *J. Comp. Neurol.* 349, 633–645.
Ramsey, I. S., Delling, M., and Clapham, D. E. (2006). An introduction to TRP channels. *Annu. Rev. Physiol.* 68, 619–647.
Robertson, H. M., and Wanner, K. W. (2006). The chemoreceptor superfamily in the honey bee, *Apis mellifera*: expansion of the odorant, but not gustatory, receptor family. *Genome Res.* 16, 1395–1403.
Robertson, H. M., Warr, C. G., and Carlson, J. R. (2003). Molecular evolution of the insect chemoreceptor gene superfamily in *Drosophila melanogaster*. *Proc. Natl. Acad. Sci. U.S.A.* 100, 14537–14542.
Rodrigues, V., and Siddiqi, O. (1981). A gustatory mutant of *Drosophila* defective in pyranose receptors. *Mol. Gen. Genet.* 181, 406–408.
Rosenzweig, M., Kang, K., and Garrity, P. A. (2008). Distinct TRP channels are required for warm and cool avoidance in *Drosophila melanogaster*. *Proc. Natl. Acad. Sci. U.S.A.* 105, 14668–14673.
Sakurai, T., Nakagawa, T., Mitsuno, H., Mori, H., Endo, Y., Tanoue, S., Yasukochi, Y., Touhara, K., and Nishioka, T. (2004). Identification and functional characterization of a sex pheromone receptor in the silkmoth *Bombyx mori*. *Proc. Natl. Acad. Sci. U.S.A.* 101, 16653–16658.
Scott, K. (2005). Taste recognition: food for thought. *Neuron* 48, 455–464.
Scott, K., Brady, J. R., Cravchik, A., Morozov, P., Rzhetsky, A., Zuker, C., and Axel, R. (2001). A chemosensory gene family encoding candidate gustatory and olfactory receptors in *Drosophila*. *Cell* 104, 661–673.
Shanbhag, S. R., and Singh, R. N. (1989). "Projections and functional implications of labellar neurons from individual sensilla of *Drosophila melanogaster*," in *Neurobiology of Sensory Systems*, eds R. N. Singh and N. J. Strausfeld (New York and London: Plenum Press), 427–437.
Shanbhag, S. R., and Singh, R. N. (1992). Functional implications of the projections of neurons from individual labellar sensillum of *Drosophila melanogaster* as revealed by neuronal-marker horseradish peroxidase. *Cell Tissue Res.* 267, 273–282.
Shimada, I., Shiraishi, A., Kijima, H., and Morita, H. (1974). Separation of two receptor sites in a single labellar sugar receptor of the flesh-fly by treatment with p-chloromercuribenzoate. *J. Insect Physiol.* 20, 605–621.
Singh, R. N. (1997). Neurobiology of the gustatory systems of *Drosophila* and some terrestrial insects. *Microsc. Res. Tech.* 39, 547–563.
Slone, J., Daniels, J., and Amrein, H. (2007). Sugar receptors in *Drosophila*. *Curr. Biol.* 17, 1809–1816.
Stocker, R. F. (1994). The organization of the chemosensory system in *Drosophila melanogaster*: a review. *Cell Tissue Res.* 275, 3–26.
Stocker, R. F., and Schorderet, M. (1981). Cobalt filling of sensory projections from internal and external mouthparts in *Drosophila*. *Cell Tissue Res.* 216, 513–523.
Suh, G. S. B., Wong, A. M., Hergarden, A. C., Wang, J. W., Simon, A. F., Benzer, S., Axel, R., and Anderson, D. J. (2004). A single population of olfactory sensory neurons mediates an innate avoidance behaviour in *Drosophila*. *Nature* 431, 854–859.
Tanimura, T., Isono, K., Takamura, T., and Shimada, I. (1982). Genetic dimorphism in the taste sensitivity to trehalose in *Drosophila melanogaster*. *J. Comp. Physiol.* 147, 433–437.
Thorne, N., and Amrein, H. (2008). Atypical expression of *Drosophila* gustatory receptor genes in sensory and central neurons. *J. Comp. Neurol.* 506, 548–568.
Thorne, N., Chromey, C., Bray, S., and Amrein, H. (2004). Taste perception and coding in *Drosophila*. *Curr. Biol.* 14, 1065–1079.
Tompkins, L., Cardosa, M. J., White, F. V., and Sanders, T. G. (1979). Isolation and analysis of chemosensory behavior mutants in *Drosophila melanogaster*. *Proc. Natl. Acad. Sci. U.S.A.* 76, 884–887.
Tracey, W. D. Jr., Wilson, R. I., Laurent, G., and Benzer, S. (2003). Painless, a *Drosophila* gene essential for nociception. *Cell* 113, 261–273.
Ueno, K., Ohta, M., Morita, H., Mikuni, Y., Nakajima, S., Yamamoto, K., and Isono, K. (2001). Trehalose sensitivity in *Drosophila* correlates with mutations in and expression of the gustatory receptor gene Gr5a. *Curr. Biol.* 11, 1451–1455.
van der Goes van Naters, W., and Carlson, J. R. (2007). Receptors and neurons for fly odors in *Drosophila*. *Curr. Biol.* 17, 606–612.
Wang, Z., Singhvi, A., Kong, P., and Scott, K. (2004). Taste representations in the *Drosophila* brain. *Cell* 117, 981–991.
Wanner, K. W., Nichols, A. S., Walden, K. K. O., Brockmann, A., Luetje, C. W., and Robertson, H. M. (2007). A honey bee odorant receptor for the queen substance 9-oxo-2-decenoic acid. *Proc. Natl. Acad. Sci. U.S.A.* 104, 14383–14388.
Wilczek, M. (1967). The distribution and neuroanatomy of the labellar sense organs of the blowfly *Phormia regina* Meigen. *J. Morphol.* 122, 175–201.
Xu, J., Sornborger, A. T., Lee, J. K., and Shen, P. (2008). *Drosophila* TRPA channel modulates sugar-stimulated neural excitation, avoidance and social response. *Nat. Neurosci.* 11, 676–682.
Zufall, F., and Leinders-Zufall, T. (2007). Mammalian pheromone sensing. *Curr. Opini. Neurobiol.* 17, 483–489.

Conflict of Interest Statement: This research was conducted in the absence of any commercial or financial relationships that could be construed as a potential conflict of interest.

Received: 02 February 2010; paper pending published: 27 February 2010; accepted: 16 May 2010; published online: 18 June 2010. Citation: Isono K and Morita H (2010) Molecular and cellular designs of insect taste receptor system. Front. Cell. Neurosci. 4:20. doi: 10.3389/fncel.2010.00020
Copyright © 2010 Isono and Morita. This is an open-access article subject to an exclusive license agreement between the authors and the Frontiers Research Foundation, which permits unrestricted use, distribution, and reproduction in any medium, provided the original authors and source are credited.

frontiers in
CELLULAR NEUROSCIENCE

REVIEW ARTICLE
published: 31 December 2010
doi: 10.3389/fncel.2010.00133

Pheromone transduction in moths

Monika Stengl*

FB 10, Biology, Animal Physiology, University of Kassel, Kassel, Germany

Edited by:
Dieter Wicher, Max Planck Institute for Chemical Ecology, Germany

Reviewed by:
Bernd Grunewald, Johann Wolfgang Goethe University, Germany
Dean P. Smith, University of Texas Southwestern Medical Center at Dallas, USA

***Correspondence:**
Monika Stengl, FB 10, Biology, Animal Physiology, University of Kassel, Heinrich-Plett-Str. 40, 34132 Kassel, Germany.
e-mail: stengl@uni-kassel.de

Calling female moths attract their mates late at night with intermittent release of a species-specific sex-pheromone blend. Mean frequency of pheromone filaments encodes distance to the calling female. In their zig-zagging upwind search male moths encounter turbulent pheromone blend filaments at highly variable concentrations and frequencies. The male moth antennae are delicately designed to detect and distinguish even traces of these sex pheromones amongst the abundance of other odors. Its olfactory receptor neurons sense even single pheromone molecules and track intermittent pheromone filaments of highly variable frequencies up to about 30 Hz over a wide concentration range. In the hawkmoth *Manduca sexta* brief, weak pheromone stimuli as encountered during flight are detected via a metabotropic PLCβ-dependent signal transduction cascade which leads to transient changes in intracellular Ca^{2+} concentrations. Strong or long pheromone stimuli, which are possibly perceived in direct contact with the female, activate receptor-guanylyl cyclases causing long-term adaptation. In addition, depending on endogenous rhythms of the moth's physiological state, hormones such as the stress hormone octopamine modulate second messenger levels in sensory neurons. High octopamine levels during the activity phase maximize temporal resolution cAMP-dependently as a prerequisite to mate location. Thus, I suggest that sliding adjustment of odor response threshold and kinetics is based upon relative concentration ratios of intracellular Ca^{2+} and cyclic nucleotide levels which gate different ion channels synergistically. In addition, I propose a new hypothesis for the cyclic nucleotide-dependent ion channel formed by insect olfactory receptor/coreceptor complexes. Instead of being employed for an ionotropic mechanism of odor detection it is proposed to control subthreshold membrane potential oscillation of sensory neurons, as a basis for temporal encoding of odors.

Keywords: insect olfaction, second messengers, octopamine, circadian rhythms, signal transduction cascades, field potentials, subthreshold membrane potential oscillations, temporal encoding

MALE MOTHS DETECT PHEROMONES WITH ASTOUNDING SENSITIVITY AND HIGH TEMPORAL RESOLUTION, BUT UNDERLYING TRANSDUCTION CASCADES ARE NOT UNDERSTOOD

Sensitive odor detection is a prerequisite to survival and reproduction in many insect species, especially in short-lived moths. While they rest during the day late at night female moths release pulses of a sex-pheromone blend to attract their mates (Itagaki and Conner, 1988). Pheromones are species-specific odors with properties of hormones. They signal the physiological state of the individual insect to their conspecifics. Air turbulences tear and whirl the pheromone blend pulse pattern into intermittent odor filaments of varying blend concentrations and frequencies. Time-dependently in synchrony with the female, male moths detect the pheromone filaments at astounding sensitivity with specialized hair-like sensilla on their antennae (Kaissling and Priesner, 1970; Sanes and Hildebrand, 1976; Almaas et al., 1991; reviews: Kaissling and Thorson, 1980; Kaissling, 1987). With forward pointed antennae male moths fly upwind, brushing the air with long trichoid sensilla. They adsorb about 30% of the lipophilic pheromones in a surrounding air stream on the waxy surface of the antennal cuticle (Kaissling, 1987). Hawkmoths fly with a velocity of about 3.5 m/s and beat their wings at a high frequency of about 30 Hz. Flight velocity and wing beat frequency affect sampling of odorants. It is assumed that each downstroke of the wing accelerates airflow over the olfactory sensilla and, thus, periodically allows for odor sampling, about every 30 ms (Tripathy et al., 2010).

Next to the species-specific pheromone blend composition, this intermittency of the pheromone signal is a critical prerequisite for eliciting arousal in the male moth, for starting and maintaining the male's characteristic zig-zagging anemotaxis (Kennedy et al., 1981; Murlis and Jones, 1981; Baker et al., 1985; Baker and Haynes, 1989; Tumlinson et al., 1989; Vickers and Baker, 1992; Vickers, 2000; Koehl, 2006; Lei et al., 2009). Constant or very strong pheromone stimulation results in cessation of the males search, possibly caused by adaptation of the sensory cells (Baker et al., 1988). Owing to the turbulent air, distance to the female is encoded in the mean frequency of pheromone filaments rather than in a concentration gradient. From behavioral experiments it was calculated that male moths can assess pheromone blend ratios within less than 100 ms, possibly comparing two consecutive antennal "sniffs" (review: De Bruyne and Baker, 2008). Upon loss of pheromone during zig-zag upwind flight they respond with cross wind-casting within 300–500 ms (Baker and Vogt, 1988). Apparently, sensitized silkmoth antennal olfactory receptor neurons (ORNs) can detect single pheromone molecules and hawkmoth ORNs differentiate pheromone

concentrations over at least 4 log units (Kaissling and Priesner, 1970; Kaissling, 1987; Dolzer et al., 2003). In addition, the olfactory system appears to follow intermittent odor signals of about 30 Hz (Justus et al., 2005; Ito et al., 2008; Tripathy et al., 2010). Therefore, evolution shaped the olfactory system to be as sensitive as possible and to allow reaction times within the range of 30 ms.

Still it is not resolved which olfactory signal transduction cascades are responsible for the astounding sensitivity and for the fast temporal resolution of pheromone blend detection and discrimination. There is strong controversy in the field of olfaction in the interpretation of apparently conflicting genetic and physiological data. Especially the characterization of receptor–ion channel complexes raised the hypothesis that insects smell via speedy ionotropic signal transduction in contrast to vertebrates which employ sensitive G-protein coupled, metabotropic odor transduction cascades. This review focuses on sex-pheromone-detection in the hawkmoth *Manduca sexta* due to an available primary cell culture system which greatly facilitated physiological studies (Stengl and Hildebrand, 1990), while only briefly brushing over perireceptor events which were reviewed recently (Kaissling, 2009). In this review I suggest novel explanations for the surprising variety of different signal transduction cascades reported in moth pheromone transduction which differ greatly from a previously suggested quantitative model of insect transduction (Gu et al., 2009). I propose a new testable hypothesis of receptor–ion channel complex-function in the control of subthreshold membrane potential oscillations and, thus, in the control of temporal encoding in moth pheromone transduction.

FUNCTIONAL ANATOMY OF PHEROMONE-SENSITIVE ANTENNAL SENSILLA

Insects detect odorants mostly with their antennae (von Frisch, 1921). In moths the sexually dimorphic antennal flagellum of the male is enlarged to house extra arrays of pheromone-specific long trichoid sensilla. In addition, it contains cholinergic, shorter sensilla basiconica which detect general odorants and sensilla of other modalities (Altner and Prillinger, 1980; Keil and Steinbrecht, 1984; Lee and Strausfeld, 1990; Stengl et al., 1990).The extreme sensitivity of moth pheromone detection observed is obtained by a number of different mechanisms, including the specific morphology of the moth's antennal sensilla. The pheromone-sensitive trichoid sensilla (**Figure 1**) are the longest and most abundant (38% of 2100 sensilla per annulus in *M. sexta*) cuticular hairs which form regular brush-like arrays on each annulus of the antennal flagellum (Keil, 1989; Lee and Strausfeld, 1990). About 32% of 3.6×10^5 sensory neurons of the hawkmoth antenna are pheromone-sensitive ORNs which innervate long trichoid sensilla. In *M. sexta* antennae two ORNs innervate each trichoid sensillum. One of them (Dolzer et al., 2003) responds to (E,Z)-10,12-hexadecadienal (=bombykal), the main sex pheromone component which makes up 31% of the sex-pheromone blend. The other of the two ORNs responds to other components of the pheromone blend such as to (E,E,Z)-10,12,14-hexadecatrienal (14.7%; Kaissling et al., 1989). Next to the ORNs each sensillum trichodeum contains about three non-neuronal cells: the trichogen, the tormogen, and the thecogen cells (**Figure 1**). All cells of an olfactory sensillum are born from ganglion mother cells in the antennal epithelium (Keil, 1999). During development

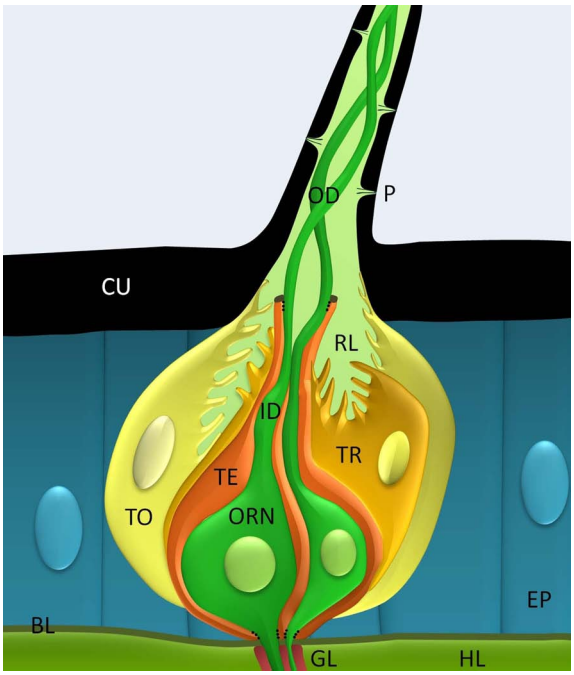

FIGURE 1 | In the hawkmoth the long trichoid sensillum is innervated by two pheromone-sensitive olfactory receptor neurons (ORNs), one responding to bombykal the main pheromone component. The non-neuronal tormogen (TO) and trichogen cells (TE) build the hollow hair shaft of the long sensory hair. Pores (P) in the cuticle (CU) of the hair allow pheromone to enter the receptor lymph (RL). The ORNs (green) are partitioned via tight membrane junctions (dotted lines) into an outer dendrite (OD), an inner dendrite (ID) and soma, both covered by a thecogen cell (TE), and a glia-wrapped axon. Thus, only the outer dendrite contacts the RL containing high potassium concentration and odorants. Hemolymph (HL); basal lamina (BL), epithelial cells (EP).

the trichogen and tormogen cells generate the hollow cuticular hair shaft with the inner sensillar lymph cavity. The dendrites of the ORNs are partitioned into an outer and inner dendrite by a short ciliary structure. The thecogen cell wraps around the inner dendrite and soma of the sensory neurons. Only the naked outer dendrites of the two bipolar ORNs extend into the sensillum lymph cavity. The outer dendrite is a modified cilium which lacks the central microtubule pair and does not contain an endoplasmic reticulum or any other organelles. It is motile and can perform oscillatory elongations and constrictions (Keil, 1993). The sensory neuron's axon, which is covered by a glial sheet, projects to the antennal lobe of the brain (**Figure 1**). The somata of moth ORNs are embedded between epithelial cells underneath the cuticular hair. Thus, each moth ORN is partitioned into three separate compartments: (1) the outer dendrite, (2) the inner dendrite with soma, and (3) the axon. The different compartments are isolated from each other. Very likely they maintain different external ionic milieus and different membrane compositions. The sensillum lymph contains a very high potassium concentration of about 200 mM (reviews: Kaissling and Thorson, 1980; Thurm and Küppers, 1980; Kaissling, 2009). This intracellular-like potassium concentration is generated by vacuolar-type H^+-ATPases in the copious membrane folds of the tormogen and trichogen cells walling the sensillum lymph cavity. Thus, a

transepithelial potential (TEP) of up to 40 mV between sensillum lymph and hemolymph adds to the negative resting potential of the ORNs and increases the electrical driving force for the receptor current. This TEP shows oscillations which are affected by biogenic amines circulating in the hemolymph (Dolzer et al., 2001). Little is known about ion channels in the supporting cells. But it is clear that also the non-neuronal cells contribute to odor-dependent sensillum potentials since no direct correlation between odor-dependent sensillum potential changes and action potential responses of the sensory neurons are found (Dolzer et al., 2003).

In conclusion: The lipophilic cuticle and surface maximization of many long trichoid sensilla assure accumulation of airborne pheromones at high efficiency to improve sensitivity. It remains to be studied whether slow oscillatory elongations of the dendrite and slow TEP-oscillations are phase-locked to the moth's fast wing beat frequency and whether oscillatory wing beats ensure oscillatory odor stimulation. Furthermore, it remains to be examined whether oscillatory odor stimulation results in synchronization of ORNs to improve frequency resolution and blend assessment via mechanisms of temporal encoding. Compartmentalization of the ORN implicates differential distribution of membrane proteins and extracellular milieus which also need to be evaluated further. Finally, the nitty-gritty of non-neuronal supporting cells should not be neglected because they considerably contribute to olfactory transduction not only via generation of a modifiable TEP.

PERIRECEPTOR EVENTS: FROM STIMULUS ENTRY TO PASSAGE TO OLFACTORY RECEPTOR MOLECULES

Through pores and lipophilic pore tubules which extend into the cavity of the sensory hairs the hydrophobic pheromones enter the hair shaft and face the aqueous sensillum lymph with high protein concentrations (Keil and Steinbrecht, 1984). Supporting cells secrete these millimolar concentrations of pheromone-binding proteins (PBPs; odorant-binding proteins = OBPs in sensilla basiconica) into the sensillum lymph of trichoid sensilla (Forstner et al., 2006, 2009; Pelosi et al., 2006). The moth PBPs bind specific pheromone components with high affinity and thereby contribute to the specificity and sensitivity of the pheromone responses (Stengl et al., 1992; Steinbrecht et al., 1995; Ziegelberger, 1995; Mohl et al., 2002; Pophof, 2004; Leal et al., 2005; Grosse-Wilde et al., 2006, 2007; Kaissling, 2009). Their various functions are not yet completely resolved but the PBPs appear to act as scavenger of unspecific odorants and as carrier of specific pheromone compounds to their dendritic receptor molecule complexes. Apparently, PBPs undergo a conformational shift after pheromone binding (Ziegelberger, 1995). Then, they are enabled to transiently interact with dendritic pheromone receptor molecule-complexes (containing various molecules, see below) which allows for another conformational change which initiates pheromone degradation via enzymes (Vogt and Riddiford, 1981, 1986; Ziegelberger, 1995). Thus, moth PBPs/OBPs appear to be selectivity filters, as well as temporal filters, contributing to the specific, transient, and single interaction with dendritic olfactory receptor molecule-complexes before the odor molecules are inactivated. Studies with loss of function and gain of function mutants of the OBP LUSH in *D. melanogaster* generally support this notion (Laughlin et al., 2008). In addition to affecting odor detection, *lush* loss of function mutants decrease spontaneous activity of the ORNs (Xu et al., 2005). It is assumed that LUSH is absolutely required for the detection of the fruitfly's aggregation pheromone 11-*cis* vaccenyl acetate (Xu et al., 2005). Alternatively, it is possible that LUSH lowers the detection threshold of odors and prevents adaptation of receptors because it allows for only very transient binding of the odor to the receptor. Without LUSH an odorant might not be transiently bound and quickly removed from the odor receptor complex which then desensitizes. This assumption was supported by respective observations in the hawkmoth (Stengl et al., 1992). Still, the different functions of the PBPs/OBPs are under debate and remain to be investigated further. Modeling studies by Kaissling (2009) predicted that 17% of the total pheromone concentration is enzymatically degraded and 83% is bound to the PBPs within 3 ms after entering the sensillum lymph. In his kinetic model the half-life of the activated dendritic receptor–pheromone–PBP complex was calculated to be 0.8 s, the EC50 was 6.8 μM.

In conclusion: Moth ORNs are flux detectors because antennal odor adsorption depends not only on the external odor concentration but also on the relative velocity of the air stream, the speed, and the wing beat frequency of the flying insect (Kaissling, 2009). Therefore, the latency and kinetics of the odor-dependent potential responses are also governed by the kinetics of odor entry, odor-PBP(OBP)-odor receptor complex interactions, and odor inactivation/enzymatic degradation. Further quantitative studies need to resolve the dynamical impact of perireceptor events in odor detection within more detail.

OLFACTORY RECEPTOR MOLECULE COMPLEXES IN OUTER DENDRITES OF MOTH ORNs

After reaching the outer dendritic membrane of ORNs pheromone–PBP complexes specifically interact with olfactory receptor molecule (OR)–complexes, initiating signal transduction cascades. There are different classes of chemosensory receptor molecules described, next to other specific sensory neuron membrane proteins (SNMPs).

INSECT ORs ARE UNRELATED IN SEQUENCE TO VERTEBRATE ORs

Insect ORs appear to be largely insect-specific proteins which do not share sequence similarity to vertebrate ORs or other G-protein coupled receptors. Nevertheless, also insect ORs have predicted seven transmembrane domains, but they appear to adopt a different topology in contrast to vertebrate ORs (review: Nakagawa and Vosshall, 2009; Silbering and Benton, 2010). Studies in molecular genetics combined with immunocytochemistry revealed that dendrites of a single silkmoth ORN contain at least two different olfactory receptor molecules (ORs), apparently forming complexes at unknown density with unresolved stoichiometry (Krieger et al., 2002, 2004, 2005, 2009; Sakurai et al., 2004; Grosse-Wilde et al., 2007; Brigaud et al., 2009; review: Nakagawa and Vosshall, 2009). One of them is a widely conserved coreceptor (COR) termed OR83b in the fruitfly and *Msexta*OR2 in the hawkmoth (Krieger et al., 2003; Malpel et al., 2008; *M. sexta*: Patch et al., 2009; review: Nakagawa and Vosshall, 2009). In *D. melanogaster* this COR is a chaperon that is obligatory for directing ORs into dendritic membranes and thus, its destruction deletes odor responses in the fruitfly (Larsson et al., 2004; Benton et al., 2006). In moths *in situ* hybridizations suggested

that *MsextaOR2* is also located to pheromone-sensitive long trichoid sensilla and, thus, appears to play a role in pheromone transduction (Patch et al., 2009). This hypothesis is confirmed by Nakagawa et al. (2005) who found the COR colocalized with pheromone receptors in *Bombyx mori*. However, relative levels of *MsextaOR2* expression are much higher in the female antenna than in the male antenna. This result suggests that the COR is either not expressed in all pheromone-sensitive trichoid sensilla of male hawkmoths or that it is expressed at considerably lower level in the pheromone system as compared to the general odor detecting system (Patch et al., 2009). Due to these conflicting results it is necessary to perform more studies in different insect species to resolve whether pheromone transduction indeed depends on an OR/COR complex.

THE SENSORY NEURON MEMBRANE PROTEINS IN DENDRITIC MEMBRANES OF ORNs

The SNMPs were identified in the dendritic membrane of male and female moth ORNs and supporting cells (Rogers et al., 1997, 2001a,b; Forstner et al., 2008). The SNMPs are related to the CD36 receptor family of glycoproteins, which recognize long-chain fatty acids, oxidized phospholipids, and lipoproteins (review: Silverstein and Febbraio, 2009). Their functions in olfaction are not yet resolved but it is hypothesized that SNMPs might be additional coreceptors which are involved in the transfer of lipophilic pheromones or pheromone–PBP-complexes to ORs (Rogers et al., 2001b; Vogt et al., 2009). This assumption is supported by studies in *D. melanogaster* which demonstrated that a SNMP is required for pheromone responses (Benton et al., 2007). Because SNMP mutants showed increased spontaneous activity it was suggested that SNMP inhibits the receptor in absence of pheromone (Benton et al., 2007; Jin et al., 2008). However, the additional expression of SNMPs in non-neuronal supporting cells of trichoid sensilla suggests additional functions (Forstner et al., 2008). Because supporting cells show pheromone-induced cGMP elevations and NADPH-diaphorase activity (which is indicative of nitric oxide synthase) only after very strong, long pheromone stimuli, it remains to be examined whether SNMPs might be pheromone-sensitive coreceptors of receptor guanylyl cyclases (GCs) in supporting cells (Stengl and Zintl, 1996; Stengl et al., 2001).

OTHER RECEPTORS FOUND IN DENDRITES OF ORNs

Next to the ORs and to gustatory receptors, a third family of chemosensory receptors was identified in the fruitfly; the ionotropic receptors (IRs). The IRs share homology to a class of ligand-gated ion channels (Benton, 2009). Their functions in the antenna still need to be resolved. Whether the IRs are present also in the moth antenna is unknown. In addition, different types of receptor GCs and of octopamine receptors were located in moth antennae (Von Nickisch-Rosenegk et al., 1996; Simpson et al., 1999; Nighorn et al., 2001; Morton and Nighorn, 2003; Dacks et al., 2006). Whether CO_2-, or oxygen-receptors as described in fruitflies are also present in moth pheromone-sensitive ORNs remains to be examined (Benton, 2009).

In conclusion: The outer dendrites of pheromone-specific moth ORNs comprise apparently heteromeric OR/COR complexes. These complexes appear also to be associated with SNMPs, which might aggregate PBPs loaded with pheromone. Furthermore, octopamine-receptors and receptor-type-, but not soluble GCs are present in the dendrites of moth ORNs. The functional implications of these large receptor complexes in temporal encoding of odor transduction are discussed below.

SUBTHRESHOLD MEMBRANE POTENTIAL OSCILLATIONS OF ORNs AND TEMPORAL ENCODING OF ODORS

First odors bind to their specific receptors (ORs), then, conformational changes of ORs initiate signal transduction cascades which transduce the chemical signal to a graded potential change (receptor potential) in the sensory neuron. If this receptor potential reaches a threshold of about −40 mV at the axon hillock it elicits opening of voltage-dependent Na^+ and K^+ channels, and thus action potentials (=spikes). To understand odor transduction cascades in insects it is important to determine which schemes of information encoding they employ. Thus, before conflicting hypotheses of odor transduction cascades are being discussed, first, I briefly compare "rate codes" and "temporal encoding" in chemosensory neurons. Then, I will summarize evidence for the type of coding employed by insect odor transduction cascades.

"Rate codes" imply that increasing odor concentrations result in increasing action potential frequencies in ORNs. Dose–response curves of ORNs are semi-logarithmic with a linear increase of the response with 10× rising odor concentration (bombykal cell in *M. sexta*: Dolzer et al., 2003). Thus, odor concentration is encoded in the action potential rate of a single ORN. In the hawkmoth the first five interspike intervals, but not the average action potential frequency over the pheromone stimulus duration encode pheromone quantity over at least 4 log units (Dolzer et al., 2003).

Next to the "rate code," olfactory information can also be encoded in the time domain, called "temporal encoding" (Milner, 1974; Singer and Gray, 1995; Knüsel et al., 2007; Ito et al., 2008, 2009). In temporal encoding one assumes that more important than the frequency of action potentials elicited in single cells is at what time the action potentials occur in a population of cells which respond to the same input. Thus, the information is encoded, e.g., in the latency of the first odor-dependent action potential elicited at the level of a neuronal population. The latency may be calculated with respect to a local field potential oscillation, generated via synchronized subthreshold membrane potential oscillations in the respective neurons. On the population level it is assumed that all cells which process the same stimulus express synchronized first action potentials with zero phase difference or constant phase relationship (Nadasdy, 2010). The phase implies the time when the action potential occurs. To obtain synchronization of spikes within the range of ms amongst a population of neurons different mechanisms of coupling (=synchronization) can be employed. Most commonly self-organized coupling is obtained with interacting neuronal oscillators. A neuronal oscillator generates endogenous subthreshold membrane potential oscillations which underlie spontaneous spike activity. Subthreshold membrane potential oscillations provide a temporal preference for input detection. Stimulus-induced receptor potentials as well as neurotransmitter-induced postsynaptic potentials will reach action potential threshold earlier, if they superimpose at the depolarizing phase of endogenous subthreshold membrane potential oscillations, rather than at the hyperpolarizing phase. As soon as any two oscillators have similar periods (interspike intervals) any type of

interaction will synchronize both oscillators causing a stable phase relationship and a common period. For example in the cockroach brain gap junctions maintain synchronized periods of neuronal oscillators at a stable phase difference (Schneider and Stengl, 2005, 2006, 2007). If these coupled oscillators are transiently inhibited at the same time via an inhibitory interneuron zero phase difference results. Thus, a transient neuronal ensemble is generated which contains synchronized neurons which all fire their action potentials at the same time or at integer multiples of the same time. This means, depending on the input (the odor applied) transient neuronal ensembles can be obtained which are recruited into variable functions from the same population of coupled neurons. Thus, an "across fiber pattern" of ORNs could mean that not a single neuron encodes a specific odor quality and quantity, but rather a specific neuron can encode sequentially different odor qualities/quantities depending on the ensemble it is recruited to (Johnson et al., 1991; Ito et al., 2009; Raman et al., 2010).

In the olfactory system of vertebrates Junek et al. (2010) demonstrated that temporal encoding is prevalent over rate codes. They found that latency rank patterns of odor responses specifically encode odor quality and quantity, more reliably than action potential firing rates. They proved that the latency of the first action potential of an odor response is most instrumental for odor encoding already at the periphery. In addition, the importance of latency rank patterns suggested that the phase relationships of the first odor-dependent action potential elicited amongst different ORNs is important and needs to be tightly controlled, possibly via different mechanisms which couple ORNs. That also in the olfactory system of insects temporal encoding is important was shown mostly in recordings of the olfactory pathway in the brain (review: Laurent, 2002) and more recently also for ORNs (Ito et al., 2009; Raman et al., 2010). Also in ORNs of *M. sexta* and *B. mori* the latency of the first action potential elicited decreases with increasing odor concentration (Kaissling and Priesner, 1970). However, in moths it has not been thoroughly examined yet over which concentration range latencies encode odor concentration on the level of a single ORN or on the population level. But because insect ORNs, as well as vertebrate ORNs are spontaneously active and generate bursts of action potentials they very likely employ temporal encoding strategies (Gesteland, 1971; Kaissling, 1987; De Bruyne et al., 2001; Dolzer et al., 2001; Duchamp-Viret et al., 2005). The interspike intervals of spontaneous activity in ORNs of *M. sexta* are not randomly distributed and phases of action potentials are advanced via current injection (Dolzer et al., 2001; Nadasdy, 2010). This hints that the ORNs resting potential produces subthreshold membrane potential oscillations with different superimposed ultradian frequencies: one controls the frequency of bursts, one interspike intervals within bursts, and another interspike intervals between bursts. These ultradian membrane potential oscillations appear to be endogenous since regularly oscillating membrane potentials were recorded intracellularly in isolated ORNs from *M. sexta in vitro*, in addition to very regularly oscillating Ca^{2+} currents in the same frequency range which were observed in patch clamp recordings (Stengl, 1990). Comparably to cockroach circadian pacemaker cells (Schneider and Stengl, 2005, 2007), next to ultradian oscillations ORNs also show daytime-dependent changes in the spontaneous activity with the highest frequency during the moth's activity phase (Flecke and Stengl, 2009). Since moth ORNs express circadian rhythms and circadian clock genes, as do fruitfly and cockroach ORNs, it is likely that also moth ORNs are endogenous circadian oscillators (Krishnan et al., 1999, 2008; Tanoue et al., 2004, 2008; Merlin et al., 2006, 2007; Schuckel et al., 2007; Saifullah and Page, 2009). In moths it is not known whether I_h currents (Krannich, 2008) or other ion channels provide the pacemaking inward currents at hyperpolarizing potentials, underlying these different, superimposed, spontaneous oscillations of the resting potential.

Not only in *D. melanogaster* heteromeric OR/COR complexes mediate spontaneous activity because they form constitutively open non-specific cation channels even at negative resting potentials which leak depolarizing Ca^{2+} currents into ORNs (Sato et al., 2008; Wicher et al., 2008). Rising intracellular Ca^{2+} concentrations and increasing depolarization then might open voltage- and Ca^{2+}-dependent cation and Cl^- channels found in ORNs (Zufall et al., 1991a; Dolzer et al., 2008; Pézier et al., 2010). Possibly, these ion channel openings might underlie the elementary receptor potentials (bumps) observed in moth ORNs (Minor and Kaissling, 2003). The Ca^{2+}-dependent de- or hyperpolarizing ion channels cause ultradian oscillations of the membrane potential. Since the OR–COR ion channel complexes appear to be gated via cAMP (Wicher et al., 2008) they could be modulated via adenylyl cyclase-activating hormones such as octopamine (**Figure 2**). Furthermore, in *D. melanogaster* the availability of OR complexes in dendrites is controlled via an endogenous circadian clock (Tanoue et al., 2008). Therefore, experimental evidence is provided that OR–COR complexes are a prerequisite to metabotropically modifiable subthreshold membrane potential oscillations with superimposed ultradian and circadian periods in fruitflies.

According to theories of temporal encoding (Nadasdy, 2010) it is likely that ultradian subthreshold membrane potential oscillations in insect ORNs are an obligatory prerequisite to the phase control of the first action potential elicited in odor responses and are used for temporal encoding of odor blend quality and quantity. In addition, regularly patterned odor stimuli as might be generated by the beating wings of the flying moth will entrain ultradian membrane potential oscillations of ORNs to resonate in synchrony, thus providing phase-coupling on the population level of ORNs. Stimulus-dependent synchronization significantly increases the temporal resolution of the insect olfactory system and its fidelity in fast odor blend assessment (Tripathy et al., 2010). In addition, synchronization of many sensory neurons would decrease odor detection threshold, because more antennal cells could be recruited into an ensemble by the same stimulus, providing synchronized summed input into postsynaptic antennal lobe neurons (Ito et al., 2009; Raman et al., 2010).

In conclusion: Hallmarks of temporal encoding are endogenous subthreshold membrane potential oscillations generating spontaneously active neurons as well as different means of synchronization to recruit neuronal ensembles into a specific function. Also insect ORNs are endogenous oscillators which express ultradian and circadian subthreshold membrane potential oscillations which result in a temporal preference for odor detection. I propose that the leaky, metabotropically modifiable OR–COR ion channel complex is instrumental for these important properties which could underlie temporal encoding of odors also in insects (**Figure 2**).

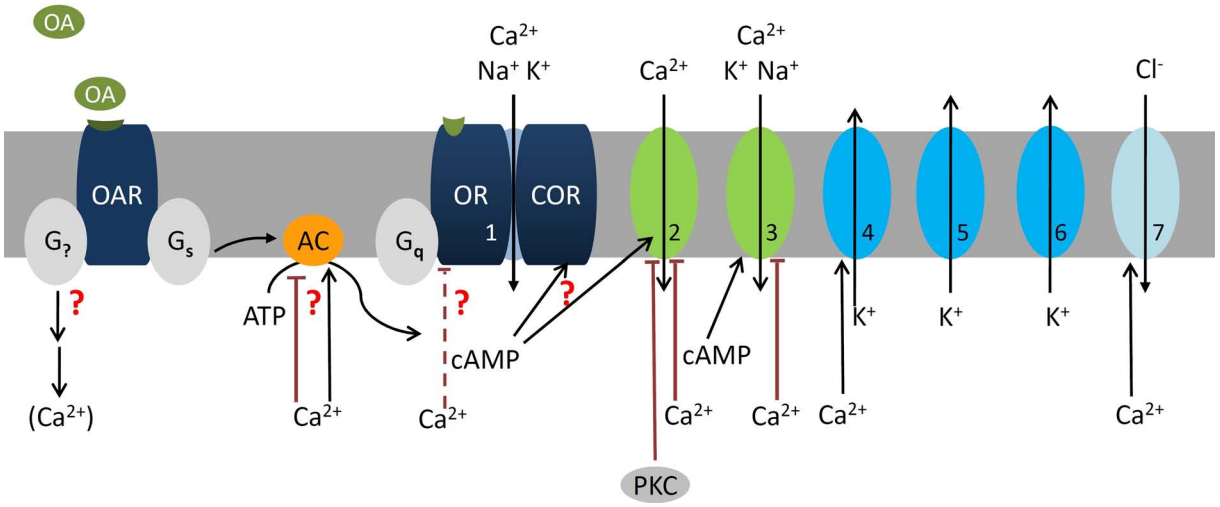

FIGURE 2 | At night the stress hormone octopamine (OA) lowers odor detection threshold and accelerates response kinetics of olfactory receptor neurons (ORNs) possibly via second messenger-dependent modulation of subthreshold membrane potential oscillations (SMPOs). The SMPOs are suggested to be driven via the leaky olfactory receptor–coreceptor ion channel complex (OR–COR, 1) as pacemaker current. The OR–COR causes steady influx of Ca^{2+} and monovalent cations into the ORN. It drives the resting potential of the hyperpolarized ORN to more depolarized potentials and to higher intracellular Ca^{2+}-concentrations. Depolarizations activate different types of repolarizing fast, transient (5, I_A, ~30 pS), and delayed rectifier K^+-channels (6, ~30 pS; Zufall et al., 1991a). Elevations of intracellular Ca^{2+} activate large Ca^{2+}-dependent K^+ (4) and Cl^- channels (7) (Dolzer et al., 2008). resulting in SMPOs. If SMPOs reach spike threshold of –40 mV spontaneous action potentials are elicited. OA increases spontaneous activity via modulation of intracellular messengers (Flecke and Stengl, 2009). One OA-receptor (OAR) couples to a trimeric G_s protein which activates an apparently Ca^{2+}-dependent adenylyl cyclase (AC). In addition, OA couples to at least one other so far undescribed G-protein ($G_?$) which very likely couples to PLCβ and affects Ca^{2+} levels. This hypothetical branch of the cascade including PLCβ-dependent ion channels (**Figure 3**) is not shown. The OA-dependent rise in cAMP is assumed to increase the open probability of the leaky OR–COR (1). In addition, cAMP rises open a transient, protein kinase C (PKC)-dependently blocked L-type Ca^{2+} channel (2) and a less transient cyclic nucleotide gated cation channel (3) (Krannich and Stengl, 2008). All three of these channels permeate Ca^{2+} which then exerts negative feedback, possibly indirectly (interrupted lines) also to (1). Thus, OA-dependent rises in the intracellular cAMP- and Ca^{2+}-concentration would increase amplitude and frequency of SMPOs. Since SMPOs determine temporal encoding properties of ORNs OA determines detection threshold and kinetics of odor responses. Question marks indicate less well documented parts of the cascade. The numbers indicate the same ion channels in all Figures.

OLFACTORY SIGNAL TRANSDUCTION CASCADES

In insects odor-dependent signal transduction cascades that transduce the odor stimulus into a graded receptor potential and action potential responses are still under lively debate. Based on genetic and physiological analysis of *D. melanogaster*, *B. mori*, and mosquito ORs expressed in vertebrate cell lines Sato et al. (2008) claimed that the main mechanism of insect odor and pheromone transduction is a rapid ionotropic pathway employing the OR/COR complex as odor-gated ion channel without involvement of any G-protein-coupled metabotropic cascades which would amplify the signal. In contrast to this hypothesis several different metabotropic cascades were reported to affect odor and pheromone transduction in different insect species. Here, I will summarize experimental evidences in support of either hypothesis. Then, I will interpret the apparently conflicting results for each cascade and will put forward my own hypothesis of pheromone transduction in moths (**Figures 2–5**).

HETEROLOGOUS OR/COR COMPLEX-DEPENDENT SIGNAL TRANSDUCTION CASCADES

Studies suggested that *D. melanogaster* ORs signal independently of heterotrimeric G-proteins (Sato et al., 2008; Smart et al., 2008). Based on previous evidence it was proposed that a directly odor-gated fast ionotropic mechanism via OR/OR83b-formed ion channels is the main odor-dependent transduction pathway eliciting receptor potentials (Nakagawa et al., 2005; Sato et al., 2008). This was claimed not only for general odorants in the fruitfly but also for pheromone-transduction in moths. This hypothesis is based upon the observation that insect ORs are seven-transmembrane receptors which are inversely inserted into the dendritic membrane with the N-terminal reaching into the inside of the cell (Benton et al., 2006; Lundin et al., 2007). Thus, the known G-protein binding motif on the C-terminal is located at the extracellular site and cannot account for a metabotropic cascade. In addition, odor-dependent but GTP-/ATP-independent inward currents were recorded after expression of fruitfly, silkmoth, and mosquito ORs coexpressed with the respective OR83b (COR)/-homologs in HeLa and HEK293 cells (Sato et al., 2008; Wicher et al., 2008). However, unphysiologically strong and long pheromone stimuli of 10 μM bombykol for several seconds which do not occur in natural surroundings of the moths were necessary to elicit a fast, small ionotropic current via bombykol-receptor–COR complexes (Sato et al., 2008). In comparison, dependent on the expression of OR22a/OR83b, 100 nM ethyl butyrate pulses of 1 s duration elicited an ionotropic current which peaked at 1 s and terminated after 10 s. It was followed by a stronger metabotropic current component which developed after about 10 s, peaked at about 60 s, and terminated after about 80 s (Wicher et al., 2008). The less sensitive ionotropic current component appeared to be a current via the OR/OR83b-formed

ion channels, gated via binding of odor to the OR-subunit. This ionotropic current did not depend on the presence of ATP or GTP, in contrast to the slower and more sensitive metabotropic current component. The metabotropic current appeared to be mediated via binding of cyclic nucleotides to the OR–COR-formed ion channel, which apparently increased its probability to open. Whether G-protein-dependent activation of an adenylyl cyclase was mediated via OR homodimers with C-termini intracellularly or via a new G-protein-binding domain at the intracellular N-terminus, or via another G_s-coupled receptor remains to be examined more thoroughly. The time courses of both of these current components, the ionotropic as well as the cGMP/cAMP-dependent metabotropic currents do not match the time course of non-adapted phasic odor responses in intact ORNs or of odor sampling of moths, which both last less than 100 ms (Kaissling, 1987). Possibly, this temporal discrepancy results from the heterologous expression systems used. Alternatively, these currents serve other purposes, such as the modulation of spontaneous activity shown in fruitflies (review: Nakagawa and Vosshall, 2009). The function of the COR is not easy to resolve since specific blockers are missing which solely delete the ionotropic component of the current leaving its chaperon function intact. Because the COR functions as a chaperon which is required for insertion of ORs into dendritic membranes (Larsson et al., 2004) deletions of the COR will delete odor responses and will not necessarily provide evidence for the need of ionotropic odor transduction cascades.

In conclusion: Only two reports using unphysiologically high stimulus concentrations and vertebrate expression systems for fruitfly ORs are in support of a solely ionotropic signal transduction cascade, which, however, is much slower than odor transduction *in situ*. As an alternative hypothesis I suggest that cyclic nucleotide-dependent, leaky heteromeric OR/COR complexes are involved in a depolarizing influx of Ca^{2+} and other cations into ORNs to drive spontaneous subthreshold membrane potential oscillations and, thus, spontaneous activity daytime-dependently (**Figure 2**). Subthreshold membrane potential oscillations keep ORNs close to the action potential threshold and constitute a temporal filter. Thus, they control sensitivity as well as temporal response characteristics of ORNs. Future experiments will examine whether the modulation of the heteromeric OR/COR complexes via a cyclic nucleotide-binding domain on the COR is instrumental for the regulation of daytime-dependent temporal resolution of the ORNs via hormones, neuropeptides, and biogenic amines (Flecke and Stengl, 2009). Therefore, many more studies in different species are needed to resolve the function of the OR/COR complexes for insect olfactory transduction.

G-PROTEIN COUPLED PHOSPHOLIPASE Cβ-DEPENDENT ODOR TRANSDUCTION CASCADES

Many studies obtained with various techniques from different laboratories support the role of colocalized heterotrimeric G-protein-coupled signal transduction cascades in insect ORNs. Most evidence is provided for a phospholipase Cβ (PLCβ)-dependent signal transduction cascade (**Figure 3**). Overwhelming evidence suggest that it underlies the sensitive phasic pheromone responses of the males late at night during their search for the female. In contrast, second-long, strong pheromone stimuli appear to decrease the sensitivity of the ORNs and involve protein kinase C (PKC)-dependent actions which appear to downregulate and terminate PLCβ-dependent signal transduction (Stengl, 1993, 1994; Schleicher et al., 1994).

In different insects cloning experiments, *in situ* hybridizations, and also immunocytochemical studies provided evidence for the presence of G_s (which activates adenylyl cyclase), G_i (which inhibits adenylyl cyclase), G_q (which activates phospholipase Cβ), and G_o (which targets are not well characterized) in antennae (Raming et al., 1989; Boekhoff et al., 1990; Talluri et al., 1995; Laue et al., 1997; Schmidt et al., 1998; Kalidas and Smith, 2002; Miura et al., 2005; Rützeler and Zwiebel, 2005; Kain et al., 2008; Chatterjee et al., 2009; Boto et al., 2010). Four G-proteins: G_s, G_i, $G_{q/11}$, $G_{\beta 13F}$ were colocalized in dendrites of ORNs of *D. melanogaster* (Boto et al., 2010). In addition, G_o is present in fruitfly ORNs, increasing their sensitivity to all odors tested (Chatterjee et al., 2009). Also in the silkmoth *B. mori* application of G-protein activating fluoride increased activity in single pheromone-sensitive sensilla (Laue et al., 1997). Because G_q was located via molecular cloning studies and in immunocytochemical experiments in dendrites of *B. mori*, *Antheraea pernyi*, and *Mamestra brassicae*, fluoride appeared to activate PLCβ (Jacquin-Joly et al., 2002).

Also other studies support a pheromone-transduction cascade via PLCβ which hydrolyzes phospholipids generating inositol trisphosphate (IP_3) and diacylglycerol (DAG). The enzyme PLCβ was cloned and *in situ* hybridizations showed that PLCβ is transcribed in adult pheromone-sensitive ORNs of the moth *Spodoptera littoralis* (Chouquet et al., 2010). In addition, immunocytochemical studies located a PLCβ-subtype in homogenates of isolated pheromone-sensitives sensilla of *A. polyphemus* (Maida et al., 2000). This PLCβ appears to mediate insect odor transduction, because odor-dose-dependently physiological concentrations and time courses of pheromones as well as general odors caused rapid, transient rises of IP_3 in antennal homogenates within several milliseconds. The IP_3 rises occur in the dendritic fraction of antennal tissue in the same millisecond time window as phasic odor-dependent action potential responses to brief, millisecond-long physiological stimuli (Breer et al., 1990; Boekhoff et al., 1993; Kaissling and Boekhoff, 1993). Consistently, IP_3-receptors were located in the dendritic membrane of moth ORNs (Laue and Steinbrecht, 1997). In addition, perfusion of cultured ORNs from *M. sexta* with IP_3 opened a specific sequence of at least three inward currents which resembled pheromone-dependent currents (**Figure 3**; Stengl et al., 1992; Stengl, 1993, 1994). Pheromone opened a very transient IP_3-dependent Ca^{2+} current (#9, **Figure 3**) which is blocked via intracellular Ca^{2+} rises within less than 50 ms. The rise in Ca^{2+} rapidly opens a Ca^{2+}-activated cation channel (#10) which is blocked within seconds via further intracellular Ca^{2+} rises. In addition, the increase in Ca^{2+} opens fast, large Ca^{2+}-dependent K^+ channels (#4) and a Cl^- channel (#7) possibly involved in re-/hyperpolarization of the receptor potential (Dolzer et al., 2008; Pézier et al., 2007, 2010). When the receptor potential reaches spike threshold Na^+ influx occurs at the spike initiation zone of the axon. Then, voltage-sensitive K^+ channels (#5, 6) and possibly also second messenger-dependent K^+- (#4, 8) and Cl^--channels (#7) repolarize and guarantee phasic pheromone responses (Zufall et al., 1991a). In cell-attached patch clamp recordings of ORNs from *M. sexta* as the first pheromone-response an increase in the open probability of the ATP/cGMP-blocked K^+

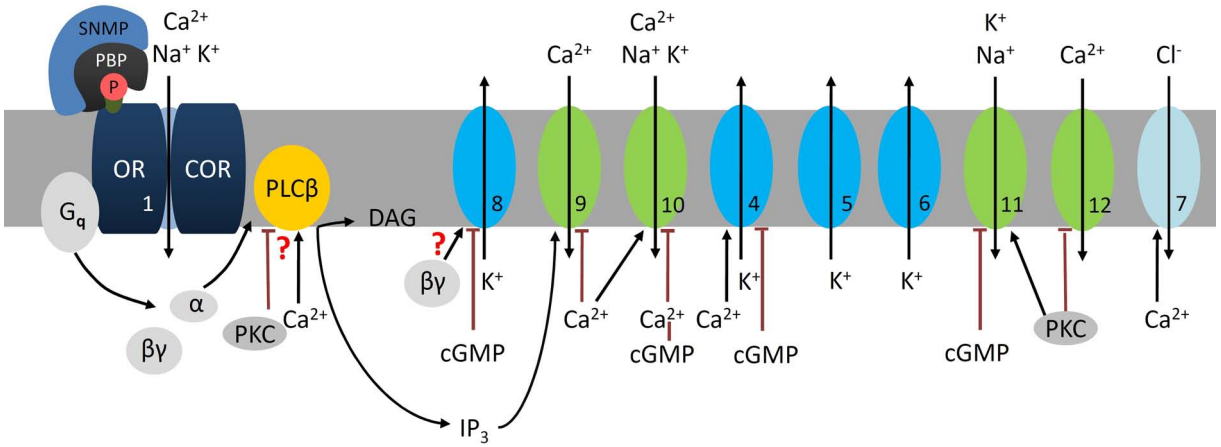

FIGURE 3 | At night sensitive pheromone detection involves phospholipase Cβ (PLCβ) cascades in the hawkmoth *M. sexta*. During the moth's activity phase low, brief pheromone stimuli elicit phasic, sensitive odor responses. Pheromone–pheromone binding protein (P-PBP) binds to the pheromone receptor complex (OR–COR, 1) which activates a G_q-protein. The $G_{q(\alpha)}$ subunit activates a Ca^{2+}-dependent PLCβ which hydrolyses phospholipids (PIP_2) to IP_3 and DAG. The $G_{q(\beta\gamma)}$ subunit opens a delayed rectifier-type K^+ channel (8, ~30 pS), which is blocked by high levels of cGMP (Stengl et al., 1992). Depending on channel density it hyperpolarizes the ORN and decreases its spontaneous activity. Steep IP_3 rises open a transient Ca^{2+} channel (9, <20 pS) in the outer dendrite. The resulting influx of Ca^{2+} triggers activation of nearby Ca^{2+}-gated cation channels (10, ~53 pS) before closing both channels (9, 10) via negative feedback causing desensitization (Stengl et al., 1992; Stengl, 1993, 1994). The resulting high amplitude, rapidly rising Ca^{2+}-oscillations (depending on feedforward activation of PLCβ via Ca^{2+}) and the depolarizations activate additional voltage- or Ca^{2+}-gated channels: Ca^{2+}-dependent K^+-channels (4, ~66 pS) and Cl^- channels (7), voltage-dependent fast, transient I_A-type (5, ~30 pS), and delayed rectifier K^+-channels (6, ~30 pS), as well as Ca^{2+}-channels (12) (Zufall et al., 1991a). Resulting hyperpolarizations together with Ca^{2+}-dependent negative feedback, directly or indirectly via protein kinase C (PKC) terminate this pheromone-transduction cascade. Stronger, second-long Ca^{2+} rises via adapting pheromone stimuli activate PKC. The PKC-dependent down-regulation of PLCβ (Schleicher et al., 1994), closure of voltage-sensitive Ca^{2+} channels (12), and the gating of different cation channels which are not Ca^{2+} permeable (11, ~40 pS, ~60 pS not shown) causes slower, decreased depolarizations and decreased intracellular Ca^{2+} levels resembling conditions of short-term adaptation (Stengl, 1993; Dolzer et al., 2003, 2008). Because dropping intracellular Ca^{2+} levels will not activate the large, fast Ca^{2+}-dependent K^+ or Cl^- channels, repolarizations will be slowed down, decreasing pheromone response kinetics. The PKC-dependently activated ion channels are closed via rises of cGMP-levels as occur under conditions of long-term adaptation (**Figure 3**). The numbers indicate the same ion channels in all Figures.

channel (#4, **Figure 3**) was observed (Stengl et al., 1992). Thus, this channel might be opened via $G_{\beta\gamma}$ subunits and might be present in the outer dendrite, in contrast to the voltage-dependent K^+ channels which rather might be located in the soma and axon compartments (Stengl et al., 1992). It remains to be examined whether this channel (#8) is employed in pheromone-dependent hyperpolarizations as observed in intracellular recordings of ORNs *in vitro* (Stengl, 1990). In contrast, IP_3 was ineffective in excised inside-out patches of dendritic membranes from silkmoth ORNs, very likely because IP_3-dependent ion channels were blocked Ca^{2+}-dependently via sustained, adapting incubation with pheromone (Zufall and Hatt, 1991).

Next to IP_3, DAG is also a potential second messenger of odor transduction in moths. It appears to serve different functions, either as activator of PKC (**Figure 3**) or as activator of transient receptor potential (TRP)-type ion channels (not shown). Immunocytochemical experiments provided evidence for the colocalization of phospholipase Cβ together with a PKC in trichoid sensilla of *A. polyphemus* (Maida et al., 2000). The PKC appears to be employed in transduction of long, adapting pheromone stimuli because in homogenates of antennal sensilla of *A. polyphemus* second- to minute-long incubation with pheromone increased PKC but not PKA activity (Maida et al., 2000). Also, constant, second- to minute-long presence of low pheromone concentrations in extruded dendrites of trichoid sensilla from *A. polyphemus* cation channels were activated which resembled DAG-, PKC- and cGMP-dependently activated channels (Zufall and Hatt, 1991). In addition, DAG application *in situ* and *in vitro* in tip recordings and patch clamp recordings depolarized ORNs or activated depolarizing inward currents in *B. mori*, *A. polyphemus*, and *M. sexta* (Maida et al., 2000; Pophof and van der Goes van Naters, 2002; Krannich, 2008). Since in biochemical assays PKC activation decreased PLCβ-activity and rendered it less transient PKC may play a role for gain control and down-regulation of pheromone responses under conditions of overstimulation, possibly resembling conditions of short-term adaptation (Schleicher et al., 1994). In accordance with this notion PKC activity appears to underlie pheromone-dependent currents activated via second- to minute-long adapting pheromone application in patch clamp recordings *in vitro* (Stengl, 1994; Dolzer et al., 2008). Thus, activation of PKC appears to guarantee signal termination and adjustment of responsiveness of ORNs under conditions of strong, long-lasting Ca^{2+} rises which close IP_3- and Ca^{2+}-activated channels. Because PKC closes voltage-sensitive Ca^{2+} channels and opens cation channels which are not Ca^{2+}-permeable PKC activity decreases intracellular Ca^{2+}-concentrations (Dolzer et al., 2008). Thus, the PKC-dependent cascade favors conditions of low intracellular Ca^{2+} and will not trigger opening of large Ca^{2+}-dependent K^+or Cl^- channels. Therefore, ORNs will repolarize more slowly and will show less phasic, reduced action potential frequencies, as observed during conditions of short-term adaptation.

In contrast, other work suggests that DAG can also activate a PKC-independent pathway. A PKC-independent DAG-gated cation current was described in patch clamp recordings from cultured ORNs of *S. littoralis* and *M. sexta* (Lucas and Pézier, 2006; Krannich, 2008). In accordance, a diacylglycerol kinase (which converts DAG to phosphatidic acid and recycles phosphatidylinositols) was located in olfactory sensilla trichodea of *S. litt ralis* (Chouquet et al., 2008). Because IP_3- and DAG-gated ion channels most likely belong to the TRP-superfamily of ion channels (review: Dong et al., 2010) the localization of TRP channels in moth antennae further substantiates the importance of the PLCβ-dependent signal transduction pathway in moth olfaction (Ackermann, 2004; Chouquet et al., 2009). A PLCβ-dependent cascade might be employed not only in pheromone-transduction but also in general odor transduction. This is supported by an IP_3-dependent conductance, measured in locusts, which resembled a general odor-dependent conductance (Wegener et al., 1997). This assumption is further supported by patch clamp experiments of *M. sexta* ORNs *in vitro*. While 36% of all *M. sexta* ORNs in culture responded to pheromone, more than 90% of the cultured ORNs responded to GTPγS (activator of G-protein-dependent cascades), more than 90% responded to IP_3, and about 64% responded to DAG with inward currents (Stengl, 1993, 1994; Krannich, 2008). These findings indicate that in *M. sexta* both, ORNs which respond to pheromone as well as ORNs which respond to general odors use G-protein-coupled metabotropic signal transduction cascades via activation of a PLCβ (Stengl et al., 1999). Because the number of food odor-sensitive ORNs correlated with the number of DAG-responsive cells *in vitro* it needs to be examined whether food odor-dependent ORNs in *M. sexta* employ DAG-gated TRP-channels, instead of IP_3-gated channels. Whether pheromone transduction in the hawkmoth employs both dendritic IP_3- and DAG-gated ion channels remains to be examined.

In conclusion: There is convincing evidence, provided by many groups based upon different techniques, for sensitive, phasic PLCβ-dependent signal transduction cascades in pheromone- and also in general odor transduction in moths (**Figure 3**). Apparently, IP_3-, DAG-, and Ca^{2+}-gated TRP-like ion channels underlie fast, phasic responses to millisecond-long, weak odor stimuli. Desensitization (=the decline of the response during ongoing stimulation) via Ca^{2+}-dependent negative feedback allows for phasic action potential responses. Stronger or longer odor stimuli cause short-term adaptation via longer-lasting Ca^{2+} rises which activate PKC. Activation of PKC reduced Ca^{2+} influx and slowed down odor responses shifting from phasic to more tonic response patterns. Furthermore, elevation of cGMP levels inactivated PLCβ-dependent signal transduction cascades (Stengl et al., 2001). Thus, depending on stimulus length and strength different second messengers determine threshold and kinetics of the odor response.

cGMP-DEPENDENT ODOR TRANSDUCTION CASCADES IN MOTH ORNs

Different studies suggested that cGMP-dependent signal transduction cascades in moth olfaction are employed for long-term adaptation of the olfactory system during minute-long or very strong odor exposure (**Figure 4**). Several different types of GCs were cloned and characterized from hawkmoth antennae and *in situ* hybridization located some of them to ORNs (Simpson et al., 1999; Nighorn et al., 2001; Stengl et al., 2001; Morton and Nighorn, 2003; Morton, 2004). In homogenates of different insect antennae only very strong, long pheromone stimuli caused delayed, slow rises of cGMP (Ziegelberger et al., 1990; Boekhoff et al., 1993). Immunocytochemistry revealed that pheromone-dependent cGMP-rises occurred in neuronal and non-neuronal cells of pheromone-sensitive trichoid sensilla (Stengl et al., 2001). The cGMP rises in ORNs strongly depended on

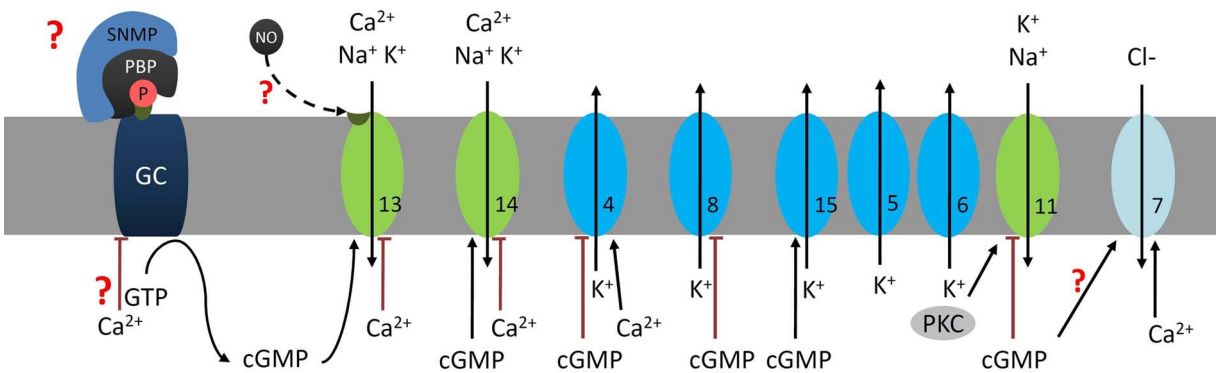

FIGURE 4 | Elevations in cGMP underlie long-term adaptation. Strong or minute-long pheromone stimuli result in more tonic, less sensitive cGMP-dependent pheromone responses in hawkmoth ORNs. The adapting pheromone doses cause long-lasting rises in intracellular cGMP- and Ca^{2+}-concentrations which inactivate PLCβ-dependent signal transduction cascade (**Figure 3**). Possibly SNMP-mediated pheromone-PBP-dependent activation of a receptor-type guanylyl cyclase (GC) elevates cGMP levels in ORNs NO-dependently (Stengl et al., 2001). Elevations in cGMP and possibly also NO (dashed line) activate non-specific cation channels (13, 14, ~55 pS) which differ in their Ca^{2+}-permeability and Ca^{2+}-dependent inactivation (Krannich and Stengl, 2008). The Ca^{2+}-dependent K^+-channels (4, ~66 pS), as well as the cGMP/ATP-dependent K^+ channels (8,~ 30 pS) are blocked via cGMP rises (Dolzer, 2002). In contrast, a slow K^+ channel (15) is opened via cGMP (Dolzer, 2002) and other voltage-dependent delayed rectifier K^+ channels (5, 6) are opened depolarization-dependently. In addition, the cGMP rises close a 40 pS cation channel (11) previously activated by PKC (Dolzer et al., 2008). It remains to be examined whether cGMP-dependent activation of Ca^{2+}-dependent Cl^- channels or just sustained rises in Ca^{2+} underlie the faster repolarization of adapted cells. All together, cGMP rises elevate baseline levels of intracellular Ca^{2+} and shift the resting potential to more depolarized values. The numbers indicate the same ion channels in all Figures.

the duration and strength of the pheromone stimulus, as well as on the presence of nitric oxide (NO). Because *in situ* hybridizations showed that NO-dependent soluble GCs are not expressed in pheromone-sensitive ORNs it is likely that NO opened Ca^{2+} permeable CNG channels instead (**Figure 4**, #13; Broillet and Firestein, 1997; Stengl et al., 2001). The elevated cGMP-levels close fast K^+ channels (**Figure 4**, #8), large, fast Ca^{2+}-activated K^+ channels (#4), as well as PKC-dependent ion channels (**Figure 4**, #11), while opening slower K^+ channels (#15) and less transient Ca^{2+}-permeable cation channels (#13, 14) in moth ORNs (Zufall and Hatt, 1991; Zufall et al., 1991a; Stengl, 1994; Dolzer, 2002; Dolzer et al., 2008; Krannich and Stengl, 2008). Because cGMP-infusion into trichoid sensilla decreased the pheromone-dependent action potential frequency daytime-dependently and rendered pheromone responses less phasic, cGMP rises adapt and slow down ORNs (Flecke et al., 2006). Interestingly, there is considerable cross-talk between PLCβ – and GC-dependent signal transduction cascades because cGMP affected Ca^{2+}-activated and PKC-activated ion channels (Zufall et al., 1991a,b; Dolzer et al., 2008). Based on our data obtained from tip recordings (Dolzer et al., 2003; Flecke et al., 2006) and biochemical assays I propose that in insects endogenous cGMP elevations during the inactivity phase are at least partially responsible for increased odor-thresholds and decreased ability to resolve odor pulses (**Figure 5**). In addition, it needs to be examined whether resting moths can be disadapted via octopamine-mediated stressors. Possibly, fast, large Ca^{2+} transients due to stress hormone release during the inactivity phase inhibit receptor-GCs and activate phosphodiesterases to decrease cGMP levels. Finally, it remains to be examined whether receptor-GCs in moth ORNs are activated SNMP-dependently via PBP-dimers loaded with pheromone.

In conclusion: Very strong, long pheromone stimuli are possibly encountered in close contact with the female moth causing conditions of long-term olfactory adaptation in the male. These adapting stimuli can be detected via cGMP-dependent signal transduction cascades. The cGMP-dependent odor transduction cascades (**Figure 4**) appear to exclude PLCβ-dependent cascades and result in less sensitive, less phasic pheromone responses as compared to IP_3-, DAG-, Ca^{2+}-, or PKC-dependent responses (Stengl et al., 1992; Dolzer, 2002; Dolzer et al., 2008). Circadian rhythms of cGMP baseline levels could regulate activity-rest cycles of moths (**Figure 5**).

OCTOPAMINE AND cAMP-DEPENDENT TRANSDUCTION CASCADES IN MOTH ORNs

While in vertebrates a cAMP-dependent odor transduction cascade is predominant in the main olfactory epithelium, in moths there is less evidence for cAMP-dependent signal transduction cascades (review; Fleischer et al., 2009; Kaupp, 2010). However, in moth antennae octopamine receptors were cloned which appear to couple to adenylyl cyclases (Von Nickisch-Rosenegk et al., 1996; Dacks et al., 2006; Huang et al., 2008). Biochemical experiments showed that hemolymph concentration of the stress hormone octopamine express endogenous circadian rhythms with its maximal concentration during the activity phase of the moths late at night (Lehman, 1990). In addition, octopaminergic neurons project into the antenna and appear to contact

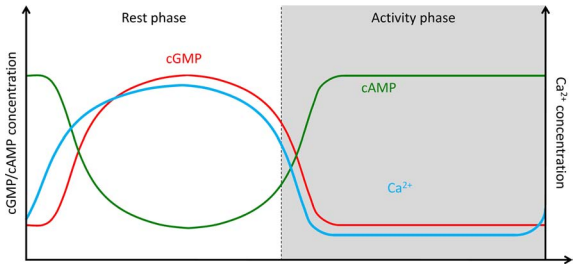

FIGURE 5 | Hypothesis of endogenous circadian rhythms in baseline levels of intracellular Ca^{2+}- and cyclic nucleotide-levels at different Zeitgeber times controlling spontaneous activity in the absence of odor stimulation. During the activity phase at night baseline levels of intracellular Ca^{2+} are low, of cGMP are low, and of cAMP are high. At the rest phase during the day elevated baseline levels in intracellular Ca^{2+}-concentration are maintained, as well as high cGMP-, and low cAMP-concentrations. The endogenous rhythms are not gated by light, but anticipate light–dark rhythms. While our preliminary experiments support cyclic nucleotide-rhythms, it remains to be examined whether rhythms in intracellular baseline Ca^{2+} concentration phase-lead or phase-lag the other rhythms .

ORNs. In different moth species octopamine improves pheromone source location daytime-dependently in behavioral studies (Linn Jr. and Roelofs, 1986). Octopamine disadapts ORNs and renders pheromone responses more phasic, apparently via a cAMP-dependent transduction cascade and an additional possibly Ca^{2+}-dependent cascade in tip recordings of intact trichoid sensilla (Pophof, 2000, 2002; Flecke and Stengl, 2009; Flecke et al., 2010). In addition, octopamine increased the spontaneous activity of the pheromone-sensitive ORNs. This increase was only partly mimicked by cAMP-rises (**Figure 2**; Flecke and Stengl, 2009; Flecke et al., 2010). Possibly, cAMP increased the open probability of the leaky OR/COR ion channel complex as reported in the fruitfly (Wicher et al., 2008). The leaky OR/COR (**Figure 2**, #1) would cause a steady influx of Ca^{2+} into ORNs pulling the membrane potential to more depolarized potentials while increasing baseline Ca^{2+}concentrations. In addition cAMP would cause superimposed transient Ca^{2+}-rises via opening of a very transient, PKC-inhibited L-type Ca^{2+}-channel (#2) and a less transient CNG-channel (#3) both of which would transiently depolarize ORNs (Krannich and Stengl, 2008). The rapid, transient Ca^{2+} rises as well as the resulting depolarizations would initiate repolarizations via activation of voltage-dependent K^+ channels (#5, 6), and fast, large Ca^{2+} dependent K^+- (#4) and Cl^- channels (**Figure 2**, #7). Thus, OA would increase subthreshold membrane potential oscillations in amplitude and frequency, which might underlie the observed OA-dependent increase in spontaneous activity (Flecke and Stengl, 2009). It remains to be examined whether the OA-dependent decrease in odor threshold and the increased odor-response kinetics are due to second messenger-dependent modulation of subthreshold membrane potential oscillations.

In conclusion: So far, no odor-dependent cAMP-rises were described in moths. But the stress hormone octopamine couples via G_s to adenylyl cyclase in moth antennae. Thus, endogenous, circadian rhythms in octopamine concentration possibly generate

circadian rhythms of cAMP baseline levels in ORNs. Possibly together with activation of a G_q-protein dependent pathway (not shown in **Figure 2**) octopamine allows for more phasic, more sensitive pheromone responses during the night (**Figure 2**) (Flecke and Stengl, 2009; Flecke et al., 2010). In addition, octopamine can also acutely elevate cAMP-concentrations in antennae in response to stressors at all daytimes via centrifugal octopaminergic neurons. Stress-dependent activation of these octopaminergic cells during the day disadapts ORNs and allows for pheromone responses of awakened moths. Whether OA-dependent cAMP rises in synergism with specific Ca^{2+} levels increase the spontaneous activity of ORNs and, thus, improve their ability to follow high frequency odor pulses, remains to be examined.

ARE THERE SIGNALOSOMES IN INSECT OLFACTION?

The dispute over rapid ionotrophic versus signal enhancing metabotropic signal transduction cascades can be boiled down to the question whether there is a need for speed or a need for sensitivity maximization in pheromone transduction. While ionotropic signal transduction cascades work in the microsecond time range and are employed, e.g., in the auditory system, metabotropic cascades are employed to allow for signal amplification and response range enlargement such as in the visual system. In the fruitfly visual system where scaffolding proteins aggregate the members of the metabotropic signal transduction cascade to form fast-acting signalosomes reaction times as fast as 20 ms are reached (Hardie and Raghu, 2001). Thus, the response time of signalosome-employing metabotropic signal transduction cascades would be in the time range maximally employed by the insect olfactory system. In addition, sensitivity maximization allowing for the detection of single pheromone molecules as calculated by Kaissling (1987) cannot be reached with an ionotropic cascade but requires signal amplification via metabotropic cascades. So far, it is not known yet, whether insect olfactory signal transduction cascades are spatially aggregated via scaffolding molecules to form fast-acting signalosomes (Hardie and Raghu, 2001). However, scanning electron microscopy and atomic force microscopy could resolve large complexes of molecules in the outer dendritic membrane of moth ORNs of the moths *A. polyphemus* and *A. pernyi* (Klein and Keil, 1984; Eschrich et al., 1998). Next to different pores of 14–18 nm diameter with a density of about 20/μm^2 also dots and membrane patches could be resolved. It remains to be examined whether these dots and patches are signalosomes, which could speed up metabotropic signal transduction machinery. The presence of signalosomes is supported by patch clamp analysis of ORNs which suggests close local neighborhood of different pheromone-dependent ion channels and enzymes which remained together after patch excision (Stengl, 1993, 1994). In addition, scaffolding molecules were cloned from antennae of the hawkmoth. But still, the presence of signalosomes in insect olfaction remains to be examined.

To summarize: Moth pheromone transduction requires reaction times in the range of 30 ms, large, adaptable dynamic range, and extreme sensitivity maximization. Thus, signalosome-dependent metabotropic signal transduction cascades would fit these requirements best.

CONCLUSIONS

Accumulating evidence suggests that there is not only one predominant odor transduction cascade in insect olfactory sensory neurons. Rather, there are different colocalized, equally important signal transduction cascades which allow for sliding adjustment of odor response threshold and kinetics, in response to endogenous physiological rhythms, to different behavioral states, and to various different odor stimulus properties (**Figures 2–5**). Preliminary evidence suggests that endogenous circadian rhythms of cyclic nucleotides occur in insect ORNs, synchronized with the activity-rest cycle of the insect with maximal cAMP concentrations during the activity phase and maximal cGMP concentrations during the rest phase (**Figure 5**). Elevated cGMP levels increase baseline levels of intracellular Ca^{2+}. Thus, a circadian rhythm in the baseline of intracellular Ca^{2+} concentrations, with the maximum at rest, during the day would accompany cyclic nucleotide rhythms. Whether additional mechanisms control rhythms in intracellular Ca^{2+} levels and whether circadian rhythms in intracellular baseline Ca^{2+} concentrations phase-lead or phase-lag cyclic nucleotide rhythms remains to be examined. Hormones and possibly also neuropeptides which represent a specific physiological, metabolic state such as hunger or sexual drive might couple to G_i or G_s, and possibly also to receptor GCs, thereby changing baseline levels of the respective second messengers. Superimposed on these slow rhythms of the baseline levels of cyclic nucleotide- and Ca^{2+} concentrations high frequency, large amplitude oscillations of the respective second messengers occur during odor "sniffing" with each stroke of the wings in flight. These ultradian oscillations depend on strength and time course of odor stimuli. The resulting relative concentration ratios of intracellular messengers and activated enzymes then open or close different ion channels and, thus, define the response threshold and temporal resolution of ORNs. Therefore, for each internal physiological state and each external stimulus condition there is a specific ratio of these second messengers and activated enzymes, and a corresponding complementary set of depolarizing and hyperpolarizing ion channels which support odor responses. This model differs greatly from current models of insect odor transduction (Gu et al., 2009; Nakagawa and Vosshall, 2009) and needs to be challenged in computational simulations to allow for quantitative predictions.

But what is the role of the "ionotropic" pathway via OR/COR-dependent ion channels in moth ORNs? I suggest that the main function of this metabotropically mediated OR/COR-ion channel complex is the control of subthreshold membrane potential oscillations and thus of the spontaneous activity of ORNs to allow for temporal encoding of odor blends. However, more comparative work in different insect species needs to be accomplished to resolve its functions and to challenge my hypothesis.

ACKNOWLEDGMENTS

Thanks to Dr. Uwe Homberg, Dr. Christian Flecke, Andreas Nolte, Ursula Reichert, and to the referees for critically reading and improving of the manuscript. All Figures were generously provided by Andreas Nolte. The research was supported by grants from the Deutsche Forschungsgemeinschaft (DFG).

REFERENCES

Ackermann, F. (2004). *Ionenkanäle in der Antenne des Tabakschwärmers Manduca sexta. Identifizierung eines Homologs der TRP-Kanalfamilie*. Dissertation, University of Marburg.

Almaas, T. J., Christensen, T. A., and Mustaparta, H. (1991). Chemical communication in heliothine moths. I. Antennal receptor neurons encode several features of intra- and interspecific odorants in the male corn earworm moth *Helicoverpa zea*. *J. Comp. Physiol. A* 169, 249–258.

Altner, H., and Prillinger, L. (1980). Ultrastructure of invertebrate chemo-, thermo-, and hygroreceptors and its functional significance. *Int. Rev. Cytol.* 67, 69–139.

Baker, T. C., Hansson, B. S., Löfstedt, C., and Löfquvist, J. (1988). Adaptation of antennal neurons in moths is associated with cessation of pheromone-mediated upwind flight. *Proc. Natl. Acad. Sci. U.S.A.* 85, 9826–9830.

Baker, T. C., and Haynes, K. F. (1989). Field and laboratory electroantennographic measurements of pheromone plume structure correlated with oriental fruit moth behavior. *Physiol. Entomol.* 14, 1–12.

Baker, T. C., and Vogt, R. G. (1988). Measured behavioral latency in response to sex-pheromone loss in the large silk moth *Antheraea polyphemus*. *J. Exp. Biol.* 137, 29–38.

Baker, T. C., Willis, M., Haynes, K. F., and Phelan, P. L. (1985). A pulsed cloud of sex pheromone elicits upwind flight in male moths. *Physiol. Entomol.* 10, 257–265.

Benton, R. (2009). Evolution and revolution in odor detection. *Science* 326, 282–283.

Benton, R., Sachse, S., Michnick, S. W., and Vosshall, L. B. (2006). Atypical membrane topology and heteromeric function of *Drosophila* odorant receptors *in vivo*. *PLoS Biol.* 4, e20. doi: 10.1371/journal.pbio.0040020

Benton, R., Vannice, K. S., and Vosshall, L. B. (2007). An essential role for a CD36-related receptor in pheromone detection in *Drosophila*. *Nature* 450, 289–293.

Boekhoff, I., Seifert, E., Göggerle, S., Lindemann, M., Krüger, B.-W., and Breer, H. (1993). Pheromone-induced second messenger signalling in insect antennae. *Insect Biochem. Mol. Biol.* 23, 757–762.

Boekhoff, I., Strotmann, J., Raming, K., Tareilus, E., and Breer, H. (1990). Odorant-sensitive phospholipase C in insect antennae. *Cell. Signal.* 2, 49–56.

Boto, T., Gomez-Diaz, C., and Alcorta, E. (2010). Expression analysis of the 3 G-protein subunits, G_α, G_β, G_γ, in the olfactory receptor organs of adult *Drosophila melanogaster*. *Chem. Senses* 35, 183–193.

Breer, H., Boekhoff, I., and Tareilus, E. (1990). Rapid kinetics of second messenger formation in olfactory transduction. *Nature* 345, 65–68.

Brigaud, I., Montagne, N., Monsempes, C., Francois M.-C., and Macquin-Joly, E. (2009). Identification of an atypical insect olfactory receptor subtype highly conserved within noctuids. *FEBS J.* 276, 6537–6547.

Broillet, M.-C., and Firestein, S. (1997). β Subunits of the olfactory cyclic nucleotide-gated channel form a nitric oxide activated Ca^{2+} channel. *Neuron* 18, 951–958.

Chatterjee, A., Roman, G., and Hardin, P. E. (2009). G_o contributes to olfactory reception in *Drosophila melanogaster*. *BMC Physiol.* 9, 1–7. doi: 10.1186/1472-6793-9-22

Chouquet, B., Bozzolan, R., Solvar, M., Duportets, L., Jacquin-Joly, E., Lucas, P., and Debernard, S. (2008). Molecular cloning and expression patterns of a putative olfactory diacylglycerol kinase from the noctuid moth *Spodoptera littoralis*. *Insect Mol. Biol.* 17, 485–493.

Chouquet, B., Debernard, S., Bozzolan, R., Solvar, M., Maibeche-Coisne, M., and Lucas, P. (2009). A TRP channel is expressed in *Spodoptera littoralis* antennae and is potentially involved in insect olfactory transduction. *Insect Mol. Biol.* 18, 213–222.

Chouquet, B., Lucas, P., Bozzolan, R., Solvar, M., Maibeche-Coisne, M., Durand, N., and Debernard, S. (2010). Molecular characterization of a phospholipase C {beta} potentially involved in moth olfactory transduction. *Chem. Senses.* 35, 363–373.

Dacks, A. M., Dacks, J. B., Christensen, T. A., and Nighorn, A. J. (2006). The cloning of one putative octopamine receptor and two putative serotonin receptors from the tobacco hawkmoth *Manduca sexta*. *Insect Biochem. Mol. Biol.* 36, 741–747.

De Bruyne, M., and Baker, T. C. (2008). Odor detection in insects: volatile codes. *J. Chem. Ecol.* 34, 882–897.

De Bruyne, M., Foster, K., and Carlson, J. R. (2001). Odor coding in the *Drosophila* antenna. *Neuron* 30, 537–552.

Dolzer, J. (2002). *Mechanisms of Modulation and Adaptation in Pheromone-Sensitive Trichoid Sensilla of the Hawkmoth Manduca sexta*. Dissertation, University of Marburg, 1–120.

Dolzer, J., Fischer, K., and Stengl, M. (2003). Adaptation in pheromone-sensitive trichoid sensilla of the hawkmoth *Manduca sexta*. *J. Exp. Biol.* 206, 1575–1588.

Dolzer, J., Krannich, S., Fischer, K., and Stengl, M. (2001). Oscillations of the transepithelial potential of moth olfactory sensilla are influenced by octopamine and serotonin. *J. Exp. Biol.* 204, 2781–2794.

Dolzer, J., Krannich, S., and Stengl, M. (2008). Pharmacological investigation of protein kinase C and cGMP-dependent ion channels in cultured olfactory receptor neurons of the hawkmoth *Manduca sexta*. *Chem. Senses* 33, 803–813.

Dong, X.-P., Wang, X., and Xu, H. (2010). TRP channels of intracellular membranes. *J. Neurochem.* 1013, 313–328.

Duchamp-Viret, P., Kostal, L., Chaput, M., Lansky, P., and Rospars, J. P. (2005). Patterns of spontaneous activity in single rat olfactory receptor neurons are different in normally breathing and tracheotomized animals. *J. Neurobiol.* 65, 97–114.

Eschrich, R., Kumar, G. L., Keil, T. A., and Guckenberger, R. (1998). Atomic-force microscopy on the olfactory dendrites oft he silkmoths *Antheraea polyphemus* and *A. pernyi*. *Cell Tissue Res.* 294, 179–185.

Flecke, C., Dolzer, J., and Stengl, M. (2006). Perfusion with cGMP adapts the action potential response in pheromone-dependent trichoid sensilla in the moth *Manduca sexta*. *J. Exp. Biol.* 209, 3898–3912.

Flecke, C., Nolte, A., and Stengl, M. (2010). Perfusion with cAMP analog affects pheromone-sensitive trichoid sensilla of the hawkmoth *Manduca sexta* in a time-dependent manner. *J. Exp. Biol.* 213, 842–852.

Flecke, C., and Stengl, M. (2009). Octopamine and tyramine sensitize pheromone-sensitive olfactory sensilla of the hawkmoth *Manduca* sexta in a daytime-dependent manner. *J. Comp. Physiol. A* 195, 529–545.

Fleischer, J., Breer, H., and Strotmann, J. (2009). Mammalian olfactory receptors. *Front. Cell. Neurosci.* 3:9. doi: 10.3389/neuro.03.009.2009

Forstner, M., Breer, H., and Krieger, J. (2009). A receptor and binding protein interplay in the detection of a distinct pheromone component in the silkmoth *Antheraea polyphemus*. *Int. J. Biol. Sci.* 5, 745–757.

Forstner, M., Gohl, T., Breer, H., and Krieger, J. (2006). Candidate pheromone binding proteins of the silkmoth *Bombyx mori*. *Invert. Neurosci.* 6, 177–187.

Forstner, M., Gohl, T., Gondesen, I., Raming, K., Breer, H., and Krieger, J. (2008). Differential expression of SNMP-1 and SNMP-2 proteins in pheromone-sensitive hairs of moths. *Chem. Senses* 33, 291–299.

Gesteland, R. C. (1971). "Neural coding in olfactory receptor cells," in *Handbook of Sensory Physiol*, Vol. IV, *Chem. Senses*, ed. L. M. Beidler (Berlin: Springer), 132–150.

Grosse-Wilde, E., Gohl, T., Bouche, E., Breer, H., and Krieger, J. (2007). Candidate pheromone receptors provide the basis for the response of distinct antennal neurons to pheromonal compounds. *Eur. J. Neurosci.* 25, 2364–2373.

Grosse-Wilde, E., Svatos, A., and Krieger, J. (2006). A pheromone-binding protein mediates the bombykol-induced activation of a pheromone receptor *in vitro*. *Chem. Senses* 31, 547–555.

Gu, Y., Lucas, P., and Rospars, J.-P. (2009). Computational model of the insect pheromone transduction cascade. *PLoS Comput. Biol.* 5, e1000321. doi: 10.1371/journal.pcbi.1000321

Hardie, R. C., and Raghu, P. (2001). Visual transduction in *Drosophila*. *Nature* 413, 186–193.

Huang, J., Hamasaki, T., Ozoe, F., and Ozoe, Y. (2008). Single amino acid switch for distinct G protein couplings. *Biochem. Biophys. Res. Commun.* 371, 610–604.

Itagaki, H., and Conner, W. E. (1988). Calling behavior of *Manduca sexta* (Lepidoptera: Sphingidae) with notes on the morphology of the female sex pheromone gland. *Ann. Entomol. Soc. Am.* 81, 798–807.

Ito, I., Bazhenov, M., Ong, R. C., Raman, B., and Stopfer, M. (2009). Frequency transitions in odor-evoked neural oscillations. *Neuron* 64, 692–706.

Ito, I., Ong, R. C., Raman, B., and Stopfer, M. (2008). Olfactory learning and spike timing dependent plasticity. *Commun. Integr. Biol.* 1, 170–171.

Jacquin-Joly, E., Francois, M. C., Burnet, M. Lucas, P., Bourrat, F., and Maida, R. (2002). Expression pattern in the antennae of a newly isolated lepidopteran G_q protein alpha subunit cDNA. *Eur. J. Biochem.* 269, 2133–2142.

Jin, X., Ha, T. S., and Smith, D. P. (2008). SNMP is a signaling component required for pheromone sensitivity in *Drosophila*. *Proc. Natl. Acad. Sci. U.S.A.* 105, 10996.

Johnson, B. R., Vligt, R., Merrill, C. L., and Atema, J. (1991). Across-fiber patterns may contain a sensory code for stimulus intensity. *Brain Res. Bull.* 26, 327–331.

Junek, S., Kludt, E., Wolf, R., and Schild, D. (2010). Olfactory coding with patterns of response latencies. *Neuron* 67, 872–884.

Justus, K. A., Carde, R. T., and French, A. S. (2005). Dynamic properties of antennal responses to pheromone in two moth species. *J. Neurophysiol.* 93, 2233–2239.

Kain, P., Chandrashekaran, S., Rodrigues, V., and Hasan, G. (2008). *Drosophila* mutants in phospholipid signaling have reduced olfactory responses as adults and larvae. *J. Neurogenet.* 23, 303–312.

Kaissling, K.-E. (1987). "Stimulus transduction," in *R. H. Wright Lectures on Insect Olfaction*, ed. K. Colbow (Burnaby, BC: Simon Fraser University Press), 1–190.

Kaissling, K.-E. (2009). Olfactory perireceptor and receptor events in moths: a kinetic model revised. *J. Comp. Physiol. A Neuroethol. Sens. Neural Behav. Physiol.* 195, 895–922.

Kaissling, K.-E., and Boekhoff, I. (1993). "Transduction and intracellular messengers in pheromone receptor cells of the moth *Antheraea polyphemus*," in *Sensory Systems of Arthropods*, eds K. Wiese, F. G. Gribakin, A. V. Popov, and G. Renninger (Berlin: Birkhäuser), 489–502.

Kaissling, K.-E., Hildebrand, J. G., and Tumlinson, J. H. (1989). Pheromone receptor cells in the male moth *Manduca sexta*. *Arch. Insect Biochem. Physiol.* 10, 273–279.

Kaissling, K.-E., and Priesner, E. (1970). Smell threshold of the silkmoth. *Naturwissenschaften* 57, 23–28.

Kaissling, K.-E., and Thorson, J. (1980). "Insect olfactory sensilla: structural chemical and electrical aspects of the functional organization," in *Receptors for Neurotransmitters, Hormones, and Pheromones in Insects*, eds D. B. Satelle, L. M. Hall, and J. G. Hildebrand (Amsterdam: Elsevier/North-Holland Biomedical Press), 261–282.

Kalidas, S., and Smith, D. P. (2002). Novel genomic cDNA hybrids produce effective RNA interference in adult *Drosophila*. *Neuron* 33, 177–184.

Kaupp, U. B. (2010). Olfactory signaling in vertebrates and insects: differences and commonalities. *Nat. Rev. Neurosci.* 11, 188–200.

Keil, T. (1989). Fine structure of the pheromone-sensitive sensilla on the antenna of the hawkmoth, *Manduca sexta*. *Tissue Cell* 21, 139–151.

Keil, T. A. (1993). Dynamics of "immotile" olfactory cilia in the silkmoth *Antheraea*. *Tissue Cell* 25, 573–587.

Keil, T. A. (1999). "Morphology and development of the peripheral olfactory organs," in *Insect olfaction*, ed. B. S. Hansson (Berlin: Springer), 6–47.

Keil, T. A., and Steinbrecht, R. A. (1984). "Mechanosensitive and olfactory sensilla of insects," in *Insect Ultrastructure*, Vol. 2, eds R. C. King and H. Akai (New York: Plenum Press), 435–475.

Kennedy, J. S., Ludlov, A. R., and Sanders, D. J. (1981). Guidance of flying male moths by wind-born sex pheromone. *Physiol. Entomol.* 6, 395–412.

Klein, U., and Keil, T. A. (1984). Dendritic membrane from insect olfactory hairs: isolation method and electron microscopic observations. *Cell. Mol. Neurobiol.* 4, 385–396.

Knüsel, P., Carlsson, M. A., Hansson, B. S., Pearce, T. C., and Verschure, P. R. M. J. (2007). Time and space are complementary encoding dimensions in the moth antennal lobe. *Network* 18, 35–62.

Koehl, M. A. R. (2006). The fluid mechanics of arthropod sniffing in turbulent odor plumes. *Chem. Senses* 31, 93–105.

Krannich, S. (2008). *Electrophysiological and Pharmacological Characterization of Ion Channels Involved in Moth Olfactory Transduction Cascades*. Dissertation, University of Marburg, 1–114.

Krannich, S., and Stengl, M. (2008). Cyclic nucleotide-activated currents in cultured olfactory receptor neurons of the hawkmoth *Manduca sexta*. *J. Neurophysiol.* 100, 2866–2877.

Krieger, J., Gondesen, I., Forstner, M., Gohl, T., Dewer, Y. M., and Breer, H. (2009). HR11 and HR13 receptor-expressing neurons are housed together in pheromone-responsive sensilla trichodea of male *Heliothis virescens*. *Chem. Senses* 34, 469–477.

Krieger, J., Grosse-Wilde, E., Gohl, T., and Breer, H. (2005). Candidate pheromone receptors of the silkmoth *Bombyx mori*. *Eur. J. Neurosci.* 21, 2167–2176.

Krieger, J., Grosse-Wilde, E., Gohl, T., Dewer Y. M. E., Raming, K., and Breer, H. (2004). Genes encoding candidate pheromone receptors in a moth (*Heliothis virescens*). *Proc. Natl. Acad. Sci. U.S.A.* 101, 11645–11850.

Krieger, J., Klink, O., Mohl, C., Raming, K., and Breer, H. (2003). A candidate olfactory receptor subtype highly conserved across different insect orders. *J. Comp. Physiol. A* 189, 519–526.

Krieger, J., Raming, K., Dewer, Y. M. E., Bette S., Conzelmann, S., and Breer, H. (2002). A divergent gene family encoding candidate olfactory receptors of the moth *Heliothis virescens*. *Eur. J. Neurosci.* 16, 619–628.

Krishnan, B., Dryer, S. E., and Hardin, P. E. (1999). Circadian rhythms in olfactory responses of *Drosophila melanogaster*. *Nature* 400, 375–378.

Krishnan, P., Chatterjee, A., Tanoue, S., and Hardin, P. E. (2008). Spike amplitude of single-unit responses in antennal sensillae is controlled by the *Drosophila* circadian clock. *Curr. Biol.* 18, 803–807.

Larsson, M. C., Domingos, A. L., Jones, W. D., Chiappe, M. E., Amrein, H., and Vosshall, L. B. (2004). Or83b encodes a broadly expressed odorant receptor essential for *Drosophila* olfaction. *Neuron* 43, 703–714.

Laue, M., Maida, R., and Redkozubov, A. (1997). G-protein activation, identification and immunolocalization in pheromone-sensitive sensilla trichodea of moths. *Cell Tissue Res.* 288, 149–158.

Laue, M., and Steinbrecht, R. A. (1997). Topochemistry of moth olfactory sensilla. *Int. J. Insect Morphol. Embryol.* 26, 217–228.

Laughlin, J. D., Ha, T. S., Jones, D. N. M., and Smith, D. P. (2008). Activation of pheromone-sensitive neurons is mediated by conformational activation of pheromone-binding protein. *Cell* 133, 1255–1265.

Laurent, G. (2002). Olfactory network dynamics and the coding of multidimensional signals. *Nat. Rev. Neurosci.* 3, 884–895.

Leal, W. S., Chen, A. M., Ishida, Y., Chiang, V. P., Erickson, M. L., Morgan, T. I., and Tsuruda, J. M. (2005). Kinetics and molecular properties of pheromone binding and release. *Proc. Natl. Acad. Sci. U.S.A.* 102, 5386–5391.

Lee, J. K., and Strausfeld, N. J. (1990). Structure, distribution, and number of surface sensilla and their receptor cells on the antennal flagellum of the male sphinx moth *Manduca sexta*. *J. Neurocytol.* 19, 519–538.

Lehman, H. K. (1990). Circadian control of *Manduca sexta* flight. *Abstr. Soc. Neurosci.* 16, 1334.

Lei, H., Riffell, J. A., Gage, S. L., and Hildebrand, J. G. (2009). Contrast enhancement of stimulus intermittency in a primary olfactory network and its behavioral significance. *J. Biol.* 8, 1–15.

Linn, C. E. Jr., and Roelofs, W. L. (1986). Modulatory effects of octopamine and serotonin on male sensitivity and periodicity of response to sex pheromone in the cabbage looper moth, *Trichoplusia ni*. *Arch. Insect. Biochem. Physiol.* 3, 161–171.

Lucas, P., and Pézier, A. (2006). DAG, calcium and chloride: partners involved in insect olfactory transduction. *Chem. Senses* 31, E81.

Lundin, C., Käll, L., Kreher, S. A., Kapp, K., Sonnhammer, S. L., Carson, J. R., Heijne, G., and Nilsson, I. (2007). Membrane topology of the *Drosophila* OR83b odorant receptor. *FEBS Lett.* 581, 5601–5604.

Maida, R., Redkozubov, A., and Ziegelberger, G. (2000). Identification of PLC beta and PKC in pheromone receptor neurons of *Antheraea polyphemus*. *Neuroreport* 11, 1773–1776.

Malpel, S., Merlin, C., François, M. C., and Jacquin-Joly, E. (2008). Molecular identification and characterization of two new Lepidoptera chemoreceptors belonging to the *Drosophila melanogaster* OR83b family. *Insect. Mol. Biol.* 17, 587–596.

Merlin, C., François, M. C., Queguiner, I., Maibèche-Coisné, M., and Jacquin-Joly, E. (2006). Evidence for a putative antennal clock in *Mamestra brassicae*: molecular cloning and characterization of two clock genes – *period and cryptochrome* – in antennae. *Insect. Mol. Biol.* 15, 137–145.

Merlin, C., Lucas, P., Rochat, D., François, M. C., Maibèche-Coisne, M., and Jacquin-Joly, E. (2007). An antennal circadian clock and circadian rhythms in peripheral pheromone reception in the moth *Spodoptera littoralis*. *J. Biol. Rhythms* 22, 502–514.

Milner, P. (1974). A model for visual shape recognition. *Psychol. Rev.* 81, 521–535.

Minor, A. V., and Kaissling, K.-E. (2003). Cell responses to single pheromone molecules may reflect the activation kinetics of olfactory receptor molecules. *J. Comp. Physiol. A* 189, 221–230.

Miura, N., Atsumi, S., Tabunoki, H., and Sato, R. (2005). Expression and localization of three G protein subunits, Go, Gq, and Gs, in adult antennae of the silkmoth (*Bombyx mori*). *J. Comp. Neurol.* 485, 143–152.

Mohl, C., Breer, H., and Krieger, J. (2002). Species-specific pheromonal compounds induce distinct conformational changes of pheromone binding protein subtypes from *Antheraea polyphemus*. *Invert. Neurosci.* 4, 165–174.

Morton, D. (2004). Invertebrates yield a plethora of atypical guanylyl cyclases. *Mol. Neurobiol.* 29, 97–116.

Morton, D., and Nighorn, A. (2003). MsGC-II, a receptor guanylyl cyclase isolated from the CNS of *Manduca sexta* that is inhibited by calcium. *J. Neurochem.* 84, 363–372.

Murlis, J., and Jones, C. (1981). Fine-scale structure of odour plumes in relation to insect orientation to distant pheromone and other attractant sources. *Physiol. Entomol.* 6, 71–86.

Nadasdy, Z. (2010). Binding by asynchrony: the neuronal phase code. *Front. Neurosci.* 4:51. doi: 10.3389/fnins.2010.00051

Nakagawa, T., Sakurai, T., Nishioka, T., and Touhara, K. (2005). Insect sex pheromone signals mediated by specific combinations of olfactory receptors. *Science* 307, 1638–1642.

Nakagawa, T., and Vosshall, L. (2009). Controversy and consensus: noncanonical signaling mechanisms in the insect olfactory system. *Curr. Opin. Neurobiol.* 19, 284–292.

Nighorn, A., Simpson, P. J., and Morton, D. B. (2001). The novel guanylyl cyclase Ms GC-I is strongly expressed in higher order neuropils in the brain of *Manduca sexta*. *J. Exp. Biol.* 204, 305–314.

Patch, H., Velarde, R. A., Walden, K. K. O., and Robertson, H. M. (2009). A candidate pheromone receptor and two odorant receptors of the hawkmoth *Manduca sexta*. *Chem. Senses* 34, 305–316.

Pelosi, P., Zhou, J. J., Ban, L. P., and Calvello, M. (2006). Soluble proteins in insect chemical communication. *Cell. Mol. Life Sci.* 63, 1658–1676.

Pézier, A., Acquistapace, A., Renou, M., Rospars, J.-P., and Lucas, P. (2007). Ca^{2+} stabilizes the membrane potential of moth olfactory receptor neurons at rest and is essential for their fast repolarization. *Chem. Senses* 32, 305–317.

Pézier, A., Grauso, M., Acquistapace, A., Monsempes, C., Rospars, J.-P., and Lucas, P. (2010). Calcium activates a chloride conductance likely involved in olfactory receptor neuron repolarization in the moth *Spodoptera littoralis*. *J. Neurosci.* 30, 6323–6333.

Pophof, B. (2000). Octopamine modulates the sensitivity of silkmoth pheromone receptor neurons. *J. Comp. Physiol. A* 186, 307–313.

Pophof, B. (2002). Octopamine enhances moth olfactory responses to pheromones, but not those to general odorants. *J. Comp. Physiol. A* 188, 659–662.

Pophof, B. (2004). Pheromone-binding proteins contribute to the activation of olfactory receptor neurons in the silkmoths *Antheraea polyphemus* and *Bombyx mori*. *Chem. Senses* 29, 117–125.

Pophof, B., and van der Goes van Naters, W. (2002). Activation and inhibition of the transduction process in silkmoth olfactory receptor neurons. *Chem. Senses* 27, 435–443.

Raman, B., Tang, J. J., and Stopfer, M. (2010). Temporally diverse firing patterns in olfactory receptor neurons underlie spatiotemporal neural codes for odors. *J. Neurosci.* 30, 1994–2006.

Raming, K., Krieger, J., and Breer, H. (1989). Molecular cloning of an insect pheromone-binding protein. *FEBS Lett.* 256, 215–218.

Rogers, M. E., Steinbrecht, R. A., and Vogt, R. G. (2001a). Expression of SNMP-1 in olfactory neurons and sensilla of male and female antennae of the silkmoth *Antheraea polyphemus*. *Cell Tissue Res.* 303, 433–446.

Rogers, M. E., Krieger, J., and Vogt, R. G. (2001b). Antennal SNMPs (sensory neuron membrane proteins) of Lepidoptera define a unique family of invertebrate CD36-like proteins. *J. Neurobiol.* 49, 47–61.

Rogers, M. E., Sun, M., Lerner, M. R., and Vogt, R. G. (1997). SNMP-1, a novel membrane protein of olfactory neurons of the silk moth *Antheraea polyphemus* with homology to the CD36 family of membrane proteins. *J. Biol. Chem.* 272, 14792–14799.

Rützeler, M., and Zwiebel, I. J. (2005). Molecular biology of insect olfaction: recent progress and conceptual models. *J. Comp. Physiol. A* 191, 777–790.

Saifullah, A. S., and Page, T. L. (2009). Circadian regulation of olfactory receptor neurons in the cockroach antenna. *J. Biol. Rhythms* 24, 144–152.

Sakurai, T., Nakagawa, T., Mitsuno, H., Mori, H., Endo, Y., Tanoue, S., Yasukochi, Y., Touhara, K., and Nishioka, T. (2004). Identification and functional characterization of a sex pheromone receptor in the silkmoth *Bombyx mori*. *Eur. J. Neurosci.* 21, 2167–2176.

Sanes, J. R., and Hildebrand, J. G. (1976). Origin and morphogenesis of sensory neurons in an insect antenna. *Dev. Biol.* 51, 300–319.

Sato, K., Pellegrino, M., Nakagawa, T., Nakagawa, T., Vosshall, L. B., and Touhara, K. (2008). Insect olfactory receptors are heteromeric ligand-gated ion channels. *Nature* 452, 1002–1006.

Schleicher, S., Boekhoff, I., Konietzko, U., and Breer, H. (1994). Pheromone-induced phosphorylation of antennal proteins from insects. *J. Comp. Physiol. B* 164, 76–80.

Schmidt, C. J., Garen-Fazio, S., Chow, Y. K., and Neer, E. J. (1998). Neuronal expression of a newly identified *Drosophila melanogaster* G protein alpha o subunit. *Cell Regul.* 1, 125–134.

Schneider, N.-L., and Stengl, M. (2005). Pigment-dispersing factor and GABA synchronize insect circadian clock cells. *J. Neurosci.* 25, 5138–5147.

Schneider, N.-L., and Stengl, M. (2006). Gap junctions between accessory medulla neurons appear to synchronize circadian clock cells. *J. Neurophysiol.* 95, 1996–2002.

Schneider, N.-L., and Stengl, M. (2007). Long term recordings of the isolated circadian pacemaker center of the cockroach *Leucophaea maderae* reveals circadian and ultradian rhythms. *J. Comp. Physiol. A* 193, 35–42.

Schuckel, J., Siwicki, K. K., and Stengl, M. (2007). Putative circadian pacemaker cells in the antenna of the hawkmoth *Manduca sexta*. *Cell Tissue Res.* 330, 271–278.

Silbering, A. F., and Benton, R. (2010). Ionotropic and metabotropic mechanisms in chemoreception: "chance or design"? *EMBO Rep.* 11, 173–179.

Silverstein, R. L., and Febbraio, M. (2009). CD36, a scavenger receptor involved in immunity, metabolism, angiogenesis, and behavior. *Sci. Signal.* 2, re3.

Simpson, P. J., Nighorn, A., and Morton, D. B. (1999). Identification of a novel guanylyl cyclase that is related to receptor guanylyl cyclases, but lacks extracellular and transmembrane domains. *J. Biol. Chem.* 274, 4440–4446.

Singer, W.., and Gray, C. (1995). Visual feature integration and the temporal correlation hypothesis. *Annu. Rev. Neurosci.* 18, 555–586.

Smart, R., Kiely, A., Beale, M., Vargas, E., Carraher, C., Kralicek, A. V., Christie, D. L., Chen, C., Newcomb, R. D., and Warr, C. G. (2008). *Drosophila* odorant receptors are novel seven transmembrane domain proteins that can signal independently of heterotrimeric G proteins. *Insect Biochem. Mol. Biol.* 38, 770–780.

Steinbrecht, R. A., Laue, M., and Ziegelberger, G. (1995). Immunocytochemistry of odorant-binding protein and general binding protein in olfactory sensilla of the silk moths *Antheraea* and *Bombyx*. *Cell Tissue Res.* 282, 203–217.

Stengl, M. (1990). *Development of an In Vitro Model System to Study Primary Sensory Transduction Mechanisms*. Dissertation, ARL, University of Arizona, 1–177.

Stengl, M. (1993). Intracellular-messenger-mediated cation channels in cultured olfactory receptor neurons. *J. Exp. Biol.* 178, 125–147.

Stengl, M. (1994). Inositol-trisphosphate-dependent calcium currents precede cation currents in insect olfactory receptor neurons. *J. Comp. Physiol. A* 174, 187–194.

Stengl, M., and Hildebrand, J. G. (1990). Insect olfactory neurons *in vitro*: morphological and immunocytochemical characterization of male-specific antennal receptor cells from developing antennae of male *Manduca sexta*. *J. Neurosci.* 10, 837–847.

Stengl, M., and Zintl, R. (1996). NADPH-diaphorase staining in the antenna of the moth *Manduca sexta*. *J. Exp. Biol.* 199, 1063–1072.

Stengl, M., Homberg, U., and Hildebrand, J. G. (1990). Acetylcholinesterase activity in antennal receptor neurons of the sphinx moth *Manduca sexta*. *Cell Tissue Res.* 262, 245–252.

Stengl, M., Ziegelberger, G., Boekhoff, I., and Krieger, J. (1999). "Perireceptor events and transduction mechanisms in insect olfaction," in *Insect Olfaction*, ed. B. S. Hansson (Berlin: Springer), 49–66.

Stengl, M., Zintl, R., de Vente, J., and Nighorn, A. (2001). Localization of cGMP-immunoreactivity and of soluble guanylyl cyclase in antennal sensilla of the hawkmoth *Manduca sexta*. *Cell Tissue Res.* 304, 409–421.

Stengl, M., Zufall, F., Hatt, H., and Hildebrand, J. G. (1992). Olfactory receptor neurons from antennae of developing male *Manduca sexta* respond to components of the species-specific sex pheromone *in vitro*. *J. Neurosci.* 12, 2523–2531.

Talluri, S., Bhatt, A., and Smith, D. P. (1995). Identification of a *Drosophila* G protein alpha subunit (dG_q alpha-3) expressed in chemosensory cells and central neurons. *Proc. Natl. Acad. Sci. U.S.A.* 92, 11475–11479.

Tanoue, S., Krishnan, P., Chatterjee, A., and Hardin, P. E. (2008). G protein-coupled receptor kinase 2 is required for rhythmic olfactory responses in *Drosophila*. *Curr. Biol.* 18, 787–794.

Tanoue, S., Krishnan, T., Krishnan, B., Dryer, S. E., and Hardin, P. E. (2004). Circadian clocks in antennal neurons are necessary and sufficient for olfaction rhythms in *Drosophila*. *Curr. Biol.* 14, 638–649.

Thurm, U., and Küppers, J. (1980). "Epithelial physiology of insect sensilla," in *Insect Biology in the Future*, eds M. Locke and D. S. Smith (New York: Academic Press), 735–763.

Tripathy, S., Peters, O. J., Staudacher, E. M., Kalwar, F. R., Hatfield, M. N., and Daly, K. C. (2010). Odors pulsed at wing beat frequencies are tracked by primary olfactory networks and enhance odor detection. *Front. Cell. Neurosci.* 16:1. doi: 10.3389/neuro.03.001.2010

Tumlinson, J. H., Brennan, M. M., Doolittle, R. E., Mitchell, E. R., Brabham, A., Mazomemos. B. E., Baumhover, A. H., and Jackson, D. M. (1989). Identification of a pheromone blend attractive to *Manduca sexta* (L.) males in a wind tunnel. *Arch. Insect Biochem. Physiol.* 10, 255–271.

Vickers, N. J. (2000). Mechanisms of animal navigation in odor plumes. *Biol. Bull.* 198, 203–212.

Vickers, N. J., and Baker, T. C. (1992). Male *Heliothis virescens* maintain upwind flight in response to experimentally pulsed filaments of their sex pheromone *(Lepidoptera: Noctuidae)*. *J. Insect Behav.* 5, 669–687.

Vogt, R. G., Miller, N. E., Litvack, R., Fandino, R. A., Sparks, J., Staples, J., Friedman, R., and Dickens, J. C. (2009). The insect SNMP gene family. *Insect Biochem. Mol. Biol.* 39, 448–456.

Vogt, R. G., and Riddiford, L. M. (1981). Pheromone binding and inactivation by moth antennae. *Nature* 293, 161–163.

Vogt, R. G., and Riddiford, L. M. (1986). "Pheromone reception: a kinetic equilibrium," *Mechanisms in Insect Olfaction*, eds T. L. Payne, M. C. Birch and E. J. Kennedy (Oxford: Clarendon), 201–208.

von Frisch, K. (1921). Über den Sitz des Geruchssinnes bei Insekten. *Zool. Jahrb. Abt. Allgem. Zool. Physiol. Tiere* 38, 449–516.

Von Nickisch-Rosenegk, E., Krieger, J., Kubick, S., Laage, R., Strobel, J., Stotmann, H., and Breer, H. (1996). Cloning of biogenic amine receptors from moths (*Bombyx mori* and *Heliothis virescens*). *Insect Biochem. Mol. Biol.* 26, 817–827.

Wegener, J. W., Hanke, W., and Breer, H. (1997). Second messenger-controlled membrane conductance in locust (*Locusta migratoria*) olfactory receptor neurons. *J. Insect. Physiol.* 43, 595–605.

Wicher, D, Schäfer, R., Bauernfeind, R., Stensmyr, M. C., Heller, R., Heinemann, S. H., and Hansson, B. S. (2008). *Drosophila* odorant receptors are both ligand-gated and cyclic-nucleotide-activated cation channels. *Nature* 452, 1007–1011.

Xu, P. X., Atkinson, R., Jones, D. N. M., and Smith, D. P. (2005). *Drosophila* OBP LUSH is required for activity of pheromone-sensitive neurons. *Neuron* 45, 193–200.

Ziegelberger, G. (1995). Redox-shift of the pheromone-binding protein in the silkmoth *Antheraea polyphemus*. *Eur. J. Biochem.* 232, 706–711.

Ziegelberger, G., Van den Berg, M. J., Kaissling, K.-E., Klumpp, S., and Schultz, J. E. (1990). Cyclic nucleotide levels and guanylate cyclase activity in pheromone-sensitive antennae of the silkmoths *Antheraea polyphemus* and *Bombyx mori*. *J. Neurosci.* 10, 1217–1225.

Zufall, F., and Hatt, H. (1991). Dual activation of a sex pheromone-dependent ion channel from insect olfactory dendrites by protein kinase C activators and cyclic GMP. *Proc. Natl. Acad. Sci. U.S.A.* 88, 8520–8524.

Zufall, F., Stengl, M., Franke, C., Hildebrand, J. G., and Hatt, H. (1991a). Ionic currents of cultured olfactory receptor neurons from antennae of male *Manduca sexta*. *J. Neurosci.* 11, 956–965.

Zufall, F., Franke, C., and Hatt, H. (1991b). A calcium-activated nonspecific cation channel from olfactory receptor neurons of the silkmoth *Antheraea polyphemus*. *J. Exp. Biol.* 161, 455–468.

Conflict of Interest Statement: The author declares that the research was conducted in the absence of any commercial or financial relationships that could be construed as a potential conflict of interest.

Received: 31 May 2010; paper pending published: 07 September 2010; accepted: 16 December 2010; published online: 31 December 2010.

*Citation: Stengl M (2010) Pheromone transduction in moths. Front. Cell. Neurosci. **4**:133. doi: 10.3389/fncel.2010.00133*

Copyright © 2010 Stengl. This is an open-access article subject to an exclusive license agreement between the authors and the Frontiers Research Foundation, which permits unrestricted use, distribution, and reproduction in any medium, provided the original authors and source are credited.

frontiers in
CELLULAR NEUROSCIENCE

ORIGINAL RESEARCH ARTICLE
published: 16 November 2012
doi: 10.3389/fncel.2012.00054

Temporal response dynamics of *Drosophila* olfactory sensory neurons depends on receptor type and response polarity

Merid N. Getahun, Dieter Wicher, Bill S. Hansson† and Shannon B. Olsson*†

Department of Evolutionary Neuroethology, Max Planck Institute for Chemical Ecology, Jena, Germany

Edited by:
Barry W. Connors, Brown University, USA

Reviewed by:
Jane L. Witten, University of Wisconsin-Milwaukee, USA
Alfredo Fontanini, Stony Brook University, USA

****Correspondence:***
Shannon B. Olsson, Department of Evolutionary Neuroethology, Max Planck Institute for Chemical Ecology, Hans-Knöll-St. 8, D-07745 Jena, Germany.
e-mail: solsson@ice.mpg.de

† These authors share senior authorship.

Insect olfactory sensory neurons (OSN) express a diverse array of receptors from different protein families, i.e. ionotropic receptors (IR), gustatory receptors (GR) and odorant receptors (OR). It is well known that insects are exposed to a plethora of odor molecules that vary widely in both space and time under turbulent natural conditions. In addition to divergent ligand specificities, these different receptors might also provide an increased range of temporal dynamics and sensitivities for the olfactory system. To test this, we challenged different *Drosophila* OSNs with both varying stimulus durations (10–2000 ms), and repeated stimulus pulses of key ligands at various frequencies (1–10 Hz). Our results show that OR-expressing OSNs responded faster and with higher sensitivity to short stimulations as compared to IR- and Gr21a-expressing OSNs. In addition, OR-expressing OSNs could respond to repeated stimulations of excitatory ligands up to 5 Hz, while IR-expressing OSNs required ∼5x longer stimulations and/or higher concentrations to respond to similar stimulus durations and frequencies. Nevertheless, IR-expressing OSNs did not exhibit adaptation to longer stimulations, unlike OR- and Gr21a-OSNs. Both OR- and IR-expressing OSNs were also unable to resolve repeated pulses of inhibitory ligands as fast as excitatory ligands. These differences were independent of the peri-receptor environment in which the receptors were expressed and suggest that the receptor expressed by a given OSN affects both its sensitivity and its response to transient, intermittent chemical stimuli. OR-expressing OSNs are better at resolving low dose, intermittent stimuli, while IR-expressing OSNs respond more accurately to long-lasting odor pulses. This diversity increases the capacity of the insect olfactory system to respond to the diverse spatiotemporal signals in the natural environment.

Keywords: odorant receptors, ionotropic receptors, pulse resolution, single sensillum recording

INTRODUCTION

Insect olfactory sensory neurons (OSN) express a large number of receptor proteins of different types. These receptor types include ionotropic receptors (IR), gustatory receptors (GR), and odorant receptors (OR) (Clyne et al., 1999; Vosshall et al., 1999; Benton et al., 2009). IRs are composed of three trans-membrane proteins and co-receptors, while GRs and ORs are seven trans-membrane proteins (Vosshall et al., 1999; Benton et al., 2006, 2009). ORs are co-expressed with the ubiquitous co-receptor Orco, while Gr21a, a CO_2 sensor, is co-expressed with Gr63a (Benton et al., 2006; Jones et al., 2007). All OSNs are housed within different morphological types of olfactory hairs, known as sensilla. There appear to be important organizational differences between OSNs that express IRs, GRs, or ORs. Multiple IRs and GRs can be co-expressed per neuron, while OR expression generally follows a one neuron-one receptor rule (Thorne et al., 2004; Wang et al., 2004; Couto et al., 2005; Benton et al., 2009). Receptors from different protein families can also be co-localized in the same sensillum (Couto et al., 2005; Song et al., 2012). For example, in *Drosophila*, the ab1 sensillum houses four OSNs, three expressing ORs and one expressing Gr21a. Also, in the *Drosophila* coeloconic sensillum ac3 an OSN expressing Or35a is co-localized with an OSN expressing Ir75abc (Yao et al., 2005; Silbering et al., 2011).

These diverse receptors have evolved at different points in evolutionary time (Robertson et al., 2003; Croset et al., 2010). Recent research also suggests that many have broad affinity to different chemical classes (Hallem et al., 2004; Yao et al., 2005; Benton et al., 2009; Ai et al., 2010). Yet specificity might not be the only reason for receptor diversification. In the natural environment, insects are constantly challenged with odors not only of diverse molecular types, but with diverse spatio-temporal dynamics. At some distances, odor plumes can present brief and intermittent stimuli (Kaissling et al., 1987; Vickers et al., 2001) with low molecular flux, while at close range or high molecular flux, odors could present a nearly continuous stimulus (Murlis et al., 2000; Louis et al., 2008; Gomez-Marin et al., 2011). These spatiotemporal factors could also be a significant driving force for diversification. The behavior of an insect is a result of the integration of responses from several OSNs expressing a variety of receptor

types (Silbering et al., 2011). Thus it is worthwhile to characterize the response dynamics across the OSN repertoire.

To address whether these different receptor types exhibit differences in temporal response kinetics, we assess the response dynamics of *Drosophila* OSNs expressing various receptor types to both different stimulus durations and frequencies. We evaluate the temporal dynamics of antennal OSNs expressing ORs (Or59b and Or35a), IRs (Ir84a, Ir75abc, and Ir41a), and GRs (Gr21a). Or59b-OSNs and Ir41a-OSNs respond with either excitation or inhibition to different ligands, and were chosen to assess the effect of response polarity on temporal kinetics. Or35a- and Ir75abc-OSNs are housed in the same sensillum, and are tested to control for the effects of the perireceptor environment on the temporal response. Finally, Gr21a-expressing OSNs are the only GR-expressing OSNs found on the antenna. Here we show that sensory neurons expressing receptors from different protein families also exhibit different dynamics to brief and intermittent stimuli.

MATERIALS AND METHODS

Both male and female flies at 2–6 days of age were used. Stocks were maintained on conventional cornmeal agar medium under a 12 h light: 12 h dark cycle at 25°C.

ELECTROPHYSIOLOGY

A fly was mounted in a cut pipette tip with the head protruding and small amount of wax placed into the tip end to prevent movement. The pipette was then fixed onto a microscope slide with wax and the antennae fixed on a cover slip with a sharpened glass micropipette, similar to (Hallem et al., 2004; Yao et al., 2005; Pellegrino et al., 2010). An electrolytically sharpened tungsten electrode was placed in the eye for grounding and a sharpened tungsten recording electrode was brought into contact with the base of the sensillum using a Luigs and Neumann, SM-59 manipulator (Ratingen, Germany) at 1000× magnification with an Olympus BX-51 microscope (Olympus Corporation, Tokyo, Japan).

ODOR STIMULI

Methyl acetate (>98%), citral (>95%), phenyl acetaldehyde (>90%), butyric acid (>99%), 1, 4-diaminobutane and isoamylamine (>98%), 1-hexanol (>99%), and ethyl hexanoate (>99%) were purchased from Sigma Aldrich Germany. Phenyl acetaldehyde, methyl acetate, 1-hexanol and ethyl hexanoate were diluted in mineral oil (BioChemika Ultra, Fluka), and butyric acid, 1, 4-diaminobutane, and isoamylamine were dissolved in water. Citral was dissolved in hexane (>99%, Fluka Analytical, Buchs, Switzerland). We chose odor concentrations within the linear portion of the dose response curve and the tested concentrations are indicated with circles (**Figure 1**). All concentrations are reported as log [odor] v/v. For Gr21a stimulation, a 1.5 ml glass vial was filled with pure CO_2 and placed into the stimulus system similar to the other stimuli. After each frequency set (1–10 Hz), the CO_2 was refilled.

For frequency stimulation, we used a custom-built multicomponent stimulus system similar to (Olsson et al., 2011). Briefly, 400 ul of appropriate dilutions of each odorant was added to an Eppendorf tube and placed in the bottom of a PEEK vial (4.6 cm × 2.5 cm × 2.5 cm dimensions). Each vial was sealed with a stainless steel plug (Olsson et al., 2011). The pulse duration, inter-stimulus interval and number of pulses were adjusted through a custom built Labview program (Olsson et al., 2011). The odors were delivered from the headspace via Teflon tubing 150 cm long with an inner diameter of 1 mm and positioned as close as possible (∼1.5 cm) to the antennae. The flow rate of air was 0.5 L/min. For stimulation, the stimulus system was connected to the IDAC (Syntech, Ockenfels, Germany) and through USB connection to a PC. Stimulation was controlled by an OEM (EDP 0504, thinXXS) pump control system and DAQ (USB 6008

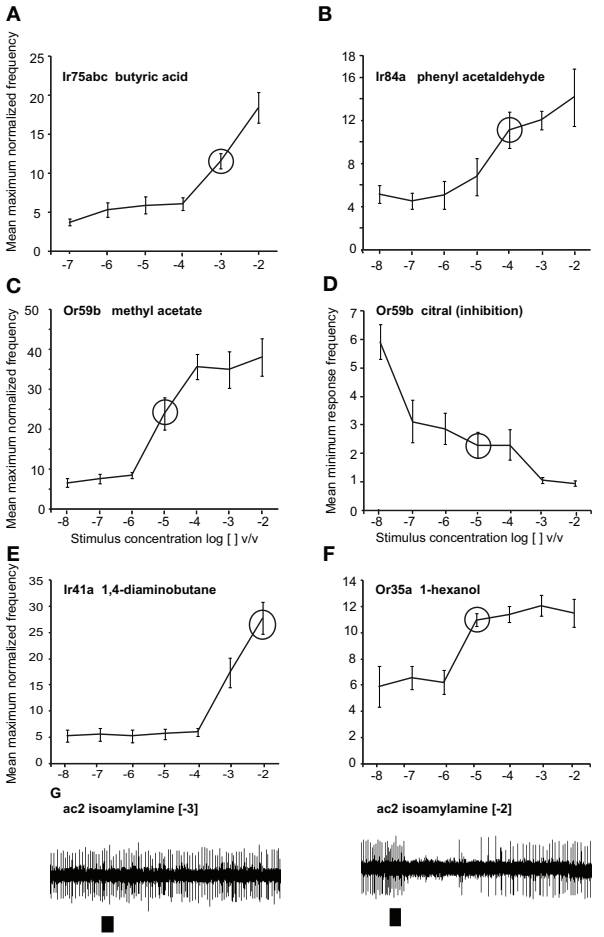

FIGURE 1 | Responses to odors at different doses. Dose-response curves presented as normalized maximum frequency response for **(A)** Ir75abc-expressing neurons to butyric acid $n = 8–13$ **(B)** Ir84a-expressing neurons to phenylacetaldehyde, $n = 9–12$. **(C)**, Or59b-expressing neurons to methyl acetate, $n = 8–17$ **(D)** Or59b-expressing neurons to citral presented as the minimum frequency, $n = 6–10$. **(E)** Ir41a-expressing neurons to 1, 4-diaminobutane $n = 6–8$ **(F)**. Or35a-expressing OSNs to 1-hexanol, $n = 6–8$. **(G)** Representative traces showing the response of OSNs of ac2 sensilla to isoamylamine at two different concentrations (responses to lower concentrations were not observed). Please note that while only Ir41a-expressing neurons are excited by 1, 4-diaminobutane in this sensillum (ac2), all neurons are inhibited by isoamylamine, and we thus label the inhibitory responses with the entire sensillum label.

data acquisition hardware, National Instruments, Austin, TX, USA) with custom-built Labview 8.5 software (built by Daniel Veit; National Instruments). For frequency stimulation the on time was 50 ms for OR- and Gr21a-OSNs and the off time was adjusted from 950 ms or 50 ms for 1–10 Hz, respectively. For IR-OSNs stimulated with [−4] and [−3] stimulus concentrations, the pump on time was 200 ms and off time 800, 300, or 50 ms for 1–4 Hz, respectively. At [−2], the protocol was identical to the OR-OSNs and Gr21a-OSNs. The consistency of odor delivery for different pulse durations and frequencies was confirmed using PID (200a, Aurora Scientific Ontario, Canada).

DATA ANALYSIS

All raw spike data were acquired and converted to digital spikes using Autospike 3.7 (Syntech). Co-localized neurons were identified based on spike amplitude. Peri-stimulus time histograms (PSTHs) were obtained by averaging spike activities in 25 ms bins from the start of the stimulation and normalized to the average frequency for 2 s before stimulation (Olsson et al., 2011; Sargsyan et al., 2011). The OSN responses between consecutive pulses were compared using repeated measure ANOVA by assessing the normalized mean of area under curve (AUC) spike frequency per each stimulus duration, i.e. pump on time + off time. Consecutive pulses were normalized to the response of 1st pulse. Between treatments, a Mann-Whitney U test or *t*-test was used depending on the normality of the data. To evaluate the capacity of receptors to resolve pulsed stimuli, we visualized the response using normalized peri-stimulus histograms and quantified the % return to the spontaneous activity (baseline), using the ratio between the first value in the 2nd pulse and the maximum peak value of the first (previous) pulse converted to a percentage: Percent return to baseline = 1−(1st value of the 2nd pulse/maximum frequency of the 1st pulse) × 100 (Bau et al., 2002). A One-Way ANOVA followed by a Tukey *post-hoc* test was performed to determine if the return to baseline was significantly reduced between the different stimulation frequencies. Latency was measured as the time from the onset of the odor stimulus to the maximum response frequency (mechanical delay was not considered). Response width was calculated as the time between half-maximal response for excitation and half-minimal response in the case of inhibition. Spearman's correlation was used to assess the relationship between repeated pulses and latency as well as between response width and intensity with stimulus duration. All analyses were performed using SPSS version 17 (IBM Corporation, Armonk, New York, US).

RESULTS

RESPONSE DYNAMICS OF DIFFERENT SENSORY NEURONS TO VARYING STIMULUS DURATIONS

We first assessed the response of OSNs carrying ORs, Gr21a, or IRs to key ligands presented with varying stimulus durations at concentrations found in the linear portion of the dose-response curve for each OSN (**Figure 1**). OSNs expressing Or59b housed in basiconic sensillum type ab2 were stimulated with methyl acetate at [−5] concentration, with stimulus durations varying from 10 ms to 2 s. At 20 ms, the mean normalized frequency of Or59b-expressing OSNs was greater than the spontaneous activity ($t = 3.482$, $P = 0.005$), indicating that a 20 ms stimulation was sufficient to elicit a response (**Figure 2A** asterisk right). A maximal stimulus response was obtained with a 50 ms stimulation ($P < 0.05$), however, stimulations of 1 s or more significantly reduced the OSN response maximum ($t = 3.482$, $P = 0.005$, mean normalized maximum frequency for 500 ms vs. 1 s stimulation and $t = 5.047$, $P < 0.001$ for 500 ms vs. 2 s, Student's *t*-test). Similar response dynamics were observed in Or35a-expressing OSNs ($t = 5.007$, $P < 0.001$ mean normalized maximum frequency for 500 ms vs. 2 s stimulation; **Figure 2B**). Adaptation to long stimulus durations (>1 s) was also apparent for Or22a-OSNs (data not shown). There was also a positive and significant correlation between response width at half-maximal response and stimulus duration for both OR-expressing OSNs ($r = 0.853$, $P < 0.001$ for Or59b-OSNs and $r = 0.93$, $P < 0.001$ for Or35a-OSNs; both Spearman's correlation **Figures 2A,B** left panels).

OSN expressing Ir84a (**Figure 2C**) were stimulated with [−4] phenyl acetaldehyde and a significant response was obtained at 100 ms ($P < 0.001$, Mann–Whitney *U*-test; **Figure 2B**). A maximal response was reached at 500 ms ($P = 0.001$, Mann–Whitney *U*-test, as compared to 100 ms), and the maximum response intensity did not decrease at longer stimulation durations ($t = 0.605$, $P = 0.554$ at 500 ms stimulation vs. 1 s, and $t = 0.394$, $P = 0.699$ for 500 ms vs. 2 s; Student's *t*-test). The response of Ir75abc-expressing neurons was similar when stimulated with [−3] butyric acid, (significant response at 100 ms; Mann–Whitney U, $P = 0.016$, **Figure 2D**), and reached a maximum response at 500 ms ($t = 2.286$, $P = 0.036$ compared to 100 ms). Furthermore, the response did not change at longer stimulus durations ($t = 0.096$, $P = 0.924$, 500 ms vs. 1 s, $t = 0.068$, $P = 0.946$, 500 ms vs. 2 s; **Figure 2D** right panel). There was also a positive and significant correlation between stimulus duration and response width at half maximal response ($r = 0.905$, $P < 0.001$ for Ir84a-OSNs, and $r = 0.917$, $P < 0.001$ for Ir75abc-OSNs, Spearman's correlation; **Figures 2C** and **D** left panel). Similarly, the Ir41a-OSN response to 1,4-diaminobutane at [−2] did not show adaptation at longer stimulus durations ($t = 0.073$, $P = 0.944$ for 500 ms vs. 1 s stimulations; $t = 0.01$, $P = 0.992$ for 500 ms vs. 2 s stimulations).

OSNs expressing Gr21a, which are housed in ab1 sensilla on the *Drosophila* antenna, respond to pure CO_2 beginning at a 20 ms stimulation (Mann–Whitney *U*-test, $P = 0.009$ **Figure 2E**). Peak response was obtained at 1 s ($t = 4.641$, $P = 0.002$, Student's *t*-test compared to 20 ms), while at a 2 s stimulation the maximum response frequency decreased significantly ($t = 2.63$, $P = 0.02$, Student's *t*-test, 1 s vs. 2 s). However, the response latency also became shorter with stimulus duration, decreasing from the 20 ms duration (with a mean half-maximal response on set time of 400 ± 26.35 ms), to 1 s (with a mean half maximal response on set time 300 ± 17.67 ms, $t = 3.028$, $P = 0.016$, Student's *t*-test; **Figure 2E** left panel). This is opposite to both OR- and IR-expressing OSNs, where there was no difference (**Figures 2A–D**). Similarly, the response width also increased with stimulus duration ($r = 0.781$, $P < 0.001$, Spearman's correlation, **Figure 2E** left panel).

Increasing stimulus concentrations reduced the duration required to elicit a response regardless of the receptor expressed.

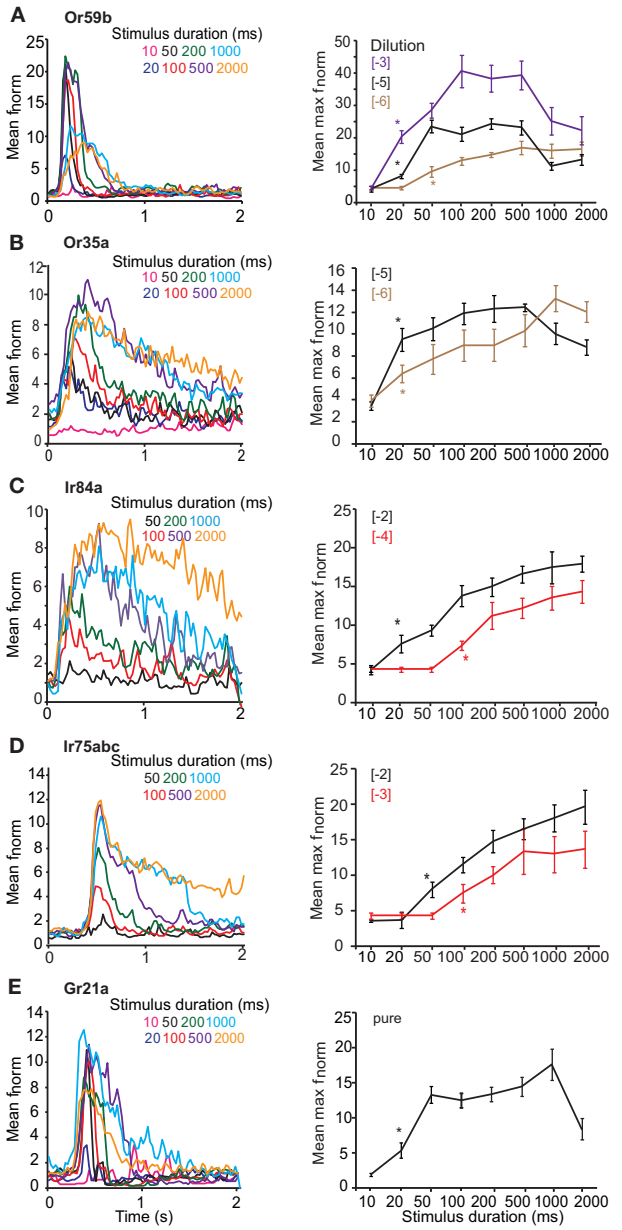

FIGURE 2 | Response of OSNs to varying stimulus durations. (**A**, left) Mean peri-stimulus time histograms (PSTHs, 25 ms bins) showing the response of Or59b-expressing OSNs to various stimulus durations of log [−5] v/v methyl acetate. (**A**, right) Mean normalized maximum frequency for Or59b-expressing neurons plotted vs. stimulus duration ($n = 8$–15) for three different concentrations. Asterisks indicate the minimum stimulus duration that elicited a significant response, $P < 0.05$. (**B**, left) Mean peri-stimulus time histograms as in **(A)** showing the response of Or35a-expressing OSNs to various stimulus durations of log [−5] v/v 1-hexanol. (**B**, right) Mean normalized maximum frequency for Or35a-expressing neurons plotted versus stimulus duration for log [−5] and [−6] v/v of 1-hexanol ($n = 6$–14). (**C**, left) Response of Ir84a-expressing neurons to various durations of log [−4] v/v phenyl acetaldehyde as in **(A)**, $n = 8$–10 (**C**, right) as in A for two different concentrations. (**D**, left) Response of Ir75abc-expressing neurons to various durations of log [−3] v/v butyric acid ($n = 6$–15) and (**D**, right) as in **(C)**. **(E)** Response of Gr21a-expressing neurons to pure CO_2 at different stimulus durations ($n = 6$–10).

For example, Or59b-OSNs required 50 ms at [−6] to elicit a significant response ($t = 2.486$, $P = 0.025$; **Figure 1A** right), but only 20 ms at [−3] ($P < 0.001$, Mann–Whitney *U*-test, asterisk in **Figure 2A** right). Similarly, Ir84a-expressing OSNs stimulated with phenyl acetaldehyde at [−2] required only 20 ms to elicit a significant response (Mann–Whitney U, $P = 0.02$, **Figure 2C**), while Ir75abc-expressing OSNs required a 50 ms stimulation when the concentration of butyric acid increased by 10× [−2] (Mann–Whitney U, $P = 0.002$, **Figure 2D**, asterisk right).

However, the dose-dependency of OSN adaptation to long stimulus durations was dependent on the receptor expressed. At [−6] long stimulus durations did not reduce the response of Or59b-expressing OSNs ($t = 0.292$, $P = 0.776$ for 500 ms vs. 1 s; $t = 0.33$, $P = 0.745$ for 500 ms vs. 2 s) or Or35a-expressing OSNs ($t = 1.151$, $P = 0.147$ for 500 ms vs. 1 s; $t = 0.948$, $P = 0.356$ for 500 ms vs. 2 s; **Figures 2A,B** right). However, at [−3] concentration, stimulations of 1 s or more significantly reduced the Or59b-expressing OSN response maximum ($t = 2.235$, $P = 0.045$ for 500 ms vs. 1 s; $t = 2.658$, $P = 0.021$ for 500 ms vs. 2 s, **Figure 2A**). In contrast, longer stimulus durations did not reduce the response of IR-expressing OSNs regardless of concentration (Ir84a-expressing OSNs at [−2]: Mann–Whitney U, $P = 0.847$ for 500 ms vs. 1 s; Ir75abc-expressing OSNs at [−2]: $t = 0.644$, $P = 0.531$ for 500 ms vs. 1 s; Ir41a-expressing OSNs at [−2], $t = 0.073$, $P = 0.944$ for 500 ms vs. 1 s; **Figures 2C,D** right panels).

PULSE RESOLUTION OF DIFFERENT SENSORY NEURONS

After investigating the response of OSNs to various stimulus durations, we presented the neurons with repeated stimulations of varying frequency. The latency to repeated stimulations at 1 Hz increased for all OSN types ($r = 0.742$, $P < 0.001$ for Or59b-OSNs; $r = 0.94$, $P < 0.001$ for Gr21a-OSNs; $r = 0.787$, $P < 0.001$ for Ir75abc-OSNs; $r = 0.652$, $P < 0.001$ for Ir84a-OSNs; Spearman's correlation; **Figures 3A–E**). However, a variability in latency was observed between the tested OSNs; e.g., Ir75abc-OSNs showed more delayed time to maximum than all other neurons tested, $P < 0.001$, ANOVA followed by Tukey *post-hoc* test (**Figure 3E**). At 100× stimulus concentrations or a 5 s interstimulus interval, the latency for Or59b-expressing OSNs did not change with repeated stimulation ($r = 0.09$, $P = 0.475$; $r = -0.006$, $P = 0.952$, respectively, Spearmans's correlation; **Figure 3F**). Similarly, Ir75abc-expressing OSN response onset recovered with a higher concentration ($r = 0.01$, $P = 0.90$, Spearmans's correlation). However, at 5 s interstimulus intervals the response onset became significantly faster for the later pulses ($r = -0.885$, $P < 0.001$, Spearmans's correlation; **Figure 3G**). The latency also decreased with subsequent stimulations of CO_2 for Gr21a-expressing OSNs at 5 s interstimulus intervals ($r = -0.976$, $P < 0.001$, Spearmans's correlation; **Figure 3H**). In summary, this shows that changes in response onset kinetics to repeated stimuli are similar across all tested OSNs and response latencies can be regulated either by altering stimulus concentrations or inter-stimulus intrervals.

Ir84a and Ir75abc-OSNs, housed in ac4 and ac3 sensilla respectively, could resolve repeated 200 ms pulses of [−4] and [−3] stimulus concentrations, respectively, up to 4 Hz (the maximum testable frequency due to stimulation length). The mean

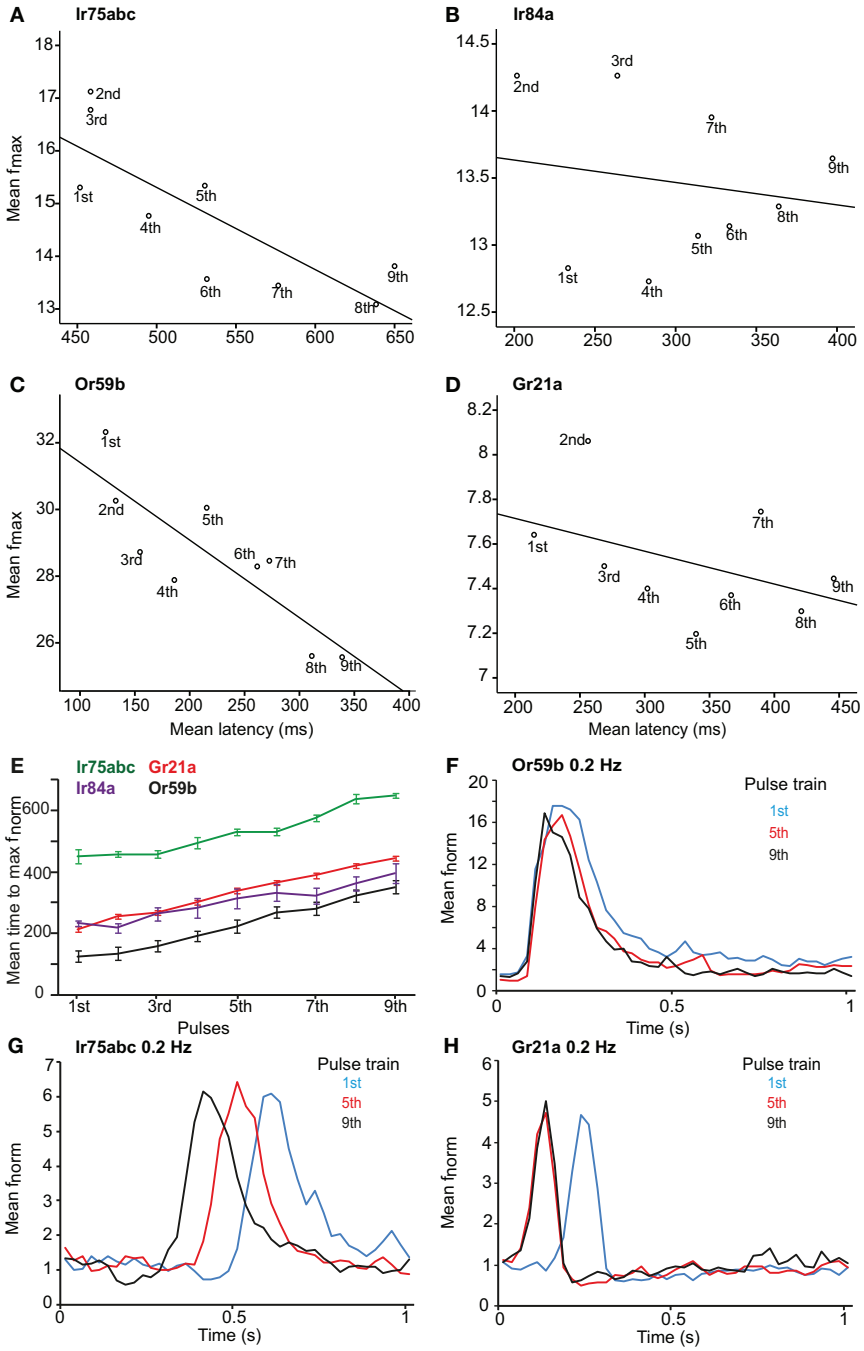

FIGURE 3 | Latency and maximum response of OSNs to repeated stimuli. Maximum response frequency vs. time to peak (latency), with best fit line, for OSNs carrying various receptors in response to repeated 1 Hz stimulations. **(A)** Ir75abc, **(B)** Ir84a, **(C)** Or59b and **(D)** Gr21a. Pulse number (1–9) indicated below each point. **(E)** Mean time to maximum response frequency for neurons in **(A–D)** at a 1 Hz repeated stimulation. **(F)** The response onset recovery of Or59b-expressing OSNs when stimulated at 0.2 Hz, $n = 10$ **(G)** as in **(F)** for Ir75abc-expressing OSNs, $n = 7$ and **(H)** as in **(F)** for Gr21a-expressing OSNs, $n = 10$.

return to base line during repeated stimulation was significantly reduced at 4 Hz as compared to 1 and 2 Hz stimulation, ($P < 0.05$ ANOVA followed by Tukey *post-hoc* test; **Figures 4A,B**). At an increased concentration of [−2], Ir75abc OSNs could resolve pulsed stimuli up to 5 Hz at a 50 ms pulse duration (**Figure 4C**).

Gr21a-expressing OSNs housed in ab1 sensilla resolved intermittent pulses of CO_2 as fast as 8 Hz with no significant difference in return to baseline between 1 Hz and 5 Hz stimulations. At 8 Hz, the mean return to base line was significantly reduced, and at 10 Hz only 2.4% recovery to the base line occurred

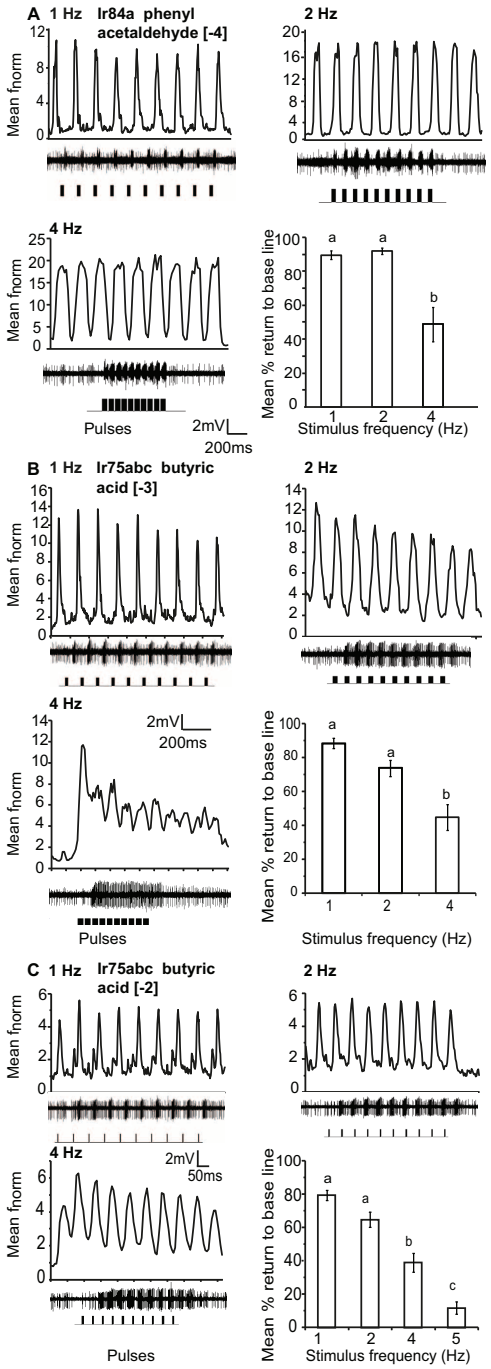

FIGURE 4 | Response of OSNs to repeated stimulus pulses at varying frequencies. (A) Average normalized PSTH responses for Ir84a-expressing neurons in response to repeated pulses of log [−4] v/v phenyl acetaldehyde at listed frequencies. Traces below each panel show sample 200 ms recordings. Square pulses indicate stimulus presentation. The final panel shows the mean percent return to base line across all pulses at listed frequencies; error bars indicate SEM (ANOVA, $P < 0.05$, followed by Tukey *post-hoc*, $n = 7$–9). **(B)** Response of Ir75abc-expressing neurons to repeated stimulations of log [−3] v/v butyric acid stimulation as in **(A)** (ANOVA, $P < 0.05$, followed by Tukey *post-hoc* ($n = 8$–10). **(C)** Response as in **(B)** to a 10× concentration of butyric acid (log [−2]); ANOVA, $P < 0.05$, followed by Tukey *post-hoc*, $n = 14$–15).

($P < 0.001$, ANOVA followed by Tukey *post-hoc* test; **Figures 5A** and **B**). Gr21a-expressing OSNs also exhibited short term adaptation based on AUC (see "Materials and methods") that was frequency dependent, i.e. at 1 Hz stimulation the 9th pulse resulted in a significantly reduced response compared to the 1st pulse (repeated measure ANOVA, $P < 0.001$), while at 2 Hz the 4th pulse was reduced ($P = 0.039$), at 4 Hz the 5th ($P = 0.001$), and at 5 and 8 Hz the 2nd ($P < 0.01$, repeated measure ANOVA; **Figure 5** asterisks).

PULSE RESOLUTION OF STIMULI ELICITING OPPOSITE RESPONSE POLARITY

We also tested the pulse following capacity to single excitatory and inhibitory odor ligands in Or59b-expressing OSNs. We applied [−5] methyl acetate as an excitatory and [−5] citral as an inhibitory ligand. Or59b-expressing OSNs could resolve the excitatory stimulus up to 5 Hz (**Figure 6A**). The mean return to base line was significantly reduced at 5 Hz stimulation as compared to 1 and 2 Hz ($P < 0.05$, ANOVA followed by Tukey *post-hoc* test; **Figure 6C**). However, the pulse resolution was also affected by concentration, as a 100× increase in concentration reduced the pulse resolution to 2 Hz ($P < 0.05$). In contrast to the excitatory responses, Or59b-cells were able to resolve pulses of the inhibitory ligand citral only up to 2 Hz, and at 4 and 5 Hz the OSNs showed total inhibition and did not recover when stimulated repeatedly with the inhibitory ligand ($P < 0.05$ ANOVA followed by

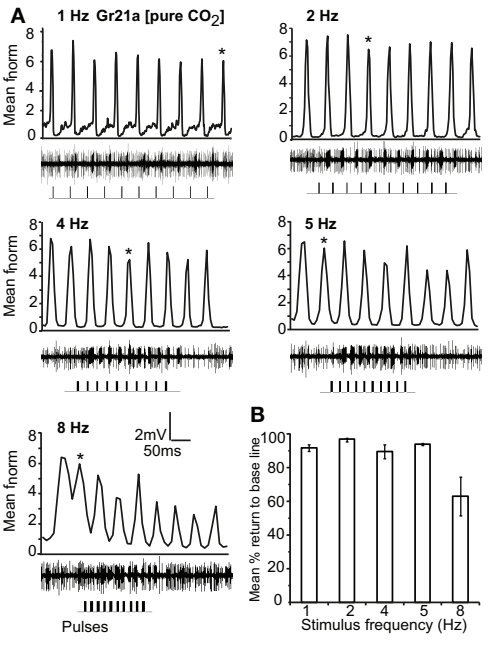

FIGURE 5 | Response of Gr21a-expressing OSNs to repeated stimulus pulses at varying frequencies. (A) Average normalized PSTH responses of Gr21a-expressing neurons to repeated pulses of pure CO_2 at listed frequencies. Traces below each panel show sample 50 ms recordings. Square pulses indicate stimulus presentation. **(B)** Mean percent return to base line across all pulses of listed frequencies, error bars indicate SEM (ANOVA, $P < 0.05$, followed by Tukey *post-hoc* test, $n = 11$–12).

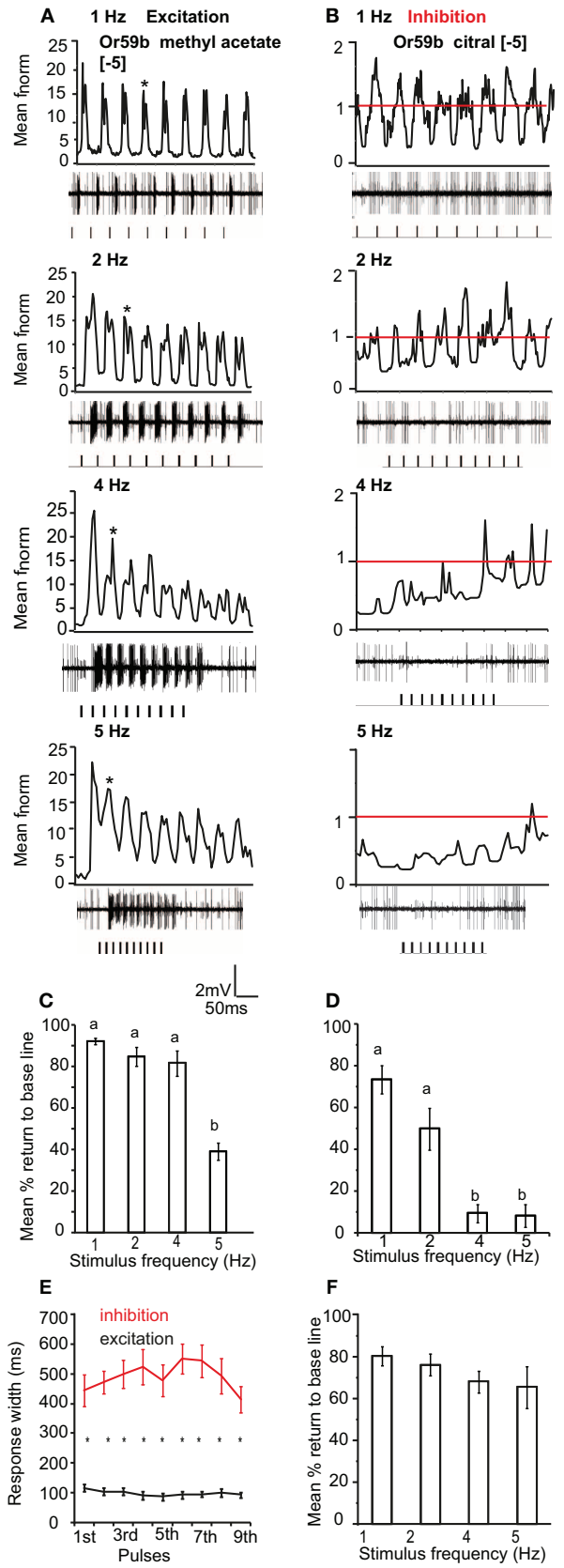

FIGURE 6 | Continued

FIGURE 6 | OR-expressing OSN response polarity and pulse resolution. **(A)** Mean normalized PSTH response of Or59b-expressing OSNs to repeated pulses of log [−5] v/v methyl acetate at listed frequencies. Traces below each panel show sample 50 ms recordings. Square pulses indicate stimulus presentation. **(B)** Mean normalized PSTH response of Or59b-expressing OSNs to repeated pulses of log [−5] v/v citral (an inhibitory odor) at listed frequencies as in **(A)**. Red line indicates baseline frequency. **(C)** Mean percent return to base line across all pulses for Or59b-OSN response to methyl acetate, error bars indicate SEM (ANOVA, $P < 0.05$, followed by Tukey *post-hoc* test, $n = 9$–13) and **(D)** as in **(C)** for citral (ANOVA, $P < 0.05$, followed by Tukey *post-hoc* test, $n = 13$–15). **(E)** Mean response width of Or59b-expressing OSNs for excitation and inhibition. **(F)** Mean percent return to base line in response to a pulsed binary mixture of methyl acetate and citral, error bars indicate SEM, ($P > 0.05$ ANOVA, $n = 8$–9).

Tukey *post-hoc* test; **Figures 6B** and **D**). The inhibitory ligand also resulted in a larger response width as compared to the excitatory ligand, even though both ligand concentrations were at similar points in the dose response curve (see **Figure 1**). This indicates that a given OSN response to an inhibitory or excitatory ligand can differ not only in polarity but also in temporal dynamics (**Figure 6E**). Furthermore, Or59b-OSNs showed short-term adaptation to the excitatory ligand that was frequency dependent (repeated measure ANOVA, $P < 0.05$). At increasing frequencies, short-term adaptation occurred earlier in the stimulus train (**Figure 6A** asterisk). In contrast, we did not find short-term adaptation based on response width to the inhibitory ligand (repeated measure ANOVA, $P > 0.05$).

We also asked if the total inhibition of the neuron at high frequencies of citral (>4 Hz) could interfere with odor coding of the excitatory ligand when presented simultaneously to the OSN. We thus stimulated the neurons with the binary mixture of the two ligands at the concentrations listed above. Stimulation with the two component blend resulted in an improved pulse resolution over either separate odor, with no significant difference in pulse resolution between 1 and 5 Hz ($P > 0.05$ ANOVA (**Figure 6F**). The effect of response polarity on pulse resolution was also observed in OSNs that express IRs. Ir41a-OSNs exhibited an excitatory response to 50 ms pulses of [−2] 1,4-diaminobutane and resolved pulsed stimuli as fast as 2 Hz, (ANOVA, $P < 0.05$; **Figures 7A** and **D**). However, the pulse resolution to the inhibitory ligand isoamylamine at [−2] (the concentration at which the neurons are inhibited by the ligand, **Figure 1G**) was only maintained at 1 Hz (ANOVA $P < 0.05$; **Figures 7B** and **E**). In addition, the binary mixture of 1, 4-diaminobutane and isoamylamine at the same concentration [−2], sharpened the response of Ir41a-OSNs especially at 4 Hz (**Figures 7C** and **F**).

DISCUSSION

Odor stimuli contain three elements of information: odor identity; odor intensity, and a temporal component (Hallem et al., 2004). To respond to these stimuli, insect OSNs express a wide variety of receptors. Here we investigate the response dynamics of OSNs expressing receptors from different protein families to stimuli of both different durations and frequencies. We find that ORs, IRs, and Gr21a exhibit distinct response characteristics that could increase the response range of the insect to the temporally dynamic natural odor environment.

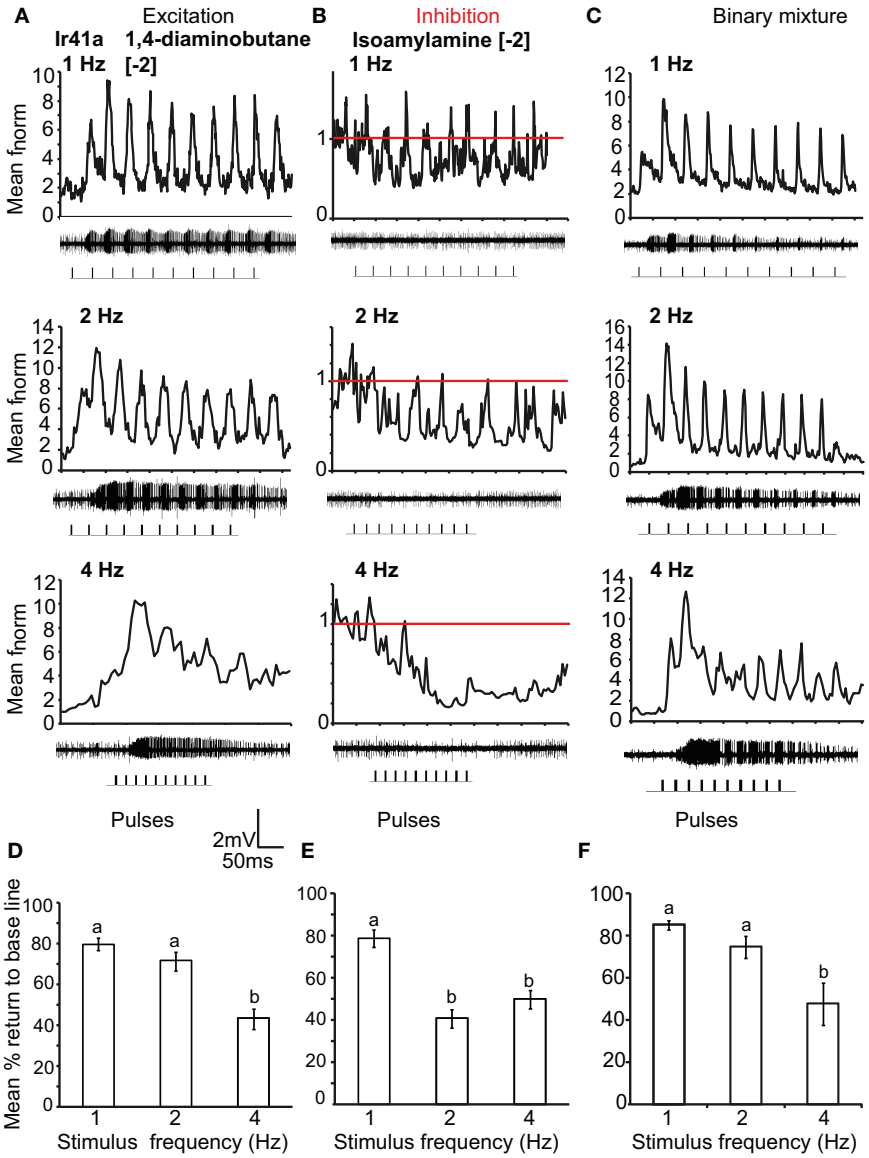

FIGURE 7 | IR-expressing OSN response polarity and pulse resolution. **(A)** Mean normalized PSTH response of Ir41a-expressing OSNs to repeated pulses of log [−2] v/v 1, 4-diaminobutane at listed frequencies. Traces below each panel show sample 50 ms recordings. Square pulses indicate stimulus presentation. **(B)** As in **(A)** for log [−2] v/v of the inhibitory odor isoamyl amine. Red line indicates baseline frequency. **(C)** Mean normalized PSTH response of Ir41a-expressing OSNs to a binary mixture of 1, 4-diaminobutane and isoamyl amine at [−2] v/v. **(D)** Mean percent return to base line to the excitatory ligand across all pulses at listed frequencies, error bars indicate SEM (ANOVA, $P < 0.05$, followed by Tukey *post-hoc* test, $n = 7$–8) **(E)**, as in **(D)** for log [−2] v/v of the inhibitory odor isoamyl amine (ANOVA, $P < 0.05$, followed by Tukey *post-hoc* test; $n = 7$–9). **(F)** as in **(D)** for the binary mixture (ANOVA, $P < 0.05$, followed by Tukey *post-hoc* test, $n = 7$–9).

RESPONSE DYNAMICS TO DIFFERENT STIMULUS DURATIONS ARE A FUNCTION OF RECEPTOR TYPE

We found that the response of *Drosophila* OSNs to varying stimulus durations (**Figure 2**) depends on the type of receptor expressed in that neuron. OR-expressing OSNs showed adaptation to higher concentrations of long stimulus pulses (>1 s), both in maximum frequency and latency. This response feature was also independent of ligand (data not shown). In contrast, when IR-expressing OSNs were tested with the same protocol, they required longer stimulus durations to respond, and there was no desensitization even up to 2 s stimulation either in response intensity or latency regardless of stimulus concentration. As a consequence, OSNs that express IRs are able to transmit information concerning the presence of long-lasting odors in their environment better than OR-expressing OSNs. However, this could also present a trade off, because the signal transduction in these OSNs appears to be slower, as seen in **Figure 3E**, where the time to maximum frequency was

longer in IR-expressing OSNs as compared to OR-expressing OSNs.

The difference in response between IR- and OR-expressing OSNs to longer pulses was not a function of stimulus presentation, which was assessed by PID (see "Materials and methods"). It is therefore a property of the OSNs themselves. Are these differences a function of the peri-receptor environment, or rather a property of internal OSN kinetics? To test this, we assessed the response of Or35a-OSNs, which are housed in coeloconic sensillum ac3 together with Ir75abc-OSNs. As with other OR-expressing OSNs, Or35a-OSNs also responded to stimulations as brief as 20 ms and showed desensitization at longer pulses (2 s) in maximum response frequency (**Figure 2B**). The response kinetics of these OSNs is therefore less influenced by the environment where they are expressed and rather by intrinsic properties of the neurons themselves.

The broad protostome conservation of IRs contrasts sharply with the restriction of ORs to insect genomes. This phylogenetic evidence suggests that IRs were the first olfactory receptor repertoire in insects (Robertson et al., 2003; Croset et al., 2010). IRs are also restricted to coeloconic sensilla, whereas ORs are found in several morphological sensillum types (Gupta and Rodrigues, 1997; Goulding et al., 2000; zur Lage et al., 2003; Benton et al., 2009). Our results show that IR-expressing OSNs required longer stimulation times to respond to key odorants, and responded with lower response intensities. This could imply that IRs are less efficient and less sensitive in detecting and transducing a chemical signal. OR activation results in both ionotropic and metabotropic signaling (Wicher et al., 2008; Deng et al., 2011), while IRs are thought to be purely ionotropic (Benton et al., 2009). Iontropic signaling is also known to be less sensitive (Sato et al., 2008, 2011; Wicher et al., 2008). The requirement for higher concentrations in IR-expressing OSNs has been also shown in Yao et al. (2005). The signal transduction in Gr21a has been shown to involve $G\alpha_q$ protein, but not $G\alpha_s$ (Yao and Carlson, 2010; Deng et al., 2011). Thus, it is possible that the transduction cascade itself leads to these differences in response to varying stimulus durations.

The desensitization/adaptation at longer stimulus durations could affect the temporal accuracy of OR-expressing OSNs in reporting long-lasting odor strands, but it may also enrich the coding possibilities for odor discrimination (DeBruyne and Baker, 2008; Nagel and Wilson, 2011) by allowing the neuron to return to its resting state more quickly. This could provide additional possibilities for odor discrimination such as under background odor, or for resolution of intermittent pulsed stimuli. Adaptation extends the operating range of sensory systems, in some cases over an enormous span of stimulus intensities (Torre et al., 1995). It may also play a role in complex functions of neuronal systems such as stimulus location (Kaissling et al., 1987). Similar results were reported in the locust where the electrophysiological response of projection neurons also depended on stimulus duration (Brown et al., 2005; Mazor and Laurent, 2005). In contrast, the long-lasting response of IR-expressing OSNs could allow for close range detection while on or very near the stimulus source where stimulus durations could persist for much longer periods of time (Murlis et al., 2000; Louis et al., 2008; Gomez-Marin et al., 2011).

PULSE RESOLUTION IS RECEPTOR TYPE DEPENDENT

The different classes of OSNs also showed differences in their pulse resolution to repeated stimuli. Brief intermittent stimuli were not detected by IR-expressing OSNs, in contrast to those expressing ORs (which could respond up to 5 Hz). This response characteristic was mainly due to a difference in sensitivity, as increasing the stimulus concentration for IR-expressing OSNs improved the detection and resolution to 5 Hz. In contrast, a 100× increase in concentration actually reduced the OR-OSNs pulse resolution. The accuracy of encoding rapidly fluctuating intermittent odorant stimuli above 5 Hz was significantly reduced for all OSNs regardless of receptor type. Similarly, other insects resolved up to 5 Hz pulses of general odors or pheromones (e.g., Lemon and Getz, 1997; Barrozo and Kaissling, 2002; Bau et al., 2002), even at the antennal lobe (e.g., Christensen and Hildebrand, 1997; Lei and Hansson, 1999; Lei et al., 2009).

Short term adaptation and latency to peak response to repeated stimuli were independent of the receptor expressed in the OSN (**Figures 3A–E**). In addition, the time to peak response and the response intensity were recovered in all OSNs either by increasing the inter-stimulus interval to 5 s or by increasing the concentration. This suggests that adaptation to repeated stimulation is a general feature of all OSNs, regardless of the receptor expressed. Adaptation is assumed to be an early step in information processing and decision making (Kaissling et al., 1987; Baker et al., 1988; Dolzer et al., 2003; Theodoni et al., 2011), and appears to affect the response of all OSN types in a similar manner.

RESPONSE POLARITY AFFECTS PULSE RESOLUTION

Both OR- and IR-expressing OSNs were unable to resolve pulsed inhibitory ligands at frequencies as high as excitatory ligands (**Figures 6B** and **7B**). This could be because the response inhibition lasted longer than excitation (**Figure 6E**), even though the concentrations tested were at the same point in the dose response curve (**Figure 1**). According to Ghatpande and Reisert (2011), fast response termination improves pulse resolution. Similarly, Su et al. (2011) showed that the inhibitory responses of OSNs lasted much longer than their excitatory responses, but the reason for this difference is not clear. Interestingly, a mixture of both excitatory and inhibitory odors improved pulse resolution at high frequencies (**Figures 6F** and **7F**). As a consequence, OSNs may respond to intermittent blends at faster rates, which may increase their ability to track complex natural stimuli.

The fast-terminating biphasic response exhibited by Gr21a-OSNs in response to CO_2 stimulation could be the reason why Gr21a-OSNs resolved more rapid stimulations as compared to OR- and IR-expressing OSNs (**Figure 5**). A biphasic response improved pulse resolution in antennal lobe neurons (Lei and Hansson, 1999). Besides the OSN itself, the chemistry of CO_2 could also contribute to

better pulse resolution as it will readily hydrate to bicarbonate (Kwon et al., 2007), and the degree of odor clearing is one of the challenges for resolving rapidly fluctuating odorant stimuli (Ishida and Leal, 2005; Ghatpande and Reisert, 2011).

CONCLUSION

Terrestrial olfaction requires the tracking of brief, intermittent airborne stimuli in a turbulent and dynamic environment. Fast reaction times to pockets of clean air are suggested to be behaviorally important for successful and rapid source location; hence, the selection over evolutionary time for sensitive and high-fidelity odor strand detection and resolution in the insect olfactory system is crucial (Baker and Vickers, 1997). Equally, the temporal structure of olfactory information has been shown to be critical for odor coding in a variety of systems (Laurent et al., 2001). Here we show that IR-expressing OSNs are better in detecting long-lasting odor pulses, but they are less sensitive. That could suggest that they are better at close range odor detection where odor-OR interaction time is not a limiting factor (high molecular flux). In contrast OR-expressing neurons are more sensitive and better at resolving brief (low molecular flux) pulsed stimuli. This diversity in temporal characteristics could provide a broad palette of response kinetics for the insect olfactory system to respond to the high-dimensional temporal input found in an insect's odor environment.

IRs are the only receptors found in basal insects and conserved between unicellular and multicellular organisms (Croset et al., 2010). ORs appear to have derived from the gustatory receptor family (Robertson et al., 2003; Nordström et al., 2011), which is present in insects as well as in aquatic arthropods such as water fleas (Peñalva-Arana et al., 2009). Besides increasing the diversity of chemicals that could be detected, OR-OSNs also allow the olfactory system to rapidly detect and transduce brief airborne odor information. This is especially important for flying insects, for which stimulus contact is brief and fast response in time is most critical. OR-expressing OSNs were indeed more sensitive to intermittent stimuli than IRs and Gr21a. The sensitive and fast neuronal response observed in OR-expressing OSNs could result from Orco-dependent transduction, which may have evolved through selective pressure to increase sensitivity and speed of odor detection while in flight.

ACKNOWLEDGMENTS

This study was supported by the International Max Planck Research School (Merid N. Getahun) and the Max Planck Society (Dieter Wicher, Bill S. Hansson, and Shannon B. Olsson).

REFERENCES

Ai, M., Min, S., Grosjean, Y., Leblanc, C., Bell, R., Benton, R., et al. (2010). Acid sensing by the *Drosophila* olfactory system. *Nature* 468, 691–695.

Baker, T. C., Hansson, B. S., Löfsted, C., and Löfqvist, J. (1988). Adaptation of antennal neurons in moths is associated with cessation of pheromone-mediated upwind flight. *Proc. Natl. Acad. Sci. U.S.A.* 85, 9826–9830.

Baker, T. C., and Vickers, N. J. (1997). "Pheromone-mediated flight in moths," In *Pheromone Research: New Directions.* ed R. T. Cardé (Minks AK. New York: Chapman and Hall), 248–264.

Barrozo, R. B., and Kaissling, K.-E. (2002). Repetitive stimulation of olfactory receptor cells in female silkmoths *Bombyx mori* L. *J. Insect Physiol.* 48, 825–834.

Bau, J., Justus, K. A., and Carde', R. T. (2002). Antennal resolution of pulsed pheromone plumes in three moth species. *J. Insect Physiol.* 48, 433–442.

Benton, R., Sachse, S., Michnick, S. W., and Vosshall, L. B. (2006). Atypical membrane topology and heteromeric function of *Drosophila* odorant receptors *in vivo*. *PLoS Biol.* 4:e20. doi: 10.1371/journal.pbio.0040020

Benton, R., Vannice, K. S., Gomez-Diaz, C., and Vosshall, L. B. (2009). Variant ionotropic glutamate receptors as chemosensory receptors in *Drosophila*. *Cell* 136, 149–162.

Brown, S. L., Joseph, J., and Stopfer, M. (2005). Encoding a temporally structured stimulus with a temporally structured neural representation. *Nat. Neurosci.* 8, 1568–1576.

Christensen, T. A., and Hildebrand, J. G. (1997). Coincident stimulation with pheromone components improves temporal pattern resolution in central olfactory neurons. *J. Neurophysiol.* 77, 775–781.

Clyne, P. J., Warr, C. G., Freeman, M. R., Lessing, D., Kim, J., and Carlson, J. R. (1999). A novel family of divergent seven-trans- membrane proteins: candidate odorant receptors in *Drosophila*. *Neuron* 22, 327–338.

Couto, A., Alenius, M., and Dickson, B. J. (2005). Molecular anatomical and functional organization of the *Drosophila* olfactory system. *Curr. Biol.* 15, 1535–1547.

Croset, V., Rytz, R., Cummins, S. F., Budd, A., Brawand, D., Kaessmann, H., et al. (2010). Ancient protostome origin of chemosensory ionotropic glutamate receptors and the evolution of insect taste and olfaction. *PLoS Genet.* 6:e1001064. doi: 10.1371/journal.pgen.1001064

DeBruyne, M., and Baker, T. C. (2008). Odor detection in insects: volatile codes. *J. Chem. Ecol.* 34, 882–897.

Deng, Y., Zhang, W., Farhat, K., Oberland, S., Gisselmann, G., and Neuhaus, E. M. (2011). The stimulatory Gαs protein is involved in olfactory signal transduction in *Drosophila*. *PLoS ONE* 6:e18605. doi: 10.1371/journal.pone.0018605

Dolzer, J., Fischer, K., and Stengl, M. (2003). Adaptation in pheromone sensitive trichoid sensilla of the hawkmoth *Manduca sexta*. *J. Exp. Biol.* 206, 1575–1588.

Ghatpande, A. S., and Reisert, J. (2011). Olfactory receptor neuron responses coding for rapid odour sampling. *J. Physiol.* 589, 2261–2273.

Gomez-Marin, A., Greg, J., Stephens, G. J., and Louis, M. (2011). Active sampling and decision making in *Drosophila* chemotaxis. *Nat. Commun.* 2, 441.

Goulding, S. E., zur Lage, P., and Jarman, A. P. (2000). Amos, a proneural gene for *Drosophila* olfactory sense organs that is regulated by lozenge. *Neuron* 25, 69–78.

Gupta, B. P., and Rodrigues, V. (1997). Atonal is a proneural gene for a subset of olfactory sense organs in *Drosophila*. *Genes Cells* 2, 225–233.

Hallem, E. A., Ho, M. G., and Carlson, J. R. (2004). The molecular basis of odor coding in the *Drosophila* antenna. *Cell* 117, 965–979.

Ishida, Y., and Leal, W. S. (2005). Rapid inactivation of a moth pheromone. *Proc. Natl. Acad. Sci. U.S.A.* 102, 14075–14079.

Jones, W. D., Cayirlioglu, P., Kadow, I. G., and Vosshall, L. B. (2007). Two chemosensory receptors together mediate carbon dioxide detection in *Drosophila*. *Nature* 445, 86–90.

Kaissling, K. E., Zack Strausfeld, C., and Rumbo, E. R. (1987). Adaptation processes in insect olfactory receptors. Mechanisms and behavioral significance. *Ann. N.Y. Acad. Sci.* 510, 104–112.

Kwon, J. Y., Dahanukar, A., Weiss, L. A., and Carlson, J. R. (2007). The molecular basis of CO_2 reception in *Drosophila*. *Proc. Natl. Acad. Sci. U.S.A.* 104, 3574–3578.

Laurent, G., Stopfer, M., Friedrich, R. W., Rabinovich, M. I., Volkovskii, A., and Abarbanel, H. D. (2001). Odor encoding as an active, dynamical process: experiments, computation, and theory. *Annu. Rev. Neurosci.* 24, 263–297.

Lei, H., and Hansson, B. S. (1999). Central processing of pulsed pheromone signals by antennal lobe neurons in the male moth *Agrotis segetum*. *J. Neurophysiol.* 81, 1113–1122.

Lei, H., Riffell, J. A., Gage, S. L., and Hildebrand, J. G. (2009). Contrast enhancement of stimulus intermittency in a primary olfactory network and its behavioral significance. *J. Biol.* 8, 21.

Lemon, W. C., and Getz, W. M. (1997). Temporal resolution of general odor pulses by olfactory sensory neurons in American cockroaches. *J. Exp. Biol.* 200, 1809–1819.

Louis, M., Huber, T., Benton, R., Sakmar, T. P., and Vosshall, L. B.

(2008). Bilateral olfactory sensory input enhances chemotaxis behavior. *Nat. Neurosci.* 11, 187–199.

Mazor, O., and Laurent, G. (2005). Transient dynamics versus fixed points in odor representations by locust antennal lobe projection neurons. *Neuron* 48, 661–673.

Murlis, J., Willis, M. A., and Carde', R. T. (2000). Spatial and temporal structures of pheromone plumes in fields and forests. *Physiol. Entomol.* 25, 211–222.

Nagel, K. I., and Wilson, R. I. (2011). Biophysical mechanisms underlying olfactory receptor neuron dynamics. *Nat. Neurosci.* 14, 208–216.

Nordström, K. J., Almen, M. S., Edstam, M. M., Fredriksson, R., and Schioth, H. B. (2011). Independent HHsearch, Needleman-Wunsch-based and motif analyses reveals the overall hierarchy for most of the G protein-coupled receptor families. *Mol. Biol. Evol.* 28, 2471–2480.

Olsson, S. B., Getahun, M. N., Wicher, D., and Hansson, B. S. (2011). Piezo-controlled microinjection: an *in vivo* complement for *in vitro* sensory studies in insects. *J. Neurosci. Methods* 201, 385–389.

Olsson, S. B., Kuebler, L. S., Veit, D., Steck, K., Schmidt, A., Knaden, M., et al. (2011). A novel multicomponent stimulus device for use in olfactory experiments. *J. Neurosci. Methods* 195, 1–9.

Pellegrino, M., Nakagawa, T., and Vosshall, L. B. (2010). Single sensillum recordings in the insects *Drosophila melanogaster* and *Anopheles gambiae*. *J. Vis. Exp.* 17, 1–5.

Peñalva-Arana, D. C., Lynch, M., and Robertson, H. M. (2009). The chemoreceptor genes of the waterflea *Daphnia pulex*: many GRs but no ORs. *BMC Evol. Biol.* 9:79. doi: 10.1186/1471-2148-9-79

Robertson, H. M., Warr, C. G., and Carlson, J. R. (2003). Molecular evolution of the insect chemoreceptor gene superfamily in *Drosophila melanogaster*. *Proc. Natl. Acad. Sci. U.S.A.* 100, 14537–14542.

Sargsyan, V., Getahun, M. N., Llanos. S. L., Olsson, S. B., Hansson, B. S., and Wicher, D. (2011). Phosphorylation via PKC regulates the function of the *Drosophila* odorant coreceptor. *Front. Cell. Neurosci.* 5:5. doi: 10.3389/fncel.2011.00005

Sato, K., Pellegrino, M., Nakagawa, T., Nakagawa, T., Vosshall, L. B., and Touhara, K. (2008). Insect olfactory receptors are heteromeric ligand-gated ion channels. *Nature* 452, 1002–1006.

Sato, K., Tanaka, K., and Touhara, K. (2011). Sugar-regulated cation channel formed by an insect gustatory receptor. *Proc. Natl. Acad. Sci. U.S.A.* 108, 11680–11685.

Silbering, A. F., Rytz, R., Grosjean, Y., Abuin, L., Ramdya, P., Jefferis, G. S., et al. (2011). Complementary function and integrated wiring of the evolutionarily distinct *Drosophila* olfactory subsystems. *J. Neurosci.* 31, 13357–13375.

Song, E., de Bivort, B., Dan, C., and Kunes, S. (2012). Determinants of the *Drosophila* odorant receptor pattern. *Dev. Cell* 22, 363–376.

Su, C. Y., Martelli, C., Emonet, T., and Carlson, J. R. (2011). Temporal coding of odor mixtures in an olfactory receptor neuron. *Proc. Natl. Acad. Sci. U.S.A.* 108, 5075–5080.

Theodoni, P., Kovacs, G., Greenlee, M. W., and Deco, G. (2011). Neuronal adaptation effects in decision making. *J. Neurosci.* 31, 234–246.

Thorne, N., Chromey, C., Bray, S., and Amrein, H. (2004). Taste perception and coding in *Drosophila*. *Curr. Biol.* 14, 1065–1079.

Torre, V., Ashmore, J. F., Lamb, T. D., and Menini, A. (1995). Transduction and adaptation in sensory receptor cells. *J. Neurosci.* 75, 7757–7768.

Vickers, N. J., Christensen, T. A., Baker, T. C., and Hildebrand, J. G. (2001). Odour-plume dynamics influence the brain's olfactory code. *Nature* 410, 466–470.

Vosshall, L. B., Amrein, H., Morozov, P. S., Rzhetsky, A., and Axel, R. (1999). A Spatial map of olfactory receptor expression in the *Drosophila* antenna. *Cell* 96, 725–736.

Wang, Z., Singhvi, A., Kong, P., and Scott, K. (2004). Taste representations in the *Drosophila* brain. *Cell* 117, 981–991.

Wicher, D., Schafer, R., Bauernfeind, R., Stensmyr, M. C., Heller, R., Heinemann, S. H., et al. (2008). *Drosophila* odorant receptors are both ligand-gated and cyclic-nucleotide-activated cation channels. *Nature* 452, 1007–1011.

Yao, C. A., and Carlson, J. R. (2010). Role of G-Proteins in odor-sensing and CO_2-sensing neurons in *Drosophila*. *J. Neurosci.* 30, 4562–4572.

Yao, C. A., Ignell, R., and Carlson, J. R. (2005). Chemosensory coding by neurons in the coeloconic sensilla of the *Drosophila* antenna. *J. Neurosci.* 37, 8359–8367.

zur Lage, P. I., Prentice, D. R., Holohan, E. E., and Jarman, A. P. (2003). The *Drosophila* proneural gene *amos* promotes olfactory sensillum formation and suppresses bristle formation. *Development* 130, 4683–4693.

Conflict of Interest Statement: The authors declare that the research was conducted in the absence of any commercial or financial relationships that could be construed as a potential conflict of interest.

Received: 02 August 2012; paper pending published: 06 September 2012; accepted: 28 October 2012; published online: 16 November 2012.

Citation: Getahun MN, Wicher D, Hansson BS and Olsson SB (2012) Temporal response dynamics of Drosophila olfactory sensory neurons depends on receptor type and response polarity. Front. Cell. Neurosci. ***6****:54. doi: 10.3389/fncel.2012.00054*

Copyright © 2012 Getahun, Wicher, Hansson and Olsson. This is an open-access article distributed under the terms of the **Creative Commons Attribution License**, *which permits use, distribution and reproduction in other forums, provided the original authors and source are credited and subject to any copyright notices concerning any third-party graphics etc.*

frontiers in
CELLULAR NEUROSCIENCE

ORIGINAL RESEARCH ARTICLE
published: 08 October 2012
doi: 10.3389/fncel.2012.00042

Plant odorants interfere with detection of sex pheromone signals by male *Heliothis virescens*

Pablo Pregitzer[1], Marco Schubert[2,3], Heinz Breer[1], Bill S. Hansson[2], Silke Sachse[2†] and Jürgen Krieger[1*†]

[1] *Institute of Physiology, University of Hohenheim, Stuttgart, Germany*
[2] *Department of Evolutionary Neuroethology, Max Planck Institute for Chemical Ecology, Jena, Germany*
[3] *Department of Biology, Chemistry and Pharmacy, Institute of Biology/Neurobiology, Free University Berlin, Berlin, Germany*

Edited by:
Dieter Wicher, Max Planck Institute for Chemical Ecology, Germany

Reviewed by:
Sylvia Anton, Institut National de la Recherche Agronomique, France
Bente G. Berg, Norwegian University of Science and Technology, Norway
Thomas Baker, The Pennsylvania State University, USA

****Correspondence:***
Jürgen Krieger, Institute of Physiology (230), University of Hohenheim, Garbenstraße 30, 70599 Stuttgart, Germany.
e-mail: krieger@uni-hohenheim.de

† Silke Sachse and Jürgen Krieger share the last authorship

In many insects, mate finding relies on female-released sex pheromones, which have to be deciphered by the male olfactory system within an odorous background of plant volatiles present in the environment of a calling female. With respect to pheromone-mediated mate localization, plant odorants may be neutral, favorable, or disturbing. Here we examined the impact of plant odorants on detection and coding of the major sex pheromone component, (Z)-11-hexadecenal (Z11-16:Ald) in the noctuid moth *Heliothis virescens*. By *in vivo* imaging the activity in the male antennal lobe (AL), we monitored the interference at the level of olfactory sensory neurons (OSN) to illuminate mixture interactions. The results show that stimulating the male antenna with Z11-16:Ald and distinct plant-related odorants simultaneously suppressed pheromone-evoked activity in the region of the macroglomerular complex (MGC), where Z11-16:Ald-specific OSNs terminate. Based on our previous findings that antennal detection of Z11-16:Ald involves an interplay of the pheromone binding protein (PBP) HvirPBP2 and the pheromone receptor (PR) HR13, we asked if the plant odorants may interfere with any of the elements involved in pheromone detection. Using a competitive fluorescence binding assay, we found that the plant odorants neither bind to HvirPBP2 nor affect the binding of Z11-16:Ald to the protein. However, imaging experiments analyzing a cell line that expressed the receptor HR13 revealed that plant odorants significantly inhibited the Z11-16:Ald-evoked calcium responses. Together the results indicate that plant odorants can interfere with the signaling process of the major sex pheromone component at the receptor level. Consequently, it can be assumed that plant odorants in the environment may reduce the firing activity of pheromone-specific OSNs in *H. virescens* and thus affect mate localization.

Keywords: pheromone detection, antennal lobe, pheromone receptor, pheromone binding protein, olfaction

INTRODUCTION

The ability of many insect species to use plant volatiles and pheromones to locate food, sexual partners, and appropriate egg-laying places is crucial for survival and reproduction (Zwiebel and Takken, 2004; Vosshall, 2008; Carey and Carlson, 2011; Hansson and Stensmyr, 2011). The remarkable pheromone detection system of male moths (Schneider, 1992; Hansson, 1995) allows them to recognize female-released sex pheromone blends from long distances (David et al., 1983; Vickers and Baker, 1997); in addition, it triggers and controls upwind flight behavior and guides the sexual partner to the calling female (Vickers et al., 1991; Vickers, 2006; Carde and Willis, 2008).

Components of female sex pheromone blends are detected by specialized sensilla on the male antenna (Almaas and Mustaparta, 1991; Baker et al., 2004). These porous, hair-like structures house the dendrites of pheromone-responsive olfactory sensory neurons (Ph-OSNs) bathed in sensillum lymph containing a high concentration of pheromone binding proteins (PBP) (Vogt and Riddiford, 1981; Steinbrecht and Gnatzy, 1984; Zhang et al., 2001). Specific PBPs take distinct pheromone molecules from the air and transfer them through the lymph toward specific pheromone receptors (PRs) in the dendritic membrane of Ph-OSNs (Leal, 2003; Vogt, 2003; Grosse-Wilde et al., 2006, 2007; Forstner et al., 2009). The Ph-OSNs for different pheromone components are endowed with specific PRs (Krieger et al., 2004; Nakagawa et al., 2005; Grosse-Wilde et al., 2010; Wanner et al., 2010) and converge their axons into separate compartments of the macroglomerular complex (MGC), the male-specific pheromone-processing center within the antennal lobe (AL) (Hansson et al., 1992; Berg et al., 1998; Hansson and Anton, 2000). In contrast, signals from general odorants, e.g., plant volatiles, are detected by general OSNs and transferred to sexually isomorphic ordinary glomeruli in the AL (Galizia et al., 2000; Hansson et al., 2003).

Abbreviations: AL, antennal lobe; HR, *Heliothis virescens* receptor; PBP, pheromone binding protein; Z11-16:Ald, (Z)-11-hexadecenal; OSNs, olfactory sensory neurons; Ph-OSNs, pheromone-responsive olfactory sensory neurons.

When they are released the female-produced sex pheromones are embedded within a background of general odorants, mainly plant volatiles. The air concentration of odorants depends on various environmental parameters: the abundance of vegetation, time of day, and weather (Kesselmeier and Staudt, 1997; Müller et al., 2002). Therefore, a male's sex pheromone detecting system is exposed simultaneously to mixtures of pheromone components and general odorants at varying ratios. The highest concentrations of both pheromone and plant odorants are likely to be present near to the calling female, which is often situated on a host plant. Although many studies of insect olfaction have addressed antennal detection and central coding of single compounds, as well as of mixtures of plant odorants or of pheromone blends, (e.g., Galizia and Menzel, 2000; Galizia et al., 2000; Hallem and Carlson, 2006; Lei and Vickers, 2008; Wang et al., 2010; Kuebler et al., 2012), few studies have examined pheromone/plant odorant mixtures. Recent electrophysiological studies on the pheromone sensilla of *Heliothis virescens* (Hillier and Vickers, 2011), *Spodoptera littoralis* (Party et al., 2009) and *Agrotis ipsilon* (Deisig et al., 2012) have found that the firing activity of Ph-OSNs to specific pheromone components was suppressed when plant odorants were co-applied. In contrast, an earlier study on *Helicoverpa zea* indicated enhancement of the pheromone-evoked spike activity of Ph-OSNs in the presence of plant odorants (Ochieng et al., 2002). Stimulation of the antenna with the plant odorant heptanal was found to reduce the pheromone response in the MGC of *Agrotis ipsilon* on both the input (Ph-OSNs) and output side (projection neurons, PNs) (Chaffiol et al., 2012; Deisig et al., 2012); conversely, in the silk moth *Bombyx mori*, sex pheromone responses in PNs of the MGC were enhanced in the presence of the host plant odor Z3-hexenol (Namiki et al., 2008).

Current data indicate that the interference of plant odorants with pheromone responses may appear already at the level of antennal sensilla—suppressing or enhancing Ph-OSN firing activity which is conveyed to the AL. The molecular targets at which plant odorants may interfere with pheromone-induced activities of OSNs are unknown, but key elements involved in pheromone detection, such as PBPs in the sensillum lymph or PRs in the dendrites of Ph-ORNs, are considered as candidates (Party et al., 2009; Deisig et al., 2012). Our previous studies have indicated that an interplay of the PBP HvirPBP2 and the PR HR13 is important for eliciting cellular responses by the major sex pheromone component Z11-16:Ald (Grosse-Wilde et al., 2007). In the present study we set out to explore if plant volatiles may interact with any of these key elements. In order to identify plant odorants, which may affect pheromone detection in *H. virescens* we performed *in vivo* imaging experiments monitoring pheromone-evoked activity in the so-called cumulus region of the MGC, where Z11-16:Ald-specific OSNs terminate (Galizia et al., 2000). Using a fluorescence-based competitive binding assay we examined how identified plant odorants and pheromone/plant odorant mixtures bind to HvirPBP2. Furthermore, a cell line expressing the PR HR13 was employed in fura-2-based calcium imaging studies to test whether plant odorants interfere with Z11-16:Ald detection at the level of the PR.

MATERIALS AND METHODS

ANIMALS

H. virescens pupae were kindly provided by Bayer CropScience, Frankfurt, Germany. Pupae were sexed and allowed to develop at room temperature. After emergence, moths were fed on 10% sucrose solution.

PHEROMONE AND PLANT ODORANTS

(Z)-11-hexadecenal (Z11-16:Ald) was purchased from Fluka or Bedoukian. Plant odorants (β-caryophyllene, geraniol, Z3-hexenol, isoamyl acetate, linalool, linalyl acetate) were purchased from Fluka, Sigma, and Merck at the highest purity available. β-caryophyllene, geraniol, Z3-hexenol, and linalool were selected because of their physiological and ecological relevance to heliothine moths. For these chemicals previous studies on male and female *H. virescens* have identified responsive OSNs on the antenna, processing glomeruli in the AL or effects on behavior (De Moraes et al., 2001; Skiri et al., 2004; Hillier et al., 2005; Rostelien et al., 2005; Hillier and Vickers, 2007). Isoamyl acetate was chosen as a typical fruit odor. Linalyl acetate was selected because it is chemically related to linalool and emitted as a principle component from many flowers and spice plants. For optical imaging experiments, plant odorants were diluted in mineral oil (Sigma-Aldrich) to a concentration of 1:10 (v/v) which equates to 85–90 μg/μl. The pheromone component Z11-16:Ald was diluted to a final concentration of 1 μg/μl.

OPTICAL IMAGING OF THE ANTENNAL LOBE

Moths were 1- to 5-day-old male *H. virescens*. Animals were gently pushed into a 1000 μl pipette whose tip had been cut open and then fixed with dental wax. After the scales were removed, the labial palps and proboscis were fixed to reduce movement artifacts. A window was cut into the head cuticle between the compound eyes. Glands and trachea were carefully removed to get access to the brain. A fluorescent calcium indicator (Calcium Green-1 or 2 AM, Invitrogen) was dissolved in Ringer solution (150 mM NaCl, 3 mM KCl, 3 mM $CaCl_2$, 25 mM sucrose, 10 mM TES buffer, pH 6.9) with 6% Pluronic F-127 (Invitrogen) to a concentration of 30 μmol. The brain was incubated with ∼20 μl of this solution at 4°C. After incubation for 60 min, the brain was rinsed several times with Ringer solution.

Imaging experiments were performed using a Till Photonics imaging setup (TILL imago, Till Photonics GmbH) with a CCD-camera (PCO imaging, Sensicam) and a fluorescence microscope (Olympus, BX51WI) equipped with a 20× water immersion objective (NA 0.95, XLUM Plan FI, Japan). Calcium Green™ was excited at 475 nm (500 nm SP, xenon arc lamp, Polychrome V, Till Photonics), and fluorescence was detected at 490/515 nm (DCLP/LP). The whole setup was placed on a dumping table. Fourfold binning on the CCD-camera chip gave a resolution of 1.25 μm/pixel with an image size of 344 × 260 pixels.

Six μl of plant odorants (i.e., 510–540 μg) or 10 μl of pheromone component (i.e., 10 μg) was pipetted on a filter paper (12 mm diameter), which was inserted into a glass pipette; these were renewed every day. A stimulus controller (Syntech, Stimulus Controller CS-55) was used to apply the odor in a continuous airstream, whose flow of 0.6 l/min was monitored by a flow

meter (Cool Parmer). An acrylic glass tube guided the airflow to the moth's antenna. For mixture application, plant odorant and pheromone component were applied in two separate pipettes which were inserted into the continuous airstream (stimulus flow: 0.4 l/min). In case of single odor application, the second pipette was empty. Each recording had a continuance of 10 s with an acquisition rate of 4 Hz. Odors were applied after 2 s for 2 s. Single moths were imaged for up to 1 h, with interstimulus time intervals (ISI) of 1–3 min. The sequence of stimulations was randomized from insect to insect and repeated in a few cases to test for reproducibility of the odor-evoked activity patterns.

The imaging data were processed as previously described (Bisch-Knaden et al., 2012) using custom-written software in IDL (ITT Visual Information Solutions). To quantify odor-evoked calcium signals, we identified the cumulus because of its clear response to Z11-16:Ald and its proximity to the antennal nerve entrance. In each animal, the responses were normalized to the maximal response over all odorants. We defined the average of frames 10–18 (i.e., 0.5 s after stimulus onset until 0.5 s after stimulus offset) as the odor-evoked signal intensity.

EXPRESSION AND PURIFICATION OF *H. virescens* PBP2

The bacterial expression of *H. virescens* PBP2 (HvirPBP2) (Krieger et al., 1993) and purification of the protein from a periplasmic fraction of *E. coli* BL21 (DE3) was performed as described previously (Campanacci et al., 2001; Grosse-Wilde et al., 2007). Recombinant HvirPBP2 was delipidated to remove possible hydrophobic ligands, which may co-purify with PBP expressed in bacteria (Oldham et al., 2001), and finally dissolved in Ringer solution (138 mM NaCl, 5 mM KCl, 2 mM $CaCl_2$, 1.5 mM $MgCl_2$, 10 mM Hepes, 10 mM glucose, pH 7.3). The protein concentration was determined using a spectrometer at 280 nm applying the absorption co-efficient determined by the ProtParam program (ExPASy molecular biology server: http://www.expasy.org). Finally, the protein solution was aliquoted and stored at −70°C until use. Once unfrozen, the HvirPBP2 solution was kept at 8°C.

COMPETITIVE FLUORESCENCE BINDING ASSAY WITH HvirPBP2

To evaluate the binding of plant odorants to HvirPBP2 and an interference of plant odorants with pheromone binding, a competitive fluorescence binding assay that had previously been used to characterize ligand binding to various PBPs and odorant binding proteins (OBPs) of insects, including moth, flies, locust, and mosquitoes was applied (Campanacci et al., 2001; Ban et al., 2003; Zhou et al., 2004; Qiao et al., 2010).

Fluorescence emission spectra (360–600 nm) after excitation at 337 nm were recorded on a PerkinElmer LS 50B spectrofluorimeter using a quartz cuvette with a 1 cm light path fluorimeter in a right angle configuration and emission slit width of 5 nm were used. The binding of 1-N-phenylnapthylamine (1-NPN) to HvirPBP2 was determined by titrating 2 μM protein with increasing concentrations of the chromophore dissolved in dimethyl sulfoxide (DMSO).

For competitive binding experiments, HvirPBP2 (2 μM) in Ringer solution was loaded with 2 μM 1-NPN. The change in 1-NPN fluorescence was monitored after increasing amounts of Z11-16:Ald, plant odorants, or combinations of both from stock solutions (10 mM each; freshly prepared in methanol) were added to a final concentration of 10 μM. In control experiments, we observed no significant effects of the solvents in use (methanol for the pheromone component and plant odorants; DMSO for 1-NPN) on 1-NPN binding to HvirPBP2. To evaluate how different compounds and pheromone/plant odorant mixtures bound to HvirPBP2, the maximum 1-NPN fluorescence at a given concentration was determined and related to the maximum 1-NPN fluorescence in the absence of competitor (= 100%). For data analysis and graphic plotting, the program GraphPad Prism version 4.0 (GraphPad Software, San Diego, CA, USA) was used. The K_{diss} for Z11-16:Ald binding to HvirPBP2 was calculated according to $K_{diss} = [IC50]/(1 + [1\text{-NPN}]/K_{1\text{-NPN}})$ with [1-NPN] = 1-NPN concentration and $K_{1\text{-NPN}}$ = 1-NPN dissociation constant for PBP/1-NPN.

CALCIUM IMAGING OF HR13-EXPRESSING CELLS

To analyze the effect of plant-derived odorants on Z11-16:Ald detection by the PR HR13 (Krieger et al., 2004), we used a stable receptor-expressing cell line. The generation and functionality of HR13/Flp-In T-REx293/Gα15 cells have been described previously (Grosse-Wilde et al., 2007). HR13/Flp-In T-REx293/Gα15 cells were cultured using DMEM media (Invitrogen) supplemented with 10% fetal calf serum and either 100 mg/L hygromycin, 10 mg/L blasticidin, or 200 mg/L geneticin in regular alternation.

Calcium imaging experiments were performed as described previously (Grosse-Wilde et al., 2006, 2007; Forstner et al., 2009). Briefly, 48 h before imaging, 0.7×10^5 cells were plated onto poly-L-lysine coated glass coverslips (Ø15 mm, Hecht, Sondheim, Germany), harbored in a 24 well plate. After 24 h, receptor expression was induced by adding 5 mg/ml tetracycline. Twenty-four hours later, cells were washed with warmed Ringer solution (138 mM NaCl, 5 mM KCl, 2 mM $CaCl_2$, 1.5 mM $MgCl_2$, 10 mM Hepes, 10 mM Glucose, pH 7.3) and incubated with 4 μmol/L fura-2 AM (Invitrogen) in Ringer solution at 37°C for 30 min. A flow chamber was used to place a coverslip with cells loaded with fura-2 onto the stage of an inverted microscope (Olympus IX70) equipped for epifluorescence. Cells were permanently rinsed with Ringer solution (warmed to 37°C) at a flow rate of 1 ml/10 s. Control and test solutions (400 μl each) were applied at the same flow rate using a three-way valve system with connected syringes.

In a single experiment, cells were first rinsed for at least 5 min with Ringer solution, after which a control stimulus was applied (Ringer solution with 0.1% DMSO and 0.1% *n*-Hexane). This procedure allowed us to monitor responses to DMSO or *n*-hexane and to eliminate spontaneously active cells from later data analysis. After rinsing cells for another 5 min with Ringer solution, test odorants were applied. Z11-16:Ald and plant odorants were diluted from stock solutions in *n*-hexane using Ringer solution with 0.1% DMSO. All dilutions were prepared freshly before imaging started. Following the application of test substances, the viability of the cell was tested by applying 10 mM ATP in Ringer solution directly to the cell chamber. To monitor changes in the intracellular Ca^{2+} concentration in individual cells, light emission at 510 nm was measured over time following excitation

at 340 nm and 380 nm. Data analysis and acquisition were performed with the Metafluor imaging system and Metafluor 4 software (Visitron Systems, Puchheim, Germany). Changes in fluorescence intensity at 340 nm/380 nm excitation were used as an index of increasing calcium concentrations. Ratios of fluorescence intensity for at least 30 cells per experiment were determined before (F_0) and after stimulation (F; peak of response). F/F_0 values of individual cells were determined and averaged in a single experiment.

RESULTS

PLANT ODORANTS AFFECT PHEROMONE-INDUCED RESPONSES IN THE AL

In order to analyze the interference between volatiles of host plants that are present in the environment of calling females and the major sex pheromone component Z11-16:Ald, we performed functional *in vivo* calcium imaging of the AL of male *H. virescens*. We compared odor-evoked calcium activity patterns after separately or simultaneously stimulating the antenna with Z11-16:Ald and different plant odorants. Stimulation of the antenna with Z11-16:Ald alone revealed clear calcium signals in the cumulus of the MGC, the place where Z11-16:Ald-reactive OSNs terminate (**Figure 1A**). In contrast, none of the plant odorants tested clearly activated the cumulus. Instead, the various plant odorants generated calcium signals in distinct yet partly overlapping sets of ordinary glomeruli (**Figure 1A**, upper row). This observation was substantiated in time course measurements (**Figure 1B**, upper row). Simultaneously stimulating the antenna with mixtures of the pheromone component and a plant odorant revealed different spatio-temporal activity patterns in the AL (**Figure 1A**, lower row). The combination of Z11-16:Ald and isoamyl acetate elicited calcium signals that were almost the sum of the responses obtained by stimulation with the single compounds. In contrast, application of Z11-16:Ald in combination with linalool or geraniol led to a significantly reduced pheromone-induced activity in the cumulus region, whereas the calcium response in the ordinary glomeruli appeared almost unaltered. These results were supported by the time courses of the measurements (**Figure 1B**, lower row).

The inhibitory effect of linalool and geraniol onto the pheromone-induced response in the cumulus was reproducible between different individuals (**Figure 2**). In addition, we observed a clear inhibitory effect for the two odorants Z3-hexenol and linalyl acetate. For isoamyl acetate, a slight inhibitory effect was observed in a few animals, but did not prove to be statistically significant (**Figure 2**). Thus, our experiments demonstrated that several, but not all plant odorants clearly inhibit the induced activity pattern in the first processing center for pheromone signals.

INTERFERENCE OF PLANT ODORANTS WITH MOLECULAR ELEMENTS OF PHEROMONE SIGNALING

The observation that plant odorants reduce pheromone-induced spiking activity of Ph-OSNs (Party et al., 2009; Hillier and Vickers, 2011; Deisig et al., 2012) suggests that the inhibitory effects of plant odorants on the Z11-16:Ald-evoked activity we monitored in the MGC (**Figures 1** and **2**) may result from an interference of plant odorants with molecular elements of pheromone detection in the antenna. It has recently been shown that in *H. virescens* the Z11-16:Ald detection involves the PBP HvirPBP2 and the PR HR13 (Grosse-Wilde et al., 2007). Therefore, we asked if plant-related odorants may affect these two components of the pheromone recognition system.

PLANT ODORANTS DO NOT BIND TO HvirPBP2

First, we have analyzed if plant odorants may be able to occupy the binding pocket of HvirPBP2 and thereby prevent binding of Z11-16:Ald. To estimate the binding of odorants to HvirPBP2, we conducted fluorescence displacement assays employing 1-NPN as fluorescence reporter. When excited at 337 nm, 1-NPN in aqueous buffer emits fluorescence only weakly. However, in a hydrophobic environment, such as the hydrophobic binding pocket of PBPs (Sandler et al., 2000), the fluorescence intensity increases and the emission maximum blue-shifts. Accordingly, the titration of 1-NPN to HvirPBP2 in Ringer solution resulted in a large increase in fluorescence intensity (**Figure 3A**) and a shift of the emission maximum from 465 nm to 402 nm (not shown). The concentration-dependent binding of 1-NPN can be described by a hyperbolic curve (**Figure 3A**), which is consistent with a one-site binding model and a calculated K_{diss} value of 1.4 μM.

To test the functionality of the assay system and the integrity of the purified HvirPBP2, we monitored the ability of Z11-16:Ald to displace 1-NPN (**Figure 3B**). We found that upon titration of the pheromone component, the 1-NPN fluorescence was reduced in a concentration-dependent manner, indicating the pheromone component had bound to the hydrophobic binding pocket of HvirPBP2. Half-maximum 1-NPN displacement was obtained at a pheromone component concentration of 0.8 μM. Calculation of the relative dissociation constant revealed a K_{diss} of 0.33 μM. A binding affinity for pheromones in the micromolar range was also found for the PBPs of other insects (Plettner et al., 2000; Campanacci et al., 2001). Thus, the competitive 1-NPN displacement assay demonstrated that Z11-16:Ald binds to HvirPBP2; this finding confirms and extends previous results (Grosse-Wilde et al., 2007).

To address the question if plant odorants are able to occupy the binding pocket of HvirPBP2, we tested the ability of different plant volatiles to displace 1-NPN. In most cases, plant odorants did not markedly decrease 1-NPN fluorescence even at the highest concentration (**Figure 4**). Displacement was seen only after application of higher doses of linalyl acetate or β-caryophyllene. Together these results indicate that plant odorants do not (linalool, geraniol, Z3-hexenol, and isoamyl acetate) or only very weakly (linalyl acetate and β-caryophyllene) bind to the hydrophobic binding pocket of HvirPBP2.

PLANT ODORANTS DO NOT ALTER Z11-16:ALD BINDING TO HvirPBP2

Despite the inability to displace 1-NPN, it is possible that plant odorants could affect the Z11-16:Ald binding of HvirPBP2 in a different way; for example, acting as allosteric effectors plant odorants may bind outside the Z11-16:Ald binding pocket and cause conformational changes of HvirPBP2, which may alter pheromone binding in a non-competitive manner.

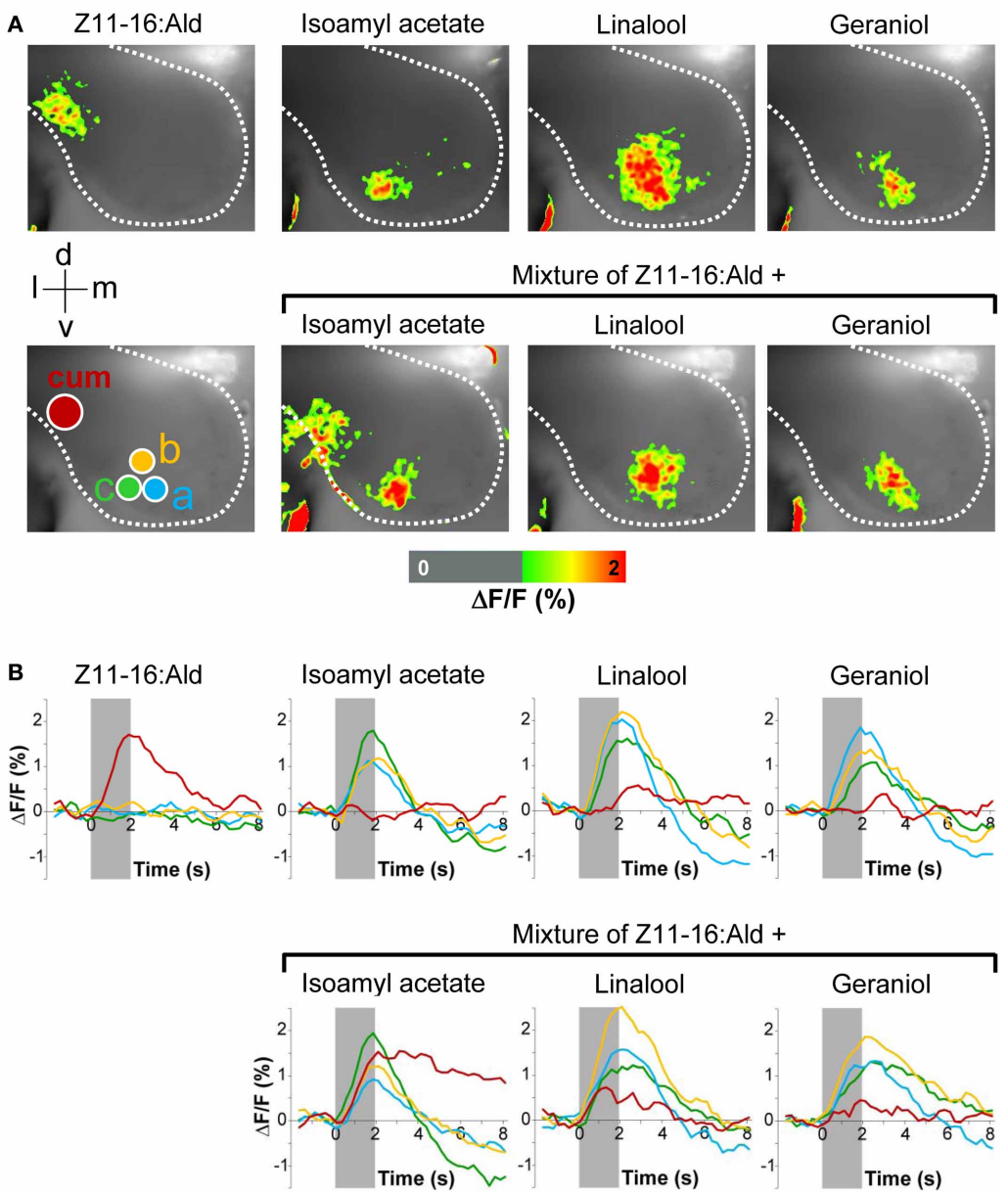

FIGURE 1 | Effect of plant odorants on pheromone-induced calcium signals in the moth antennal lobe. The antenna of a *H. virescens* male was stimulated separately with single compounds or simultaneously with Z11-16:Ald (10 μg) and plant odorants [1:10 (v/v) diluted in mineral oil]. Activity patterns in the antennal lobe were monitored using calcium imaging. **(A)** Representative false-color coded spatial response patterns. The positions of the cumulus (cum) region in the macroglomerular complex and of three ordinary glomeruli (a–c) are indicated by colored circles. All images are scaled to the overall maximum of all measurements. Images represent Δ*F*/*F* (in % change from background) superimposed onto the raw fluorescence images according to the scale below of one representative male moth. The directions medial (m), lateral (l), dorsal (d), and ventral (v) are indicated. **(B)** Time courses of glomerular calcium responses shown as Δ*F*/*F* (in %) of the cumulus (red line) and three ordinary glomeruli (yellow, green, and blue lines) as marked with circles in **(A)**. The odor stimulation is indicated by the gray bar.

Searching for possible non-competitive effects of plant odorants on pheromone binding to HvirPBP2, we tested mixtures of Z11-16:Ald and odorants in a second series of 1-NPN displacement experiments. When the displacement curves for Z11-16:Ald alone are compared to the curves obtained for pheromone plus plant odorant, no statistically significant difference in the binding curves were found (**Figure 5**). From these experiments we conclude that these plant odorants do not interfere with the ability of pheromones to bind to HvirPBP2 thus, indicating that it seems not to be a perturbed pheromone-binding protein which causes a plant odorant-mediated attenuation of the pheromone-induced response of Ph-OSNs on the antenna (Hillier and Vickers, 2011) and in the cumulus region of the AL (**Figures 1**, **2**).

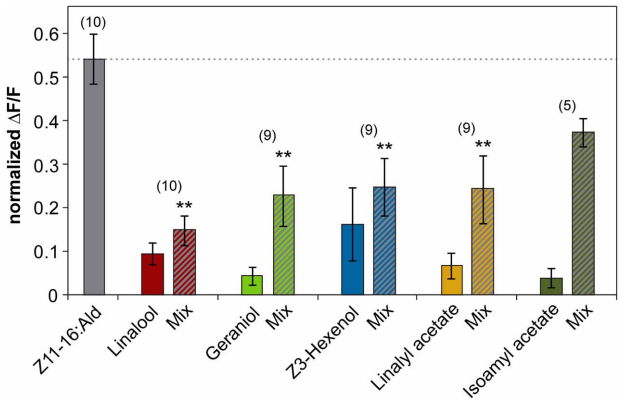

FIGURE 2 | Plant odorants inhibit the pheromone-induced activity in the cumulus region of the antennal lobe. Relative fluorescence changes in the cumulus region of the antennal lobe upon stimulation with Z11-16:Ald (10 μg, gray bar), or with the plant odorant indicated [1:10 (v/v) diluted in mineral oil, colored bars] or with a mix of both (striped bars). Data represent the mean response including the standard error of mean (SEM) based on 5–10 *H. virescens* males. $\Delta F/F$ [%] values have been normalized for each individual over all odors and glomeruli by setting the maximum response to 1. All plant odorants except isoamyl acetate significantly reduce the pheromone-induced response in the cumulus (**$p < 0.01$; ANOVA followed by Dunnett Multiple Comparisons Test).

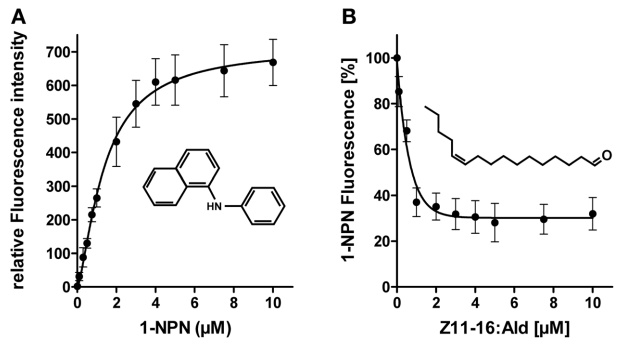

FIGURE 3 | 1-NPN binds to HvirPBP2 and is displaced by Z11-16:Ald. (A) Relative fluorescence intensity as a function of 1-NPN concentration. HvirPBP2 in Ringer solution (2 μM) was titrated with increasing amounts of 1-NPN to a final concentration of 10 μM. **(B)** Competitive fluorescence binding assay on HvirPBP2 (2 μM in Ringer solution) using 1-NPN (2 μM). Maximum emission of 1-NPN fluorescence was monitored after increasing concentrations of Z11-16:Ald (0–10 μM) were added. Fluorescence intensities at different pheromone component concentrations are shown as percentages of the maximum 1-NPN fluorescence in the absence of the pheromone component. Data represent the mean of three independent measurements. Standard deviations are indicated by error bars.

PLANT ODORANTS AFFECT THE PHEROMONE-INDUCED RESPONSE OF HR13-EXPRESSING CELLS

To determine whether plant odorants may affect the PR for Z11-16:Ald on the antenna, we next examined whether a HR13-mediated pheromone response is altered in the presence of plant odorants. We used HEK293/Gα15 cells stably expressing HR13 and performed fura-2-based calcium imaging experiments in order to compare the responsiveness of the cells upon stimulation with the pheromone component or pheromone/plant odorant mixtures. In a first set of experiments we monitored changes in the level of intracellular [Ca^{2+}] of HR13 cells after stimulation with plant odorants used in the AL experiments (see above). Previous dose-response experiments (Grosse-Wilde et al., 2007) had shown that the threshold concentration for stimulating HR13 cells with Z11-16:Ald solubilized with DMSO in Ringer solution was about 10 pM. To detect any possible response of HR13 cells to plant odorants, we therefore used a 10,000-fold higher odorant concentration (100 nM). Stimulation of the HR13 cells with 100 nM of the various plant odorants did not elicit any calcium signals that differed significantly from the control (**Figure 6**). In accordance with previous work (Grosse-Wilde et al., 2007), cells stimulated with a 1 nM solution of Z11-16:Ald revealed a clear calcium response (**Figure 6**); such a response indicates the presence of a functional HR13 receptor protein, which binds the pheromone component and activates reaction cascades leading in turn to a rise in intracellular [Ca^{2+}].

Next, we analyzed the responses of HR13 cells to a stimulation with mixtures of Z11-16:Ald and single plant odorants. First, the odorant linalool was tested, which caused a strongly attenuated pheromone response at the level of the AL (**Figures 1**, **2**). Stimulating HR13-expressing cells with 1 nM Z11-16:Ald elicited a clear calcium response (**Figure 7A**), while linalool (100 nM) alone did not alter their calcium levels (**Figure 7B**). Interestingly, simultaneous application of Z11-16:Ald and linalool led to a significantly weaker calcium response (**Figure 7C**). To confirm the specificity of the linalool effect we used different ratios of Z11-16:Ald to plant odorant (1:1, 1:10, and 1:100) (**Figure 7D**). The results revealed that the pheromone-induced calcium responses of HR13 cells were significantly reduced at 10- and 100-fold excess of plant odorants. Even a 1:1 ratio of pheromone component to plant odorant resulted in a weaker, though not significant calcium signal. Thus, linalool reduced the pheromone-induced calcium response of HR13 cells in a dose-dependent manner.

In a further series of calcium imaging experiments, we tested if other plant odorants that suppressed pheromone-induced activity in the cumulus region of the MGC (**Figure 2**) also affected the pheromone responses of HR13 cells. We found that a mixture containing 100-fold excess of linalyl acetate, Z3-hexenol, or geraniol significantly reduced the pheromone-induced calcium signal (**Figure 8**). In contrast, the odorant isoamyl acetate, which did not affect pheromone-evoked signals in the MGC, did not significantly change the pheromone-induced calcium responses of HR13 cells. Similarly, β-caryophyllene did not alter the pheromone-induced response (**Figure 8**). Together these results suggest that in *H. virescens*, the plant odorant-provoked suppression of pheromone-induced firing of Ph-OSNs as reported by Hillier and Vickers (2011) and the inhibition of the pheromone-induced response in the Ph-OSNs projection area in the AL are mainly due to a plant odorant-dependent interference at the level of the PRs.

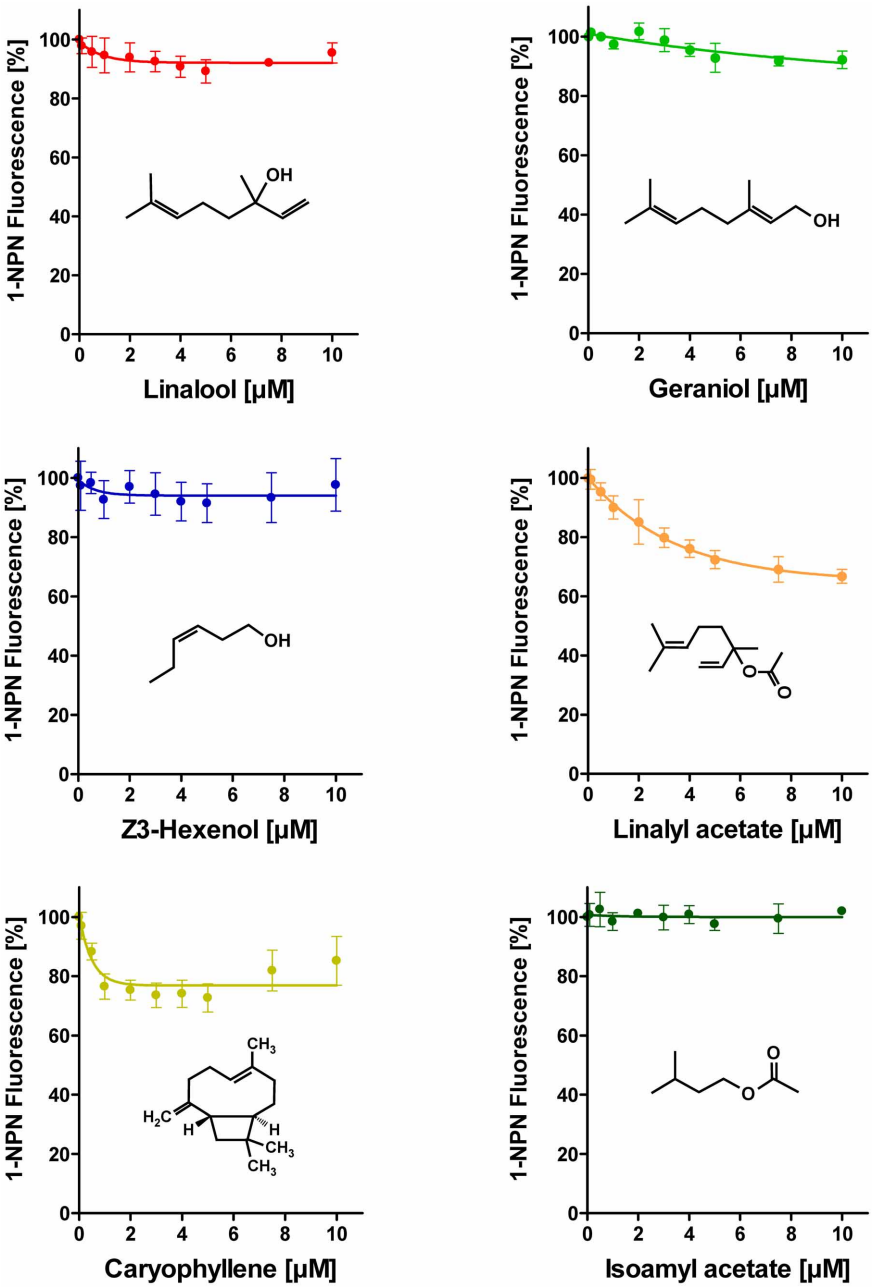

FIGURE 4 | Plant odorants do not bind or bind only very weakly to HvirPBP2. In competitive fluorescence-binding assays, a mixture of HvirPBP2 and 1-NPN (both at 2 µM) was titrated with increasing concentrations of the plant odorants indicated, while the emission of 1-NPN fluorescence was monitored. Maximum fluorescence intensities are reported as percentages of the value in the absence of competitor (plant odorant). Data represent the mean of three independent measurements. Error bars indicate standard deviations.

DISCUSSION

PLANT ODORANTS SUPPRESS PHEROMONE-EVOKED ACTIVITY IN THE ANTENNAL LOBE

In this study we examined the effect of plant odorants on peripheral detection and primary central coding of a sex pheromone component using the noctuid moth *H. virescens* as a model. Functional imaging studies in the moth AL revealed that stimulation of the male antenna with the major sex pheromone component, Z11-16:Ald, in the presence of distinct plant volatiles, namely linalool, linalyl acetate, Z3-hexenol, and geraniol resulted in a significantly reduced pheromone-induced calcium signal in the cumulus region of the MGC, the projection area of Z11-16:Ald-specific Ph-OSNs. In contrast, the odorant isoamyl acetate did not have a significant effect. Interestingly this odorant is the only fruit odorant in our stimulus set and might not be of ecological relevance for a male moth, while the other compounds are

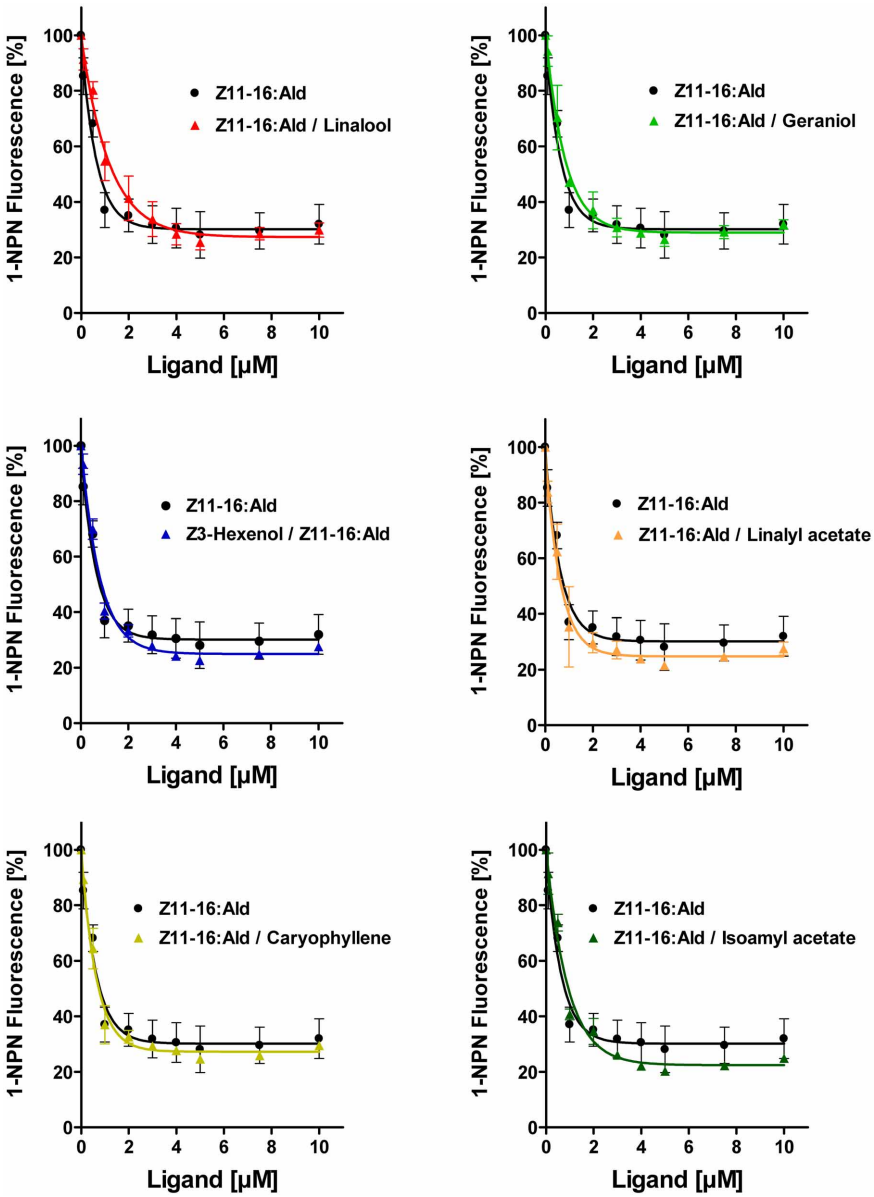

FIGURE 5 | Plant odorants do not interfere with the binding of Z11-16:Ald to HvirPBP2. Competitive fluorescence binding assays were performed, employing HvirPBP2 and 1-NPN, both at 2 µM concentration in Ringer solution. The maximum emission of 1-NPN fluorescence was monitored after increasing concentrations (0–10 µM) of Z11-16:Ald were added and the plant odorants indicated (1:1 ratio). Maximum fluorescence intensities over concentration are shown as percentages of the value in the absence of the mixture. For comparison, the displacement curve determined for the pheromone component alone is depicted in addition to the displacement curves for the mixtures.

emitted by flowers or leafs. *In vivo* calcium imaging using bath-applied Calcium Green™ allowed us to monitor spatio-temporal changes in intracellular calcium levels in the AL, mainly reflecting the presynaptic calcium influx into OSNs (Galizia et al., 2000; Bisch-Knaden et al., 2012). In line with this observation, previous single sensillum recordings from the antenna of *H. virescens* (Hillier and Vickers, 2011) revealed that stimulation with mixtures of the pheromone component and linalool or Z3-hexenol strongly reduced the spiking activity of Z11-16:Ald-specific Ph-OSNs. Contrary to *H. virescens* these plant odorants act synergistically with Z11-16:Ald in the heliothine moth *Helicoverpa zea* leading to an increased spiking activity (Ochieng et al., 2002). Whether these differences in mixture responses in the two heliothine species may be due to differences in their odorant receptors for Z11-16:Ald or result from other mechanisms have yet to be identified. Mentionable, in *H. virescens* an increase in spike frequency of Ph-OSNs after stimulation with a mixture of Z11-16:Ald and β-caryophyllene was noted (Hillier and Vickers, 2011). We did not test this compound in our AL experiments but found no β-caryophyllene-produced synergy in

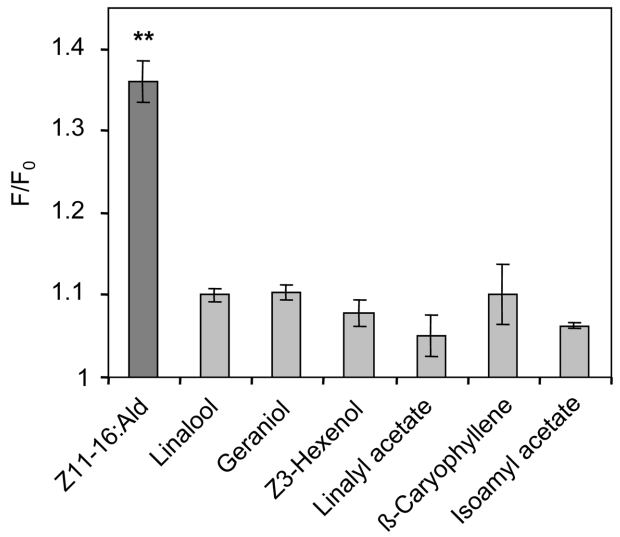

FIGURE 6 | Responses of HR13-expressing cells to Z11-16:Ald and plant odorants. HR13 cells respond to stimulation with Z11-16:Ald (1 nM) but not to linalool, linalyl acetate, Z3-hexenol, geraniol, isoamyl acetate, and β-caryophyllene even at 100-fold higher doses (100 nM). Data represent the mean calcium responses of cells expressed as $F/F_0 \pm$ SE ratios determined from at least three independent experiments with a minimum of 30 cells each. Data were normalized against control measurements using Ringer with 0.1% DMSO and 0.1% *n*-hexane for stimulation. Responses which differed significantly from those of the control are indicated by asterisks (**$p < 0.01$; One-Way ANOVA followed by Dunnett's post-test).

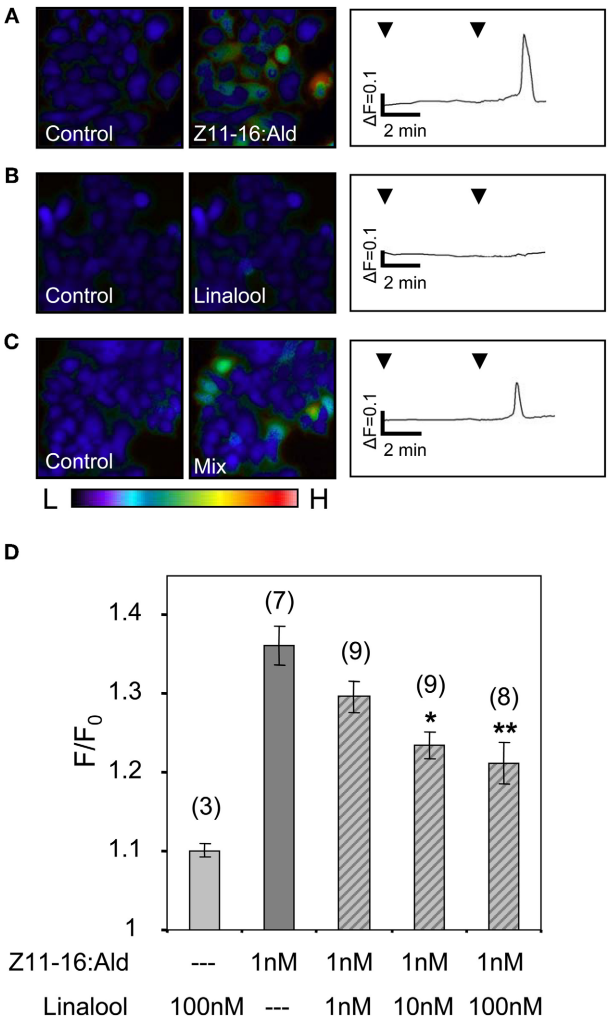

FIGURE 7 | Linalool reduces the responses of HR13-expressing cells to Z11-16:Ald. (A–C) Pseudocolor images on the left indicate calcium levels in HR13-expressing cells after the application of Ringer with 0.1% DMSO, 0.1% *n*-hexane (control) or stimulation with solutions containing 1 nM Z11-16:Ald **(A)**, 100 nM linalool **(B)** or a mixture of both **(C)**. The color bar indicates low (L) and high (H) calcium concentration in blue and red, respectively. Calcium responses of representative cells from the experiments are shown to the right as changes of fura-2 fluorescence intensity ratios (340/380 nm) over time. HR13-expressing cells displayed clear calcium responses to Z11-16:Ald **(A)**, whereas these cells did not respond to linalool **(B)** and showed reduced responses to a mixture **(C)** of the pheromone component and the plant odorant (ratio 1:100). **(D)** Responses of HR13-expressing cells to Z11-16:Ald/linalool mixtures at different ratios. Cell responses were monitored after stimulation with solutions containing 1 nM Z11-16:Ald and 1, 10 or 100 nM linalool, respectively. (For comparison, data for linalool and pheromone component alone were adopted from **Figure 6**.) HR13 cells do not respond to linalool (100 nM) but show a clear calcium signal after stimulation with Z11-16:Ald (1 nM). The pheromone-induced calcium response of the cells is significantly reduced in the presence of a 10- and 100-fold excess of linalool. Bars represent the mean responses of cells reported as $F/F_0 \pm$ SE ratios determined from 3 to 9 independent replicates with at least 30 cells in each experiment. Values have been normalized to the control. Responses to mixtures, which were significantly decreased compared to the response to the pheromone component alone, are indicated by asterisks (*$p < 0.05$, **$p < 0.01$; One-Way ANOVA followed by Dunnett's post-test).

our experiments with HR13-expressing cells, suggesting that the plant odorant elicits a synergistic effect via a HR13-independent mechanism.

Interestingly, and similar to the results for linalool and Z3-hexenol in *H. virescens*, a reduction of Ph-OSN spiking and a suppression of the pheromone-evoked activity in the AL was recently found for the plant odorant heptanal in the moth *Agrotis ipsilon* (Deisig et al., 2012). Although the reduced firing rate of OSNs correlate with reduced responses in the MGC we cannot rule out the possibility that inhibitory neural circuits, mediated by GABAergic local interneurons in the moth AL, also contribute to the observed inhibition of pheromone-evoked signals. Since local interneurons form multiglomerular wide-field arborizations and connect the MGC with ordinary glomeruli (Christensen et al., 1993; Anton et al., 1997; Seki and Kanzaki, 2008), they might inhibit the MGC when a plant odor is applied. However, since our data strongly suggest that the inhibitory effect is already taking place at the PR site, we assume that the contribution of the inhibitory AL network to the observed effect is probably rather minor. Nevertheless, we will silence GABA-mediated inhibition in the AL in future experiments to investigate its contribution or feedback signaling.

PLANT ODORANTS INTERFERE WITH PHEROMONE BINDING TO HR13

Our data indicate that the attenuating effect of plant odorants in detection of the major sex pheromone component occurs at the level of the PR HR13. This is reminiscent of recent findings of the

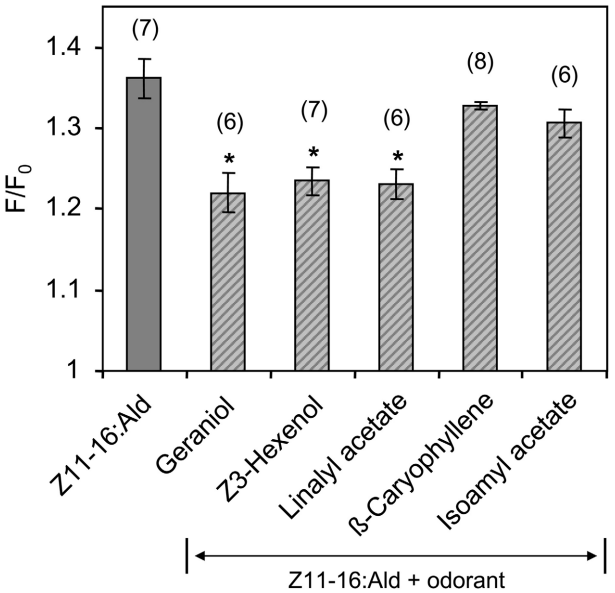

FIGURE 8 | Responses of HR13-expressing cells to mixtures of Z11-16:Ald with different plant odorants. HR13 cells were stimulated with solutions containing 1 nM Z11-16:Ald and 100 nM of the respective plant odorant (1:100 ratio). The pheromone response was significantly reduced in the presence of linalyl acetate, Z3-hexenol, and geraniol, but not in mixtures containing isoamyl acetate and β-caryophyllene. Data represent the mean calcium responses of cells expressed as $F/F_0 \pm$ SE ratios determined from 6 to 8 independent experiments with a minimum of 30 cells each. Data were normalized to the control. Asterisks indicate mixture responses, which differed significantly from the responses to the pheromone component alone (*$p < 0.05$; One-Way ANOVA followed by Dunnett's post-test).

fruit fly *Drosophila melanogaster* and the mosquitoes *Anopheles gambiae* and *Aedes aegypti*: in these insects, the responses of various olfactory receptor (OR) types to odorants were inhibited in the presence of several insect repellents (Ditzen et al., 2008; Bohbot and Dickens, 2010, 2012; Bohbot et al., 2011). For some mosquito ORs the data suggest a competitive antagonism or an allosteric inhibition of the repellents. Both mechanisms could also account for the interference of plant odorants with the Z11-16:Ald response; plant odorants could occupy the pheromone binding site of the HR13 receptor or affect the receptor activity by allosteric inhibition.

Using a competitive binding assay, we confirmed and extended previous results demonstrating that HvirPBP2 is the binding protein for the major sex pheromone component (Grosse-Wilde et al., 2007). In contrast, none of the plant odorants was bound or did affect the binding of the pheromone component to HvirPBP2. These results suggest that plant odorants do not interfere with the solubilization and transfer of the major sex pheromone component in the sensillum lymph.

The finding that HvirPBP2 does not bind non-pheromone odorants in its ligand binding pocket raises the question of how inhibitory plant odorants overcome the aqueous sensillum lymph to elicit their effects at the receptor site. Although some of the compounds used here—for example, linalool—are soluble in aqueous solutions, others are hardly soluble or even non-soluble, e.g., linalyl acetate. Conceivably, the transfer of such compounds may be mediated by other proteins present in the sensillum lymph surrounding the HR13-expressing Ph-OSN. In support of this notion, previous *in situ* hybridization studies have shown that HvirPBP1 is co-expressed with HvirPBP2 in support cells associated with the same sensillum (Grosse-Wilde et al., 2007) and three PBPs coexist in pheromone responsive hairs of *Antheraea polyphemus* (Forstner et al., 2009). In addition, certain sensilla in the silk moth *Bombyx mori* co-express BmorPBP and the antennal binding protein X (ABPX) (Maida et al., 2005). Thus, HvirPBP1 or other yet not identified PBPs and OBPs coexisting in the sensillum lymph with HvirPBP2 may account for the solubilization and transfer of plant odorants.

Although non-pheromone odorants do not bind to the pheromone-binding pocket it cannot be excluded that they may interact with the surface of HvirPBP2 and thus be transported through the sensillum lymph. Considering such a possibility, one has to take into consideration that a plant odorant/PBP interaction may block conformational changes, which may be necessary for pheromone release (Wojtasek and Leal, 1999) or receptor activation by PBP/ligand complexes (Laughlin et al., 2008). In this way, the plant odorant/PBP interaction could directly contribute to the suppression of pheromone-evoked responses observed in single sensillum recordings (Party et al., 2009; Hillier and Vickers, 2011; Deisig et al., 2012) and calcium imaging of the AL (this study).

ECOLOGICAL RELEVANCE OF PHEROMONE/PLANT ODORANT INTERFERENCE

Female-released pheromones trigger and control upwind flight behavior and guide the male to the mating partner. According to our study and the work of others, the sex pheromone detection system of male moths seems unexpectedly susceptible to plant odorants in the environment. Most studies have reported that pheromone detection is suppressed in the presence of plant odorants (Party et al., 2009; Hillier and Vickers, 2011; Deisig et al., 2012).

With regard to a sensitive detection of the female-released pheromone and mate localization, the mostly found inhibition of the male pheromone detection system by plant odorants appears to be counterproductive. However, data suggest that suppression of the pheromone response by plant odorants may be of advantage. In electrophysiological studies of male antennae a background of plant odorants decreased the intensity of pheromone signals and improved the separation of pheromone pulses by the Ph-OSNs (Party et al., 2009). Furthermore, due to the reduced response rate both during and between pheromone pulses, a plant odorant background contributes to preserve the temporal structure of the pheromone signal (Rouyar et al., 2011). Because information encoded in the temporal structure of a pheromone plume is particularly important for orientation of male moths toward a pheromone source (Vickers, 2006), a higher odor background in the vicinity of a calling female sitting on a plant may positively affect mate localization by males approaching her.

ACKNOWLEDGMENTS

The authors would like to thank the insect rearing unit at Bayer CropScience AG Frankfurt for providing *Heliothis virescens* pupae. We further thank Nelli Dick for excellent technical assistance, Katarina Dittrich, Maik Althans, and Hannes Merten for performing functional imaging experiments, and Sonja Bisch-Knaden for statistical advice. This work was supported by the Deutsche Forschungsgemeinschaft, SPP1392 by grants to Jürgen Krieger (KR1786/4-1) and Silke Sachse (SA909/3-1), the Max Planck Society and a BMBF grant to Silke Sachse.

REFERENCES

Almaas, T. J., and Mustaparta, H. (1991). *Heliothis virescens*: response characteristics of receptor neurons in sensilla trichodea type 1 and type 2. *J. Chem. Ecol.* 17, 953–972.

Anton, S., Löfstedt, C., and Hansson, B. (1997). Central nervous processing of sex pheromones in two strains of the European corn borer *Ostrinia nubilalis* (Lepidoptera: Pyralidae). *J. Exp. Biol.* 200, 1073–1087.

Baker, T. C., Ochieng, S. A., Cosse, A. A., Lee, S. G., Todd, J. L., Quero, C., et al. (2004). A comparison of responses from olfactory receptor neurons of *Heliothis subflexa* and *Heliothis virescens* to components of their sex pheromone. *J. Comp. Physiol. A* 190, 155–165.

Ban, L., Scaloni, A., D'Ambrosio, C., Zhang, L., Yahn, Y., and Pelosi, P. (2003). Biochemical characterization and bacterial expression of an odorant-binding protein from *Locusta migratoria*. *Cell. Mol. Life Sci.* 60, 390–400.

Berg, B. G., Almaas, T. J., Bjaalie, J. G., and Mustaparta, H. (1998). The macroglomerular complex of the antennal lobe in the tobacco budworm moth *Heliothis virescens*: specified subdivision in four compartments according to information about biologically significant compounds. *J. Comp. Physiol. A* 183, 669–682.

Bisch-Knaden, S., Carlsson, M. A., Sugimoto, Y., Schubert, M., Missbach, C., Sachse, S., et al. (2012). Olfactory coding in five moth species from two families. *J. Exp. Biol.* 215, 1542–1551.

Bohbot, J. D., and Dickens, J. C. (2010). Insect repellents: modulators of mosquito odorant receptor activity. *PLoS ONE* 5:e12138. doi: 10.1371/journal.pone.0012138

Bohbot, J. D., and Dickens, J. C. (2012). Odorant receptor modulation: ternary paradigm for mode of action of insect repellents. *Neuropharmacology* 62, 2086–2095.

Bohbot, J. D., Fu, L., Le, T. C., Chauhan, K. R., Cantrell, C. L., and Dickens, J. C. (2011). Multiple activities of insect repellents on odorant receptors in mosquitoes. *Med. Vet. Entomol.* 25, 436–444.

Campanacci, V., Krieger, J., Bette, S., Sturgis, J. N., Lartigue, A., Cambillau, C., et al. (2001). Revisiting the specificity of *Mamestra brassicae* and *Antheraea polyphemus* pheromone-binding proteins with a fluorescence binding assay. *J. Biol. Chem.* 276, 20078–20084.

Carde, R. T., and Willis, M. A. (2008). Navigational strategies used by insects to find distant, wind-borne sources of odor. *J. Chem. Ecol.* 34, 854–866.

Carey, A. F., and Carlson, J. R. (2011). Insect olfaction from model systems to disease control. *Proc. Natl. Acad. Sci. U.S.A.* 108, 14849–14854.

Chaffiol, A., Kropf, J., Barrozo, R. B., Gadenne, C., Rospars, J. P., and Anton, S. (2012). Plant odour stimuli reshape pheromonal representation in neurons of the antennal lobe macroglomerular complex of a male moth. *J. Exp. Biol.* 215, 1670–1680.

Christensen, T. A., Waldrop, B. R., Harrow, I. D., and Hildebrand, J. G. (1993). Local interneurons and information processing in the olfactory glomeruli of the moth *Manduca sexta*. *J. Comp. Physiol. A* 173, 385–399.

David, C. T., Kennedy, J. S., and Ludlow, A. R. (1983). Finding of a pheromone source by gypsy moths released in the field. *Nature* 303, 804–806.

Deisig, N., Kropf, J., Vitecek, S., Pevergne, D., Rouyar, A., Sandoz, J. C., et al. (2012). Differential interactions of sex pheromone and plant odour in the olfactory pathway of a male moth. *PLoS ONE* 7:e33159. doi: 10.1371/journal.pone.0033159

De Moraes, C. M., Mescher, M. C., and Tumlinson, J. H. (2001). Caterpillar-induced nocturnal plant volatiles repel conspecific females. *Nature* 410, 577–580.

Ditzen, M., Pellegrino, M., and Vosshall, L. B. (2008). Insect odorant receptors are molecular targets of the insect repellent DEET. *Science* 319, 1838–1842.

Forstner, M., Breer, H., and Krieger, J. (2009). A receptor and binding protein interplay in the detection of a distinct pheromone component in the silkmoth *Antheraea polyphemus*. *Int. J. Biol. Sci.* 5, 745–757.

Galizia, C. G., and Menzel, R. (2000). Odour perception in honeybees: coding information in glomerular pattern. *Curr. Opin. Neurobiol.* 10, 504–510.

Galizia, C. G., Sachse, S., and Mustaparta, H. (2000). Calcium responses to pheromones and plant odours in the antennal lobe of the male and female moth *Heliothis virescens*. *J. Comp. Physiol. A* 186, 1049–1063.

Grosse-Wilde, E., Gohl, T., Bouche, E., Breer, H., and Krieger, J. (2007). Candidate pheromone receptors provide the basis for the response of distinct antennal neurons to pheromonal compounds. *Eur. J. Neurosci.* 25, 2364–2373.

Grosse-Wilde, E., Stieber, R., Forstner, M., Krieger, J., Wicher, D., and Hansson, B. S. (2010). Sex-specific odorant receptors of the tobacco hornworm *Manduca sexta*. *Front. Cell. Neurosci.* 4:22. doi: 10.3389/fncel.2010.00022

Grosse-Wilde, E., Svatos, A., and Krieger, J. (2006). A pheromone-binding protein mediates the bombykol-induced activation of a pheromone receptor *in vitro*. *Chem. Senses* 31, 547–555.

Hallem, E. A., and Carlson, J. R. (2006). Coding of odors by a receptor repertoire. *Cell* 125, 143–160.

Hansson, B. S. (1995). Olfaction in Lepidoptera. *Experientia* 51, 1003–1027.

Hansson, B. S., and Anton, S. (2000). Function and morphology of the antennal lobe: new developments. *Annu. Rev. Entomol.* 45, 203–231.

Hansson, B. S., Carlsson, M. A., and Kalinova, B. (2003). Olfactory activation patterns in the antennal lobe of the sphinx moth, *Manduca sexta*. *J. Comp. Physiol. A Neuroethol. Sens. Neural Behav. Physiol.* 189, 301–308.

Hansson, B. S., Ljungberg, H., Hallberg, E., and Lofstedt, C. (1992). Functional specialization of olfactory glomeruli in a moth. *Science* 256, 1313–1315.

Hansson, B. S., and Stensmyr, M. C. (2011). Evolution of insect olfaction. *Neuron* 72, 698–711.

Hillier, N. K., Kleineidam, C., and Vickers, N. J. (2005). Physiology and glomerular projections of olfactory receptor neurons on the antenna of female *Heliothis virescens* (Lepidoptera: Noctuidae) responsive to behaviorally relevant odors. *J. Comp. Physiol. A. Neuroethol. Sens. Neural Behav. Physiol.* 192, 199–219.

Hillier, N. K., and Vickers, N. J. (2007). Physiology and antennal lobe projections of olfactory receptor neurons from sexually isomorphic sensilla on male *Heliothis virescens*. *J. Comp. Physiol. A Neuroethol. Sens. Neural Behav. Physiol.* 193, 649–663.

Hillier, N. K., and Vickers, N. J. (2011). Mixture interactions in moth olfactory physiology: examining the effects of odorant mixture, concentration, distal stimulation, and antennal nerve transection on sensillar responses. *Chem. Senses* 36, 93–108.

Kesselmeier, J., and Staudt, M. (1997). Biogenic volatile organic compounds (VOC) an overview on emission, physiology and ecology. *J. Atmos. Chem.* 33, 22–88.

Krieger, J., Gaenssle, H., Raming, K., and Breer, H. (1993). Odorant binding proteins of *Heliothis virescens*. *Insect Biochem. Mol. Biol.* 23, 449–456.

Krieger, J., Grosse-Wilde, E., Gohl, T., Dewer, Y. M. E., Raming, K., and Breer, H. (2004). Genes encoding candidate pheromone receptors in a moth (*Heliothis virescens*). *Proc. Natl. Acad. Sci. U.S.A.* 101, 11845–11850.

Kuebler, L. S., Schubert, M., Karpati, Z., Hansson, B. S., and Olsson, S. B. (2012). Antennal lobe processing correlates to moth olfactory behavior. *J. Neurosci.* 32, 5772–5782.

Laughlin, J. D., Ha, T. S., Jones, D. N., and Smith, D. P. (2008). Activation of pheromone-sensitive neurons is mediated by conformational activation of pheromone-binding protein. *Cell* 133, 1255–1265.

Leal, W. S. (2003). "Proteins that make sense," in *Insect Pheromone Biochemistry and Molecular Biology. The Biosynthesis and Detection of Pheromones and Plant Volatiles,* eds G. Blomquist and R. Vogt (London: Elsevier Academic Press), 447–476.

Lei, H., and Vickers, N. (2008). Central processing of natural odor mixtures in insects. *J. Chem. Ecol.* 34, 915–927.

Maida, R., Mameli, M., Muller, B., Krieger, J., and Steinbrecht, R. A. (2005). The expression pattern of four odorant-binding proteins in male and female silk moths, *Bombyx mori*. *J. Neurocytol.* 34, 149–163.

Müller, K., Pelzing, M., Gnauk, T., Kappe, A., Teichmann, U., Spindler, G., et al. (2002). Monoterpene emissions and carbonyl compound air concentration during blooming period of rape (*Brassica napus*). *Chemosphere* 49, 1247–1256.

Nakagawa, T., Sakurai, T., Nishioka, T., and Touhara, K. (2005). Insect sex-pheromone signals mediated by specific combinations of olfactory receptors. *Science* 307, 1638–1642.

Namiki, S., Iwabuchi, S., and Kanzaki, R. (2008). Representation of a mixture of pheromone and host plant odor by antennal lobe projection neurons of the silkmoth *Bombyx mori*. *J. Comp. Physiol. A Neuroethol. Sens. Neural Behav. Physiol.* 194, 501–515.

Ochieng, S. A., Park, K. C., and Baker, T. C. (2002). Host plant volatiles synergize responses of sex pheromone-specific olfactory receptor neurons in male *Helicoverpa zea*. *J. Comp. Physiol. A Neuroethol. Sens. Neural Behav. Physiol.* 188, 325–333.

Oldham, N. J., Krieger, J., Breer, H., and Svatos, A. (2001). Detection and removal of an artefact fatty acid from the binding site of recombinant *Bombyx mori* pheromone-binding protein. *Chem. Senses* 26, 529–531.

Party, V., Hanot, C., Said, I., Rochat, D., and Renou, M. (2009). Plant terpenes affect intensity and temporal parameters of pheromone detection in a moth. *Chem. Senses* 34, 763–774.

Plettner, E., Lazar, J., Prestwich, E. G., and Prestwich, G. D. (2000). Discrimination of pheromone enantiomers by two pheromone binding proteins from the gypsy moth *Lymantria dispar*. *Biochemistry* 39, 8953–8962.

Qiao, H., He, X., Schymura, D., Field, L., Dani, F. R., Michelucci, E., et al. (2010). Cooperative interactions between odorant-binding proteins of *Anopheles gambiae*. *Cell. Mol. Life Sci.* 68, 1799–1813.

Rostelien, T., Stranden, M., Borg-Karlson, A. K., and Mustaparta, H. (2005). Olfactory receptor neurons in two Heliothine moth species responding selectively to aliphatic green leaf volatiles, aromatic compounds, monoterpenes and sesquiterpenes of plant origin. *Chem. Senses* 30, 443–461.

Rouyar, A., Party, V., Presern, J., Blejec, A., and Renou, M. (2011). A general odorant background affects the coding of pheromone stimulus intermittency in specialist olfactory receptor neurones. *PLoS ONE* 6:e26443. doi: 10.1371/journal.pone.0026443

Sandler, B. H., Nikonova, L., Leal, W. S., and Clardy, J. (2000). Sexual attraction in the silkworm moth: structure of the pheromone-binding-protein-bombykol complex. *Chem. Biol.* 7, 143–151.

Schneider, D. (1992). 100 years of pheromone research/An essay on lepidoptera. *Naturwissenschaften* 79, 241–250.

Seki, Y., and Kanzaki, R. (2008). Comprehensive morphological identification and GABA immunocytochemistry of antennal lobe local interneurons in *Bombyx mori*. *J. Comp. Neurol.* 506, 93–107.

Skiri, H. T., Galizia, C. G., and Mustaparta, H. (2004). Representation of primary plant odorants in the antennal lobe of the moth *Heliothis virescens* using calcium imaging. *Chem. Senses* 29, 253–267.

Steinbrecht, R. A., and Gnatzy, W. (1984). Pheromone receptors in *Bombyx mori* and *Antheraea pernyi*. I. Reconstruction of the cellular organization of the sensilla trichodea. *Cell Tissue Res.* 235, 25–34.

Vickers, N. J. (2006). Winging it: moth flight behavior and responses of olfactory neurons are shaped by pheromone plume dynamics. *Chem. Senses* 31, 155–166.

Vickers, N. J., and Baker, T. C. (1997). Flight of *Heliothis virescens* males in the field in response to sex-pheromone. *Physiol. Entomol.* 22, 277–285.

Vickers, N. J., Christensen, T. A., Mustaparta, H., and Baker, T. C. (1991). Chemical communication in heliothine moths. III. Flight behavior of male *Helicoverpa zea* and *Heliothis virescens* in response to varying ratios of intra- and interspecific pheromone compounds. *J. Comp. Physiol. A* 169, 275–280.

Vogt, R. G. (2003). "Biochemical diversity of odor detection: OBPs, ODEs and SNMPs," in *Insect Pheromone Biochemistry and Molecular Biology. The Biosynthesis and Detection of Pheromones and Plant Volatiles*, eds G. Blomquist and R. G. Vogt (London: Elsevier Academic Press), 391–445.

Vogt, R. G., and Riddiford, L. M. (1981). Pheromone binding and inactivation by moth antennae. *Nature* 293, 161–163.

Vosshall, L. B. (2008). Scent of a fly. *Neuron* 59, 685–689.

Wang, G., Carey, A. F., Carlson, J. R., and Zwiebel, L. J. (2010). Molecular basis of odor coding in the malaria vector mosquito *Anopheles gambiae*. *Proc. Natl. Acad. Sci. U.S.A.* 107, 4418–4423.

Wanner, K. W., Nichols, A. S., Allen, J. E., Bunger, P. L., Garczynski, S. F., Linn, C. E., et al. (2010). Sex pheromone receptor specificity in the European corn borer moth, *Ostrinia nubilalis*. *PLoS ONE* 5:e8685. doi: 10.1371/journal.pone.0008685

Wojtasek, H., and Leal, W. S. (1999). Conformational change in the pheromone-binding protein from *Bombyx mori* induced by pH and by interaction with membranes. *J. Biol. Chem.* 274, 30950–30956.

Zhang, S., Maida, R., and Steinbrecht, R. A. (2001). Immunolocalization of odorant-binding proteins in noctuid moths (Insecta, Lepidoptera). *Chem. Senses* 26, 885–896.

Zhou, J. J., Zhang, G. A., Huang, W., Birkett, M. A., Field, L. M., Pickett, J. A., et al. (2004). Revisiting the odorant-binding protein LUSH of *Drosophila melanogaster*: evidence for odour recognition and discrimination. *FEBS Lett.* 558, 23–26.

Zwiebel, L. J., and Takken, W. (2004). Olfactory regulation of mosquito-host interactions. *Insect Biochem. Mol. Biol.* 34, 645–652.

Conflict of Interest Statement: The authors declare that the research was conducted in the absence of any commercial or financial relationships that could be construed as a potential conflict of interest.

Received: 27 July 2012; accepted: 20 September 2012; published online: 08 October 2012.

Citation: Pregitzer P, Schubert M, Breer H, Hansson BS, Sachse S and Krieger J (2012) Plant odorants interfere with detection of sex pheromone signals by male Heliothis virescens. Front. Cell. Neurosci. ***6****:42. doi: 10.3389/fncel. 2012.00042*

Copyright © 2012 Pregitzer, Schubert, Breer, Hansson, Sachse and Krieger. This is an open-access article distributed under the terms of the Creative Commons Attribution License, which permits use, distribution and reproduction in other forums, provided the original authors and source are credited and subject to any copyright notices concerning any third-party graphics etc.

frontiers in
CELLULAR NEUROSCIENCE

GENERAL COMMENTARY
published: 25 October 2012
doi: 10.3389/fncel.2012.00046

A first glance on the molecular mechanisms of pheromone-plant odor interactions in moth antennae

Sylvia Anton*[1] *and* ***Michel Renou*[2]**

[1] *Faculté des Sciences, Laboratoire Récepteurs et Canaux Ioniques Membranaires, UPRES-EA 2647 USC INRA 1330, Université d'Angers, Angers, France*
[2] *Physiologie de l'Insecte: Signalisation et Communication, Centre de Recherches de Versailles, UMR 1272 INRA/Université Paris 6, Versailles, France*
**Correspondence: sylvia.anton@angers.inra.fr*

Edited by:
Dieter Wicher, Max Planck Institute for Chemical Ecology, Germany

Reviewed by:
Dieter Wicher, Max Planck Institute for Chemical Ecology, Germany

A commentary on

Plant odorants interfere with detection of sex pheromone signals by male *Heliothis virescens*
by Pregitzer, P., Schubert, M., Breer, H., Hansson, B. S., Sachse, S., and Krieger, J. (2012). Front. Cell. Neurosci. 6:42. doi: 10.3389/fncel.2012.00042

It is widely accepted that odorants emanating from different organic sources are interacting to elicit behaviors in animals, including insects. However, the mechanisms of such interactions are largely unknown. In insects, the most prominent examples for odor interactions are mixtures of host odors and anthropogenic repellents in blood-sucking insects such as mosquitoes (Syed and Leal, 2008) and synergistic or inhibitory interactions of sex pheromones and host or non-host plant odors in moths (Byers et al., 2004; Yang et al., 2004; Schmidt-Büsser et al., 2009; Allmann and Baldwin, 2010; Varela et al., 2011). Detection of pheromone and plant odors in moths, for instance, is known to happen via highly separated channels whose input is transmitted via labeled lines to primary and even secondary processing centers (Christensen and Hildebrand, 2002). Behavioral effects issuing from this particular example of mixture interactions have therefore been thought to occur mainly through integration in higher centers within the brain (Lei and Vickers, 2008).

The literature shows, however, that olfactory signals supposed to serve as cues for different behaviors, like sex pheromone and plant odor, interact already in the peripheral detection system (Den Otter et al., 1978; Van der Pers et al., 1980; Ochieng et al., 2002; Party et al., 2009; Hillier and Vickers, 2011; Rouyar et al., 2011; Deisig et al., 2012). Moreover the information on odor mixtures might subsequently be modified throughout the olfactory pathway (Namiki et al., 2008; Barrozo et al., 2010; Chaffiol et al., 2012; Deisig et al., 2012). The pheromone-plant odor interactions have been mainly analyzed with *in vivo* optical imaging or extra- and intracellular electrophysiological recording techniques, revealing suppressive or synergistic interactions at the cellular level. However, nothing was known so far on the molecular mechanisms involved in the observed interactions. The major hypotheses were that plant odors might interfere with pheromone binding to binding proteins or olfactory receptors in a competitive or non-competitive way. A contribution of ion channels or odorant degrading enzymes, which influence the dynamics of odor responses in olfactory receptor neurons was also considered (Pophof and Van der Goes van Naters, 2002; Ishida and Leal, 2008).

In the article published in Frontiers of Cellular Neuroscience volume 6, P. Pregitzer and co-authors confirm the inhibition of sex pheromone responses by certain plant odorants, using *in vivo* calcium imaging of the antennal lobe, i.e., responses of receptor neurons from the entire antenna in their model, the noctuid moth, *Heliothis virescens*. *H. virescens* is a favorable model to investigate molecular mechanisms underlying pheromone-plant odor interactions in antennal sensilla, because the pheromone binding protein (HvirPBP2) and the olfactory receptor (HR13) binding the major pheromone compound, *Z*-11-hexadecenal (Z11-16:Ald), have been identified (Grosse-Wilde et al., 2007). The authors profited from this knowledge to investigate effects of plant odorants alone or in combination with Z11-16:Ald on HvirPBP2 and on HR13. The tested plant odorants did not themselves bind to HvirPBP2 and did not alter binding of the main pheromone component to HvirPBP2. However, pheromone-induced responses of human embryonic kidney (HEK) cells expressing HR13 changed in a dose-dependent manner, when certain plant odorants are added. Interestingly, the same plant odorants eliciting inhibition of pheromone responses in the antennal lobe also reduced pheromone responses in the HR13-expressing cells. On the other hand, a fruit odorant, without evident behavioral significance for the moth, did neither have an effect on receptor neuron responses to the sex pheromone, nor did it change pheromone responses in HR13-expressing cells. These results are a first important step towards identifying the molecular actors involved in pheromone-general odorant interactions within the highly specific pheromone detection system on the antennae of an insect. The transport of pheromone molecules through the sensillum lymph seems not to be affected by plant odorants, but pheromone binding to membrane receptors changes in the presence of plant odorants. Although the odorant types are rather different, these effects are similar to the action of the insect repellent DEET on olfactory receptors in different mosquito species and *Drosophila melanogaster* (Ditzen et al., 2008; Bohbot et al., 2011; Bohbot and Dickens, 2012).

The study by Pregitzer et al. shows that we just begin to understand peripheral interactions of different odorants. In the future it will be exciting to see if

the situation found in a heterologous system corresponds to a "real life" situation with the complex environment of an antennal sensillum, in which different molecular actors are present and where potential feedback from the antennal lobe might affect receptor neuron responses. The current results help to refine the future approaches by excluding already some players and proposing candidate molecular actors involved in environmental modulation of olfaction.

REFERENCES

Allmann, S., and Baldwin, I. T. (2010). Insects betray themselves in nature to predators by rapid isomerization of geen leaf volatiles. *Science* 329, 1075–1078.

Barrozo, R. B., Gadenne, C., and Anton, S. (2010). Switching attraction to inhibition: mating-induced reversed role of sex pheromone in an insect. *J. Exp. Biol.* 213, 2933–2939.

Bohbot, J. D., and Dickens, J. C. (2012). Odorant receptor modulation: ternary paradigm for mode of action of insect repellents. *Neuropharmacology* 62, 2086–2095.

Bohbot, J. D., Fu, L., Le, T. C., Chauhan, K. R., Cantrell, C. L., and Dickens, J. C. (2011). Multiple activities of insect repellents on odorant receptors in mosquitoes. *Med. Vet. Entomol.* 25, 436–444.

Byers, J. A., Zhang, Q. H., and Birgersson, G. (2004). Avoidance of nonhost plants by a bark beetle, *Pityogenes bidentatus*, in a forest of odors. *Naturwissenschaften* 91, 215–219.

Chaffiol, A., Kropf, J., Barrozo, R. B., Gadenne, C., Rospars, J.-P., and Anton, S. (2012). Plant odour stimuli reshape pheromonal representation in neurons of the antennal lobe macroglomerular complex of a male moth. *J. Exp. Biol.* 215, 1670–1680.

Christensen, T. A., and Hildebrand, J. G. (2002). Pheromonal and host-odor processing in the insect antennal lobe: how different? *Curr. Opin. Neurobiol.* 12, 393–399.

Deisig, N., Kropf, J., Vitecek, S., Pevergne, D., Rouyar, A., Sandoz, J. C., et al. (2012). Differential interactions of sex pheromone and plant odour in the olfactory pathway of a male moth. *PLoS ONE* 7:e33159. doi: 10.1371/journal.pone.0033159

Den Otter, C. J., Schuil, H. A., and Sander-Van Oosten, A. (1978). Reception of host-plant odours and female sex pheromone in *Adoxophyes orana* (Lepidoptera:Tortricidae): electrophysiology and morphology. *Entomol. Exp. Appl.* 24, 370–378.

Ditzen, M., Pellegrino, M., and Vosshall, L. B. (2008). Insect odorant receptors are molecular targets of the insect repellent DEET. *Science* 319, 1838–1842.

Grosse-Wilde, E., Gohl, T., Bouché, E., Breer, H., and Krieger, J. (2007). Candidate pheromone receptors provide the basis for the response of distinct antennal neurons to pheromonal compounds. *Eur. J. Neurosci.* 25, 2364–2373.

Hillier, N. K., and Vickers, N. J. (2011). Mixture interactions in moth olfactory physiology: examining the effects of odorant mixture, concentration, distal stimulation, and antennal nerve transection on sensillar responses. *Chem. Senses* 36, 93–108.

Ishida, Y., and Leal, W. S. (2008). Chiral discrimination of the Japanese beetle sex pheromone and a behavioral antagonist by a pheromone-degrading enzyme. *Proc. Natl. Acad. Sci. U.S.A.* 105, 9076–9080.

Lei, H., and Vickers, N. (2008). Central processing of natural odor mixtures in insects. *J. Chem. Ecol.* 34, 915–927.

Namiki, S., Iwabuchi, S., and Kanzaki, R. (2008). Representation of a mixture of pheromone and host plant odor by antennal lobe projection neurons of the silkmoth *Bombyx mori*. *J. Comp. Physiol. A* 194, 501–515.

Ochieng, S. A., Park, K. C., and Baker, T. C. (2002). Host plant volatiles synergise responses of sex pheromone-specific olfactory receptor neurons in male *Helicoverpa zea*. *J. Comp. Physiol. A* 188, 325–333.

Party, V., Hanot, C., Saïd, I., Rochat, D., and Renou, M. (2009). Plant terpenes affect intensity and temporal parameters of pheromone detection in a moth. *Chem. Senses* 34, 763–774.

Pophof, B., and Van der Goes van Naters, W. (2002). Activation and inhibition of the transduction process in silkmoth olfactory receptor neurons. *Chem. Senses* 27, 435–443.

Rouyar, A., Party, V., Presern, J., Blejec, A., and Renou, M. (2011). A general odorant background affects the coding of pheromone stimulus intermittency in specialist olfactory receptor neurones. *PLoS ONE* 6:e26443. doi: 10.1371/journal.pone.0026443

Schmidt-Büsser, D., von Arx, M., and Guerin, P. (2009). Host plant volatiles serve to increase the response of male European grape berry moths, *Eupoecilia ambiguella*, to their sex pheromone. *J. Comp. Physiol. A* 195, 853–864.

Syed, Z., and Leal, W. (2008). Mosquitoes smell and avoid the insect repellent DEET. *Proc. Natl. Acad. Sci. U.S.A.* 105, 13598–13603.

Van der Pers, J., Thomas, G., and Den Otter, C. J. (1980). Interactions between plant odours and pheromone reception in small ermine moths (Lepidoptera: Yponomeutidae). *Chem. Senses* 5, 367–371.

Varela, N., Avilla, J., Anton, S., and Gemeno, C. (2011). Synergism of pheromone and host-plant volatile blends in the attraction of *Grapholita molesta* males. *Entomol. Exp. Appl.* 141, 114–122.

Yang, Z. H., Bengtsson, M., and Witzgall, P. (2004). Host plant volatiles synergize response to sex pheromone in codling moth, *Cydia pomonella*. *J. Chem. Ecol.* 30, 619–629.

Received: 03 October 2012; accepted: 04 October 2012; published online: 25 October 2012.

*Citation: Anton S and Renou M (2012) A first glance on the molecular mechanisms of pheromone-plant odor interactions in moth antennae. Front. Cell. Neurosci. **6**:46. doi: 10.3389/fncel.2012.00046*

Copyright © 2012 Anton and Renou. This is an open-access article distributed under the terms of the Creative Commons Attribution License, which permits use, distribution and reproduction in other forums, provided the original authors and source are credited and subject to any copyright notices concerning any third-party graphics etc.

frontiers in
CELLULAR NEUROSCIENCE

ORIGINAL RESEARCH ARTICLE
published: 08 October 2009
doi: 10.3389/neuro.03.011.2009

Ric-8A, a Gα protein guanine nucleotide exchange factor potentiates taste receptor signaling

Claire Fenech[1†], Lila Patrikainen[1†], Daniel S. Kerr[2], Sylvie Grall[1], Zhenhui Liu[1], Fabienne Laugerette[3], Bettina Malnic[2] and Jean-Pierre Montmayeur[1,3]*

[1] *UMR 5170 CNRS, Centre des Sciences du Goût, Dijon, France*
[2] *Departamento de Bioquímica, Instituto de Química, Universidade de São Paulo, São Paulo, Brazil*
[3] *General Olfaction and Sensing Program on a European Level, Centre Européen des Sciences du Goût, Dijon, France*

Edited by:
Dieter Wicher, Max Planck Institute for Chemical Ecology, Germany

Reviewed by:
Christian Derst, Institut für Integrative Neuroanatomie der Charité, Germany
Bruno Lapied, Université d'Angers, France

****Correspondence:***
Jean-Pierre Montmayeur, Centre des Sciences du Goût, 15 rue Hugues Picardet, 21000 Dijon, France.
e-mail: montmayeur@cesg.cnrs.fr

[†]Claire Fenech and Lila Patrikainen contributed equally to this work.

Taste receptors for sweet, bitter and umami tastants are G-protein-coupled receptors (GPCRs). While much effort has been devoted to understanding G-protein-receptor interactions and identifying the components of the signalling cascade downstream of these receptors, at the level of the G-protein the modulation of receptor signal transduction remains relatively unexplored. In this regard a taste-specific regulator of G-protein signaling (RGS), RGS21, has recently been identified. To study whether guanine nucleotide exchange factors (GEFs) are involved in the transduction of the signal downstream of the taste GPCRs we investigated the expression of Ric-8A and Ric-8B in mouse taste cells and their interaction with G-protein subunits found in taste buds. Mammalian Ric-8 proteins were initially identified as potent GEFs for a range of Gα subunits and Ric-8B has recently been shown to amplify olfactory signal transduction. We find that both Ric-8A and Ric-8B are expressed in a large portion of taste bud cells and that most of these cells contain IP3R-3 a marker for sweet, umami and bitter taste receptor cells. Ric-8A interacts with Gα-gustducin and Gαi2 through which it amplifies the signal transduction of hTas2R16, a receptor for bitter compounds. Overall, these findings are consistent with a role for Ric-8 in mammalian taste signal transduction.

Keywords: Ric-8A, Ric-8B, G-protein-coupled-receptor, taste, regulators of G-protein signaling, guanine nucleotide exchange factors, bitter, gustducin

INTRODUCTION

Taste receptors are the sensors through which the tastants dissolved in the saliva are detected. Over the years evidence has accumulated supporting the importance of G-protein mediated signaling in taste detection. Initially, electrophysiological studies implicated cyclic nucleotides in taste transduction (Avenet et al., 1988; Tonosaki and Funakoshi, 1988). Subsequently, gustducin, a G-protein alpha subunit expressed in taste receptor cells was shown to be involved in bitter, sweet, and glutamate detection in mice (McLaughlin et al., 1992; Wong et al., 1996; He et al., 2004). More recently and importantly, Tas1Rs and Tas2Rs, two families of G-protein-coupled-receptors (GPCRs) that are respectively involved in the detection of certain sweet, umami and bitter tasting compounds were discovered (Hoon et al., 1999; Adler et al., 2000; Chandrashekar et al., 2000; Matsunami et al., 2000; Nelson et al., 2001, 2002; Zhao et al., 2003). GPCR signaling cascades involve the activation of G-proteins as well as subsequent stimulation of effector enzymes by the free alpha or beta-gamma subunits of the activated heterotrimeric G-protein (Oldham and Hamm, 2008). Accessory proteins such as regulators of G-protein signaling (RGS) and GDP/GTP exchange factors (GEFs) which regulate the activation state of the G-protein, have been shown to modulate GPCR signaling in a variety of cell types (Klattenhoff et al., 2003; Siderovski and Willard, 2005; Neitzel and Hepler, 2006). GEFs act as signal amplifiers by promoting the exchange of GDP to GTP on the receptor-activated Gα subunits whereas RGS promote the hydrolysis of GTP thus attenuating the activation of the effector (Wilkie and Kinch, 2005; Jean-Baptiste et al., 2006).

In vision and olfaction, two senses involving GPCRs as main detectors, RGS9-1 and RGS2 respectively have been reported to attenuate light or odorant responses (Sinnarajah et al., 2001; Nishiguchi et al., 2004) while Ric-8B a putative GEF for Gαolf that is abundant in olfactory sensory neurons amplifies odorant receptor signaling (Von Dannecker et al., 2005, 2006). Ric-8B has one other known mammalian homologue, Ric-8A, which was shown to enhance Gαq-mediated ERK activation by GPCRs (Nishimura et al., 2006) as well as interact and display GEF activity for Gαi1, Gαq and Gαo but not Gαs *in vitro* (Tall et al., 2003). The GEF activity of Ric-8A on the Gαι subunit has been extensively studied in receptor-independent G-protein-mediated events regulating microtubules pulling forces during cell division (Tall and Gilman, 2005). In this system the action of Ric-8A is similar to that of a GPCR while the GDI activity of GPR/GoLoco motif-containing proteins resemble that of Gβγ subunits (Thomas et al., 2008).

In gustation, RGS21 has been reported to be expressed specifically in taste cells and to play a role in gustducin signaling (von Buchholtz et al., 2004); however, no reports of GEFs further controlling this system have been made. To study whether GEFs are involved in the transduction of the signal downstream of the taste GPCRs we investigated the expression of Ric-8A and Ric-8B in mouse taste cells and their interaction with G-protein subunits found in taste buds.

MATERIALS AND METHODS

ANIMALS

French guidelines for the use and the care of laboratory animals were followed, and experimental protocols were approved by the animal ethic committee of the University of Burgundy. Six-week-old C57BL/6J mice housed in a controlled environment (constant temperature and humidity, darkness from 8 pm to 8 am) were used for all experiments. They were fed a standard laboratory chow *ad libitum* (UAR A04, Usine d'Alimentation Rationnelle, France).

YEAST TWO-HYBRID INTERACTIONS AND CO-IMMUNOPRECIPITATION

The entire open reading frame of mouse Ric-8A, RGS21, gustducin, Gαt2, Gαi2, Gαolf, or GPR domains 1–4 of AGS1, AGS2, AGS3 or GoLoco domain of AGS4, PBP, Pins, RGS2, RGS9, were PCR amplified from C57BL6/J mice heart, testis or circumvallate papillae cDNA using specific primers (Operon, Germany) containing a Sal I (forward primer) or Not I (reverse primer) restriction site. Ric-8B was from Von Dannecker et al. 2006.

(5′ > 3′): Ric-8A(S) CGAGGTCGACTGAGCCCCGGGCAGTTGCG,
Ric-8A(AS) CTTAGCGGCCGCTCAGTCAGGATCTGAGTCAGG,
RGS21(S) TTGTCGACCTCGAGGCCAGTGAAATGCTGTTTC,
RGS21(AS) TTGTCGACGCGGCCGCTTACAGGAAAGGCAG,
Gαgus(S) AAAGCACGCGTGATGGGAAGTGGAATTAGTTCAG,
Gαgus(AS) CAAAGCGGCCGCTCAGAAGAGCCCACAGTCTTT GAGGTT,
Gαt2(S) CGAGGTCGACTGGGAGTGGCATCAGTGCT,
Gαt2(AS) GAATGCGGCCGCTTAAAAGAGCCCACAGTCCTTGA,
Gαi2(S) GGAATTCCCACCATGGGCTGGACCTGTAG,
Gαi2(AS) AGCGGCCGCGAAGAGGCCACAGTCCTTC,
Gα*olf* (S) CGAGGTCGACTGGGTGTTTGGGCAACAGC,
Gα*olf* (AS) GAATGCGGCCGCTCACAAGAGTTCGTACTGCTTG,
AGS1(S) CGAGGTCGACGAAACTGGCCGCGATGATC,
AGS1(AS) CTTAGCGGCCGCCTAACTGATGACACAGCG,
AGS2(S) CGAGGTCGACGGAAGACTTCCAGGCCTC,
AGS2(AS) CTTAGCGGCCGCTCAGATGGACAGTCCGAAG,
AGS3(S) CGAGGTCGACTATTCCCAGGGCCCCGTC,
AGS3(AS) CTTAGCGGCCGCTTAGCTGGCACCCGGTG,
AGS4(S) CGAGGTCGACGGAGGCTGAAAGACCCCAG,
AGS4(AS) CTTAGCGGCCGCTCAGCAGGTGTGTGTAGG,
PBP(S) CGAGGAATTCTGGCCGCCGACATCAGC,
PDB(AS) CTTAGCGGCCGCCTACTTCCCTGACAGCTG,
Pins(S) CGAGGTCGACAATCAGTTCAGACACGATTG,
Pins(AS) CTTAGCGGCCGCTTATTTTCCCGAATGCTTAAA,
RGS2(S) CGAGGTCGACTATGCAAAGTGCCATGTTCCTG,
RGS2(AS) CTTAGCGGCCGCTCATGTAGCATGGGGCTC,
RGS9(S) CGAGGTCGACGGTGGAGATCCCAACCAAGATG,
RGS9(AS) CTTAGCGGCCGCTCACTGGGTGATGTCCACGG.

After amplification with PFU (Stratagene, USA) according to the manufacturer's specifications, the products of the expected size were subcloned into pSTBlue-1 according to the manufacturer's specifications (Novagen, USA) and sequenced before subsequent subcloning as a fusion into the Sal I and Not I sites of either pDBLeu (bait vector) or pEXP (prey vector) of the Proquest two-hybrid system (Invitrogen, USA).

Competent Mav203 yeast cells (Invitrogen, USA) were co-transformed with 200 ng of each prey and bait vector and grown 48 h at 30°C on minimal media plates without leucine and tryptophan. Two colonies were then collected and each was dissolved separately into 500 µl of water before spotting 10 µl of each solution side by side onto plates lacking leucine histidine and tryptophan but containing either 10, 25 or 50 mM 3-AT to test the strength of the interaction. After 24 h at 30°C, the plates were replica cleaned using a velour cloth before an additional incubation of 48–72 h at 30°C prior to scoring growth.

For co-immunoprecipitations the open reading frame of Gαi2, Gαt2 and Gαgus were subcloned into pDisplay (Invitrogen, USA) in frame with the HA epitope. Prior to subcloning into pCDNA3 (Invitrogen, USA) a Flag tag was inserted at the N terminus of Ric-8A. All constructs were verified by sequencing. These constructs as well as a Flag-tagged-Ric-8B (Von Dannecker et al., 2006) were transfected in various combinations into HEK 293T cells seeded in six well plates. Forty-eight hours later the cells were harvested and lysed following the manufacturer's directions. The lysate was incubated overnight at 4°C with 2 µg of mouse monoclonal anti-Flag (Kodak, USA) or 12CA5 mouse monoclonal anti-HA antibody (Roche, Switzerland) and protein A Sepharose (Roche, Switzerland) following the manufacturer's directions. After washing the immunoprecipitate four times with lysis buffer the samples were eluted by boiling for 5 min in sample buffer (Bio-Rad, USA) and subjected to SDS-PAGE and Western blot analysis. For Western blot hybridization the antibodies were used at a dilution of 1/1000. The membrane was subsequently processed using the components of the chemiluminescent detection kit according to the manufacturer's instructions (GE Healthcare, USA).

RT-PCR AND QUANTITATIVE RT-PCR

Total RNA was isolated from various tissues, using RNAeasy (Qiagen, Germany) according to the manufacturer's instructions. First strand cDNA was synthesized using 500 ng of total RNA with Superscript II (Invitrogen, USA). With the exception of foliate, fungiform and palate papillae, for each tissue three pools of mRNA, each from three mice, were isolated to perform triplicate RT reactions and triplicate qPRC reactions. For non quantitative PCR, the three RT reactions were pooled for each tissue.

Quantitative RT-PCR was performed on a Mini Opticon (Biorad, USA). Reactions (50 µl) contained 1× iQ™SYBR green supermix (Biorad, USA), 100 nM of each primer, and 1 µl of a 1:5 dilution of the appropriate RT reaction.

Amplification efficiency (*E*) was determined for each primer pair on triplicate 5-fold serial dilutions of mouse brain cDNA. Relative quantification was performed in relation to cyclophilin expression using the Pfaffl algorithm with kinetic PCR efficiency correction (REST-MCS) (Pfaffl, 2001; Pfaffl et al., 2002). Results are expressed as expression ratio (*R*) derived from the equation:

$$\text{Ratio}_{\text{target}} = \frac{E_{\text{target}}^{\Delta \text{Ct}_{\text{target}}(\text{control}-\text{tissue})}}{E_{\text{cyclo}}^{\Delta \text{Ct}_{\text{cyclo}}(\text{control}-\text{tissue})}}$$

where the reference gene is cyclophilin (cyclo).

RT-PCR reactions (25 µl) contained 1× Taq mastermix (Qiagen, Germany), 0.4 µM of each primer, 1 µl of appropriate RT reaction (water for control). Cycling parameters: 95°C for 2 min then 35 cycles of 95°C for 30 s; 60 or 58°C for 40 s, 72°C for 40 s, and

final elongation at 72°C for 2 min. Products (13 μl) were run onto 1.4% agarose Seakem TAE gels (Cambrex, USA). Primers used were (5′ > 3′): Ric-8A (S) CACGAAGGATCCTTAGAGTT CATG, Ric-8A (AS) GCACATTCTGTCAACACGTTCA, F78a: CAAAGAGAGAGTGGATAGCCTGC, R810b: GCAACTCCTCTT TTGGTTTTGC, cyclophilin (S): CAGACGCCACTGTCGCTTT, cyclophilin (AS): TGTCTTTGGAACTTTGTCTGCAA, F89: GCA AAACCAAACATTAATCTTATCACT, R910: AAGCAACTCCTCT CTGGAAAGTTTAT, F6: GGAAGCAGCTATAGAGAGGGTCTAA, R7: CCAGCTTATTTCTCACGGTTGA.

IMMUNOHISTOCHEMISTRY AND WESTERN BLOTTING

Four- to six-week-old male C57BL6/J mice were perfused with 4% paraformaldehyde. Circumvallate papillae were excised and allowed to soak in 30% sucrose overnight before being snap-frozen in isopentane chilled with liquid nitrogen. The tissue was then embedded in OCT compound (Tissue-Tek, Japan) and processed using a cryostat into 14-μm sections. Sections were air-dried for 2 h at room temperature and stored at −80°C. On the day of the experiment sections were rehydrated in 0.1 M phosphate saline buffer (PBS, pH 7.4) for 10 min and blocked in 5% goat serum (Sigma, USA), 0.2% Triton X-100 in PBS for 15 min at room temperature then incubated overnight at 4°C with either a 1/100 dilution of the rabbit polyclonal anti-Ric-8B antibody (Kerr et al., 2008) a 1/100 dilution of the rabbit polyclonal anti-Ric-8A antibody (Proteintech group, Inc., Chicago, IL, USA) or a 1/400 dilution of the rabbit polyclonal anti-gustducin antibody (SCBT, Santa-Cruz, USA). After washing, sections were next incubated for 2 h at room temperature with a 1/600 dilution of Alexa-488-conjugated anti-rabbit IgG secondary antibodies (Molecular probes, USA). After washing and counterstaining with Hoescht 33258 (Sigma, USA) slides were mounted in gel/mount (Biomeda Corp., USA) and analyzed under an Axioskop microscope equipped with an Axiocam MRc5 (Zeiss, Germany). For double-labelling, the sections were incubated simultaneously with a 1/200 dilution of the mouse monoclonal anti-IP3R-3 (BD Biosciences, USA) and either a 1/100 dilution of the rabbit polyclonal anti-Ric-8B antibody or a 1/100 dilution of the rabbit polyclonal anti-Ric-8A antibody (Proteintech group, Inc., Chicago, IL, USA) overnight at 4°C, washed prior to incubation with secondary antibodies for 2 h at room temperature (1/600 dilution of Alexa-488-conjugated goat anti-rabbit IgG and 1/600 dilution of Alexa-555-conjugated goat anti-mouse IgG (Molecular Probes, USA). Slides were analyzed under a TCS4D confocal microscope (Leica, Germany).

For Western blotting, circumvallate papillae from 4- to 6-week-old male C57BL6/J mice were collected and mechanically dissociated in standard lysis buffer using a dounce homogenizer on ice. 20 μg of the total protein extract was loaded on a 10% SDS-PAGE gel (Bio-Rad, USA), transferred onto a hybond-P, PVDF membrane (GE Healthcare, USA) and incubated overnight at 4°C with either a 1/100 dilution of the rabbit polyclonal anti-Ric-8B antibody, a 1/100 dilution of the rabbit polyclonal anti-Ric-8A antibody (Proteintech group, Inc., Chicago, IL, USA) or a 1/1000 dilution of a mouse monoclonal anti-β–actin antibody (Sigma, USA). The membrane was subsequently processed using the components of the ECL kit according to the manufacturer's instructions (GE Healthcare, USA).

HEK 293T cells in DMEM supplemented with 10% fetal calf serum were grown in six wells plates until 50% confluence was reached. Cells were transfected with pCDNA3 alone or containing 5′Flag-Ric8A, or 5′Flag-Ric8B. Transfections were carried out using Lipofectamine LTX (Invitrogen, USA) according to the manufacturer's protocol. 48 h after transfection the cells were harvested and lysate prepared. 15 μg of total protein extract was loaded on a denaturing 4–12% BisTris PAGE gel (Invitrogen, USA), transferred onto a hybond-P, PVDF membrane (GE Healthcare, USA) and incubated overnight with either a 1/100 dilution of the rabbit polyclonal anti-Ric-8B antibody, a 1/300 dilution of the rabbit polyclonal anti-Ric-8A antibody (Proteintech group, Inc., Chicago, IL, USA) or a 1/1000 dilution of mouse monoclonal anti-Flag (Kodak, USA). The membrane was subsequently processed using the components of the ECL kit according to the manufacturer's instructions (GE Healthcare, USA). The next day, the membranes were stripped and reprobed with a 1/1000 dilution of a mouse monoclonal anti-β–actin antibody (Sigma, USA).

IN SITU HYBRIDIZATION

The procedure used for *in situ* hybridization of 16-μm sections of fresh frozen circumvallate papillae from C57BL6/J male mice was described previously (Matsunami et al., 2000). Briefly, the sections were hybridized (58°C) overnight to hydrolysed digoxigenin-labeled cRNA probes prepared from cloned segments of cDNAs encoding Ric-8A (NCBI reference: NM_053194 nt 75-1667), Ric-8B (NCBI reference: AY940666 nt 99-1781) or gustducin (NCBI reference: BC147841 nt 125-1043). After washing, the sections were incubated with anti-Dig AP and subsequently developed using a mix of NBT-BCIP (Roche, Switzerland) according to the manufacturer's instructions. Slides were then mounted with vectamount (Vector laboratories USA) and analyzed under an Axioskop microscope equipped with an Axiocam MRc5 (Zeiss, Germany).

cAMP ASSAY

Intracellular cAMP production was monitored using a cell-based reporter gene assay relying on transcriptional regulation of secreted human placental alkaline phosphatase (SEAP) by five 5′-cyclic AMP (cAMP) response elements (CREs). This assay is based on the premise that intracellular cAMP activates protein kinase A which in turn phosphorylates the transcription factor CREB (cAMP response element binding protein) ultimately leading to SEAP production. SEAP activity is then determined using 4-methylumbelliferyl phosphate (4-MUP) as substrate.

The coding sequence of hTas2R16, a receptor activated by salicin, was PCR amplified using specific primers and fused to the first 44 amino acids of Bovine rhodopsin before subcloning into pCDNA3 (Invitrogen, USA). The coding sequence of the mouse Gαi2 or Ric-8A were PCR amplified using specific primers and subcloned into pEF6 (Invitrogen, USA) and pcDNA 3.1 (Invitrogen) respectively. All constructs were verified by DNA sequencing. HEK 293T cells in DMEM supplemented with 10% fetal calf serum were grown in 96 wells plates until 80–95% confluence was reached. Cells were transfected with different combinations of plasmid constructs coding for Tas2R16, D1R (Von Dannecker et al., 2005), Gαi2,

Ric-8A and pCRE-SEAP (Durocher et al., 2000). Transfections were carried out using Lipofectamine 2000 (Invitrogen, USA) according to the manufacturer's protocol. 24 h after transfection the media was replaced by 200 µl of serum free DMEM containing the different agonists (dopamine, salicin) and incubated for 6 h at 37°C. 200 µl of the media from each well was transferred to a new plate, heated to 65°C for 30 min and spun to remove debris. 100 µl of each sample was mixed with 100 µl of the SEAP buffer (30 mM Tris pH 8.0, 0.06%BSA, 1 mM L-homoarginine, 10 mM $MgCl_2$, 20% diethanolamine, 3.6 mg 4-methylumbelliferyl phosphate) and incubated for 1 h at 37°C. Fluorescence was measured at a wavelength of 449 nm using a Viktor 1420 microplate reader (PerkinElmer, USA). The deactivation rate was calculated by dividing each deactivation value (dopamine + salicin) by the corresponding activation value (dopamine alone). Statistical significance was evaluated by paired Student's *t*-test.

RESULTS

Ric-8A AND Ric-8B ARE EXPRESSED IN TASTE TISSUE

In the oral cavity most taste buds are found on the palate and on the tongue. The lingual structures harboring the taste buds are called taste papillae. In order to investigate Ric-8 expression in palate as well as in fungiform, foliate and circumvallate taste papillae we conducted RT-PCR using primers specific for Ric-8A and Ric-8B on RNA extracted from these tissues together with olfactory mucosa, vomeronasal organ, eye, brain and testis. As a control for taste bud rich tissue, the expression of gustducin and Gαi2, reportedly two of the most abundantly expressed G-protein alpha subunits in taste cells (Kusakabe et al., 2000), was also analyzed.

As can be seen in **Figure 1A**, messenger RNAs for Ric-8A and Ric-8B are detected in fungiform, foliate and circumvallate papillae as well as in all other examined tissues. We also find as previously reported (Kusakabe et al., 2000) that gustducin and Gαi2 are present in all three taste papillae including palatal taste buds.

In order to quantify the relative abundance of Ric-8A and Ric-8B mRNAs in taste tissue compared to that in olfactory mucosa, total brain and testis, we conducted a quantitative PCR experiment using primers specific for each gene. As seen in **Figure 1B** the relative levels of Ric-8 mRNA do not vary widely amongst the tissues examined, with the exception of the olfactory mucosa in which Ric-8B is significantly more abundant in line with a previous report focusing on olfactory neurons (Von Dannecker et al., 2005).

In foliate, palate and fungiform papillae Ric-8A mRNA is slightly more abundant than that of Ric-8B while the circumvallate papillae displays a profile similar to that of brain, testis and olfactory mucosa in which Ric-8B is prevalent over Ric-8A. In the olfactory epithelium, an alternatively spliced variant of Ric-8B called Ric-8BΔ9 in which exon 9 is missing has also been described (Von Dannecker et al., 2005). We looked for the presence of this isoform in tissues in which Ric-8B is predominant. When using primers for Ric-8B flanking exon 9 or primers specific for the short form only we observe that both isoforms can be detected (**Figure 1C**). Interestingly, quantification of the relative abundance of both isoforms shows a predominance of the short Δ9 form of Ric-8B in all assayed tissues, but more markedly so in taste tissues, especially foliate and fungiform papillae (**Figure 1D**).

Prior to performing qPCR the specificity of all quantitative primer pairs were tested by conventional PCR to confirm the amplification of a single product of the expected size and the absence of primer-dimers (**Figure 1E**). Moreover each qPCR experiment was immediately followed by melt curve analysis for each sample to ensure amplification specificity. The primers used for differential amplification of the various Ric-8B splice variants were located at the exon-exon boundaries (**Figure 1F**).

EXPRESSION OF Ric-8A AND Ric-8B IN TASTE PAPILLAE IS CONFINED TO TASTE BUD CELLS

We next determined whether Ric-8A and Ric-8B gene expression in taste papillae is confined to the taste bud cells. To do this, we conducted *in situ* hybridization experiments on sections of circumvallate papillae using probes specific for Ric-8A or Ric-8B.

Figures 2A,B show that Ric-8A and Ric-8B mRNAs are found in cells confined within the taste buds when compared with the expression pattern of gustducin, a taste bud specific G-protein (**Figure 2C**). Although Ric-8B mRNA is clearly very abundant in taste buds we also noticed some staining in the basal layer of the tongue epidermis. This data is in line with an earlier study reporting the presence of Ric-8B messenger RNA in a human taste buds cDNA library (Rossier et al., 2004).

Using antibodies directed against Ric-8A (**Figure 2D**) or Ric-8B (**Figure 2E**) confirms that the labeling is more intense within the taste buds than in the surrounding tissue and very similar to what is observed for gustducin (**Figure 2F**). To test the specificity of the antibodies against the Ric-8 proteins we performed a Western blotting analysis with protein extracts of taste bud-enriched tissue and surrounding tissue from mouse circumvallate papillae. As shown in **Figure 2G**, the antibody against Ric-8A detected a major band at ~70 kDa while the Ric-8B antibody detected a major band of ~88 kDa. It is worth noting that the band is significantly stronger in taste bud-enriched tissue than in surrounding tongue tissue thus corroborating the staining pattern obtained in immunohistochemistry experiments. The size of the Ric-8A and Ric-8B bands are about 7 and 25 kDa bigger than the predicted molecular weight respectively indicating that these proteins likely undergo posttranslational modifications in this tissue. A similar observation has already been made in olfactory epithelium for Ric-8B (Kerr et al., 2008).

Ric-8A AND Ric-8B ARE CO-LOCALIZED WITH IP3R-3 IN TYPE II TASTE BUD CELLS

Taste bud cells are divided in at least four distinct cell types, which can be distinguished by the expression of specific markers. To analyze what type or subset of taste cells expresses Ric-8A and Ric-8B we performed double immunolabeling using an antibody specific to either Ric-8A or Ric-8B together with an antibody raised against IP3R-3, a marker of type II cells staining sweet, umami and bitter taste receptor cells. Our results (**Figure 3A**) show that 100% of IP3R-3 positive cells are stained with Ric-8A or Ric-8B (**Figure 3A** merge). The presence of Ric-8A and Ric-8B in taste-GPCR expressing cells is consistent with a role in taste transduction.

Additionally we find that a subpopulation (~15%) of taste bud cells is immunopositive for Ric-8A or Ric-8B but negative for IP3R-3 ($n = 100$). The nature of these cells remains to be determined.

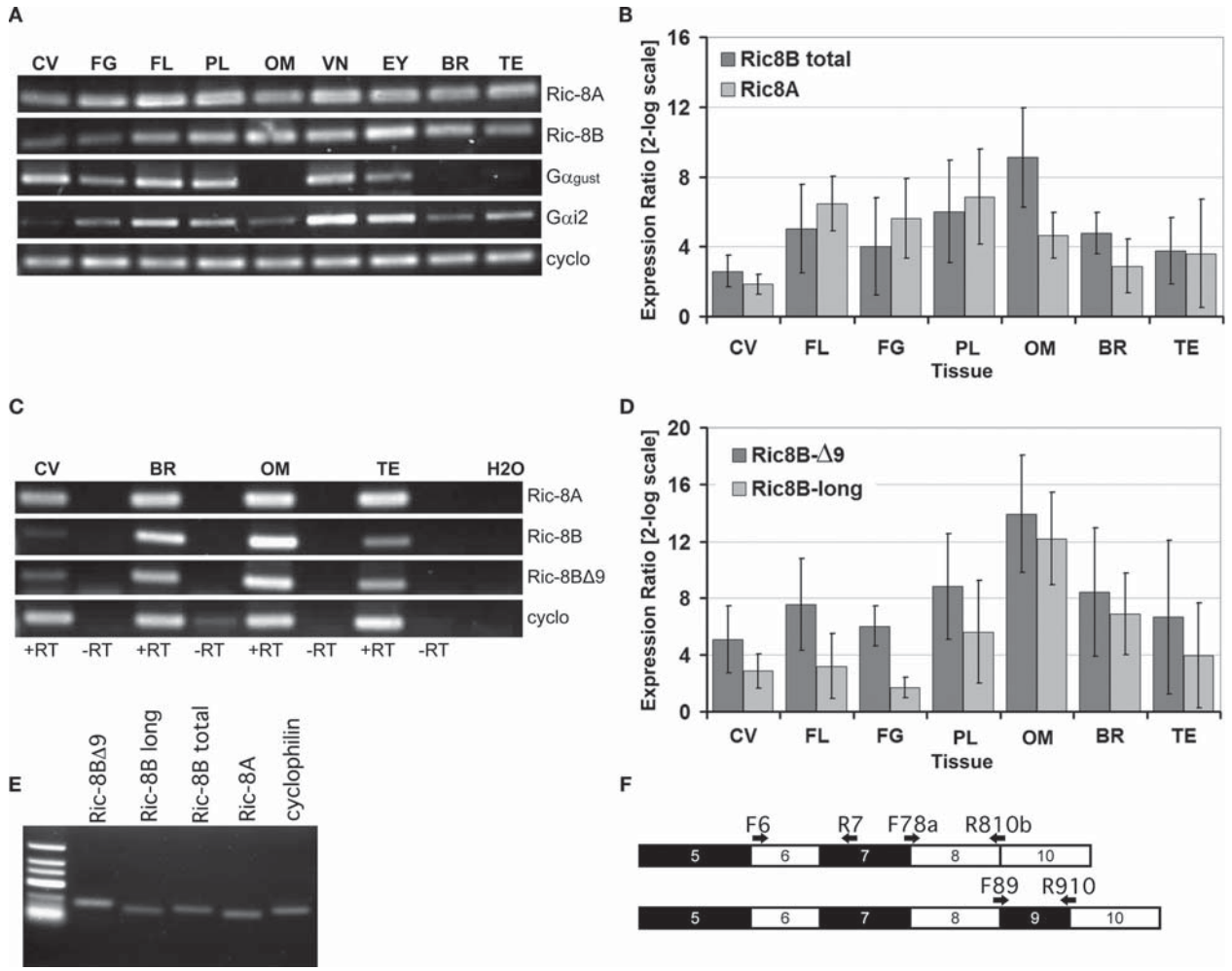

FIGURE 1 | Ric-8A and Ric-8B variants are expressed in tongue taste papillae. (A) RT-PCR on total RNA from various tissues using specific primers for Ric-8A, Ric-8B, gustducin, Gαi2 and cyclophilin. CV: circumvallate papillae, FG: fungiform papillae, FL: foliate papillae, PL: Palate, OM: olfactory mucosa, VN: vomeronasal organ, EY: Eye, BR: whole brain, TE: testis. **(B)** q-PCR showing the relative abundance of Ric-8B (both variants) and Ric-8A. Ric-8A is predominantly expressed over Ric-8B in palate, foliate and fungiform papillae but not in circumvallate papillae. **(C)** RT-PCR on a restricted panel of mRNAs using specific primers for Ric-8A, Ric-8B (long variant only), Ric-8BΔ9 only. For each tissue +RT: with Reverse transcriptase, -RT: without reverse transcriptase. CV: circumvallate papillae, BR: whole brain, OM: olfactory mucosa, TE: testis. **(D)** q-PCR showing the relative abundance of Ric-8B splicing variants. Ric-8BΔ9 is the major variant in palate, foliate and fungiform papillae but not in circumvallate papillae. **(E)** RT-PCR on brain RNA with the various primer pairs used for q-PCR. Note the presence of a single band of the expected size and the absence of primer-dimers for each primer pair tested, thus validating them for SYBR green q-PCR. **(F)** Scheme showing the strategy of amplification of the two Ric-8B isoforms. Black and white rectangles denote coding exons in the Ric-8B gene and black arrows the location of the primers used. Primer pair F6-R7 amplifies both Ric-8B isoforms (Ric-8B total). Primer pair F78a-R810b amplifies the Ric-8BΔ9 isoform only (Ric-8BΔ9) while primer pair F89-R910 amplifies the Ric-8B long form only (Ric-8B long). Primer F78a anneals to both isoforms but this is corrected by taking primer pair efficiency into account in the calculation of the ratio.

The matching expression patterns of Ric-8A and Ric-8B which are both found in 100% of IP3R-3 positive cells suggest that they might be co-expressed in these cells, a prospect that we could not test directly given the fact that both antibodies against Ric-8A and Ric-8B are raised in rabbit. Nevertheless, to rule out the possibility that this pattern could be generated by cross-reactivity of the antibodies with the paralogous proteins a western blotting analysis testing the specificity of the antibodies against the two Flag-tagged recombinant Ric-8 proteins transiently expressed in HEK 293T cells was conducted. As seen in **Figure 3B** no cross-reactivity was detected thus supporting the notion that these two proteins might be co-expressed.

Ric-8A INTERACTS WITH ALPHA-GUSTDUCIN AND ALPHA-TRANSDUCIN

Because a large percentage of IP3R-3 cells expresses gustducin (Clapp et al., 2001), we used a directed two-hybrid interaction screen to investigate whether Ric-8A or Ric-8B can interact directly with gustducin.

We initially validated our assay by testing the previously reported interaction between Ric-8A and Gai2 as well as that between Ric-8B and Gαolf (Tall et al., 2003; Von Dannecker et al., 2005).

Figure 4A shows that, as expected, Ric-8A strongly interacts with Gαi2 but not with G*αolf*. More importantly we find that Gαt2 and to a lesser extent gustducin also interact with Ric-8A.

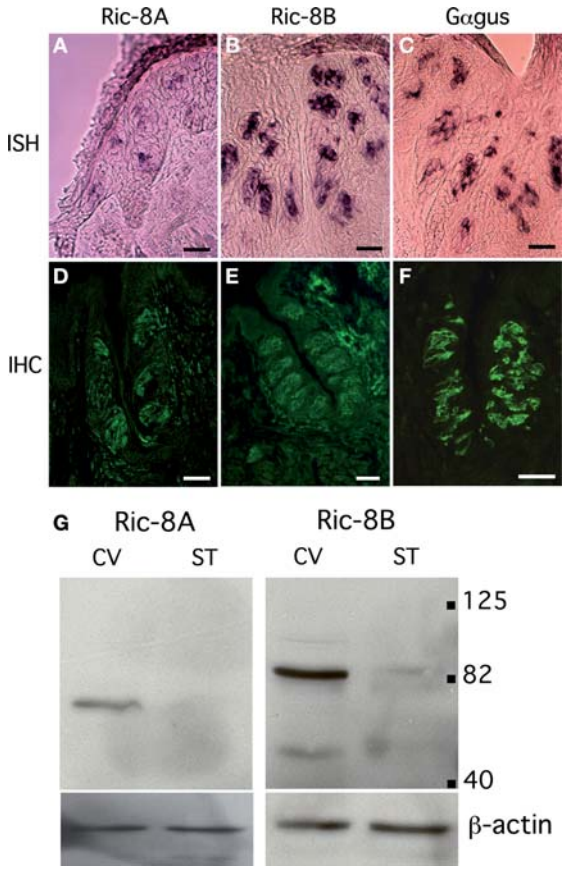

FIGURE 2 |The expression of Ric-8A and Ric-8B is confined to taste bud cells. (A–C) Sagittal sections of circumvallate papillae were hybridized with antisense probes to Ric-8A, Ric-8B or gustducin and visualized with an alkaline phosphatase colorimetric reaction. The purple signal is confined to taste buds. Section hybridized to the sense probes did not show any signal (not shown). (Scale bar = 50 μm). **(D–F)** Immunostaining of sagittal sections of circumvallate papillae using anti-Ric-8A, anti-Ric-8B or anti-gustducin rabbit polyclonal antibodies visualized with an anti-rabbit-Alexa488 secondary. The immunofluorescence is confined to the taste buds and labels 100% of taste buds. (Scale bar = 50 μm). **(G)** Western blotting analysis of circumvallate papillae (CV) or surrounding tissue (ST) extracts using anti-Ric-8A and Ric-8B antibodies. A major band around 70 kDa for Ric-8A and ~88 kDa for Ric-8B is detected in CV indicating that these proteins are concentrated in taste buds. Bottom panels show β-actin loading controls. [Right margin: molecular weight marker bands (kDa)].

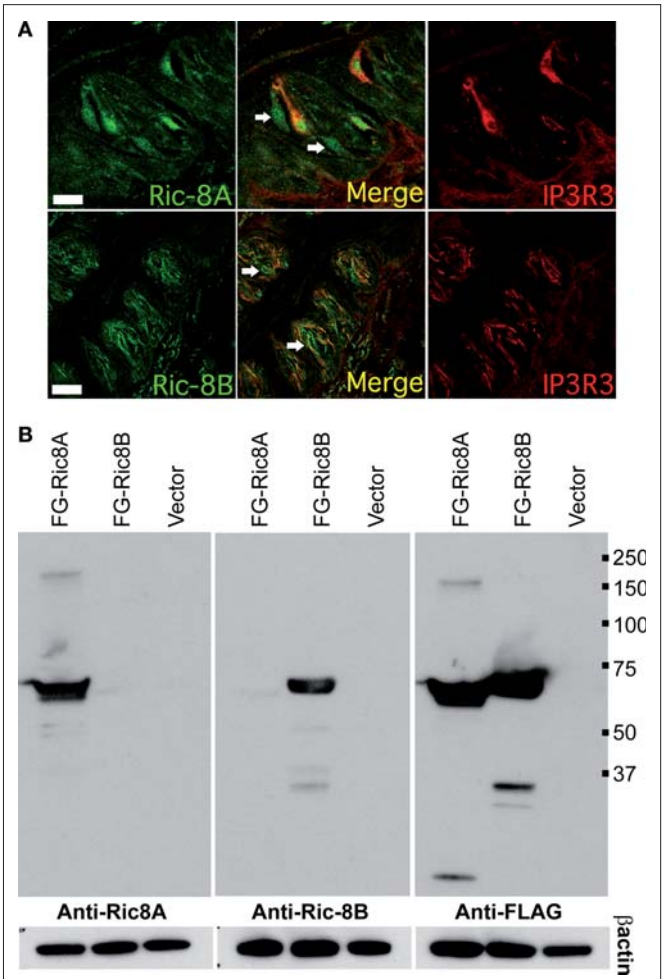

FIGURE 3 | Ric-8 expression is not strictly confined to type II taste bud cells. (A) Double labeling immunohistochemistry on sagittal sections of circumvallate papillae using an antibody raised against IP3R-3 visualized with an Alexa555 coupled secondary antibody (red) and either an anti-Ric-8A (top row) or anti-Ric-8B (bottom row) antibody visualized with an Alexa488 secondary antibody (green). Middle panels are merged images showing co-localization. All IP3R-3 cells display Ric-8A and Ric-8B labeling but not all Ric-8A or Ric-8B cells are positive for IP3R-3 (white arrows) indicating that Ric-8A and Ric-8B expression extends to other cells beside IP3R-3 positive cells. (Scale bar top row = 20 μm; bottom row = 40 μm). **(B)** Western blotting analysis of whole cell lysates from cells transiently transfected with either Flag-Ric-8A (FG-Ric8A), Flag-Ric-8B (FG-Ric8B) or the expression vector alone (Vector) using anti-Ric-8A (left panel), anti-Ric-8B (middle panel) or anti-Flag (right panel) antibodies. A single band around 64 kDa for recombinant Flag-Ric-8A and ~71 kDa for Flag-Ric-8B is detected in HEK 293T cells thus clearly showing that Ric-8 antibodies do not cross-react with the paralogous protein. Bottom panels show β-actin loading controls. [Right margin: molecular weight marker bands (kDa)].

Under the same conditions and as expected Ric-8B clearly interacts with Gα*olf* but not with Gαi2. We also observe a weak interaction with Gαt2 but none with gustducin. Ric-8BΔ9 was also included in the screen but no substantial interaction was detected (**Table 1**).

As a control for the strength of the interaction several RGS (i.e. RGS2, RGS9 and RGS21) were also tested for their ability to interact with gustducin in the same assay. Our results confirm that RGS21 physically interacts with the constitutively activated form of gustducin (QL) as previously reported using a different test (von Buchholtz et al., 2004), whereas Ric-8A is likely to interact with gustducin in its GDP-bound form as we find no interaction with the GTPase deficient Gαgus QL.

Next we validated these interactions in an heterologous expression system involving transient transfection of 5′-Flag-tagged-Ric-8 and 5′-HA-tagged-Gα-proteins expression constructs in HEK 293T cells followed by immunoprecipitation using an anti-Flag antibody. The results of this assay essentially corroborate the results obtained in yeast: Ric-8A interacts strongly with Gαi2 and Gαt2, and to a lesser extent with gustducin, while Ric-8B interacts weakly with Gαt2 but not with gustducin (**Figure 4B**). Taken

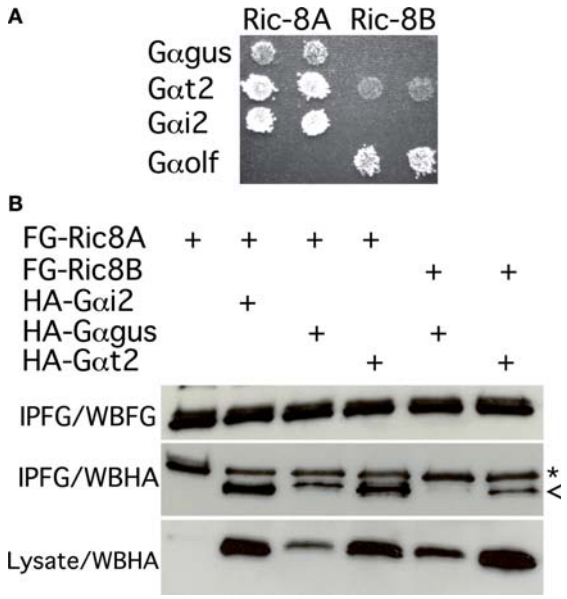

FIGURE 4 | Gustducin interacts with Ric-8A, but not Ric-8B. (A) Yeast two hybrid interaction assay. Mav203 yeasts cells were co-transformed with different combinations of bait (Gαolf, Gαt2, Gαgus or Gαi2) and prey (Ric-8A or Ric-8B) plasmids. Interaction was scored on minimal medium plates containing 3-AT and lacking histidine and tryptophan. Growth reflects the strength of the interaction. **(B)** Co-immunoprecipitation experiment showing the association between Flag-Ric-8A and HA-Gαi2 or HA-Gαgus. (*) denotes an artifact band (IgG) while (<) correspond to the Gα subunit band. IPFG: immunoprecipitation using an anti-Flag antibody; WBFG: western blotting membrane incubated with an anti-Flag antibody; WBHA: western blotting membrane incubated an anti-HA antibody.

Table 1 | Search for modulators of G-protein signaling in taste papillae.

Prey	Bait					
	Gαgus	Gαgus QL	Gαt2	Gαi2	Gαolf	Gs
Ric-8A	++		+++	++++		
Ric-8B			+		++++	+++
Ric-8BD9			+			
AGS1						
AGS2						
AGS3 (GPR1-4)			+	++++		
AGS4			+			
PBP						
Pins/LGN (GoLoco)				+++		+
RGS2						
RGS9 (RGS)						
RGS21		+				

Interaction between various modulators of G-protein signaling and G-protein alpha subunits was tested using the Proquest yeast two-hybrid system. Interaction was scored on minimal medium plates containing 25 mM 3-AT and lacking leucine histidine and tryptophan. Growth represented by stars in the table reflects the strength of the interaction. + weak, ++ moderate, +++ strong, ++++ very strong. Note that AGS3 and PBP interact strongly with Gαi2 as previously reported (Bernard et al., 2001) however except for Ric-8A none of the proteins tested interacts with gustducin under these conditions.

together these results strongly suggest that in taste buds Gαt2, and the abundantly represented gustducin and Gαi2, which have been reported to couple to taste receptors (Ueda et al., 2003) are the most likely targets of Ric-8A in this tissue.

Ric-8A AMPLIFIES THE SIGNAL DOWNSTREAM OF hTas2R16

In a previous study it was shown that Ric-8B is particularly abundant in the olfactory sensory neurons where it acts as a signal amplifier for G-protein mediated signaling cascades (Von Dannecker et al., 2005, 2006). To test the possibility that Ric-8A's expression in taste receptor cells plays a similar role in taste transduction we focused our study on hTas2R16, the human receptor for the bitter tastant salicin that was previously reported to be coupled to Gαi2 as well as Gαt2 (Ueda et al., 2003).

To monitor the effect of hTas2R16 stimulation on intracellular cAMP levels we devised an heterologous expression system in HEK 293T cells involving transient co-transfection of the dopamine D1 receptor (D1R) which is known to be coupled to Gαs, together with hTas2R16 and Gαi2. Intracellular cAMP levels were monitored by a reporter enzyme (secreted alkaline phosphatase, SEAP) under the control of CRE.

In this system stimulation of the dopamine D1R receptor with dopamine triggers a rise of intracellular cAMP which is reduced in a dose depend way by stimulation of hTas2R16 with salicin (**Figure 5**). Next we tested whether co-expression with Ric-8A affects the activity of hTas2R16. To do so HEK 293T cells were transiently transfected with D1R, hTas2R16, Gai2 and Ric-8A or a control expression construct. Upon stimulation of the cells with 10 μM dopamine and either 5 or 10 mM salicin, a dose dependent reduction in the cAMP levels was recorded (**Figure 5**). The magnitude of this reduction (~35%) was statistically significant between Ric-8A transfected versus transfected cells without Ric-8A vector suggesting that Ric-8A is able to promote hTas2R16 activity. Since this reduction in cAMP accumulation was

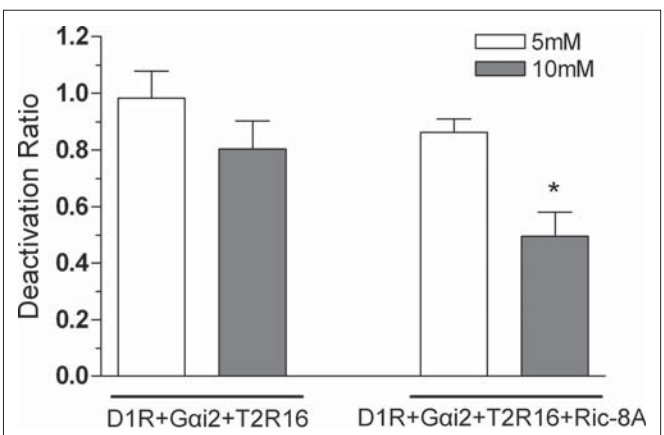

FIGURE 5 | Ric-8A enhances Gαi2 mediated decreases in cAMP concentration. Production of cAMP was measured in HEK 293T cells transfected with D1R, Tas2R16, Gαi2 with or without Ric-8A in the presence of 10 μM dopamine, or 10 μM dopamine plus 5 (white bars) or 10 mM (grey bars) salicin as indicated. The graph shows the mean and SD values of four independent experiments. The deactivation ratio is calculated by dividing values after a dopamine + salicin stimulation by the corresponding dopamine activation values. For 10 mM salicin Ric-8A enhancement of Gαi2 mediated deactivation was statistically significant. (*) $p < 0.05$, Paired Student's *t*-test.

stronger in cells transfected with Gαi2 than in cells which did not overexpress Gαi2 (data not shown) we conclude that Ric-8A is able to amplify hTas2R16 signal transduction through Gαi2.

DISCUSSION

In taste cells two main families of GPCRs are involved in tastant detection and transduction. The Tas1Rs which recognize sweet and umami compounds and the Tas2Rs which are tuned to bitter compounds (Chandrashekar et al., 2006). Upon stimulation with a tastant the receptor activates an heterotrimeric G-protein consisting of a Gα subunit and a Gβγ dimer. During that step the receptor bound Gα subunit undergoes an exchange of GDP for GTP which leads to the release of the GTP-Gα subunit from the Gβγ dimer. Both components are then capable of modulating effectors independently based on their affinity for that effector. This reaction can be further amplified by non GPCR GDP/GTP exchange factors which are specific for certain Gα subunits. The composition of the G-proteins coupled to the various GPCRs involved in taste detection is therefore germane to determining which signal transduction pathway is activated and how it might be regulated. Several studies have investigated the importance of G-proteins in taste transduction or the coupling of Tas1Rs and Tas2Rs to G-proteins. The report that knock-out mice for Gα-gustducin have diminished but not abolished sensitivity to sweet and bitter compounds (Wong et al., 1996) which can be rescued by Gα-transducin expression together with heterologous expression studies showing that Gαgus is able to couple to the Tas1Rs and Tas2Rs are consistent with an important role of this G-protein in taste signal transduction (Li et al., 2002; Ueda et al., 2003; Sainz et al., 2007b). Here we report for the first time that Gαgus and Gαt2 physically interact with Ric-8A a GDP/GTP exchange factor expressed in type II taste cells. In addition we show that Ric-8A is able to amplify Tas2R16 signaling through Gαi2. Interestingly, Tas2Rs have been reported to couple to all three Gα subunits interacting with Ric-8A namely Gαgus, Gαi2 and Gαt2 (Chandrashekar et al., 2000; Ueda et al., 2003; Sainz et al., 2007a). Therefore we anticipate that Ric-8A might be a general modulator of bitter GPCR signaling (**Figure 6**).

Furthermore, we show that Ric-8A is expressed in all IP3R-3 positive taste bud cells, a good portion of which have been reported to be type II or taste receptor cells in mice (Clapp et al., 2001). This finding and the fact that IP3R-3 links PLC-β2 signaling with bitter receptors support this argument. Note that some IP3R-3 positive cells have also been reported to express markers specific for type III cells such as SNAP-25 a synaptic protein found in mouse taste buds (DeFazio et al., 2006); since we report that 100% of IP3R-3 positive cells are also positive for Ric-8A its function in these cell types may be linked to GPCRs present in these cells. Gαgus and Gαi have been shown to couple to Tas1Rs (Li et al., 2002; Ozeck et al., 2004; Sainz et al., 2007b) and Gαt1 to play a role in behavioral and electrophysiological taste responses to umami (He et al., 2004); it is therefore plausible that Ric-8A might amplify the signaling of these receptors as well.

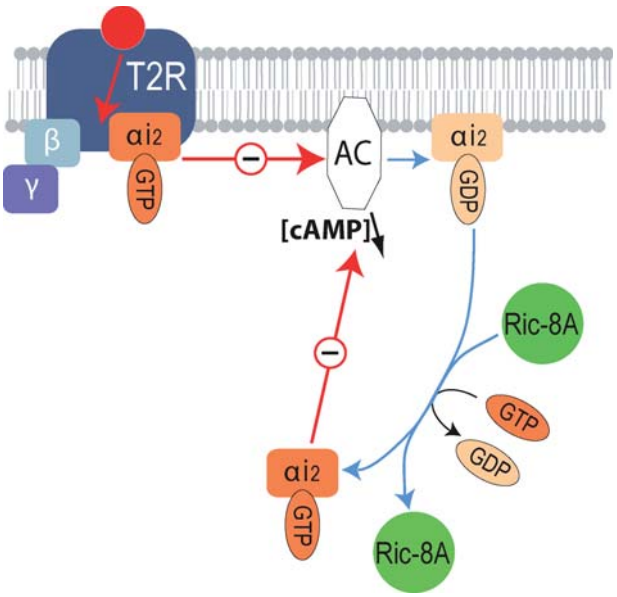

FIGURE 6 | Molecular mechanisms underlying the modulation of bitter receptor signaling by Ric-8A. Diagram illustrating the signaling cascade downstream of bitter taste GPCR (T2R) modulated by Ric-8A. Upon activation of T2R the receptor coupled heterotrimeric G-protein separates into Gα-GTP and Gβγ, Gα-GTP will then inhibit the activity of adenylyl cyclase, subsequently the GTP bound to Gα will be hydrolyzed into GDP, Gα-GDP can then reassociate with Gγβ or interact with Ric-8A. By supporting the exchange of GDP by GTP, the GEF activity of Ric-8A will allow a new cycle of inhibition of the effector thus enhancing the signal.

Previous work reporting an interaction between Ric-8B and Gγ13 (Kerr et al., 2008) or Gαq (Tall et al., 2003), both found in taste bud cells (Kusakabe et al., 1998; Huang et al., 1999) together with our data showing that it is present in all IP3R-3 positive cells suggest that Ric-8B may effect G-protein signaling in these cells. One intriguing prospect involves a possible interaction with Gα14 a G-protein recently reported as co-expressed with the sweet taste receptor (Tas1R2–Tas1R3) (Shindo et al., 2008; Tizzano et al., 2008). These possibilities and its precise role in taste cells remain to be investigated.

ACKNOWLEDGMENTS

We would like to thank Drs. V. Dionne (Boston University) and S. Simon (Duke University) for critical reading of the manuscript as well as C. Arnould and A. Gaudin for help with the confocal microscope. This work was supported by an Action Thematique Incitative sur Programme (CNRS) grant to Jean-Pierre Montmayeur, Région de Bourgogne post-doctoral fellowships to Lila Patrikainen and Zhenhui Liu as well as funds from GOSPEL to Fabienne Laugerette. Bettina Malnic and Daniel S. Kerr are supported by funds from FAPESP and CAPES.

REFERENCES

Adler, E., Hoon, M. A., Mueller, K. L., Chandrashekar, J., Ryba, N. J., and Zuker, C. S. (2000). A novel family of mammalian taste receptors. *Cell* 100, 693–702.

Avenet, P., Hofmann, F., and Lindemann, B. (1988). Transduction in taste receptor cells requires cAMP-dependent protein kinase. *Nature* 331, 351–354.

Bernard, M. L., Peterson, Y. K., Chung, P., Jourdan, J., and Lanier, S. M. (2001). Selective interaction of AGS3 with G-proteins and the influence of AGS3 on the activation state of G-proteins. *J. Biol. Chem.* 276, 1585–1593.

Chandrashekar, J., Hoon, M. A., Ryba, N. J., and Zuker, C. S. (2006). The receptors and cells for mammalian taste. *Nature* 444, 288–294.

Chandrashekar, J., Mueller, K. L., Hoon, M. A., Adler, E., Feng, L., Guo, W., Zuker, C. S., and Ryba, N. J. (2000). T2Rs function as bitter taste receptors. *Cell* 100, 703–711.

Clapp, T. R., Stone, L. M., Margolskee, R. F., and Kinnamon, S. C. (2001).

Immunocytochemical evidence for co-expression of Type III IP3 receptor with signaling components of bitter taste transduction. *BMC Neurosci.* 2, 6.

DeFazio, R. A., Dvoryanchikov, G., Maruyama, Y., Kim, J. W., Pereira, E., Roper, S. D., and Chaudhari, N. (2006). Separate populations of receptor cells and presynaptic cells in mouse taste buds. *J. Neurosci.* 26, 3971–3980.

Durocher, Y., Perret, S., Thibaudeau, E., Gaumond, M. H., Kamen, A., Stocco, R., and Abramovitz, M. (2000). A reporter gene assay for high-throughput screening of G-protein-coupled receptors stably or transiently expressed in HEK293 EBNA cells grown in suspension culture. *Anal. Biochem.* 284, 316–326.

He, W., Yasumatsu, K., Varadarajan, V., Yamada, A., Lem, J., Ninomiya, Y., Margolskee, R. F., and Damak, S. (2004). Umami taste responses are mediated by alpha-transducin and alpha-gustducin. *J. Neurosci.* 24, 7674–7680.

Hoon, M. A., Adler, E., Lindemeier, J., Battey, J. F., Ryba, N. J., and Zuker, C. S. (1999). Putative mammalian taste receptors: a class of taste-specific GPCRs with distinct topographic selectivity. *Cell* 96, 541–551.

Huang, L., Shanker, Y. G., Dubauskaite, J., Zheng, J. Z., Yan, W., Rosenzweig, S., Spielman, A. I., Max, M., and Margolskee, R. F. (1999). Ggamma13 colocalizes with gustducin in taste receptor cells and mediates IP3 responses to bitter denatonium. *Nat. Neurosci.* 2, 1055–1062.

Jean-Baptiste, G., Yang, Z., and Greenwood, M. T. (2006). Regulatory mechanisms involved in modulating RGS function. *Cell. Mol. Life Sci.* 63, 1969–1985.

Kerr, D. S., Von Dannecker, L. E., Davalos, M., Michaloski, J. S., and Malnic, B. (2008). Ric-8B interacts with G alpha olf and G gamma 13 and co-localizes with G alpha olf, G beta 1 and G gamma 13 in the cilia of olfactory sensory neurons. *Mol. Cell. Neurosci.* 38, 341–348.

Klattenhoff, C., Montecino, M., Soto, X., Guzman, L., Romo, X., Garcia, M. A., Mellstrom, B., Naranjo, J. R., Hinrichs, M. V., and Olate, J. (2003). Human brain synembryn interacts with Gsalpha and Gqalpha and is translocated to the plasma membrane in response to isoproterenol and carbachol. *J. Cell Physiol.* 195, 151–157.

Kusakabe, Y., Yamaguchi, E., Tanemura, K., Kameyama, K., Chiba, N., Arai, S., Emori, Y., and Abe, K. (1998). Identification of two alpha-subunit species of GTP-binding proteins, Galpha15 and Galphaq, expressed in rat taste buds. *Biochim. Biophys. Acta* 1403, 265–272.

Kusakabe, Y., Yasuoka, A., Asano-Miyoshi, M., Iwabuchi, K., Matsumoto, I., Arai, S., Emori, Y., and Abe, K. (2000). Comprehensive study on G protein alpha-subunits in taste bud cells, with special reference to the occurrence of Galphai2 as a major Galpha species. *Chem. Senses* 25, 525–531.

Li, X., Staszewski, L., Xu, H., Durick, K., Zoller, M., and Adler, E. (2002). Human receptors for sweet and umami taste. *Proc. Natl. Acad. Sci. U.S.A.* 99, 4692–4696.

Matsunami, H., Montmayeur, J. P., and Buck, L. B. (2000). A family of candidate taste receptors in human and mouse. *Nature* 404, 601–604.

McLaughlin, S. K., McKinnon, P. J., and Margolskee, R. F. (1992). Gustducin is a taste-cell-specific G protein closely related to the transducins. *Nature* 357, 563–569.

Neitzel, K. L., and Hepler, J. R. (2006). Cellular mechanisms that determine selective RGS protein regulation of G protein-coupled receptor signaling. *Semin. Cell Dev. Biol.* 17, 383–389.

Nelson, G., Chandrashekar, J., Hoon, M. A., Feng, L., Zhao, G., Ryba, N. J., and Zuker, C. S. (2002). An amino-acid taste receptor. Nature 416, 199–202.

Nelson, G., Hoon, M. A., Chandrashekar, J., Zhang, Y., Ryba, N. J., and Zuker, C. S. (2001). Mammalian sweet taste receptors. *Cell* 106, 381–390.

Nishiguchi, K. M., Sandberg, M. A., Kooijman, A. C., Martemyanov, K. A., Pott, J. W., Hagstrom, S. A., Arshavsky, V. Y., Berson, E. L., and Dryja, T. P. (2004). Defects in RGS9 or its anchor protein R9AP in patients with slow photoreceptor deactivation. *Nature* 427, 75–78.

Nishimura, A., Okamoto, M., Sugawara, Y., Mizuno, N., Yamauchi, J., and Itoh, H. (2006). Ric-8A potentiates Gq-mediated signal transduction by acting downstream of G protein-coupled receptor in intact cells. *Genes Cells* 11, 487–498.

Oldham, W. M., and Hamm, H. E. (2008). Heterotrimeric G protein activation by G-protein-coupled receptors. *Nat. Rev. Mol. Cell Biol.* 9, 60–71.

Ozeck, M., Brust, P., Xu, H., and Servant, G. (2004). Receptors for bitter, sweet and umami taste couple to inhibitory G protein signaling pathways. *Eur. J. Pharmacol.* 489, 139–149.

Pfaffl, M. W. (2001). A new mathematical model for relative quantification in real-time RT-PCR. *Nucleic Acids Res.* 29, e45.

Pfaffl, M. W., Horgan, G. W., and Dempfle, L. (2002). Relative expression software tool (REST) for group-wise comparison and statistical analysis of relative expression results in real-time PCR. *Nucleic Acids Res.* 30, e36.

Rossier, O., Cao, J., Huque, T., Spielman, A. I., Feldman, R. S., Medrano, J. F., Brand, J. G., and le Coutre, J. (2004). Analysis of a human fungiform papillae cDNA library and identification of taste-related genes. *Chem. Senses* 29, 13–23.

Sainz, E., Cavenagh, M. M., Gutierrez, J., Battey, J. F., Northup, J. K., and Sullivan, S. L. (2007a). Functional characterization of human bitter taste receptors. *Biochem. J.* 403, 537–543.

Sainz, E., Cavenagh, M. M., LopezJimenez, N. D., Gutierrez, J. C., Battey, J. F., Northup, J. K., and Sullivan, S. L. (2007b). The G-protein coupling properties of the human sweet and amino acid taste receptors. *Dev. Neurobiol.* 67, 948–959.

Shindo, Y., Miura, H., Carninci, P., Kawai, J., Hayashizaki, Y., Ninomiya, Y., Hino, A., Kanda, T., and Kusakabe, Y. (2008). G alpha14 is a candidate mediator of sweet/umami signal transduction in the posterior region of the mouse tongue. *Biochem. Biophys. Res. Commun.* 376, 504–508.

Siderovski, D. P., and Willard, F. S. (2005). The GAPs, GEFs, and GDIs of heterotrimeric G-protein alpha subunits. *Int. J. Biol. Sci.* 1, 51–66.

Sinnarajah, S., Dessauer, C. W., Srikumar, D., Chen, J., Yuen, J., Yilma, S., Dennis, J. C., Morrison, E. E., Vodyanoy, V., and Kehrl, J. H. (2001). RGS2 regulates signal transduction in olfactory neurons by attenuating activation of adenylyl cyclase III. *Nature* 409, 1051–1055.

Tall, G. G., and Gilman, A. G. (2005). Resistance to inhibitors of cholinesterase 8A catalyzes release of Galphai-GTP and nuclear mitotic apparatus protein (NuMA) from NuMA/LGN/Galphai-GDP complexes. *Proc. Natl. Acad. Sci. U.S.A.* 102, 16584–16589.

Tall, G. G., Krumins, A. M., and Gilman, A. G. (2003). Mammalian Ric-8A (synembryn) is a heterotrimeric Galpha protein guanine nucleotide exchange factor. *J. Biol. Chem.* 278, 8356–8362.

Thomas, C. J., Tall, G. G., Adhikari, A., and Sprang, S. R. (2008). Ric-8A catalyzes guanine nucleotide exchange on G alphai1 bound to the GPR/GoLoco exchange inhibitor AGS3. *J. Biol. Chem.* 283, 23150–23160.

Tizzano, M., Dvoryanchikov, G., Barrows, J. K., Kim, S., Chaudhari, N., and Finger, T. E. (2008). Expression of Galpha14 in sweet-transducing taste cells of the posterior tongue. *BMC Neurosci.* 9, 110.

Tonosaki, K., and Funakoshi, M. (1988). Cyclic nucleotides may mediate taste transduction. *Nature* 331, 354–356.

Ueda, T., Ugawa, S., Yamamura, H., Imaizumi, Y., and Shimada, S. (2003). Functional interaction between T2R taste receptors and G-protein alpha subunits expressed in taste receptor cells. *J. Neurosci.* 23, 7376–7380.

von Buchholtz, L., Elischer, A., Tareilus, E., Gouka, R., Kaiser, C., Breer, H., and Conzelmann, S. (2004). RGS21 is a novel regulator of G protein signalling selectively expressed in subpopulations of taste bud cells. *Eur. J. Neurosci.* 19, 1535–1544.

Von Dannecker, L. E., Mercadante, A. F., and Malnic, B. (2005). Ric-8B, an olfactory putative GTP exchange factor, amplifies signal transduction through the olfactory-specific G-protein Galphaolf. *J. Neurosci.* 25, 3793–3800.

Von Dannecker, L. E., Mercadante, A. F., and Malnic, B. (2006). Ric-8B promotes functional expression of odorant receptors. *Proc. Natl. Acad. Sci. U.S.A.* 103, 9310–9314.

Wilkie, T. M., and Kinch, L. (2005). New roles for Galpha and RGS proteins: communication continues despite pulling sisters apart. *Curr. Biol.* 15, R843–R854.

Wong, G. T., Gannon, K. S., and Margolskee, R. F. (1996). Transduction of bitter and sweet taste by gustducin. *Nature* 381, 796–800.

Zhao, G. Q., Zhang, Y., Hoon, M. A., Chandrashekar, J., Erlenbach, I., Ryba, N. J., and Zuker, C. S. (2003). The receptors for mammalian sweet and umami taste. *Cell* 115, 255–266.

Conflict of Interest Statement: The authors declare that the research was conducted in the absence of any commercial or financial relationships that could be construed as a potential conflict of interest.

Received: 18 May 2009; paper pending published: 17 June 2009; accepted: 22 September 2009; published online: 08 October 2009.

*Citation: Fenech C, Patrikainen L, Kerr DS, Grall S, Liu Z, Laugerette F, Malnic B and Montmayeur J-P (2009) Ric-8A, a Gα protein guanine nucleotide exchange factor potentiates taste receptor signaling. Front. Cell. Neurosci. **3**:11. doi: 10.3389/neuro.03.011.2009*

Copyright © 2009 Fenech, Patrikainen, Kerr, Grall, Liu, Laugerette, Malnic and Montmayeur. This is an open-access article subject to an exclusive license agreement between the authors and the Frontiers Research Foundation, which permits unrestricted use, distribution, and reproduction in any medium, provided the original authors and source are credited.

frontiers in
CELLULAR NEUROSCIENCE

ORIGINAL RESEARCH ARTICLE
published: 21 June 2012
doi: 10.3389/fncel.2012.00026

Identification of new binding partners of the chemosensory signaling protein Gγ13 expressed in taste and olfactory sensory cells

Zhenhui Liu[1†‡], Claire Fenech[1‡], Hervé Cadiou[2†], Sylvie Grall[1], Esmerina Tili[1†], Fabienne Laugerette[3], Anna Wiencis[3], Xavier Grosmaitre[2] and Jean-Pierre Montmayeur[1,3]*

[1] *Chemosensory Perception, Centre des Sciences du Goût et de l'Alimentation, UMR-6265 CNRS, UMR-1324 INRA, Dijon, France*
[2] *Functional Plasticity of Olfactory Neurons, Centre des Sciences du Goût et de l'Alimentation, UMR-6265 CNRS, UMR-1324 INRA, Dijon, France*
[3] *General Olfaction and Sensing Program on a European Level, Centre des Sciences du Goût et de l'Alimentation, UMR-6265 CNRS, UMR-1324 INRA, Dijon, France*

Edited by:
Dieter Wicher, Max Planck Institute for Chemical Ecology, Germany

Reviewed by:
Monika Stengl, Universität Kassel, Germany
Yuanquan Song, University of California San Francisco, USA

***Correspondence:**
Jean-Pierre Montmayeur, Chemosensory Perception, Unités Mixtes de Recherche, Centre des Sciences du Goût, 9E Boulevard J. D'Arc, 21000 Dijon, France.
e-mail: jean-pierre.montmayeur@u-bourgogne.fr

†Present address:
Zhenhui Liu, Marine Life College, Ocean University of China, 5 Yushan Road, 266003 Qingdao, China.
Hervé Cadiou, Nociception and Pain Department, Institut des Neurosciences Cellulaires et Intégratives (INCI), CNRS UPR3212, 5 Rue Blaise Pascal, F-67084 Strasbourg, France.
Esmerina Tili, Ohio State University, Comprehensive Cancer Center, 460 West 12th Ave, BRT 1060, Columbus, OH 43201, USA.

‡*These authors contributed equally to this work.*

Tastant detection in the oral cavity involves selective receptors localized at the apical extremity of a subset of specialized taste bud cells called taste receptor cells (TRCs). The identification of the genes coding for the taste receptors involved in this process have greatly improved our understanding of the molecular mechanisms underlying detection. However, how these receptors signal in TRCs, and whether the components of the signaling cascades interact with each other or are organized in complexes is mostly unexplored. Here we report on the identification of three new binding partners for the mouse G protein gamma 13 subunit (Gγ13), a component of the bitter taste receptors signaling cascade. For two of these Gγ13 associated proteins, namely GOPC and MPDZ, we describe the expression in taste bud cells for the first time. Furthermore, we demonstrate by means of a yeast two-hybrid interaction assay that the C terminal PDZ binding motif of Gγ13 interacts with selected PDZ domains in these proteins. In the case of the PDZ domain-containing protein zona occludens-1 (ZO-1), a major component of the tight junction defining the boundary between the apical and baso-lateral region of TRCs, we identified the first PDZ domain as the site of strong interaction with Gγ13. This association was further confirmed by co-immunoprecipitation experiments in HEK 293 cells. In addition, we present immunohistological data supporting partial co-localization of GOPC, MPDZ, or ZO-1, and Gγ13 in taste buds cells. Finally, we extend this observation to olfactory sensory neurons (OSNs), another type of chemosensory cells known to express both ZO-1 and Gγ13. Taken together our results implicate these new interaction partners in the sub-cellular distribution of Gγ13 in olfactory and gustatory primary sensory cells.

Keywords: taste bud, ZO-1, Gγ13, PDZ, olfactory sensory neurons, MPDZ, GOPC

INTRODUCTION

In rodents the peripheral gustatory system contributes to the detection of sapid molecules present in the oral cavity. This task is accomplished through taste receptors present on the apical microvilli of specialized polarized neuroepithelial taste bud cells also called taste receptor cells (TRCs) or type II cells. TRCs are one of four cell types found in the taste buds of the tongue papillae along with supporting cells (type I), presynaptic cells (type III) and basal cells (type IV) (Finger, 2005). TRCs are elongated cells extending microvilli at their apical end. These extensions which protrude from the adjacent epithelium at the taste bud pore harbor taste receptors designed to recognize the sapid compounds dissolved in saliva. At the pore, tight junctions between the cells composing the taste bud bestow polarity on the cells and seal the paracellular space thus isolating taste receptors on the apical membrane from ion channels found on the basolateral membrane. TRPM5 and voltage-gated Na^+ channels are the main types of channels found on the baso-lateral membrane of TRCs (Gao et al., 2009) where they are thought to play an important role in the generation of action potentials coding the properties of the tastants (Vandenbeuch and Kinnamon, 2009). Claudins and occludins are two of the main transmembrane proteins composing the tight junction (Furuse et al., 1998; Tsukita and Furuse, 1998). The selectivity of the paracellular barrier formed by tight junctions between neighboring cells is defined by the specific nature of the claudins composing it (Tsukita et al., 2008). It was reported recently that claudin 6 and 7 are found in microvilli and on the basolateral membrane of a subset of taste bud cells (TBCs) respectively while claudin 4 and 8, which are associated with a reduced cationic conductance, are prevalent at the taste

bud pore (Michlig et al., 2007). These proteins interact with zona occludens-1 (ZO-1), a multimodular cytoplasmic protein (Mitic and Anderson, 1998). ZO-1 was the first protein (225 kDa) shown to be specifically associated with the tight junction (Anderson et al., 1988; Stevenson and Keon, 1998). Subsequent studies identified ZO-1 isoforms as well as ZO-2 and ZO-3 as binding partners of ZO-1 (Gumbiner et al., 1991). ZO proteins belong to the large family of membrane-associated guanylate kinases (MAGUKs). All three known ZO proteins are each composed of three PDZ domains, one Src homology 3 domain (SH3), one guanylate kinase-like homologue domain (GUK) and proline-rich domains. PDZ and GUK domains interact selectively with claudins and occludins respectively (Furuse et al., 1994; Itoh et al., 1999). In addition, ZO proteins can bind to actin thus acting as scaffolds linking tight-junction proteins to the cytoskeleton (Fanning et al., 1998).

PDZ domains are typically stretches of about 100 amino acids able to recognize selectively a short peptide motif. Their role in receptor clustering and the organization of supramolecular complexes is well documented (Sheng, 1996). MPDZ also known as MUPP1, is a 13 PDZ domains-containing protein interacting selectively with a great number of PDZ binding motif-containing proteins including claudin-1 (Hamazaki et al., 2002). Single or multiple PDZ domains-containing proteins are often involved in the trafficking and localization of receptors or cytosolic signaling proteins to specialized membrane regions. A well-studied such example is the Golgi-associated protein GOPC also known as PIST. GOPC contains a single PDZ domain and two coiled-coil domains, one of which includes a leucine zipper important for homodimerization. It is known to regulate the intracellular sorting and plasma membrane location of a number of proteins (Yao et al., 2001; Cheng et al., 2002; Gentzsch et al., 2003; Hassel et al., 2003; Wente et al., 2005; Ito et al., 2006) including the adherent junction protein cadherin 23 in the highly specialized sensory hair cells of the inner ear (Xu et al., 2010).

In TRCs, bitter tastants binding to the apical membrane or membrane depolarization both lead to the secretion of adenosine 5′-triphosphate (ATP) from gap junction hemichannels located on the baso-lateral membrane (Huang and Roper, 2010). The signaling cascade downstream of taste G protein-coupled receptors (GPCRs) involves a number of well-characterized components. One of these signaling molecules is a G protein alpha subunit called gustducin (Gαgust) which plays an important role in sweet, umami, and bitter taste transduction (Gilbertson et al., 2000; He et al., 2004). Gustducin is part of an heterotrimeric complex including G beta 1 (Gβ1) and Gγ13, consequently Gγ13 much like Gαgust is abundant in a subset of type II TRCs (Huang et al., 1999; Clapp et al., 2001; Ohtubo and Yoshii, 2011). Expression of Gγ13 has also been reported in three additional types of sensory cells including retinal bipolar cells, vomeronasal, and olfactory sensory neurons (VOSNs and OSNs) (Huang et al., 2003; Kulaga et al., 2004; Kerr et al., 2008). More recently nutrient-sensing neurons of the hypothalamus were found to express Gγ13 as well (Ren et al., 2009). In OSNs Gγ13 is very abundant in cilia along with GαOlf and the guanine nucleotide exchange factor Ric-8B to which it was revealed to bind *in vitro* (Kerr et al., 2008). In TRCs, Gγ13 was reported to interact directly with the PDZ-containing scaffolding proteins PSD95, Veli-2, and SAP97 (Li et al., 2006).

Here, we report the identification of three new interaction partners for Gγ13 with various subcellular distributions in taste cells and OSNs. Through these previously unidentified interactions our results highlight partnerships between signal transduction components and multimodular proteins implicated in macromolecular complexes with possible consequences on sensory signaling.

MATERIALS AND METHODS

ANIMALS

Experiments were performed on C57BI/6J mice (P0—7 weeks old). The animals were fed a standard laboratory chow ad libitum (UAR A04, Usine d'Alimentation Rationnelle, France) and housed under constant temperature and humidity with a light-dark cycle of 12 h following French guidelines for the use and care of laboratory animals. All experimental protocols were approved by the animal ethics committee of the University of Burgundy.

EXPRESSION CONSTRUCTS

Mice were euthanized with an overdose of sodium pentobarbital and decapitated. Various tissues were collected and immediately processed for total RNA isolation using the RNAeasy kit (Qiagen, Germany) following the manufacturer's instructions. The RNA was then treated with DNase I (Promega, USA) and cleaned before reverse transcription. First strand cDNA was synthesized using 1 μg of total RNA with Superscript II (Invitrogen, USA) according to the manufacturer's protocol.

The entire open reading frame of mouse Gγ13, PDZ domains of ZO-1, Veli-2, PSD95, SAP97, RGS12, SH3 domain of ZO-1, and c-terminal intracellular regions of the junctional adhesion molecule (JAM), claudin 1, claudin 4, or claudin 8 were PCR amplified from C57BI/6J mice brain, testis, or circumvallate papillae cDNA using specific primers (Operon, Germany) containing a Sal I (forward primer) or Not I (reverse primer) restriction site. For a complete list of primers including melting temperatures and size of the expected PCR products see **Table A1.**

PCR reactions (25 μl) contained 1× PFU turbo buffer (Stratagene, USA), 0.4 μM of each primer, 10 μM dNTPs (Qiagen, Germany) and 1/20th of the appropriate RT reaction (water for control). Cycling parameters were: 95°C for 2 min then 35 cycles of 95°C for 30 s; appropriate melting temperature (**Table A1**) for 40 s, 72°C for 60 s, and final elongation at 72°C for 10 min. Following amplification (Biometra, Germany) an aliquot of the PCR products was loaded onto 1.4% agarose Seakem TAE gels (Cambrex, USA) to verify the specificity of the reaction. Single products of the expected size were then subcloned into pSTBlue-1 according to the manufacturer's directions (Novagen, USA). Recombinant clones were analyzed for accuracy by sequencing before subsequent subcloning into the Sal I and Not I sites of either pDBLeu (bait) or pEXP (prey) vectors of the Proquest two-hybrid system (Invitrogen, USA) or pDisplay-FLAG or pDisplay-HA (Invitrogen, USA) vectors. All constructs were sequenced to ensure in frame subcloning.

YEAST TWO-HYBRID INTERACTIONS

Yeast two-hybrid interactions were performed following the recommendations of the manufacturer of the Proquest two-hybrid system (Invitrogen, USA). Briefly, the appropriate combination of bait and prey plasmids (200 ng each) were co-transformed into competent MaV203 yeast cells (Invitrogen, USA) and plated onto minimal media plates without leucine and tryptophan. The plates were incubated for 48 h at 30°C before selection of two colonies, each dissolved into 500 ml of water. To test the strength of the interaction 10 μl of each slurry was spotted side by side onto plates lacking leucine, histidine, and tryptophan but containing either 0 (control plate), 12.5, 25, or 50 mM 3-Amino-1,2,4-triazole (3-AT) (Sigma, USA). After 24 h at 30°C, the plates were replica cleaned using a velour cloth and incubated an additional 48–72 h at 30°C prior to growth assessment.

CO-IMMUNOPRECIPITATION AND WESTERN BLOTTING

For co-immunoprecipitation assays with full length ZO-1 and Gγ13, 4 μg of a pcDNA3-FLAG-Gγ13 construct (generous gift of B. Malnic) were co-transfected into HEK 293 cells (60 mm dish) using Lipofectamine LTX (Invitrogen, USA) together with 4 μg of either pcDNA3, full-length pCB6-MYC-ZO-1 or a truncated pCB6-MYC-ZO-1 lacking the PDZ1 domain (pCB6-MYC-ZO-1mut) (generous gift of A. Fanning). pcDNA3-FLAG-Gγ13 + pCB6-MYC-ZO-1 or pcDNA3-FLAG-Gγ13 + pCB6-MYC-ZO-1mut transfections were performed in parallel. Two days later the transfected cells were lysed on ice in 600 μl lysis buffer containing 20 mM Tris, pH 8.0, 150 mM NaCl, 2 mM EDTA, 1% Triton *X*-100, 0.05% SDS, 1 mg/ml bovine serum albumin, 1 mM DTT and Complete protease inhibitor cocktail (Roche, Switzerland). The lysates were incubated 20 min on ice, centrifuged at 14,000 rpm in a microcentrifuge for 20 min at 4°C and the supernatant incubated overnight at 4°C with 5 μg of mouse monoclonal anti-FLAG (Kodak, USA). Antibody/proteins complexes were recovered with 50 μl protein G-coupled dynabeads (Invitrogen, USA) according to manufacturer's instructions. After three consecutive washes in PBS buffer containing Ca^{2+} and Mg^{2+} the samples were eluted by heating to 80°C for 10 min in LDS sample buffer (Invitrogen, USA) and subjected to SDS-PAGE and Western blot analysis.

For co-immunoprecipitation assays with full length Gγ13 and truncated forms of ZO-1, 3.5 μg of a pDisplay-HA-Gγ13 construct was co-transfected into HEK 293 cells plated on 60 mm dishes using Lipofectamine LTX (Invitrogen, USA) together with 3.5 μg of either pDipslay or various truncated forms of ZO-1, Veli-2, or PSD95 into pDisplay-FLAG. Forty-eight hours later cells were lysed on ice in 600 μl lysis buffer containing 25 mM Hepes, pH 7.5, 5 mM $MgCl_2$, 4 mM EDTA, 1% Triton X-100, and Complete protease inhibitor cocktail (Roche, Switzerland). Protein extracts were treated essentially as described above except that 8 μg 12CA5 mouse monoclonal anti-HA antibody (Roche, Switzerland) were used for immunoprecipitation.

For Western blotting, IP products or total protein lysates (30 μg) were typically separated on a denaturing 4–12% Bis-Tris PAGE gel (Invitrogen, USA), transferred onto a hybond-P, PVDF membrane (GE Healthcare, USA) and incubated overnight at 4°C with the appropriate primary antibody. Mouse monoclonal anti-HA (1/400; Roche, USA) or anti-FLAG (1/1000; Kodak, USA) or rabbit polyclonal anti-Ezrin H-276 (1/500; Santa Cruz, USA) or mouse monoclonal anti-myc tag 9B11 (1/1000; Cell Signaling Technology, USA). The membrane was subsequently processed using the SNAP id system (Millipore, USA) and signal was detected with an HRP-coupled secondary antibody and a chemiluminescent substrate (Supersignal West Pico, Pierce, USA) on a Chemidoc imager (Biorad, USA). Quantification and normalization was performed using ImageLab (Biorad, USA). When necessary membranes were stripped using a stripping solution (Uptima, USA) and reprobed with another primary antibody.

To analyze the expression of the PDZ domain-containing proteins and test the specificity of the antibodies used for immunohistochemistry circumvallate papillae and whole olfactory epithelia of fifteen 6–8 weeks old C57BI/6J mice were collected and pooled together. Tissue lysates were prepared in lysis buffer using a tissue lyser (Qiagen, Germany) during three cycles of 90 s each at 20 Hz. After centrifugation the soluble fraction was recovered and the protein content assessed. Seventy-five microgram of each lysate were separated on denaturing 4–12% Bis-Tris PAGE gel (Invitrogen, USA), transferred onto a hybond-P, PVDF membrane (GE Healthcare, USA) and incubated overnight at 4°C with the appropriate primary antibody. Mouse monoclonal anti-β-actin (1/1000; A5441; Sigma, USA), or rabbit polyclonal anti-GOPC (1/500; SAB3500332, Sigma, USA), or rabbit polyclonal anti-ZO-1 (1/600; 40–2200; Invitrogen, USA), or mouse monoclonal anti-MPDZ (1/250; 611558; BD Tranduction Laboratories, USA), or goat polyclonal anti-Gγ13 (1/200; sc-26781; Santa Cruz Biotechnology, USA). The membrane was subsequently processed as described above. Comparison of the expression levels of ZO-1 and Gγ13 in postnatal and adult mice was carried out by collecting olfactory epithelia from 6 P0, 3 P30, and 15 adult animals, pooling the samples from the animals of the same age and preparing tissue lysates as described above. 75, 100, and 130 μg of each extract were separated on a 4–12% Bis-Tris PAGE gel and transferred onto hypond-P. Each membranes which contained samples from either P0 and adult or P30 and adult animals were immunobloted with a rabbit polyclonal anti ZO-1 mid (1/500; 40–2200; Invitrogen, USA) or a mix of goat polyclonal anti-Gγ13 (1/200 sc-26781 + sc-26782; Santa Cruz Biotechnology, USA) and immunoreactivity evaluated by densitometry (ImageLab; Biorad, USA). The signal intensity for each protein load was expressed as the percentage of the younger animal to the adult and the median value determined.

IMMUNOHISTOCHEMISTRY

Immunostaining of taste tissue: C57BI/6J mice deeply anesthetized by intraperitoneal injections of sodium pentobarbital (60 mg/kg) were perfused with 4% paraformaldehyde (PFA). Following perfusion the tongue was removed and circumvallate papillae were excised and soaked 2 h in 4% PFA at 4°C before soaking overnight in 20% sucrose at 4°C. The next day the tissue was snap frozen in isopentane chilled with liquid nitrogen and embedded in OCT medium (Tissue-Tek, Japan) before performing sections (16 μm) on a Leica CM3050S cryostat (Leica Microsystems, Germany). Sections were air dried for 2 h at room temperature, and stored at −80°C. The day of

experiment sections were rehydrated in 0.1 M phosphate saline buffer (PBS, pH 7.4) for 10 min and blocked in 5% goat serum, 0.2% Triton *X*-100 in PBS for 30 min at room temperature before overnight incubation at 4°C with a 1/100 dilution of the appropriate primary antibodies. Commercial antibodies used were: an affinity purified goat polyclonal anti-Gγ13 (sc-26781; Santa Cruz Biotechnology, USA). This antibody was raised against an N-terminal peptide of human Gγ13 and has been validated previously on mouse taste tissue (Ohtubo and Yoshii, 2011). Immunoblotting shows that it recognizes Gγ13 and does not cross-react with ZO-1 in HEK 293 cells co-expressing both proteins (not shown). A mouse monoclonal anti-β-actin (A5441; Sigma, USA), these ascites recognize a single protein of the expected molecular weight in immunoblotting applications (see **Figure 2**). This antibody has been previously used to stain taste buds in rodents (Hofer and Drenckhahn, 1999). An affinity purified rabbit polyclonal anti-GOPC (SAB3500332; Sigma, USA) raised against a 16 amino acid peptide from near the carboxy terminus of human PIST. The specificity of this antibody was tested by the manufacturer. The specificity of this antibody and its restricted staining pattern in mouse taste buds was previously reported (Michlig et al., 2007). A rat monoclonal anti-ZO-1 (MAB1520; Chemicon International, USA). Two rabbit polyclonal anti-ZO-1 (Invitrogen, USA) one raised against amino acids 463–1109 of a human recombinant ZO-1 fusion protein (Cat # 61–7300); the other raised against a synthetic peptide of the mid region of human ZO-1 (Cat # 40–2200). The latter two antibodies recognized a ZO-1 myc tagged protein over-expressed in HEK 293T cells by western blot. Furthermore these antibodies did not cross-react with Gγ13 (not shown).

The next day sections were washed repeatedly and incubated for 2 h at room temperature with the appropriate combination of labeled secondary antibodies (1/500 dilution of Alexa 564-conjugated donkey anti-goat IgG (Molecular Probes, USA), 1/500 dilution of Alexa-488-conjugated donkey anti-rabbit IgG (Molecular Probes, USA). Staining specificity was assessed by treating slices in the absence of primary antibodies. After washing and counterstaining with Hoechst 33342 reagent (Sigma, USA), slides were mounted in gel/mount (Biomeda Corp., USA) and analyzed under a TCS-SP2 confocal microscope (Leica, Germany).

Immunostaining of the olfactory epithelium (OE): C57BI/6J mice were deeply anesthetized by injection of ketamine HCl and xylazine (150 mg/kg and 15 mg/kg body weight, respectively) and then decapitated. The nasal septum was dissected out, the OE removed and subsequently immersed in cold oxygenated ACSF containing in mM: NaCl, 124; $CaCl_2$ 2; NaH_2PO_4 1.25; $MgSO_4$ 1.3; glucose 15, and $NaHCO_3$ 26, respectively. Mice olfactory epithelia were then fixed using PFA 4% in PBS containing 0.2% glutaraldehyde. Epithelia were further dipped in 95% ethanol for 1 min, washed three times with PBS, blocked with 2% donkey serum, 2% BSA, and 0.25% Triton *X*-100 in PBS for 1 h and incubated overnight at 4°C with the primary antibodies diluted in blocking solution. Primary rabbit anti-ZO-1 and goat anti-Gγ13 (Santa-Cruz SC-26781) were used at 1:100. Sections were washed three times in PBS and incubated with the secondary antibodies (1:500, goat Alexa488-anti-rabbit, donkey Alexa488 anti-goat or donkey Alexa555 anti-rabbit, Molecular Probes, Invitrogen) in blocking solution for 2 h at room temperature. Epithelia were mounted between slide and coverslip using MOWIOL 4-88 (Merck, Germany). All Chemicals were from Sigma unless stated.

Samples were visualized using a Leica SP2 laser scanning confocal microscope and a 63× oil immersion objective. Ciliary length was used as an indicator of neuron maturity (see Schwarzenbacher et al., 2005) and for each knob the lengths of all the cilia were averaged. Results are given as mean ± SEM, n = number of olfactory knobs.

RT-PCR

To analyze the expression of the PDZ domain-containing genes in various tissues 6-weeks-old C57BI/6J mice were killed with an overdose of sodium pentobarbital, and circumvallate papillae, whole olfactory epithelia (including nasal respiratory epithelium), tongue epithelium devoid of taste buds, liver, and whole brain were dissected out of the carcass on ice. Total RNA extraction, cDNA synthesis and PCR amplification were performed as previously described (Fenech et al., 2009). Primer pairs sequences and annealing temperature are listed in **Table A1.**

RESULTS

Gγ13 PHYSICALLY INTERACTS WITH ZO-1, GOPC, AND MPDZ

Earlier work reported an interaction between the C-terminus PDZ binding CTIL motif of Gγ13 and the third PDZ domains (PDZ3) of PSD95 or SAP97, or the single PDZ domain of Veli-2 (Li et al., 2006).

To identify additional PDZ-domain containing proteins interacting with Gγ13 which might be relevant to taste biology, we conducted a yeast two-hybrid assay using Gγ13 as a bait against a selection of five PDZ-domains (Kalyoncu et al., 2010). Some PDZ domains were chosen on the basis of their relative homology to the PDZ3 of PSD95, such as for the multiple PDZ domain protein (MPDZ) PDZ10 and PDZ11 (**Figure 1A**). We also selected the PDZ domains of GOPC (golgi-associated PDZ- and coiled-coil motif-containing protein) and MPDZ PDZ12 which are related to that of Veli-2. In addition, to broadly screen for a novel interaction we also included more divergent PDZ domains such as those of RGS12 (regulator of G protein signaling 12), MPDZ PDZ13, and PDLIM2 (PDZ and Lim domain protein 2). Finally, the three PDZ domains of ZO-1, a tight junction protein belonging to the MAGUK protein family, were also incorporated. MAGUK proteins typically contain multiple PDZ domains and a GUK domain; PSD95 and SAP97 belong to that family.

Plasmids containing either the entire coding sequence of the mouse Gγ13 (pBait) or each of the PDZ domain sequences listed above (pPrey) were co-transformed into competent yeast cells and plated out on selective growth media. During an initial screen we uncovered robust interactions with the PDZ1 of ZO-1, the PDZ domain of GOPC and the PDZ12-13 of MPDZ. In contrast, the PDZ domains of RGS12, PDLIM2, PDZ2, and 3 of ZO-1 as well as PDZ10-11 of MPDZ showed weak or no interaction under those conditions (**Figure 1B** and **Table A2**). Note that the PDZ3 of PSD95 which we used as a positive control displayed a relatively weak interaction under these conditions.

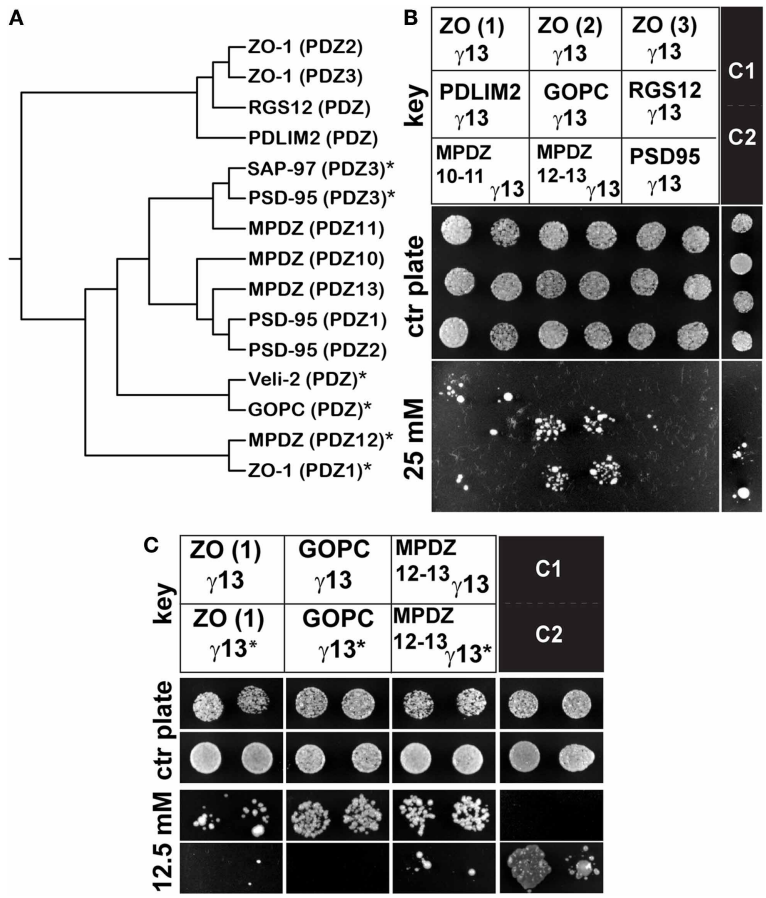

FIGURE 1 | Gγ13 interacts with the PDZ domains of GOPC, MPDZ and ZO-1. (A) Phylogenetic tree of a selection of PDZ domains. Sequences encompassing the PDZ domain region of several proteins were analyzed with clustalW 2.1. using the PAM weight matrix. The PDZ domains presenting the highest homology are closer together on the tree. (*) PDZ domains interacting with Gγ13. **(B)** Individual constructs encompassing each of the ZO-1 PDZ domains (PDZ1, PDZ2, PDZ3), PDZ10-11, and 12–13 of MPDZ, PDZ3 of PSD95 or the unique PDZ domains of PDLIM2, GOPC, and RGS12 (see key) were co-transformed together with Gγ13 into MaV203 competent yeast cells and assayed for growth on medium lacking His, Leu, and Trp supplemented with 0 (control plate) or 25 mM 3-AT. ZO-1 (PDZ1), GOPC, and MPDZ (PDZ12-13) are clearly interacting with Gγ13. C1 and C2 are weak- and moderate-strength interaction controls respectively provided by the manufacturer. The results shown are representative of three independent experiments each performed in duplicate. **(C)** Yeast two-hybrid interaction assay testing the interaction of ZO-1, GOPC, and MPDZ with a mutant Gγ13 (T56A) (γ13*). MaV203 competent yeast cells were co-transfected with either the ZO-1 (PDZ1) or GOPC or MPDZ (PDZ12-13) constructs and γ13* and assayed for growth on medium lacking His, Leu, and Trp supplemented with 0 (control plate) or 12.5 mM 3-AT. The T65A mutation clearly abrogates the interaction with these PDZ domains indicating that the c-terminal CTAL motif is critical for this interaction. The results shown are representative of three independent experiments each performed in duplicate.

It was previously reported that the PDZ binding domain of Gγ13 is selective for some but not all PDZ domains within the multi-PDZ domain proteins PSD95 and SAP97 (Li et al., 2006). Our results extend this observation to two additional multi-PDZ domain proteins, namely ZO-1 and MPDZ as well as to the mono-PDZ domain protein GOPC. In the case of ZO-1, the first PDZ domain showed the strongest interaction with Gγ13, the second PDZ domain interacted very weakly while the third did not interact at all under our experimental conditions. The interaction with MPDZ was also selective for certain PDZ domains since Gγ13 appeared more tightly bound to PDZ12-13 than to PDZ10-11 (**Figure 1B**). When relating these results to the sequence conservation between these PDZ domains (**Figure 1A**) it appears that the PDZ domains most similar to Veli-2 such as GOPC and MPDZ (PDZ12) show a strong affinity for Gγ13 whereas the divergent RGS12, PDLIM2, and ZO-1 (PDZ2) are very weak interactors.

Gγ13 INTERACTS WITH ZO-1 PDZ1 THROUGH A CLASSIC PDZ BINDING MOTIF—PDZ DOMAIN INTERACTION

It is well known that the residue in position −2 in the canonical X(S/T)XA PDZ binding motif, where X is any amino acid and A any hydrophobic amino acid, is critical for the interaction with type I PDZ domains (Bezprozvanny and Maximov, 2001). To confirm the importance of the CTIL motif of Gγ13 in the interaction with ZO-1 PDZ1, GOPC, and MPDZ PDZ12-13 we substituted the threonine in position −2 with

an alanine and subsequently tested the ability of the resulting Gγ13T65A mutant to interact with these PDZ domains in a yeast two-hybrid assay. As shown in **Figure 1C** and as predicted, the T65A substitution led to a dramatic reduction in the ability of these proteins to interact together. This result supports the notion that Gγ13 interacts with these PDZ domains through a classic PDZ binding motif—PDZ domain type interaction (**Table A2**) as previously shown for PSD95 and Veli-2 (Li et al., 2006).

Taken together these results establish for the first time to our knowledge that Gγ13 binds selectively to MDPZ PDZ12, GOPC, and ZO-1 PDZ1 via its c-terminal PDZ binding motif.

EXPRESSION OF Gγ13 BINDING PARTNERS

To address whether these newly identified PDZ-containing Gγ13 binding partners were expressed in taste tissue and therefore likely to be biologically relevant, we carried out a series of related analyses to look for gene expression and protein content in circumvallate papillae (CV), a site where both Gγ13 and bitter taste receptors are abundant (Huang et al., 1999; Matsunami et al., 2000). First we carried out an RT-PCR experiment to look for the expression of the genes coding for GOPC, MPDZ, and ZO-1 in CV, surrounding non-sensory tongue tissue, whole OE, whole brain and liver. Since many splice variants of MPDZ have been reported previously, for this gene we designed primers flanking the 12–13 PDZ domains pair to specifically confirm their expression in CV. In addition, to monitor the presence of OSNs in our OE sample we used specific primers against Gγ13 while specific primers against Gαgust, a G-protein alpha subunit selectively expressed in a subset of TRCs, allowed us to probe their presence in our CV sample. Glutaraldehyde phosphate dehydrogenase (GAPDH) amplification and a reaction that does not contain reverse transcriptase were carried out as controls to validate the quality of the cDNA reaction and specificity of primer pairs used. Our results show (**Figure 2A**) that ZO-1, GOPC, and MDPZ are broadly expressed and therefore detected in all tissues tested. In contrast Gγ13 and Gαgust's expression appear restricted to CV and OE samples despite reports of their expression in certain brain cells. We believe that too great of a dilution of the mRNAs for these genes in our whole brain extracts is the reason for the absence of detection in this tissue under our amplification conditions (25 PCR cycles).

To investigate further the localization of the Gγ13 interacting proteins in taste bud cells we prepared sections of CV taste buds which were incubated with antibodies raised against MPDZ, GOPC, or ZO-1. Prior to immunohistochemical staining the specificity of the antibodies was verified using immunoblots containing protein extracts from murine CV and OE as well as from HEK 293 cells untransfected or co-transfected with ZO-1 and Gγ13 expression constructs. Antibodies raised against MPDZ, GOPC, ZO-1, and Gγ13 revealed bands of the expected molecular weight in CV, OE, untransfected and ZO-1/Gγ13 transfected HEK 293 cells (**Figure 2B**) thus corroborating the gene expression data obtained by RT-PCR (**Figure 2A**). The presence of additional bands detected by the anti-ZO-1 (in CV, OE, and HEK 293) and anti-MPDZ antibodies in HEK 293 cells is likely linked to the presence of splice variants of these proteins in these cells/tissues. We noted that the Gγ13 protein was of higher molecular weight in CV as compared to OE. Alternative splicing is unlikely to be the reason behind this higher molecular weight since the RT-PCR product generated with primers encompassing the entire coding region of Gγ13 is of the expected size in CV and OE (**Figure 2A**). Additional investigations using another antibody directed against an epitope in the middle of the Gγ13 coding sequence points toward a post-translational modification preventing binding of the antibody at this site as the higher molecular weight band was not revealed in CV (**Figure A1**). Although, GOPC was detected both in CV and OE it was ∼4 fold more abundant in the latter (**Figure 2B**).

Next, we sought to establish whether these proteins were confined to taste bud cells as it is the case for Gγ13. Immunostaining of CV sections with the anti-MPDZ antibody revealed the presence of immunopositive taste bud cells (**Figure 2C**). MPDZ was detected mainly in the cytoplasm with a small fraction near the pore.

Gγ13 was confined to a subset (∼20%) of taste bud cells, presumably type II cells, and although distributed throughout these cells it was most abundant in the cytoplasm as previously reported. Similarly GOPC was confined to a subset of taste bud cells and its subcellular distribution appeared restricted to the cytoplasm and somewhat near the peripheral plasma membrane (**Figure 2C**).

In contrast, immunostaining with the antibody raised against ZO-1 pointed to a different sub-cellular distribution with most of the protein localized at the taste pore (**Figure 2C**). This distribution is consistent with the location of tight junctions in these cells.

Because of the proximal location of ZO-1 to the microvilli where Gγ13 is thought to operate downstream of T2Rs and its role in paracellular permeability paramount to taste cell function, we decided to focus subsequent experiments on the study of the interaction between Gγ13 and ZO-1.

SELECTIVITY AND STRENGTH OF THE INTERACTION BETWEEN Gγ13 AND ZO-1

In the next set of experiments, we sought to examine the strength of the interaction between Gγ13 with ZO-1 in a more quantitative way. To this end we took advantage of the fact that with the ProQuest yeast two-hybrid system the level of expression of the HIS3 reporter gene is directly proportional to the strength of the interaction between the two assayed proteins. To grade the strength of the interaction between the proteins tested, yeast clones were plated on selection plates lacking histidine and containing increasing concentrations of 3-AT, an HIS3 inhibitor. Yeast clones containing Gγ13 and ZO-1 (PDZ1-2) grew on selection plates containing up to 50 mM of 3-AT (**Figure 3A**). This clearly demonstrates a strong interaction between these proteins. The strength of this interaction is only slightly less robust than that observed with claudin-8 a four-transmembrane domain protein integral to taste bud tight junctions previously reported to interact with the PDZ1 of ZO-1 via its c-terminal PDZ binding domain (Itoh et al., 1999; Michlig et al., 2007). No interaction was observed between claudin-8 and ZO-1 (PDZ2-3) as expected; however, Gγ13 associated weakly with ZO-1 (PDZ2-3)

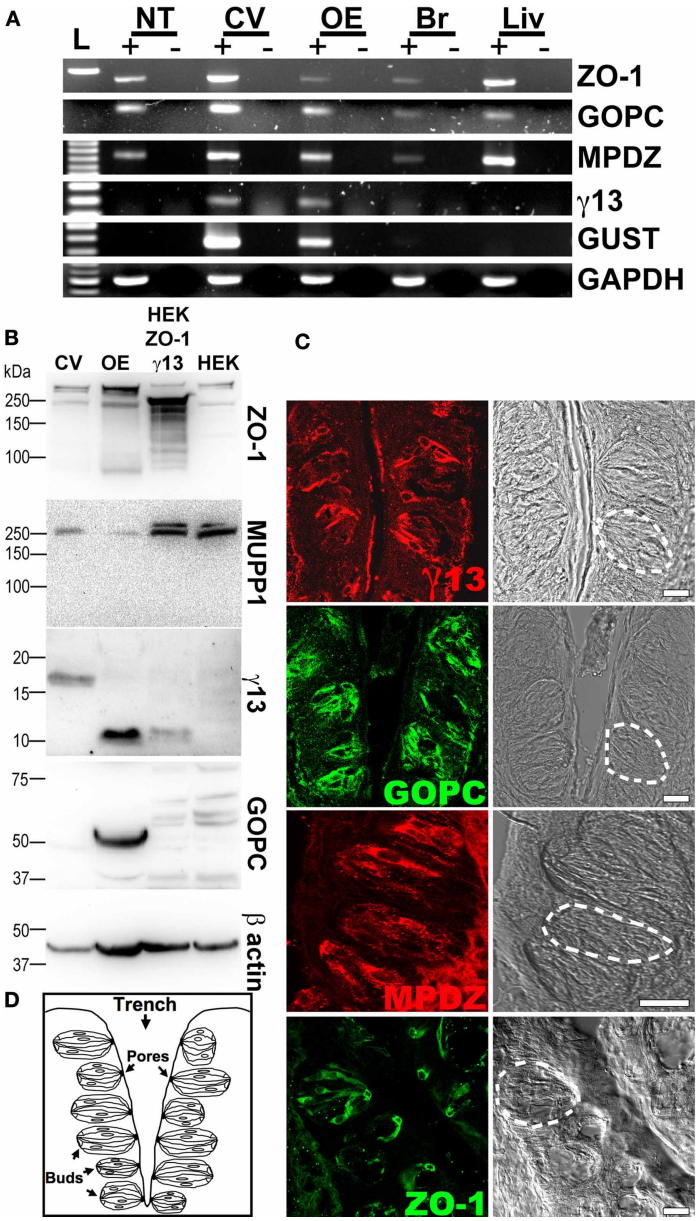

FIGURE 2 | Expression of GOPC, MPDZ, ZO-1 and Gγ13 in circumvallate papillae. (A) RT-PCR experiment demonstrating expression of ZO-1, GOPC, and MPDZ in all tissues tested. In contrast, the presence of Gγ13 and Gαgust (GUST) mRNAs appear to be restricted to taste and olfactory sensory tissues. See Section "RT-PCR" and **Table A1** for details about amplification conditions and expected sizes of PCR products. GAPDH primers were used as a control of the quality of the RNA. (+) and (–) indicate the presence or absence of reverse transcriptase in the reaction respectively. L: 100 bp ladder. NT, tongue epithelium deprived of taste buds; CV, circumvallate papillae; OE, olfactory epithelium; Br, whole brain; Liv, liver. The results presented are representative of three independent experiments. **(B)** Immunodetection of ZO-1, MPDZ, GOPC, and Gγ13 proteins in circumvallate (CV) and whole olfactory epithelium (OE) protein extracts. Sample preparation and immunodetection conditions following western blotting are as described in detail under Section "Co-immunoprecipitation and Western blotting." Protein extracts from HEK 293 cells (HEK) or HEK 293 cells stably expressing HA-Gγ13 transiently transfected with a full length Myc-ZO-1 construct (HEK ZO-1 γ13) were used as controls. As expected ZO-1 and Gγ13 are detected in CV and OE. Note that Gγ13 displays a higher apparent molecular weight in CV than in OE. Predicted molecular masses for ZO-1, MPDZ, GOPC, Gγ13, and β-actin are 220, 220, 51, 8, and 42 kDa respectively. β-actin was used as loading control. The results presented are representative of three independent experiments. **(C)** Localization of MPDZ, GOPC, Gγ13, and ZO-1 proteins in circumvallate taste buds sections. Indirect immunofluorescence on longitudinal cryosections of circumvallate papillae was performed as described under Section "Immunohistochemistry." MPDZ, GOPC, and Gγ13 are mainly distributed in the cytoplasm of a subset of taste bud cells while ZO-1 localizes mostly at the taste pore. On the Nomarski image a white dashed line highlights the size and location of one taste bud. Gγ13, MPDZ, and GOPC images are strict confocal optical sections (pinhole 82 μm, airy disk 1) while a wider pinhole was used for the ZO-1 image (pinhole 124 μm, airy disk 1.7), Scale bar = 50 μm. Staining patterns are representative of two independent experiments performed on multiple sections from at least two mice. **(D)** Drawing representing a longitudinal section of the circumvallate papillae as in **(C)**, showing the location of the taste buds along the walls of the trench under the surface of the tongue. Taste bud cells protrude into the trench through the taste pore.

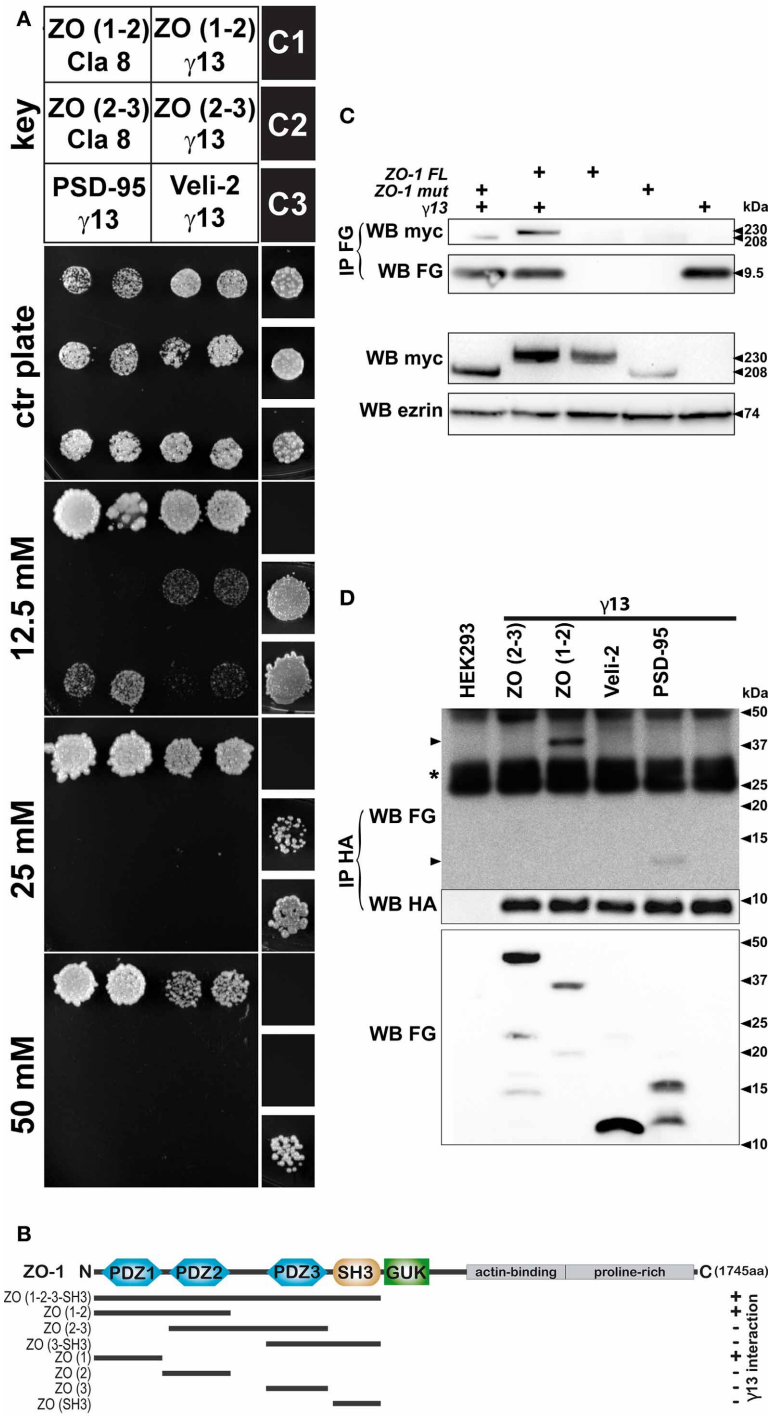

FIGURE 3 | Physical interaction between heterologously expressed Gγ13 and ZO-1. (A) To test the strength of the interaction between the proteins assayed Mav203 yeasts cells were co-transformed with different combinations of bait and prey plasmids (see key). Interaction was scored on minimal medium plates lacking His, Leu, and Trp but containing increasing concentrations of 3-AT (0–50 mM) a competitive inhibitor of the enzyme involved in histidine biosynthesis. Titration of the strength of the interaction is established by growth potential and compared to weak (C1), moderate (C2) and strong (C3) interaction controls provided by the manufacturer. The construct encompassing the first 2 PDZ domains of ZO-1 [ZO (1–2)] interacts with Gγ13 (γ13) to a similar extend as with the c-terminal tail of claudin 8 (Cla 8) a transmembrane cell–cell interaction protein integral to tight junctions. Weaker interactions between Gγ13 and the PDZ2-3 of ZO-1 [ZO (2–3)], the PDZ3 of PSD95 (PSD95), or the unique PDZ domain of Veli-2 (Veli-2) were also observed. Note that no interaction between claudin 8 and ZO (2–3) was visible as expected. The results presented are representative of three independent experiments performed in duplicate. **(B)** Schematic drawing recapitulating the different domains of ZO-1 tested for their interaction with Gγ13 by two-hybrid interaction assay. At the top simplified representation of the organization of protein domains in ZO-1 showing the PDZ1, PDZ2, PDZ3, SH3, GUK, actin-binding and proline-rich

(Continued)

FIGURE 3 | Continued
domains. The span of the constructs tested by two-hybrid are shown underneath (black line). The ability of the ZO-1 constructs to interact with Gγ13 in presence of 25 mM 3-AT were scored with a (+) when growth was observed or (–) when there was no growth. An interaction with Gγ13 was detected whenever the construct contained the first PDZ domain of ZO-1. **(C)** To ensure that Gγ13 could interact with the native ZO-1 protein, expression constructs encoding tagged full length ZO-1, or Gγ13 proteins were transiently transfected into HEK 293 cells. Protein extracts were prepared from cells expressing full length MYC-ZO-1 (ZO-1FL, lane 3), MYC-ZO-1 missing the PDZ1 domain (ZO-1mut, lane 4), FLAG-Gγ13 (lane 5) or co-expressing FLAG-Gγ13 and MYC-ZO-1FL (lane 2), or FLAG-Gγ13 and MYC-ZO-1mut (lane 1) as indicated. Examination of the expression of MYC-ZO-1 and MYC-ZO-1mut expression by western blot with anti-MYC (WB myc, second to last panel) revealed that both proteins are produced (~230 and ~208 kDa respectively). Erzin was used as a loading control (WB erzin). Protein extracts were used to immunoprecipitate the FLAG-Gγ13 protein with an anti-FLAG antibody (IP FG, WB FG). Analysis of the content of the immunoprecipitated complex (IP FG) using an anti-myc antibody (WB myc) confirms the interaction of the ZO-1FL or ZO-1mut proteins with Gγ13 in the samples co-expressing ZO-1FL or ZO-1mut and FLAG-Gγ13 (lane 1 and 2). Two additional experiments yielded the same results. **(D)** To validate the interactions uncovered using the yeast two-hybrid interaction assay and in particular the protein domains of ZO-1 important for the interaction with Gγ13, co-immunoprecipitation experiments were performed in HEK 293 cells following heterologous co-expression of HA-Gγ13 with various FLAG-ZO-1 deletion constructs. Cells were left untransfected (lane 1) or transiently transfected with HA-Gγ13 alone (lane 6) or in combination with FLAG-ZO-1(PDZ2-3) (lane 2), FLAG-ZO-1(PDZ1-2) (lane 3), FLAG-Veli-2(PDZ) (lane 4), or FLAG-PSD95(PDZ3) (lane 5) as indicated. Protein extracts from transfected cells were first analyzed for expression of the FLAG-tagged deletion constructs by western blot using an anti-FLAG antibody (WB FG, bottom panel). Then anti-HA immunoprecipitation was carried out and complexes were analyzed by western blot using an anti-FLAG antibody (IP HA, WB FG, top panel). FLAG-PSD95 and FLAG-ZO-1(PDZ1-2) are detected (arrowheads) indicating that these domains interact with Gγ13 under these conditions. Anti-HA western analysis of the samples confirms correct immunoprecipitation of HA-Gγ13 (IP HA, WB HA, middle panel). (*) IgG light chains. The experiment shown is representative of 3 independent experiments.

presumably through a direct interaction with the second PDZ domain of ZO-1 (see **Figure 1B**).

INTERACTION OF Gγ13 AND ZO-1 IN HEK 293T CELLS

To validate our yeast two-hybrid assay interaction results between ZO-1 and Gγ13 we next tested whether these proteins would co-immunoprecipitate when co-expressed in HEK 293 cells. In order to rule out the possibility that folding of the native protein would prevent this interaction, full-length ZO-1 and Gγ13 constructs were used for this experiment. HEK 293 cell lines stably expressing a MYC-ZO-1 or a MYC-ZO-1 mutant lacking the PDZ1 domain (generous gift of A. Fanning) (Fanning et al., 1998) were transiently transfected with a FLAG-Gγ13 (generous gift of B. Malnic) (Kerr et al., 2008) construct. Forty-eight hours later protein extracts from these cells were prepared and used for immunoprecipitation using an anti-FLAG antibody. Western blot analysis of simple protein extracts from transfected cells using anti-MYC and anti-FLAG antibodies confirms that all full length and mutant proteins are produced in these cells (**Figure 3B**). Immunoprecipitation of Gγ13 using an anti-FLAG antibody pulled down both intact MYC-ZO-1 and mutant constructs thus supporting further our contention that Gγ13 and ZO-1 physically interact. The interaction of the MYC-ZO-1 mutant construct with Gγ13 despite the absence of the PDZ1 domain can potentially be explained by the fact that as shown in **Figures 1B** and **3A** Gγ13 interacts weakly with the PDZ2 of ZO-1 in yeast cells. Alternatively, it is possible that the transfected MYC-ZO-1 mutant binds the endogenous ZO-1 (see **Figure 2B**) through an already documented PDZ2 mediated interaction (Utepbergenov et al., 2006). This homodimer would allow Gγ13 to be pulled down along with the MYC-ZO-1 mutant through an interaction with the ZO-1 PDZ1 of the endogenous ZO-1.

In order to further investigate these two possibilities we generated two truncated FLAG-tagged ZO-1 constructs encompassing either the first and second (PDZ1-2) or the second and third (PDZ2-3) PDZ domains of ZO-1 as well as a Gγ13 construct harboring an HA tag at the N-terminal. We also made FLAG-PSD95 (PDZ3), and FLAG-Veli-2 (PDZ) control constructs. The HA-Gγ13, along with each FLAG-tagged construct were transfected in HEK 293 cells. Forty-eight hours after transfection the cell lysates were subjected to immunoprecipitation with an anti-HA antibody. Lysates from untransfected cells and cells transfected with the HA-Gγ13 construct alone were used as controls. Analysis of the immunoprecipitates by immunoblotting using an anti-FLAG antibody showed that Gγ13 co-precipitated with ZO-1 (PDZ1-2) and PSD95 (PDZ3) but not with ZO-1 (PDZ2-3) or Veli-2 (PDZ) (**Figure 3C**). Analysis of the HEK 293 cell lysates by immunoblot using an anti-FLAG antibody indicates that all the FLAG-tagged constructs including ZO-1 (PDZ2-3) and Veli-2 (PDZ) were produced and therefore available for co-immunoprecipitation. These results corroborate our yeast two-hybrid assay results (**Figures 1B** and **3A**) and effectively rule out the possibility that binding of Gγ13 to the second PDZ domain of ZO-1 is strong enough to withstand the harsh conditions of this assay. We also note that under these conditions the weak interaction between Gγ13 and Veli-2 is not recapitulated.

Yeast two-hybrid and co-immunoprecipitation assay data strongly supporting a direct interaction between the c-terminal 4 amino-acids of Gγ13 and the first PDZ domain of ZO-1 are recapitulated in **Figure 3D.**

PARTIAL CO-LOCALIZATION OF MPDZ, GOPC, OR ZO-1 WITH Gγ13 IN MOUSE TASTE BUD CELLS

In circumvallate taste buds Gγ13′s expression is restricted to type II cells where it is thought to play a role in bitter taste signal transduction (Huang et al., 1999; Clapp et al., 2001). In addition, immunohistochemical analysis of circumvallate, fungiform or soft palate papillae indicates that Gγ13 is particularly abundant in the cytoplasm of these cells (Clapp et al., 2001; Ohtubo and Yoshii, 2011). To test whether MPDZ, GOPC, and ZO-1 are co-localized with Gγ13 in mouse taste bud cells, circumvallate papillae were dissected out and double- immunofluorescent labeling experiments on sagittal cryosections were performed.

Optical sections of tissue were acquired under a confocal microscope focusing on the region of interest and overlayed with the software.

Analysis of tissue sections co-stained with Gγ13 (**Figure 4A**) and MPDZ (**Figure 4C**) focusing on confocal optical sections near the pore shows that a small fraction of the Gγ13 staining overlaps with that of MPDZ in that area (**Figure 4B**). On tissue sections double labeled with GOPC (**Figure 4D**) and Gγ13 (**Figure 4F**) analysis of single optical sections through the cytoplasm of taste bud cells where Gγ13 is abundant, revealed an extensive co-localization with GOPC at that location (**Figure 4E**). In addition, a similar partial co-localization pattern between ZO-1 (**Figure 4G**) and Gγ13 (**Figure 4I**) was observed on single optical sections through the taste pore (**Figure 4H**). This pattern was further confirmed using two additional antibodies raised in a different host and targeting different epitopes in ZO-1 (data not shown). Partial co-localization between MPDZ, GOPC, or ZO-1, and Gγ13 in taste bud cells indicates that these proteins might be involved in a dynamic process within the cell and supports the claim that they are likely biological partners.

These experiments also revealed that all TRCs expressing Gγ13 are immunopositive for GOPC, further emphasizing a tight collaboration between these two proteins. GOPC immunoreactivity was observed as well in cells that did not express Gγ13 (**Figure 4E**), presumably in type I or III cells. Unfortunately the rather weak immunostaining with the MPDZ specific antibody and the very restricted location of ZO-1 around the tight junctions prevented an in depth study of the cell types expressing these proteins.

CO-LOCALIZATION OF ZO-1 AND Gγ13 IN OLFACTORY SENSORY NEURONS

Both ZO-1 and Gγ13 have been independently reported to be expressed in OSNs (Miragall et al., 1994; Kulaga et al., 2004). In order to investigate whether Gγ13 and ZO-1 co-localize in olfactory neurons, we set-up a flat-mount (or ≪ en face ≫) preparation of OE allowing us to image individual olfactory neuron dendritic knobs. First, in P30 mice no co-localization between Gγ13 and ZO-1 was ever seen in Gγ13 immunopositive knobs ($n = 220$, **Figure 5A**). Next, we analyzed newborn mice (P0). At this stage dendritic knobs could be split into two groups (Schwarzenbacher et al., 2005). A first group did not display any cilia and was recognizable by its round smooth aspect (**Figure 5B**). In this group co-localization was found in 66.6% of the dendritic knobs ($n = 9$ knobs). In a second more important group encompassing dendritic knobs bearing small ciliary compartments (**Figure 5C**) co-localization between Gγ13 and ZO-1 was seen in 73% of the ciliated dendritic knobs ($n = 27$ knobs). Overall co-localization could be observed in 72.2% of the Gγ13 immunopositive dendritic knobs ($n = 36$) at P0. Finally and in line with these observations, dendritic knobs where co-localization between the two proteins was seen had shorter cilia (average length per knobs 2.8 ± 0.2 mm, $n = 20$) compared to the ones where no co-localization was observed ($n = 5.5 \pm 1.0$ mm, $n = 7$, $p < 0.01$ Mann-Whitney). We, therefore, infer that co-localization between Gγ13 and ZO-1 depends upon the developmental stage of olfactory neurons. Note that the secondary antibody alone did not produce any background staining (**Figure 5D**).

Next ZO-1 and Gγ13's protein expression levels in olfactory mucosa were evaluated during development by western blot. The signal intensity expressed as the percentage of the younger animal to the adult indicates that there is a slight decrease of ZO-1 expression from 84% at P0 to 63% at P30 while Gγ13's expression increased from 15% at P0 to 33% at P30. Given these results we cannot completely rule out the possibility that the lack of co-localization observed at P30 might be linked with the slight decrease of ZO-1 expression at this stage.

DISCUSSION

A NETWORK OF PROTEINS POTENTIALLY REGULATING THE INTRACELLULAR TRAFFIC OF Gγ13 IN TASTE RECEPTOR CELLS

Following up on an earlier report demonstrating an interaction between Gγ13 and the PDZ domain containing proteins Veli-2 and SAP97, our data identified GOPC, MPDZ, and ZO-1 as binding partners of Gγ13. We also report for the first time to our knowledge the expression of GOPC and MPDZ in taste bud cells.

All three PDZ-containing proteins identified in this study are known members of macromolecular complexes or participate in protein trafficking suggesting that they are likely to determine Gγ13′s transport and/or subcellular location in taste cells.

GOPC is a Golgi-associated protein reportedly interacting with a number of transmembrane proteins including channels and GPCRs for which it is thought to modulate vesicular transport from the Golgi apparatus to the plasma membrane. In addition it is known to associate with the Rho effector Rhotekin at adherent junctions where it is thought to regulate cell-polarity development (Ito et al., 2006). These features might explain in part both the punctate staining pattern as well as the staining observed at the periphery of the taste bud cells (**Figure 2C**). Although, this is the first report of GOPC's expression in TRCs, this new finding is not totally surprising considering that TRCs are polarized neuroepithelial sensory cells much like inner ear sensory hair cells of the cochlea where GOPC regulates membrane trafficking of cadherin 23 (Xu et al., 2010), a cell-cell adhesion protein also found in retinal cells where its loss is associated with retinitis pigmentosa (Bolz et al., 2001). In hair cells GOPC retains cadherin 23 in trans-golgi networks (TGNs). Co-expression of MAGI-I and harmonin, two PDZ domain-containing proteins, competes with GOPC to cause the release of cadherin 23 from the TGN. It is plausible that in TRCs MPDZ, which we find distributed in the cytoplasm and to a small extent near the tight junctions, fulfills the same function as MAGI-I. Under this scenario we would assume that MPDZ is able to compete with GOPC for Gγ13 binding and once unloaded onto MPDZ, Gγ13 is transported to the taste bud pore. Coincidently, MPDZ has been reported to interact with the tight junction complex, particularly with claudin-1 in polarized epithelial cells; therefore, its localization at the pore is not completely unexpected (Hamazaki et al., 2002; Liew et al., 2009). Our own experiments corroborate these findings by showing that although MPDZ seems most abundant in the cytoplasm of taste bud cells, a fraction of it is detected at the pore where it is partly co-localized with ZO-1 (**Figure A2**).

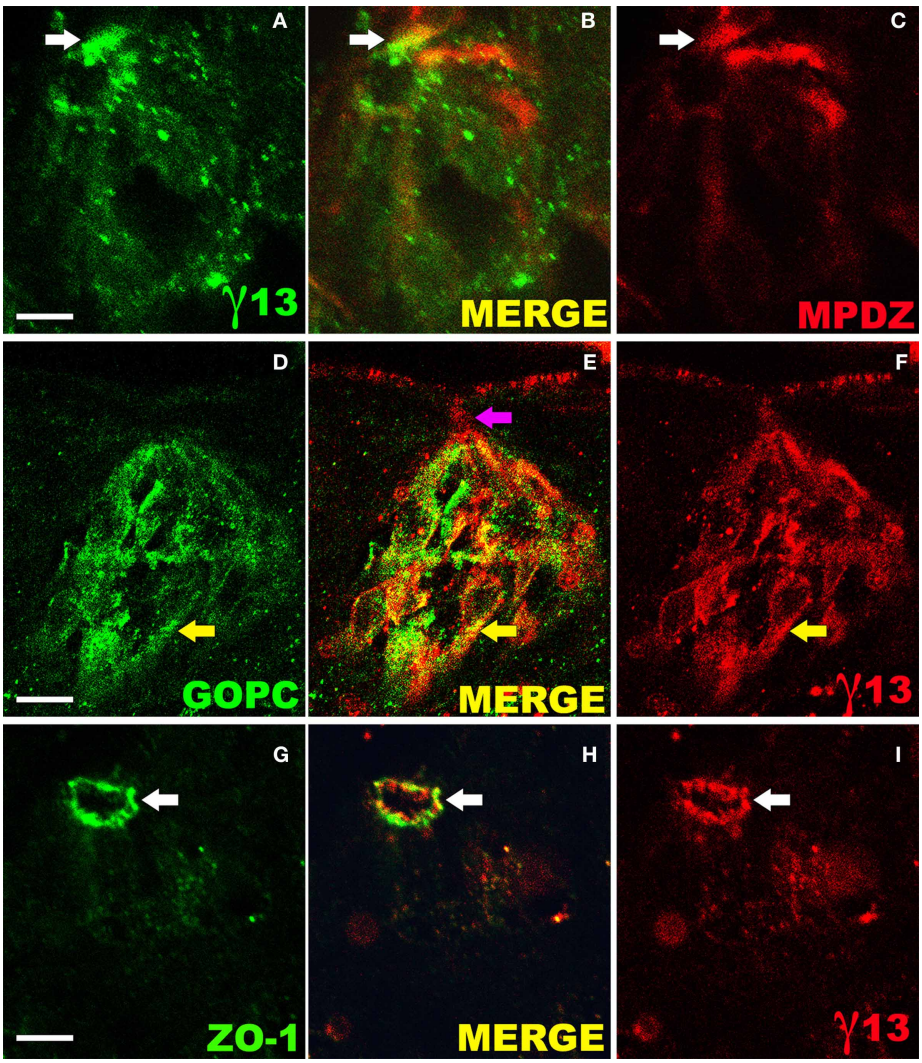

FIGURE 4 | Partial co-localization of Gγ13 with its interaction partners in mouse taste bud cells. Laser scanning confocal microscope analysis of sagittal sections of circumvallate papillae incubated simultaneously with specific antibodies raised against Gγ13 and either ZO-1, MPDZ, or GOPC and revealed with the appropriate fluorescent secondary antibodies. Each image shows one entire taste bud (apical: up, basal: down). Partial co-localization between Gγ-13 and MPDZ **(A–C)** is observed in the cytoplasm and to a small extend the pore (white arrows). GOPC and Gγ-13 staining **(D–F)** shows an extensive overlap in the cytoplasmic region (yellow arrows) but not near the pore (purple arrow). Partial co-localization of ZO-1 and Gγ-13 **(G–I)** is evident at the pore where tight junctions are located. The images presented are single optical sections (not stacks) collected under strict confocal conditions (airy disk 1, GOPC/Gγ-13 Pinhole 82 μm, GOPC or ZO-1/Gγ-13 Pinhole 115 μm). Confocal images where merged electronically using Photoshop. Scale bar 15 μm. Images are representative of staining patterns obtained in >6 taste buds from three mice.

Alternatively Veli-2, another cytosolic Gγ13 binding protein might be able to fulfill the same function (Li et al., 2006). It is interesting to note that both MAGI-I and MDPZ have several (>5) PDZ domains suggesting that in addition to Gγ13 they might concomitantly bind additional proteins such as receptors and channels. $GABA_B$ receptors which have been detected in TBCs and shown to interact with MPDZ represent such an example (Balasubramanian et al., 2007; Cao et al., 2009). Once at the tight junction, ZO-1 would allow docking of Gγ13 and perhaps regulate its entry into the microvilli. In this regard, it is worth noting that detection of Gγ13 in microvilli of TRCs appears weak compared to what is observed in olfactory cilia suggesting that entry of Gγ13 in microvilli is tightly regulated. Alternatively, this interaction might affect paracellular permeability as discussed below.

It is conceivable that within the microvilli Gγ13 could travel to the apical tip through an interaction with the PDZ domain containing protein SAP97 as previously suggested (Li et al., 2006). There Gγ13 would become anchored to the plasma membrane following prenylation of its c-terminal cystein residue. This event would signal the end of the road for Gγ13 as prenylation is preceded by the removal of the residues downstream of the cystein thus eliminating the PDZ binding site as previously noted by Li et al. (2006). At its final destination Gγ13 would presumably

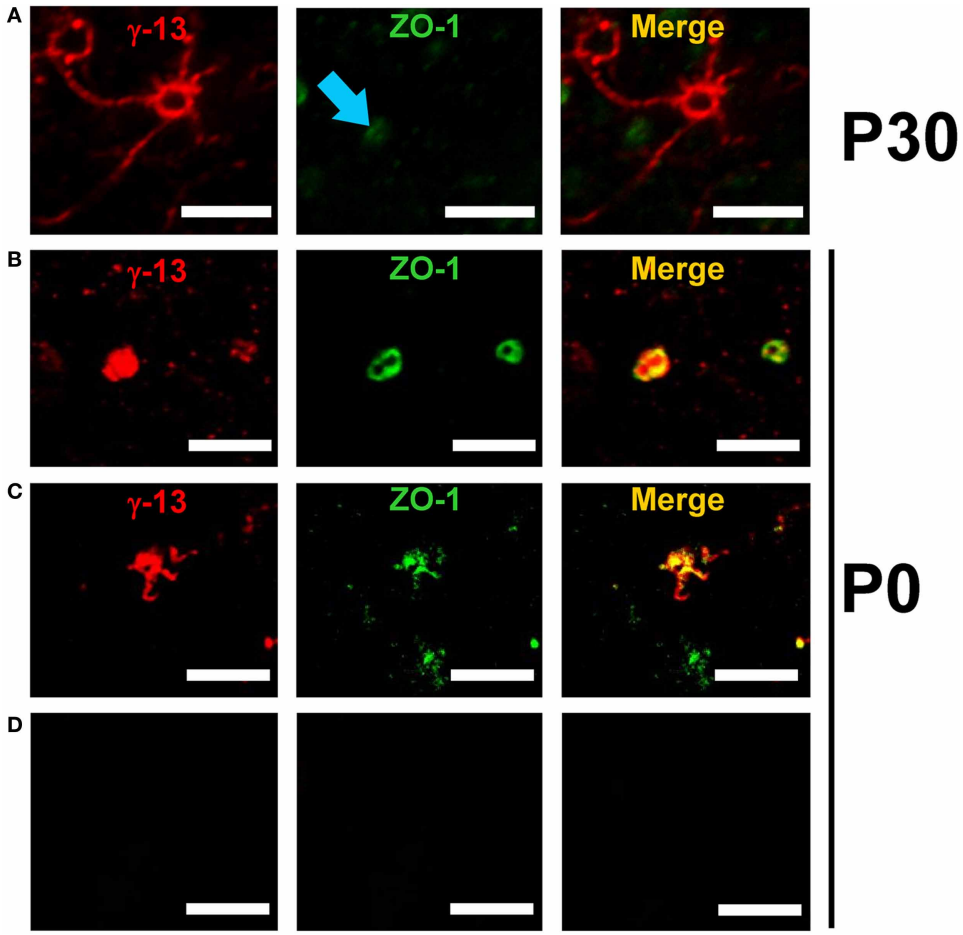

FIGURE 5 | Co-localization of ZO-1 and Gγ13 in mouse olfactory sensory neurons is age-dependent. Series of confocal images showing age-dependent co-localization between Gγ-13 (red) and ZO-1 (green) in mouse olfactory dendritic knobs. **(A)** In P30 mice the immunostaining for ZO-1 (blue arrow) does not co-localize with the Gγ-13 immunostaining. **(B)** In P0 mice a strong co-localization within olfactory dendritic knobs devoid of cilia as well as neurons bearing small-sized cilia **(C)** is observed. **(D)** Control experiment performed by omitting the primary antibody. Scale bar 5 μm.

assemble with Gβ1 and Gαgust to participate in signaling downstream of T2R receptors (Huang et al., 1999). Although the exact sequence of events remains to be confirmed we note that the short sequence between the βB and βC regions of the PDZ domains of PSD95 and Veli-2 thought to accommodate the prenyl group of Gγ13 (Li et al., 2006) is absent from ZO-1 (PDZ1) and MPDZ (PDZ12) (**Figure A3**) perhaps indicating that prenylation occurs later in this sequence.

Gγ13 AT THE TIGHT JUNCTION

The tight junction of polarized epithelial cells plays a fundamental role in the regulation of the paracellular permeability barrier as well as the maintenance of apical and basolateral compartments. Interestingly, heterotrimeric G protein signaling has been implicated in tight junction biogenesis and permeability regulation. Consistent with this a number of modulators of G protein activity (AlF4, cholera, and pertussis toxins) affect tight junction assembly (Balda et al., 1991) and several G protein α subunits including Gαi2, Gαo, Gα12, and Gαs have been located at the tight junction (Saha et al., 2001). In fact, it was recently shown that activation of Gα12, which interacts directly with ZO-1 through its SH3 domain, disrupts the tight junction through a c-Src mediated pathway thereby increasing paracellular permeability (Meyer et al., 2002; Sabath et al., 2008). Heterotrimeric G proteins mediate GPCR signaling through Gα and Gβγ subunits and as expected one GPCR has been reported to regulate tight junction permeability in a pertussis-sensitive manner. This is the case of the somatostatin 3 receptor (SSTR3) which is targeted to the tight junction through a direct interaction between a PDZ binding motif in its c-terminal tail and MPDZ PDZ10 (Liew et al., 2009). Finally, another component of the G protein cascade, namely regulator of G protein signaling 5 (RGS5) has also been reported to interact with ZO-1 (Bal et al., 2012).

Although there are no prior reports of Gβγ subunits at the tight junction, our finding that Gγ13 interacts directly with ZO-1 and MPDZ is not totally unexpected. However the role it might play on TJ assembly, maintenance of polarity, or paracellular permeability in taste bud cells remains to be established.

Gγ13 IN OLFACTORY SENSORY NEURONS

In stark contrast to what is observed in microvilli, Gγ13 is readily detected in cilia of OSNs where it is thought to be involved in sensory signaling. Our observation that Gγ13 and ZO-1 co-localize in the OE of neonates but not in that of adult animals suggests that this interaction might be important during the maturation of the epithelium in mice. In adult rat OE, ZO-1 is localized at apical tight junctions connecting the dendrites of OSNs and surrounding supporting cells (Miragall et al., 1994). Claudins 1, 3, 4, and 5 are part of the apical tight junction complex forming a selective barrier necessary for proper signaling in OSNs (Steinke et al., 2008). Despite the fact that tight junctions in TRCs and OSNs share a number of components including claudin 1, claudin 4, and ZO-1, the absence of co-localization between Gγ13 and ZO-1 in the adult OE clearly points to important organizational dissimilarities in these tissues.

Another notable difference between these tissues includes the fact that in OSNs MPDZ is mainly restricted to the cilia where it is thought to regulate odorant evoked signal duration through a direct interaction with odorant receptors (Dooley et al., 2009). As a result, MPDZ has been deemed a major component of the signalosome downstream of odorant receptors also known as "olfactosome." Our findings extend this concept by showing that another component of the olfactory signaling cascade abundant in cilia, namely Gγ13, also interacts with MPDZ.

Although, there are no current reports of GOPC in OSNs, here we present data indicating that GOPC is detected in the OE. While its precise location and sub-cellular distribution in the OE remains to be investigated, we suspect that it is involved in retention of Gγ13 in the TGN.

Gγ13 AND SENSORY SIGNALING

GPCRs couple selectively to Gα subunits which themselves associate selectively with Gβγ subunits. Upon stimulation of the receptor, both Gα- and Gβγ-mediated processes are activated. Determinants effectively governing downstream events include the repertoire of Gα, Gβ, Gγ and cellular effectors present in the cells expressing the receptor in question as well as the selectivity of the interactions between receptor and Gα subunits and that between Gγ/Gβ subunits and cellular effectors.

If we apply this reasoning to TRCs we note that both Gαgust and Gαi2 are present (McLaughlin et al., 1992; Kusakabe et al., 2000), and that functional and biochemical studies indicate that T2Rs are able to couple to and activate both Gαi/o and Gαgust subunits (Ozeck et al., 2004; Sainz et al., 2007). Experiments with gustducin knock-out (KO) animals implicate both Gαgust and additional Gα subunits in bitter transduction as the KO mice retained sensitivity to bitter substances (Wong et al., 1996). Regarding the beta and gamma subunits, both Gβ1 and Gβ3 have been detected in gustducin expressing cells together with Gγ3 and Gγ13 (Huang et al., 1999; Rossler et al., 2000).

Based on these accounts many possible Gα, Gβ, Gγ combinations may mediate bitter detection in mammals. Nevertheless, it is thought that the heterotrimer composed of Gαgust/Gβ3/Gγ13 is the main player. Under this scenario the Gβ3-Gγ13 complex activates phospholipase C-β2 (PLC-β2) or PLC-β3 (Hacker et al., 2008) while Gαgust acts in parallel on local phosphodiesterases to modulate intracellular cAMP levels. A recent report puts forward an alternative role for Gαgust in taste cells by demonstrating that its constitutive activity maintains low resting cAMP levels thereby regulating the responsiveness of bitter receptor cells (Clapp et al., 2008). This new hypothesis does not take away from the demonstrated central role of PLC-β2 in bitter transduction (Zhang et al., 2003) and the possible involvement of Gγ13 in this process. Nevertheless, a tissue-specific KO model validating the role of Gγ13 in bitter taste transduction *in vivo* is still missing.

Unlike in the taste cells where PLC signaling is paramount to GPCR-mediated tastant detection, in OSNs disruption of the cAMP pathway leads to anosmia (Brunet et al., 1996; Belluscio et al., 1998; Wong et al., 2000). In olfactory cilia Gγ13 co-localizes and is thought to interact with Gβ1 and Gαolf (Kerr et al., 2008). Although, the recombinant Gβ1γ13 dimer appears to be the second most potent activator of PLC-β isoforms after Gβ1γ7 (Poon et al., 2009), the absence of a convincing demonstration of PLC-β expression in OSNs suggests that in these cells Gγ13 might play another role. Kerr et al. reported that Gγ13 interacts with Ric-8B, a guanine nucleotide exchange factor for Gαolf, and hypothesized that by retaining Ric-8B in proximity of Gαolf-GTP, Gγ13 would facilitate re-association of Ric-8B and Gαolf-GDP which ultimately would maximize the efficiency of that pathway.

Our immunostaining experiments suggest that Gγ13 interacts with ZO-1 temporarily during the maturation of the OSN. The impact this interaction might have on sensory signaling or OSN maturation remains to be investigated. Functional maturation is known to occur in OSNs (Lee et al., 2011). This maturation could be correlated with signaling protein trafficking and involve ZO-1 as it was previously implicated in maturation and regeneration in other cell types (Castillon et al., 2002; Kim et al., 2009). Under this scenario it is conceivable that the interaction between ZO-1 and Gγ13 during OSN maturation might induce some functional changes. In this case a tissue-specific Gγ13 KO mouse model will be a valuable tool to help unravel the role of this protein in OSN function *in vivo*.

Finally, in mouse cone and rod bipolar cells Gγ13 appears to be distributed throughout the cells while Gαo is concentrated in dendrites. The co-expression of Gγ13 with Gβ3, Gβ4, and Gαo in ON cone bipolar cells which do not contain PLC-β suggests that it might be involved in yet another signaling pathway in these cells (Huang et al., 2003). In this tissue where ZO-1 expression has been reported as well (Ciolofan et al., 2006), it would be interesting to investigate whether these proteins are partly co-localized.

CONCLUSION

In the present study, we report the identification of three novel binding partners for Gγ13. In addition, we provide the first evidence of the expression of two of these proteins (GOPC and MPDZ) in taste bud cells. We anticipate that future work addressing the sequence of these interactions with Gγ13 and their temporality will help shed more light on the precise role these proteins play in efficiently targeting Gγ13 to selective subcellular locations.

By comparing the subcellular location of some of these proteins in OSNs and neuroepithelial taste cells, our study points out possible discrepancies in the mechanisms guiding protein traffic

and subcellular localization in these two cell types. These differences might not be surprising given the differences in the origin (neuronal vs. epithelial) and the architecture of neuroepithelial taste cells and OSNs. In particular, we believe that the differential location of MPDZ and Gγ13 in OSNs and TRCs reflects different mechanisms at play in both types of sensory cells and provides some clues as to what their function in these cells might be (transport vs. signalosome). Interestingly, MPDZ is thought to act as a scaffolding protein in the spermatozoa, a polarized cell capable of chemotaxis through taste and odorant receptors (Zitranski et al., 2010).

The presence of MPDZ, ZO-1, and Gγ13 at the tight junction in TRCs is intriguing and remains to be investigated further. In this context it is interesting to mention that ZO-1 has been demonstrated to associate with F-actin through an actin-binding region located in the C-terminal half of the molecule (Fanning et al., 2002) and that F-actin filaments are major structural components of taste cells microvilli (Takeda et al., 1989).

Finally, we would like to mention that given the expected importance of Gγ13 in taste cells signaling, disruption of any of the interactions reported here could have important consequences on taste reception. There is such a precedent in the OE where polymorphisms in CEP290, a protein which cargoes Gγ13, Gαs, and Gβ1 from the base of the cilia toward the tip, have been linked with anosmia (McEwen et al., 2007).

ACKNOWLEDGMENTS

We would like to thank Dr. A. Fanning (University of North Carolina at Chapel Hill, USA) for providing the Myc-tagged ZO-1 constructs and kindly sharing protocols with us, Dr. O. Keskin (Koç University, Turkey) for help with the classification of PDZ domains. Dr. E. Assémat (IBDML, Marseille) and C. Neophytou (Emergo, Cyprus) for advice on MPDZ and ZO-1 antibodies respectively, Dr. C. Arnould (INRA, Dijon) for help with confocal microscopy and A. Lefranc for help with animal husbandry. We are grateful to Dr. B. Malnic (University of Sao Paolo, Brazil) for the FLAG-Gγ13 construct, insightful comments and suggestions throughout, Dr. V. Dionne (Boston University, USA) for critical reading of the manuscript, and Dr. G. Strichartz (Brigham and Women's Hospital, USA) for support. This work was supported by Action Thematique Incitative sur Programme (CNRS) grants to Jean-Pierre Montmayeur and Xavier Grosmaitre, Région de Bourgogne and CNRS poste rouge post-doctoral fellowships to Zhenhui Liu and Esmerina Tili respectively, and funds from GOSPEL (IST-2002-507610) to Fabienne Laugerette and Anna Wiencis.

REFERENCES

Anderson, J. M., Stevenson, B. R., Jesaitis, L. A., Goodenough, D. A., and Mooseker, M. S. (1988). Characterization of ZO-1, a protein component of the tight junction from mouse liver and Madin-Darby canine kidney cells. *J. Cell Biol.* 106, 1141–1149.

Balasubramanian, S., Fam, S. R., and Hall, R. A. (2007). GABAB receptor association with the PDZ scaffold Mupp1 alters receptor stability and function. *J. Biol. Chem.* 282, 4162–4171.

Bal, M. S., Castro, V., Piontek, J., Rueckert, C., Walter, J. K., Shymanets, A., Kurig, B., Haase, H., and Blasig, I. E. (2012). The hinge region of the scaffolding protein of cell contacts, zonula occludens protein 1, regulates interacting with various signaling proteins. *J. Cell. Biochem.* 113, 934–945.

Balda, M. S., Gonzalez-Mariscal, L., Contreras, R. G., Macias-Silva, M., Torres-Marquez, M. E., Garcia-Sainz, J. A., and Cereijido, M. (1991). Assembly and sealing of tight junctions: possible participation of G-proteins, phospholipase C, protein kinase C and calmodulin. *J. Membr. Biol.* 122, 193–202.

Belluscio, L., Gold, G. H., Nemes, A., and Axel, R. (1998). Mice deficient in G(olf) are anosmic. *Neuron* 20, 69–81.

Bezprozvanny, I., and Maximov, A. (2001). Classification of PDZ domains. *FEBS Lett.* 509, 457–462.

Bolz, H., von Brederlow, B., Ramirez, A., Bryda, E. C., Kutsche, K., Nothwang, H. G., Seeliger, M., del, C. S. C. M., Vila, M. C., Molina, O. P., Gal, A., and Kubisch, C. (2001). Mutation of CDH23, encoding a new member of the cadherin gene family, causes Usher syndrome type 1D. *Nat. Genet.* 27, 108–112.

Brunet, L. J., Gold, G. H., and Ngai, J. (1996). General anosmia caused by a targeted disruption of the mouse olfactory cyclic nucleotide-gated cation channel. *Neuron* 17, 681–693.

Cao, Y., Zhao, F. L., Kolli, T., Hivley, R., and Herness, S. (2009). GABA expression in the mammalian taste bud functions as a route of inhibitory cell-to-cell communication. *Proc. Natl. Acad. Sci. U.S.A.* 106, 4006–4011.

Castillon, N., Hinnrasky, J., Zahm, J. M., Kaplan, H., Bonnet, N., Corlieu, P., Klossek, J. M., Taouil, K., Avril-Delplanque, A., Peault, B., and Puchelle, E. (2002). Polarized expression of cystic fibrosis transmembrane conductance regulator and associated epithelial proteins during the regeneration of human airway surface epithelium in three-dimensional culture. *Lab. Invest.* 82, 989–998.

Cheng, J., Moyer, B. D., Milewski, M., Loffing, J., Ikeda, M., Mickle, J. E., Cutting, G. R., Li, M., Stanton, B. A., and Guggino, W. B. (2002). A Golgi-associated PDZ domain protein modulates cystic fibrosis transmembrane regulator plasma membrane expression. *J. Biol. Chem.* 277, 3520–3529.

Ciolofan, C., Li, X. B., Olson, C., Kamasawa, N., Gebhardt, B. R., Yasumura, T., Morita, M., Rash, J. E., and Nagy, J. I. (2006). Association of connexin36 and zonula occludens-1 with zonula occludens-2 and the transcription factor zonula occludens-1-associated nucleic acid-binding protein at neuronal gap junctions in rodent retina. *Neuroscience* 140, 433–451.

Clapp, T. R., Stone, L. M., Margolskee, R. F., and Kinnamon, S. C. (2001). Immunocytochemical evidence for co-expression of Type III IP3 receptor with signaling components of bitter taste transduction. *BMC Neurosci.* 2, 6.

Clapp, T. R., Trubey, K. R., Vandenbeuch, A., Stone, L. M., Margolskee, R. F., Chaudhari, N., and Kinnamon, S. C. (2008). Tonic activity of Galpha-gustducin regulates taste cell responsivity. *FEBS Lett.* 582, 3783–3787.

Dooley, R., Baumgart, S., Rasche, S., Hatt, H., and Neuhaus, E. M. (2009). Olfactory receptor signaling is regulated by the post-synaptic density 95, Drosophila discs large, zona-occludens 1 (PDZ) scaffold multi-PDZ domain protein 1. *FEBS J.* 276, 7279–7290.

Fanning, A. S., Jameson, B. J., Jesaitis, L. A., and Anderson, J. M. (1998). The tight junction protein ZO-1 establishes a link between the transmembrane protein occludin and the actin cytoskeleton. *J. Biol. Chem.* 273, 29745–29753.

Fanning, A. S., Ma, T. Y., and Anderson, J. M. (2002). Isolation and functional characterization of the actin binding region in the tight junction protein ZO-1. *FASEB J.* 16, 1835–1837.

Fenech, C., Patrikainen, L., Kerr, D. S., Grall, S., Liu, Z., Laugerette, F., Malnic, B., and Montmayeur, J. P. (2009). Ric-8A, a Galpha protein guanine nucleotide exchange factor potentiates taste receptor signaling. *Front. Cell. Neurosci.* 3:11. doi: 10.3389/neuro.03.011.2009

Finger, T. E. (2005). Cell types and lineages in taste buds. *Chem. Senses* 30 (Suppl. 1), i54–i55.

Furuse, M., Fujita, K., Hiiragi, T., Fujimoto, K., and Tsukita, S. (1998). Claudin-1 and -2, novel integral membrane proteins localizing at tight junctions with no sequence similarity to occludin. *J. Cell Biol.* 141, 1539–1550.

Furuse, M., Itoh, M., Hirase, T., Nagafuchi, A., Yonemura, S., Tsukita, S., and Tsukita, S. (1994).

Direct association of occludin with ZO-1 and its possible involvement in the localization of occludin at tight junctions. *J. Cell Biol.* 127, 1617–1626.

Gao, N., Lu, M., Echeverri, F., Laita, B., Kalabat, D., Williams, M. E., Hevezi, P., Zlotnik, A., and Moyer, B. D. (2009). Voltage-gated sodium channels in taste bud cells. *BMC Neurosci.* 10, 20.

Gentzsch, M., Cui, L., Mengos, A., Chang, X. B., Chen, J. H., and Riordan, J. R. (2003). The PDZ-binding chloride channel ClC-3B localizes to the Golgi and associates with cystic fibrosis transmembrane conductance regulator-interacting PDZ proteins. *J. Biol. Chem.* 278, 6440–6449.

Gilbertson, T. A., Damak, S., and Margolskee, R. F. (2000). The molecular physiology of taste transduction. *Curr. Opin. Neurobiol.* 10, 519–527.

Gumbiner, B., Lowenkopf, T., and Apatira, D. (1991). Identification of a 160-kDa polypeptide that binds to the tight junction protein ZO-1. *Proc. Natl. Acad. Sci. U.S.A.* 88, 3460–3464.

Hacker, K., Laskowski, A., Feng, L., Restrepo, D., and Medler, K. (2008). Evidence for two populations of bitter responsive taste cells in mice. *J. Neurophysiol.* 99, 1503–1514.

Hamazaki, Y., Itoh, M., Sasaki, H., Furuse, M., and Tsukita, S. (2002). Multi-PDZ domain protein 1 (MUPP1) is concentrated at tight junctions through its possible interaction with claudin-1 and junctional adhesion molecule. *J. Biol. Chem.* 277, 455–461.

Hassel, B., Schreff, M., Stube, E. M., Blaich, U., and Schumacher, S. (2003). CALEB/NGC interacts with the Golgi-associated protein PIST. *J. Biol. Chem.* 278, 40136–40143.

He, W., Yasumatsu, K., Varadarajan, V., Yamada, A., Lem, J., Ninomiya, Y., Margolskee, R. F., and Damak, S. (2004). Umami taste responses are mediated by alpha-transducin and alpha-gustducin. *J. Neurosci.* 24, 7674–7680.

Hofer, D., and Drenckhahn, D. (1999). Localisation of actin, villin, fimbrin, ezrin and ankyrin in rat taste receptor cells. *Histochem. Cell Biol.* 112, 79–86.

Huang, L., Max, M., Margolskee, R. F., Su, H., Masland, R. H., and Euler, T. (2003). G protein subunit G gamma 13 is coexpressed with G alpha o, G beta 3, and G beta 4 in retinal ON bipolar cells. *J. Comp. Neurol.* 455, 1–10.

Huang, L., Shanker, Y. G., Dubauskaite, J., Zheng, J. Z., Yan, W., Rosenzweig, S., Spielman, A. I., Max, M., and Margolskee, R. F. (1999). Ggamma13 colocalizes with gustducin in taste receptor cells and mediates IP3 responses to bitter denatonium. *Nat. Neurosci.* 2, 1055–1062.

Huang, Y. A., and Roper, S. D. (2010). Intracellular Ca(2+) and TRPM5-mediated membrane depolarization produce ATP secretion from taste receptor cells. *J. Physiol.* 588, 2343–2350.

Ito, H., Iwamoto, I., Morishita, R., Nozawa, Y., Asano, T., and Nagata, K. (2006). Identification of a PDZ protein, PIST, as a binding partner for Rho effector Rhotekin: biochemical and cell-biological characterization of Rhotekin-PIST interaction. *Biochem. J.* 397, 389–398.

Itoh, M., Furuse, M., Morita, K., Kubota, K., Saitou, M., and Tsukita, S. (1999). Direct binding of three tight junction-associated MAGUKs, ZO-1, ZO-2, and ZO-3, with the COOH termini of claudins. *J. Cell Biol.* 147, 1351–1363.

Kalyoncu, S., Keskin, O., and Gursoy, A. (2010). Interaction prediction and classification of PDZ domains. *BMC Bioinformatics* 11, 357.

Kerr, D. S., von Dannecker, L. E., Davalos, M., Michaloski, J. S., and Malnic, B. (2008). Ric-8B interacts with G alpha olf and G gamma 13 and co-localizes with G alpha olf, G beta 1 and G gamma 13 in the cilia of olfactory sensory neurons. *Mol. Cell. Neurosci.* 38, 341–348.

Kim, J. H., Kim, J. H., Yu, Y. S., Kim, D. H., and Kim, K. W. (2009). Recruitment of pericytes and astrocytes is closely related to the formation of tight junction in developing retinal vessels. *J. Neurosci. Res.* 87, 653–659.

Kulaga, H. M., Leitch, C. C., Eichers, E. R., Badano, J. L., Lesemann, A., Hoskins, B. E., Lupski, J. R., Beales, P. L., Reed, R. R., and Katsanis, N. (2004). Loss of BBS proteins causes anosmia in humans and defects in olfactory cilia structure and function in the mouse. *Nat. Genet.* 36, 994–998.

Kusakabe, Y., Yasuoka, A., Asano-Miyoshi, M., Iwabuchi, K., Matsumoto, I., Arai, S., Emori, Y., and Abe, K. (2000). Comprehensive study on G protein alpha-subunits in taste bud cells, with special reference to the occurrence of Galphai2 as a major Galpha species. *Chem. Senses* 25, 525–531.

Lee, A. C., He, J., and Ma, M. (2011). Olfactory marker protein is critical for functional maturation of olfactory sensory neurons and development of mother preference. *J. Neurosci.* 31, 2974–2982.

Li, Z., Benard, O., and Margolskee, R. F. (2006). Ggamma13 interacts with PDZ domain-containing proteins. *J. Biol. Chem.* 281, 11066–11073.

Liew, C. W., Vockel, M., Glassmeier, G., Brandner, J. M., Fernandez-Ballester, G. J., Schwarz, J. R., Schulz, S., Buck, F., Serrano, L., Richter, D., and Kreienkamp, H. J. (2009). Interaction of the human somatostatin receptor 3 with the multiple PDZ domain protein MUPP1 enables somatostatin to control permeability of epithelial tight junctions. *FEBS Lett.* 583, 49–54.

Matsunami, H., Montmayeur, J. P., and Buck, L. B. (2000). A family of candidate taste receptors in human and mouse. *Nature* 404, 601–604.

McEwen, D. P., Koenekoop, R. K., Khanna, H., Jenkins, P. M., Lopez, I., Swaroop, A., and Martens, J. R. (2007). Hypomorphic CEP290/NPHP6 mutations result in anosmia caused by the selective loss of G proteins in cilia of olfactory sensory neurons. *Proc. Natl. Acad. Sci. U.S.A.* 104, 15917–15922.

McLaughlin, S. K., McKinnon, P. J., and Margolskee, R. F. (1992). Gustducin is a taste-cell-specific G protein closely related to the transducins. *Nature* 357, 563–569.

Meyer, T. N., Schwesinger, C., and Denker, B. M. (2002). Zonula occludens-1 is a scaffolding protein for signaling molecules. Galpha(12) directly binds to the Src homology 3 domain and regulates paracellular permeability in epithelial cells. *J. Biol. Chem.* 277, 24855–24858.

Michlig, S., Damak, S., and Le Coutre, J. (2007). Claudin-based permeability barriers in taste buds. *J. Comp. Neurol.* 502, 1003–1011.

Miragall, F., Krause, D., de Vries, U., and Dermietzel, R. (1994). Expression of the tight junction protein ZO-1 in the olfactory system: presence of ZO-1 on olfactory sensory neurons and glial cells. *J. Comp. Neurol.* 341, 433–448.

Mitic, L. L., and Anderson, J. M. (1998). Molecular architecture of tight junctions. *Annu. Rev. Physiol.* 60, 121–142.

Ohtubo, Y., and Yoshii, K. (2011). Quantitative analysis of taste bud cell numbers in fungiform and soft palate taste buds of mice. *Brain Res.* 1367, 13–21.

Ozeck, M., Brust, P., Xu, H., and Servant, G. (2004). Receptors for bitter, sweet and umami taste couple to inhibitory G protein signaling pathways. *Eur. J. Pharmacol.* 489, 139–149.

Poon, L. S., Chan, A. S., and Wong, Y. H. (2009). Gbeta3 forms distinct dimers with specific Ggamma subunits and preferentially activates the beta3 isoform of phospholipase C. *Cell. Signal.* 21, 737–744.

Ren, X., Zhou, L., Terwilliger, R., Newton, S. S., and de Araujo, I. E. (2009). Sweet taste signaling functions as a hypothalamic glucose sensor. *Front. Integr. Neurosci.* 3:12. doi: 10.3389/neuro.07.012.2009

Rossler, P., Boekhoff, I., Tareilus, E., Beck, S., Breer, H., and Freitag, J. (2000). G protein betagamma complexes in circumvallate taste cells involved in bitter transduction. *Chem. Senses* 25, 413–421.

Sabath, E., Negoro, H., Beaudry, S., Paniagua, M., Angelow, S., Shah, J., Grammatikakis, N., Yu, A. S., and Denker, B. M. (2008). Galpha12 regulates protein interactions within the MDCK cell tight junction and inhibits tight-junction assembly. *J. Cell Sci.* 121, 814–824.

Saha, C., Nigam, S. K., and Denker, B. M. (2001). Expanding role of G proteins in tight junction regulation: Galpha(s) stimulates TJ assembly. *Biochem. Biophys. Res. Commun.* 285, 250–256.

Sainz, E., Cavenagh, M. M., Gutierrez, J., Battey, J. F., Northup, J. K., and Sullivan, S. L. (2007). Functional characterization of human bitter taste receptors. *Biochem. J.* 403, 537–543.

Schwarzenbacher, K., Fleischer, J., and Breer, H. (2005). Formation and maturation of olfactory cilia monitored by odorant receptor-specific antibodies. *Histochem. Cell Biol.* 123, 419–428.

Sheng, M. (1996). PDZs and receptor/channel clustering: rounding up the latest suspects. *Neuron* 17, 575–578.

Steinke, A., Meier-Stiegen, S., Drenckhahn, D., and Asan, E. (2008). Molecular composition of tight and adherens junctions in the rat olfactory epithelium and fila. *Histochem. Cell Biol.* 130, 339–361.

Stevenson, B. R., and Keon, B. H. (1998). The tight junction: morphology to molecules. *Annu. Rev. Cell Dev. Biol.* 14, 89–109.

Takeda, M., Obara, N., and Suzuki, Y. (1989). Cytoskeleton in the apical region of mouse taste bud cells. *Shika Kiso Igakkai Zasshi* 31, 317–323.

Tsukita, S., and Furuse, M. (1998). Overcoming barriers in the study of tight junction functions: from occludin to claudin. *Genes Cells* 3, 569–573.

Tsukita, S., Yamazaki, Y., Katsuno, T., Tamura, A., and Tsukita, S. (2008). Tight junction-based epithelial microenvironment and cell proliferation. *Oncogene* 27, 6930–6938.

Utepbergenov, D. I., Fanning, A. S., and Anderson, J. M. (2006). Dimerization of the scaffolding protein ZO-1 through the second PDZ domain. *J. Biol. Chem.* 281, 24671–24677.

Vandenbeuch, A., and Kinnamon, S. C. (2009). Why do taste cells generate action potentials? *J. Biol.* 8, 42.

Wente, W., Stroh, T., Beaudet, A., Richter, D., and Kreienkamp, H. J. (2005). Interactions with PDZ domain proteins PIST/GOPC and PDZK1 regulate intracellular sorting of the somatostatin receptor subtype 5. *J. Biol. Chem.* 280, 32419–32425.

Wong, G. T., Gannon, K. S., and Margolskee, R. F. (1996). Transduction of bitter and sweet taste by gustducin. *Nature* 381, 796–800.

Wong, S. T., Trinh, K., Hacker, B., Chan, G. C., Lowe, G., Gaggar, A., Xia, Z., Gold, G. H., and Storm, D. R. (2000). Disruption of the type III adenylyl cyclase gene leads to peripheral and behavioral anosmia in transgenic mice. *Neuron* 27, 487–497.

Xu, Z., Oshima, K., and Heller, S. (2010). PIST regulates the intracellular trafficking and plasma membrane expression of Cadherin 23. *BMC Cell Biol.* 11, 80.

Yao, R., Maeda, T., Takada, S., and Noda, T. (2001). Identification of a PDZ domain containing Golgi protein, GOPC, as an interaction partner of frizzled. *Biochem. Biophys. Res. Commun.* 286, 771–778.

Zhang, Y., Hoon, M. A., Chandrashekar, J., Mueller, K. L., Cook, B., Wu, D., Zuker, C. S., and Ryba, N. J. (2003). Coding of sweet, bitter, and umami tastes: different receptor cells sharing similar signaling pathways. *Cell* 112, 293–301.

Zitranski, N., Borth, H., Ackermann, F., Meyer, D., Viewig, L., Breit, A., Gudermann, T., and Boekhoff, I. (2010). The "acrosomal synapse": subcellular organization by lipid rafts and scaffolding proteins exhibits high similarities in neurons and mammalian spermatozoa. *Commun. Integr. Biol.* 3, 513–521.

Conflict of Interest Statement: The authors declare that the research was conducted in the absence of any commercial or financial relationships that could be construed as a potential conflict of interest.

Received: 03 April 2012; paper pending published: 13 April 2012; accepted: 31 May 2012; published online: 21 June 2012.

*Citation: Liu Z, Fenech C, Cadiou H, Grall S, Tili E, Laugerette F, Wiencis A, Grosmaitre X and Montmayeur J-P (2012) Identification of new binding partners of the chemosensory signaling protein Gγ13 expressed in taste and olfactory sensory cells. Front. Cell. Neurosci. **6**:26. doi: 10.3389/fncel.2012.00026*

Copyright © 2012 Liu, Fenech, Cadiou, Grall, Tili, Laugerette, Wiencis, Grosmaitre and Montmayeur. This is an open-access article distributed under the terms of the Creative Commons Attribution Non Commercial License, which permits non-commercial use, distribution, and reproduction in other forums, provided the original authors and source are credited.

APPENDIX

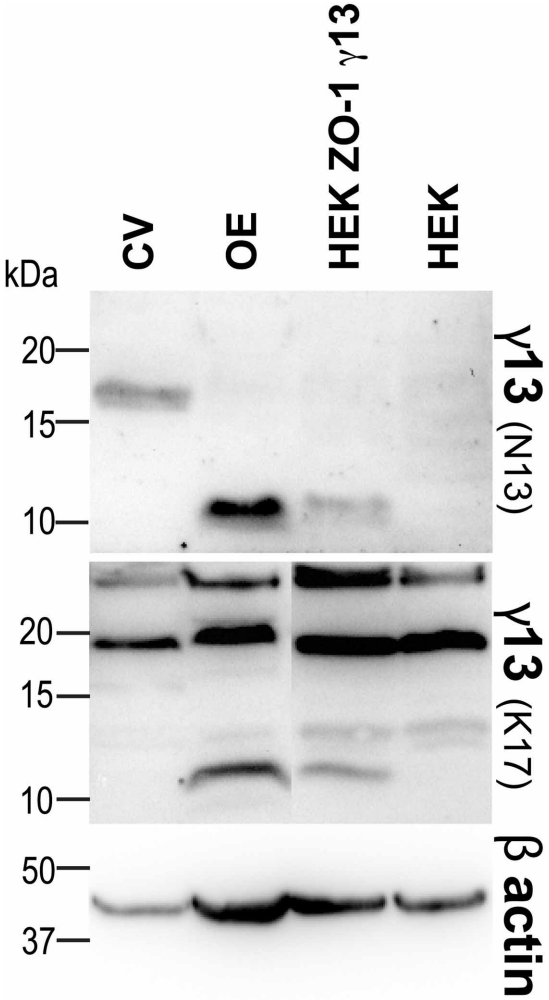

FIGURE A1 | Different features for Gγ13 in CV and OE. Immunodetection of Gγ13 protein in circumvallate (CV) and whole olfactory epithelium (OE) protein extracts. Protein extracts of HEK 293 cells (HEK) or HEK 293 cells stably expressing HA-Gγ13 transiently transfected with a full length Myc-ZO-1 construct (HEK ZO-1 γ13) were used as controls. Note that Gγ13 displays a higher apparent molecular weight in CV than in OE or HEK ZO-1 γ13 cells where the detected band runs at the predicted molecular mass (8 kDa). An antibody raised against the N-terminal region of Gγ13 does not recognize Gγ13 in CV while it does in OE and HEK ZO-1 γ13 cells. β-actin (42 kDa) was used as loading control. The results presented are representative of two independent experiments.

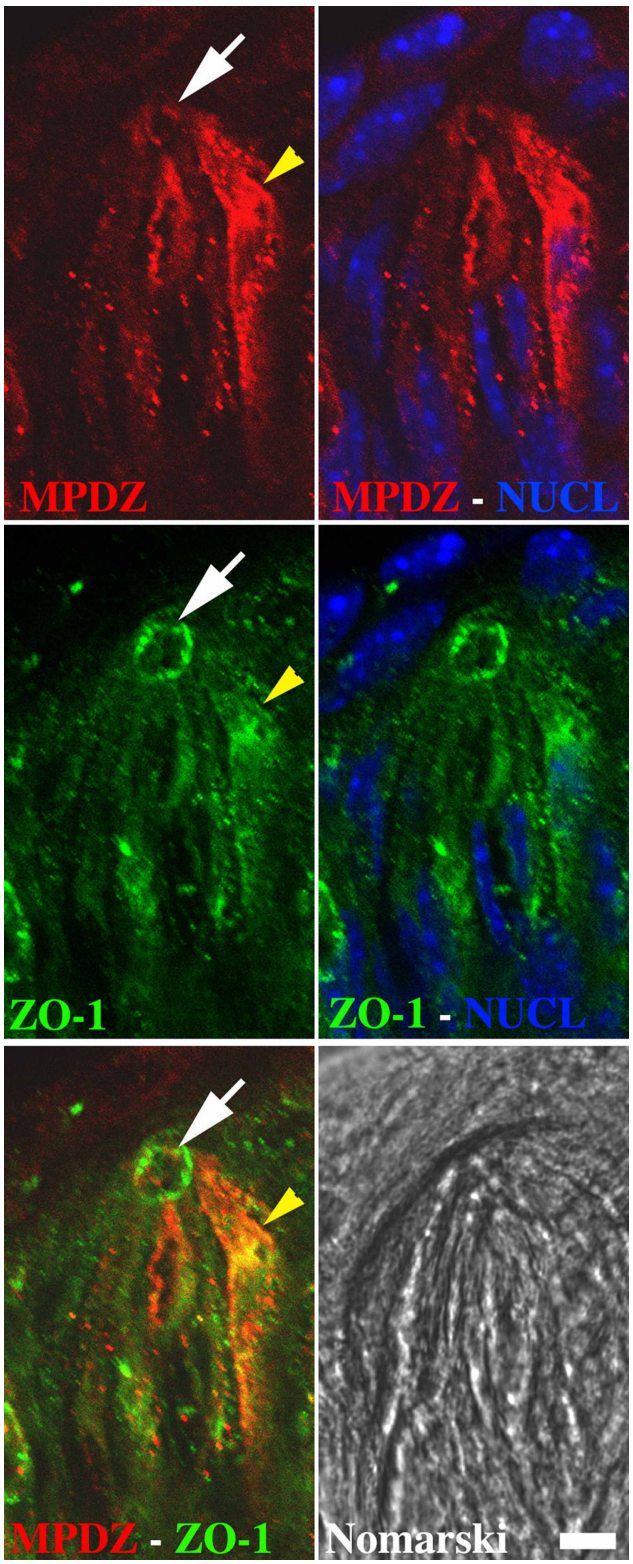

FIGURE A2 | Partial co-localization between ZO-1 and MPDZ in CV taste bud cells. Immunolocalization of MPDZ (red) and ZO-1 (green) in circumvallate taste buds. Indirect immunofluorescence on saggital cryosections of circumvallate papillae was performed as described under Section "Immunohistochemistry." Each image shows one entire taste bud (apical: up, basal: down). Nuclei (blue) were visualized using nuclear stain. MPDZ and ZO-1 staining overlaps partly in the cytoplasm (yellow arrowhead) and at the taste pore (white arrow). The Nomarski image shows the location of the taste bud. Scale bar = 15 μm. Images are representative of staining patterns from at least 5 taste buds.

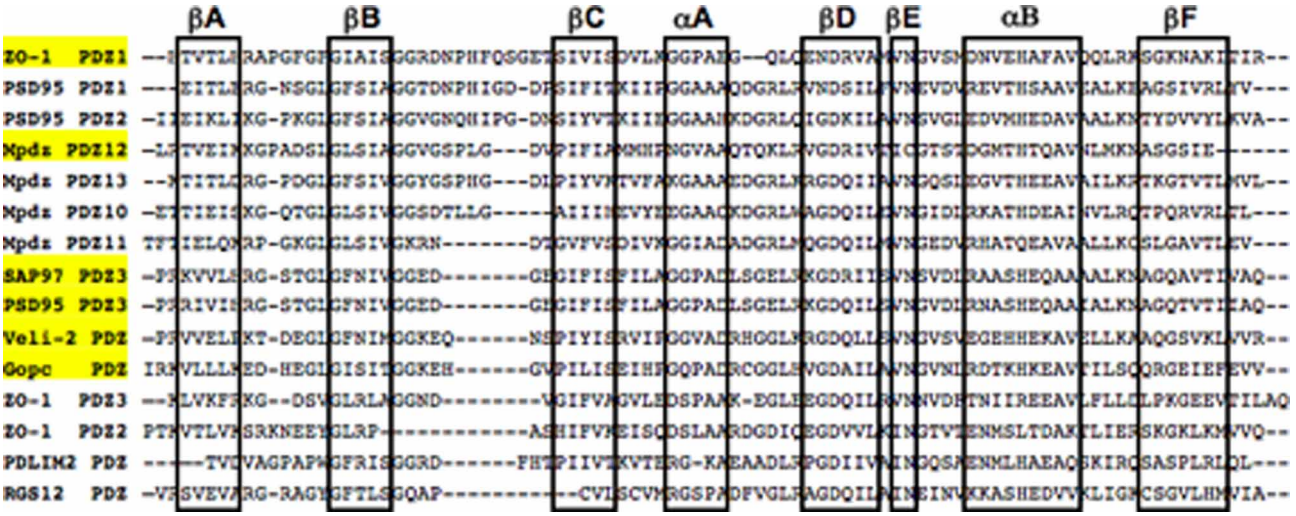

FIGURE A3 | PDZ domains sequence alignment. The amino acid sequence of select PDZ domains from GOPC, MPDZ, PDLIM2, PSD95, RGS12, SAP97, and Veli-2 used in our initial yeast-two hybrid screening were aligned using clustalW 2.1. Residues involved in α-helices and β-sheet structures are boxed. PDZ domains interacting with Gγ13 are highlighted in yellow. Note that the stretch of amino acids present between the βB and βC sheet is of variable length between the various binding partners of Gγ13 thus making it unlikely that this region plays a critical role in the interaction as suggested by Li et al.

Table A1 | List of primer sequences and corresponding annealing temperatures used for PCR experiments.

Gene	Forward primer sequence	Reverse primer sequence	Template Acc#	Ampl. size (bp)	Tm (°C)
Gng13	CGAGGTCGACTGAGGAGTGGGATGTGCC	CTTAGCGGCCGCTCATAGGATGGTGCACTT	AY029485	200	56
Gng13TA	CGAGGTCGACTGAGGAGTGGGATGTGCC	CTTAGCGGCCGCTCATAGGATGGCGCACTT	AY029485	200	54
Tjp1 (PDZ1)	CGAGGTCGACTGCAATGGAGGAAACAGCTA	CTTAGCGGCCGCTTAACTTACAGGGATCTGAACTTTC	BC138028	317	58
Tjp1 (PDZ2)	CGAGGTCGACTTCCGTGGCCTCCAGTCAG	CTTAGCGGCCGCTTAAATTTCTGAAATGTCATCTCTTTCC	BC138028	353	58
Tjp1 (PDZ3)	CGAGGTCGACTCCGAAACCTGTGTATGCT	CTTAGCGGCCGCTTAAACGTCCTTCTTCTTCTG	BC138028	365	55
#Tjp1 (PDZ1-2)	CGAGGTCGACTGCAATGGAGGAAACAGCTA	CTTAGCGGCCGCTTAAATTTCTGAAATGTCATCTCTTTCC	BC138028	842	58
Tjp1 (PDZ2-3)	CGAGGTCGACTTCCGTGGCCTCCAGTCAG	CTTAGCGGCCGCTTAAACGTCCTTCTTCTTCTG	BC138028	995	55
Tjp1 (PDZ3-SH3)	CGAGGTCGACTCCGAAACCTGTGTATGCT	CTTAGCGGCCGCTTAAGCTGGGAACTTAGTTTGAA	BC138028	743	56
Tjp1 (SH3)	CGAGGTCGACTGTGACCATACTGGCTCAG	CTTAGCGGCCGCTTAAGCTGGGAACTTAGTTTGAA	BC138028	410	56
Tjp1 (PDZ1-SH3)	CGAGGTCGACTGCAATGGAGGAAACAGCTA	CTTAGCGGCCGCTTAAGCTGGGAACTTAGTTTGAA	BC138028	1862	56
Tjp1 (PDZ1-PDZ3)	CGAGGTCGACTGCAATGGAGGAAACAGCTA	CTTAGCGGCCGCTTAAACGTCCTTCTTCTTCTG	BC138028	1484	55
Cldn1	CGAGGTCGACTCGGAAAACAACCTCTTAC	CTTAGCGGCCGCTCACACATAGTCTTTCCC	EU076705	74	55
Cldn4	CGAGGTCGACTCCTCGTAGCAACGACAAG	CTTAGCGGCCGCTTACACATAGTTGCTGGCGG	AF087822	74	60
Cldn8	CGAGGTCGACTACTGAAAGGAGCAACAGTTA	CTTAGCGGCCGCCTACACATACTGACTTTTGG	AF087826	113	56
F11r	CGAGGTCGACCAGCCGTGGATACTTTGAAAGAAC	CTTAGCGGCCGCTCACACCAGGAACGACGA	BC021876	119	60
Lin7b	CGAGGTCGACTCCCAGGGTCGTGGAACTA	CTTAGCGGCCGCTCAAGTGTAGCGCACCACCAG	AF087694	251	62
Dlg1 (PDZ3)	CGAGGTCGACTATCACTAGGGAACCTAGA	CTTAGCGGCCGCTTAACGACTGTACTCTTCGGG	AY159380	279	55
Dlg4 (PDZ3)	CGAGGTCGACTAGGCGGATCGTGATCCAT	CTTAGCGGCCGCTTACTCTTCTGGTTTATACTGAGC	BC014807	256	58
Mpdz (PDZ10-11)	CGAGGTCGACTTCCTCCACACCAGCAGTC	CTTAGCGGCCGCTTAGGGGGAGTGAAAGATGACAG	BC145117	682	62
#Mpdz (PDZ12-13)	CGAGGTCGACTGGAATAAATACATCAGAGTCA	CTTAGCGGCCGCTCAAGAGAGAACCATGAG	BC145117	704	55
Pdlim2	CGAGGTCGACTATGGCGTTGACTGTGGATG	CTTAGCGGCCGCTTATGTTTGGGACCGGTCCAG	BC024556	254	60
#Gopc	CGAGGTCGACTATTAGAAAAGTTCTCCTCCTT	CTTAGCGGCCGCTTAGACTACTTCAAACTCAATC	AF287894	250	54
Rgs12	CGAGGTCGACTGTGCGGAGCGTCGAAGTG	CTTAGCGGCCGCTCACTCAGCAATCACCATGTGCAG	BC40396	233	62
*Gng13	ATGGAGGAGTGGGATGT	TCATAGGATGGTGCACTTG	AY029485	203	54
*Gnat3	TCAGGAGGATGCTGAGCG	ATGCCCTTTCAAAGCAGGC	BC147841	361	56
*Gapdh	TGGTCACCAGGGCTGC	GTGGCAGTGATGGCATG	GU214026	501	59

(*) Primers and annealing temperatures used for RT-PCR only.

(#) Primers and annealing temperatures used for both cloning and RT-PCR experiments.

(Acc#) GenBank accession number.

Table A2 | Table summarizing the results (from at least three independent experiments) of the yeast two-hybrid interaction assays performed with different combinations of baits and preys.

Bait	Prey	3-AT (12.5 mM)	3-AT (25 mM)	3-AT (50 mM)
Gγ13	ZO-1 PDZ1	+	+	−
Gγ13	ZO-1 PDZ2	+	−	
Gγ13	ZO-1 PDZ3	−		
Gγ13	ZO-1 SH3	+	−	
Gγ13	ZO-1 PDZ1-2	+	+	+
Gγ13	ZO-1 PDZ2-3	+	−	
Gγ13	ZO-1 PDZ3-SH3	+	−	
Gγ13	ZO-1 PDZ1-2-3-SH3	+	+	
Gγ13	Veli-2	+	−	
Gγ13	PSD95 PDZ3	+	−	
Gγ13	SAP97 PDZ3	+	−	
Gγ13	PDLIM2	-		
Gγ13	GOPC	+	+	
Gγ13	RGS12	+	−	
Gγ13	MPDZ PDZ10-11	+	−	
Gγ13	MPDZ PDZ12-13	+	+	
Gγ13*	ZO-1 PDZ1	−		
Gγ13*	ZO-1 PDZ1-2	−		
Gγ13*	GOPC	−		
Gγ13*	MPDZ PDZ12-13	−		
Claudin 1	ZO-1 PDZ1	−		
Claudin 1	ZO-1 PDZ2	−		
Claudin 1	ZO-1 PDZ3	−		
Claudin 1	ZO-1 PDZ1-2	+	−	
Claudin 1	ZO-1 PDZ3-SH3	−		
Claudin 1	MPDZ PDZ8-9	+	−	
Claudin 1	MPDZ PDZ10-11	+	−	
Claudin 1	MPDZ PDZ12-13	−		
Claudin 4	ZO-1 PDZ1	−		
Claudin 4	ZO-1 PDZ2	−		
Claudin 4	ZO-1 PDZ3	−		
Claudin 4	ZO-1 PDZ1-2	+	+	−
Claudin 4	ZO-1 PDZ3-SH3	−		
Claudin 4	MPDZ PDZ8-9	+	−	
Claudin 4	MPDZ PDZ10-11	+	−	
Claudin 4	MPDZ PDZ12-13	−		
Claudin 8	ZO-1 PDZ1	+	+	+
Claudin 8	ZO-1 PDZ2	−		
Claudin 8	ZO-1 PDZ3	−		
Claudin 8	ZO-1 PDZ1-2	+	+	+
Claudin 8	ZO-1 PDZ3-SH3	−		
Claudin 8	MPDZ PDZ8-9	+	−	
Claudin 8	MPDZ PDZ10-11	+	−	
Claudin 8	MPDZ PDZ12-13	−		
JAM	ZO-1 PDZ3	−		
JAM	ZO-1 PDZ1-2	−		
JAM	ZO-1 PDZ2-3	−		
JAM	ZO-1 PDZ3-SH3	−		

The strength of the interaction was assessed by analyzing growth at 30° C in the presence of increasing concentrations of 3-AT. (+) indicates growth (−) indicates absence of growth. Cells were left empty when the experiment was not performed. Gγ13 is for the T65A mutant. JAM: Junctional adhesion molecule 1.*